



Swansea University
Prifysgol Abertawe



Swansea University E-Theses

The stratigraphy and sedimentology of Middle and Late Eocene carbonates of the Nile Valley, Egypt: A basinal analysis.

Abdou Soliman, Fathy Hussien

How to cite:

Abdou Soliman, Fathy Hussien (1988) *The stratigraphy and sedimentology of Middle and Late Eocene carbonates of the Nile Valley, Egypt: A basinal analysis..* thesis, Swansea University.

<http://cronfa.swan.ac.uk/Record/cronfa42551>

Use policy:

This item is brought to you by Swansea University. Any person downloading material is agreeing to abide by the terms of the repository licence: copies of full text items may be used or reproduced in any format or medium, without prior permission for personal research or study, educational or non-commercial purposes only. The copyright for any work remains with the original author unless otherwise specified. The full-text must not be sold in any format or medium without the formal permission of the copyright holder. Permission for multiple reproductions should be obtained from the original author.

Authors are personally responsible for adhering to copyright and publisher restrictions when uploading content to the repository.

Please link to the metadata record in the Swansea University repository, Cronfa (link given in the citation reference above.)

<http://www.swansea.ac.uk/library/researchsupport/ris-support/>

**THE STRATIGRAPHY AND SEDIMENTOLOGY
OF MIDDLE AND LATE EOCENE
CARBONATES OF THE NILE VALLEY,
EGYPT; A BASINAL ANALYSIS**

by

Fathy HUSSIEN ABDOU SOLIMAN

B.Sc. & M.Sc. (Assiut, Egypt)

**Thesis Submitted to the University of Wales
for the Degree of Doctor of Philosophy.**

**Earth Sciences Department
University College of Swansea
University of Wales
September, 1988.**

ProQuest Number: 10805300

All rights reserved

INFORMATION TO ALL USERS

The quality of this reproduction is dependent upon the quality of the copy submitted.

In the unlikely event that the author did not send a complete manuscript and there are missing pages, these will be noted. Also, if material had to be removed, a note will indicate the deletion.



ProQuest 10805300

Published by ProQuest LLC (2018). Copyright of the Dissertation is held by the Author.

All rights reserved.

This work is protected against unauthorized copying under Title 17, United States Code
Microform Edition © ProQuest LLC.

ProQuest LLC.
789 East Eisenhower Parkway
P.O. Box 1346
Ann Arbor, MI 48106 – 1346

1950

1951

DECLARATION

I declare that the contents of this thesis submitted for the Degree of Philosophiae Doctor are largely the result of my own independent investigations in the Nile Valley and Fayum provence, Northern Egypt.

The results have not been submitted in substance for any other degree, and it is not concurrently being submitted in candidature for any other degree.

All other works referred to in this thesis have been acknowledged.

Fathy H. Abdou Soliman
(Candidate)

Dr. A. T. S. Ramsay
(Director of Studies)



To my parents

ABSTRACT

Carbonate sediments in the northern Nile Valley were subjected to stratigraphical and sedimentological studies which led to a complete basinal analysis. Initiation of this basin occurred in the early Late Eocene at 40 MY.

A workable lithostratigraphy is developed to group the various Formations (Beni Suef, Birket Qarun, Saqqara, the Qurn, and the Wadi Hof) under one regional rock unit; the Middle Mokattam Unit. Biostratigraphical zonations were adapted, by means of nannoplankton and (both micro and larger) foraminifera, to date the strata as closely as possible and to achieve chronostratigraphical correlations. Onlap-offlap and facies interfingering relationships are recorded and discussed. The stratigraphical investigation has shown the presence of a depositional basin (Middle Mokattam basin) and detected its outline.

Sedimentological studies and detailed modal analysis of carbonate grains have identified 12 major facies and 36 microfacies associations. These have clarified the depositional environments which occupied the basin.

Careful basinal analysis, for both stratigraphical and sedimentological investigations, together with paleoecological determination of carbonate grains and communities, were used to reveal the basin configuration. Soft sediment deformation is also recorded and used to interpret the pattern of syndepositional subsidence which was controlled by rejuvenated deep-seated faults. Recurring uplift of the external northwestern block shaped the basin and controlled the depositional processes. This was responsible for an influx of resedimented deposits derived either from nearby shelves or from adjacent paleohighs. The resedimented deposits formed deeply channelled fans and clastic barriers. The basin exhibits abundant evidence of synchronous tectonic uplift and sedimentation. Features such as growth faults, syn-sedimentary and syn-tectonic unconformities, debris and mass gravity flow deposits demonstrate a direct link between sedimentation and tectonism, and highlight the episodic nature of uplift in the external parts of the basin. This uplift resulted in the syn-sedimentary southward shifting of the depositional axis.

P R E F A C E

- 1 - This thesis comes in one volume and occurs in nine chapters plus Appendix and references .
- 2 - Geographic coordinates for all locality names mentioned in the text are in Appendix "A" .
- 3 - Locations of logged sections are in Fig 2-1, and their numbers are referred to through the thesis figures numerically on top of their log lines .

CONTENTSPage

Abstract	
List of Figures	
List of Tables	
List of Plates	
Acknowledgments	

CHAPTER ONE1. INTRODUCTION

1-1	Preamble	1
1-2	Problem culmination	1
1-3	Research approach	2
1-4	General location	5
1-5	Topographic and Geological setting	5
1-6	History of Previous Research	9
1-6-1	Stratigraphy	11
1-6-1,1	Lithostratigraphic studies	11
1-6-1,2	Biostratigraphy	20
1-6-2	Sedimentological studies	25
1-7	Scope of the present work	28

CHAPTER TWO2. METHODOLOGY AND TECHNIQUES

2-1	Methods of collecting field Data	30
2-2	Laboratory techniques	32
2-2-1	Sedimentological techniques	32
2-2-1-1	Stained acetate peels of carbonate rocks.....	32
2-2-1-2	Thin sections	35
2-2-1-3	Point-counting.....	36
2-2-1-4	Facies analysis	38
2-2-1-5	Carbonate rock classification	39
2-2-2	Stratigraphical techniques	40
2-2-2-1	Calcareous Nannofossils	41
2-2-2-2	Micro and Larger foraminifers	42
2-2-2-3	Macro-fossils	43

CHAPTER THREE3. LITHOSTRATIGRAPHIC ANALYSIS

3-1	The term "Mokattam"	44
3-2	The Lower Mokattam Unit	46
3-3	The Middle Mokattam Unit	50
3-3-1	The Cairo Area.....	51
3-3-2	East Helwan Area	56
3-3-3	EL Saff-Beni Suef Area	61
3-3-4	The Fayum Area	68
3-4	The Upper Mokattam Unit	71

CHAPTER FOUR4. BIOSTRATIGRAPHIC ANALYSIS
& CHRONOSTRATIGRAPHIC
CORRELATIONS

4-1	Calcareous Nannoplankton Zonation	75
4-2	Foraminiferal Zonation	82
4-2-1	Planktonic Foraminiferal Zones.....	83
4-2-2	Larger Foram (Nummulitic) Zonation	93
4-2-3	Micro-Benthonic Foraminiferal Zonation	101
4-3	Chronocorrelation and Age Assignment.....	104

CHAPTER FIVE5. STRATIGRAPHIC RELATION AND
BASIN CONCEPT

5-1	Introduction	111
5-2	The onlap-offlap relationships	111
5-2(A)	The onlapping relationships	114
5-2(B)	The offlapping relationships	115
5-2(C)	Interpretation	116
5-3	Basin outline	118
5-4	Datum of correlation	120
5-5	Stratigraphic correlations	121

CHAPTER SIX6. FACIES & MICROFACIES ANALYSIS
AND THEIR DEPOSITIONAL
ENVIRONMENTS

6-1	<u>The marl facies (F1)</u>	130
6-1-1	Description	130
6-1-2	Distribution	132
6-1-3	Microfacies Associations	133
6-1-3-1	Marly lime mudstone microfacies (M1F1)	133
6-1-3-2	Marl microforaminiferal mudstone microfacies (M2F1)	135
6-1-3-3	Marly miliolid bioclastic lime-wackestone microfacies (M3F1)	136
6-1-3-4	Marly formainiferal molluscan lime-wackestone microfacies (M4F1)	137
6-1-3-5	Marly ostracod microforam lime-wackestone microfacies (M5F1)	138
6-1-3-6	Marl spiculific lime-wackestone microfacies (M6F1)	139
6-1-4	Depositional Environment of the marl facies	140
6-2	<u>Marly clay facies (F2)</u>	145
6-2-1	Description	145
6-2-2	Distribution	146
6-2-3	Microfacies Associations	146

	<u>Page</u>
6-2-3-1 Marly clay microforam lime-wackestone microfacies (M2F2)	148
6-2-3-2 Marly clay molluscan lime-wackestone microfacies (M8F2)	149
6-2-3-3 Marly clay clastic lime-wackestone microfacies (M9F2)	150
6-2-3-4 Calcareous shale microfacies (M10F2)	151
6-2-4 Depositional Environment of the marly clay facies	152
6-3 <u>The Wavy Bedded Carbonate Facies (F3)</u>	155
6-3-1 Description	155
6-3-2 Distribution	156
6-3-3 Microfacies Associations	157
6-3-3-1 Echinodermal bryozoan lime-mudstone wackestone microfacies (M11F3)	157
6-3-3-2 Nummulitic bioclastic lime-mudstone microfacies (M12F3)	161
6-3-3-3 Spiculitic Bryozoan lime-mudstone microfacies (M13F3)	162
6-3-3-4 Arenaceous Bioclastic lime-wackestone to grainstone microfacies (M14F3)	163
6-3-3-5 Nummulitic bioclastic lime-wackestone microfacies (M15F5)	166
6-3-3-6 Opercalinid arenaceous wackestone microfacies (M16F3)	168
6-3-3-7 Molluscan sandy lime-wackestone microfacies (M17F3)	168
6-3-4 Submarine Fans and their microfacies: An interpretation (fig 6-8)	169
6-4 <u>Mixed sandy clay carbonate facies (F4)</u>	178
6-4-1 Description	178
6-4-2 Distribution	180
6-4-3 Microfacies Associations	180
6-4-3-1 Sandy-clay foraminiferal lime-wackestone microfacies (M18F4)	180
6-4-3-2 Bioclastic silty sands lime-wackestone microfacies (M19F4)	182
6-4-3-3 Calcareous sand lime-packstone microfacies (M20F4)	183
6-4-3-4 Arenaceous silty lime-wackestone microfacies (M21F4)	184
6-4-3-5 Shale microfacies (M22F4)	185
6-4-4 Depositional environment of the ruxed sandy clay carbonate	185
6-5 <u>Bivalve carbonate facies (F5)</u>	189
6-5-1 Description	189
6-5-2 Distribution	191
6-5-3 Microfacies Association of facies (F5)	191
6-5-3-1 Bivalve packstone microfacies (M23F5)	191
6-5-3-2 Bivalve Bryozoan packstone microfacies (M24F5)	193
6-5-3-3 Bivalve Lithoclastic wackestone microfacies (M25F5)	195
6-5-3-4 Molluscan dolomitic wackestone microfacies (M26F6)	196
6-5-4 Depositional environment for the bivalve facies..	197

	<u>Page</u>	
6-6	<u>Nummulitic Facies (F6)</u>	200
6-6-1	Description	200
6-6-2	Distribution	200
6-6-3	Microfacies Associations	204
6-6-3-1	Nummulitic Arenaceous wackestone-packstone microfacies (M28F6)	205
6-6-3-2	Nummulitic echinodermal bryozoan wackestone packstone microfacies (M28F6)	205
6-6-4	Depositional environment of the nummulitic facies (F6)	207
6-7	<u>Pelletal Facies (F7)</u>	212
6-7-1	Description	212
6-7-2	Distribution	213
6-7-3	Microfacies Association	213
6-7-3-1	The pelletal nummulitic packstone microfacies (M29F7)	213
6-7-4	Depositional environment of the pelletal facies	217
6-8	<u>The conglomerate debris facies (F8)</u>	221
6-8-1	Description	221
6-8-2	Distribution	221
6-8-3	Microfacies Association	223
6-8-3-1	The conglomerate nummulitic packstone microfacies (M30F8)	223
6-8-4	Depositional Environment of the debris facies (F8)	225
6-9	<u>The coralline facies (F9)</u>	228
6-9-1	Description	228
6-9-2	Distribution	228
6-9-3	Microfacies association of facies (F9)	230
6-9-3-1	Coralline nummulitic boundstone to bafflestone microfacies (M31F9)	230
6-9-4	Depositional environment of the coral facies	231
6-10	<u>The serpulid facies (F10)</u>	233
6-10-1	Description	233
6-10-2	Distribution	234
6-10-3	Microfacies association of the facies (F10)	234
6-10-3-1	Serpulid foraminiferal packstone microfacies (M32F10)	234
6-10-4	Depositional environment of the serpulid facies	236
6-11	<u>Planktonic foraminiferal facies (F11)</u>	237
6-11-1	Description	237
6-11-2	Distribution	238
6-11-3	Microfacies association	238
6-11-3-1	Foraminiferal mudstone-wackestone microfacies (M33F11)	240
6-11-3-2	Pelagic wackestone microfacies (M34F11)	240
6-11-4	Depositional environments of the planktonic foraminifera	241
6-12	<u>Calcareous evaporitic shale facies (F12)</u>	242
6-12-1	Description	242
6-12-2	Distribution	243
6-12-3	Microfacies associations	243
6-12-3-1	The unfossiliferous shale microfacies (M35F12)	245

	<u>Page</u>
6-12-3-2 The operculina shale microfacies (M36F12)	245
6-12-4 Depositional Interpretation of the calcareous evaporitic shale facies (F12)	247

CHAPTER SEVEN

7. BASIN ANALYSIS

7-A	<u>Basin configuration of the Middle Mokattam facies .</u>	251
7-A-1	<u>Analysis of carbonate grains and communities</u>	251
(a)	The platform community	258
(b)	The coral community	260
(c)	Bioclastic-mud community.....	260
(d)	Planktonic foraminifera community	262
(e)	Micro-benthonic foraminifera community	262
7-A-2	<u>Basin Detection from microfacies</u>	264
7-A-3	<u>Stratigraphic thicknesses and basin configuration</u>	268
7-A-4	<u>Evaluation of the used methods in estimating basin configuration</u>	273
7-B	<u>Syn-Depositional Deformation structures from the Middle Mokattam of Egypt</u>	277
7-B-1	Slump structures	277
7-B-2	Gravity Block Sliding	283
7-B-3	Gravity Grain and Debris Flow	286
7-B-4	Syn depositional Unconformities	290
7-B-5	Growth Faults	292
7-B-6	Fluidized flow-scape features	294
7-C	<u>Tectonic influence and basin sedimentation</u>	297
7-D	<u>The Middle Mokattam basin and Source of Sediments .</u>	306

CHAPTER EIGHT

8.	<u>DEPOSITIONAL EVOLUTION OF THE MIDDLE MOKATTAM BASIN</u>	312
----	--	-----

CHAPTER NINE

9.	<u>GENERAL SUMMARY & RECOMENDATIONS</u>	
9-1	<u>GENERAL SUMMARY & CONCLUSIONS</u>	324
9-2	<u>RECOMENDATIONS FOR FURTHER RESEARCH</u>	329

<u>Appendix No.</u>	<u>APPENDICES</u>	<u>Page</u>
Appendix (A)	Geographic co-ordinates of localities and names mentioned in the text (A1-A2).....	331-332
Appendix (B)	Log graphs of measured sections (B1-B24)....	333-357
Appendix (C)	List of Point counting data (C1-C24).....	358-381
Appendix (D)	Computer programs used for plotting the variation graphs (D1-D26).....	382-409
Appendix (E)	Key and Vertical variation graphs of the carbonate components for the counted logs (E1-E25).....	410-434

REFERENCES 435-463

ARABIC SUMMARY 464-465

LIST OF FIGURES

<u>Fig. No.</u>		<u>Page</u>
1-1	Location map of the studied area.	4
1-2	Topographic map of the Nothern Nile Valley and Fayum area.	6
1-3	Principal drainage patterns for the studied area of N. Nile Valley.	7
1-4	Sketch map showing major geologic units of Nothern Nile Valley, Egypt.	8
2-1	Location map for the field sections and correlation trends	31
3-1	Map showing locations of the Middle Mokattam unit for the collected logs around Cairo.	54
3-2	Block diagram to show the change in facies thickness of the Middle Mokattam unit around Cairo.	55
4-1	Correlation chart of nannoplanktonic zones in the Middle, late Eocene sections of the N. Nile Valley Basin.	76
4-2	Lithostratigraphic correlation for the Middle Mokattam rock units in the studied basin, of Nothern Nile Valley, Egypt, along N-S direction.	105
5-1	Stratigraphical sequential relationships in the southeastern part of the studied Nile Valley basin, Egypt.	112
5-2	Stratigraphic sequential relationships in the northwestern parts of the studied Nile Valley Eocene basin, Egypt.	113
5-3	The outline shape of the studied basin of the Nothern Nile Valley and the Fayum area, Egypt.	119
5-4	General correlation of the Middle Mokattam unit.	122
5-5	Areal distribution of the different rock formations throughout the Middle Mokattam unit, Nile Valley and the Fayum basin, Egypt.	122
5-6	Lithostratigraphic correlation sections throughout the studied basin along A-A, B-B, C-C and D-D lines.	123
5-7	Isopach maps of the Middle Mokattam unit in the Nothern Nile Valley and the Fayum Basin, Egypt.	125
6-1	Facies distribution and correlation throughout the Nothern Nile Valley and the Fayum basin.	129

<u>Fig. No.</u>	<u>Page</u>
6-2	Log graph of the marly facies and normal graded sequences. 131
6-3	Schematic representation of sediment microfacies distribution of facies (F1) on the deep shelf margin of Nothern Nile Valley basin. 141
6-4	Diagrammatic representation of the marl facies (F1) shore line. 143
6-5(A)	Suggested stratigraphic and sedimentological model for the occurrence and interfingering of the different microfacies associations, with facies (F2) on the shelf platform. 153
(B)	Inferred seaward directions of the located platform margin slope facies (F2). 153
6-6	Diagram illustrating the sequence of the wavy bedded facies (F3) with its associated microfacies (M11-M17). 158
6-7(A)	General skematic diagram of facies (F3) and the lateral variation in a southeast to northwest direction. 170
6-7 (B)	Upper channel facies migration over the levee deposits to establish a new distributary. 173
6-8	Reconstruction model of fan and lobes environments of the modular beddes facies carbonate facies and the distribution of its microfacies. 174
6-9	Fining-up and coarsing-up sequence of mixed sandy clay facies (F4). 179
6-10	The inferred of barren complex through the deposition of the siliaclastic carbonate facies (F4), within the upper member facies of the Beni Suef formation 187
6-11	The molluscan facies (F5) in the southern and northern parts of the studied basin of Nothern Nile Valley Egypt. 190
6-12	Inferred idealized diagram illustrating the bivalue build up facies on a nummulitic carbonate platform, crossed by feeder channels. 198
6-13	Graphic log of the sequence of nummulitic facies (F6) and facies associations in section 61. 201
6-14	Distribution of nummulitic facies throughout the nothern part of the studied basin. 203

<u>Fig. No.</u>		<u>Page</u>
6-15	Distribution of nummulites according to the size variation in the neritic zone.....	208
6-16	Distribution of small nummulites around nummulitic banks.	208
6-17	Inferred diagrammatic representation of the nummulitic microfacies throughout the shelf.	210
6-18	Schematic representation of carbonate matrix distribution in contemporaneous to the nummulitic shelf facies deposition.	210
6-19	Depositional model and distribution of the pelletal, nummulitic and coral facies along the late Eocene carbonate shelf of the Guishi formation, Nile Valley, Egypt.	218
6-20	Model of growth and lateral avulsion of the pelletal fan lobes, and sequence characteristic of inactive pelletal lobe of deep water plain facies.	218
6-21	Upward coarsening sequences of facies f2, f4 and f8 in East Helwan area.	222
6-22	Sequences characteristic and inferred depositional environments of the debris facies.	226
6-23	Inferred stages of coral build up formation, on the carbonate platform edge of the Eocene Nile Valley, Egypt.	232
6-24	General characters of both M35 and M36.	246
6-25	Restricted lagoonal phase with a tear-drop pattern of operculina - shale facies imposed by the positioning of the sea-water (top of the studied Middle Mokattam facies, Egypt).	248
7-1	Lateral distribution of the highest percentages of the carbonate components. (Along direction No. 1)...	252
7-2	Lateral distribution of the highest percentages of the carbonate components (Along direction No. 3). ..	253
7-3	Lateral distribution of the highest percentages of the carbonate components (Along direction No. 2)....	254
7-4	Lateral distribution of the highest percentages of the carbonate components (Along direction No. 4). ..	255
7-5	Areal distribution of the carbonate grains on the studied datum of Northern Nile Valley and the Fayum Basin.	259

<u>Fig. No.</u>	<u>Page</u>	
7-6	Communities of the important carbonate skeletal on the studied datum plane.	261
7-7	Reconstruction of the Middle Mokattam facies bottom, in terms of skeletal grain communities.	261
7-8	Areal distribution of the studied facies and micro- facies, and then depositional environments throughout the datum plane of the basin.	265
7-9	Diagrammatic representation for the depositional environments responsible for the formation of the datum plane along nearby S-N direction (A-A').	266
7-10	Diagrammatic representation for the depositional environments responsible for the formation of the datum plane along B-B', C-C' and D-D' directions.	267
7-11(A)	Stratigraphic cross-section through the studied area of the Northern Nile Valley, Egypt, showing the basin configuration in a different direction.	269
7-11(B)	Basin shape in C-C' (SE-NW) direction (Northern limb of the basin.)	270
7-11(C)	Basin shape in B-B' (SE-NW) direction (Middle part of the basin).	271
7-11(D)	Basin shape in D-D' (NE-SW) direction (Southern limb of the basin).	271
7-12	Inferred paleogradients of the basin floor extracted from fig (7-11).	275
7-13	Slumped horizon in a nummulitic facies.	282
7-14	Idealised cross-section of the submarine failure in the Middle Mokattam basin, Egypt.	282
7-15	The mean direction of slumps and gravity block slide, movement, indicates the paleoslope strike trend around the deeper areas of the Middle Mokattam basin, Egypt.	284
7-16	Inferred major block faulted units and framework of the deep seated subblocks which constructed the basin..	299
7-17	Compiled subsurface and geophysical evidence for the deep seated faulted subblocks and the basin framework.	305
7-18	Reconstruction of the palio-provenance and source areas for the Middle Mokattam basin sediments.	309

<u>Fig. No.</u>		<u>Page</u>
8-1(A)	Major facies distribution along S-N direction.....	313
8-1(B)	Major facies distribution along SE-NW direction....	314
8-1(C)	Major facies distribution along the middle part of the basin.....	315
8-1(D)	Major facies distribution along the southern limb of the basin	315
8-2	Depositional model indicating the depositional history and developing of the Middle Mokattam unit.	317&318

LIST OF TABLES

<u>Table</u>		<u>Page</u>
1-1	Lithostratigraphic correlation of the Middle and Late Eocene rocks of the Nile Valley and Fayum, Egypt. ..	10
3-1	Proposed lithostratigraphic correlation for the rock units of the Northern Nile Valley and Fayum area...	45
4-1	Biostratigraphic correlation of the Upper Middle and Late Eocene sequences in Egypt.	74
4-2	Calcareous nannoplankton zonation of the studied basin sequences in the Northern Nile Valley, Egypt.	78
4-3	Distribution chart of the nannoplanktonic species in the studied area.	79
4-4	Planktonic foraminiferal zonations of the studied rock sequences in the Northern Nile Valley Eocene basin.	84
4-5	Distribution chart of the upper Middle and Late Eocene planktonic foraminiferal species in the studied rocks.	85
4-6	Large foraminiferal (nummulites) zones in the studied sequences of the Northern Nile Valley, basin.....	94
4-7	Nummulite species range chart of the studied rock sequences in Northern Egypt.	95
4-8	General biostratigraphic correlation for the upper Middle-Late Eocene of the Northern Nile Valley and Fayum in Egypt.....	107
4-9	Planktonic correlation between this work and both standard and regional workable zones in Egypt.....	109

LIST OF PLATES

<u>Plate No.</u>		<u>Page</u>
3-1	Giushi formation, top division of the lower Mokattam unit, East of Cairo. Both the Middle and Upper Mokattam overlie on right top of photo.....	48
3-2(A)	The Middle Mokattam unit (M) underlies the Upper Mokattam (U) in Gabal Mokattam, east of Cairo. Looking East. Scale box is 5 metres.	52
(B)	Top of the Middle Mokattam unit, where the man stands, in Gabal Mokattam, east of Cairo. Looking east.....	52
3-3	Middle Mokattam unit in Wadi Hof, east of the Helwan area. The Quern formation (Q) at base and the Wadi Garawi Formation (W) on the top. Looking North.....	57
3-4(A)	The Middle Mokattam facies at Gabal Qibli El-Arram; South of the Giza Pyramids (M), precedes younger Pliocene Sediments (P), looking south (scale is 3 meters).	59
(B)	The Middle Mokattam unit at Gabal El-Maskara, east of the Helwan area, looking south west.....	59
3-5	The Beni Suef formation, Middle Mokattam unit, with the Qurn Member (A) at its lower part, and the Tarbul Member (B) at the top (Gabal Tarbul).....	62
6-1	Marl microfacies associations (F1).....	134
6-2	Marly clay microfacies (F2).	147
6-3	Wavy bedded carbonate facies (F3).....	160
6-4(A)	Upper body of polymictic disorganised conglomerate. Residimented grain supported, Calcurudite turbidite. Clastic rotation, growth faults and slump structures occur. The lower layers are of proximal levee deposits.	164
(B)	Migrating of upper fan deposits to a new active prograding channel.....	164
6-5	Mixed sandy-clay facies associations (F4).....	181
6-6	The bivalve facies (F5).	192
6-7	Bivalval facies associations (F5).....	194
6-8	Nummulite facies (F6).	202
6-9	Nummulite microfacies associations (F6).	206
6-10	Pelletal microfacies associations (F7).	214&21

<u>Plate No.</u>	<u>Page</u>
6-11	224
6-12	229
6-13	235
6-14	239
6-15	244
7-1	278
7-2	279
7-3(A)	281
(B)	281
7-4	285
7-5	287
7-6(A)	289
(B)	289
7-7	293

<u>Plate No.</u>	<u>Page</u>
7-8	295
7-9	296
7-10	301
7-11	302
7-12	303

ACKNOWLEDGEMENTS

I wish to thank Dr. A.T.S. Ramsay for supervising this project. His help in identifying the nannoplanktons and reading the manuscript are greatly appreciated. My thanks are also due to Professor D.V. Ager and Professor R.B. Kidd for their continuous help, valuable discussions and for providing various departmental facilities.

I would also like to express my appreciation of the help received from Dr. C.G. Adams in the British Museum, for his assistance in identifying the nummulites and for allowing the author to study foraminiferal collections and topotype materials at the Museum. Professor F. Banner of London University have kindly checked some planktonic foraminiferal species, for which I am grateful.

Thanks also to Drs. G. Owen and S. Nolan for stimulating discussions on sedimentology. Thanks are also to my friend Dr. S. Hanna for his beneficial discussions on tectonism, reading few verses of the draft, and for his continuous and willing help in labelling some diagrams.

I wish to credit Mr. S. Hibbs (Dark Room) for providing helpful assistance with the reproduction of plates and photographs. My thanks are also extended to my research colleagues, the staff members, technicians, and to the secretaries of Swansea Earth Science Department for their help.

Thanks are also due to the staff of the Natural Sciences library and the computer centre, University College of Swansea for their kind assistance.

I am especially grateful to some of my friends :- Dr. A. El-Agha for his support and reading parts of the final draft, which proved so helpful; and to Heba who provided great assistance and lots of fun during the last stages of the work.

I am also grateful to the Egyptian Government and to the Geology Department, Minia University, Egypt, for financing and supporting this research project. The receipt of an O.R.S. award in the last two years of research, is gratefully acknowledged.

My sincere gratitude goes to my family in Egypt, and to my wife and daughters Dalia, Deena, Dauaa, without whose sacrifice and patience this work could not have been possible. There great enthusiasm, tireless efforts in seeing the thesis completion, and their endless love will never be forgotten.

INTRODUCTION

CHAPTER ONE

1. INTRODUCTION

1.1 Preamble

The sedimentology of the Eocene carbonate rocks of Egypt is not yet understood. There have been few attempts to elucidate depositional environments and their sedimentary processes and the evolutionary history of the Middle-Late Eocene carbonates. However, a research project has been carried out on some of the exposed carbonate sequences along the Nile Valley banks by the sedimentology sections of Assiut and Minia Universities in Egypt. Yet the stratigraphical relationships between the rock units in many parts of the Nile Valley - and between this region and other parts of the country - has not been studied in detail.

1.2 Problem culmination

In the last 30 years, much has been written about the Middle-Late Eocene rock units, although from different localities. In this respect, there have been two main working research groups on the surrounding limestones which border the Nile Valley. One group, the Upper Egypt geologists, started research in their home adjacent deserts extending their work from the far south to the north [Bishay (1961,1966), Boukhary (1973), Omara *et al.*, (1972, a, & b)]. The second group, the Capital

geologists, started their rock investigations around Cairo and extended these studies southwards [Farag and Ismail (1959), Said (1962, 1971), Strougo (1979) and Abdel-Kireem (1985)]. At the same time, a third group of researchers were interested in the rocks which surround the Fayum [Said (1962, 1971), Bishay (1966), Abdou and Abdel-Kireem (1972), Strougo (1977; 1979) Shama (1976) and Shama et al., (1982)]. They all published a large number of informal formational names but reached a point where now it is very difficult to match their formation schemes and to correlate these even within one unit of a long exposed section (Table 1-1). Moreover, neither the rock units names nor their ages were stable even within most subsequent works by the same authors. As a result, the misleading correlations paralysed the research on the Mid-Late Eocene stratigraphical column of Egypt. This confusion in correlation has increased through time as each author developed individual stratigraphical sections for different localities. To tie up the results of the three groups became a major problem and offered a question of comparing the incomparable. The result was that the overall view of depositional history and of regional events throughout the basin became obscured.

1.3 Research Approach

When the author was studying the carbonates of the Beni Suef area [Abdou-Soliman, 1980], the key point which aroused his interest for further research was to study the Middle-Late Eocene with the view of understanding the

depositional basin and its history. So the term "sedimentary basin" is in constant use in this work. Using this term, we imply a basin that comprises a sequence of layers of sedimentary rocks which occupies an area that is more or less oval to trough-shaped. Also, the sequence thins considerably or pinches out completely along the edge of this area [Conybeare, 1979].

Consequently, the theme of this work has been to choose and locate a suitable sedimentary basin, detect its configuration and then analyse the main elements of the basin. In order to achieve this, our principal aim was to depict the solid geometry, structural, and stratigraphical framework of a basin as it is at present. For this purpose, the northern Nile Valley and the Fayum basin were chosen for the present project since the boundary between the Middle-Late Eocene is well represented in these localities. We believe that the detailed carbonate sedimentology and environmental study will certainly help in clarifying these relationships and will throw more light upon the history of the Middle and Late Eocene in the Nile Valley and the Fayum basin. It is also hoped that elucidation of the depositional environments and the basinal analysis would lead to better understanding of the sedimentology and stratigraphy of the Middle-Late Eocene throughout Egypt, especially by investigating the effect of their syndepositional tectonism.

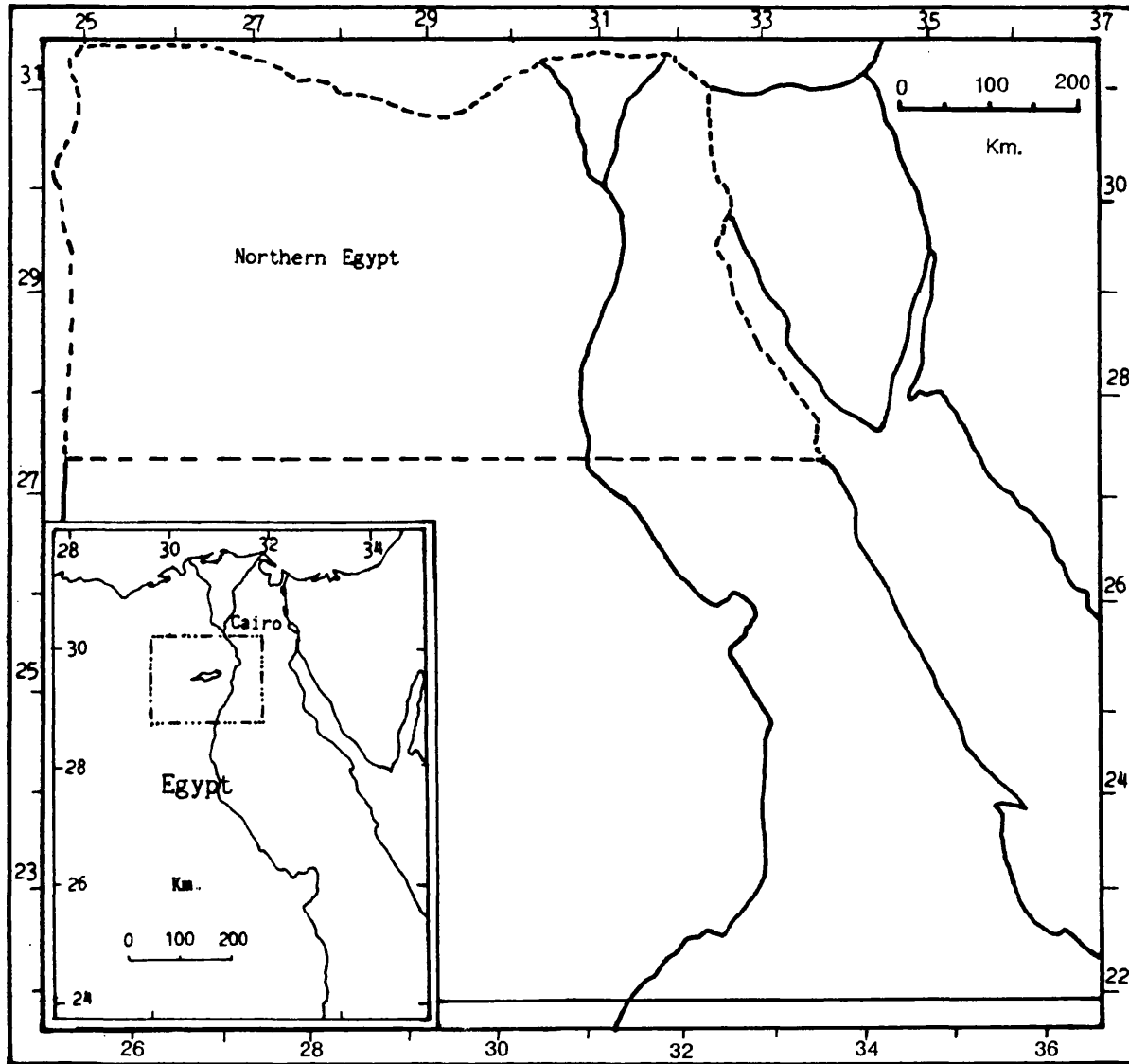


Fig.(1-1): Location map for the studied area, northern Egypt.

— Studied area - - - Northern Egypt

1.4 General Location

The main region pertinent to this study is included within the northern Nile Valley and the Fayum area in both the Eastern and Western Deserts of Egypt. This region may be defined as that part of the Nile Valley borders which lies to the north of Maghagha. The area of concern, in this study, covers approximately 15.375 square kilometers and lies between longitudes 30°30' and 32°00' east and latitudes 28°40' and 30°10' north (Fig. 1-1).

1.5 Topographic and Geological Setting

The Eocene rocks form a major topographic feature across the Nile Valley of Egypt. The studied area, as indicated in the general topographic map (Fig. 1-2), shows excellent exposure from 60% to 80% in many places. Physically, much of the area is inaccessible except by camel or on foot. The topographic elevation of the area indicates a general topographic slope towards the west-northwest. The relief ranges from 2920 feet (above sea level) to 141 feet (below the sea level). The topographic relief features of the area consist mainly of plateaux, scarps, plains, and ridges. The area is dissected by a number of main valleys or drainage lines (Fig. 1-3) which represent the principal drainage patterns in the area of study.

The generalised geological setting of the field area is indicated in Fig. 1-4. The Middle-Late Eocene rocks are encountered in the northern parts of the Eocene rocks

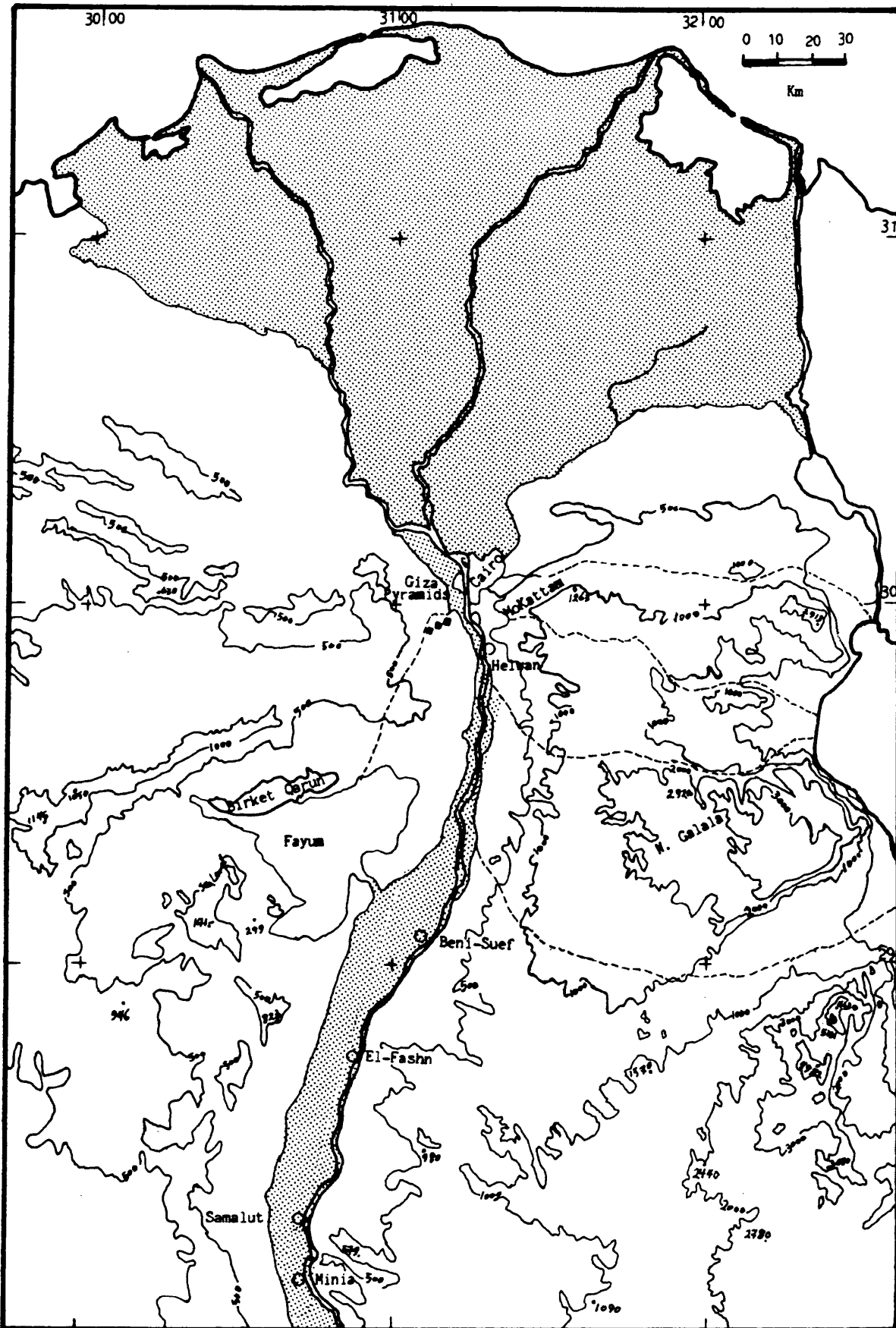


Fig. (1-2): General topographic map of the northern Nile Valley and Fayum, Egypt (heights in feet).

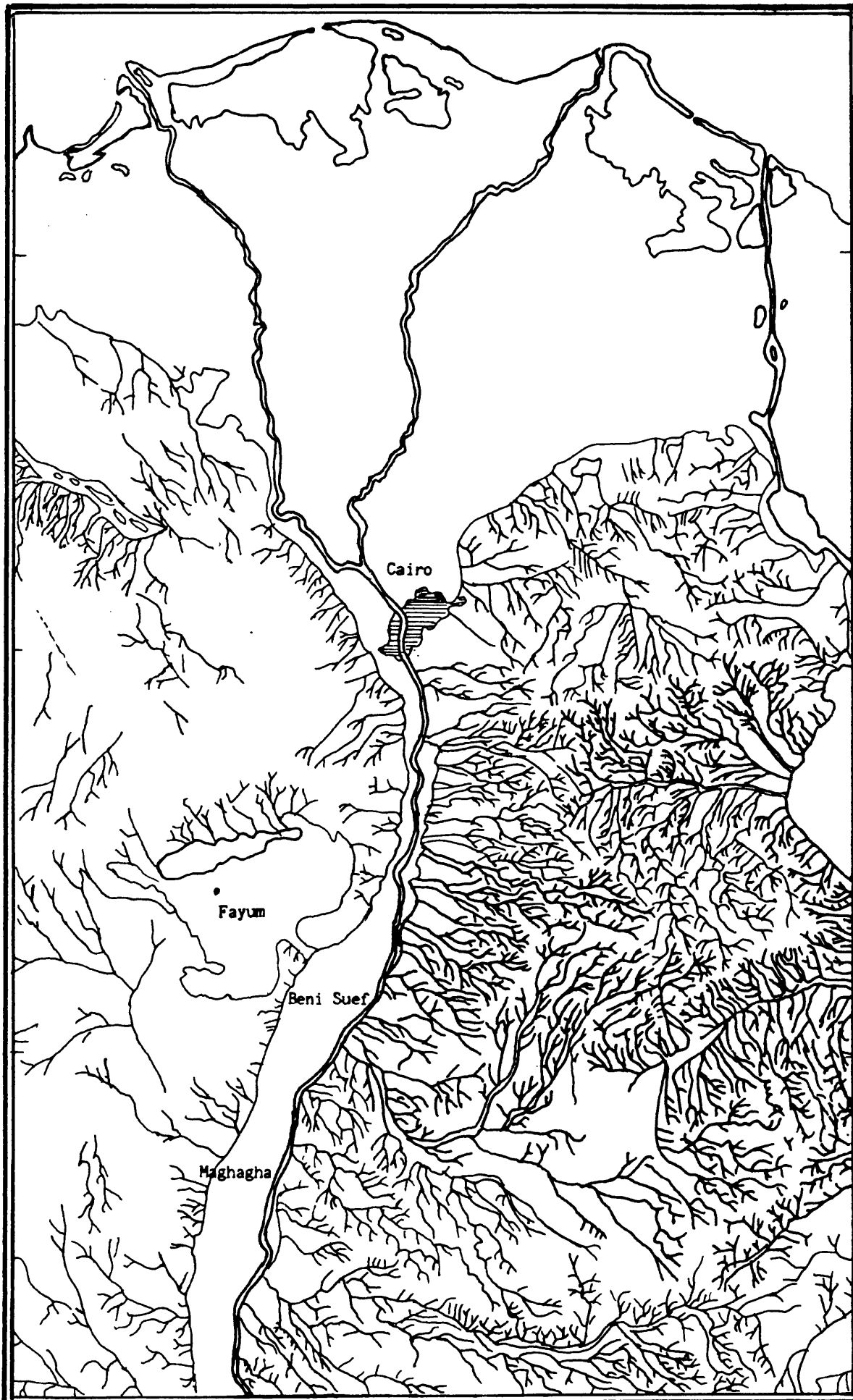


Fig. (1-3): Principal drainage patterns for the studied area of N. Nile Valley.

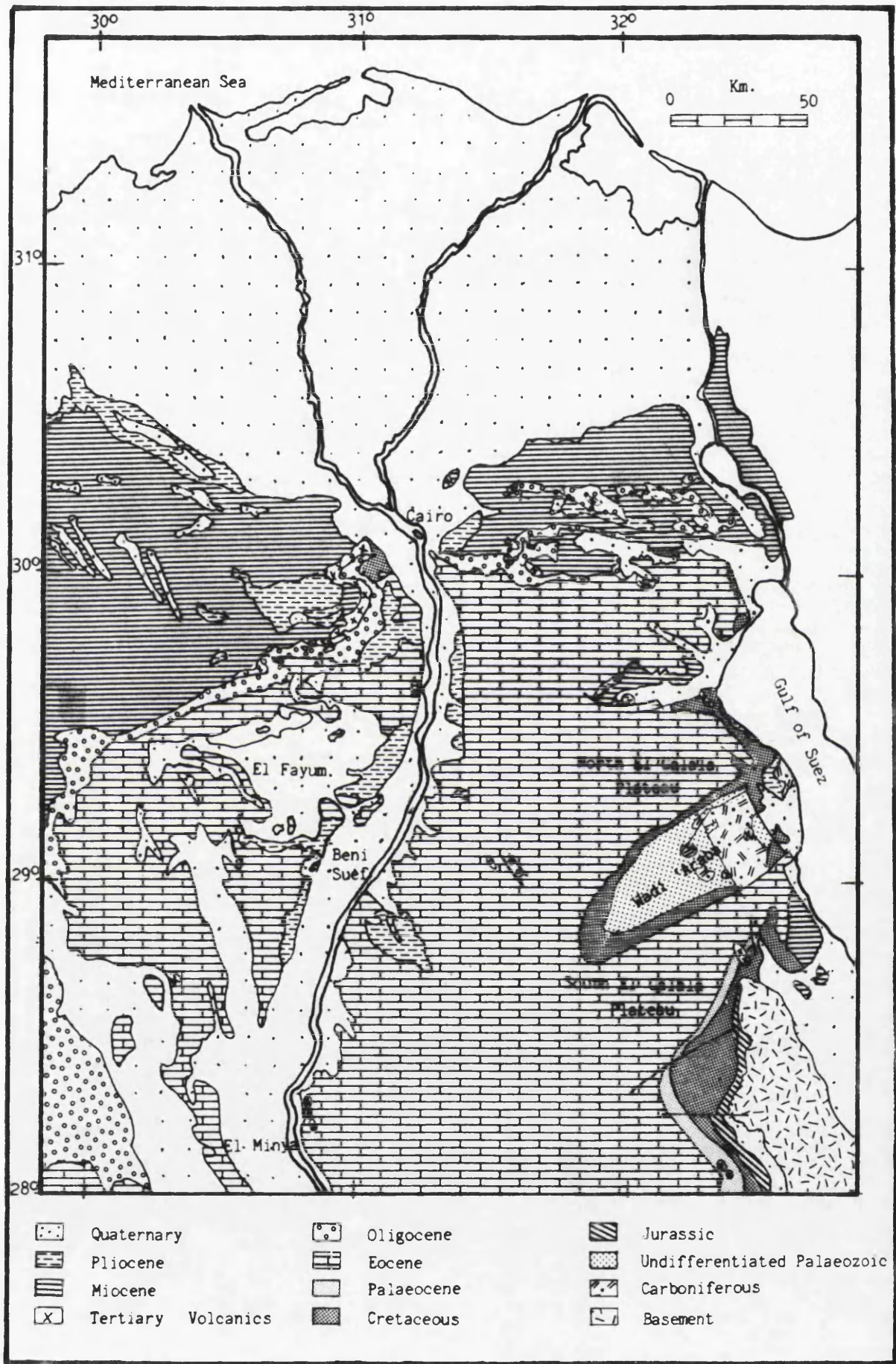


Fig. (1-4): Sketch map showing major geologic units of Northern Nile Valley, Egypt (Survey Department, Cairo, 1981).

in the country. Most of these rocks are represented by limestones of monotonous appearance, marls and calcareous clastics. However, Said (1971, p.22) mentioned that attempts to map or zone the Eocene in a satisfactory and reasonably natural way had not so far been successful. The mapping is difficult because the detailed stratigraphy is poorly known and faults are not easy to trace [Said, 1971, p.22].

1.6 History of Previous Research

The history of geological research in Egypt has been revealed in quite extensive published and unpublished literature. The most distinguished of these are: Sherborn (1910), Hume (1925), Keldani (1939), Said and El-Shazly (1957), Said (1962) and the publication list of the Geological Survey of Egypt (Anon., 1981). The geology of the area lying between Cairo and Minia in the Northern Nile Valley and Fayum has received only little detailed attention. However, the area was included in more regional as well as limited separately local studies carried out by Zittel (1883), Schweinfurth (1883), Fourtau (1897, 1912, and 1916), Blanckenhorn (1900), Oppenheim (1903), Beadnell (1905), Barron (1907), Boussac (1910), Hume (1911, 1912, and 1925), Cuvillier (1924, 1930), Little (1936), Barker (1945), Ansary (1955), Ghorab and Ismail (1957), Ismail and Farag (1957), Nakkady (1958), Farag and Ismail (1959), Said (1961, 1962, 1963 and 1971), Said and Martin (1964), Krashennnikov and Ponikarov (1964), Bishay (1966), Furon (1968), Tadros (1968),

Beckmann *et al.*, (1969), Boukhary (1970, 1973), El-Naggar (1970), Ismail and Abdel-Kireem (1971), Abdou and Abdel-Kireem (1972), Bassiouni *et al.*, (1974), Hanna (1974), Fahmy (1975), Salem (1976), Strougo (1977, 1979), Hassan *et al.*, (1978), Kenawy *et al.*, (1978), Omara *et al.*, (1978), El-Dawoody (1979), Abdou-Soliman (1980), Aigner (1982, 1983), Bown (1982), Boukhary *et al.*, (1982, 1983), Shamah *et al.*, (1982), Strougo *et al.*, (1982), Philobos (1984) and Abdel-Kireem (1985).

1.6.1 Stratigraphy

A detailed review of the stratigraphic history of the area under consideration and its surroundings is given by Said (1962), Bishay (1966), Boukhary (1970, 1973), Hassan *et al.*, (1978) and Abdou-Soliman (1980). A short review of some salient stratigraphic studies (Table 1-1) of the Middle and Late Eocene on the rocks of the studied area and its surroundings is given in this chapter.

1.6.1.1 Lithostratigraphic studies

The history of lithostratigraphic research on the Palaeogene sections of the Nile Valley dates back to the end of the nineteenth century. The Nile Valley cliffs and the Fayum depression surrounding plateaux have attracted the attention of many workers either for their accessibility or for the fame of some localities as archeological sites. The work during this period up until the present time, somehow, reflects the development of the geology of the area as a whole. The history of research, in the studied area, may be divided into two stages.

The first stage is the interval from 1883 onwards, up until 1929. This can be considered as the regional descriptive period. This stage was closely associated with the foundation of the Geological Survey of Egypt in 1896. The pioneer systematic study of the Palaeogene sections of the Nile Valley started by Zittle (1883) who, in the east of Cairo, referred the "Mokattam Stufe" for all the rock sequences of the Mokattam area to the Middle Eocene. The strata at the Mokattam area are, however, differentiated into a lower two thirds consisting of white limestones, and an upper grayish to reddish brown sequence that is characterised by numerous beds of clastic rocks. This marked lithological separation led Schweinfurth (1883) to subdivide these strata to "Unter" and "über" Mokattam. He dated them as Middle Eocene. Blanckenhorn (1900), subdivided the Middle Eocene Mokattam rocks into Lower Mokattam with *N. gizehensis* beds, and Upper Mokattam with *Carolia* beds. The status of the area within the Middle Eocene was reconsidered by Hume (1911), but at that time a third term, the "Middle Mokattam" was defined - for the first time - for the beds with *Exogyra*, which form the lower part of the *Carolia* beds. Later on, Boussac (1916) recognized the equivalent of the Priabonian of Europe within the Upper Mokattam and that was also proved by Fourtau (1916) when she recorded Late Eocene echinoidal faunas from the Upper Mokattam. In 1924, Cuvillier updated the whole Upper Mokattam to be of Late Eocene

describing it as of brown beds with *Carolia*. He (*op. cit.*) added a new point by referring to the Middle Mokattam of Hume, as the limestone with *Operculina pyramidum* and bryozoa of Lutetian age, representing the top part of the Lower Mokattam.

The Helwan and Beni Suef areas were included within the Lower Mokattam on Hume's map (1911, Table VI), and remained during this period without lithologic classification.

In the Fayum area, Beadnell (1905) divided the Eocene rocks into Qasr El Sagha series, at the top, Birket Qarun series, Ravine beds, and Wadi El Rayan series, at the base. He (*op. cit.*) reported the Birket Qarun and Qasr El sagha series as belonging to the Late Eocene. That classification has been considered as a very important reference in most subsequent work up to the present. In his work, Hume (1911) correlated Beadnell's (1905) divisions with his Mokattam classifications. He compared his Lower Mokattam with the Wadi El Rayan beds, the Middle Mokattam with the Birket Qarun beds, and the Upper Mokattam with the Qasr El Sagha beds.

By 1925, Hume culminated this period by the publication of his "Geology of Egypt". After that, the foundations of the regional geology of Egypt were firmly laid down during this first period which ended by the publication of the Geological Map of the Geological Survey of Egypt in 1928.

The second stage extended from 1930 until the present time and is closely associated with the extensive work of petroleum exploration and with the establishment of the Egyptian universities. During this period, detailed and elaborate studies have been carried out. Cuvillier (1930) was the first to lead the way in this stage by his publication about "Révision du nummulitique Egyptien". His work was a real encyclopedia for the Eocene stratigraphy of Egypt. The Mokattam unit occupied the major part of Cuvillier's (1930) work. He (*op. cit.*) mentioned that the Middle and Upper Mokattam, in the Cairo area, belonged to the Lower Bartonian (Late Eocene in his sense). The relationship between the Late Eocene and the underlying Middle Eocene was described and the geographic distribution of that boundary, according to Cuvillier (1930), was found to occur in Gabal Qibli el Ahram (South Giza Pyramids), Gabal Giushi of Mokattam, and in east Maadi. Nakkady (1958) included the Eocene stratigraphy within his teaching book of 'Geology of Egypt' without substantial division.

Around the 1960's, another stage of different rock unit naming started and thus the stratigraphical correlation seemed to be lost through the generosity of the used unit names. Said (1962) tried to make use of collecting all the efforts of his staff of geologists, as the director of the Egyptian survey, and launched his book

"The Geology of Egypt", which is considered as the bible of Egyptian geology. In that book, Said (1962), subdivided the Eocene succession of the Mokattam area and southwards to the Beni Mazar area into two main divisions; the Mokattam Formation (Middle to Late Eocene) and the Maadi Formation (Late Eocene). According to Said (1962), his Mokattam and Maadi Formations are equivalent to both the Lower and Upper Mokattam of Schweinfurth (1883). Said and Martin (1964) subdivided the Mokattam Formation of Said (1962) into 4 rock members starting from the base upwards as (1) Lower building-stone Member, (2) Gizehensis Member, (3) Upper building-stone Member, and (4) Giushi Member. The lower three members are dated Upper Lutetian (Middle Eocene), whereas the uppermost member (Giushi Member) is dated Bartonian (Late Eocene). Tadros (1968) followed the previous divisions in Gabal Mokattam but he subdivided the Mokattam formation into new member names starting from below by (A) Kait-Bay limestone Member, (B) Khalifa building-stone Member, and (C) Giushi Member. Said (1971) changed his view and subdivided the Mokattam Formation of Said (1962) into Gabal Hof Member, at the base, and Building-Stone member at the top. He (*op. cit.*, table III), in the same work, stated that the Late Eocene was subdivided into two rock formations: the Giushi Formation (base), and the Maadi Formation (top). Strougo (1977) was not contented with Said's (1962-1971) classifications. He employed Hume's (1911) divisions as

Lower, Middle and Upper Mokattam. The Middle Mokattam is used by Strougo (1977) in Gabal Mokattam in a different sense to include both of Hume (1911) and Cuvillier (1930). That means Strougo's Middle Mokattam extends downwards to lump the Bryozoan limestone (Giushi Formation of Said) together with the marly horizons which underlie the *Carolia placunoides* beds. In 1979, Strougo suggested that the Middle Mokattam corresponded with the "Biarritzian" (uppermost middle Eocene) age.

Abdel-Kireem (1985), in the Gabal Mokattam area, preferred applying the divisions of the Lower and Upper Mokattam Formations and adopted 3 subdivisions for the Lower Mokattam Formation (a) Gizehensis Member (base), (b) Building Stone Member, and (c) Giushi Member.

The Late Eocene boundary, according to Abdel-Kireem (*op. cit.*), coincides with the upper part of the Giushi Member.

In the Helwan area, as early as 1930, Cuvillier recorded the Late Eocene boundary of undifferentiated rocks in Wadi Hof, but no details of this sequence were given. The only piece of previous detailed work is given by Farag and Ismail (1959) in the Helwan area, where the Eocene succession is divided into 5 rock series. The first older unit is the Gabal Hof Series which is overlain by the Observatory Series (Middle Eocene age). The latter is overlain by the Qurn Series, the Wadi Garawi Series and the Wadi Hof series (Late Eocene age). Said (1971) used

the terminology of Farag and Ismail (1959) in formal names. He (*op. cit.*) correlated his Giushi Formation, in the Mokattam area, with the Qurn Formation and the Maadi Formation with the Wadi Garawi Formation only. That latter relationship contradicts what he himself admitted before in 1962 (p. 137) when he mentioned that the Maadi Formation was equivalent to both the Wadi Garawi and the Wadi Hof Formations.

In the Beni Suef area, during this second stage, Cuvillier (1930) described a lithological section from the northern side of Gabal Shaibun (east of Beni Suef). He (*op. cit.*) indicated that the approximate limit of the Late Eocene rocks was found east of Biba in the Wadi Sannure, El Fashn, Beni Suef, El-Wasta areas. The first differentiated trail, in this period, started by Barker (1945) when he included the area from El-Fashn and northwards to El-Wasta within his Eocene studies. He subdivided the Eocene rocks in the previous area into 3 formations of cartographic value, to which he gave the following names: Formations D, E (Middle Eocene), and F (Late Eocene). Bishay (1966) identified those of Barker (1945) and subdivided the succession into: Late Eocene, represented by the Fayum Formation, and Middle Eocene, represented by El Fashn and the Beni Suef Formations. Said (1971) included the Beni Suef and its surrounding area on his map as undifferentiated Eocene rocks.

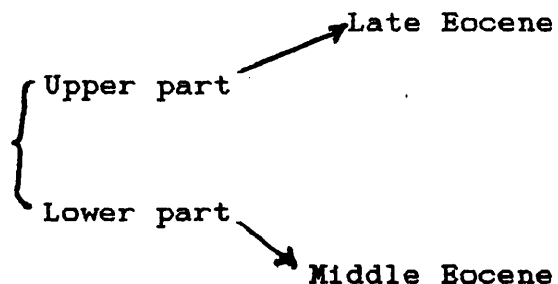
Boukhary (1973) related the Eocene succession of the Beni Suef area to the Mokattam Formation and subdivided it from the top downwards into (a) Shaibun Member (lower Late Eocene), Upper Building stone Member, which he believed to be equivalent to the Beni Suef Member, and (c) Upper Gizehensis Member (Middle Eocene).

Hassan *et al.*, (1978) gave the following classification for the Eocene of the area east of Beni Suef.

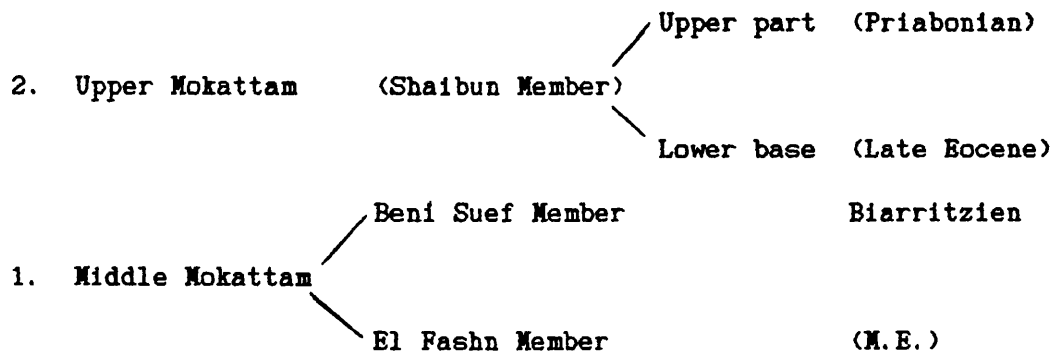
3. Wadi Hof Formation

2. The Qurn formation

1. Mokattam formation



Strougo (1977, p. 60) divided the succession of Gabal Hamret Shaibun into two divisions:



He (*op. cit.*, p. 89) added that the Shaibun Member extended northwards to the east and west Cairo areas.

Abdou-Soliman (1980) divided the Late Eocene succession of the northeast Beni Suef area to:

3. Maadi Formation

2. Beni Suef Formation

→ Tarbul Member

→ Qurn Member

In the Fayum area, Cuvillier (1930) recorded the lower boundary of the Bartonian (Late Eocene) in the top of Wadi Moela, Gabal Gehannam and Birket Qarum. Little (1936) mapped an indifferetiated Eocene rocks of the Fayum depression. Bishay (1966) described the Birket Qarum section as the type section for the Fayum Formation. Said (1962) used Beadnell's (1905) classification, but in a formal sense. He referred to the Middle Eocene rocks as the Wadi Rayan Formation which is overlain by the Ravine Formation, and the Late Eocene succession as the Birket Qarum Formation overlain by the Qasr El-Sagha Formation. In 1971, Said changed his view and used the Gar Gehannam Formation instead of the Ravine Formation.

In 1972, Abdou and Abdel-Kireem and Abdel-Kireem (1985) divided the Late Eocene of the Fayum sections from top to base into two formations: the Qasr El Sagha Formation, and the Gehannam Formation. The latter

formation is subdivided into two members; the Gehannam shale Member (top) and the Gehannam marl Member (base).

Strougo (1977) indicated that the Middle Mokattam can be correlated with the Fayum area to include both the Gehannam and the Birket Qarum Formations, whereas the Upper Mokattam will be equivalent to the Qasr El sagha Formation. Strougo (1977, 1979) pointed out that the counterparts of the Middle Mokattam in the Fayum area were of Middle Eocene "Biarritzian" age.

1.6.1.2 Biostratigraphy

Hume (1911) considered the Late Eocene of Egypt to be characterised by *Nummulites fabianii*, A and B forms (but respectively under the names *N. fichtelii* Mich., and *N. intermedius*, D'Arch.), and *N. chavannesi* De La Harpe.

Cuvillier (1930) separated the Late Eocene succession of Egypt into two main divisions; the Upper Bartonian, which includes the beds with *Nummulites fabianii*, and *N. chavannesi*, represented by the Qasr El Sagha series of Fayum. The Lower Bartonian, represented by the limestone with *Nummulites contortus-striatus* and bryozoa, corresponds to the Upper Mokattam and the terminal beds of the Lower Mokattam stage.

Ansary (1955) and Ansarry and Ismail (1956) studied the microforaminiferal contents of different stratigraphic sections measured in the Late Eocene at Wadi Tayiba (Sinai), Fayum, the Maadi and east of Helwan areas. Ansary (1955) recorded two foraminifera zones; (1) *Robulus-Bolivina-Nonion* Zone, and (2) *Bolivina-Nonion*

Zone. He (*op. cit.*) in the Fayum area distinguished another two biozones; (1) *Gyroidina cibaoensis* Zone and, (2) *Haplophragmoides emaciatus* Zone. The age assigned by Ansary (1955) for these biozones is Late Eocene age.

Ansary and Ismail (1956) attempted to define the Middle-Late Eocene boundary of the succession east of Helwan based on its microbenthonic foraminiferal content. They drew their boundary line between the two epochs at the contact between their Observatory Series and their Qurn Series.

Bishay (1966) gave regional larger foraminiferal zonations for the Middle-Late Eocene of the Nile Valley and southwest Sinai. According to his view, the Middle-Late Eocene boundary can be revealed through the following zones:

- | | | | | |
|----|------------------------------|------|---|-----------------|
| 1. | <i>Nummulites gizehensis</i> | Zone | } | (Middle Eocene) |
| 2. | <i>N. beaumonti</i> | Zone | | |
| 3. | <i>N. striatus</i> | Zone | | (Late Eocene) |

Tadros (1968) studies the Middle and Late Eocene rocks of Gabal Mokattam and gave the following biostratigraphic zonation for the Late Eocene succession:

- Base 1 *Bulimina jacksonensis* - *Uvigerina mediterranea*
 Zone
- (i) *Chilogumblina cubensis* Subzone
- (ii) *Anomalina afinis* Subzone
- (iii) *Bulimina jarvisi misrensis* Subzone
2. *Cancris cocasensis* - *Massilina decorata* Zone
3. *Pyrgo subspharica* Zone

Boukhary (1970) defined the following biozones from Minia to Beni Suef adjacent to the Nile Valley area:-

- Top 4. *Nummulites contortus/Sphaerogypsina globulus* Zone
3. *Truncorotaloides rohri* Zone = *Nummulites beaumonti*
 / *Gypsina carteri* Zone
2. *Nummulites gizehensis* Zone
1. *Alveolina frumentiformis* Zone

The uppermost zone (No. 4) is considered to be of the Late Eocene and the underlying two zones (Nos. 3 and 2) belong to the upper Middle Eocene. The lowermost zone, however, is represented at the Minia area and considered as lower Middle Eocene age.

Abdou and Abdel-Kireem (1972) identified the following planktonic foraminiferal zones:

- Top 1. *Globigerinatheka semiinvoluta* Zone
 2. *Truncorotaloides rohri* Zone
 3. *Globorotalia lehneri* Zone
 4. *Globigerapsis kugleri* Zone

The upper zones (Nos. 1 and top of 2) are assigned to the Late Eocene, while the rest is of the Middle Eocene.

Fahmy (1975) divided the Eocene of the Nile Valley into:

1. *Bolivina ventricosa* Zone as a Late Eocene. This zone comprises the Fayum Formation and the top part of the Beni Suef Formation.
2. *Truncorotaloides rohri* Zone, as Lutetian (Middle Eocene) age. This zone yields the lower part of the Beni Suef Formation.

Bassiouni et al., (1974) were able to define two biozones in the Minia-Beni Suef area:

1. *Nummulites striatus* (*Sphaerogysina globulosa* zone of Late Eocene).
2. *Truncorotaloides rohri* (Late Lutetian).

Strougo (1977) reported the following biozones on Bivalve bases from the Middle - Late Eocene of Egypt:-

- Top 1. *Nicaisolopha clotbeyi/Felaniella (Zemysia) cycloidea* Zone.
2. *Plicatula (Darteplicatula) polymorpha* Zone
 3. *Carolia placunoides* Zone
 4. *Cossmannella fajumensis* Zone

The boundary between the Middle-Late Eocene is placed between zone No. 3 and zone No. 4.

Omara *et al.*, (1978b) in the area south west of Beni Suef, reported the following biozones, arranged from base to top.

1. *Nummulites gizehensis* Zone (Late Lutetian)
2. *N. beaumonti* Zone (Late Lutetian)
3. *Truncorotaloides rohri* Zone
(uppermost Middle Eocene)

Strougo (1979) has the opinion that the beds of the Mokattam, with *Nummulites striatus*, belong to Biarritzian (uppermost Middle Eocene). On the other hand, the upper beds of the Mokattam, with *Carolia placunoides* and *Nummulites fabianii*, belong to the Priabonian (Late Eocene). He (*op. cit.*) emphasized that the occurrence of the bivalves *Carolia placunoides* was essential to define the Late Eocene in Egypt.

Kenaway (1978) recorded some new species of foraminifera from the early Late Eocene of the Fayum area.

Abdou-Soliman (1980) recorded the following biozones from the area northeast of Beni Suef:

8. *Nummulites striatus* Zone
7. *Operculina pyramidum* Zone
6. *Cancris cocaensis/Massilina decorata* Zone
5. *Bulimina jacksonensis/Uvigerina mediterranea* Zone
4. *Truncorotaloides rohri* Zone
3. *Mesophyllum/Lithothamnium* Zone

2. *Orbitolites complanatus* Zone

1. *Nummulites gizehensis* zone

Zones 1-4 are of Middle Eocene, while zones 5-8 are of Late Eocene.

Omara and Kenawy (1984) identified new species *Nummulites rohlfi*, from the early Late Eocene of the Nile Valley.

Abdel-Kireem (1985) recorded the following biozones from the Eocene of Gabal Mokattam:

- | | | |
|---|---|-----------------|
| 1. <i>Globigerina corpulenta</i> Zone | } | (Late Eocene) |
| 2. <i>Globigerinatheka seminvoluta</i> Zone | | |
| 3. <i>Truncorotaloides rohri</i> Zone | | (Middle Eocene) |

1.6.2. Sedimentological studies

The sedimentology of the upper Middle and Late Eocene carbonate of the northern Nile Valley and the Fayum area, north of the latitude of El Fashn, has received very little attention. Most of the work done has been either patchy and localized, or may be categorized as general faunal paleoecology. Starting with Ball (1939), he generally believed in a gradual rise in the land and a northward retreat in the sea during the later times of the Late Eocene epoch.

An early primitive attempt to study microfacies associations was carried out by Ghorab and Ismail (1957) in the east Helwan area. They argued that it was not

possible to establish proper microfacies, at least not before more studies for similar Eocene microfacies were done and a proper correlation was established. According to their point of view, the Gabal Hof and the Observatory Series indicated shallow neritic and warm conditions, and shallow neritic to littoral sea conditions during the deposition of the Qurn series. The Wadi Garawi series indicated littoral shoreline and the same with the Wadi Hof series, but with much shallower conditions.

Said (1962) mentioned that regression must have started at least by Lower Eocene time and must have continued probably to the end of the Oligocene time. This indicates shallower conditions of deposition and nearness to a slow-rising landmass and a fast regressing and disappearing sea.

Hassan *et al.*, (1978) believed that a regressive phase was dominating over the area during the Middle-Late Eocene times which probably continued to early stages of the Late Eocene.

Salem (1976) on the sedimentation patterns of the Eocene in the north Western Desert, indicated that the Late Eocene marked the first phase of terrigenous deposition. He proposed a depositional model for the Late Eocene time, ranging from deltaic sediments to prodelta and basinal muds and passing through marginal and basinal marls as well as through shoreline or paralic sediments.

The only piece of detailed work was done locally in the area northeast of Beni Suef by the author Abdou-Soliman (1980). He studied the carbonate microfacies and their depositional environments. He (*op. cit.*) believed that the Middle Eocene ended by facies reflecting a gentle slope on a bank and open shelf facies for the observatory member. The Late Eocene started by shelf marginal followed by the sheltered fore slope facies of the Beni Suef formation. The Maadi formation was, then, deposited in a platform subenvironment.

Aigner (1983, 1984) indicated that the top of the Middle Eocene carbonate, around the Giza pyramids, represented back-bank facies, while the Late Eocene was of littoral-lagoonal facies. Aigner (1983, Figs. 10-11) believed that the paleoslope in the pyramids area was towards the south and southeast. He (1984, Figs. 1, 2) contradicted himself when he mentioned that the paleoslope was towards the northeast direction. His fore-bank slope (Fig. 1) indicated southwest direction.

Philobos (1984), in the Beni Mazar to Cairo area, believed that the Middle Eocene shore was migrating towards the west and northwest. He also believed that a carbonate-siliciclastic was deposited in deltaic cones which were swinging towards the north and giving rise to a shallow marine and fluviomarine Late Eocene siliclastic carbonate. However, no details about the lateral and vertical distribution of the carbonate associations or

microfacies and sedimentary environments were given by any of the above-mentioned authors except Abdou-Soliman (1980). The detailed regional view of sedimentology on a basinal basis has also never been discussed.

1.7 Scope of the present work

The review of the literature, as given in the previous section and table (1-1), has shown the urgent need for further detailed study of the area of the northern Nile Valley and Fayum, north of latitude of Maghagha, especially from the stratigraphical and sedimentological points of view. The absence of a basinal approach to the study of the Middle-Late Eocene rocks created confusion. The exact relationships between the Middle and Late Eocene and their accurate correlation throughout the basin also need further investigation. This issue was previously discussed from different points of view by Hume (1911), Cuvillier (1930), Barker (1945), Farag and Ismail (1959), Said (1962, 1971), Strougo (1977, 1979).

Following a detailed discussion of the previously proposed classifications of the stratigraphic succession, a new classification is proposed in this study. Correlation of the proposed rock units is attempted in cross-section [Fig. 4.2].

A biostratigraphic zonation based on smaller and larger foraminifera, and also on nannoplanktons, has been attempted and a correlation charts with the faunal distribution are also given [Fig. 4.1 and tables 4-1 to 4-3]. Moreover, the nannoplankton of the Middle-Late

Eocene are identified for the first time in the studied area. The micro-benthonic and planktonic foraminifera, besides the Nummulites, are also identified and used in providing a perfect correlation and age assignments.

The use of the stratigraphic analysis to detect the basin of deposition is also discussed. For a detailed sedimentological study, the data from 82 columnar sections covering the different rock units were measured. Careful counting of all the carbonate components and facies study were carried out. The vertical and lateral distribution of the different limestone components are presented. The variation in the water energy index is also calculated and used. The lateral distribution of the main microfacies associations identified has led to study the slope influence and the related depositional environments.

New approach for basinal configuration is discussed and soft sediment features are studied. Basinal analysis is also carried out.

The tectonic influences are also detected and studied. Paleogeographic maps and models were constructed. The possible sedimentological history of the Middle Mokattam Unit is discussed. The involved depositional basin is identified and its controlling factors are elucidated.

In this work, rocks are dealt with in their primary state of deposition. Thus all diagenetic processes have been avoided as possible however these have only been considered where they may affect recognition of depositional features. These diagenetic processes, as believed, are recommended for further research.

METHODOLOGY
&
TECHNIQUES

CHAPTER TWO

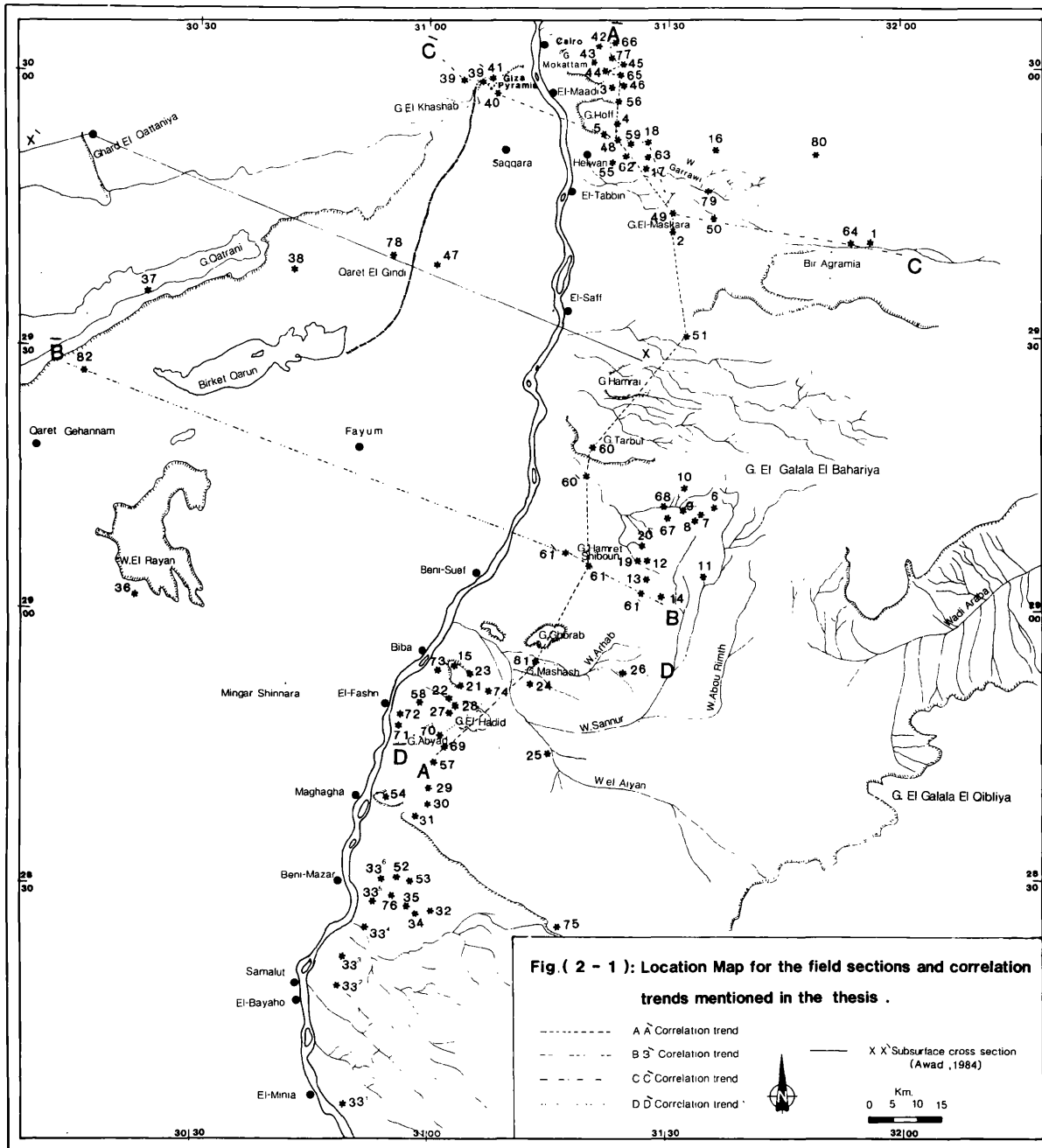
2. METHODOLOGY AND TECHNIQUES

During the course of this project a number of research methods and/or techniques have been employed for studying the sedimentology and stratigraphy of the Middle and Late Eocene carbonates both in the field and in the laboratory. The aim of this Chapter is to outline the most important of these methods.

2.1 Methods Of Collecting Field Data

A total of 82 vertical sections has been studied, some of which were measured and/or sampled in details. Twenty three of the total number of sections, which lie within the Middle-Late Eocene, were studied in detail. The rest (59 sections) were measured outside the studied time range in order to understand the development of the basin. Only a few of these (3 sections) were studied for the sake of stratigraphical correlation. Because of the nature of the outcrop pattern, some of the studied sections do not cover the whole sequence.

Due to the nature of the exposure and the difficulty of access, the selection of all localities, on the basis of a strict grid plan, was not possible. However, it is believed that an accurate picture of facies changes and modal analysis has been built up wherever exposure and access permitted. The actual locations of the studied sections permit correlations in four different directions; indicated in Fig. (2-1) .



Field logging has involved bed-by-bed measurement of sections and the recording of visible parameters such as lithology, texture, fossil content, bedding, sedimentary structures, and the geometry of individual beds of each exposure. Generally, samples have been taken at visible lithological or facies changes. However, when dealing with thick sequence of similar lithologies, additional intermediate samples have been collected. The pattern of collecting several representative samples per facies, in addition to anything unusual, was followed. The samples were then shipped to University College of Swansea for laboratory investigations.

Field data have been supplemented by petrographical and palaeontological information from laboratory studies of these samples. Data from the most important sections are presented on the log sheets (Appendix, B).

2.2 Laboratory Techniques

In this section, some of the laboratory techniques which were used are described.

2.2.1 Sedimentological techniques

2.2.1.1 Stained acetate peels of carbonate rocks.

Flügel (1982) has reviewed some techniques for preparing stained acetate peels. The method of preparation used in this work was an adaptation (with some modification) of the methods described by Bissel (1957), Friedman (1959), Warne (1962), Ayan (1965), Dickson (1965), Katz and Friedman (1965), Dickson (1966) and Davis

and Till (1968). Most staining processes use Alizarin red-S and Potassium ferricyanide in acid solutions. A prepared transparent acetate sheet, with a solvent solution on the stained specimen surface, is used in this study to obtain the peel.

For the preparation of peels, the following method was used:-

- (a) Highly friable and porous limestones were hardened by impregnation. A mixture of araldite (not soluble in acetone) and a hardener was used to fill any holes in the rock sample using the method of Müller (1967).
- (b) The rock samples were cut using the rock-cutting machine to obtain a fresh surface.
- (c) The cut surface of the specimen was prepared by grinding with 400 and then 800 grade carborundum powder. The use of 1000 grade white Aluminium oxide powder for polishing in the final stage proved to be highly successful. It also helps remove any contamination by carborundum powder from inside the porous rock surface or even from fossil and other cavities.
- (d) The prepared sample was left to soak in distilled water for some time until air bubbles cease to appear.
- (e) The polished slabs were etched in Hydrochloric acid (HCl) solution. The strength of the solution was varied according to the lithology, for most lithologies a 1.5% solution was adequate, but in

micrite samples, a solution of 0.5% produced the best results. Most samples were etched for 30 seconds, dolomitic or crystalline limestone were etched for 40 seconds. The etched samples were rinsed in distilled water.

(f) The samples were first stained in a mixture of two solutions: Potassium ferricyanide and Alizarin red-S with a ratio of 2:3, respectively. The former solution was prepared using 2.0 grammes of Potassium ferricyanide dissolved in a 100 ml of 1.5% HCl solution. The latter was prepared similarly, but using only 0.2 grammes of Alizarin red-S.

The staining lasted for 30 seconds. Softer and/or finer samples, however, need a shorter staining time.

The mixing of solutions should be made shortly before use as the stains would become stale rather rapidly.

(g) The surface was then rinsed thoroughly in distilled water.

(h) The second staining, for 10 to 15 seconds, in a solution of 0.2 g Alizarin red-S dissolved in a 100 ml of 1.5% HCl was followed by gentle rinsing in distilled water.

(i) The sample was again immersed in a bath of distilled water for at least 10 seconds to stop the etching and staining effect of the previous stages.

(j) The sample was removed from water and left in air to let any excess water on the surface to evaporate.

Care was taken, however, to keep it wet and not to allow any part of the etched and stained face to dry.

(k) The stained surface was flooded with acetone to remove all traces of water and excess stain.

(l) An acetate film (recommended thickness 0.01mm) was carefully rolled onto the wet surface and left to dry for 20 to 30 minutes.

(m) On drying, the film was peeled off carefully, cut to size, and mounted between glass plates using adhesive tape.

As a result of this staining, the different carbonate grains and cement, spar and neomorphic spar can be distinguished. Calcite stains pink to red and ferroan calcite stains blue to mauve. Dolomite remains unstained if it is iron-free, and stains pale-deep turquoise if it is iron-rich. The acetate peel method for studying carbonates is considered here to be the fastest and simplest. A total of about 514 samples has been prepared in this way and the technique is highly recommended for the good results obtained. Above all, the method enables the examination of larger areas from the rock surface. This would increase the possibility of including large and coarse grains on the cut plane.

2.2.1.2. Thin Sections

To supplement acetate peels, thin sections were prepared. More than 427 thin sections, each up to 70 microns thick, were used. We had to use thin sections

where the staining of some samples was difficult to perform properly or for a mineralogical check of some facies.

We have used a plastic spray to cover the thin sections. This gave excellent results for microscopic examination. For this purpose, a coating spray of "Merckoglas" liquid coverglass for microscopy (Art. 3972) was chosen. This is a product of BDH Diagnostics Chemicals Ltd. Stores.

The spraying process started by placing all slides, side by side, leaning 45° against the wall of a laboratory bench (covered by sheets of paper to protect it from the spray). The spray was used under a fume hood. The slides were moistened by xylene and sprayed with the "Merckoglas" spray. This took only a matter of minutes. The spray was left to dry at room temperature for 10-15 minutes. The slides were then ready for examination. The resulting film can be easily removed by wiping it off with a tissue dampened with xylene.

Care was taken to make only a very thin layer of coating by spraying the slides only once. We have found that applying the plastic coating did not take any considerable time.

2.2.1.3 Point-Counting

Point-counting, as a quantitative method of studying thin sections or peels in petrology, has long been used for the determination of various rock minerals or

carbonate grains. This technique has long been applied in research and is summarised in Galehouse (1971). The most widely used method (Sander, 1951; and Müller, 1967) to count grains along linear equidistantly-spaced traverses by moving the section automatically using a mechanical stage. A stereo-microscope "Wild Heerbrugg M5A" is recommended. Also a "Swift" automatic point-counter, model F.415C, has been used in the final stage of this research, when it was available. This counter provides practical facilities for the presentation of the percentage of the total count for each of its channels throughout the counting procedure. However, in the early stages of counting, both "swift" ordinary microscope and point counter were used but found to be of no practical use. They are time-consuming and inconvenient when a large number of samples are involved. A Nikon profile projector (Model V-16D) was also used with the help of a proposed grid of squares on a transparent sheet. This seemed to produce good results, particularly with respect to the representation of smaller components in a point count.

In all studied cases, at least 1000 points of counting were carried out for each sample. All methods for avoiding counting errors, as described by Dryden (1931), Dennison and Shea (1966), and Jaanusson (1972), have been followed.

2.2.1.4 Facies Analysis

The rock types observed in the study area, were assigned to facies "F". The usage of the term "facies" is on the basis of the description of the rocks according to their lithology, rock colour, bedding and lamination, sedimentary structures, grain size biogenic content, geometry, and stratigraphic relationships. Microscopically, all collected samples were divided into microfacies "MF" and given symbols as M_1F_1 , M_2F_1 , ..., etc. to facilitate their description. In this study, microfacies are considered as the total of all the palaeontological and sedimentological criteria, observed in peels, thin sections, and/or polished slabs. In naming the microfacies, we have taken the following into consideration:

- (1) Carbonate grain types (as counted in percentage and arranged in a descending order for the highest two or sometimes three essential components), were used to form the first syllables of the name of the microfacies, and
- (2) Their depositional texture, using the names given by Dunham (1962), was used to form the remaining syllables.

The word "lime", as a lithological sense for limestone (which can be replaced by marl or sand), is introduced between both previous syllables to form the microfacies name. For example, the carbonate may

contain 40% skeletal grains, 30% oolitic grains, 5% detrital grains, 25% micrite matrix and all having packstone depositional texture; this would be termed skeletal oolitic lime packstone.

The water energy for the carbonate facies, is calculated using the energy index (EI) and the grain matrix ratio (GMR) of Bissel and Chilingar (1967). That helps to indicate the amount of physical (mechanical) energy necessary to transport and deposit the carbonate sediment. The vertical and lateral variation of the energy index (EI) are used to interpretate the change of depositional environment throughout the studied area.

Correlation diagrams (Appendix B and Figs. 7-1 to 7-4) were constructed to study the vertical and lateral distribution of the different carbonate textures, components and microfacies.

2.2.1.5 Carbonate rock classification

A number of important suggestions for systems of classification are presented by Ham (1962). A review for the most important of these suggestions is found in Flügel (1982). In this study, the classification used is that of Dunham (1962) together with suggested modifications by Embry and Klovan (1972). This was chosen for the following reasons:-

- (a) The classification has a wide application in thin section or hand specimen and in the field. Thus a rapid "spot" identification in the field can be achieved.

(b) It is believed to have environmental significance in that the textural features which form the basis of the classification were presumably strongly influenced by depositional processes.

(c) The Dunham classification was used by other workers, Philobbs (1984), and Abdou-Soliman (1980) in the southern parts of the Eocene basin. So the use of the same classification in this work allows an easy and convenient comparison and correlation between the results of this study and earlier studies.

A slight modification of Dunham's nomenclature is used to define finer textures.

In describing mixed siliciclastic carbonates, the method of Mount (1985) is sometimes followed with modifications.

2.2.2 Stratigraphical techniques

The stratigraphical divisions, as well as the biozones within the studied basin, depend on the rock dating. For chronological studies in the basin, both the microfacies, i.e. lithostratigraphy and the palaeontological data have been used. Nannoplanktons, microforams, as well as macrofossils, have been identified. There is no detailed palaeontology in this study since the fossils were used only for generating a biostratigraphical framework within which the sedimentology could be studied.

2.2.2.1 Calcareous nannofossils

In order to study the calcareous nanoplankton in the basin, the following methods have been followed:

A. Normal smearing method

- (1) The samples to be studied have been collected with extreme care in the field.
- (2) In the laboratory, a reasonable degree of cleanliness, to avoid contamination of the sediments, was taken. Everything used has been cleaned between stages in a 10% HCl solution.
- (3) A sample was taken and snapped to produce a fresh surface, and using a small blade, a pinch of sediment from its centre was taken and mounted on a fresh slide.
- (4) The sediment was wetted with a blob of water using a glass rod.
- (5) Then, the sediment was crushed and smeared across the slide, dried in an oven and left to cool.
- (6) A blob of balsam followed by another of xylene was dropped onto the smeared slide.
- (7) Finally, the slide was cooked in an oven for 5 to 7 hours at 100°C.

A total of 198 samples have been prepared in this way.

B. Concentration method

Preparation of samples was done with extreme care to avoid contamination. A pinch of sample was carefully taken from a fresh surface and crushed using a clean small spatula. Each sample of sediment was placed in a long (10cm) glass vial and soaked overnight in a neutralized

liquid of distilled water after adding a drop or two of ammonia. When the sediment was completely disaggregated and totally dispersed, the suspension was vigorously shaken. It was then allowed to settle for four minutes and the decanted suspension was transferred to another (6cm) tube. In this process, the coarse residue was removed. Clay particles were removed later from the suspension by resettling for 8 hours and decanting the liquid and suspended clays. The use of an ultrasonic bath to disaggregate sediments was avoided, as it may harm the state of preservation of the nannofossil species. No attempt was made to remove either the salt or the organic material from the samples. Fortunately, ammonia was a reasonably good dispersant to overcome most of the suspension problems. A drop or two of the suspension was placed and smeared over the slide. The samples were permitted to dry. They were then mounted and cooked in the same way as mentioned in steps 6 and 7. of the previous method. A total of 46 samples were prepared this way in order to check whether or not barren samples from critical horizons were really unfossiliferous.

All the slides have been inspected under a high-powered light microscope.

2.2.2.2 Micro and Larger Foraminifers

Fresh uncontaminated samples were carefully collected. Most of these were friable marls or shales, and marly limestones. A small portion of each sample was soaked in water for a few days, then washed in a very fine mesh.

The residue was then dried, picked up, using a fine brush and a binocular microscope, and mounted on a slide using gum tragacanth. Most species were related to both microbenthonic and planktonic foraminifera. In the case of large foraminifera, a number of thin sections were prepared in different planes. Free specimens of *Nummulites* were used when tests recovered from a loose matrix. All samples have been identified and checked by the Palaeontology Department of the British Museum ((C.G. Adams, p.c.)).

2.2.2.3 Macro-fossils

The macrofossils recognized in the field were collected. Most of them were found to belong to bivalves, gastropods, echinoderms, and corals. They were identified using the published data and catalogues for the area. All identified samples were used for the sake of stratigraphical dating.

LITHOSTRATIGRAPHIC

ANALYSIS

CHAPTER THREE

3. LITHOSTRATIGRAPHIC ANALYSIS

In this chapter, we will discuss the lithostratigraphy of the Middle and Late Eocene rocks, in the northern Nile Valley and the Fayum area of Egypt, in detail with their age dating.

The detailed field and laboratory work of the Northern Nile Valley and the Fayum basin have shown that the main exposed rock units are of Middle and Late Eocene and younger rocks. The previously proposed lithostratigraphic units are given in Table (3-1). The more recent classifications are adapted and modified, when necessary, in order to reach a lithostratigraphic classification that can be used in the area of the Northern Nile Valley and the Fayum basin.

3.1 The term Mokattam.

As mentioned in Chapter One, the name "Mokattam Stufe" was first introduced by Zittle (1883) to describe the limestone and clastic beds of Gabal Mokattam east of Cairo. Schweinfurth (1883) subdivided the same section exposed at Gabal Mokattam into "lower Mokattam", comprising the limestone beds at the base of the hill making the main scarp face, while to the upper limestone and clastic intercalations were designated the term "Upper Mokattam". Hume (1911) was able to subdivide the Mokattam

Mokattam Stufe				Zittle 1883 (Mokattam)	
"Unter" Mokattam			"Ober" Mokattam		Schueinfurth 1883 "Mokattam"
Wadi Rayan beds	Ravine beds	Birket El-Qurun beds		Qasr El-Sagha beds "Carolia beds"	Beadnell 1905 "Fayum"
Lower Mokattam "Gizehenis beds"		Middle Mokattam "Exogyra beds"		Upper Mokattam "Carolia beds"	Hume 1911 "Mokattam"
Lower Mokattam		Middle Mokattam Operculina & Bryzoan limest.	Upper Mokattam "Brown beds with Carolia"		Cuvillier, 1924, 1930, "Mokattam"
Formation "C"	Formation "D"	Formation "E"		Formation "F"	Barker, 1945 "minia Beni Suef"
Gabal Hof Series	Observatory Series	El-Qurn Series	Wadi Garawi Series	Wadi Hof Series	Farag & Ismail 1959 "Helwan area"
Mokattam Formation			Maadi Formation		Said, 1960, 1962 "Cairo-Minia"
Wadi El- Rayan Formation	Gehannam Formation	Birket El-Qarun Formation		Qasr El- Sagha Formation	Said, 1962 "Fayum area"
Qarara Formation	El-Fashn Formation	Beni Suef Formation		Fayum Formation	Bishay, 1966 Assiut-Vasta
Mokattam Formation			Maadi Formation		Said and Martin, 1964 (G. Mokattam)
Lower subst. member	Gizehenis member	Upper building stone member	Giushi member		
Mokattam Formation					Boukhary 1970, 1973 (Beni Suef)
Upper gizehenis M.	Upper building stone		or Beni Suef Member	Shaibun Member	
Mokattam Formation		Giushi Formation	Maadi Formation		Said, 1971 Cairo Helwan areas
Gabal Hof Member	Building stone or Obs Member	Qurun Formation	Garwi Formation	Wadi Hof Formation	
Lower Mokattam		Middle Mokattam		Upper Mokattam	Strougo 1977, 1979 "Cairo area"
Mokattam Formation		Qurn Formation		Wadi Hof Formation	Hassan <i>et al.</i> 1978 E. Beni Suef
Mokattam Formation		Beni Suef Formation		Maadi Formation	Abdou-Soliman 1980 N.E. Beni Suef
Gabal Hof Member	Observatory Member	Qurn Member	Tarboui Member		
Lower Mokattam Formation			Upper Mokattam Formation		Abdel-Kireem 1986 (Mokattam)
Gizehensis Member	Building stone M.	Giushi M.			
Lower Mokattam Unit		Middle Mokattam Unit		Upper Mokattam Unit	Present work N. Nile Valley & Fayum basin

Table 3.1 Proposed lithostratigraphic correlation for the rock units of the Northern Nile Valley and Fayum area.

of Zittle to the "Lower Mokattam", "Middle Mokattam" and "Upper Mokattam" series. In this study, and because of the law of priority in naming a lithostratigraphic unit following the stratigraphic code of nomenclature (Article 5.4, Hedberg, 1972, 1976; and Article 5 of Holland *et al.*, 1978), the terminology used in this work is that of Zittle (1883) and the subdivisions of Hume (1911) with some modification under Unit hierarchy. Accordingly, the Middle Eocene and Late Eocene rocks, of the area of study, are found to include the following rock units, proceeding from top to bottom:

3. Upper Mokattam Unit (dirty, yellowish clastic sand and limestone)
2. Middle Mokattam Unit (gray to greenish marls)
1. Lower Mokattam Unit (white limestones)

Since the theme of this study is to concentrate on the Middle-Late Eocene transitional event and follow it along the studied basin, only the Middle Mokattam rock unit has been studied in detail. A general outline, for both older (Lower Mokattam) and younger (Upper Mokattam), is also included, however, briefly:

3.2 The Lower Mokattam Unit

The "Lower Mokattam" of Schweinfurth (1883) is restricted and replaced by two rock formations, the Mokattam formation at the base and the Giushi formation at the top., [Said, 1971].

Generally, the "Lower Mokattam" unit is characterized by its light colour, soft to hard limestones, which change to chalky or marly, to marls and sandy shales in some places. The unit can be distinguished into three different rock divisions. The base of that unit is characterised by the presence of the larger *Nummulite gizehensis* shells. These gizehensis beds, as described by Said (1962) form a basal uniform sequence of beds in the studied basin. Whether this statement is true or not, the gizehensis zone was useful in the field to a great extent as a coordination datum throughout the studied basin. This zone consists of limestone, packed with the large shells of *Nummulites* (up to 4cm in diameter) interbedded with shales or replaced by marly shales in the southern (Maghagha) and western (Wadi El-Rayan) provinces of the basin. The second division of the Lower Mokattam is known as the "Observatory" series [Farag and Ismail, 1956] or "Building Stone or Observatory" Member [Said, 1971]. These facies are composed of hard, well-bedded fine grained limestones with white to yellowish white colours. The larger *Nummulites* shells are rarely present. In some places, these facies change laterally to marly or arenaceous limestone (El-Fashn area) and marly limestone with marl intercalation (Gehannam Formation of Fayum).

The third or top division of the Lower Mokattam unit is the "Giushi Formation" [Said, 1971]. That division (Plate 3-1) is the only member of the Lower Mokattam which

PLATE (3-1)



Plate (3-1): Glushl Formation , top division of the Lower Mokattam Unit , East of Cairo . Both the Middle and Upper Mokattam overlie on right top of photo .

is considered to be of some interest and dealt with in some detail in this study, since it underlies the Middle Mokattam. It is mainly composed of thinly bedded, yellowish white fossiliferous limestones. The limestones are flooded with small size *Nummulites*. In the Mokattam section, there are some shaley marl intercalations (up to 40cm thick) which were found to be increasing laterally southwards throughout the basin in east Helwan and up to Beni Suef. These marls are of some importance and divide the "giushi formation" in the Gabal Mokattam section into two distinct parts. The lower part is characterized by the abundance of bryozoa and serpulid tubes. This part can be traced southwards in Wadi Hof (East Helwan), Wadi El-Baum (east of Beni Suef), Gabal El-Abyad (east El-Fashn) and in north of Gabal El-Rayan (Fayum). The upper part is distinguished by the presence of *Operculina pyramidium*. It is only represented in the Gabal Mokattam section and replaced southwards by the overlying Middle Mokattam Unit. In east Maadi the Giushi division changes laterally to coralline facies, while in Abou-Salleh (east of Beni Suef), it is composed of formainiferal fine grained limestone. The thickness of this division varies from place to place. In Gabal Giushi (east of Cairo), the Giushi beds are about 30m thick, in Helwan, nearly 60m in Wadi Hof and 24.8m in Wadi Abou Moliyssatt, and in east Beni Suef, 29.20m in Abou Saleh section and 21.4m in El Allalma section. In some places, the Giushi beds are not

represented as in the pyramids plateau and the outer borders of the studied basin. This suggests an uplifting trend in these regions.

The Giushi type unit reflects an environmental change from facies formed on shallow to open shelf environment (Chapter 6). The faunal content of the Giushi beds indicates that it includes some planktonic and micro-benthonic foraminifera, operculines abundant nummulites, bryozoa, serpiolid worms tubes at the base, some algae, gastropods, and bivalves. It is important to point out that, though the biofacies of the upper part of the Giushi type in Gabal Mokattam are more similar to those of the Middle Mokattam in the middle and south of the basin, they occur in completely different lithologies. This phenomenon could rather reflect chronstratigraphic relation than any lithostratigraphic tracability and relativity.

3.3 The Middle Mokattam Unit

The "Middle Mokattam" was introduced by Hume (1911) to describe the pale-grayish green marls with small *Nummulites* and *Exogyra fraasi* bands in Gabal Mokattam. Hume (*op. cit.*) pointed out (Table 3.1) that his "Middle Mokattam" type overlies the white limestones of the "Lower Mokattam" and underlies the brown beds with *Carolia placunoides* of the "Upper Mokattam". Cuvillier (1924, 1930), in the same type of locality of Mokattam used the same term of "Middle Mokattam" to completely different underlying beds. Cuvillier used his term to coincide with

the "Giushi" type (top of the "Lower Mokattam") and he considered all the upper clastics as of "Upper Mokattam" unit. This confusion has led Strougo (1977, 1979) to use the name "Middle Mokattam" for the combined areas of Hume (1911) and Cuvillier (1924, 1930). The present author does not agree with either the Cuvillier or Strougo subdivisions, which have created misleading boundary stratotype and prefers to follow Hume's subdivision.

What both Cuvillier and Strougo said about confirming the Middle Mokattam was somehow true, but the problem is rather more complex than they thought. In the Gabal Mokattam section, it is difficult to separate the top of the "Lower Mokattam" for any but all in one unit. Therefore, the lower boundary of Cuvillier and Strougo, "Middle Mokattam" contact, was not clearly marked. On the other hand, Hume's (1911) subdivision has priority. So, the term "Middle Mokattam", in this chapter, is adopted as used by Hume (1911).

In our study, the "Middle Mokattam" is found to exist throughout the northern Nile Valley and the Fayum basin under different stratigraphic names. It extends from Cairo to east Helwan, El-Saff - Beni Suef, and the Fayum areas. The following is a description for the "Middle Mokattam" in each of the above-mentioned areas.

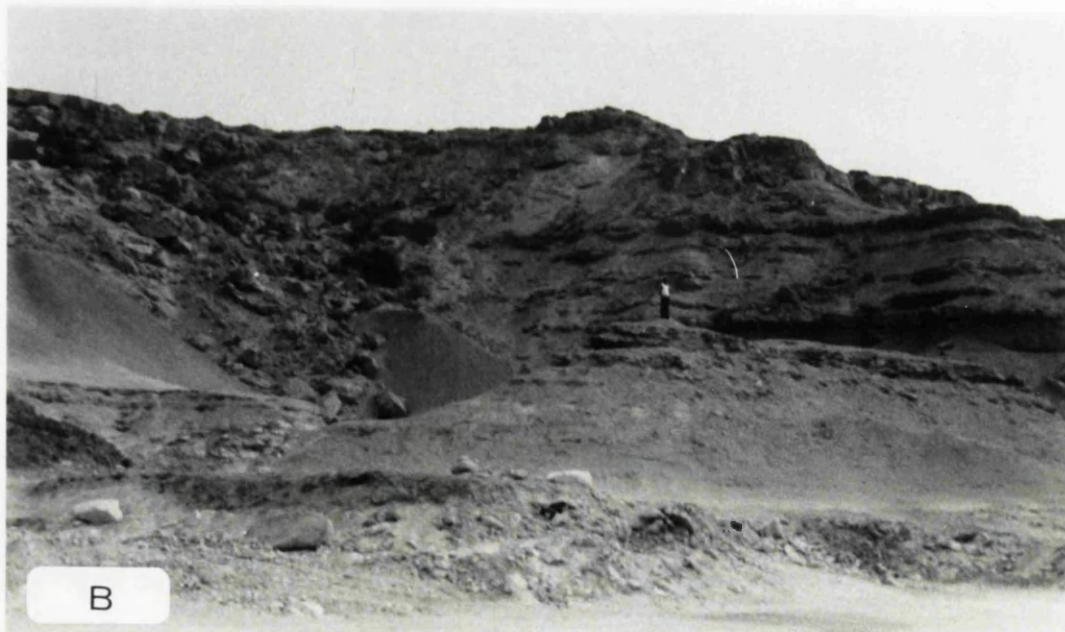
3.3.1 The Cairo Area

The true "Middle Mokattam Unit" described so far in Gabal Mokattam, East Cairo, is that of Hume (1911).

PLATE (3-2)



A- The Middle Mokattam Unit (M) underlies the Upper Mokattam (U) in Gabal Mokattam , east of Cairo . Looking East . Scale bar is 5 meters .



B- Top of the Middle Mokattam Unit , where the man stands , in Gabal Mokattam east of Cairo . Looking East .

However, it is included within the upper horizon of Strougo (1977,1979) at its type locality near the Citadel. It is distinguished by the pale greenish-gray to grayish-green marl rocks (Plate 3-2) overlying the white limestones of the "Lower Mokattam" and underlying the dirty yellowish clastics of the "Upper Mokattam". The Middle Mokattam Unit is well exposed all along the Mokattam scarp and can be traced from north of the citadel and southerly to east Maadi area, with a lense-shape facies. The thickness of the Middle Mokattam facies varies (Figs 3-1 & 3-2) where it reaches 9m in north of the Citadel (Section 66), 14m at El Mokattam Casino (Section 77), 14.75m at the Mokattam Hotel (Section 45), 32.7m at one Km south of the Hotel section (Section 65) and thinning again down to 10m in East Maadi; Kattamia Road (Section 56). The Middle Mokattam in these areas comprises soft to moderately hard marls, crossed with gypsum veinlets and interbedded with more hard marly limestone facies. These facies change laterally to clastic sandy shales northwards and with thin gypsum bands southwards (East Maadi). The recorded fauna included some bivalves, gastropods and clastic shell debris.

In the south pyramids area, at Gabal Qibli El-Ahram (Section 40), the Middle Mokattam facies become up to 17.70m thick (Plate 3-4,A). The facies are composed of yellowish gray greenish marl limestone, highly bioclastic, bioturbated, and crossed with gypsum. These beds are

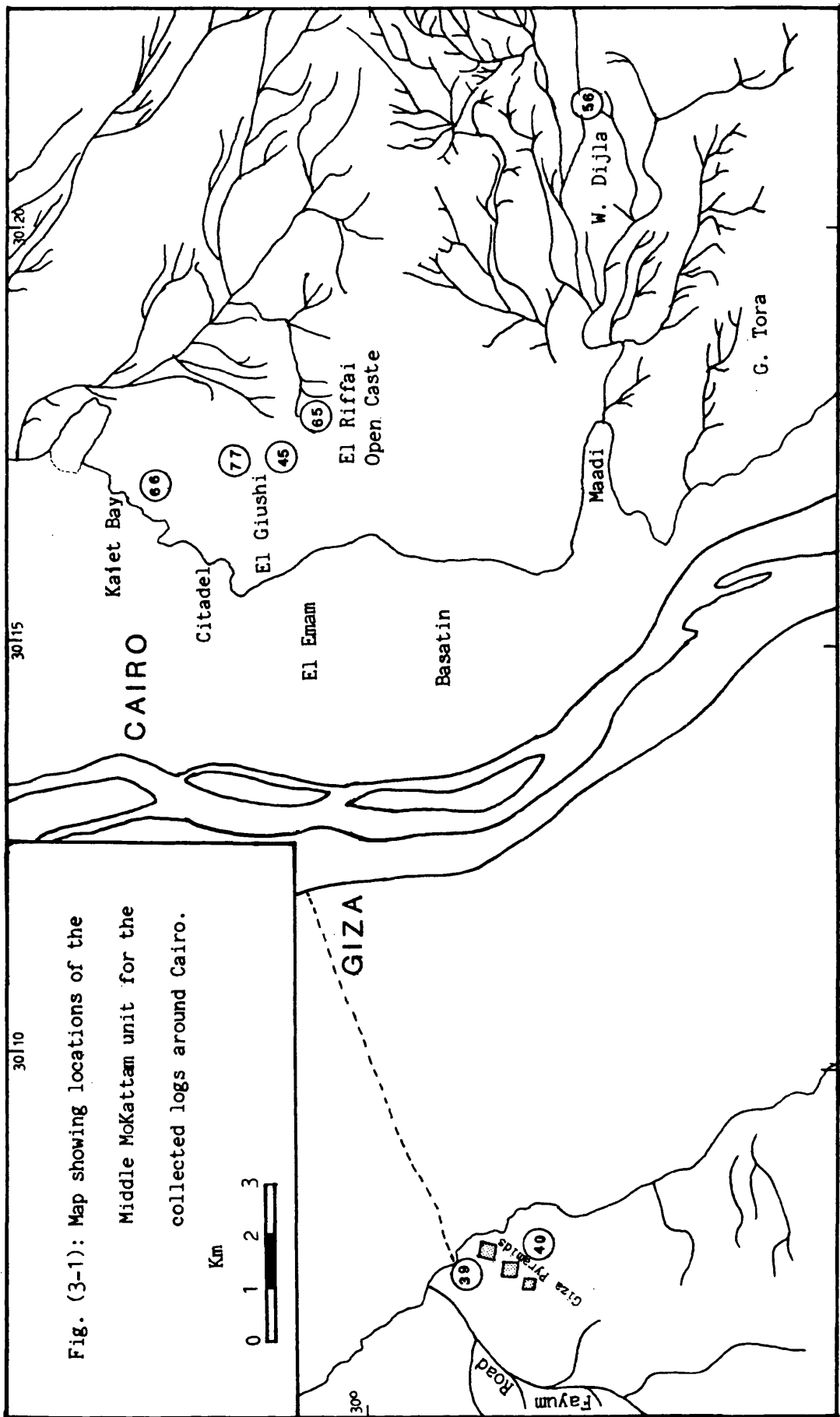


Fig. (3-1): Map showing locations of the Middle Mokattam unit for the collected logs around Cairo.

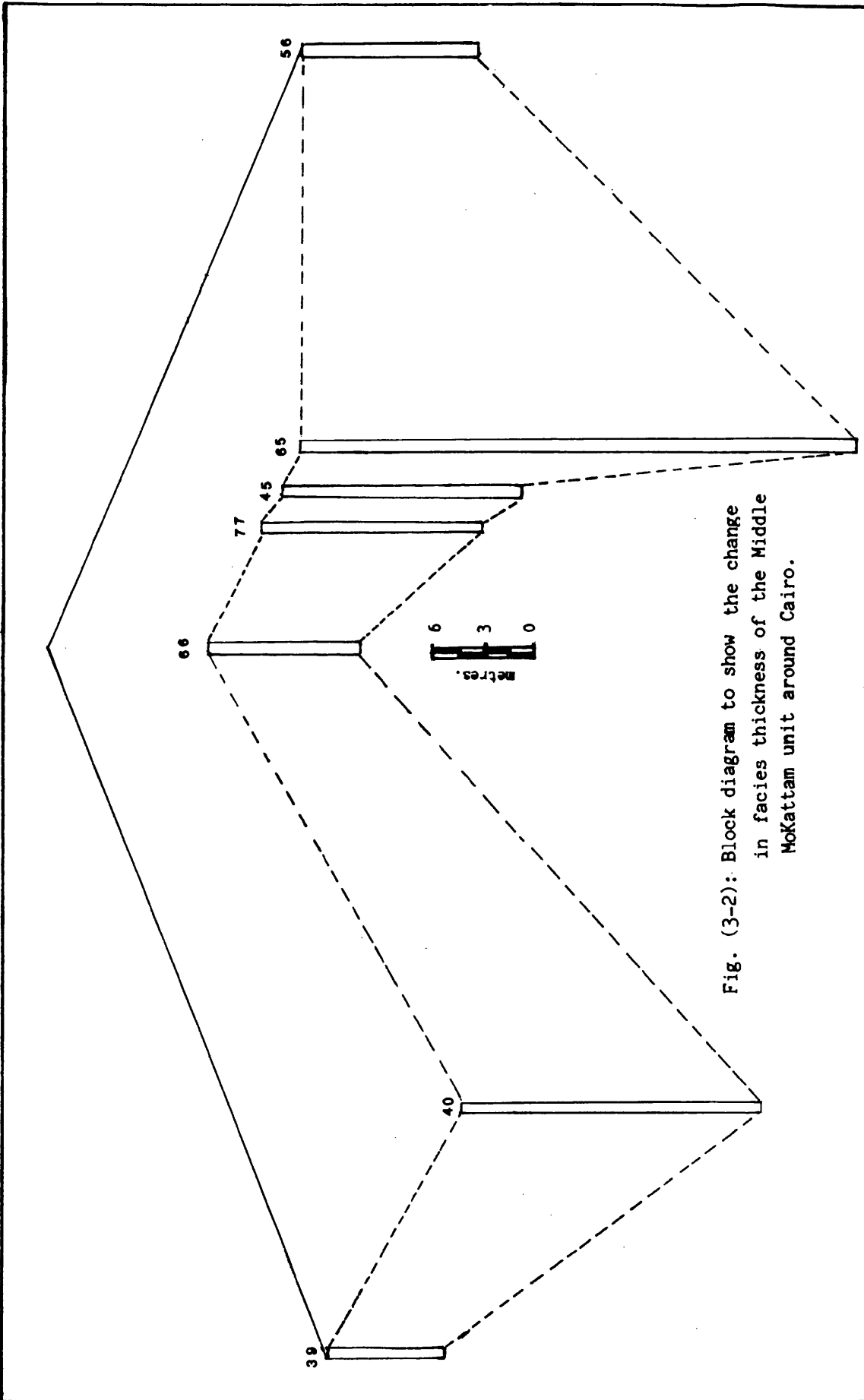


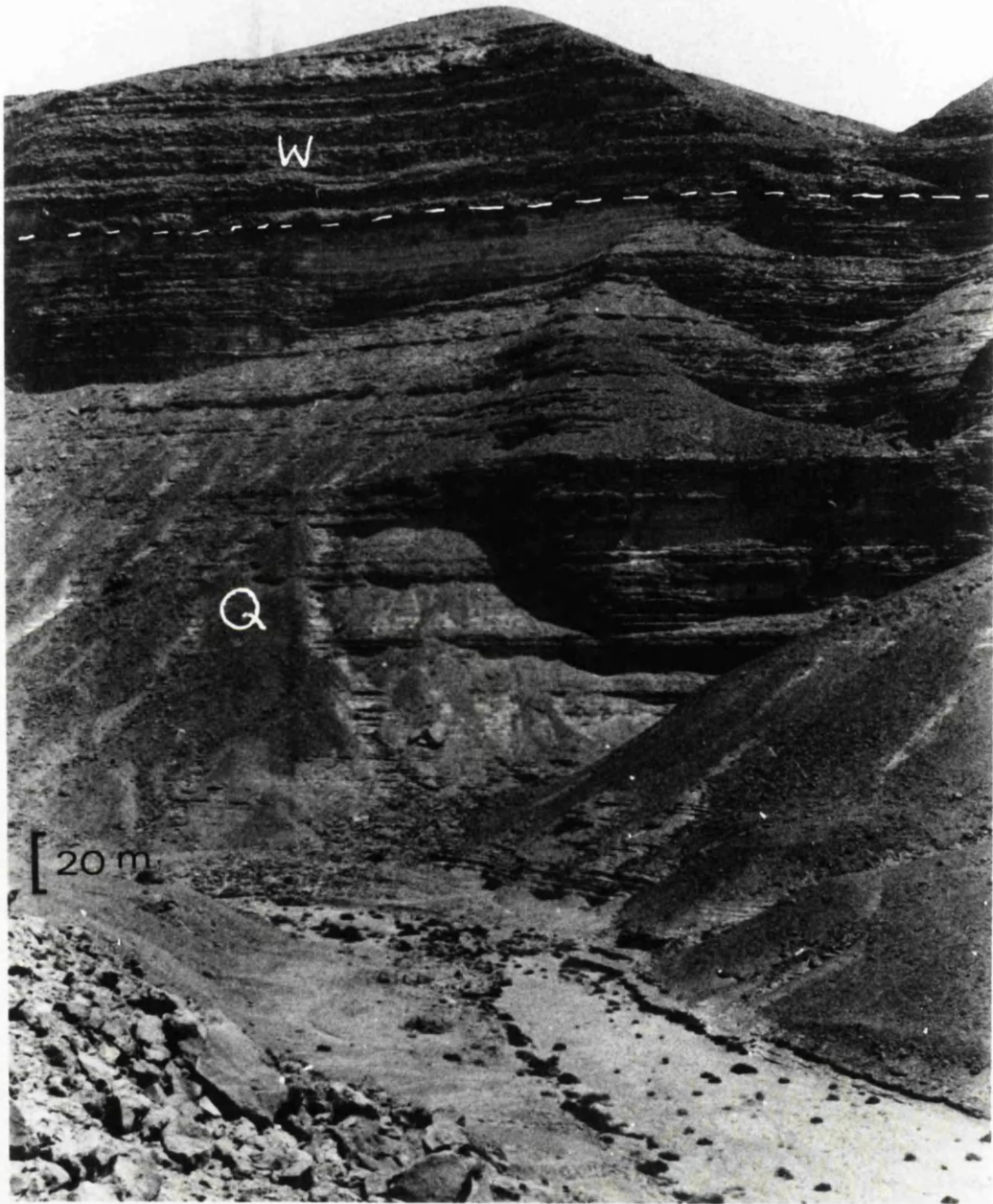
Fig. (3-2): Block diagram to show the change in facies thickness of the Middle MoKattam unit around Cairo.

interbedded with hard cross laminated limestones. The upper surface is well indicated by a conglomerate band, 3.5m thick, which succeeds the marly facies (Plate 3-4,A) and precedes, younger Pliocene shore clastics. The facies exist in Gabal Qibli El-Ahram and are more restricted than in Mokattam. The Middle Mokattam unit extends southwards to the western Nile bank in Saggara comprising most of the Saggara limestones of Hume (1911) and up to below the Carolia bed. The fauna recorded with Middle Mokattam in the Cario area belong to articulated bivalves, gastropods, ostracods, formainifera, and bryozoa.

3.3.2 East Helwan Area

The "Middle Mokattam" Unit in east Helwan (Plate 3-3) is represented by both the Qurn series, at the base, and the Wadi Garawi" series at the top [Farag & Ismail, 1959]. In this study, and according to field observations, the same rock unit names of Farag and Ismail (1959) are used but with a reduced formational rank (Table 3.1). Such formal names have been documented on the same area of Helwan by Said (1971) in a different sense of correlation (Table 3.1).

The Qurn Formation succeeds the Giushi Division of the Lower Mokattam Unit and precedes the Wadi Garawi Formation. The thickness of this formation reaches up to 96m in its type locality in the Qurn heights, where it is composed of chalky and nodular marly limestone alternating with sandy marls (section 48). The base of this section

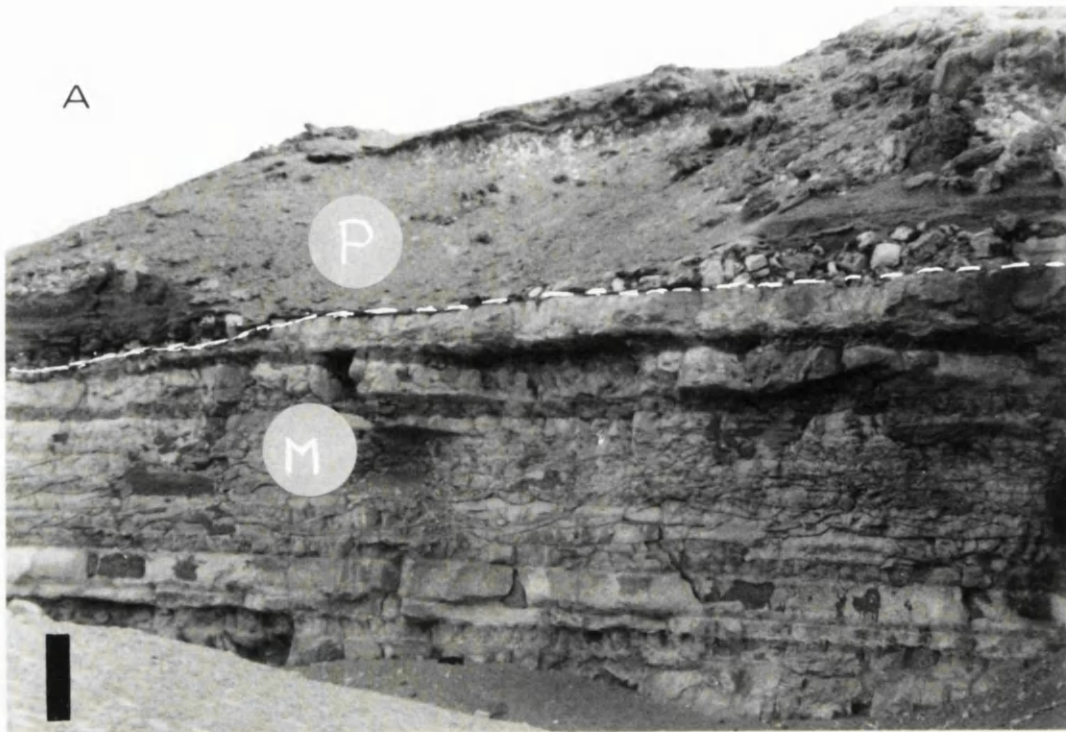


Middle Mokattam Unit in Wadi Hof , east of the Helwan area .The Qurn Formation (Q) at the base and the Wadi Garawi Formation (W) on the top . Looking North .

includes clastic limestone, with sandy size fragmented shells, which changes upwards to nummulitic nodular marly limestone with clastic content. The maximum recorded thickness for those facies was up to 128.5m in Wadi Hof (section 48,) which is thinning rapidly northwards. The Qurn formation facies has laterally changed southwards to marly limestone, marls and sandy marls, at Gabal El Maskhara (section 49, plate 3-4, B); beginning of Abou Serriaa-Suez Road, reflecting 30.1m thick carbonate facies. These latter facies extend farther south of the Helwan to El-Saff areas exhibiting softer marls, weathered shaley appearance, interbedded with more hard benches of marly nummulitic limestone bands. These nummulitic limestone bands are full of small nummulites and changing southerly to brownish dolomitic facies. The thickness of the Qurn Formation facies is generally reduced south of the Helwan area and can be traced for long distances. The same phenomenon is recorded eastwards with an increase of clastic content covering all over the eastern parts of the Helwan area along Abou Serriaa-Suez Road in east-northerly trends from 18km to 50km deeper than Helwan and increasing again easterly to reach a thickness of up to 60m in section 64 (80km deep). The fauna recorded were mainly small nummulites, gastropods, bivalves, bryozoa and echinoderms.

The "Wadi Garawi" formation in east Helwaan overlies the Qurn Formation and underlies the "Wadi Hof" Formation

PLATE (3-4)



A- The Middle Mokattam facies at Gabal Qibli El-Ahram ; south of the Giza Pyramids (M) ,precedes younger Pliocene sediments (P) . Looking south . Scale is 3 meters long .



B- The Middle Mokattam Unit at Gabal El-Maskara , east of the Helwan area . Looking south-west .

[Farag and Ismail, 1959 and amended by Said, 1962, 1971]. The Wadi Garawi Formation, as mentioned by the above authors, is used to describe the limestone, marls and sandy shales in the Wadi Garawi area reaching a thickness of 25m. This rock type in the desert of the east Helwan area (section 49) is characterized by yellowish to brownish colour, bedded stuff of marls crossed with gypsum (started from the base) nodular hard sandy limestones and soft calcareous sandstones. The previous strata are overlain by a well distinguished conglomeratic carbonate of about 3.0 to 4.0 meters in thickness. This conglomerate bed is composed of hard limestone nodules ranging from 7cm to 15cm and even to 30cm in diameter in northwards (section 48) and westwards and also with subrounded shaped thin fining and rounded southwards (section 49). These nodules in the Helwan area are embedded in nummulitic, echinodermal or fragmented shelly matrix. The section passing vertically to white grey clastic bedded with echinoderms and bivalves, bioturbated and cross laminated eastwards with dolomite bands and dolomitic boulders capped by highly cross bedded bivalve beds. The upper horizon of the Wadi Garawi formation is of marls to marly limestone and clastic nummulitic limestone, bioturbated with *Turritella* bivalves, nummulites and bryozoa. This horizon becomes softer in places and erodes away completely in others. The Wadi Garawi formation facies are represented by up to 56 meters thick carbonate which

thin to the east and south where they are represented by a yellowish to brownish clastic limestone facies. Southwards, in the area between Helwan and EL-Saff, the facies become more bedded with a fine clastic content and contains nummulites, operculines and bryozoa.

The Wadi Garawi facies change laterally to a fine crosslaminated chalky limestone at 80 Km deeper from Abou Serria - Suez Road (Section.64.).

Field observations in deeper parts of Wadi Garawi and Wadi Sisaba have shown that the above mentioned formations of the Middle Mokattam merge together and decrease in thickness eastwards forming one distinguishable unit only.

3.3.3 El Saff - Beni Suef Areas.

The southern counterpart of the Middle Mokattam Unit in the studied basin is represented by the Beni Suef Formation of Bishay (1966) and Abdou-Saliman (1980) (Table 3.1). The term Beni Suef Formation was first introduced by Bishay (1966), who described it as uniformly overlying his El Fashn Formation (top of the Lower Mokattam Unit of this study) and underlying his Fayum Formation (the Maadi Formation of Abdou-Soliman, 1980). Barker (1945) described this unit as (E) Formation. Bishay (1966) considered its type section as lying northwest of Beni Suef, where it reaches a thickness of 100 meters. Boukhary (1973), considered the same sequence as a member of the Lower Mokattam Unit and as the lateral variation of the Observatory Member.

In the area northeast of Beni Suef, the Middle Mokattam Unit (Plate, 3-5) is distinguished by its grey greenish grey colour which overlies the white limestones

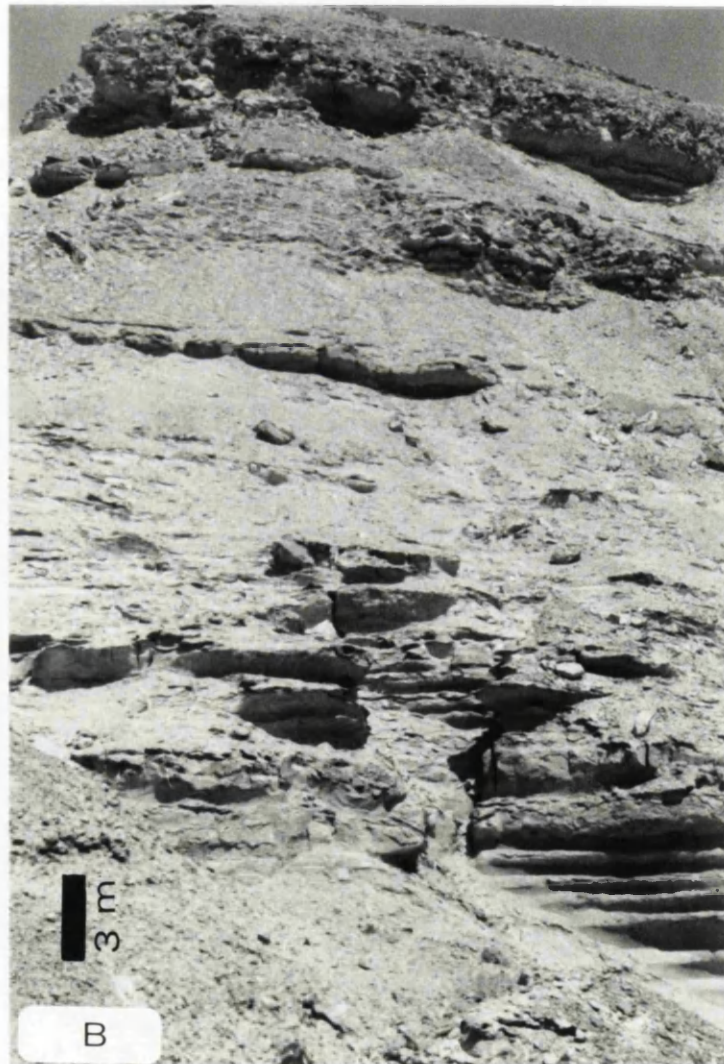
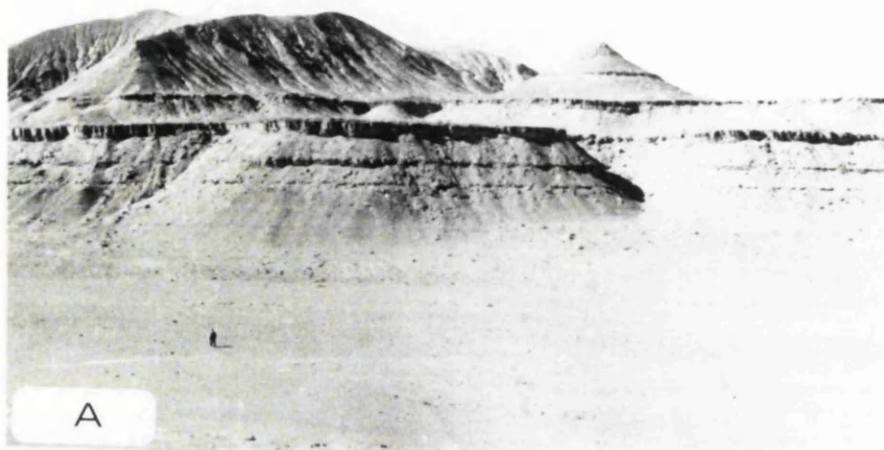


Plate (3-5): The Beni-Suef Formation ; Middle Mokattam Unit , with the Qurn Member (A) at its lower part , and the Tarbul Member (B) at the top [Gabal Tarbul] .

of the lower Mokattam and underlies the yellowish clastic of the Maadi Formation (Abdou-Soliman, 1980).

Lithologically the Middle Mokattam (Beni Suef Formation) is formed of a highly fossiliferous succession of marl and calcareous shale with clastic dolomitic limestone intercalations. This is overlain by well bedded, clastic, marly micritic limestones with *Operculina* which enclose some sandy shale and marl intercalations. The succession is capped by nummulitic limestone very rich nummulites, bryozoa, *Turritella* (gastropods), bivalves, and micro foraminifera. The field investigation of this study has shown that the Beni Suef Formation is considered as having the widest area distribution where its facies cover up to two thirds of the studied basin area of the Middle Mokattam Unit.

The Middle Mokattam, Beni Suef Formation, is represented in the area of El Saff-Beni Suef in the north, at north and the east of El saff, Gabal Hamarai, Gabal Tarbul, Tarbul Abu Khashirat, Hamret Shaibun, El-Mashash, Wadi El-Aghbig, Wadi El Arhab, at the top of Gabal El Abyad, north-western top of Gabal El Merair, and other patchy hillocks scattered over the Lower Mokattam. In the west Nile bank, the formation is well developed in the desert stretch separating the Fayum from the Nile Valley and fringing westward with the Birket Qurun facies.

The fossil content of the Beni Suef Formation dates it as of Priabonian (late Eocene) age. Bishay (1966) and

Boukhary (1970,1973), however, considered it as of Upper Lutetian (Middle Eocene) age depending upon the nummulitic content of the underlying Observatory Member, of the Lower Mokattam Unit, which they were confused in considering it as its lateral counterpart. Later on, Hassan *et al*, (1978), considered its lower part as of Middle Eocene age, whereas its upper part as of Late Eocene age.

In the east Beni Suef area, the author (Abdou-Soliman, 1980) was able to subdivide the succession of the Beni Suef Formation into two mappable units of member status, namely the Qurn Member at its base and the Tarbul Member at its upper part.

A. The Qurn Member

The term Qurn Series is retained after Farag and Ismail (1959), and is reduced in rank as a member of the Beni Suef Formation by Abdou-Soliman (1980). The Qurn Member (Plate 3-5,A) in the area from El Saff to Beni Suef and southwards, is formed of marls, shales, sandy argillaceous marl with a grey to greenish or brownish grey colours. Rhythmic bands of creamy white clastic micritic limestone, sometimes dolomitic which weather reddish brown, occur within the sequence of marly beds. These facies may change laterally to greyish green sandy shale and thins rapidly towards the south and southeast where they are sometimes absent. The thickness of this unit at its type locality (Gabal Tarbul) reaches about 50 meters.

The Qurn Member is well represented in the low escarpments of Gabal Tarbul, Tarbul Abu Kashirat, Hamret

Shaibun, and Hamrai. It is also found as isolated patches or large hillocks, at Gabal El Mashash, and at the top of Gabal El Abyad, Gabal Hadid and the north western part of Gabal El Merair. This member extends northwards to El Wasta and El Saff forming the lower part of El Saff-Helwan area on the eastern side of the Nile. In east El Saff area, the marl facies thin and interbed with more dolomitic bands and the fauna is more restricted. Nowhere has such a basal dolomitic unit been seen at the base of the Middle Mokattam from northwards. The implication is that the Qurn limestone and marls were deposited across this region on an subdued relief which was acting as paleo high probably during the deposition of the Giushi facies. On the western Nile bank the Qurn Member extends westwards covering the Nile Valley - Fayum district with more clastic facies.

The Qurn Facies, in Gabal Hamret Shaibun, was included within a section described by Cuvillier (1930, P.198-202) as of late Eocene, whereas considered since that as of Middle Eocene by relatively more recent workers as Bishay (1961, 1966), Said (1962, 1971), Boukhary (1970, 1973) and all of the unpublished work of the Geological Survey of Egypt. Hassan *et al* (1978, P.131 and P.136) in the Beni Suef area, gave this rock unit a Late Eocene age. In spite of their statement, Hassan *et al*, (1978), contradict themselves in the same work (1978, P.142 and P.143), stating that it is not wholly of upper Eocene, but it

extends downward to the Middle Eocene. Abdou-Soliman (1980) reassigned the Qurn Member, on faunal aspects, to the Late Eocene. The faunal content of the Qurn Member in the Beni Suef area contains mainly pelecypods, gastropods, ostracods and rich bottom dwelling benthonic foraminifera.

The faunal content of this unit is re-examined, in this study, using nanoplanktons and a Late Eocene (Priabonian) age is confirmed for the Qurn Member (Biostratigraphic analysis, Chapter 4).

B. Tarbul Member

The Tarbul Member (Plate, 3-5, B) represents the upper part of the Beni Suef Formation and is introduced by Abdou-Soliman (1980), from Gabal Tarbul, east of El Wasta, to describe the yellowish white, well bedded, lime arenaceous limestone with *Operculina pyramedium*. The Tarbul facies are sometimes nodular and greyish yellow marls and sandy marl. Sandy micritic limestone intercalations rich in bivalves and small *Nummulites striatus* tops the succession and is interbedded with dolomitic bands of 1 to 1.5 meters in diameter. These sandy micritic limestone beds increase in thickness northward at the expense of the underlying beds, of El Qurn Member, and reach their maximum in Helwan area to merge with the Wadi Garawi Formation east El Tebbin. The thickness of the Tarbul Member, in its type locality Gabal Tarbul, reaches up to 60 meters. To the south at

Gabal Hamret Shaibun, this unit thins out and reaches 5 meters southeast at Gabal El Mashash, and is absent further south. It conformably overlies the Qurn Member with an abrupt contact and precedes the Maadi Formation of the Upper Mokattam with a sharp lithological contact. However, this contradicts what Hassan *et al*, (1978), believed (Table 3-1) about the occurrence of unconformity; conglomeratic zone, through the upper contact of the Qurn unit. Such phenomenon does not exist in the field of his studied areas and cannot be deduced from biostratigraphy.

The Tarbul Member is composed of sandy limestones rich in *Operculina pyramedium*, *Nummulites striatus*, *Lucina pharaonis*, *Ostrea reili*, *Ostrea fraasi*, *Turritella desertica*, *T. angulata*, and *Cerithium lamellosum*. Accordingly, the Tarbul Member, is considered by Abdou-Soliman (1980) as of Late Eocene age. It is also reconsidered in this study on a nannoplanktonic basis (Chapter 4), to be of Priabonian (Late Eocene) age.

It is found that the eastern parts of the Tarbul Member merge with the underlying Qurn Member and decrease in thickness with increasing in size of the clastic content. In east El Saff area, the size and number of *Operculina pyramidum* tend to increase. On the other hand, in the west of the Nile bank, the fauna suffered more restricted environments and the facies become marly and or calcareous shale.

As mentioned above, the Tarbul Member facies in Beni Suef area (Gabal Hamret Shaibun) passes upwards to dolomitic bands and a bank bed of bivalves of up to 5 meters then gradually changed upwards to nummulitic fine grained beds full of small sized *Nummulites striatus*. This variation marks the top of this unit which could reflect more or less similar depositional conditions to those of the top Wadi Garawi Formation in Wadi Hof area (as mentioned in the case of the Helwan area). This similarity in conditions indicates the end of the depositional story of this rock unit throughout the studied basin.

3.3.4 The Fayum Area.

In the west side of the Fayum area, the Middle Mokattam Unit is represented by the Birket Qarun Formation. The use of Birket Qarun beds (or series), as a term, is back as early as 1905 when it was used by Beadnell to describe a unit of 500 meters thick in Gabal Gehannam, composed of sandstones and shales with a few bands of limestone. Said (1962) used the same term but in a formal meaning as "The Birket Qarun Formation". The Birket Qarun Formation (Table 3.1) overlies the Ravine beds of Beadnell (1905), which was called the Gehannam Formation by Said (1962), and underlies the Qasr El-Sagha Formation of Said (1962). For being difficult to identify, the lower boundary of the Birket Qarun Formation in Gabal Gehannam (Gar Gehannam), has led a research group

such as Abdou and Abdel-Kireem (1972) and Abdel-Kireem (1985) to include that formation within the underlying Gehannam Formation. This lower boundary problem, however, could be solved differently by considering the boundary to extend down to reach the hard limestone cap of the underlying (Gehannam) formation. Thus, the boundary in this new situation will underlie well defined calcareous sandy shale horizons. In doing so, the term "Birket Qarun Formation" will survive and the formation itself will be considered as a complete separate and mappable unit with two well defined boundaries.

The above shale horizons, 8 meters thick, change upwards to calcareous fine sands and marly sandstone (50 meters thick). The last beds are overlain by 5 meters of calcareous shales followed by up to 18 meters thick sandy marls.

In the north of Birket (lake) Qarun, the lower part of the formation becomes sandy marls while the upper part changes to sandy calcareous shale and fine marly sands occasionally intercalated by harder sandy clastic limestones. In both north and west of Birket Qarun, the rock unit is gradually buried as if dips beneath the overlaying Qasr El-Sagha Formation.

The Middle Mokattam (Birket Qarun Formation) facies in the Fayum area are well developed in the area fringing the northern boundary of the Fayum cultivation and Birket Qarun and the hill mass of Gabal (Gar) Gehannam.

The facies are also recorded as a siliceous carbonates with marls near the base of the rock unit, at southeast Kalamcha of Fayum and north of Birket Qarun.

The faunal content of the Birket Qarun Formation includes *Nummulites striatus*, *Operculina* cf. *discoidea*, *Ostrea reili*, *O. fraasi*, *Carolia placunoides*, and some gastropod species.

The age of the Middle Mokattam (Birket Qarun) according to the studied faunal biozones is found to be of Late Eocene (Priabonian) age. This is also considered and recorded in most of the previous work starting with Cuvillier (1930), Ansary (1955), Said (1962, 1971), Krashennnikov and Ponikarov (1964), Beckmann et al (1969), Ismail and Abdel-Kireem (1971), Abdou and Abdel-Kireem (1972), Boukhary and Abdelmalik (1983), and most unpublished and subsequent work.

In regional sense, the fauna identified from the "Middle Mokattam" facies include; *Nummulites striatus* Bruguiere, *Nummulites fayumensis* Bishay, *Operculina priabonica* Bishay, *Operculina pyramidum* Schw., *Sphaerogypsina globulus* Reuss, *Echinolampas crameri* De Ler, *Echinolampas protaeus* Fourt, *Lucina sinuosa* Bell, *Lucina* cf. *qurnaensis* Oppenheim, *Saxolucina metableta* Cossmann, *Saxolucina rai* Oppenheim, *Arcopagia (Macaliopsis) plicatulla* Mayer-Eymar, *Turritella polytoeniata* Cossmann, *Turritella pharaonica* Cossmann, and *Cerithium lamellosum* Brug.

It is also important to point out here that the Middle Mokattam facies contains various types of reworked fossils from older rocks ranging in age from Middle Eocene to Paleocene or even older. These are eliminated during biostratigraphic analysis (Chapter 4) to avoid age mixing.

3.4 The Upper Mokattam Unit.

In brief, the Upper Mokattam of Hume (1911), is characterized by its dirty yellowish brown clastic limestone, sand and shales with abundant shells of *Carolia placunoides* Cantr. These beds, forming the upper part of Gabal Mokattam to the east of Cairo, are known in the literature as the Maadi Formation, following Said (1962). The Maadi Formation in the Mokattam area extends south to the east of the Maadi City and farther south to Helwan provinces to be known under a different name (Table 3.1). In the east Helwan area, the Upper Mokattam is represented by the "Wadi Hof" series (Farag and Ismail, 1959), where it is characterized by shales and sandstones with a clastic limestone. The Upper Mokattam extends southwards to Beni Suef area forming the Maadi Formation, Abdou-Soliman (1980), a unit which was described in the southern parts of the studied basin as Formation "F"; Barker (1945), the Fayum Formation; Bishay (1966), Shaibun Member; Boukhary (1970, 1973), and Wadi Hof Formation; Hassan et al, (1978).

In the Fayum area the Upper Mokattam is represented by the Qasr El-Sagha or *Carolia* beds, Beadnell (1905). The

same unit in the Fayum area has been reported in the literature under different rock unit names; Qasr El-Sagha Formation; Said (1962) and also the Fayum Formation; Bishay (1966), which lumps both the Birket Qarun and Qasr El-Sagha series together. The Upper Mokattam Unit, throughout the studied basin is formed from different facies, mostly clastics with a brownish yellow colour and started from the base by shales or clastic sandy shales which generally overlay harder light coloured clastic limestones; top of the Middle Mokattam Unit. That field phenomenon with its regional area distribution makes the lower boundary of the Upper Mokattam easily distinguishable at the top of the Middle Mokattam.

It is important to point out that we have discussed the Upper Mokattam Unit in this study only briefly. More detailed work is needed. Also whether or not the term "unit" for Upper Mokattam could exist, still needs more research.

BIOSTRATIGRAPHIC

ANALYSIS

CHAPTER FOUR

4. BIOSTRATIGRAPHIC ANALYSIS AND CHRONOSTRATIGRAPHIC CORRELATIONS

In the previous chapter we discussed the lithostratigraphy of the northern Nile Valley and the Fayum area while in this chapter we will discuss the biostratigraphy and the chronostratigraphic correlation for the rock units of the studied area.

In order to throw more light on the accurate time lines framework of the Middle - Late Eocene in Egypt, the area of the present study is chosen as an ideal basin for having most of the Middle and Late Eocene carbonates conformably represented, Although, through time new data are constantly accumulating on the biozones (Table 4.1), the establishment of correlations between the biozones has become more and more difficult because of using mixed, reworked fauna and ignoring the nature of the basin on a regional basis. Therefore, in this chapter, the faunal contents were identified and considered for both calcareous nannoplankton and foraminiferida. The latter are based upon micro planktonic foraminifera, larger benthonic foraminifera; mainly nummulites, and to some extent on the distribution of micro-benthonic foraminifera. Proposed range distributions for the faunal species and a sequence of biozones are shown in Tabs. 4-2 to

The author has, also, attempted (in Table 4-5), to present correlations between the biozones established by means of foraminifera and calcareous nanoplankton with the rock units studied.

The classification of each stratotype of the upper and late Eocene stages is considered following those of Western Europe (Cavellier and Powerol, 1936) and Paleocene time scale.

Table (4-1): Biostratigraphic correlation of the upper Middle and Late Eocene sequences in Egypt.

AGE		Cuvillier (1930)	Ansary (1955)		Said (1963)	Bishay (1966) (Nile Valley)	Tadros (1966) (G. Mokatta)
Series	Stage		Wadi Tayiba (Sinai)	Maadi area			
Late Eocene	Bertonian (Prionian)	<i>N. chavenssi</i>		2- <i>Bolivina</i> Nonion Zone	9- <i>Anisaster gibberulus</i> Zone		III. <i>Pyrgo</i> <i>subspheric</i>
		<i>N. fabianii</i>	3- <i>Bulimina jacksonensis</i> <i>Uvigerina Mediterranea</i> Zone	1- <i>Robulus</i> <i>Bolivina</i> Nonion Zone	8- <i>Carolia placunoides</i> <i>Ostrea clot-beyi</i> Zone		II. <i>Cancris co</i> <i>Passilina</i> Zone
		<i>N. contortus</i> / <i>striatus</i>	2- <i>Lituolidea</i> Zone		7- <i>Turritella angulata</i> Zone	10- <i>N. striatus</i> Zone	
		Bryozoa	1- <i>Anomalina cocaensis</i> Zone		6- <i>N. contortus</i> <i>striatus</i> Zone		I. <i>Bulimina</i> <i>jacksonensis</i> <i>Uvigerina</i> <i>Mediterranea</i>
Middle Eocene	Lutetian				5- <i>Uperculina pyramidum</i> Zone		
		Late			4- <i>N. lyelli</i> Zone	9- <i>N. beaumonti</i> Zone	
					3- <i>N. gizehensis</i> Zone	8- <i>N. gizehensis</i> Zone	
					2- <i>N. zitteli</i> - <i>Callaudi</i> Zone	7- <i>Dictyoconus</i> <i>agyptiensis</i> Zone	
	Early				1- <i>N. marietti</i> - <i>vigueeneli pachoi</i> Zone		
						6- <i>N. obesa</i> Zone	

This zone is firstly introduced by Bay et al., (1967), and amended later by Martini (1970, a). The proposed age

4-8. The author has, also, attempted (in Table 4-8), to present correlations between the biozones established by means of foraminifera and calcareous nannoplankton with the rock units studied.

The classification of each stratotype of the upper and Late Eocene stages is considered following those of Western Europe (Cavelier and Pomerol, 1986) and Palaeogene time scale of Harland *et al.*, 1982.

The age assignment of the studied rock units and the Middle - Late Eocene boundary in the studied area are discussed separately.

The following is a discussion for the calcareous nannoplanktonic and foraminiferal biozones of the Eocene of the northern Nile Valley and the Fayum basin.

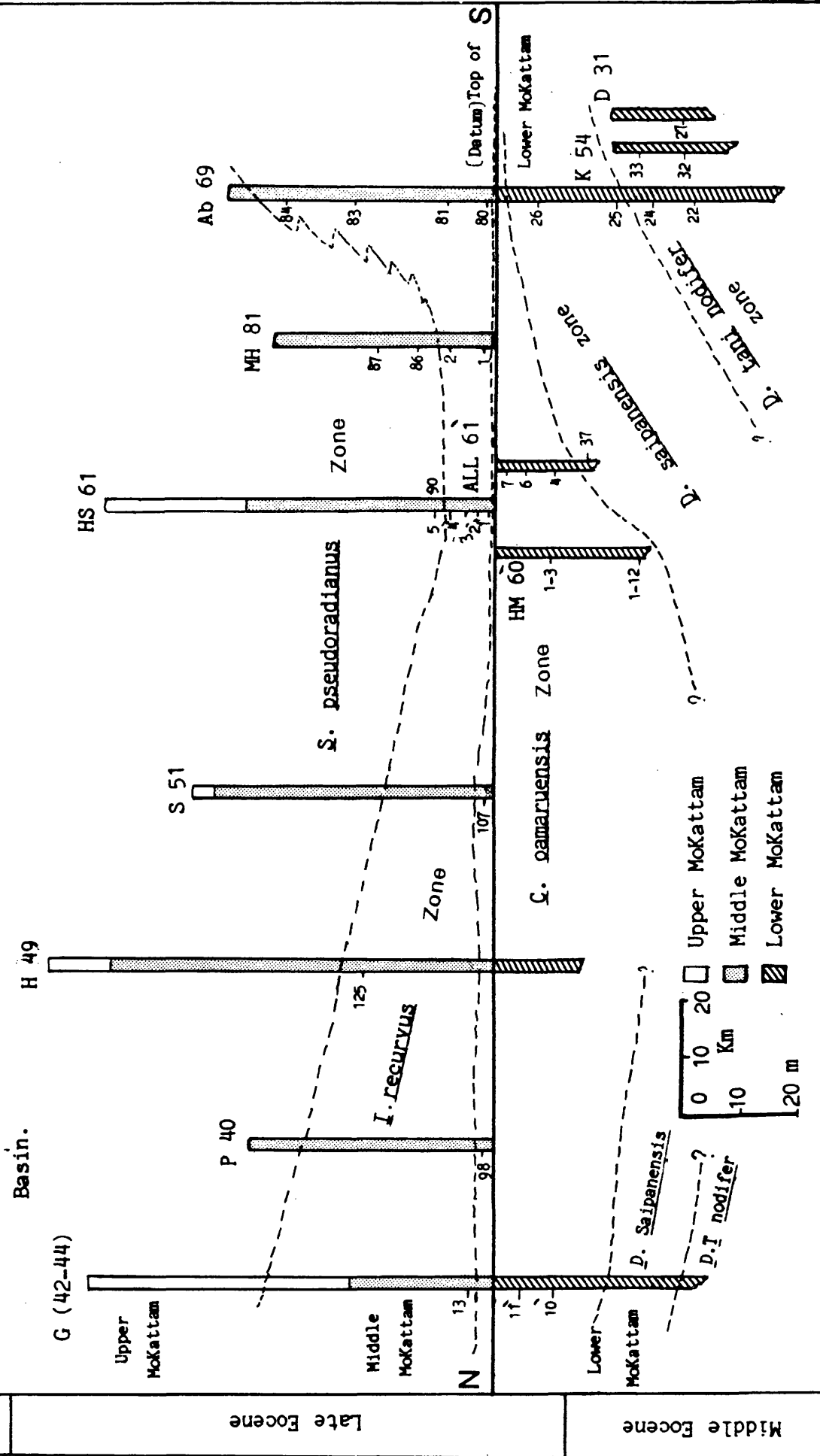
4.1 Calcareous Nannoplankton Zonation.

Calcareous nannoplankton assemblages were found and studied, for the first time, in the rocks of the northern part of Egypt. The analysed samples were collected from the carbonate sections of the Nile Valley basin exposed between Minia and Cairo. The nannoplankton species are assigned in this work to biozones (Fig. 4.1) which correlate with the standard nannoplankton zonations of Martini, 1971; and Cavelier and Pomerol, 1985 (Tables 4-2&3).

Discoaster tani nodifer Zone (NP16).

This zone is firstly introduced by Hay *et al.*, (1967), and amended later by Martini (1970,a). The proposed age

Fig. (4-1): Correlation chart of nannoplanktonic zones in the Middle and Late Eocene sections of N. Nile Valley Basin.



Age

Late Eocene

Middle Eocene

for this zone, in the studied area, is considered to be of Middle Eocene.

Definition: As defined by the author, it coincides with the last occurrences of *Rhobdolithus gladius*, and besides that, in the studied area, with the first occurrence of *Reticulofenestra umbilica*. The upper limit is defined by the last occurrences of *Chiasmolithus solitus*.

Reference localities: Samples 24, 27, 32 and 33 in the shale beds and carbonates of Gabal El-Abyad and Diya, Gabal El-Rayan of Fayum, lower part of the Pyramids section and in Gabal El-Mokattam.

Common assemblage: *Discoaster tani nodifer*, *D. barbadiensis*, *Chiasmolithus solitus*, *C. grandis*, *C. consueta*, *Reticulofenestra umbilica*, *Zygodolites dubius*, and *Sphenolithus radians*.

Correlation: This zone is correlated with the standard zone (NP16). The zone has been recorded in Belgium, Denmark, Bairritz of France, the Helmstedt-Treue of Germany, Mexico and west of the English Channel (Martini, 1971).

Discoaster saipanensis Zone (NP17).

Definition: Interval from the last occurrence of *Chiasmolithus solitus* (Bramlette and Sullivan) to the last occurrence of *C. staurion*.

Table (4-27). Calcareous nanoplankton zonation of the studied basin sequences in the Northern Nile Valley, Egypt.

Age	Stages	Rock Units	Nonnoplankton Zones.	
LATE EOCENE	PRIABONIAN	Upper Mokattam	NP20	Sphenolithus pseudoradians Zone
		Middle Mokattam	NP19	Isthmolithus recurvus Zone
		Giushi Member	NP18	Chasolithus oamaruensis Zone
MIDDLE EOCENE	BARTONIAN	LOWER MOKATTAM Observatory Member	NP17	Discoaster saipanensis Zone
			NP16	Discoaster tan1 nodifer Zone
	UPPER LATE LUTETIAN	Gizehensis Member		

Table (4-3): Distribution chart of the nannoplanktonic species in the studied area.

AGE		ZONES	C. solitus	Z. bijugatus	D. cf. deflandrei	C. neogammation	S. radians	D. cf. diastypus	D. strictus	D. cf. tani	D. cf. lodoensis	C. consuetus	E. subdisticha	C. amaruensis	C. grandis	B. bigelowi	Z. dubius	R. umbilica	M. attenuatus	C. formosus	D. barbadiensis	D. tani nodifer	D. tani	D. saipanensis	I. recurvus	H. lophota	S. pseudoradianus	H. reticulata																														
MIDDLE EOCENE	LATE	PRIABONIAN																																																							
																															S. pseudoradianus NP 20																											
																															I. recurvus NP 19																											
MIDDLE EOCENE	LATE	PRIABONIAN	C. amaruensis NP 18																																																							
			D. saipanensis NP 17																																																							
MIDDLE EOCENE	LATE	PRIABONIAN	D. saipanensis NP 17																																																							
			Discoaster tani nodifer NP 16																																																							
MIDDLE EOCENE	LUTETIAN																																																									

Author: Martini, 1970a.

Reference locality: In the middle plateau of Gabal-El Abyad (East of Fashn), basal beds of El-Allalma section (East of Beni Suef); samples numbers 25, 26 and 37.

Common species: *Braarudosphaera bigelowi*, *Chiasmolithus consueta*, *C. grandis*, *Discoaster barbadiensis*, *D. sublodoensis*, *D. cf. lodensis*, *D. cf. tani*, *D. tani nodifer*, *D. saipanensis*, *D. strictus*, *D. gemmifer*, *D. cf. diastypus*, *D. martinii*, *Helicopontosphaera lophota*, *Sphenolithus radians* and *Reticulofenestra umbilica*.

Correlation: It can be traced all over the Nile Valley scarp from East Fashn to Mokattam (East Cairo). The zone has a similar flora to that of zone (NP17) of Germany, France, Hungary, U.S.A., Atlantic and Pacific Oceans.

Chiasmolithus oamaruensis Zone (NP18)

Definition: From the first occurrence of *C. oamaruensis* (Deflandre) to the first occurrence of *Isthmolithus recurvus* (Deflandre).

Author: Martini, 1970a.

Age: All of the zone occurs in the Late Eocene except the lower base which is of the Middle Eocene.

Reference locality: Along the chalky limestone scarp east of Beni Suef in Abou-Salih and Allalma top beds; samples "HM" (1-3 to 1-12), "ALL" from samples (1-2 to 1-19), (and with thickness of up to 26.4m). The zone also occurs in E. El-Saff; sample 107, Helwan area (Gabal Hof);

sample 125, Gabal Qibli El Ahram; sample 98 and Gabal El Giushi, sample "MG"1.

Common species: *Braarudosphaera bigelowi*, *Chaiasmolithus oamaruensis*, *C. grandis*, *C. solitus*, *Discoaster tani*, *D. saipanensis*, *D. tani nodifer*, *D. barbadiensis*, *Reticulofenestra umbilica* and *Zygodolithus dubius*.

Correlation: This zone is correlated with France, Germany, Hungary and the U.S.S.R. Locally it coincides with the top part of the Lower Mokattam Unit.

Isthmolithus recurvus Zone (NP19)

Definition: From the first occurrence of *Isthmolithus recurvus* Deflandre to the first occurrence of *Helicopontosphaera reticulata* (Bramlette and Wilcoxon).

Authors: Hay, Moher and Wade (1966), amended by Martini, 1970a.

Reference locality: The top beds of Gabal El Abyad (E. El Fashn); samples "Ab" 4 to 10 (80 to 84), Gabal El Mashash in Wadi Sannur; samples "Mh" 1 and 2, and in Gabal Shaibun; samples "H.S." 1 to 3-2 (1 to 4).

Common species: *Braarudosphaera bigelowi*, *Chaiasmolithus oamaruensis*, *C. grandis*, *Discoaster tani*, *D. saipanensis*, *D. barbadiensis*, *Reticulofenestra umbilica*, *Isthmolithus recurvus*, and *Ericsonia subdisticha*.

Correlation: This zone attains maximum thickness in the south of the studied area. It can be correlated with

(NP19) in Germany, Hungary, Italy, U.S.S.R., Atlantic and Pacific Oceans, Martini, 1971.

Sphenolithus pseudoradins Zone (NP20)

Definition: Started from the first occurrence of *Helicosphaera reticulata* and upwards.

Author: Martini, 1970a.

Reference locality: This zone forms the highest zone in the studied sections. All species assemblage highly occurred in peculiar samples "Mh"3, and 4 (86 and 87), and in Gabal Shaibun East of Beni Suef; sample 3-3 (90).

Common species: *Helicosphaera reticulata*, *H. Lophota*, *Discoaster tani*, *D. tani nodifer*, *D. saipanensis*, *D. barbadiensis*, *Reticulofenestra umbilica*, *Microntholithus attenuatus*, *Zycolithus dubins* and *Isthmolithus recurvus*.

Correlation: This zone has been recorded in Belgium, Germany, U.S.S.R., Atlantic and Pacific Oceans. (Haq, 1971 and Martini, 1971).

4.2. Foraminiferal zonation.

The Middle Late Eocene foraminifera of Egypt have recently been described by Ansary (1955), and Abdel-Kireem (1985).

We examined the foraminiferid collections housed in the British Museum (Natural History). These include the Ansary collections. Many of the holotypes of species mentioned in this work, together with those of equivalent

regional planktonic and larger foraminifera, were examined and compared with our investigated material. For briefness, each named species is listed with the original name, author and date. This provides all the information necessary to find the species in the Catalogue of Index Foraminifera (Ellis and Messina, 1966, et al., 1969), Nummulites and Assilines of the Tethys palaeogen (Shaub, 1981), and all available up to date publications.

The scope of this work, does not entail detailed taxonomic or systematic descriptions and the reader is referred to Ellis and Messina, 1966, et al., 1969), Shaub (1981), Abdel-Kireem (1985), and Ansary (1955) for illustrations and descriptions of these species.

4.2.1 Planktonic Foraminiferal Zones.

Most species names are updated following Bolli, et al., 1985. The biozones used in this study are referred to in the works by Berggren et al., 1985, Cavelier and Pomerol, 1986, and these are correlated with the description of zones by Abdou and Abdel-Kireem (1972), and Abdel-Kireem (1985).

Five biozones were recognised: (Tables 4-4&5).

Morozovella lehneri Zone (P12)

Age: Middle Eocene.

Type reference: Globorotalia lehneri Cushman and Jervis, 1929.

Age	Stages	Rock Units	Planktonic biozones, modified from Abdel-Kireem (1985)
L A T E E O C E N E	P R I A B O N I A N	Upper Mokattam	Turborotalia cerroazulensis Zone (P16-P17)
		Middle Mokattam	Globigerinatheka seminvoluta (P15)
		Giushi Member	
M I D D L E E O C E N E	B A R T O N I A N	L O W E R M O K A T T A M Observatory Member	Truncorotaloides rohri (P14)
			Orbulinoides bekmanni (P13)
		Gizehensis Member	Morozovella lehneri (P12)

Table (4-5) Distribution Chart of the Upper Mid and Late Eocene Planktonic Foraminiferal Species in the Studied Rocks.

Standard Zones	AGE	Planktonic Zones	Sample Number	Species range in sections
P17 & P16	Priabonian	Turborotalia cerroazulensis zone	MA 3-3	T. cerroazulensis cushmani Cushman 1928 Turborotalia cerroazulensis cerroazulensis Cole 1928
			HS 9-3 HS 2-6	
P15	Priabonian	Globigerinatheta semiinvoluta zone	Ab4	Turborotalia cerroazulensis pomeroli (Tomarkin & Bolli, 1970) Turborotalia spinulosa Cushman, 1927 Morozovella lehnerei Cushman & Jarvis, 1929 Globigerinatheta index index Finlay, 1935
			Ab2	
P14	Bartonian	Truncorotaloides rohri zone	P3c	Morozovella venezuelana Hedberg, 1937 Morozovella lehnerei Cushman & Jarvis, 1929 T. haynesi Samanta, 1970 T. rohri Bronnmann & Bernudez, 1953 Pseudohastigerina micra Cole, 1927 Globorotaloides suteri Bolli, 1957 Globigerina gravelli Bronnmann, 1952
			M3-7 Kh7 M61	
P13	Bartonian	Orbulinoides beckmanni zone	A11 1-4	Morozovella spinulosa Cushman, 1927 Morozovella lehnerei Cushman & Jarvis, 1929 Globoquadrina venezuelana Hedberg, 1937 T. haynesi Samanta, 1970 T. rohri Bronnmann & Bernudez, 1953 Pseudohastigerina micra Cole, 1927 Globorotaloides suteri Bolli, 1957 Globigerina gravelli Bronnmann, 1952 Globigerina linaperta Bolli, 1957 Cetapsydrax dissimilis Cushman & Bernudez, 1937 Globigerinita africana Blow & Banner, 1962
			A 5-2	
P12	Upper Late Lutetian	Morozovella lehnerei zone	W 5-6	Morozovella spinulosa Cushman, 1927 Morozovella lehnerei Cushman & Jarvis, 1929 Globoquadrina venezuelana Hedberg, 1937 T. haynesi Samanta, 1970 T. rohri Bronnmann & Bernudez, 1953 Pseudohastigerina micra Cole, 1927 Globorotaloides suteri Bolli, 1957 Globigerina gravelli Bronnmann, 1952 Globigerina linaperta Bolli, 1957 Cetapsydrax dissimilis Cushman & Bernudez, 1937 Globigerinita africana Blow & Banner, 1962
			MB 6-4 A 1-1	
			B 2-2	
			B 1-13	
			B 1-1	
				Globigerina eocaena Guenbel, 1968
				Globigerina ampliapertura Bolli, 1957
				Globigerina corpulenta Subbotina, 1953
				Globigerina angiporoides Hornibrook, 1965
				Globigerina azarbadjanica Chailov, 1956
				Globigerina galavisi Bernudez, 1961

This zone was first described by Cushman and Jervis (1929). In the area of study, this zone is found to be the oldest assemblage represented. The base of the zone is not determined, but the top is well defined by the first occurrence of *Orbulinoides bekmani* Saito, 1962.

Turborotalia cerroazulensis pomeroli (Toumarkine and Bolli, 1970), and *Truncorotaloides Libyaensis* El-Khoudary, 1977, started near the top of this zone. The common species assemblage in this zone are *Acarinina spinuloinflata* Bandy, 1949, *Globigerinatheka mexicana kugleri* (Bolli, Loeblich and Tappan, 1957), *Morozovella spinulosa* Cushman, 1927, *M. lehneri* Cushman and Jervis, 1929, *Truncorotaloides rohri* Bronnimann and Bermudez, 1953.

The *Morozovella lehneri* zone is found with the base member of the Lower Mokattam Unit along the Nile Valley Basin. It is also recorded in the Beni Mazar area, EL-Medawara and Wadi El-Rayan in the Fayum area. The zone has been reported in the Fayum area by Abdou and Abdel-Kireem (1972) under the old name of *Globorotalia lehneri*.

For correlation, this zone is found to correspond to the standard P12 zone (Toumarkine and Bolli, 1970, Harland et al., 1982, Berggren et al., 1985 and Cavelier and Pomerol, 1986).

Orbulinoides beckmanni Zone (P13).

Age: Middle Eocene.

This was first named by Bolli (1957) and renamed by Cordey (1968) and Blou and Saito (1968). As defined by them it is found to have the total range of *Orbulinoides beckmanni* Saito, 1962. The common assemblage of the zone contains *Orbulinoides beckmanni* Saito, 1962, *Globigerinatheka mexicana kugleri* (Bolli, Loeblich and Tappan, 1957) *G. m. barri* Bronniman, 1952, *Acarina spinuloinflata*, Bandy, 1949, *Turborotalia cerroazuensis pomeroli* (Toumarkine and Bolli, 1970), *Morozovella spinulosa* Cushman, 1927, *M. lehneri* Cushman and Jarvis, 1929, *Truncorotaloides rohri* Bronnimann and Bermudez, 1953, *T. haynesi* Samanta, 1970, *Pseudohastigerina micra* Cole, 1927, *Globigerina linaperta* Bolli, 1957, *G. eocaena* Guembel, 1968, *G. yeguaensis* Weinzierl and Applin, 1929.

The zone is widely distributed in the area of study in the El-Midawara section and base of El-Mishigeiga Member of Adbou and Abdel-Kireem (1972) in Wadi El-Rayan, Qaret Gehannan of Fayum, Qarara and Shinnara shales, Wadi Sannur and base of building stone Member in the Cairo area (Said, 1962) and base of the Observatory Member in both the Helwan (Farag and Ismail, 1959) and Beni Suef areas (Abdou-Soliman, 1980).

The *Orbulinoides beckmanni* zone is correlated with the standard P13 zone by Blow, 1979, Harland *et al.*, 1982,

Bergreen *et al.*, 1985, Toumarkine and Luterbacher, 1985 and Cavelier and Pomerol, 1986, all over the world.

Truncorotaloides rohri Zone (P14)

Age: Middle Eocene.

This zone was first defined by Bolli, 1957b. Its top is defined by the extinction of *Truncorotaloides rohri* and appearance of *Globigerinatheka seminvoluta* Keijzer. This is found to be more or less sharply defined in the studied area. The common recognized assemblage, besides the zonal marker *Truncorotaloides rohri* Bronnimann and Bermudez, 1953, contain *T. haynesi* Samanta, 1970, *Turborotalia cerroazulensis pomeroli* (Toumarkine and Bolli, 1970), *Globogadrina venezulensis* Hedberg, 1937, *Globerinatheka index index* Finlay, 1939, *G. mexicana barri* Bronnimann, 1952, *Globigerina eocaena* Guembel, 1868, *G. linaperta* Bolli, 1957, *G. yeguaensis* Weinzierl and Applin, 1929, *Globigerinita africana* Blow and Banner, 1962 and *Globorotaloides suteri* Bolli, 1957.. *Acarinina spinuloinflata* Bandy, 1949, *Morozovella spinulosa* Cushman, 1927, and *M. lehneri* Cushman and Jervis, 1929, all of which end at the top of this zone. *Globigerina corpulenta* Subbotina, 1953, is noticed to be met with frequently in this zone, however, it may be delicate and of less quantity in the previous *Orbulinoides beckmanni* zone. Also associated to the zone is *Catapsydrax dissimilis* Cushman and Bermudez, 1937.

The *Truncorotaloides rohri* zone is distributed over a very wide area in the studied basin. The second member of the Lower Mokattam Unit; Observatory or Building stone division up to the lower part of the Giushi Formation in Cairo-Helwan areas are assigned to this zone. In the Beni Suef area, the zone can be found in the base of El Allalma and Abou-Saleh sections. In Gabal El-Abyed and Gabal El-Merier; east of El-Fashn, it occurs within the lower third of the middle plateau beds and top of Qatara section. In the Fayum area it occupies El Mishigeiga, Ravine beds of Qaret Gehannam and base of the marl Member.

The *Truncorotaloides rohri* zone corresponds with the standard P14 zone of Berggren *et al.*, 1985, Toumarkine and Luterbacher, 1985, and Cavalier and Pomerol, 1986. The extinction of mostly all spinose planktonic foraminifera (Acarina, Morozovella, *Truncorotaloides*) of the Middle Eocene marks the boundary between the Middle and Late Eocene in the studied area in Egypt (Omara *et al.*, 1978b) and throughout the world (Bolli, 1957, and Haak and Postuma, 1975).

The *Truncorotaloides rohri* zone was previously reported by El-Boukhary (1973), from the Nile Valley and by Abdel-Kireem, 1985, in Gabal Mokattam, but these workers exaggerated the limits of this zone.

Globigerinatheka semiinvoluta Zone (P15)

Age: Late Eocene.

Firstly named by Bolli, 1957, and modified by Proto, Decima and Bolli, 1970. It is considered as a range zone. The lower limit starts at the extinction of *T. rohri* zone and ends at the extinction of *Globigerinatheka semiinvoluta* Keijzer, 1945.

The common assemblage of this zone, besides the zonal marker, contains *Turborotalia cerroazulensis pomeroli* (Toumarkine and Bolli, 1970, *T.C. cerroazulensis* Cole, 1928, *Globogadrina venezuelana* Hedberg, 1937, *Globigerinatheka index index* Finlay, 1939, traces of *G. mexicana barri* Bronnimann, 1952, *Globigerina gravelli* Bronnimann, 1952, *G. linaperta* Bolli, 1957, *G. yeguaensis* Weinzierl and Applin, 1929, *G. corpulenta* Subbotina, 1953, *G. azerbadjanica* Chalilov, 1956, *G. galavisi* Bermudez, 1961, *G. escaena* Guembel, 1868, *Globorotaloides suteri* Bolli, 1957, *Pseudohastigerina micra*. Cloe, 1927, *Catapsydrax dissimilis* Cushman and Bermudez, 1937.

This zone is commonly distributed in nearly the upper two thirds of the Giushi limestones in the Mokattam area and the overlying marls of the Middle Mokattam in the east Helwan area and Wadi Hof, Wadi Garawi and El-Saff. It extends south to Beni Suef area where the white limestone top of Allalma and Abou Saleh sections are assigned to the zone. Also related to this zone are Gabal El-Abyed, towards the hard top and the shaley cap and the top of

Gabal El-Merier east El-Fashn area. In the Fayum area, the zone is found within the top shales of the Qaret Gehannam shales and the Birket Qarun shales and marls.

The *Globigerinatheka seminvoluta* zone corresponds to the standard Zone P15 (Blow, 1979 and Cavalier and Pomerol, 1986). However, it was considered in other studies to be equivalent to Zone P15 and to part of Zone P16 (Harland et al., 1982, Berggren, 1985 and Bolli et al., 1985).

In the area of study, it is considered to correspond to Zone P15. Abdel-Kireem (1985) also referred to the zone in the Mokattam section as Zone P15 and recorded the same zone to occur in the Fayum section.

In all cases, Zone P15 is considered to be of Priabonian age. (Toumarkine and Luterbacher, 1985, Berggren et al., 1985, Cavalier and Pomerol, 1986, and Pomerol and Premoli-Silva, 1986).

Turborotalia cerrozulensis Zone

This zone is assigned to the Late Eocene and is of Priabonian age. The *Turborotalia cerrozulensis* Zone was firstly described by Bolli (1957) and renamed by Bolli (1966, 1972). The zone is defined from the last occurrence of *Globigerinatheka seminvoluta* to the last occurrence of *Turborotalia cerrozulensis*. In the area of study, the normal assemblage occurring in this zone includes *Turborotalia cocoaensis* Cushman, 1928 and *T.C. cerrozulensis*, Cole, 1928.

Also as a common species *Globigerina corpulenta* Subbotina, 1953, *G. galavisi* Bermudez, 1961, *G. azerbadjanica* Chalilov, 1956, *G. angiporoides* Hornibrook, 1965, *G. yeguaensis* Weinzierland Applin, 1929, *G. linaperta* Bolli, 1957, *G. gravelli* Bronnimann, 1952, *G. eocaena* Guembel, 1868, *Globorotaloides suteri* Bolli, 1957, and *Pseudohastigerina micra* Cole, 1927, *Turborotalia cerrozulensis pomeroli* Toumarkine and Bolli, 1970; *Globogadrina venezuelana* Hedberg, 1937; and *Globigerinatheka index* Finlay, 1939, all of which occur in the lower part of the zone. However, *Globigerina ampliapertura* Bolli, 1957, is characteristic of the top part of this zone at the Hamret|Shaibun section, east Beni Suef. In the Nile Basin carbonates, the *Turborotalia cerrozulensis* Zone is met with the Upper Mokattam Unit in El Maadi; in Gabal Mokattam, at the beginning of the Cairo-Fayum Road, in the Hamret Shaibun section, and at 50km from El Kurrimat to Zaafarana Road east of Beni Suef. It represents the last stage of the Late Eocene of Egypt. For local correlation, the zone has been assigned in the Mokattam section to the *Globigerina corpulenta* zone (Abdel-Kireem, 1985). This assignment creates confusion for the following reasons: Firstly *G. corpulenta* ranges downwards into the Middle Eocene. Secondly, the worker, also, reported the species markers of the *Turborotalia cerrozulensis* within his newly named zone, but chose to ignore the law of priority when naming the zone. Thirdly,

all of the species he recorded within his zone, i.e. *G. corpulenta*, were only a typical assemblage to the *Turborotalia cerrozulensis* Zone.

Regionally, the *Turborotalia cerrozulensis* Zone corresponds to both the standard P16 and P17 Zones (Berggren et al., 1985, and Cavalier and Pomerol, 1986).

4.2.2 Larger Foram (Nummulitic) Zonations.

The widely spread, recorded larger foraminifera in the Mid-Late Eocene carbonates was Nummulities. They were highly diversified with large shell size, especially those within the Middle Eocene age (Tables 4-6&7) .

The northern Nile Valley carbonate basin has been divided in this work into the following Nummulities zones:

Nummulities gizehensis Zone.

Author: Forskal, 1775.

The oldest zone in the area of study is found to be represented by *N. gizehensis* of Lutetian, Middle Eocene age. This zone is defined as a total range zone for the marker species of *Nummulities gizehensis* both micro and megalospheric forms.

The top of the zone is well known by the last occurrence of the very big sized (up to 4cm diameter) *Nummulities gizehensis* species. The normal assemblage of this zone, besides to the zonal marker, includes *Nummulities miliecaput* and *N. discorbinus*. *Nummulities beaumonti*, *N. perforatus* and *N. biaritzensis* appeared with the top part of that zone. The zone is associated with

Table (4-6). Large foraminiferal (Nummulites) Zones in the studied sequences of the Northern Nile Valley Basin.

Age	Stages	Rock Units	Nummulitic Zones.
L A T E E O C E N E	P R I A B O N I A N	Upper Mokattam	Nummulites fabianii Zone
		Middle Mokattam	Nummulites striatus Zone
		Giushi Member	
M I D D L E E O C E N E	B A R T O N I A N	Observatory Member	Nummulites beaumonti Zone
		U P P E R I A T E L U T E T I A N	Gizehensis Member

Table 4
 Nummulite species range chart of the studied rock sequences of the Nile Valley basin in Northern Egypt

Age	Stages	Nummulitic Zones	Species ranges		
LATE EOCENE	PRIABONIAN	N. fabianii Zone	N. fabianii		
		N. striatus Zone	N. striatus	N. lyelli	N. fabianii
MIDDLE EOCENE	BARTONIAN	N. beaumonti Zone	N. perforatus N. discorbis	N. beaumonti	N. biaritzensis
		N. gizehensis Zone	N. milliecaput N. gizehensis	N. discorbis	

some larger foraminifera such as *alviolines*, *discocyclines* and *orbitoloides*.

The thickness of the zone reaches up to 80 metres but its distribution is rather localized. This zone is well represented in the foot scarp of the Giza pyramids, in the base of the Mokattam section, in the Beni Suef area; east and west of the Nile, in east Biba, in Qarara and Diya sections, El Gabal, El-Ahmar, Samalout to Minia, west of Beni Mazar, Wadi Mowillah and Gabal El-Rayyan.

The *N. gizehensis* zone in this study is confined to the lower division of the lower Mokattam unit, the Gizehensis limestones.

The *Nummulities gizehensis* zone was previously described in the Nile Valley, Egypt, by Said, 1963; Bishay, 1966; Boukhary, 1970 and Omara *et al.*, 1978, from the Middle Eocene, Lutetian, succession. It is considered as an index fossil for the Late Lutetian sections in and outside Egypt (Bishay, 1966; Kenaway *et al.*, 1978; Omara *et al.*, 1978). It has been reported by Haak and Postuma, 1975 from the Far East, the Middle-Late Lutetian rocks, upper Middle and Late Lutetian (Schaub, 1981).

Nummulities beaumonti Zone

Author: d'Archiac and Haime, 1853.

This zone overlies the previous one with its relatively smaller sized shells.

It is defined as the interval which commences at the last occurrence of *Nummulites gizehensis* and ends at the first appearance of *Nummulites striatus*. The common species which are found in this zone assemblage are *N. beaumonti*, *N. perforatus*, *N. biaritzen*, and *N. Mokatomensis*. This zone is associated with *Orbitolites complanatus*, *Discocyclus granulata*, *D. taramellii*, *D. varicostata*, *Operculina schwageri*, *O. orientalis*, *Gypsina carteri*, *Dictyoconus aegyptiensis*, and *Alveolina* aff. *delicatissima*. Also an abundance of miliolids coincide with the top of this zone in some places and calcareous algae intermix with the zone in other environments [Abdou-Soliman, 1980].

The average thickness of this zone ranges from about 57-69m.

In the present study, the *Nummulites beaumonti* zone is confined to the Observatory division of the Lower Mokattam unit or its equivalent lateral counterparts, all along the Northern Nile basin.

This zone was first introduced by Bishay (1966) from the Upper Middle Eocene (Late Lutetian) succession of the Nile Valley. *Nummulites beaumonti* is considered, in Egypt, as an index fossil for the uppermost Lutetian [Kenawy et al., 1978].

Regionally, this species has a wide distribution and occurs throughout the Mediterranean Province, Aquitaine,

Europe, Somalia, India, Senegal and Madagascar, [Blondeau, 1972], Syrte Basin of Libya [Schaub, 1981], where it is believed to have late Lutetian and Biarritzian age.

In many parts of the studied basin, it is observed that the *Nummulites beaumonti* zone coincides with the *Truncorotaloides rohri* zone. This zone, in this work, is considered to be of later Middle Eocene, Bartonian age.

Nummulites striatus zone

Author: Bruguiere, 1792

This zone is of Middle Eocene in its lower part but most of it is of Late Eocene.

It is considered, more or less, as a total range zone defined by the first appearance of *Nummulites striatus*; A and B forms, up to its extinction.

A very helpful assemblage is used to, carefully, define the range limits of that zone. This assemblage commences in contemporaneous to *Nummulites striatus* and ends with the proper top line of that zone. Rare forams of *Nummulites beaumonti* exist in the lower part of the zone. Their complete disappearance delineates the Middle-Late Eocene boundary in the studied area. *Nummulites fabianii* is recorded as scattered assemblage species. The abundant occurrence of *Operculina pyramidum* Schw and *O. priabonica* [Bishay, 1966] define certain horizons within this zone. Bryozoa also is found to be associated with different levels in the *Nummulites striatus* zone. Generally, in the field, it is a very good reference zone,

well recognized by its large numbers of small sized nummulitic shells.

The thickness of this zone is variable. On average it is about 80m. The top of the Observatory limestones and its lateral counterparts are assigned to this zone. The Giushi limestones (or the top division of the Lower Mokattam Unit), and the Middle Mokattam Unit are also encountered within this zone.

The *Nummulites striatus* zone was introduced to the Egyptian stratigraphy by Said, 1963; Bishay, 1966; El-Boukhary, 1970; Abdou-soliman, 1980 and El-Boukhary and Abdelmalik, 1983. It is considered by Said (1962, 1963), Bishay (1966) and Abdou-Soliman (1980) to be of Late Eocene. Along the Mediterranean basin, Atlantic Ocean and Alpes, *Nummulites striatus* is considered to be of Late Eocene [Blondeau, 1972]. However, Strougo (1979) has given a Middle Eocene age to the beds with *Nummulites striatus* in the Gabal Mokattam section.

The fossil associations and chronological correlation in the studied Nile basin, indicate that this zone is of Middle Eocene (Bartonian) age in its basal part while the rest of the zone is of Late Eocene (Priabonian) age. This age range, for the *Nummulites striatus* zone has already been recorded by Curry et al., (1978) and Schaub (1981) throughout the world.

Nummulites fabianii Zone

The name of *Nummulites fabianii* was first introduced by Prever in Fabiani (1905) as *Bruguieria fabianii*. Prever then under *Nummulites fabianii* Prever in Fabiani by Boussac (1911, p. 79).

This zone is considered in this work as an interval zone. The lower limit is characterized by the last appearance of the *Nummulites striatus* zone, while the upper is indicated by the last occurrence of *Nummulites fabianii*. In the studied area, besides the marker species, an abundant assemblage of tiny nummulitic species shells are observed, of which, *Nummulites fayumensis* [Bishay, 1966] is the only identified species.

Commonly associated macrofossils are represented by *Osteria clot-beyi*, *Turritella* spp., *Miliola prisca*, *Carolia placunoides*, corals, some green algae, miliolids, *Anisaste gibberulus*, *Echinolamps crameria*, *E. ovalis*, and *E. globulus*, mostly occur in a lower horizon.

It is important to mention that some alveolines species are recorded in a 10cm thick horizon in the Maadi Formation (Upper Mokattam) of the Gabal Mokattam section. Alveolina bands up to 80cm thick are recorded at three levels in the Upper Mokattam of the Beni Suef area. Unfortunately, we were unable to confirm whether or not they could be assigned to the "Neoalveolina" of Hottinger (1960).

The distribution of this zone is rather patchy and many areas are recorded to be barren of any foraminifera. The only recorded areas with this zone were Hamret Shaibun

section (as a type locality) and the Mokattam Hotel section, for the zone assemblage.

The *Nummulites fabianii* is included within the *Nummulites striatus/ N. chavannesi/ N. fabianii* zone from the Late Eocene of Egypt by Boukhary and Abdelmalik (1983). However, Zittel (1883) was the first researcher who has recorded *Nummulites fabianii* from the Priabonian of Siwa Oasis, Aradj and Sittra, all in the North Western Desert of Egypt.

Nummulites fabianii is considered as an index fossil for the Priabonian throughout the world. It is known as one of the assemblage zone from the type section of the Priabonian stage [Roveda, 1961]. The *Nummulites fabianii* zone is also recorded from the Late Eocene of the Western English Channel and southern Europe [Curry et al., 1978]. It is also considered as marker fauna for the Priabonian (Late Eocene) of Georgia [Kacharava, 1980], Italy, Swiss Alps, French Alps, Spain and Somalia [Schaub, 1981].

In the Northern Nile Valley Basin, the general chronological correlation indicates a Late Eocene; Priabonian, age for the *Nummulites fabianii* zone in the area of study.

4.2.3 Micro-Benthonic foraminiferal zonation

The micro-benthonic foraminiferal distribution in the upper Middle-Late Eocene of the Nile Valley and Fayum Basin is rather variable. The Maadi sections have a



limited microfaunal associations while these associations are abundant in the Beni-Suef area. In the Fayum area, the type of assemblage, as well as the abundance, are found to be different from those of Beni-Suef. It is believed that these differences are probably due to changing in environments and consequently the ecological conditions all along the studied basin.

The micro-benthonic forams recorded are compared with those studied before by Ansary (1955) from the Upper Eocene of Egypt. The author has examined the type of species of Ansary (1955) which are deposited in the British Museum and carefully compared them with those of the studied basin. The result was that there is a complete similarity between them. This similarity could provide another piece of evidence on the existence of Late Eocene assemblage on the basis of micro-benthonic foraminifera.

The microforaminiferal association is found to include, *Ammobaculites cubensis* Cushman and Bermudez, *Anomalina fayomensis* Ansary, *Bolivina modysensis* Cushman & Todd, *bolivian obliqua* Barbat & Johnson, *Bulimina jacksonensis* Cushman, *Bulimina inflata* Sequenza, *Cancris cf. amplus* Finlay, *Cancris cf. turgidus* Cushman & Todd, *Cibicides fletcheri* Galloway & Wisler, *Cibicides lobatulus* Walker & Jacob, *Cibicides mississippiensis*, var. *ocalamus*, Cushman, *Cibicides mabahethi* Said, *Eponides ellisorae* Garrett, *Eponides praecinotus* Karrer, *Guttulina communis*

d'Orbigny, *Guttulina yamazatii* Cushman, *Gyroidina aegyptiaca* Ansary *Gyroidina cibaoensis* Bermudez, *Haplophragmoides emaciatus* Brady, *Haplophragmoides subglobosum* Sars, *Lagena hexagona* Williamson, *Lagena laevis* Montagu, *Lagena sulcata* Walker & Jacob, *Marginulina pediformis* Bornemann, *M. costatus* Batsch, *M. similis* d'Orbigny, *Massilina decorata*, Cushman, *Nonion acutidorsatum* ten-Dam, *N. belridgensis* Barbat & Johnson, *N. maadiensis* Ansary, *N. microumbilicatus* Le Roy, *N. scarpum* Fichtel & Moll, *N. trompi*, Ansary, *Quinqueloculina seminulum* Lime, *Robulus alabamensis* Cushman, *R. chitani*, Yade & Asano, *R. mayi* Cushman & Parker, *Sigmoilina tenuis* Gzjzek, *Textularia communis* d'Orbigny, *T. halkyardi* Lalicker, *T. concava* Karrer, *Uvigerina mediterranea* Hofker, *U. squamos* d'Orbigny, and *Virgulina squamosa* d'Orbigny.

The distribution range of species is found to be non-uniform. Thus, a general zonation scheme is found to be impossible. These formaminifera, however, correlate very well with those described before either by Ansary (1955) from the Late Eocene of Egypt, or Tadros, 1968, from Gabal Mokattam, and Abdou-Soliman, 1980, from the Late Eocene of E. Beni Suef ; Egypt and also recorded by Gregory & Barret (1931) , and Cushman (1933 , 1940) from definite Late Eocene sections in America and Europe .

The localities for which those forams have been collected were from the rocks of Gabal Giushi, top of Lower Mokattam, and both of Middle and Upper Mokattam and their correspondings in Helwan, El-Saff, Beni Suef, top of

Gabal El-Abyad, and Fayum areas. Since those areas are found to be characterized by those previously indexed Late Eocene benthonic foraminiferal species, therefore, the above-mentioned sections are considered to be of the Late Eocene.

4.3 CHRONOCORRELATION AND AGE ASSIGNMENT

The standard chronostratigraphic stratotypes followed in this study are those of Harland *et al.*, (1982); Berggren *et al.*, (1985) Cavelier and Pomerol (1986) and Pomerol and Premoli-Silva (1986) for the Middle-Late Eocene stages. The Bartonian, of Egypt, is herein updated and reduced in rank to constitute a later stage for the Middle Eocene. That is well observed from the correspondence of the studied nannoplanktonic zones, and also by the geochronological correlation of the Nile Valley Bartonian with both the French Auversian-Marinesian of the Paris Basin [Chateauneuf (1980); Pomerol (1980 a, b) and Aubry (1983)] and revision of the English Bartonian [Curry (1981) and amended by Cavelier and Pomerol (1986)].

The above described biozones, in the Northern Nile Valley and the Fayum basin, have clarified the Middle-Late Eocene biostratigraphic relationship (Tab.4.8) They are now confined to well defined lithologic units (Fig.4-2). The oldest unit in the studied area is the Lower Mokattam Unit, which is divided into the Gizehensis limestones at the base, the Observatory limestones in the middle, and the Giushi limestones at the top. The lower Gizehensis

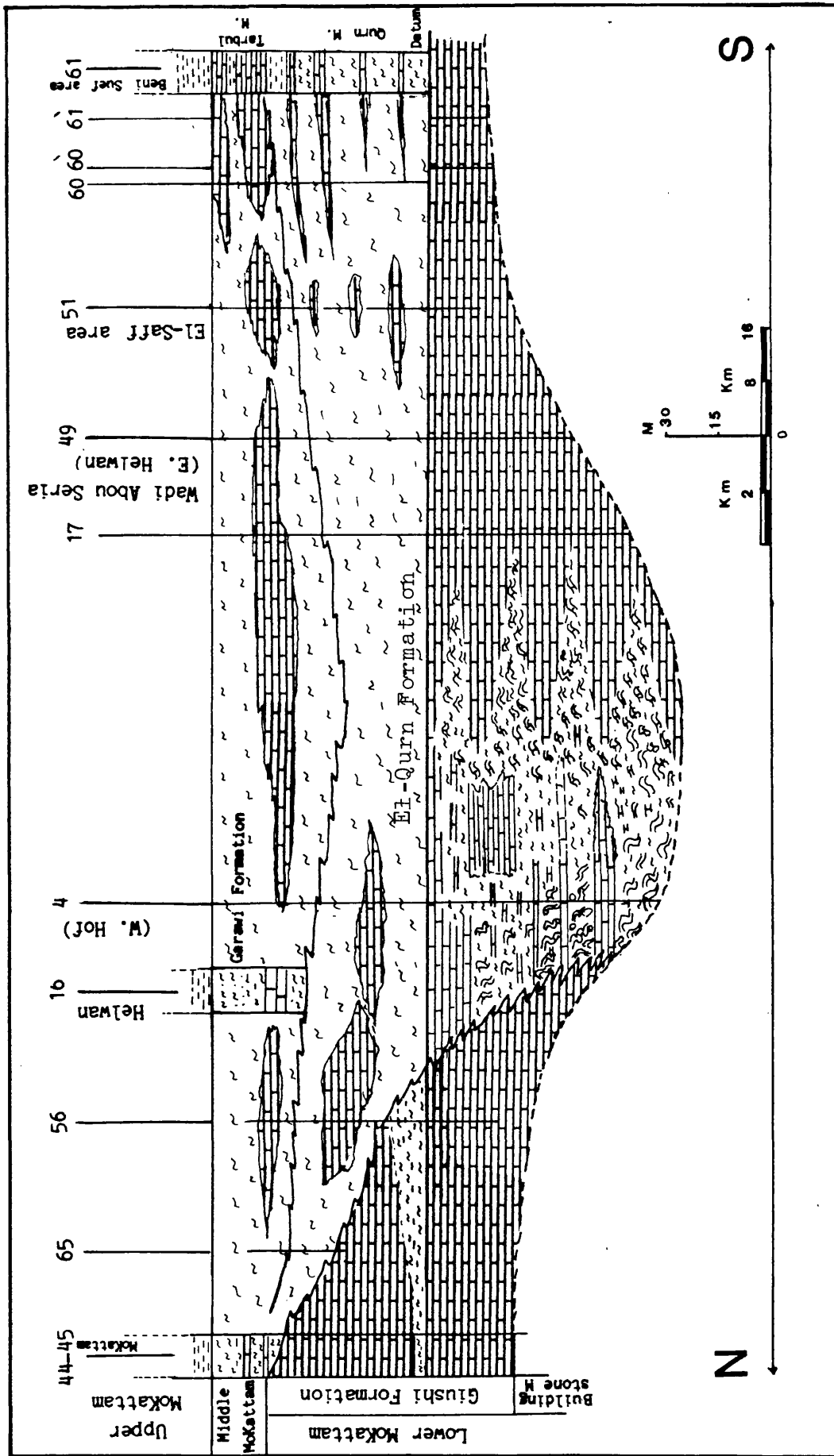


Fig. (4-2): Lithostratigraphic correlation for the Middle Mokattam rock units in the studied basin, of the Northern Nile Valley, Egypt, along N-S direction.

limestones comprises the *Nummulites gizehensis* zone and most of both *Morozovella lehneri* and *Discoaster tani nodifer* zones. Those represent the top part of the Late lutetian age either in Egypt [Said, 1963; Kenawy et al., 1976; Omara et al., 1978b; and Shama et al., 1982] or throughout the world [Haak and Postuma, 1975; Schaub, 1981; Harland et al., 1982; and Cavelier and Pomerol, 1986].

The Observatory limestones are stratigraphically parallel to the *Nummulites beaumonti* zone and the base of *Nummulites striatus* zone. It also includes the top part of P12, P13 and most of P14 planktonic zones. In the meantime the upper part of NP 16 and NP 17 of the nannoplanktonic zones are found to occupy this rock member. Accordingly, the Observatory limestones are considered, for the first time, as of Bartonian age, which represents the top stage for the Middle Eocene. The upper part of the Lower Mokattam Unit, the Giushi limestone, has yielded the nannoplankton of most *chasolithus oamaruensis* zone (NP18), and the lower half of *Nummulites striatus* zone. In terms of planktonic foraminifera, their base is at the top of *Truncorotaloides rohri* zone (P14) and the top two thirds are equivalent to part of *Globigerinatheka seminvoluta* zone (P15). Accordingly, the Middle-Late Eocene boundary is indicated by the contact between the P14 and P15 planktonic zones and in terms of nannoplankton passing through the base part of NP18 zone [Murray et al.,

Table (4-8): General biostratigraphic correlation for the Upper Middle - Late Eocene of the Northern Nile Valley and Fayum basin in Egypt.

AGE	STAGE	ROCK UNITS	PLANKTONIC FORAMINIFERA ZONES	NUMMULITIC FORAMINIFERAL ZONES	NANNOPLANKTON ZONES
LATE EOCENE	PRIBONIAN	Upper Mokattam	P 16-17 Turbotalia cerroazulensis Zone	Nummulites fabianii Zone	Sphenolithus pseudoradians Zone NP 20
MIDDLE EOCENE	GIUSHI L.S.	P 14 Truncorotaloides rohri Zone	Nummulites beaumonti Zone NP 17	Discoaster saipanensis Zone	
					MIDDLE EOCENE
MIDDLE EOCENE	GIZEHEN-SIS MEMBER	P 12 Morozovella lehneri Zone	Nummulites gizehensis Zone NP 16	Discoaster tani nodifer Zone	
					MIDDLE EOCENE
MIDDLE EOCENE	GIZEHEN-SIS MEMBER	P 12 Morozovella lehneri Zone	Nummulites gizehensis Zone NP 16	Discoaster tani nodifer Zone	
					MIDDLE EOCENE

1981; Harland *et al.*, 1982; Berggren *et al.*; 1985; Bolli *et al.*, 1985; Cavalier and Pomerol, 1986; and Pomerol and Premoli-Silva, 1986]. For the above reasons, the Giushi limestone, in this study, is believed to have Middle Eocene age (of about one fourth) from its base, while the remaining upper part is truly of Late Eocene (Priabonian) age. Nearly similar conclusions were reached by Abdel-Kireem (1986) around the Gabal-Mokattam area. Said (1962, 1971) considered all of the Giushi limestone belonging to the Late Eocene, however, Strougo (1977, 1979) included it, within the overlying unit, into the Middle Eocene. It does seem, however, that some faunal mixing, through reworking, has caused confusion.

The Middle Mokattam Unit in the studied area comprises the top half of (P15) *Globigerinatheka seminvoluta* zone and *Nummulites striatus* zone. It also yields both the top *Chaseolithus damaruensis* zone (P18) and a large part of *Isthmolithus recurvus* zone (NP19). These biozones are known to coincide with a verifiable Priabonian (Late Eocene) either in Egypt [Ansary, 1955; Said, 1962, 1971; and Abdel-Kireem, 1986] or also outside Egypt [Ramsay, 1971; Harland *et al.*, 1982; Murray *et al.*, 1981; Haq, 1983; Bolli *et al.*, 1985 and Cavalier and Pomerol, 1986].

Thus, in this work, we consider the age of the Middle Mokattam as of Late Eocene (Priabonian) age. The top unit is the Upper Mokattam which comprises the *Nummulites fabianii*, P16 and P17 planktonic zones, and NP20

Table (4-9): Planktonic correlation between this work and both standard and regional workable zones in Egypt.

Cavelier & Pomerol (1986)	Beckmann <i>et al.</i> , 1969 in Egypt	This Work		Age
		Zones		
Globigerina gortanii P17 & 16 Cribrohantkenina inflata	Cribrohantkenina P17 danvillensis Zone ----- Globorotalia P16 cerroazulensis Zone	Turborotalia cerroazulensis Zone P 16 & 17		L A T E E O C E N E
		Globigerinatheka P15 semiinvoluta		
Globigerinatheka P15 semiinvoluta	Globigerapsis P15 semiinvoluta Zone	Globigerinatheka P 15 semiinvoluta Zone		M I D D L E E O C E N E
Truncorotaloides P14 rohri	Truncorotaloides P14 pseudodubius Zone	Truncorotaloides P 14 rohri Zone		
Orbulinoidea P13 beckmanni	Globorotalia P13 lehneri Zone + Orbulinoidea beckmanni Zone	Orbulinoidea P 13 beckmanni Zone		L A T E T E R T I A R Y
Morozovella P12 lehneri Zone	Morozovella P12 lehneri Zone beckmanni Zone	Morozovella P 12 lehneri Zone		

nannoplankton zones, which were dated Late Eocene (Priabonian) by Blondeau (1972), Curry *et al.*, (1978), Kapellos and Schaub (1975), Schaub (1981), Bigg (1982) Cavelier and Pomerol (1986). That age was previously described in the area of study, by Cuvillier (1930), Said (1962, 1963) Bishay (1966) and Beckmann *et al.*, (1969) , and updated with the standard workable biozones (Tabs.4-1&9).

**STRATIGRAPHIC
RELATIONS
&
BASIN CONCEPT**

CHAPTER FIVE

5. STRATIGRAPHIC RELATIONS AND BASIN CONCEPT

5.1 INTRODUCTION

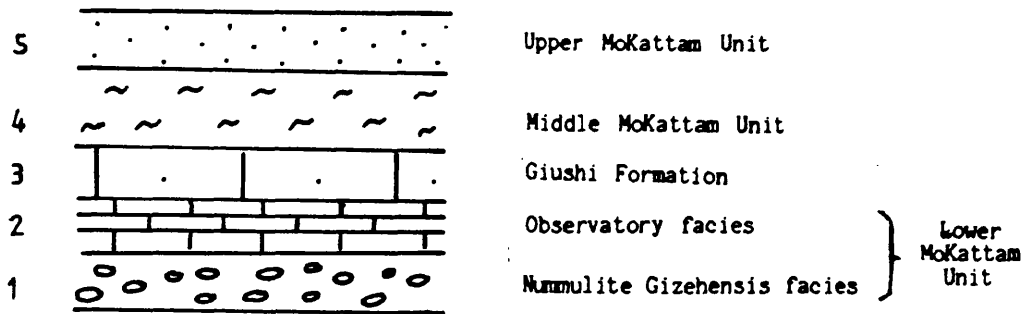
The main objective of the previous stratigraphic chapters is directed towards basin analysis, whereas the aim of this chapter is to show how the development of the basin has influenced its stratigraphic record (i.e. to link stratigraphy and basin analysis). This involves some circular argument because;

1. The stratigraphy is needed to study the basin.
2. Meanwhile, stratigraphy is a consequence of the history of the basin.

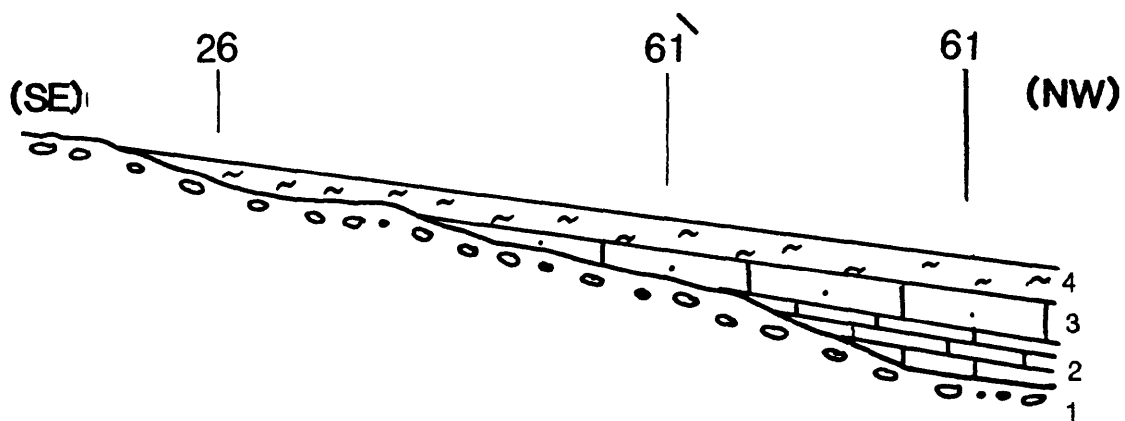
In this chapter, an attempt is made to shed light on the most important stratigraphic relationships. The approach followed to select a marker datum, to be used as a reference in this study and to enable correlations to be made, will be discussed. The stratigraphical analysis revealed in previous chapters, will be also used to detect the basin of deposition.

5.2 THE ONLAP-OFFLAP RELATIONSHIPS

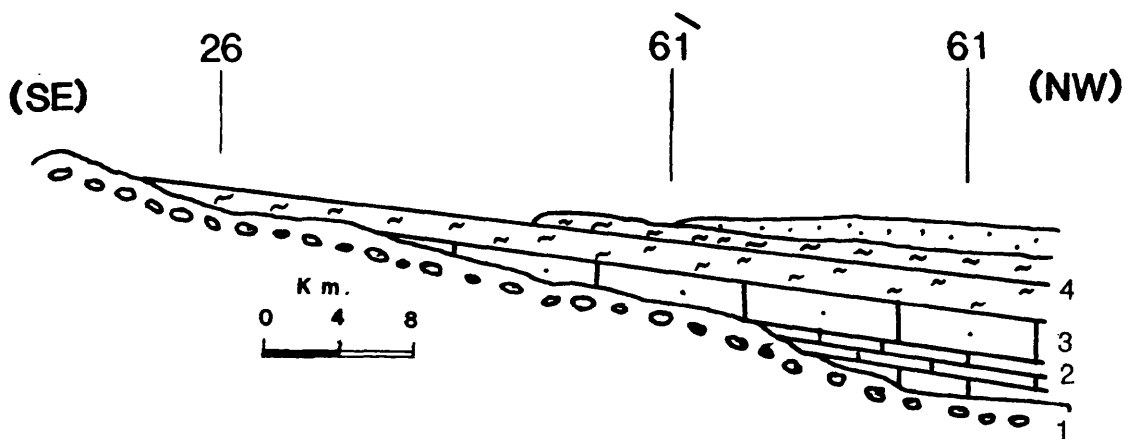
Many examples of onlap-offlap relationships are recorded from the outer margins of the study area. In this chapter, emphasis is laid on the two large southeastern and northwestern areas. (Figs 5-1 and 5-2). Each of the onlap and offlap relationships in both localities will be



(A) Conformable sequence of the studied rock units.

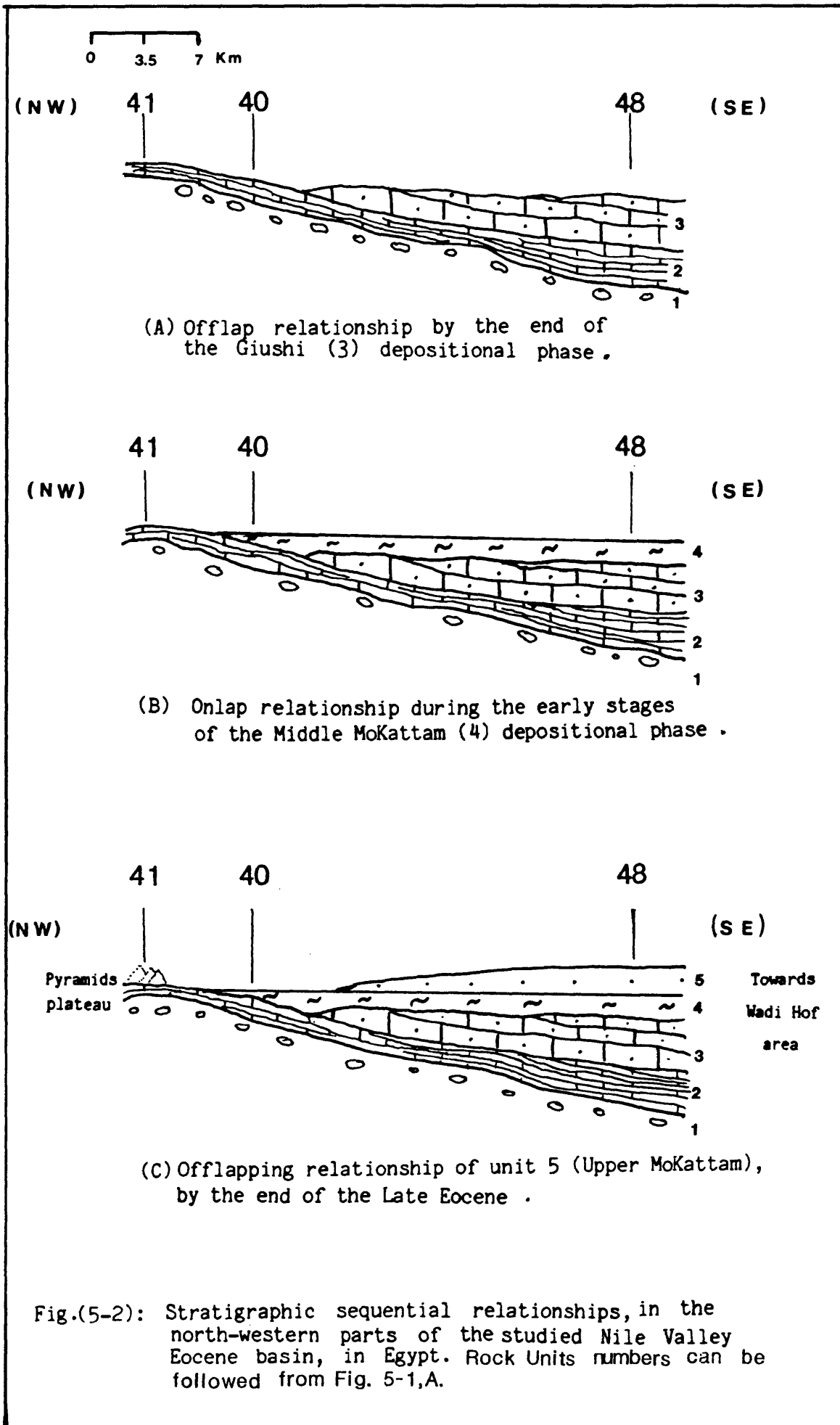


(B) Onlap relationship occurred until the early stages of deposition of the Middle MoKattam facies.



(C) Offlap relationship, by the end of the Late Eocene.

Fig. (5-1): Stratigraphical sequential relationships, in the southeastern part of the studied Nile Valley basin, Egypt.



discussed.

5.2(A) The Onlapping Relationship

The conformable sequence of the studied rock units is shown in Fig. 5-1,A). Facies onlap relationships are observed around both of the east Beni-Suef (sections 61, 26, Fig. 5-1,B) and Giza Pyramids Plateau (sections 40,41, Fig. 5-2,B) areas. This stratigraphic relationship occurs at the facies base of the Middle Mokattam Unit. In the south-eastern part of the study area (Fig. 5-1,B), the middle Mokattam Unit may overlie the *Nummulitic gizehensis* facies and the Giushi facies (section 61) or it may overlie the *gizehensis* facies alone (section 26). In this case, a complete absence of either the Observatory facies (section 61) or both the Observatory and the Giushi facies (section 26) is recorded. Meanwhile, all of the stratigraphic units conformably overlie each other (section 61) in a basin-ward direction. The best example of this relationship is noticed in the eastern parts of Wadi El-Arhab through Gabal Hamret Shaibun (in a S.E.-N.W. direction).

The other example (Fig. 5-2,B) of onlap relationship occurs in the north-western part of the study area, from the Giza Pyramids plateau (section. 41) along both the Gabal Mokattam (N.E.) direction and the Wadi Hof (S.E.) direction. In this locality, the Middle Mokattam Unit overlies the Observatory facies in Gabal Qibli El-Ahram (south of the Sphinx; section 40). Meanwhile, the Giushi

Formation is represented by thick sequence in the Wadi Hof area (section 48).

5.2(B) The Offlapping Relationship

The offlap stratigraphic relationship occurs in both the previously mentioned localities; north-western (Figs 5-2, A and C) and south-eastern (Fig. 5-1, C), parts of the study area.

In the north-western part of the study area (Fig. 5-2), around the Giza Pyramids in a N.W. - S.E. direction, the offlapping relationship occurs in two stages (Figs 5-2, A and B).

The early stage took place during the deposition of the Giushi facies (Fig. 5-2, A). This facies is completely absent to the N.W. (section 40) but occurs as a thick sequence towards the S.E. direction (section 48).

By the end of Eocene, a latter offlapping stage was developed during the deposition of the younger members of the Middle Mokattam Unit (sections 26 and 61) throughout the study area (fig 5-2, C). This regression of facies continued even during the deposition of the Upper Mokattam Unit (section 61). So the upper part of the Middle Mokattam and the Upper Mokattam Units indicate basin-ward facies migration.

On the other hand, towards the south-eastern part of the study area only the late stages and products of offlap are recorded (Fig. 5-1, C). The upper members of the Middle

Mokattam and the Upper Mokattam Units exist in section 61 and die out towards section 26 in a S.E. direction.

5.2(C) Interpretation.

The above described onlap-offlap relationships can be easily distinguished at the shallow peripheries of the basin of study. The early offlap relationship occurred during the deposition of the Giushi Facies. This was followed by a sequence of onlapping and offlapping units through the deposition of the Middle Mokattam formation and until the end of the Eocene.

The early offlapping relationship is recorded only in the Pyramids area (fig. 5-2,A). This phenomenon may account for the absence of the typical Giushi facies from the Pyramids area due to a progressive migration of that facies seawards. This facies migration is believed to have formed due to an abrupt change in the shelf slope which forced the sediments to slump and advance seaward. Such a change in the shelf gradient may be the result of drastic syndepositional subsidence in the basinal area. Alternatively, the increase in the shelf slope may be due to pulses of syndepositional uplifting in the Abou-Rawash massif, which may have been a positive feature during deposition. Such movements have been suspected by, Said (1962), and Strougo (1979).

The latter onlap-offlap relationships, which are believed to have formed during the deposition of the Middle

Mokattam and younger sediments, could have resulted from marine transgression and regression. These are commonly local phenomena that have nothing to do with absolute changes in sea level. They are believed to be formed due to the progradation of the coastal areas. Syn-tectonic pulses could cause a regional tilting to the basin margins. Consequently, the shelf gradient could possibly be changed. The sea then flooded low-lying areas, resulting in the deposition of a transgressive sequence. This might have occurred in the early depositional stages of the Middle Mokattam facies (Figs. 5-1,B and 5-2,B). On the other hand, in the areas of rapid sedimentation near the mouth of a deep channel distributary, the fan advances seaward and a regressive sequence is deposited. This may also explain the last depositional stages of the Middle Mokattam and up to the end of Eocene sequences (Fig. 5-1,C).

In Fig. (5-2,C), the onlap occurs towards the northwest direction during the deposition of the Middle Mokattam facies is separated from the underlying sedimentary wedge by an angular unconformity. This type of unconformity has been termed angular syntectonic unconformity (Riba, 1976). Riba (1976) and Anadon *et al* (1985) defined this type of unconformity as one that forms adjacent to an uplifting structure and associates with onlap-offlap stratal units. Accordingly, the onlap relation observed in Fig. (5-2,C) is believed to be developed during intervals of decreased uplift of the

adjacent Abou-Rawash complex. On the other hand, the offlapped strata (top of Middle and the Upper Mokattam Units) are believed to be formed during intervals of accelerated uplift of the same adjacent Abou-Rawash unstable shelf of Said, 1962. Several examples of that onlap-offlap relationship which associated with syn-tectonic unconformity, are observed with the outside zonal margins of the studied area. Occurrence of these relations with the sediments of the Northern Nile Valley basin, is considered as stratigraphic evidence for a diachronous tectonic event. These episodes have taken place at the end of Middle Eocene and continued during Late Eocene times.

5.3 BASIN OUTLINE

To outline the basin of deposition and detect its configuration with respect to the topography of the sea bed, a combination of three factors have to be considered. These are; the thickness of the lithostratigraphic units, the nature and distribution of the individual facies and their depositional environment. The thickness distribution of the units studied reveals the shape (or outline) of the sedimentary basin (fig. 5-3). However, this factor alone provides insufficient evidence of the nature of the sea floor topography. Therefore, we have to consider all of the above three factors (see Chapter 7) and relate them to a stratigraphic datum.

The procedure of cross-sectioning the studied basin,

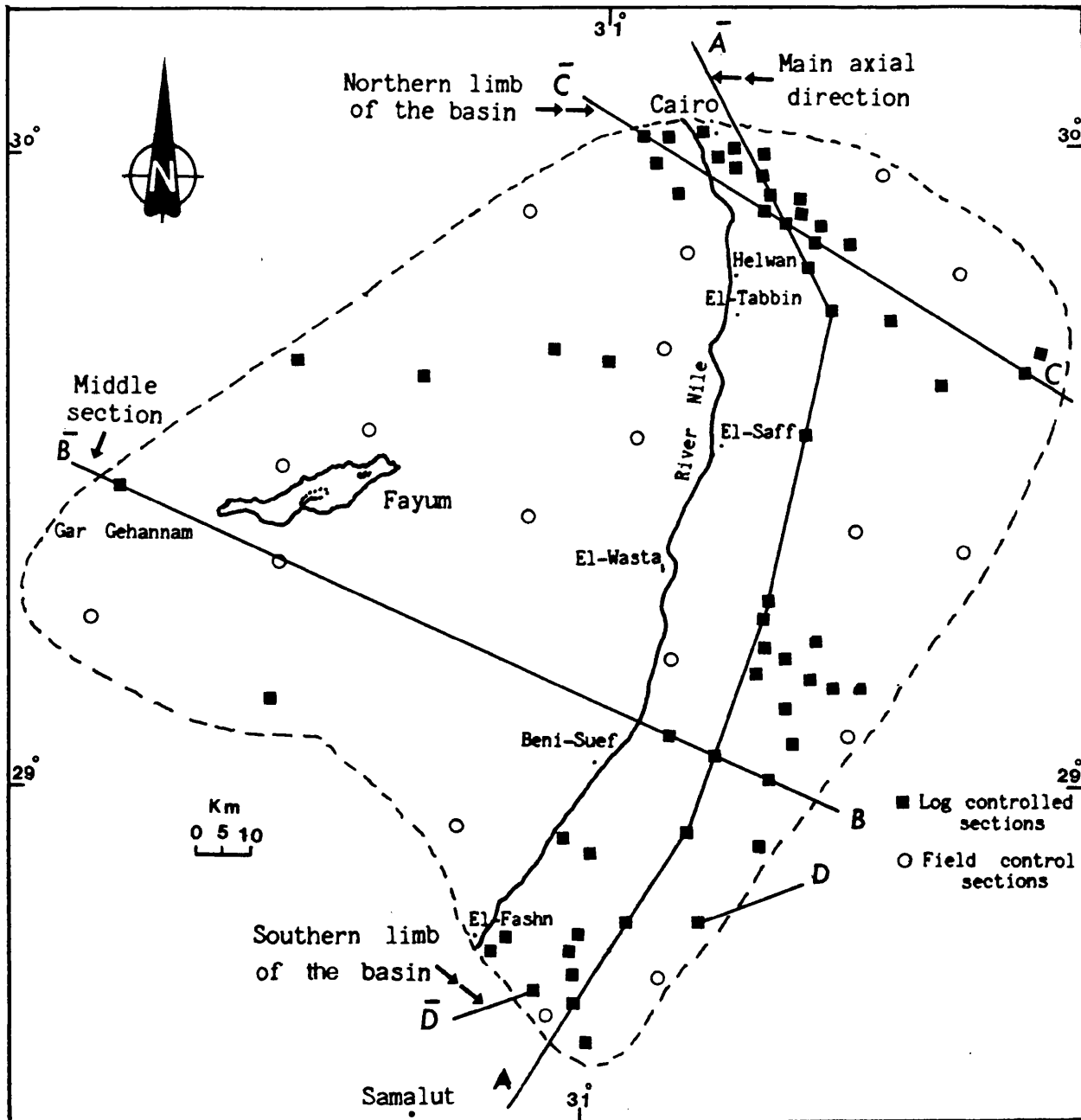


Fig. (5-3): The outline shape of the studied basin of the northern Nile Valley and the Fayum area, Egypt.

is based on establishing a datum which is assumed to be horizontal across the basin at the time of deposition (see 5-4&6). However, the depositional surface represented by this datum may have sloped or undulated. The shape of a datum plane may depend, to some extent, on the purpose for which it is employed. Where, only the correlation of beds is required, the profile of the datum may not be critical and it is usually regarded as horizontal. However, it is essential to know the slope of the datum, at the time of deposition, to define the palaeotopography of the basin floor (Conybeare, 1979). The areal depositional province, throughout the datum will be discussed later (Chapter 6 and 7). The distribution of the abundant carbonate component will also be considered (Chapter 7). A calibration of the chosen datum and the tested factors will result in an understanding of the topography of the basin floor (see Chapter 7).

5.4 DATUM OF CORRELATION

The chosen datum marks the lithological contact between two major rock units, the Lower Mokattam Unit and the overlying Middle Mokattam Unit. This datum has been chosen because it can be easily identified in and followed through most of the field area. It permits a tentative correlation between all the profiles of the northern Nile Valley and the Fayum basin.

Field recognition of that datum in the trough parts of

the study basin around Wadi Hof area, is impractical. Therefore, palaeontological identification was required. That datum is characterized by the occurrence of microbenthonic foraminifera; especially *Bulimina jacksonensis* and *Uvigerina mediterranea*. This datum also marks the top of the lower half of the *Globigerinatheka seminvoluta* (P.15), planktonic foraminifera zone. Furthermore, calcareous nannoplaktonics study confirms that the datum occurs shortly before the top part of the *Chaismolithus oamaruensis*, NP19, zone.

5.5 STRATIGRAPHIC CORRELATIONS

In this section an attempt is made to correlate the different facies of the Middle Mokattam Unit in the northern Nile Valley and the Fayum basin. Weller (1960) defined the correlation of the succession as the establishment of the mutual relationships between various rock units with respect to time. This is necessary before an environmental or basinal synthesis can be carried out.

The stratigraphical correlation scheme for the Middle Mokattam Unit in this study is shown in Fig. 5-4. Profiles are established for the horizontally assumed, chosen datum. The distribution of the different formations which represent the Middle Mokattam Unit throughout the studied basin is given in Fig. 5-5. Correlation is made, for the Middle Mokattam facies, along four different directions (Fig. 5-6). The locations of these directions were

MoKattam	Birket Qarum Formation	Saqqara Formation	Wadi Garawi Formation	Beni Suef Formation
			El-Qurn Formation	
Lower MoKattam	Giushi limestone			

Fig. (5-4): General correlation of the Middle MoKattam Unit.

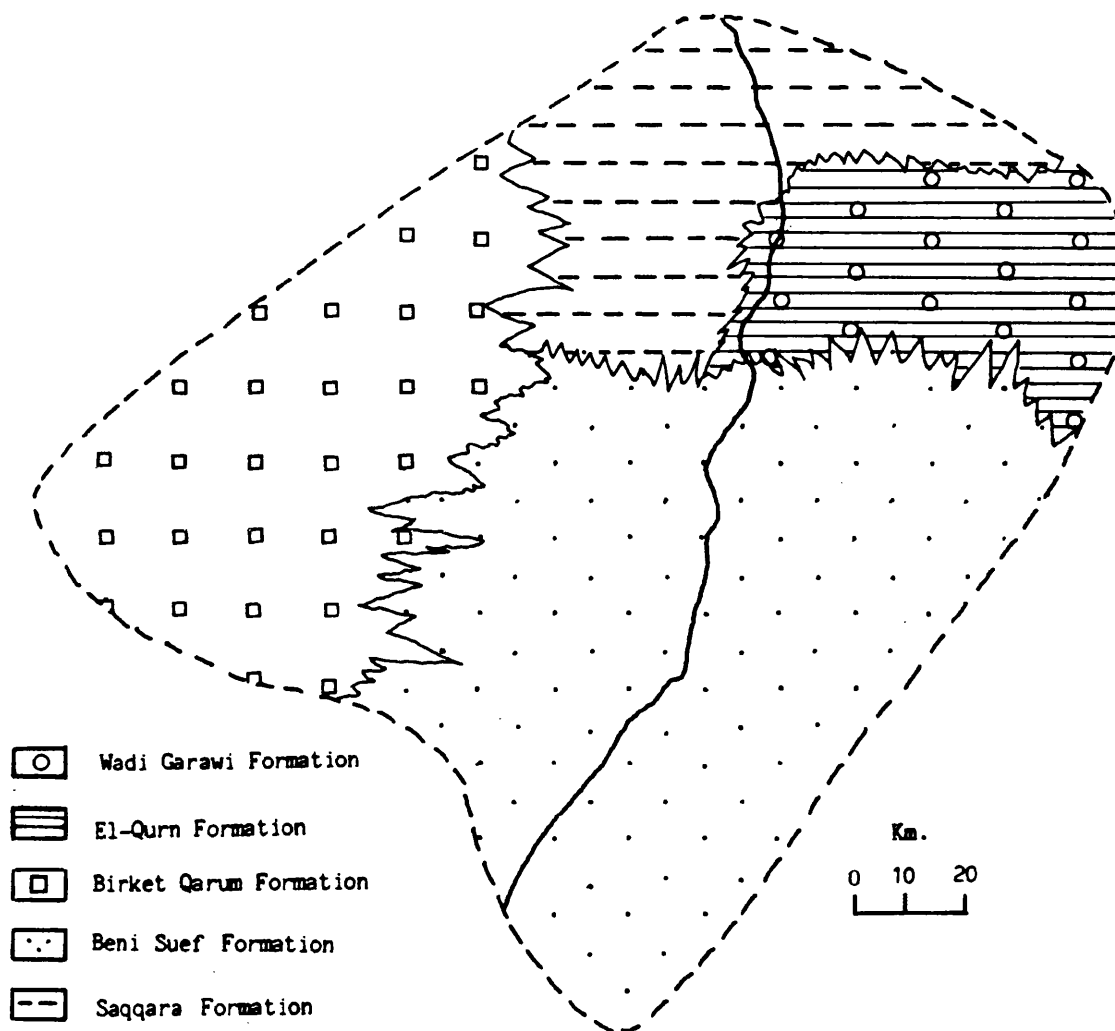


Fig. (5-5): Areal distribution of the different rock formations throughout the Middle MoKattam Unit, Nile Valley and the Fayum basin, Egypt.

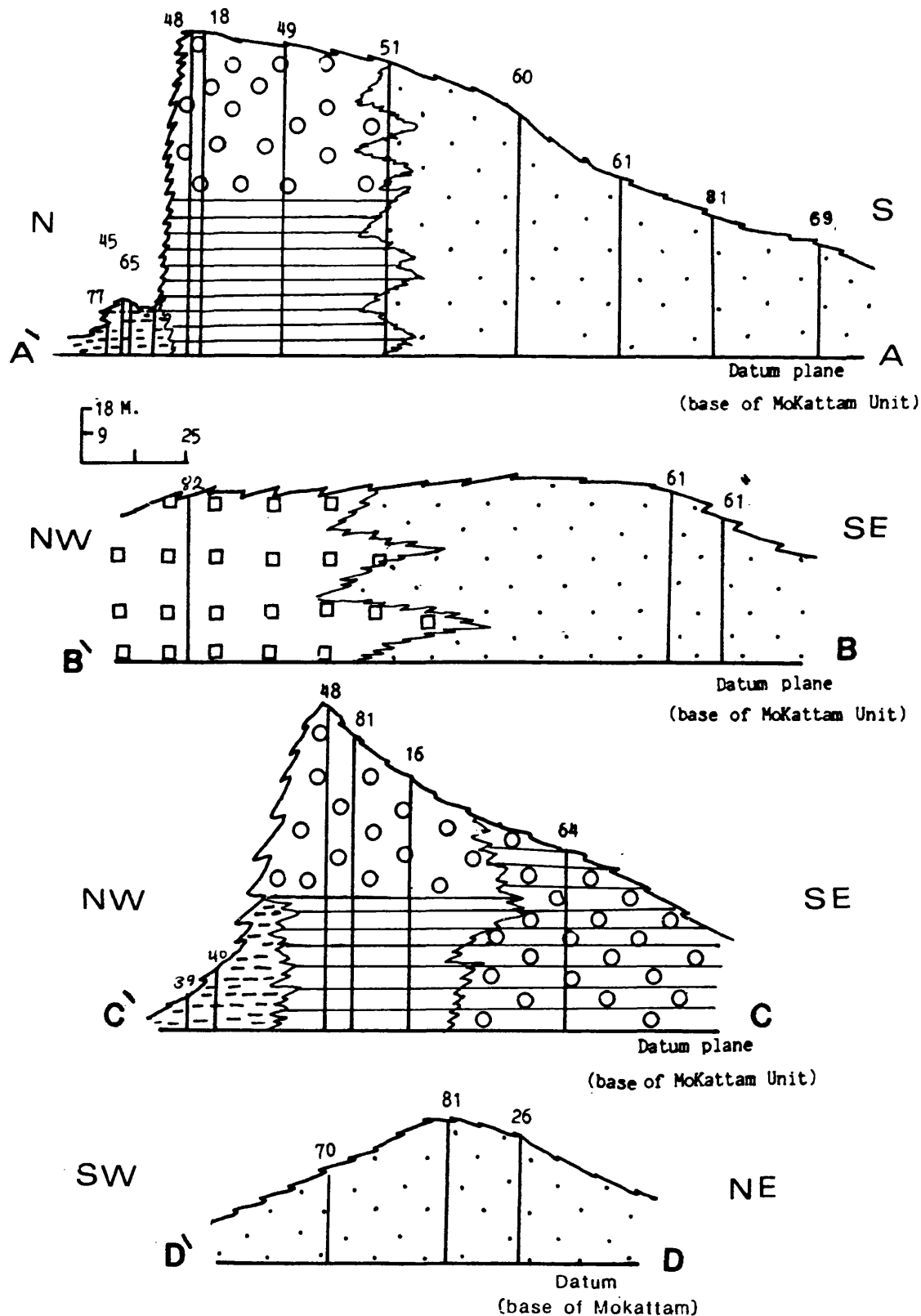


Fig. (5-6): Lithostratigraphic correlation sections throughout the studied basin along A-A'; B-B'; C-C'; and D-D' lines. Profiles are drawn to the established datum reference which supposed to form horizontal plane. (See Fig. 5-5 for key)

carefully chosen to permit an overall correlation and to reflect the basinal aspects of the analysis in the preceding chapters, see Figs. 5-3 and 2-1. The main direction (A-A) represents the basin axis which runs approximately south-north (see Fig. 2-1 for location). The second trend (B-B) represents approximately the middle part of the studied basin in a SE-NW direction. The third correlation is reflected through a SE-NW direction (C-C) for the northern part of the studied basin. The last direction is (D-D) which figures out the southern limb of the basin.

At the northern part of the basin, the Saqqara limestone formation (Hume, 1911 and Said, 1962), of the Middle Mokattam of this study, extends from the western Nile through south of the Giza Pyramids to Gabal Mokattam and the top of East El Maadi sections. In Wadi Hof-east Helwan areas, the Middle Mokattam facies is represented by both the El-Qurn and the Wadi Garawi formations. Both can be distinguished around the Wadi Hof to the east of the El-Tebbin areas, but they mix in one unit farther east.

At the southern parts of the study basin (Figs. 5.5 and 5.6), the Middle Mokattam facies is represented by the Beni Suef formation in the eastern side and around the Nile Valley. The Beni Suef formation extends westwards almost to the Fayum area, where lithologically changes to the Birket Qarun formation. Facies inter-fingering observed on the northern side of wadi Abu Sera area, east El Tebbin,

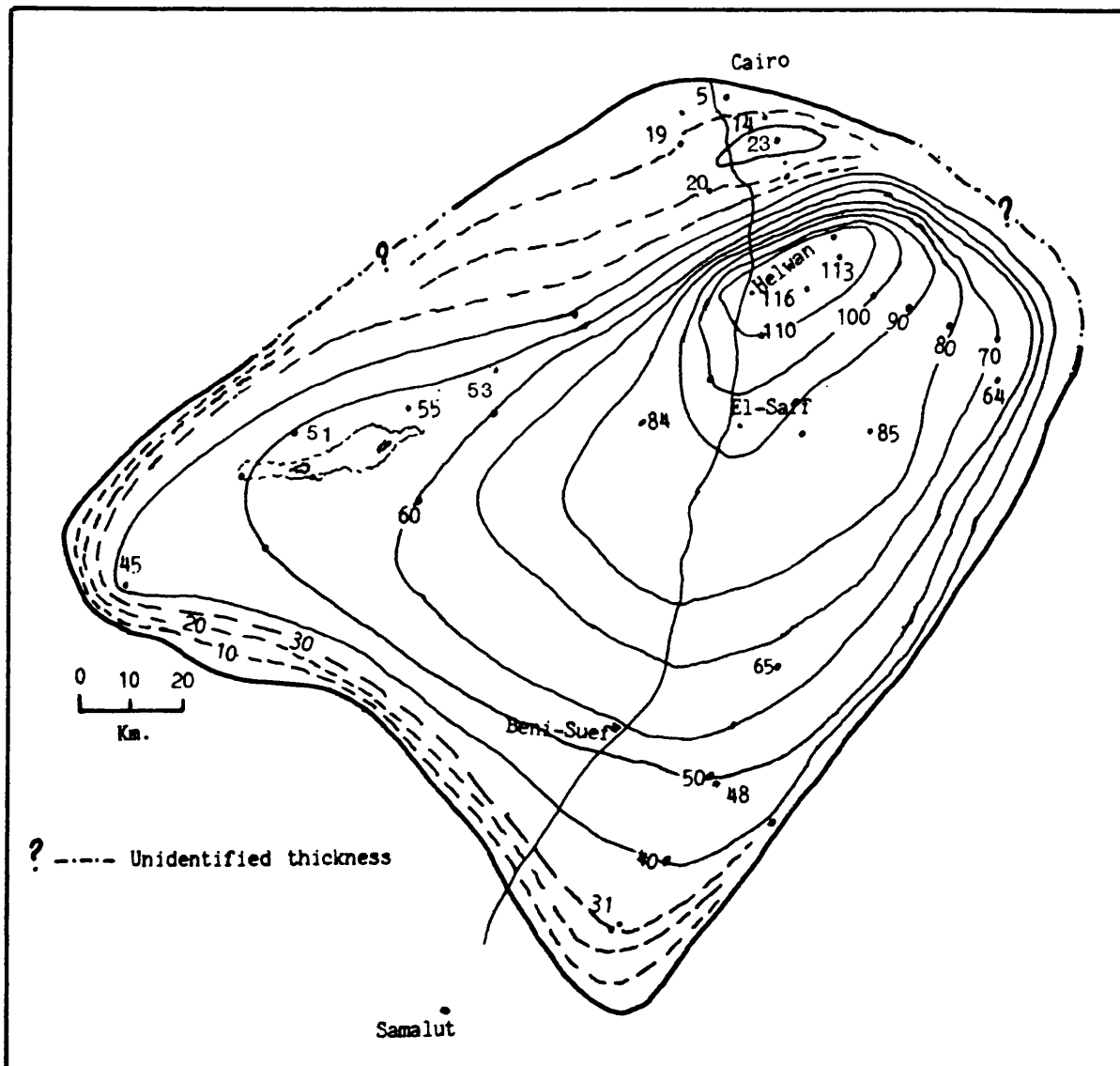


Fig. (5-7): Isopach map of the Middle Mokattam Unit in the Northern Nile Valley and the Fayum Basin, Egypt. Note shape and thickening of sediments towards the trough area of the basin. Contour interval 10 metres.

where the marl facies of the Beni Suef Formations intercalates the El-Qurn facies and wedges out northwards. The Beni Suef Formation thins southwards and is represented (as the Qurn Member only) on top of the Gabal El-Abyad, northern top of Gabal El-Merier, and the top of Wadi El-Aghbag section.

Therefore, from the stratigraphic correlations of the Middle Mokattam Unit it seems likely that the different mentioned formations represent accurate records of contemporaneous chronological facies variations. The isopach map (Fig. 5.7) indicates a marked facies thickening in the central locality of the northern part of the basin. The facies thins again towards the basin perimeter.

In the light of the biostratigraphic zonation, mentioned in the last chapter, it has been suggested that the Middle Mokattam Unit covers a span of the upper part of NP18 to the upper part of NP19 nannoplankton zones (Table 4-8). On this assumption, the total length of time for the deposition of the Middle Mokattam Unit may have been about 1 to 2 million years (following Harland *et al*, 1982; Berggren *et al*, 1985; and Cavalier and Pomerol, 1986).

**FACIES & MICROFACIES
ANALYSIS
AND
THEIR DEPOSITIONAL
ENVIRONMENTS**

CHAPTER SIX

6. FACIES AND MICROFACIES ANALYSIS & THEIR DEPOSITIONAL ENVIRONMENTS

INTRODUCTION

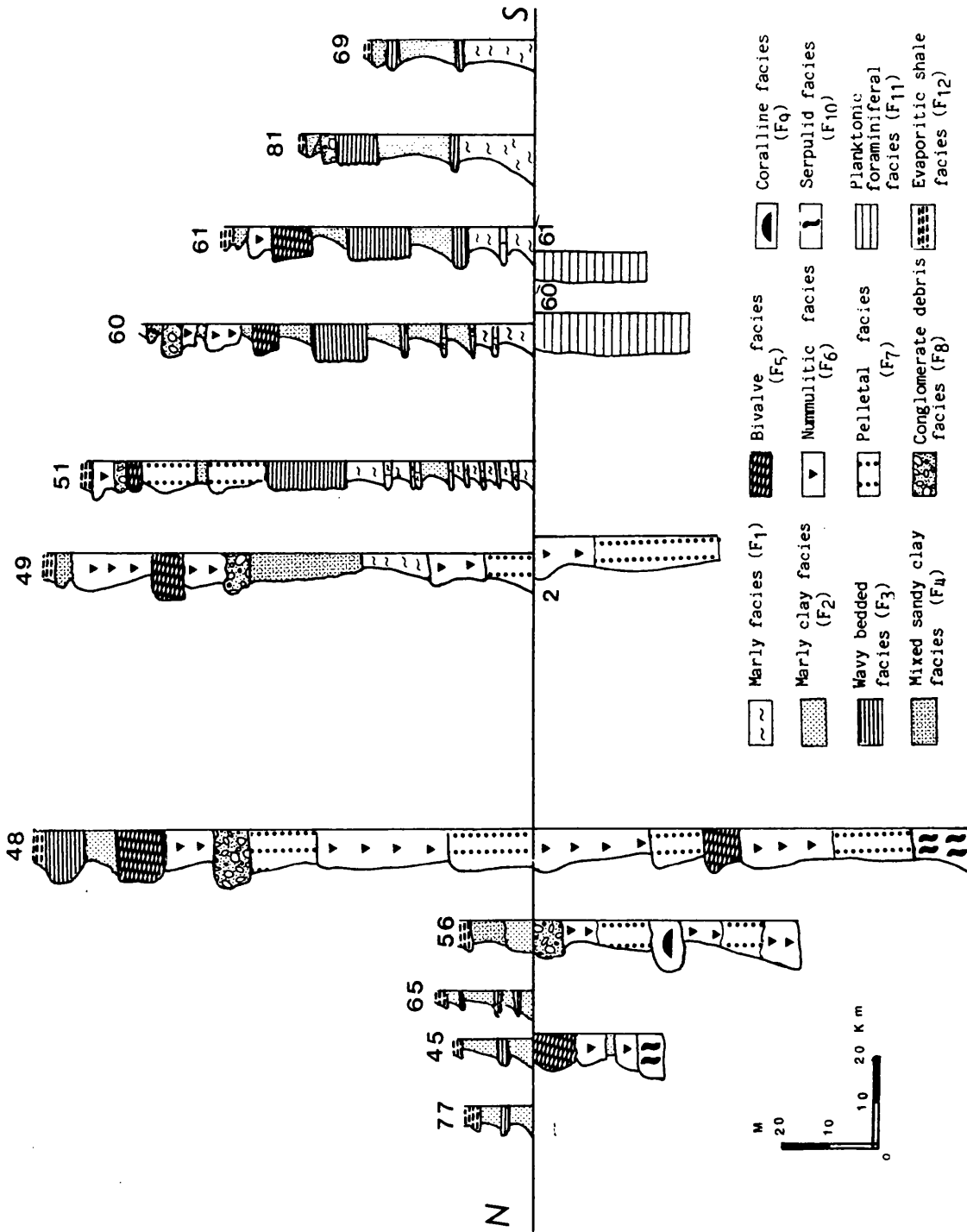
It is common knowledge that most, if not all, strata vary laterally. These variations are used to define facies. The concept of lateral variation in bodies of rock is the facies concept. The Eocene rocks of the northern Nile Valley and the fayum basin, Egypt, are characterised by distinct facies changes.

To understand more clearly the development of the basin and the distribution of the different depositional environments, in the area of study, the carbonate facies and microfacies are studied in detail in this chapter. The facies were defined, in the field, on the basis of colour, bedding, composition, texture, fossils, sedimentary structures and geometry. Each facies is subdivided into subfacies associations or microfacies. Microfacies were defined on the basis of all of the palaeontological and sedimentological criteria which could be distinguished in thin sections, peels and polished slabs. This study involved the detailed point-counting of 941 peels and thin sections representing 23 columnar sections. The percentages of the different grains and matrix components, derived from the point count analysis, were calculated

(Appendix C) plotted on diagrams with the help of a computer program to show their vertical variation (Appendix D). The general approach used in the preparation of these figures has been to keep the individual logs as factual as possible so that they, in effect, serve as basic data summary sheets. The carbonate grain types are, then, assigned to microfacies following the technique mentioned before (Article 2.2.1.4). To name and classify the carbonate microfacies, in this study, the Dunham scheme (1962), as amended by Embry and Klovan (1972) classifications, was used. The classification schemes of Barth *et. al.* (1939) and Mount (1985) were sometimes used for the clay-lime and the mixed siliciclastic carbonate lithologies. The vertical variations of the energy index "EI", of Chilingar *et. al.* (1967) were calculated and also used.

The carbonate types observed in the study area, were assigned (Fig. 6.1) to the following 12 major facies (F1-F12). These facies, in turn, were subdivided into 36 subfacies on the basis of the microfacies analysis (M1F1-M36F12). The aim of this chapter is to outline the description and distribution of these facies and the associated microfacies. One of the main objectives of this study is to interpret the origin of sedimentary facies in terms of sediment supply, sedimentary processes, and depositional environments.

Fig. (6-1): Facies distribution and correlation throughout the northern Nile Valley and the Fayum basin (S-N direction).



6.1 The Marl Facies (F1) (Plate 3-5, A)

6.1.1 Description: The Marl (as a field definition or term) has a distinctive light grey colour. The average thickness of this facies is up to 30 meters thick. It is represented by a cyclic sequence of (3-7 meters) thick segregated soft marl, capped by (relatively thin 0.4-0.8 meters) hard bank of limestone (Fig. 6.2). Above the base of each cycle, grain size decreases upwards, typically from medium sand to fine mud, resulting in a graded bedding. However, due to the well-sorted nature of beds, this grading is often difficult to detect. The marly beds contain bioclastics and are occasionally fossiliferous and highly gypsiferous in places. These have a distinctive surface due to spherical weathering, and fine cross lamination structures are recorded.

The hard limestone bands are of fine grained mudstone with very faint fine-lamination. These beds exhibit soft sediment deformation of a boudinage-like nature, and contain rare fossils. Pelagic bivalval casts, micro-shell debris and plant remains are recorded.

The important carbonate grains, or allochemical constituents which characterize the major marl facies are mainly foraminifera, some bivalves, gastropods, ostracods of both smooth and ornamented types, miliolids, sponge spicules and other unidentified shell fragments. Most of the fauna is of open marine type but some contain a mixed

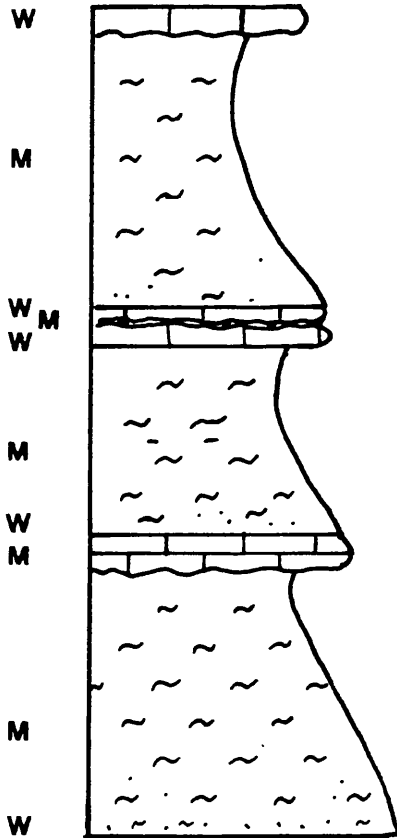
2m.

Depositional texture

Log. graph

Palaeocurrents (readings and directions)

Grading



Marls



Sandy marls



Limestone

W Wackestone

M Mudstone

Fig. (6-2): Log graph of the marly facies indicates normal graded sequences.

reworked population from older sediments. The bioclastic content of the marl facies, show grain size variation from fine sand to very coarse gravel. A few detrital quartz grains of fine silty and sandy sizes are present disseminated within the allochems. These become coarser and more angular in the upper cycles. Lime mudstone and wackestone are the dominant depositional textures for this facies. Geometrically it is represented by a sheet-like body with wedge shaped segregated beds. This marl facies, also, has very sharp conformable contacts with other facies towards the basin centre, whereas it unconformably overlies older sediments in the inner parts (outer frame) of the studied basin.

6.1.2 Distribution

The marl facies comprises most of the lower part of both the Qurn Member of the Beni-Suef Formation and the Birket Qarun Formation of Fayum area. It is recorded mainly in sections, 69, 81, 61, 60, 51, 49, 65, 45, 77, 40, and 82 (Fig. 6.2). At Gabal Tarbul Abu Khashirat, the facies is well represented where it increases in thickness towards the northern and western parts of the studied area. It thins towards the west and northwest in Fayum and Gabal Qibli El-Ahram. The facies also decreases in thickness towards the south and south-east in Gabal El Mashash and Gabal Abyad where it is represented by a small tongue. Towards the east, these facies thin again east

Gabal Tarboul Abou-Khashirat then disappeared completely along Wadi El-Aghbig.

6.1.3 Microfacies Associations

The following microfacies associations (Plate 6-1) are recognized in the studied basin:

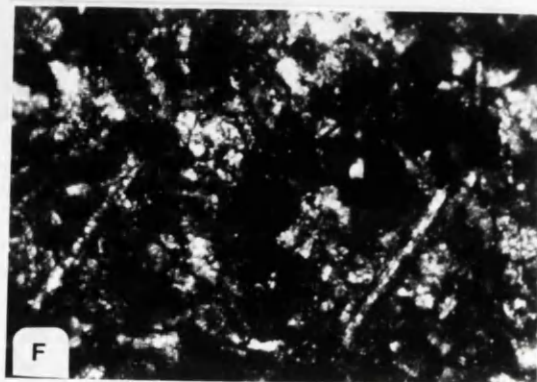
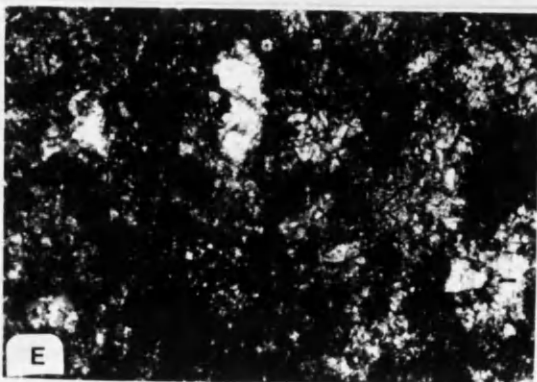
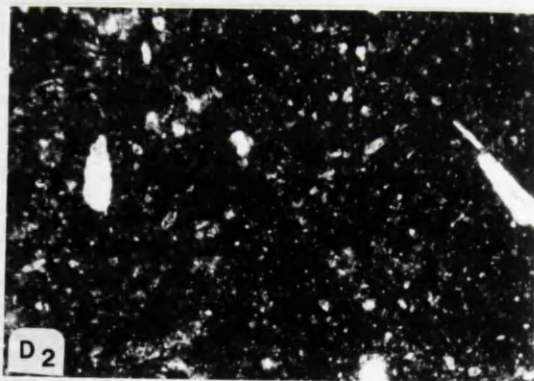
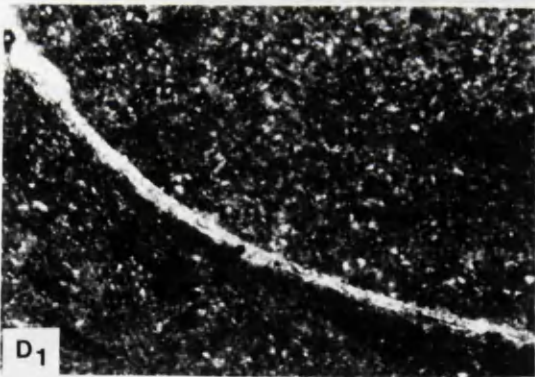
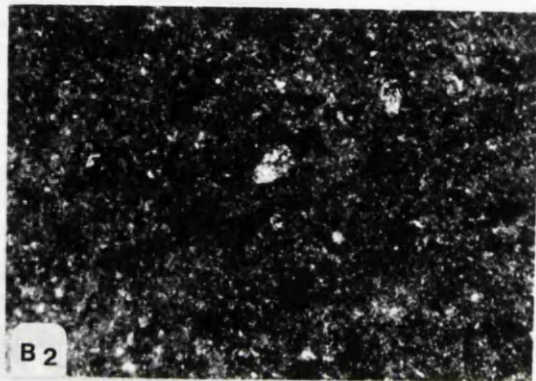
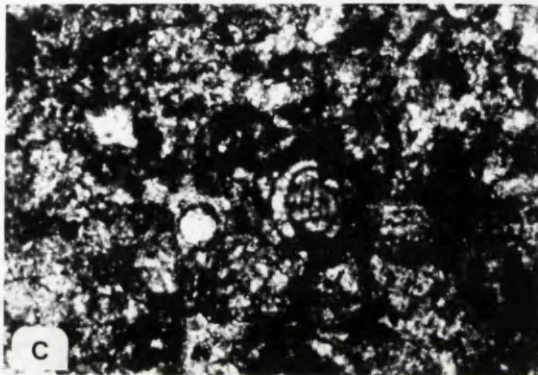
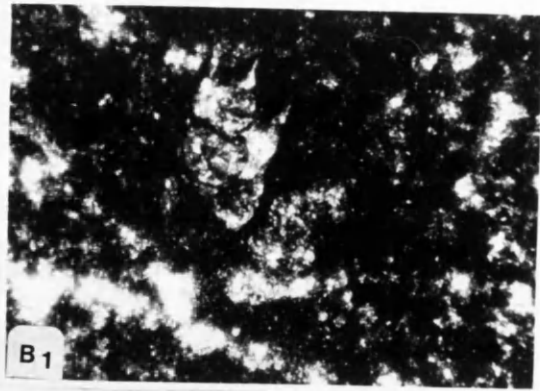
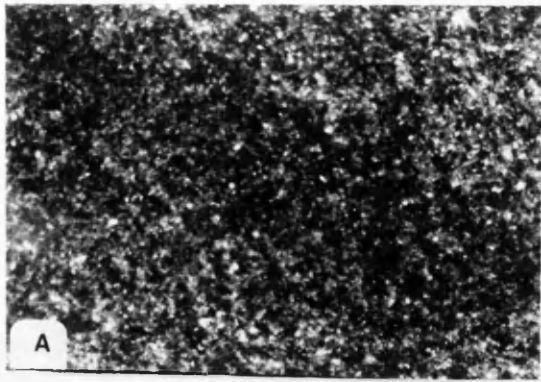
1. Marly lime mudstone microfacies (M1F1)
2. Marl microforaminiferal lime-mudstone microfacies (M2F1)
3. Marl miliolid bioclastic lime-wackestone microfacies (M3F1)
4. Marly foraminiferal molluscan lime-wackestone microfacies (M4F1)
5. Marly ostracod-microforam lime-wackestone microfacies (M5F1)
6. Marl spiculitic lime-wackestone microfacies (M6F1)

6.1.3.1 Marly lime mudstone microfacies (M1F1)

This microfacies (Plate 6-1A) is very distinctive. It appears in Gabal Hamret Shaibun and is represented by a unit 80cm thick. It is also represented at the base of Gabal Tarbul Abu-Khashirat (up to 60cm thick). This microfacies extends northwards to El-Saff and Wadi Hoff areas. In the Fayum area, the microfacies reaches up to 150cm in thickness. Geometrically, it occurs as very hard, yellowish white, massive thin beds interbedded with pale greyish green sheets of thinly laminated marls. The main constituents are |reworked *Globigerina* species (1-3%)

- Plate (6-1) : (Marl microfacies associations "F₁")
- A - Marly lime mudstone microfacies (M1) X20.
 - B - Marl microforaminiferal mudstone microfacies (M2).
 - (1- with Hantaknina sp., Late Eocene planktonic foraminifera, X50.
 - 2- with microforam tests, X20.)
 - C - Marl miliolid bioclastic wackeston microfacies (M3) X80.
 - D - Marly foraminiferal molluscan wackestone microfacies (M4)
 - (1- with Bivalves,
 - 2- with microforaminifera and molluscan debris; both 1&2 are X20.)
 - E - Marly ostracod-microforam wackestone microfacies (M5) X80.
 - F - Marl spiculitic wackeston microfacies (M6).., siliceous(bi & triaxons) sponge spicules.X80.

PLATE 6-1



biserial benthonic foraminifera (1-3%), bivalves (up to 2%), besides rare detrital quartz grains (up to 1.3%), embedded in marly micrite (Over 90%).

The main diagenetic features are the staining of the ground mass by iron oxides and the partial recrystallization of the micrite matrix into sparite. The marly mudstone microfacies probably reflects gently agitated water with an energy index of (EI)=1. The absence of abraded fine debris in this microfacies (M1F1) could indicate the winnowing by bottom turbulence. The nature of this microfacies suggests deep depositional environment (Fig. 6-3).

This microfacies may have sharp or gradational boundaries with M2F1 and M4F1 microfacies.

6.1.3.2 Marl microforaminiferal mudstone microfacies (M2F1)

This microfacies (Plate 6-1B) is mainly exposed at Wadi Bayad, Wadi Abu Treifi, Wadi Lishyab, Wadi Matin and Wadi Abu Khashirat. Geometrically, this microfacies is represented by thin laminated or well segregated beds. The main constituents are very fine grained marl matrix (more than 90%), benthonic foraminifera (1-6%) of well preserved forms mainly *Bulimina*, *Bolivina*, *Uvigerina*, *Robulus* and *Textularia* species, reworked ill-preserved planktonics (1-4%) besides few bivalves, black organic remains, and some ostracods (up to 1%). The foraminiferal

content suggests a deep depositional environment (Hendrix, 1958 and Moore, 1964). The components of this microfacies are affected by some silica replacement. The microfacies reflects deposition in gently agitated water with an energy index of $(EI)=1$. This could also be demonstrated by the fine marl matrix and the presence of thin lamination. The occurrence of the bioclastic debris reflects a decrease in turbulence of bottom waters with depth, which is believed to be the likely controlling factor in deposition of this microfacies.

Laterally this microfacies (M2F1) changes to marly lime mudstone microfacies (M1F1). It is believed to have a gradational boundary with this microfacies. The above characters suggest a probable deep basinal subenvironment (Fig. 6-3).

6.1.3.3 Marly miliolid bioclastic lime-wackestone microfacies (M3F1)

This microfacies (Plate 6-1C) is well represented at Gabal Hamret Shaibun, Tarbul, Tarbul Abu Khashirate and Gabal Abyad sections, as a sheet 3m thick which increases in thickness towards the south western parts of the studied basin. In the southeastern part it is represented by tongues wedging out towards the northeast and north direction.

The main constituents are planktonic foraminifera (2%), benthonic foraminifera (3%), miliolids (2-3%),

ostracods (1-2%), a few bivalves and gastropods (2%), and a few molluscan fragments (1-2%) besides a few detrital quartz grains, all are embedded in a marl matrix.

This microfacies reflects deposition in gently agitated water with an energy index of $(EI)=1$. The grain-matrix characters point to a quiet, landwards subenvironment. Such depositional conditions initially prevailed over the whole outer deep shelf and predominated throughout carbonate deposition in the southern landward area (Fig. 6.3). The microfacies has a gradational, upper and lower boundaries.

6.1.3.4 Marly foraminiferal molluscan lime-wackestone
microfacies (M4F1)

This microfacies (Plate 6-1D) occurs in beds that are traceable for hundreds of meters. It is met within sections 69, 81, 61, 60, 51, 49, 45, 77 and 82. It occurs as yellowish brown or greyish brown, thinly cross-laminated highly gypsiferous and bioturbated beds. The main constituents are molluscan shells (bivalves up to 6%, gastropods up to 3%), molluscan debris (6-10%), benthonic foraminifera (3-6%), planktonic foraminifera (2-4%), fine detrital quartz grains (about 3%) and all are embedded in marl (20-80%). Ferrugination is a major, possibly early, diagenetic feature which characterizes this microfacies. The occurrence of ferric oxides and the red colouration and the abundant benthos, indicates an oxygenated

environment. Gastropods, some bivalves and molluscan debris are derived from near shore environments.

The microfacies reflects deposition in water with energies ranging between gently agitated and intermittently agitated with an energy index (EI) of 1-2. That could lead us to assume that a lowering in the sea level was responsible for the deposition of this microfacies (Fig. 6-3).

The rocks of this microfacies are overlain by the marly miliolid bioclastic wackestone microfacies. Both are associated in a cyclic pattern.

6.1.3.5 Marly ostracod microforam lime-wackestone
microfacies (M5F1)

This microfacies (Plate 6-1, E) is characterized by its greyish green colour. This colour changes upwards to grey in some sections and has a range of weathered colours. It is well represented at sections 61, 60, 49, and 51 as sheets of greyish green, laminated calcareous beds having a shaley appearance on the weathered surfaces. Its thickness reaches up to 5.5 meters and units of this microfacies intercalate with harder massive tongues of the marly foraminiferal molluscan wackestone microfacies (M4F1). The microfacies thickness generally decreases towards section 61 (southwards), where it is represented by only 0.5 meters. The main components are: benthonic forams (20%), planktonic forams (7%), ostracods are

represented by smooth types of deeper, calmer water (Gall, 1983). The main diagenetic feature is represented by the partial replacement of the groundmass and ostracod tests by silica. The microfacies is highly bioturbated. The faunal content reflects an intermittently agitated depositional environment with an energy index (EI) of 2. The microfacies characters reveal a transitional phase between the outer (seaward) and inner (landward) subenvironments of the marly facies recorded throughout the studied area (Fig. 6-3).

6.1.3.6 Marl spiculitic lime-wackestone microfacies

(M6F1)

This microfacies (Plate 6-1F) is represented at Gabal Tarbul and Tarbul Abu Khashirat by a thickness of about 3 meters. The microfacies extends north to El-Saff area, where it is represented by beds of 1.2 metre which are repeated twice at different levels. It is interbedded with the microformamiferal marl mudstone microfacies (M2F1) and is capped by marly lime mudstone microfacies (M1F1) or massive cross laminated marls. The main constituents are calcareous sponge spicules (up to 4%) containing mono and biaxonal very fine spicules, shell fragments (up to 4.5%), very small nummulites (about 2%), and very fine detrital quartz (up to 4%). These components are embedded in marly lime-mud (up to 85%).

The microfacies reflects deposition in gently

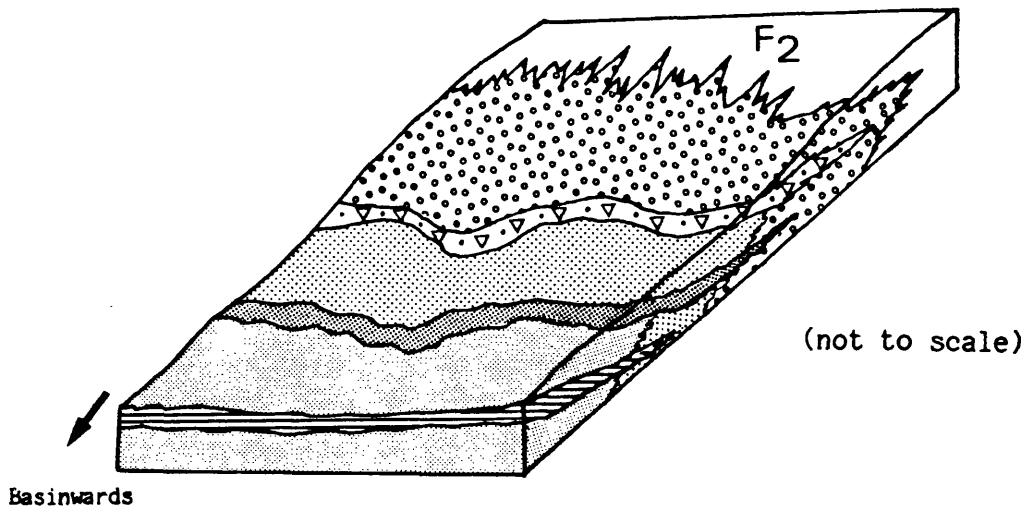
agitated to slightly agitated water with an energy index of $(EI) = 1-3$. Spicules accumulated below wave base in quiet water and occur in conditions of normal marine salinity, as is also believed by Wilson (1975). The microfacies could reveal that their spicules were a product of a reworked pelagic accumulation in the deeper troughs of the shelf margin (fig. 6-3). This deep water probably had sufficient current to orient the spicules but not enough to winnow the micrite and calcisiltite.

6.1.4 Depositional Environment of the Marl Facies

The above data and its associated microfacies suggest rapid deposition by suspended sediment fall-out on a deep wide shelf marginal to a deeper basin, as that described by Wilson (1975). Smith (1974) attributes similar facies to deposition within a normal marine environment. This environment (Fig 6-3) could be formed at the top of a carbonate producing homoclinal ramp (as suggested by Read, 1985).

The unconformable occurrence of the marl facies observed in the basin-outflanking successions, suggests deposition in a transgressive sea conditions. These conditions likely, demonstrate the facies divergent recorded in the lower part of the facies sediments (Fig. 6.4A).

The thin lamination and the small scale cross lamination suggest that this marl facies deposited in an






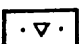

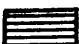
-  Marly lime mudstone microfacies (M₁F₁)
-  Marl. microforaminiferal mudstone microfacies (M₂F₁)
-  Marl miliolid bioclastic wackestone microfacies (M₃F₁)
-  Marl foraminiferal molluscan wackestone microfacies (M₄F₁)
-  Marly ostracod microforam wackestone microfacies (M₅F₁)
-  Marl spiculitic wackestone microfacies (M₆F₁)
- F2** Marly clay facies

Fig. (6-3): Schematic representation of sediment microfacies distribution of facies (F₁) on the deep shelf margin of northern Nile Valley basin.

environment with a quiet water energy. This is also demonstrated from the calculated energy indices of the associated microfacies and from the occurrence of the fine marl matrix. The producing environment is generally below wave base and barely at or just above oxygen level (Wilson, 1975). The fining-upwards sequence is interpreted to reflect waning flow velocities (Reineck and Singh, 1980). Sediment was derived from nearshore environments, as indicated by the presence of a transported benthonic macrofauna and plant remains. All the fine bioclastic detritus, associated with this facies, are believed to have been derived from adjacent shallow shelves. These fine debris were probably provided as a result of abrasion and grain breakage (Bathurst, 1970). Winnowing by bottom turbulence is demonstrated by the absence of abraded fine debris. Microbenthonic foraminifera, ostracods, and some bivalves, are autochthonous with this facies. The abundance occurrence of *Bullimina*, *Bolivina*, *Uvigerina*, and smooth ostracods within the faunal community reflect deeper water, probably more than 150 meters, as has been recorded by Murray (1973). The distribution of the different recorded microfacies associations on the ramp itself (Fig. 6-3) is believed to represent subenvironmental phases. The sequential occurrence of microfacies, within this depositional environment, may suggest an oscillation in the sea level during the time of deposition of the major

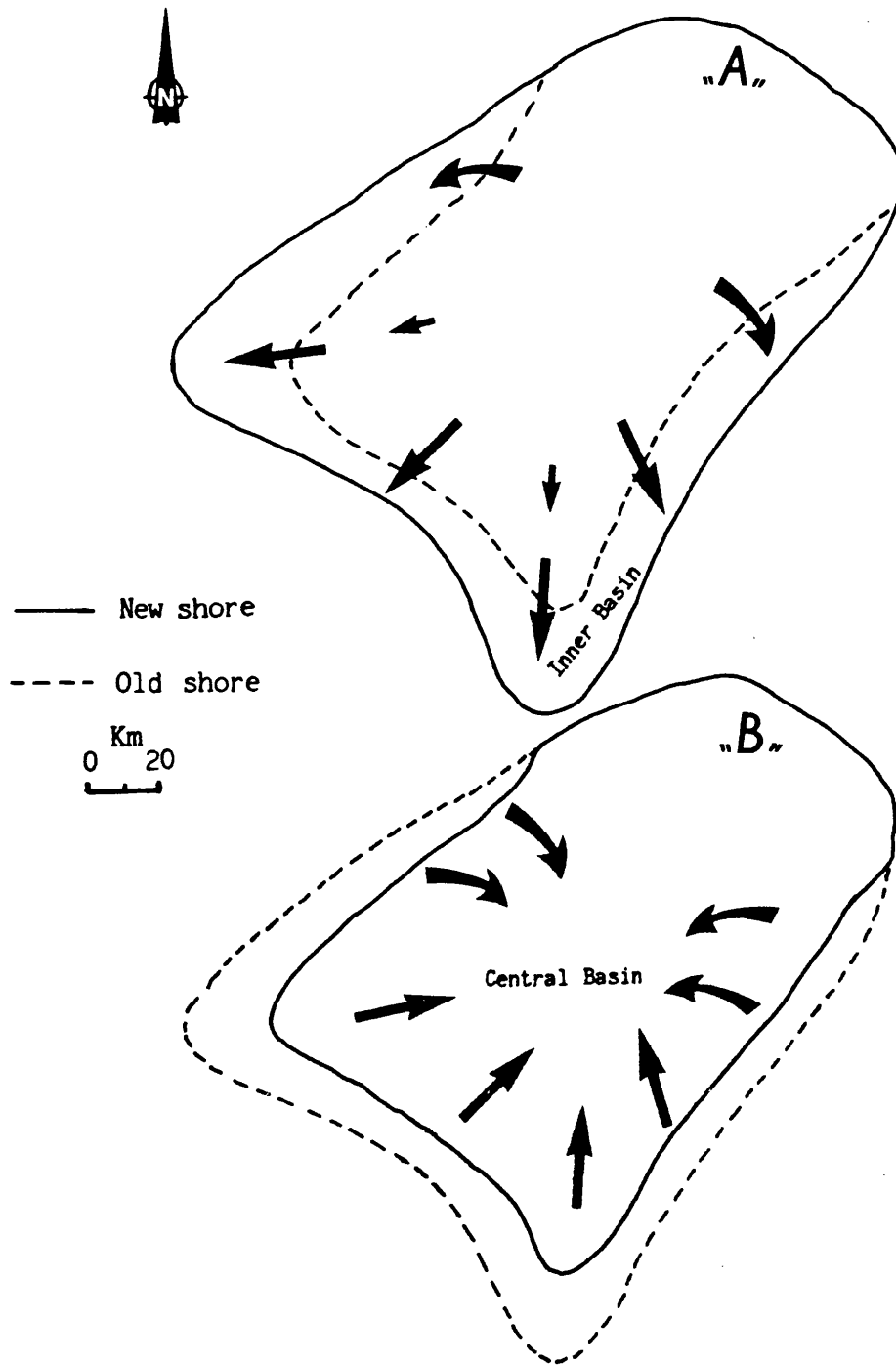


Fig. (6-4): Diagrammatic representation of the marl facies (F_1) shore line:-

- A. Divergent start of the Marl Facies sea to flood landward over new areas.
- B. Convergent end of the Marl facies shore line.

facies. This oscillation may explain the cyclic pattern of the marl limestone observed (Fig. 6-2). However, the rate of oscillation is not likely to fluctuate rapidly over the generally relatively short time represented by this facies, and would also contradict the global rising of the sea through the Late Eocene (Vail *et al*, 1977). Seismically-triggered pulses are a second possibility. The marl beds could, then, represent the deepening episodes of the basin while the limestone is the product of the quiescent intervals of these pulses. The soft sediment deformation and the boudinage-nature of the hard limestone beds within the marl facies, appears to be the result of a temporary non-completed slumping of unconsolidated sediments. The fact that this facies has the following characters: (1) it occurs on top of both a slump-scarred horizon (in the outer shelf) and unconformity surface (in the inner shelf), and (2) it exists as a lateral equivalent to basinal facies (northwards) full of gravity slump and glide blocks. All of which are convincing evidence of tectonic instability. Therefore, this evidence may suggest that seismically-triggered pulses are the more likely origin of cyclicity. Consequently a periodic high clay input into the carbonate-dominated environment probably is the most common mechanism to explain the occurrence of thin limestone layers alternating with thick marl beds (Einsele, 1982). Similar marl-limestone sequences were

thought to be formed through high-energy tectonic events in the Albian of France (Gebhard, 1982).

The marl facies may record a regressional event during the deposition of the upper part of the sequence. This could be demonstrated from the angularity and coarsening of the detrital quartz in the upper layers of the facies. This regression could arouse the shore facies convergence recorded (Fig. 6-4,B) in the top part of the marl facies and the upper sequences.

It is important to mention here, that local sediments belong to this marl facies, east of Beni Suef area, were described as basinal marginal marls (Abdou-Soliman, 1980).

6.2 Marly Clay Facies (F2)

6.2.1 Description: This facies is characterized by rocks with a grey greenish or olive grey yellowish colour and has a range of weathered colours (Plate 6-2,E). The thickness of this major facies is about 20 meters thick. It also has a distinctive blocky character both in weathered and fresh exposures. The facies is often silty and very rarely contains thin siltstone interbeds. It is highly burrowed and locally possesses a mottled appearance perhaps due to bioturbation. This facies contains terrigenous clastic constituents ranging in size from silty to sandy size and even more (up to 7cm long). The biogenic contents of this facies are mainly ostracods,

microbenthonic foraminifera, miliolids and molluscs. The facies also contains nannoplankton. The beds of this facies wedge out northwards. The facies sometimes has gradational or sharp boundaries with the marl facies (F1) and the siliciclastic carbonate facies (F3).

6.2.2 Distribution

The marly clay facies is well represented in sections 69, 81, 26, 61 and 61. The main occurrence of the carbonates of this facies is recorded in the southern parts of the studied basin. It grades laterally in the northern sections with the previous marl facies (F1). It, also, forms most of the Qurn member of the Beni Suef Formation, in the southern and southeastern parts of the studied basin. In the Cairo area, the rocks of this facies occur in one or two levels in sections 45, 44, 65 and top of section 56, all of which belong to the Saqqara formation.

6.2.3 Microfacies Associations

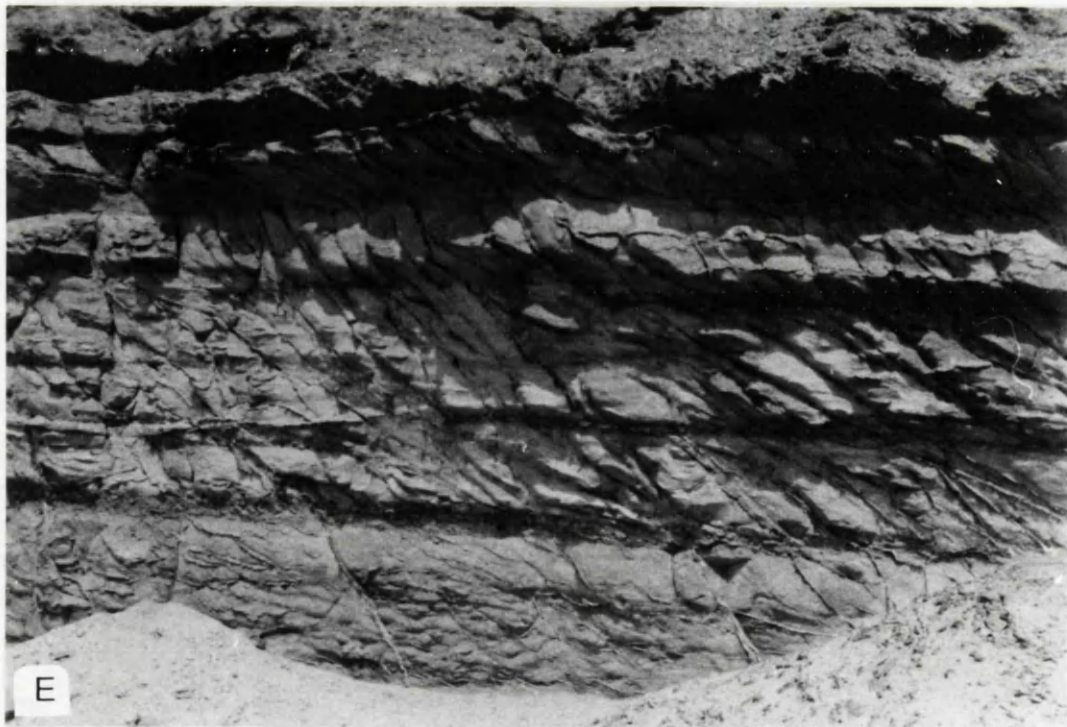
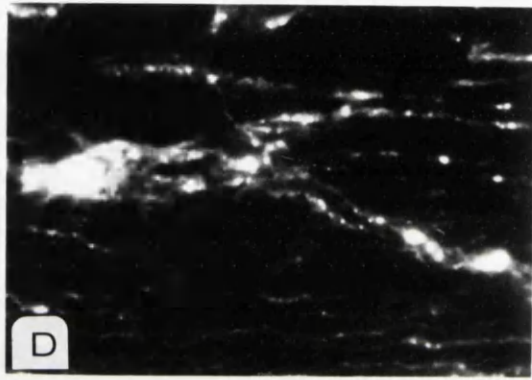
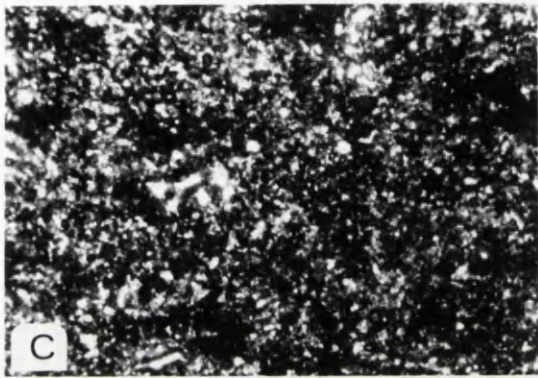
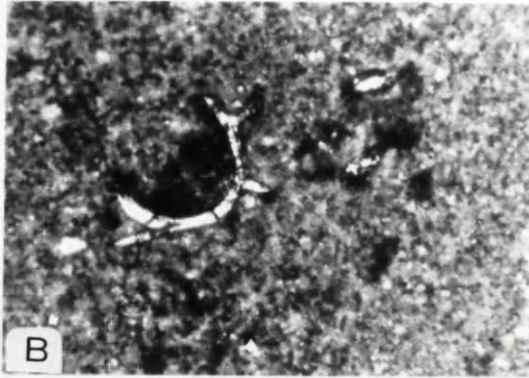
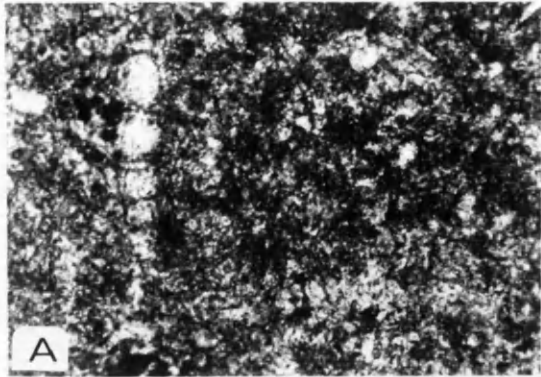
The following sub facies (Plate 6-2), are recognized as associations within the marly clay facies:

1. Marly clay microforam lime-wackestone microfacies (M7F2).
2. Marly clay molluscan lime-wackestone microfacies (M8F2).
3. Marly clay clastic lime-wackestone microfacies (M9F2).
4. Calcareous shale microfacies (M10F2).

Plat (6-2) : (Marly clay microfacies "F2")

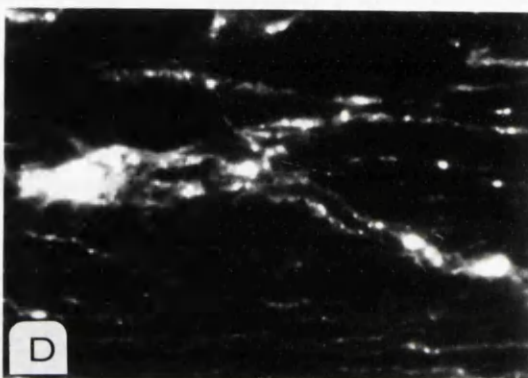
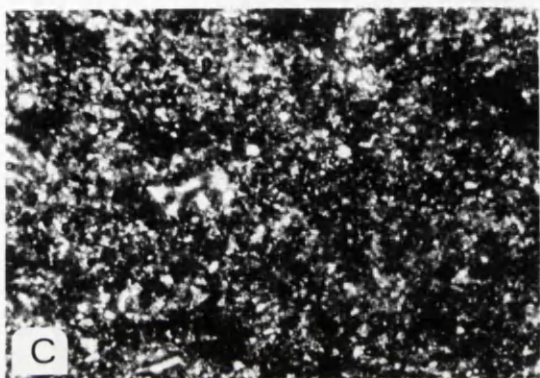
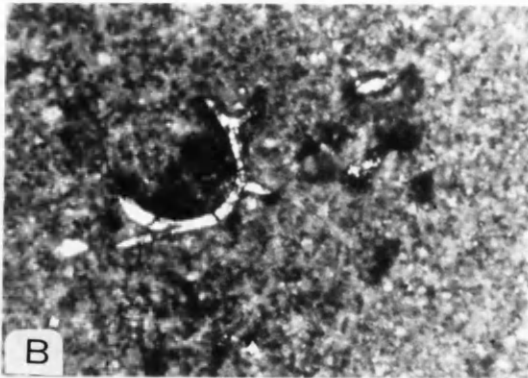
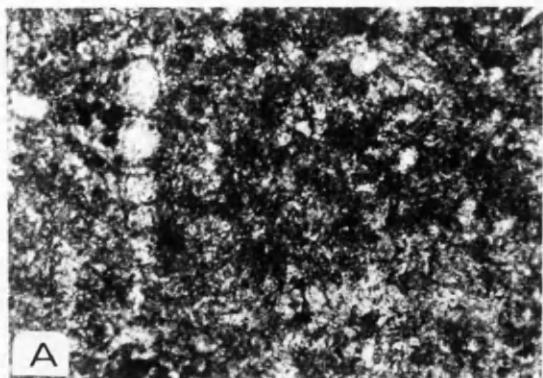
- A - Marly clay microforam wackestone microfacies
(M7) X80.
- B - Marly clay molluscan wackestone microfacies
(M8) X25.
- C - Marly clay clastic wackestone microfacies (M9) X32.
- D - Calcareous shale microfacies (M10) X20.
- E - Photograph of the marly clay facies outcrop
at Gabal El Maskara, East of the Helwan area.

PLATE 6-2



Plat (6-2) : (Marly clay microfacies "F2")

- A - Marly clay microforam wackestone microfacies
(M7) X80.
- B - Marly clay molluscan wackestone microfacies
(M8) X25.
- C - Marly clay clastic wackestone microfacies (M9) X32.
- D - Calcareous shale microfacies (M10) X20.
- E - Photograph of the marly clay facies outcrop
at Gabal El Maskara, East of the Helwan area.



6.2.3.1 Marly Clay Microforam Lime-Wackestone Microfacies

(M7F2)

The foraminiferal marly clay wackestone microfacies (Plate 6-2A) is represented at Gabal Hamret Shaibun, Gabal Tarbul, Gabal-El-Mashash, along Wadi El-Arhab, and as sheets as well as tongues capping Gabal Abyad. It is represented by moderate hardness (fresh surface) to soft (weathered surface), fine grained succession of about 50 to 60cm thick. The main constituents are micro-benthonic forams (11-20%), reworked planktonic foraminifera (up to 8%) and pelecypods of pelagic type (2 to 3%), of low diversity. All are embedded in a marly clay matrix (about 72-85%). Very rare silt sized detrital quartz grains are represented. The main diagenetic features affecting the ground mass are furrugination, pyritization, and gypsification.

This microfacies reflects deposition in intermittently agitated to slightly agitated water with energy index of (EI)=2-3. The characteristic oxidized colour, and generally lower fossil diversity are believed to characterize lower platform margin subenvironment to this microfacies. The micro-pelagic (floating) bivalves and the reworked faunal assemblage could be a useful environmental indicator. As Van Straaten (1971) indicates that the previous phenomenon could be originated during gales, where the water rises well above the mean high tide level and consequently all of

these floated shells were washed over the shallow surfaces. This assumption is highly supported by the high occurrence of broken shells associated with that kind of facies, and also from their occurrence in a landward wedging-out beds over a distance of only a few meters. That mode of formation seems to be in concord with the observed onlap or the transgressive accumulation nature of that microfacies (Fig. 6-5).

6.2.3.2 Marly Clay Molluscan Lime-Wackestone Microfacies

(M8F2)

This microfacies (Plate 6-2B) is shale like when weathered, and is olive grey in colour. This may change upward to grey or tan and red. The thickness of the carbonate assigned to this microfacies reaches up to 1.6 meters. It is well represented in Gabal Hamret Shaibun, Gabal Tarbul, Gabal Tarbul Abu-Khashirat, Wadi El-Aghbig, Wadi El-Arhab, small hillocks along Wadi Sannure, top of Gabal Abyad (east Fashn) and Gabal Qibli El-Ahram.

The microfacies is often silty and very rarely contains thin siltstone interbeds. The main components of this microfacies are bivalves (5-8%), benthonic microforaminifera (2-3%) ostracods (1-2%) and bioclastis (up to 4%). The constituents of this microfacies are surrounded by a marly clay matrix. The upper and lower boundaries of this microfacies are gradational with the other microfacies.

The above carbonate assemblage probably reflect a gently agitated depositional environment as indicated from the calculated energy index of $\langle EI \rangle = 1$. The lack of primary sedimentary structures and the homogenized state of the microfacies may be due to bioturbation. As suggested by Ziegler (1972), the faunal content of this microfacies indicates a probable water depth from 70-80 meters. The sheet-like (large scale) geometry of that microfacies, suggests a flat sub-depositional basin of wide areal extent. It is therefore suggested that the microfacies could be formed in a moderately deep platform subenvironment (Fig. 6-5).

6.2.3.3. Marly Clay Clastic Lime-Wackestone Microfacies

(M9F2)

This microfacies (Plate 6-2,C) forms beds changing in thickness from 6 meters at Gabal Abyad to 28 meters at Gabal Um-Rakaba in Wadi Sannure. The colour of this microfacies is light grey or yellowish green to grey green. It has a distinctive blocky character both in weathered and fresh exposures with a generally shaley appearance. Cross lamination is common, and locally the microfacies appears mottled. The main constituents are benthonic microforaminifera (up to 2%), fossil fragments (about 4%), micro-molluscs (3%) and some transported planktonic foraminifera. The components also include about 9% of sandy clastic detritus and are embedded in a calcisiltite matrix mixed with argillaceous components. The benthonic

foraminifera are represented in this microfacies by species of *Nodosaria*, *Marginulina* together with the arenaceous forams. All these foraminiferal assemblage may suggest shallow depositional environment (Moore *et al*, 1952, Hendrix, 1958 and Moore, 1964). The benthonic forams at Gabal El Mashash samples are found coated with iron oxides, which are possibly due to the continuous solution and precipitation process within the chemical gradient that exists near the sediment-water interfaced (Price, 1967; Garrison and Fischer, 1969; and Morgenstein, 1973). At Gabal El-Ahram, the microfacies has a nodular character, which may indicate a near shore transported source.

The microfacies usually has a gradational upper contact with the calcareous shale microfacies (M10F2) and a sharp lower contact with the marl Facies (F1). The sediment of this microfacies is believed to be formed in gently agitated water with an energy index of (EI)=1. Therefore the nature of this microfacies suggests deposition within an upper platform margin-slope subenvironment (Fig. 6-5).

6.2.3.4 Calcareous shale microfacies (M10F2)

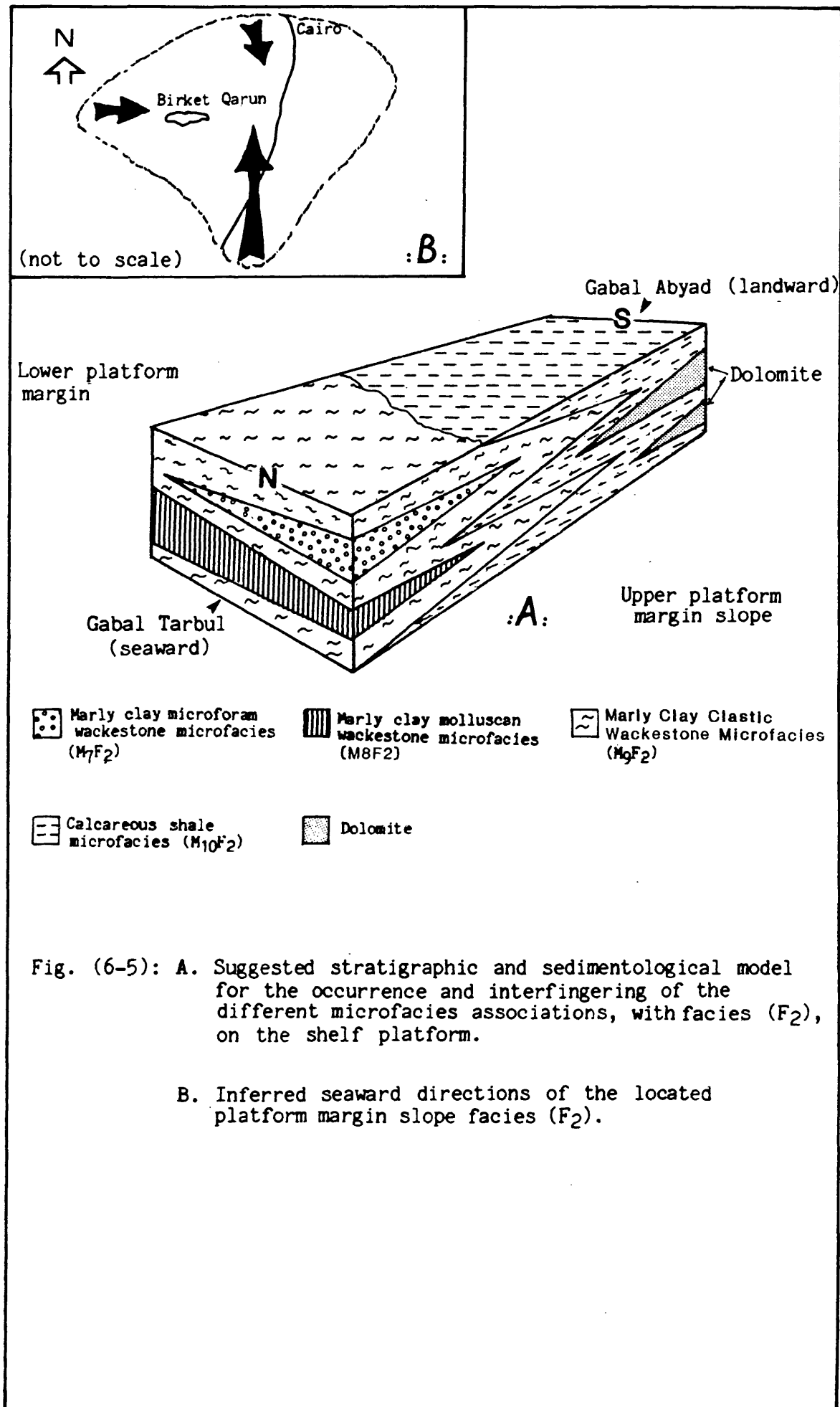
This microfacies (0.3-6.0m thick) is the most common microfacies within the Qurn facies in both the southern and north western corners of the studied basin. The microfacies (Plate 6-2,D) changes colour upward from greyish green to dirty green and has a range of weathered

colours. It is blocky and contains cross-lamination. In places, there are interbedded dolomicrites. The microfacies is usually unfossiliferous but very rarely has traces of bioclastic shell fragments. It occurs in beds that are traceable for hundreds of meters and in some places grades laterally into the siliciclastic carbonate facies (F3). It is represented in the East Fashn area, along Wadi El-Arhab, Gabal El-Hadid, East Biba, East Beni Suef, south of the Sphinx, Birket Qarun, eastern parts of the East Helwan area, and El-Saff basal facies.

The microfacies is believed to be formed in moderately to strongly agitated water with an energy index of $(EI)=4-5$. The carbonate of this microfacies are interpreted as shallow upper platform margin deposits (Fig. 6-5).

6.2.4. Depositional Environment of the Marly Clay Facies

The different associations within this marly clay facies were probably deposited on a wide platform margin slope (Fig. 6-5). This interpretation is supported by the highly bioturbated and mottled appearance recorded. The multiple generation of burrows, suggest that the dominant organisms in the marly clay facies were soft-bodied deposit feeders. The lack of primary sedimentary structures and the homogenized nature of this facies may be due to a strong burrowing effect. The bioclastic wackestone (Dunham, 1962) or bioclastic micrite (Flügel, 1972)



invariably contains a low diversity of fauna and shell debris which are believed to be jumbled and homogenized through burrowing. Bioturbation may be, also, responsible for the absence of bedding in the upper part of the sequence. Using the features described above, a fine grained lower and coarser grained upper shelf-slope depositional environment can be recognized. These are comparable with the shallow and outer barrier foreslope environments recognized in association with rudist reefs of the Caribbean area (Kauffman and Sohl, 1974). Similar facies in middle eastern Cretaceous carbonates were believed to be formed in a matching depositional environment (Burchette and Britton, 1985). The rocks of the upper marginal slope microfacies (M10F2) are found to occur in three different parts of the studied basin (Figure 6-5B). The lower platform margin microfacies (M7F2, M8F2 and M9F2), on the other hand, are found to occur in a belt seaward to the upper platform margin deposits. The microfacies associated with this facies, are intercalated with each other in a combination of onlap and offlap features (Fig. 6-5,A). This probably formed during a transgressive flooding phase which was followed by a later regression or might represent sea level fluctuations on a prograding carbonate platform slope environment. The best examples for this facies are recorded at Gabal El-Hadid, Wadi El-Arhab, Gabal Qibli El Ahram, the Birket Qarun and the lower part of the Middle Mokattam Unit in Gabal

Mokattam sections. The southern parts of the studied basin represents the major wide part (nearly 80 kms long) of the deposits of this facies.

6.3 The Wavy Bedded Carbonte Facies (F3)

6.3.1 Description

Rocks assigned to this facies are greyish green and occur in massive 20 to 100cm thick beds with wavy nodular boundaries. These are intercalated with more softer mudstone or marl partings (20-30 cm thick) (Fig. 6-6). The facies changes upward to yellowish grey, massive beds, but with local friable intercalations. The total thickness of this facies ranges from 6.0 to up to 32 meters. The least recorded thicknesses (south-east direction) are conglomeratic with 20-30 cm diameter clasts. There is also a significant total thickness increase in north-northwest direction where layer thinning and fining becomes abundant. Thickening and thinning-upward are recorded. The facies is characterised by horizontal to inclined burrowing, which becomes vertical towards the top. Ripples, cross lamination, convolute bedding, gravity slide, slump, block rotation and growth faults are also recorded. The biotic content is mainly bioclastic and is represented by fragmented bryozoa, echinoderms, operculines and nummulitic foraminifera, few bivalves and gastropods and reworked plant remains. These reworked biota are mixed with

planktonic forams and nannoplanktons. The depositional texture of this facies is represented by lime-mudstone and wackestone. Grain supported texture also occurred. The facies reflects deposition in gently agitated to slightly agitated waters with an energy index (EI) of 1-3. Geometrically this facies is represented by a large scale wedge, lobes and ribbons. Towards the north direction the facies grades laterally with pelagic and pelleted facies. Clastic turbidites deposits, commonly, intercalate with this facies. The lower and upper boundaries of this facies consist of sharp contacts with the marly clay facies (F2) below and the sandy clay above (F4). ^oErosional surfaces occur in N. W. sections 10 & 68. In east the Beni Suef area, this facies was described as the product of sheltered fore-slope environments, (Abdou-Soliman, 1980).

6.3.2 Distribution

This facies forms the lower part of the Tarbul Member in the Beni Suef area and top of the Wadi 'Garawi Formation in the Wadi Hof area. It is represented by a few meters or more in Gabal Hamret Shaibun and up to 26 meters in Gabal Tarbul and Gabal Tarbul Abu Khashirat. In the El-Saff area, this facies is represented by thicker sequences of the mudstone microfacies. The facies is also represented by coarse bioclastic wackestones in Gabal Qibli El-Ahram and the hard top of the Wadi Hof facies.

6.3.3 Microfacies Associations

This facies can be divided into the following microfacies (Plates 6-3 and 6-4).

1. Echinoderm-bryozoan lime - mudstone wackestone microfacies (M11F3)
2. Nummulitic bioclastic lime-mudstone microfacies (M12F3)
3. Spiculitic bryozoan, lime-mudstone microfacies (M13F3)
4. Arenaceous bioclastic lime-wackestone to grainstone microfacies (M14F3)
5. Nummulitic bioclastic lime-wackestone microfacies (M15F3)
6. Operculinid, arenaceous lime-wackestone microfacies (M16F3)
7. Mullascan sandy lime-wackestone microfacies (M17F3)

6.3.3.1 Echinodermal bryozoan lime-mudstone wackestone microfacies (M11F3)

The microfacies (Plate 6-3,A) is well represented (Fig. 6-6) by moderately friable, wavy pale-yellow, laminated, locally bioturbated beds which are interbedded with massive wackestone beds. The microfacies is met within Gabal's Tarbul, Tarbul Abou Khashirat, Qibli El-Ahram, Gibbo, and Saqqara, with thickness reaching up to 100cm. The maximum thickness (3 meters) is recorded in the El-Saff area. The main coarse constituents are fine detrital quartz grains (1-2%), shell fragments (2%),

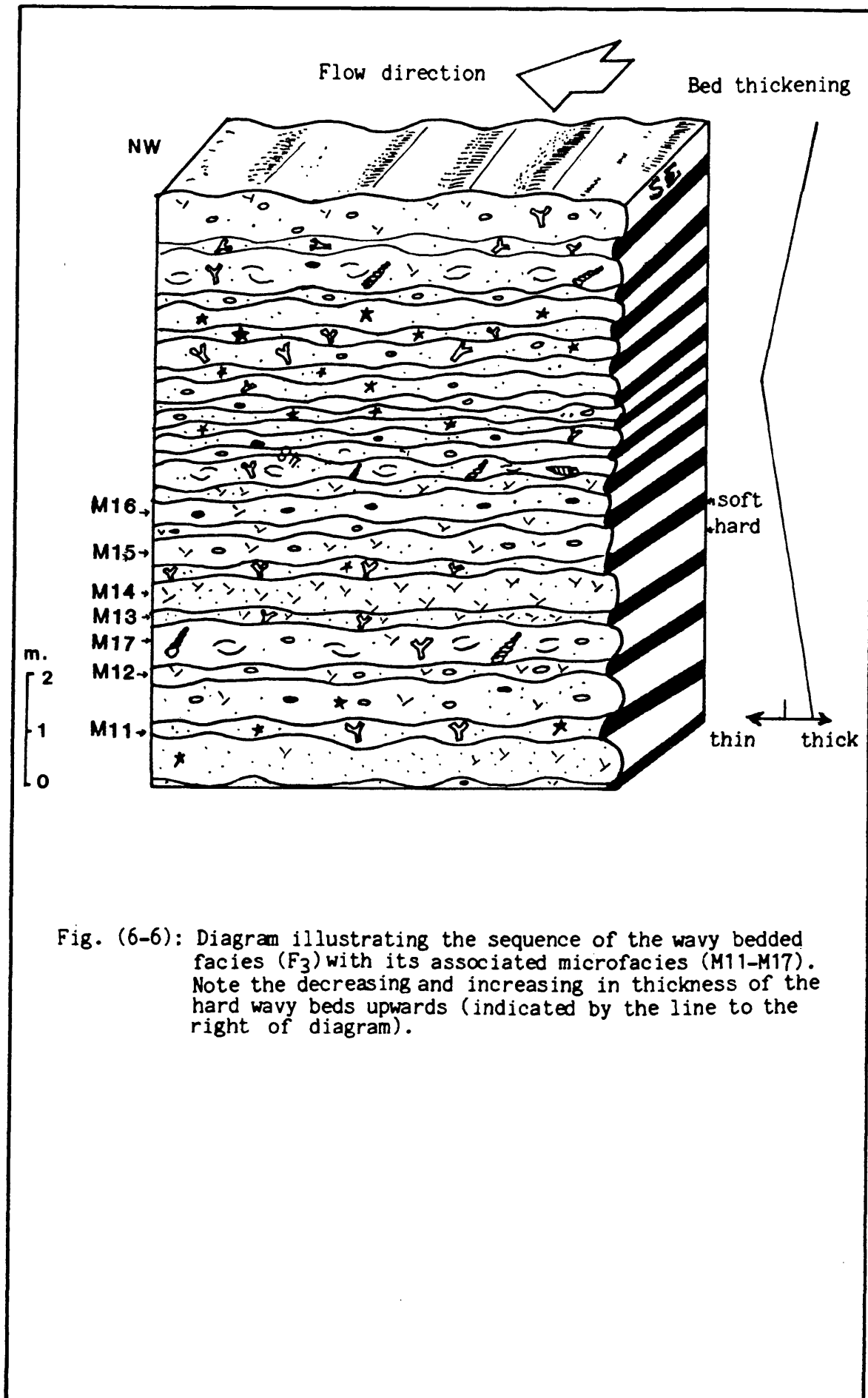


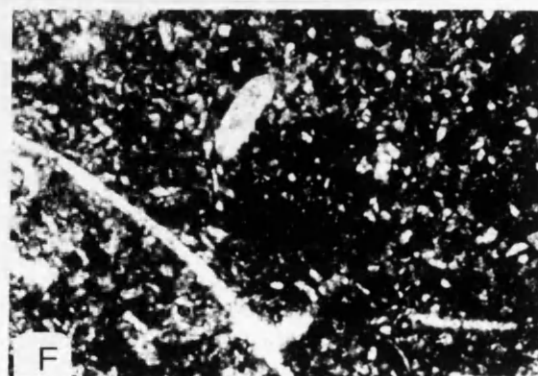
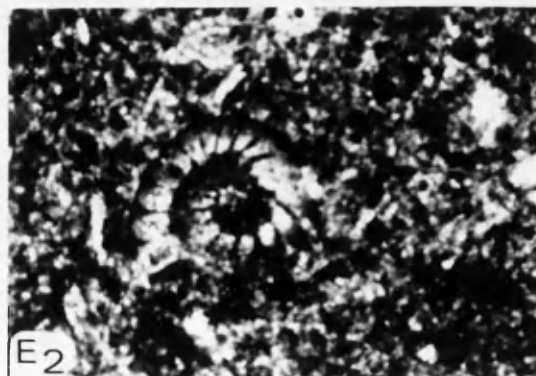
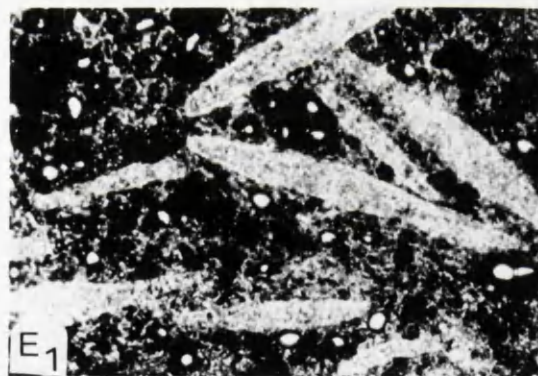
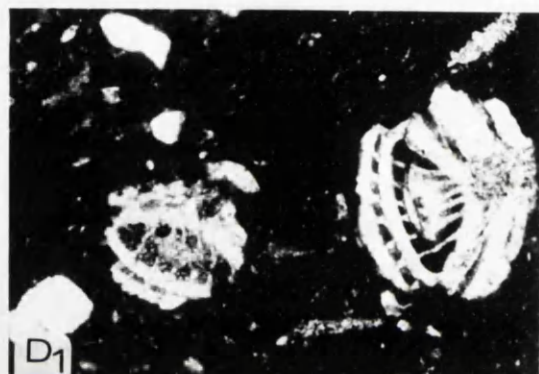
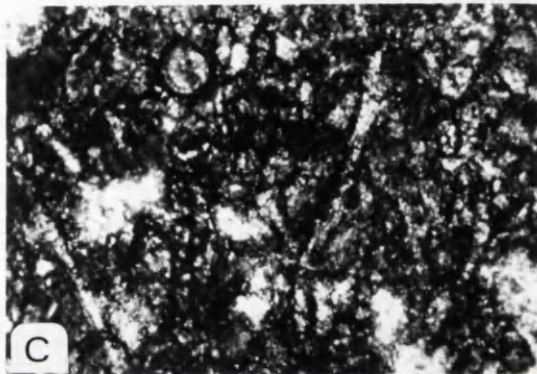
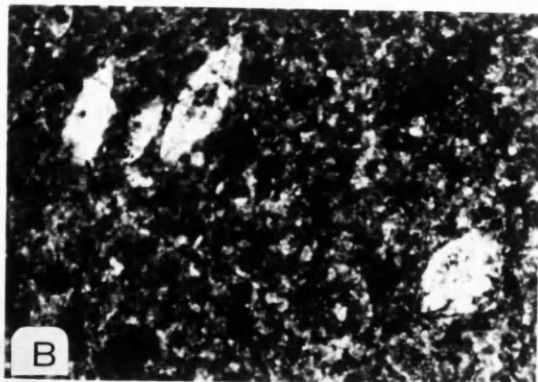
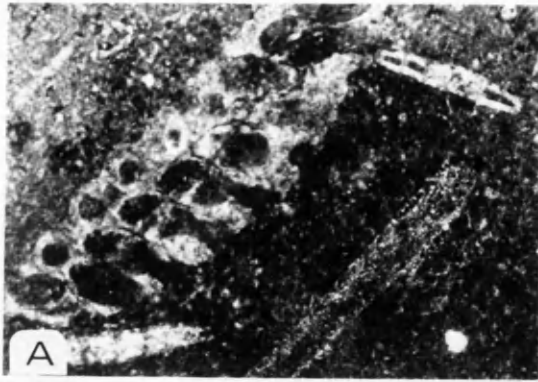
Fig. (6-6): Diagram illustrating the sequence of the wavy bedded facies (F_3) with its associated microfacies (M11-M17). Note the decreasing and increasing in thickness of the hard wavy beds upwards (indicated by the line to the right of diagram).

echinoderms (2.5%), bryozoans (2.7-8%) and nummulites (up to 1%), embedded in a marly lime-mudstone matrix (up to 90%). Bryozoan contents increase in places and are embedded in micrite matrix with wackestone texture. These carbonate grains show evidence of reworking which could be due to current transportation. The microfacies occurs as lobes which are either rounded or elongated. Some of these lobes have a higher sand grains content (up to 9%) which is believed to have developed parallel to depositional strike. This indicates that the transporting current suspended the shelf sediment which might be also enhanced by a north-west flowing discharge. This discharge displaced the sediment component from the inner-shelf, to wash down slope, towards the outer shelf. Such slope wash (a term used by McGowen and Garner, 1970, Fig. 3, p. 81) sediments were transported across the shelf slope, as lobes, to alternate with wavy sediments of the proximal microfacies (Fig. 6.8). These lobes seem to be formed in relatively deep water, which is supported from the calculated energy index of $(EI)=1$ and the microfacies deposition in gently agitated water. Reactivation surfaces are very abundant, indicating interruption of continuous bedform movement. The resultant slope wash lobes were most dense, probably during maximum sea discharge.

Plate(6-3) : (Wavy bedded carbonate facies "F3")

- A - Echinoderm-bryozoan lime-mudston wackeston microfacies (M11) X20.
- B - Nummulitic bioclastic lime mudstone microfacies (M12) X20.
- C - Spiculitic bryozoan lime-mudstone microfacies (M13). Both C1 & C2 are X80 .
- D - Nummulitic bioclastic wackestone microfacies (M15). (1 & 2 are tow different Nummulite species , both X20 .
- E - Operculina arenacious wackestone microfacies (M16), X20 (1;longitudunal section& 2; equatorial or tungetional section)
- F - Molluscan sandy wackestone microfacies (M17) , X20 .

PLATE 6-3



6.3.3.2 Nummulitic bioclastic lime-mudstone microfacies

(M12F3)

This is distributed as wavy sheets or lenses (Fig. 6.6) in Gabal Hamret Shaibun and in Gabal Tarbul, has a thickness of up to 100cm and extends northwards to El-Saff, Helwan, Gabal Qibli El-Ahram, Saqqara, and Birket Qarun. The microfacies (Plate 6-3,B) is represented by greyish green sheets with cross lamination and vertical to inclined burrowing. These may grade upwards becoming hard massive nodular lense like in shape. The soft and hard beds are repeated 13 times in cyclic fashion in Gabal Hamret Shaibun. In Gabal Tarbul, this microfacies changes laterally to a spiculite lime-mudstone microfacies (M13F3). The softer microfacies is crossed with vertical, very fine veinlets of gypsum which is a secondary diagenetic phenomenon.

The main constituents are very fine nummulites (up to 3%), shell debris (4-5%), benthonic forams (1-2%), fine detrital quartz (3%) and gastropod fragments (1%), embedded in a micrite matrix (90-92%). The microfacies reflects deposition in intermittently agitated water with an energy index of (EI)=2. The characteristic shape and nature of this micro facies leads to interpret it as mid-fan or proximal association (Fig. 6.8). The thinning-up sequence, recognized in the eastern parts of the microfacies (Fig. 6-6) is interpreted as the upper part (distributing channel)

of a mid fan. The upwards thickening sequences (Fig. 6-6) which dominate in the lower parts were the product of the prograding depositional lobes (Mutti & Ricci-Lucchi, 1972; Reading, 1978; Walker, 1978 and Reineck & Singh, 1980).

6.3.3.3 Spiculitic bryozoan lime-mudstone microfacies

(M13F3)

This microfacies (Plate 6-3,C) is represented by two lenses of friable, laminated marly mudstones, each of up to 60 cm in Gabal Tarbul and interbedded with more hard grey fossiliferous beds (50-80cm thick). The microfacies is abundant in East El-Saff sections. It is characterized by fine asymmetrical ripples and small scale cross lamination. The bed thickness increases upwards in most of the studied sections. The boundary between this microfacies and the previous microfacies (M12F3) is indistinct, however it merges at the north of Gabal Tarbul, to micro-laminated mud, silt, and sandy facies of turbidite origin (Rupke, 1978; Reineck and Singh, 1980, and Stow, 1986).

The main constituents are sponge spicules (2-4%), shell fragments (4-6%), bryozoa (1-2%), and detrital quartz (1-3%), embedded in a lime-mud matrix (92-97%).

The microfacies reflects deposition in gently agitated water with an energy index of $(EI)=1$. In the Birket Qarun area of Fayum, the microfacies is also recorded in a bed with an average thickness of 75 cm.

The fine to medium grained components, the thickening-

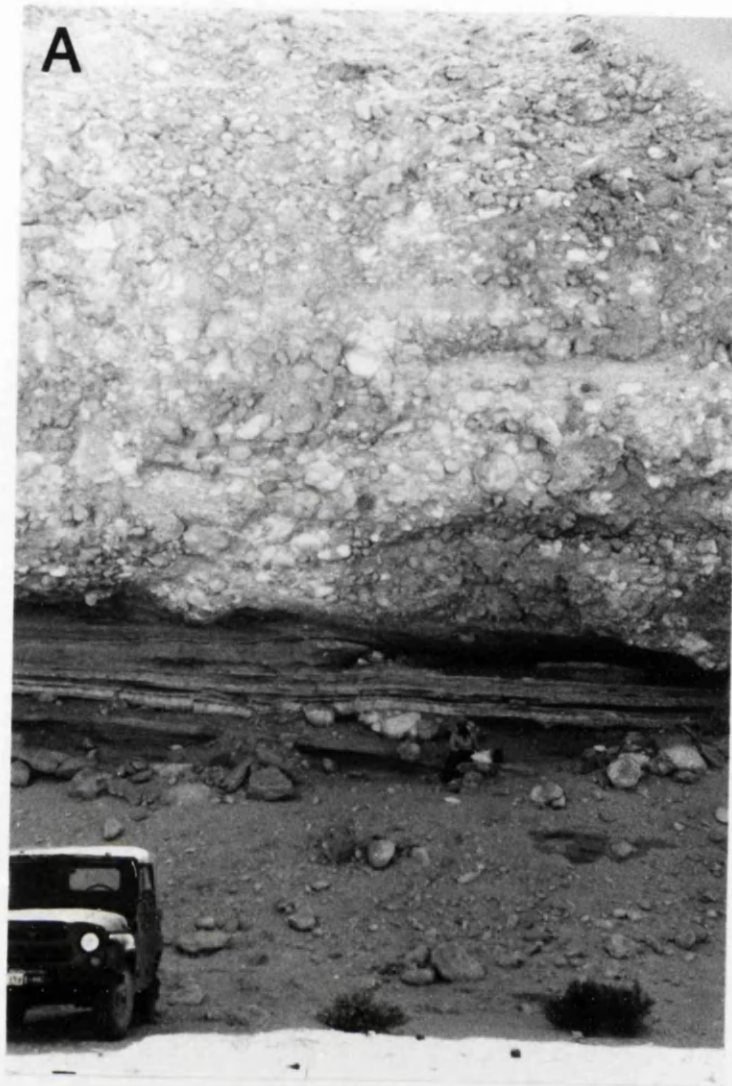
up sequences and the lateral merging with a basinal turbidite facies, demonstrate for an outer (distal) fan (Figs. 6-7 and 6-8) subenvironment (Walker and Mutti, 1973; Nelson and Nilsen, 1974; and Mutti, 1977). This is supported by the indistinct boundary between this microfacies and the mid fan microfacies (M12F3). Meanwhile, the later microfacies (M12F3) overlies M13F3 which is interpreted as fan prograding deposition.

6.3.3.4 Arenaceous Bioclastic Lime-Wackestone to Grainstone Microfacies (M14F3)

This is represented by sheets or lenses which are locally nodular and conglomeratic (Plate 6-4). In the borders of Wadi El-Arhab, Hamret Shaibun, Gabal Tarbul, East El-Saff and the Helwan area, Qibli El-Ahram and in Birket Qarun, thickness ranges between 20cm and 250cm. This thickness increases in places to 14 meters thick (Plate 6-4,A). This later sediment occurs as elongate ribbons or shoestring (Tucker, 1982) bodies with widths ranging from a few meters to 150 meters of and up to 5 kilometers long. The sediments are of disorganized polymictic rubble with syndimentary growth structures block rotation and slumps. These deposits are characterized by massive bedding, sharp top and bottom surfaces and the presence of reverse grading at the base. It is formed of grain supported calcrudite. This lithotype pattern attributed to debris flow deposition (Middleton,

Plate (6-4): A - Upper body of polymictic disorganised conglomerate is recorded in east Beni Suef area. Resedimented grain supported, calcirudite turbidite is the main facies type. Clastic rotation, growth faults, and slump structures also occur. The lower layers are of proximal levee deposits.

B - Migrating of the upper fan deposits to a new active prograding channel is predicted in this photograph from the same previous locality.



1970; Stow, 1986). The process of gravity flow is believed to be initiated by slumping and sliding. The lower surface is erosional and has a channel form with the underlying thin laminated carbonate siltstone and sandstone beds. These beds are intercalated by conglomeratic tongues or pockets and sandy lenses. Cross-lamination and small scale cross bedding occur within the fine sandy beds. These are inter-laminated with muddy layers. Convolute bedding also occurs with a fine sandy bed near the top of this lower sequence. In a cross section (Fig. 6-7,B), the width of this lower bed is about 30 meters with maximum thickness of up to 10 meters in the north wedging and dipping southerly. Flow direction in these lower layers was from north to south (Fig. 6-7,B).

The main constituents of this microfacies are a mixture of benthonic foraminifera (0.9-7%) with shell debris (2.3-4.1%), and stained reworked planktonic foraminifera (1-3%), all are embedded in a micritic muddy matrix (50-80%). At Gabal Tarbul Abu Khashirat, the groundmass of this microfacies is affected by gypsum replacement, and the overall texture is rudstone .

This microfacies reflects deposition in intermittently to slightly agitated water with an energy index of (EI)=1-2.

The above characters and nature of this microfacies are interpreted as the product of sediment flow operating in a deep submarine upper fan subenvironment (Fig. 6-8).

The main flow direction of these sediments was towards the northwest (Fig. 6-7,B, locality 1).

The lower thinly bedded sequence is interpreted as the proximal levee deposits of an old channel. Flow velocity declined away from the channel, giving rise to the thinning and wedging trend described. The alternation of thin sandy and muddy turbidite sequences were formed when flow overlapped the channel bank. This deep turbulent flow and its associated liquification were the reason for convolute bedding disturbance (Coleman, 1969; Reineck and Singh, 1980). Conglomerate pockets and sandy lenses associated with the lower part of this microfacies might be formed as deep crevasse-splay deposits which cut across the levee deposits. These crevasse channels diverted the main upper fan discharge southwards (Fig. 6-7b, Plate 6-4,A) and changed its course. So, the upper fan deposits prograded over the levee deposits towards a new active (southwest) grain flow distributary (Plate 6-4,B and Fig 6-7B,3).

6.3.3.5 Nummulitic bioclastic lime-wackestone microfacies

(M15F5), (Plate 6-3,D) .

This microfacies is represented by massive beds which form widely extending sheets. These sheets cap Gabal El-Mashash, Gabal Hamret Shaibun, G. Tarbul, G.T. Abu Khashirat, El Saff, deeper parts of Abou Serria-Suez Road, Gabal Qibli El-Ahram, Gabal El-Giushi and Birket Qarun sections. The lower beds of this microfacies sequence

thickening upwards from 60 to 150cm, then thinning near the top of a 10.6 meter succession.

The main constituents are small *Nummulite* sp. (1-9%), shell fragments (2-13%), well preserved echinoderms (0.4-3%), operculines (1%), benthonic foraminifera (2-3%) and angular to subangular fine detrital quartz grains (5-7%). All are embedded in a micritic muddy matrix (72-89%). In very rare cases the micrite matrix grades to marl.

The microfacies reflects deposition in intermittently agitated water with an energy index of (EI)=2. This microfacies has a sandy nature with medium to fine sandy grain size. The beds have a sharp hummocky surfaces and grades southwest and northwest to fine grained lobe geometry.

The microfacies reflects deposition in intermittently agitated water with an energy index of (EI)=2.

The above characters of this microfacies suggest rapid deposition. The occurrence of an upward thickening lower sequences is interpreted as prograding depositional lobes while the upward thinning up sequences are considered to represent distributary channel (Stow, 1986). The assemblage of these depositional characters is analogous to that described from turbidity current deposits (Komar, 1969; Nelson and Kulm, 1973; Stow and Bowen, 1980; and Piper et al., 1984). The features of this microfacies suggest relatively proximal deposition on a deep clastic fan (Fig. 6.8).

6.3.3.6 Operculinid arenaceous wackestone microfacies

(M16F3)

This microfacies (Plate 6-3, E and Fig. 6-6) is represented in both Gabal Hamret Shaibun and Gabal Tarbul Abu Khashirat by hard massive nodular sheets. The maximum sheet thickness is up to 100cm. This thickness increases and decreases in an upward sequence. The main constituents are Operculines (2-4%), shell fragments (1-6%) replaced by calcite, very fine detrital quartz (6-26%), benthonic foraminifera (2.6-5%), ostracods (0.2%) and with very rare nummulites, bivalves and echinoderms (0.4-3%). All are embedded in a muddy micritic matrix (70.4-77.7%).

Generally this microfacies reflects deposition in gentle to intermittently agitated water with an energy index of (EI)=2. The grain size is medium to fine sand.

This microfacies is interpreted in the same way as M15F3 as proximal facies (Fig. 6.8) but with more finer, deeper, middle fan clastics.

6.3.3.7 Molluscan sandy lime-wackestone microfacies (M17F3)

This microfacies (Plate 6-3,F) is represented by rubbly lenses of 80cm thick in Gabal Hamret Shaibun, G. Tarbul, El-Saf, and Gabal El-Maskara.

The main constituents are bivalves (2%) mainly *Lucina*, gastropods (*Turritella*) up to 2.5%, detrital quartz (5-10%), bioclasts (2-3%), embedded in a muddy matrix. The fauna is reworked and concentrated in the matrix around the

debris which are of the same source. These are subrounded to angular cobbles, poorly sorted and grain supported. The lower and upper boundaries are very sharp erosional surfaces. Soft sediment slumps occur. The occurrence of this microfacies is discontinuous and it is overlain by upper channel deposits.

The above constituents reflect intermittently agitated deposition with an energy index of $\langle EI \rangle = 2$. The angularity of clasts reflects a nearby source of upper shelf break deposits. The sharp contacts and the grain sorting suggest rapid accumulation. The bed geometry and soft sedimentary deformation structures suggest upper fan lag deposits. This is supported by the occurrence of the overlaying upper channel facies. The discontinuity of these sediments reflects the complex nature of this microfacies.

6.3.4 Submarine Fans and their Microfacies:

An Interpretation (Fig. 6-8).

Both the hard bioclastic wackestone and the softer mudstone beds contain ripple marks. These are asymmetrical with gentle slopes for both the stoss and the lee sides. The crests are generally undulatory. Their ripple index ranges between 3 and 7. They are believed to be formed by currents moving in a uniform direction over a surface of shelf margin in a shallow shelf front (Figs, 6-7 and 6-8).

Cross lamination is also relatively common and is

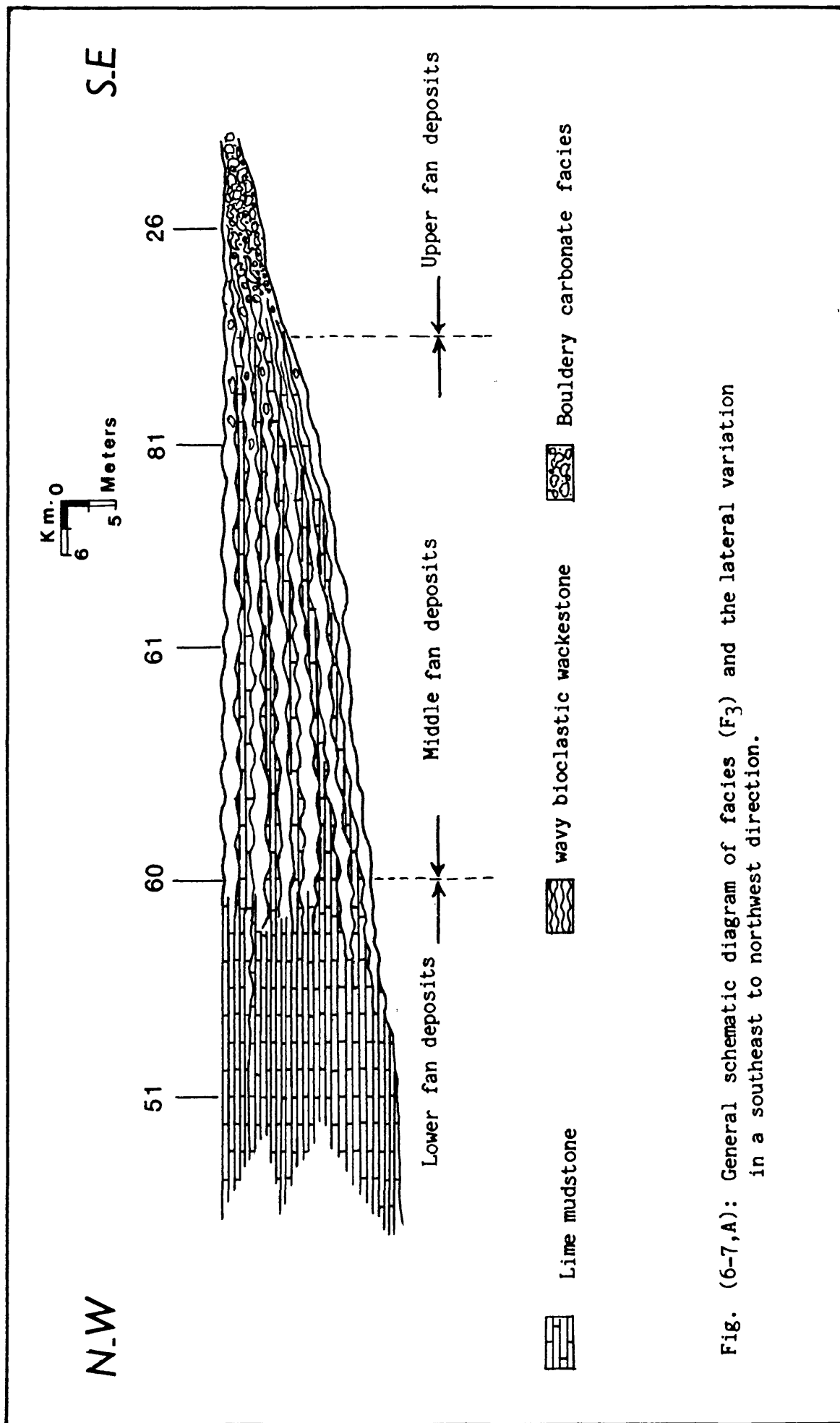


Fig. (6-7,A): General schematic diagram of facies (F₃) and the lateral variation in a southeast to northwest direction.

observed in the upper surfaces of the softer marly mudstones. It is of small scale trough cross strata with angles of dip less than 10° . These small scale cross laminations could originate from periodic currents at the interface between water and granular materials of the sea floor. They are basically current-formed, below wave base (Shrock, 1948; Pettijohn and Potter, 1964 and Wilson, 1975). The occurrence of this type of primary structure is a measure of quietness of the waters in which the sediments accumulated below wave base (Pettijohn, 1975). Wilson (1975) grouped it as a recognizable sedimentary structure of slope and basin carbonate strata.

The softer beds also contain some plant remains parallelly oriented with the sediment which might reflect an upper current oriented, upper shelf debris.

Variation in microfacies and carbonate grains could be due to a fluctuating sediment supply from different parts of the upper shelf.

The presence of the coarse material suggests transport mechanisms of sufficient competency to transport coarse sediment over great distances. Most of the coarser grained intercalations are coarsening-up sequences. This feature can be considered to indicate that currents carrying particles in suspension have progressively deposited their load according to decreasing particle size with diminishing current energy. This explains the type of grading which shows a transition to fine sediments at the top of the bed.

Sometimes, however, a normally graded unit displays a sharp boundary with the overlaying clayey sediment. This could be explained by considering that, occasionally, towards the end of the graded sedimentation, the rate of deposition decreases abruptly. In this case, traction transport of the sedimentary particles along the bottom becomes more important, and the graded unit ends abruptly. The occurrence of the above mentioned trough cross lamination at the sharp upper contacts of some such graded units would appear to support this interpretation.

Taking all this, mentioned, information into account, together with the previous characters recorded with the facies and microfacies description, it is almost certain that the wavy bedded carbonate facies accumulated as a fan facies on a wide deep shelf. The increasing of facies thickness, northwards (Fig. 6.7,B) is believed to occur in a basinward direction. Also, the increase in grain size of the terrigenous content in southeast, could reflect the source from which these deposits have entered the basin. Meanwhile, a southwest clastic source was detected.

As demonstrated before, it seems that the shelf break reworked debris, were the main fount for these fan deposits. The rapid, freefall events could be occurred in steep cliffs of faulted slopes. Initiation of these phenomena might be started by undercutting and erosion by earthquake shocks (Stow, 1986). These debris could be transported basinwards as deep channel clastics. Some of

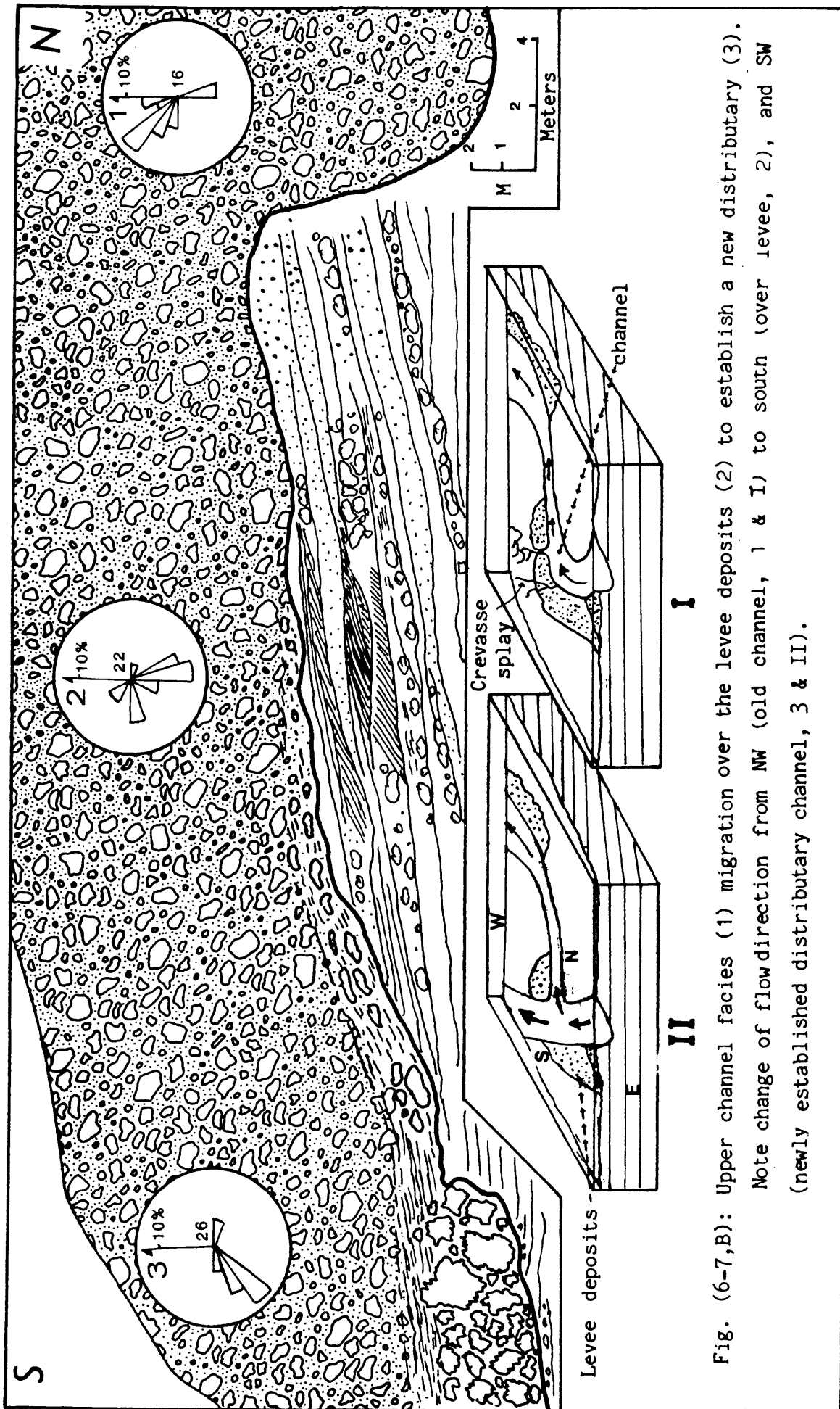


Fig. (6-7,B): Upper channel facies (1) migration over the levee deposits (2) to establish a new distributary (3). Note change of flow direction from NW (old channel, 1 & I) to south (over levee, 2), and SW (newly established distributary channel, 3 & II).

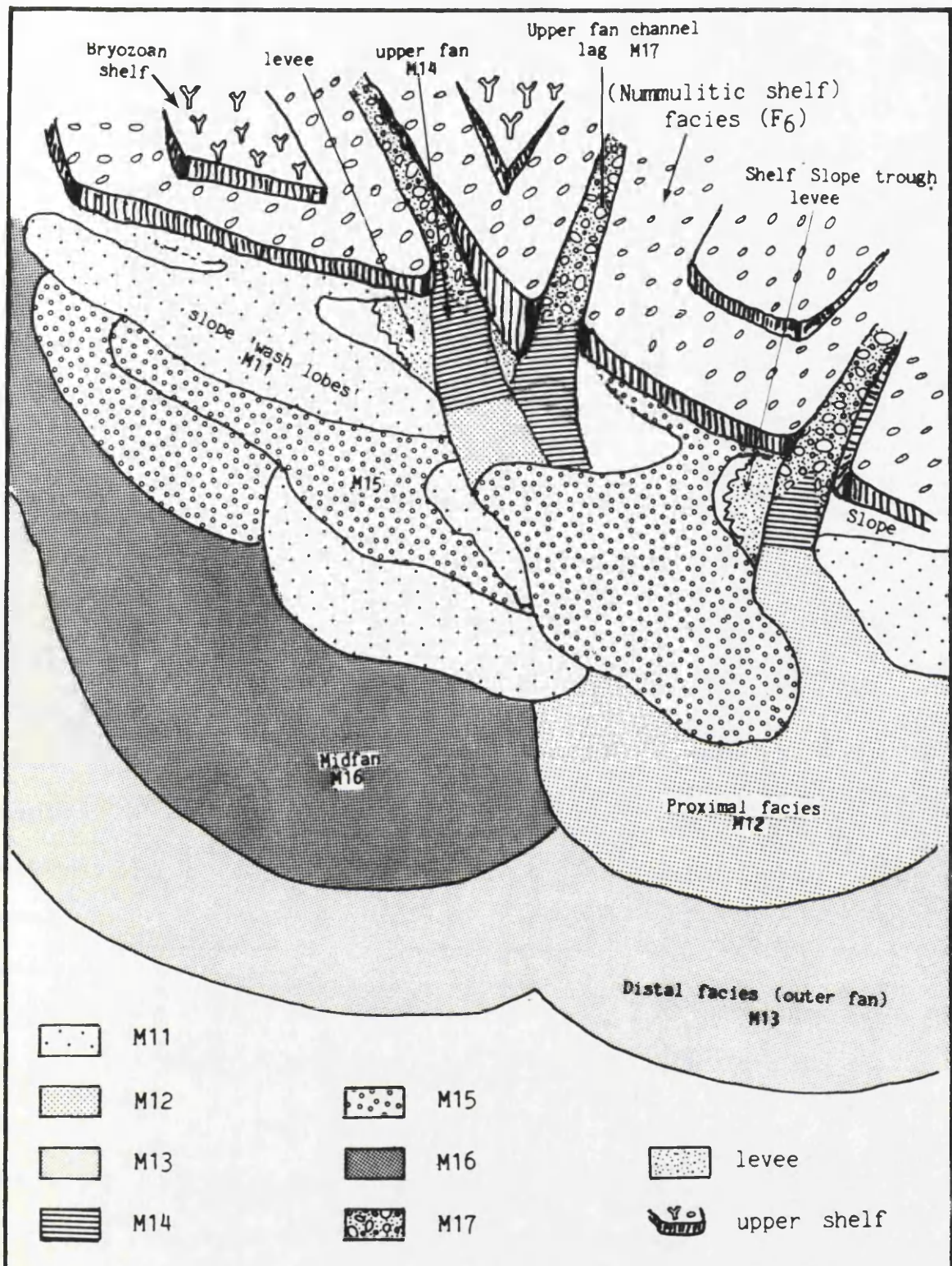


Fig. (6-8): Reconstruction model of fan and lobes environments of the nodular bedded carbonate facies and the distribution of its microfacies.

these clastics were deposited close to the sediment source as channel lag microfacies (M17). Most of the debris bounced and rolled downslope for tens or hundreds of meters before coming to rest (Abbate, et al., 1970, Johns, 1978). These debris flows eroded and constructed a driftway along the basin shelf. On the upper shelf the coarse debris deposited as upper fan microfacies (M14, Fig. 6.7,A,B, & 6.8) with its own levee deposits (Fig. 6.7,B).

These clastic sand-made turbidites are closely similar to Bouma C division, described by Hesse (1975) and Enos (1977). Fan progradation was responsible for the upper fan deposit migration to establish new distributaries over the shelf plane (Fig. 6.7,B). On the Middle shelf, proximal facies (M12 and M16) deposits accumulated as middle fan microfacies. Most of the upper shelf fauna reworked then washed down slope and deposited as slope wash-lobes, to mix with the middle fan facies producing both M11 and M15 microfacies (Fig. 6.8). The medium to finer clastics travelled deeper and accumulated as thicker mudstone (Fig. 6.7,A) microfacies (M13). These mudstones have thinner beds with parallel sided and regularly bedded succession. The sand/mud ratio of these mudstone microfacies is lower than the above mentioned proximal microfacies. These mudstones are well graded with fine lamination and current ripples. These carbonate facies are interpreted as distal facies. However, the sediments of these facies are interrupted by a (20 cm. thick) bed of pelagic facies in the

east El-Saff area (section 51). The pelagic sedimentation was probably taking place continuously during the development of the distal mudstones, but they were highly diluted by the large input of terrigenous sediments. Even during bloom periods, it would be difficult for the biogenic ooze component to surpass the rate of terrigenous input. The occurrence of the previous mentioned pelagic material, in the northern sections, could mean that they have accumulated during temporary restriction in the sediment supply (possibly related to tectonic events) or during periods of differing climatic and / or physical conditions which restricted the major processes of the fan clastic deposition.

In short, this type of fan deposit (Fig. 6.7,A) is believed to be brought in through long channels. The valley length of these buried channels and their pattern were not easily detected or measured, in field. The analysed characters of this facies reveal the following:-

1. From the channel cross section (Fig. 6.7,B), both the channel banks gradient were different. The southern bank is steep concave and the northern is gently sloping towards the axis of the channel. That could be explained respectively as the result of maximum and weaker flow velocities mechanism (Bridge, 1985).
2. The different flow direction recorded (Fig. 6.7,B) could reflect a channel splitting point (Schumm, 1985).
3. The occurrence of levee deposits recorded with

microfacies M14 (Fig. 6.7, A & B), is generally developed on the concave sides of the channels. (Reineck and Singh, 1980).

4. The major length of these channels (more than 5 Km. recorded within the study area) suggest they were not straight channels, & straight channels only exist over short distances (Reineck and Singh, 1980).

5. The length of these channels is more than 33 times the width. But as demonstrated by Leopold *et al.*, (1964) that straight channels length never exceeded 10 times their width. Therefore, that could suggest, also, that they are not admitted to straight channels.

6. The gentle slope of the studied shelf (<1°, ch.7) would have stimulated the formation of meandering rather than braided channels which develop on steeper slopes (Loepold and Wolman, 1957; Bridge, 1985).

All of the above points suggest a meander channel pattern for this deep channel facies. However, a change from meandering to braided channels is expected due to changes in the discharge sediment load, sea level and climate, as cited by Coleman (1969) and Schumm (1977). Similar examples of ancient deep-submarine channels were described by (Whitaker, 1974; Wimm and Dott, 1979).

6.4 Mixed Sandy Clay Carbonate Facies (F4)

6.4.1 Description

The mixed sandy clay facies (Fig. 6-9) is represented by a hard to medium calcareous sandstone, friable fine muddy sands, and calcareous sandy shales or silts. It is generally yellowish in colour with occasional yellowish grey, pale grey green, and brownish yellow units. The thickness of this facies is variable and ranges from 3.5 to 18 meters thick. It occurs as thick friable beds (up to 6m thick) or in a wavy bedded succession of 50cm thick units. Cross bedding is present sometimes especially with the massive facies, where both vertical and horizontal burrowing are encountered.

The bedded facies are characterized by cross lamination. Normal and reverse graded units are recorded which range from coarse to very fine sand and mud grain sizes. Biogenically the muddy or shaley intervals have vertical to inclined burrowings, near the facies base, and some foraminifera. The sandy layers are often unfossiliferous with bioclastic debris. This facies is represented by large extended wedges or lenses and repeated at different levels. It changes laterally to more finer and silty or marly shales, and northwards, changes laterally and vertically to a conglomeratic facies. The facies also has sharp boundaries.

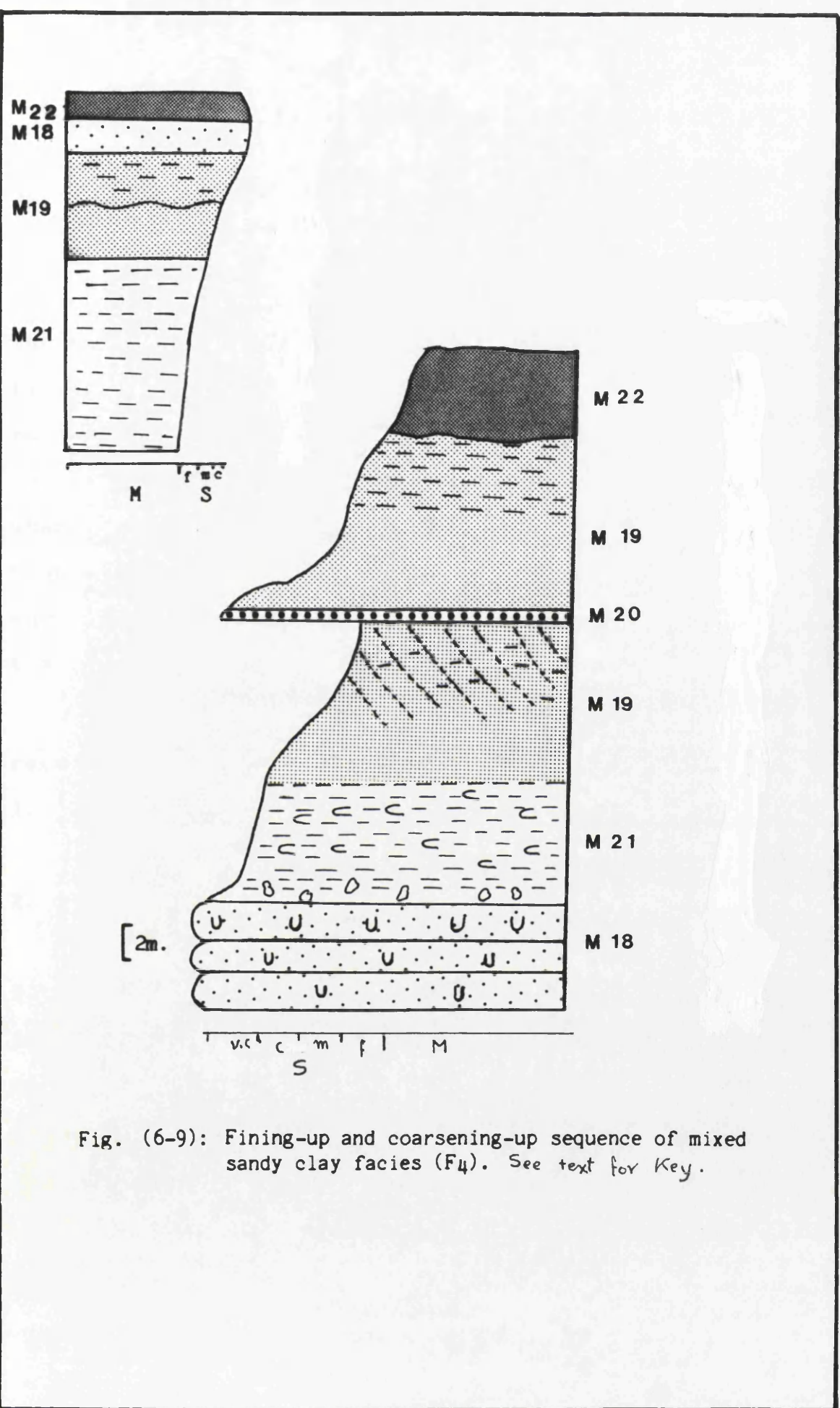


Fig. (6-9): Fining-up and coarsening-up sequence of mixed sandy clay facies (F4). See text for Key.

6.4.2 Distribution

The type section for this facies is at Gabal Hamret Shaibun, in east Beni Suef, where the beds of this facies reach up to 12.3m thick. They wedge to the northeast in Gabal Tarbul Abu-Khashirat to reach 3.50m thick and also in the north, in Gabal Tarbul, where the facies is represented by up to 8 meters of fine friable yellowish muds or sandy muds. The facies reappears in east El-Tebbin as wavy or undulated beds interbedded with highly bioturbated units where it is up to 18 meters thick. The facies occurs near the top of most sections throughout the studied area and represents the final mixed marine phase of basin fill.

6.4.3 Microfacies Associations

The following microfacies associations (Plate 6-5) are recorded with this facies:-

1. Muddy allochem foraminiferal lime-wackestone microfacies (M18F4)
2. Allochemic sands lime-wackestone microfacies (M19F4)
3. Micritic sand lime-packstone microfacies (M20F4)
4. Allochemic mud lime-wackestone microfacies (M21F4)
5. Shale microfacies (M22F4)

6.4.3.1 Muddy allochem foraminiferal lime-wackestone microfacies (M18F4)

This microfacies (Plate 6-5,A) is well represented by a hard, 2.0 meters thick bed with a greyish green colour.

Plate (6-5) : (Mixed sandy-clay facies associations " F4")

A Muddy allochem|foraminiferal wackestone microfacies
(M18) X20 .

B - Allochemic| sands wackestone microfacies
(M19) X20 .

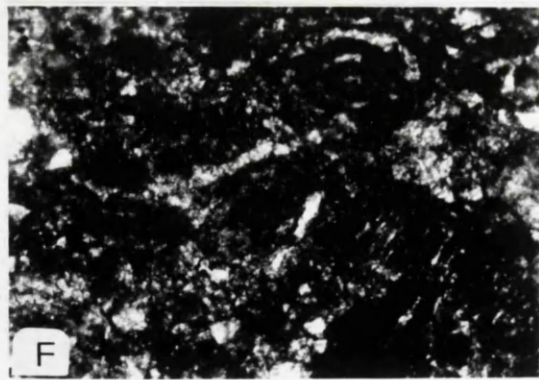
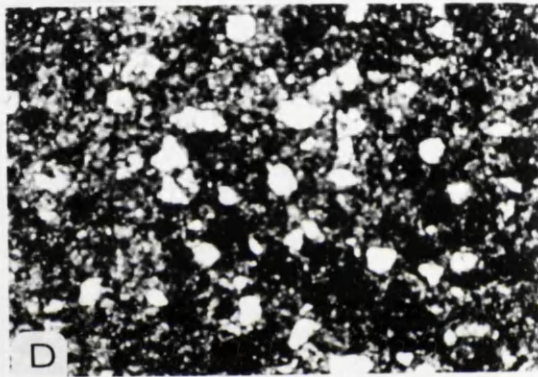
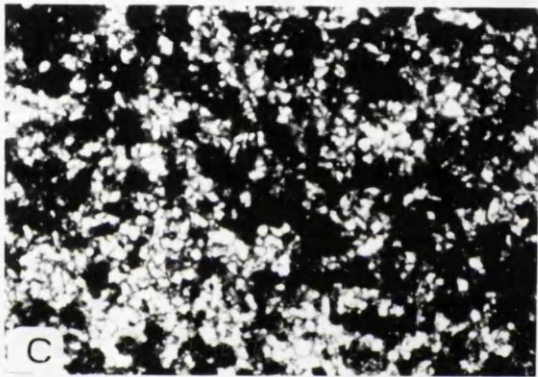
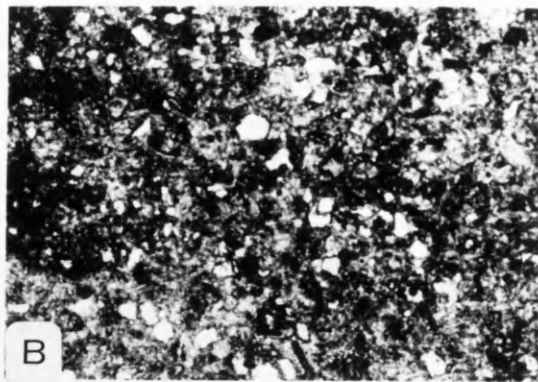
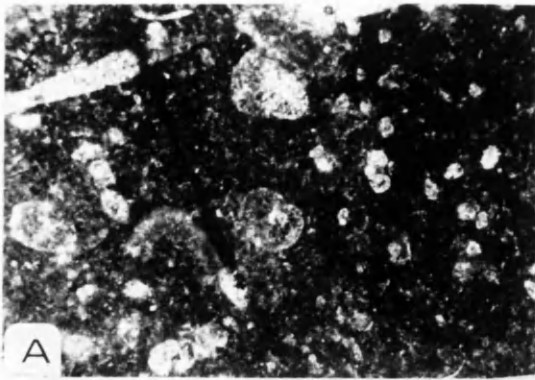
C - Micritic| sand packstone microfacies (M20)X20.

D - Allochemic mud| wackestone microfacies
(M21) X40 .

E - Shale microfacies (M22) X20. Note
occurrence of bioclastic debris .

F - Shale microfacies (M22) , with occurrence
of miliolid foraminifera . X40 .

PLATE 6-5



It occurs at the base of the whole facies (F4) and may indicate a transitional zone from the siliciclastic carbonate facies (F3) to the mixed sandy clay facies (F4). The microfacies has a sandy appearance on weathered surfaces. It is recorded within the Gabal Hamret Shaibun, Gabal Tarbul, and in the Wadi Hof sections. The main constituents are few operculines (0.5-1%), *Nummulites* (up to 0.3%), ostracodes (1%), quartz detrital grains (up to 12%), bioclastic debris (up to 40%), embedded in a mud matrix.

This microfacies changes laterally in the Beni Suef area to fine sandy silts and to the north in Wadi Hof is replaced by another arenaceous silty sand microfacies (M21F4). The microfacies has vertical burrowing and sharp boundaries and reflects deposition in slightly agitated water with an energy index of 3.

6.4.3.2 Allochemic sands wackestone microfacies

(M19F4)

This is represented by sheet like deposits (3 meters) which are repeated twice in Gabal Shaibun. The sediments are more friable and crossed with gypsum and show cross bedding. The main constituents (Plate 6-5,B) are sandy sized shell fragments (24%), silt detritals (31%) and detrital sands (45%). Sometimes the groundmass of this microfacies is affected by gypsum replacement. The microfacies fines upwards from medium to fine sands and

changes laterally to more muddy microfacies. It overlies the shale microfacies (M22F4) and underlies the calcareous sand packstone microfacies (M20F4). The main body of the sediment has a wedge shape and thins towards Gabal Tarbul, Tarbul Abu Khashirat, and Birket Qarun of the Fayum area. This microfacies reappears at the top of most sections and defines the top of the Middle Mokattam Unit. The grain content of this microfacies reflects deposition in a strongly agitated water with an energy index (EI) of 5.

6.4.3.3 Micritic sand lime-packstone microfacies (M20F4)

The calcareous sand packstone microfacies (Plate 6-5,C) is locally recognized in the east Beni Suef area, towards the western scarp of gabal Hamret Shaibun. It is represented as a brownish band of coarse grained sands (10 cm thick). The grains have a well packed texture. Microscopically, the microfacies includes detrital sand grains (55%), mud matrix (17%), with iron-oxide and ferruginous micrite in places and a few sand sized intraclasts. In the field, it is found to have sharp contacts with the underlying bioclastic silty sands wackestone microfacies (M19F4) and a gradational contact with the overlying arenaceous silty wackestone microfacies (M21F4).

Geometrically, this microfacies is a wedge like deposit which increases in thickness towards the south and east (up to 3 meters) forming elongated bodies.

This microfacies reflects deposition in moderately agitated water with an energy index (EI) of 4. This is also demonstrated from the cross bedding which occurs with the inner microfacies bodies which are interpreted as linear barrier deposits (Fig. 6-9). The outer sequences of the microfacies are bioturbated with parallel seaward dipping laminations and correlated with those described as barrier islands deposits by Howard and Reneck, (1981).

6.4.3.4 Allochemic mud lime-wackestone microfacies (M21F4)

This microfacies (Plate 6-5,D) is widespread in the studied basin of the Nile Valley and the Fayum areas. It is represented in Gabal Tarbul, Tarbul Abu Khashirat, Gabal Shaibun (of the Beni Suef area), Birket Qarun (of the Fayum area), Gabal Qibli El-Ahram (of the Giza Pyramids area), and in Gabal El-Maskara (of the Helwan area). The total thickness of these microfacies ranges from 3 meters (in the south) to 18 meters (the Helwan area). The main constituents are detrital quartz grains of sand sizes (12-30%), shell fragments (10-15%), scattered in a lime silty matrix (60-78%). Laterally this microfacies changes to a sequence of thinly interbedded hard and soft beds. This microfacies reflects deposition in a gently to intermittently agitated water with an energy index of (EI)=1-2. The grains normally grade and end with a muddy fine sandy top, highly bioturbated, ^{and} parallelly laminated.

6.4.3.5 Shale microfacies (M22F4)

The best example for this microfacies (Plate 6-5, E and F) is in Gabal Hamret Shaibun where it is 1.6 meters thick. It is also encountered in Birkjet Qarun, Gabal Tarbul and Gabal Gibli El-Ahram. It is characterized by horizontal burrowing and bioturbation. The components of this microfacies are mainly some foraminifera and shell fragments. The microfacies has plant remains and bivalve casts. Miliolid also occurs with some horizons of this microfacies (Plate 6-5, F). It has a sharp lower and upper surface. The weathered surface is yellowish grey in colour. Towards the south of the basin, contamination with muds and fine sands is recorded together with abundant miliolids and a high gypsum content. It could have been deposited in a gently agitated water with an energy index (EI) of 1.

6.4.4 Depositional environment of the mixed sandy clay carbonate

Sequences of this association are interpreted as emergent barrier islands or emergent channel-margin linear bar complexes which formed through the coalescence of landward-migrating swash bars. These sequences therefore represent a combination of off-shore swash bars and beach foreshore deposits. The major additional facies components are those deposits that form as a result of current activity through tidal inlets which pass through the

barrier into the back barrier lagoon.

The planar bedforms that characterize modern carbonate and siliciclastic beach deposits are discussed by Imbrie and Buchanan (1965) and Clifton *et al* (1971). Reineck and Singh (1980) attribute low angle seaward-dipping pebble imbrication to wave propagation along a beach. Fitzgerald (1976) described the formation of siliciclastic swash bar-channel-margin linear bar complexes along flanks of a South Carolina ebb-tidal delta. These can form emergent sand bodies which are associated with beaches and aeolian dunes (Hubbard and Barwis, 1976; Fitzgerald, 1976).

The observed features of these carbonate and clastic complexes started on a hard base or plain of an offshore microfacies (M18F4) which formed at the seaward mouth of tidal inlets. On top of that, the inlet sequence itself (M21F4) is bounded by a basal scour surface which has a coarse associated intraclast and fossil lag immediately above it. The characteristic lenticular, channel shaped isolated occurrence of these carbonate sands in the barrier islands, and their maximum dimension normal to the shoreline, all suggest a close similarity to the deep, wide shelf, inlets of Georgia, U.S.A. (Hubbard, Oertel and Nummedal, 1979). The parallel laminated sandy top is interpreted as a product of deposition in the swash zone (Reddering, 1983). The extensive thickness of this microfacies could be due to high migration rates of these tidal inlets as reported from the Fire Island, New York

linear Barrier
complex (M20)

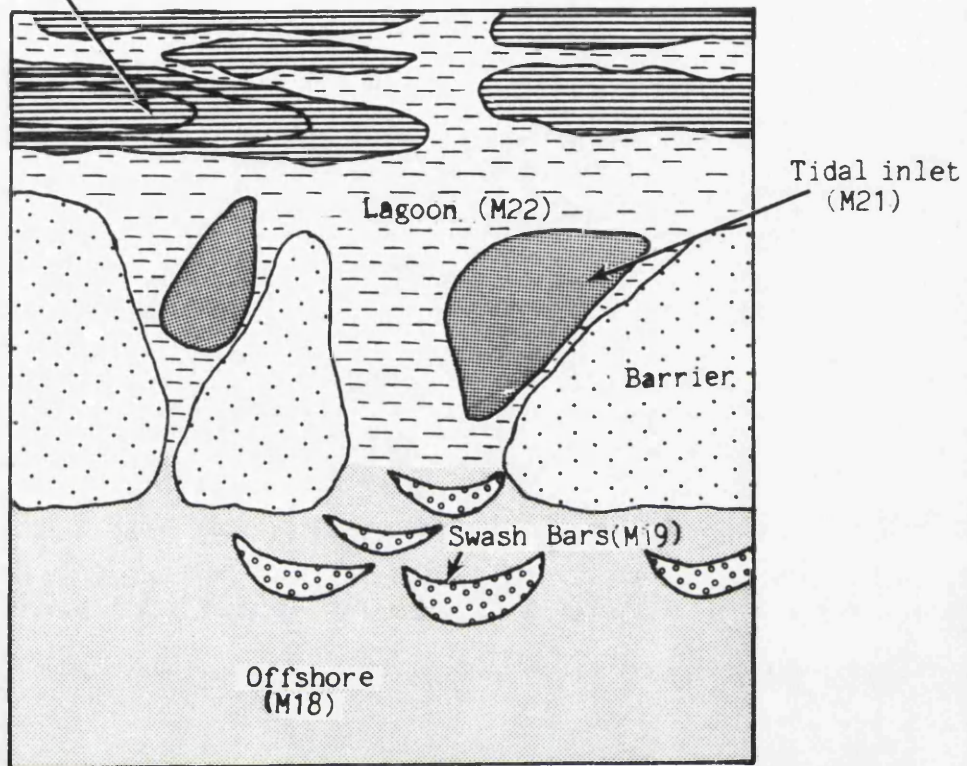


Fig. (6-10): The inferred barrier complex through the deposition of the siliciclastic carbonate facies (F₄), within the upper member facies of the Beni Suef formation.

(Kumar and Sander, 1974).

These deep inlets are overlain by large and medium scale tabular cross bedded lime wackestone (M19F4). The later microfacies, could be deposited as an emergent swash bar subenvironment. The predominance of wave processes along the margins resulted in the formation of landward-migrating swash bars. These coalesced to form emergent swash bar-channel margin linear bar complexes (Fig. 6-10). The sequence is capped abruptly by a thinly bedded (10 centimeters thick) sandstone which represents a coarsening upward shoreface (M20F4) microfacies. The top of the sequence progressively fines upward into offshore lagoonal microfacies (M22F4). In the Beni Suef area, the whole facies occur in an upward fining unit which might reflect a local prograding shore line. At the mean time, in East Helwan area, the shallow marine siliciclastic sequence occurs in a winnowed coarsening up sequence (M20F4) which could be the product of a prograding barrier shoreline. These fining and coarsening upwards, could also be due to changing in flow velocities (Reineck and Singh, 1980). All the above features have analogues in the ancient carbonate and clastic barrier complexes (Boutte, 1969; Hayes, 1976; Hubbard *et al*, 1979). The sporadic occurrence of this facies, within the middle part of the Tarbul Member of Beni Suef Formation, and the base of the Wadi Garawi formation, could suggest that these emerged carbonate and siliciclastic barriers were migrating either during storms

or during seasonal changes in the wind circulation pattern.

6.5 Bivalve Carbonate Facies (F5)

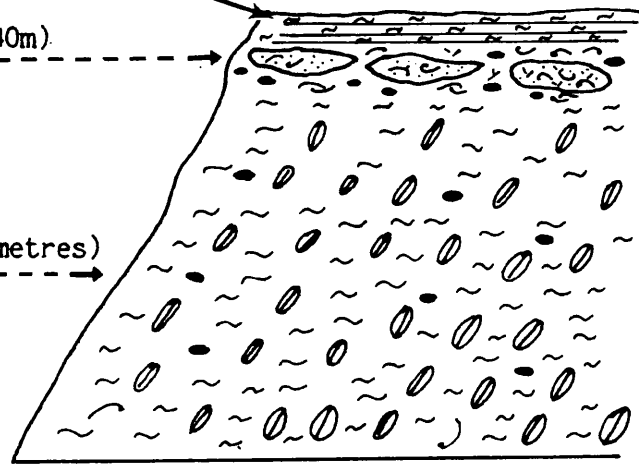
6.5.1 Description

The bivalve facies (Fig. 6-11) is represented by greyish white to greenish grey limestone bed of 5 meters thick in section 61 (Gabal Shaibun). Farther north, in section 16 of the east Helwan area, the facies is thicker (10 meters thick) and is represented by white limestone, which is cross-bedded and contains dolomitic boulders 1 to 3 meters long and up to one meter thick. These are arranged horizontally at the base of the facies. The dolomite boulders contain fine nummulites and some pockets of bivalves and gastropods. The bivalve shells are found to be concentrated towards the facies base and decrease in abundance upwards. The size of the shells varies from up to 4cm long (section 61) to up to 10cm long (section 16). Some horizontal burrowing and bioturbation is also characteristic of the facies. The facies beds are normally graded. Gastropods and small nummulites are also found associated with this facies. This facies changes near the top to boulders of hard calcareous sandstone (1 to 1.5 meters long) and lithoclastic (up to 12 cm long). The main geometry of this facies consists of lenses and wedge shaped units which pass laterally into the clastic nummulite facies (F6). The boundaries of the bivalve facies have very sharp contacts.

Unfossiliferous marl
(0.50 m)

M 26 (0.40m)

M 23 (5 metres)

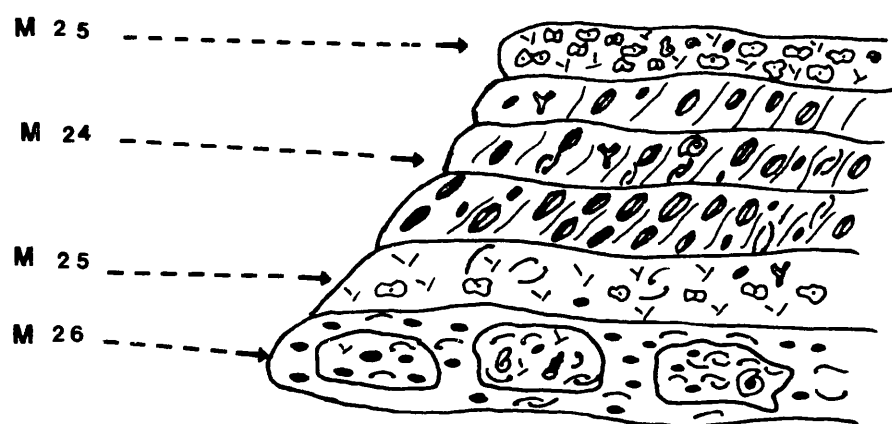


A

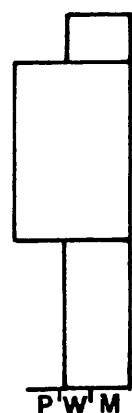
1 m.]



P'W'M



B



P'W'M

- | | | |
|----------------------|------------|---------------------|
| Articulated Bivalves | Nummulites | Intraclasts |
| Disartic Bivalves | Bryozoa | Boulders |
| Shell debris | Marl | Cross-bedded facies |
| Gastropods | Sands | fine bedded facies |

Fig. (6-11): The Molluscan facies (F₅) in the southern (A) and northern (B) parts of the studied basin of northern Nile Valley, Egypt.

6.5.2 Distribution

The bivalve facies is recorded in sections 61, 60 in the southern parts of the studied area, while it occurs in sections 44, 16, 17, 18, 4, 49 and 48 in the northern parts of the studied basin. The type section for the facies in the south is Gabal Hamret Shaibun, where the facies is represented by the dense facies of *Lucina* cf. *qurnaensis*. The thickness of the facies decreases towards the north and south and almost disappears in east and west directions. In the East Helwan area the thickness of the facies increases and attains a thickness of up to 10 meters in section 16. It decreases to a thickness of 1.20 meters in section 49. In the latter localities, the bivalve shells are represented by *Arcopagia grandis*, and *Macrosolen uniradiatus*.

6.5.3 Microfacies. Association of facies (F5)

The following microfacies associations (Plates 6-6 and 6-7) were recorded:

1. Bivalve Lime-Packstone Microfacies (M23F5)
2. Bivalve Bryozoan Lime-Packstone Microfacies (M24F5)
3. Bivalve Lithoclastic Lime-Wackestone Microfacies (M25F5)
4. Bivalve Dolomitic Lime-Wackestone Microfacies (M26F5)

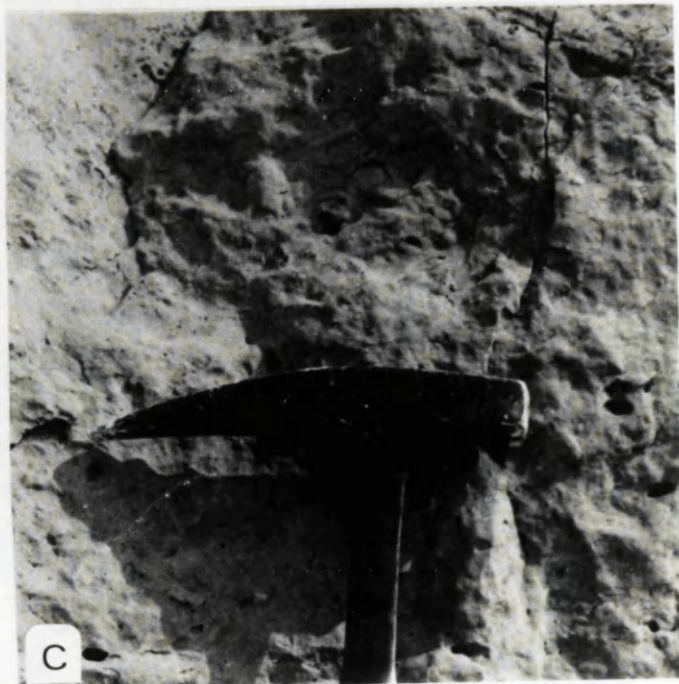
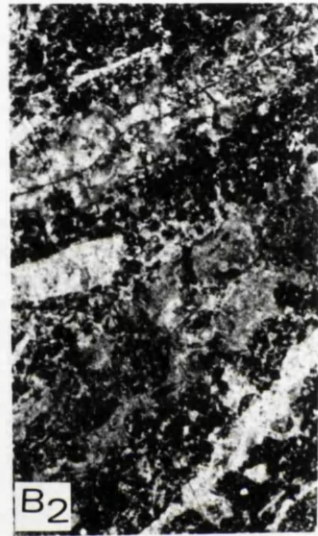
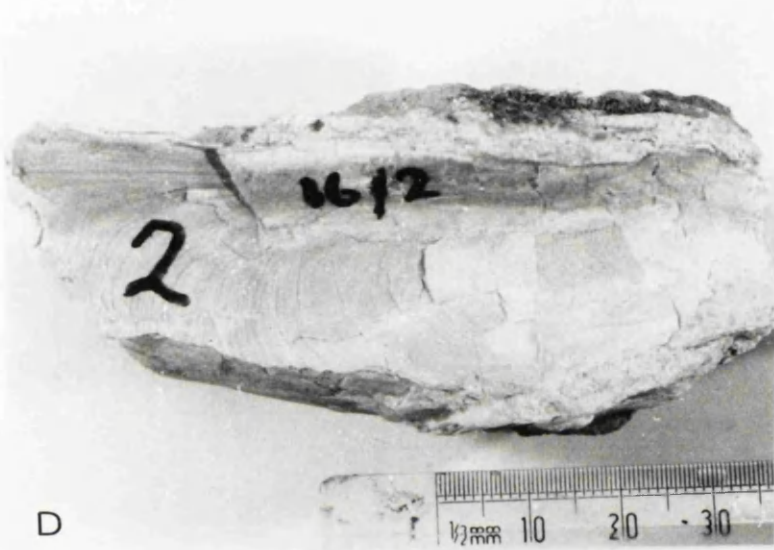
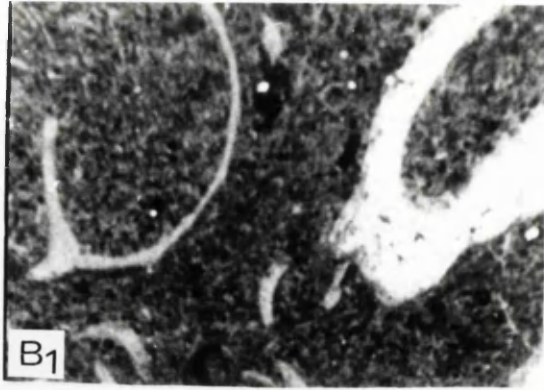
6.5.3.1 Bivalve Lime-Packstone Microfacies (M23F5)

The microfacies (Plate 6-6,A) forms massive lenses occurring in section 61, with a thickness reaching up to 8

Plate (6-6) : The bivalval facies (F5) .

- A - Bivalve packstone microfacies (M23) X20 .
- B - Bivalve bryozoan packstone microfacies (M24).
B1, X20, bivalve shells with minor bryozoa.
B2, X20, associated with bryozoan growth .
- C - Hard bed of bivalvan bryozoan packstone microfacies (M24) in Gabal El Maskara, east of El Tebbin area .
- D - Elongate bivalves characterises the bivalve bryozoan packstons microfaces, at top of Wadi Hof section (16) east of the Helwan area .
- E - Large conical gastropods associated with the bivalve bryozoan microfacies (M24), at the same locality section (16), as above. (Scale in mm.) .

PLATE 6-6



meters. It is interbedded in a cyclic manner with other microfacies. At Gabal Tarbul and Tarbul Abu Khashirat, the microfacies forms tongues within other microfacies units. The bivalves are found horizontally aligned at the base of the beds, but gradually change upwards to vertical orientations which could be due to insitu preservation. The vertically oriented valves might be produced on intertidal flats with flood and ebb currents (Reineck and Singh, 1980, p. 157.) or by tidal currents (Grinnel, 1974). The bivalves are represented by *Lucina* cf. *qurnaensis* type.

The main constituents are, well preserved bivalve (up to 12%), benthonic foraminifera (up to 4%), shell fragments (up to 7%), detrital quartz (up to 9%), miliolids (up to 1%). All are embedded in a micritic lime-mud matrix (up to 68%). The beds are disturbed by vertical gypsum veinlets.

The microfacies probably reflects deposition in intermittently agitated water with an energy index of (EI)=2.

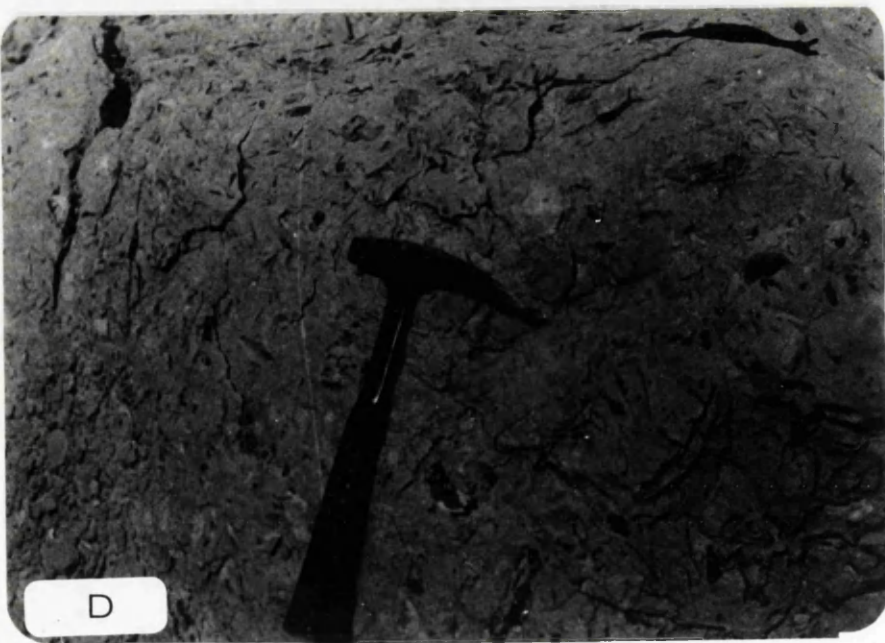
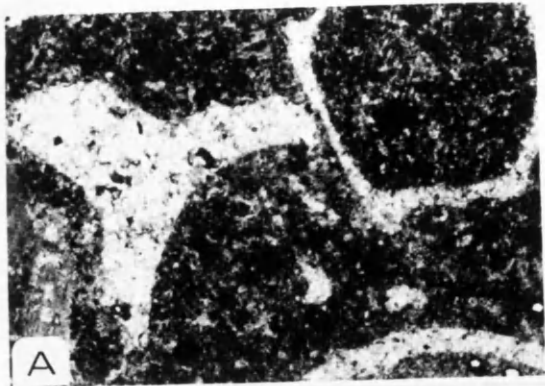
6.5.3.2 Bivalve Bryozoan Lime-Packstone Microfacies (M24F5)

This microfacies (Plate 6-6,B) consists of white limestone with an abundance of elongate bivalve shells of the *Arcopagia grandis* type. The thickness of this microfacies reaches up to 6 meters thick near the top of section 16. This thickness decreases in all directions and is reduced to 1.6 meters thick in section 49 where the microfacies is represented by a hard bed (Plate 6-6,C).

Plate (6-7): (Bivalval facies association "F5")

- A - Bivalve lithoclastic wackestone microfacies (M25) X20. The matrix is composed of fine intraclastics with some bioclastics . The whole microfacies has large lithoclastic nodules .
- B - Bivalve dolomitic wackestone microfacies (M26). The bivalve shells remain unstained with some parts of the matrix due to dolomitization .
- C - Coarsening-up throughout the bivalve lithoclastic wackestone microfacies (M25) at Wadi Hof area .
- D - Boulder of bivalve dolomitic wackestone microfacies (M26) . Dark colours are due to dolomitization which replaced the bivalve shells, of higher porosity , more than the matrix .

PLATE 6-7



The microfacies is characterized by its highly cross-bedded stratified strata. The bivalve shells range in size (Plate 6-6,D) from 12-15cm long and up to 5cm width and decrease in abundance vertically. The main components of this microfacies are bivalve shells 10-30%, conical large gastropods 2% (Plate 6-6,E), fine nummulites 5%, Bryozoa 5%, shell debris 20%, marly micrite matrix 14%, and micrite cement up to 35% with some rare echinoid shells. The energy index is estimated at (EI) = 3, which reflects slightly agitated water.

6.5.3.3 Bivalve Lithoclastic Lime-Wackestone Microfacies

(M25F5)

This microfacies (Plate 6-7,A & C) attains a thickness of up to 1.20 meters and is represented by white limestone at section 16. This microfacies occurs beneath the previous bivalve packstone microfacies and also reappears above this microfacies but with coarser lithoclasts. The lithoclasts consist of reworked subrounded to well rounded nodules which range in length from 5-17cm. Within the lithoclast nodules, the microfacies contains some rare bivalves and abundant shell fragments with some fine nummulites. The microfacies also shows reverse grading (Plate 6-7,C). This microfacies seems to decrease in thickness westwards in the East Helwan area, and has disappeared completely southwards in section 49. The microfacies has a sharp contact with the lower and upper

microfacies. It is believed that the microfacies has been formed by deposition in moderately agitated to strongly agitated water with an energy index (E1) around 4-5.

6.5.3.4 Molluscan dolomitic lime-wackestone microfacies

(M26F5)

This microfacies (plate 6-7, B & D) forms boulders of one to 3 meters long and up to 1 meter thick, arranged in horizons at Gabal Hamret shaibun and the east Helwan area in sections 16, 17, 18, 48 and 49. The main constituents are mainly molluscan debris 15%, other shell fragments 21% and some small nummulites 6%, rock fragments 2%, embedded in diagenetic dolomicrosparite matrix. The components within the boulders (Plate 6-7) show the same horizontal orientation as the components of the matrix between the boulders which consist mainly of nummulites and bivalves. The boulders also have sharp irregular contacts and weather brown. This microfacies can be traced at three different levels in the above mentioned localities in sections 49, 17, 18, and 48 of the east Helwan area.

In the Beni Suef area (section 61) the same microfacies seems to take another form (Fig. 6-10) and has detrital quartz (20-30%) with shell fragments up to 2%, bivalves 4% embedded in a diagenetic dolomicrosparite cement. The quartz grains are fine to medium sand size. They are, also, angular to subangular, and the components are stained by iron oxide. The microfacies, in particular

section 61, has boulders shaped with very hard brownish colour. It is overlain by unfossiliferous, very fine marly sands. An intermittently agitated environment, is believed, with an energy index (EI) of 2, for the deposition of this microfacies.

6.5.4 Depositional environment for the Bivalve facies

(Fig. 6-12)

This association probably formed on a shallow wide platform (Fig. 6-12) or flat, behind the inner siliciclastic carbonate barriers (F4) with open circulation and very diverse fauna. The common occurrence of molluscs and foraminifera reflect water depth of a few meters to tens of meters (Flügel, 1982). Nummulite mud facies (F6) was the main component of this carbonate platform or flat. Distributary channel feeders (F3) were cut through. Exotic blocks of (one meter thick and 3 meters across) boulders form (M26F5) form the base of the major facies. These boulders were thought to be formed during block sliding and erosion of the inner uplifted bivalval beds. That uplift is believed to be caused by tectonic effect on the upper shelf of the studied basin. This is demonstrated from the similarity of the boulders content and the host microfacies. That leads to the conclusion that the lithified substrata of the upper nummulitic bivalval microfacies, had been uplifted to the intertidal zone, where they were dolomitized, then reworked and carried

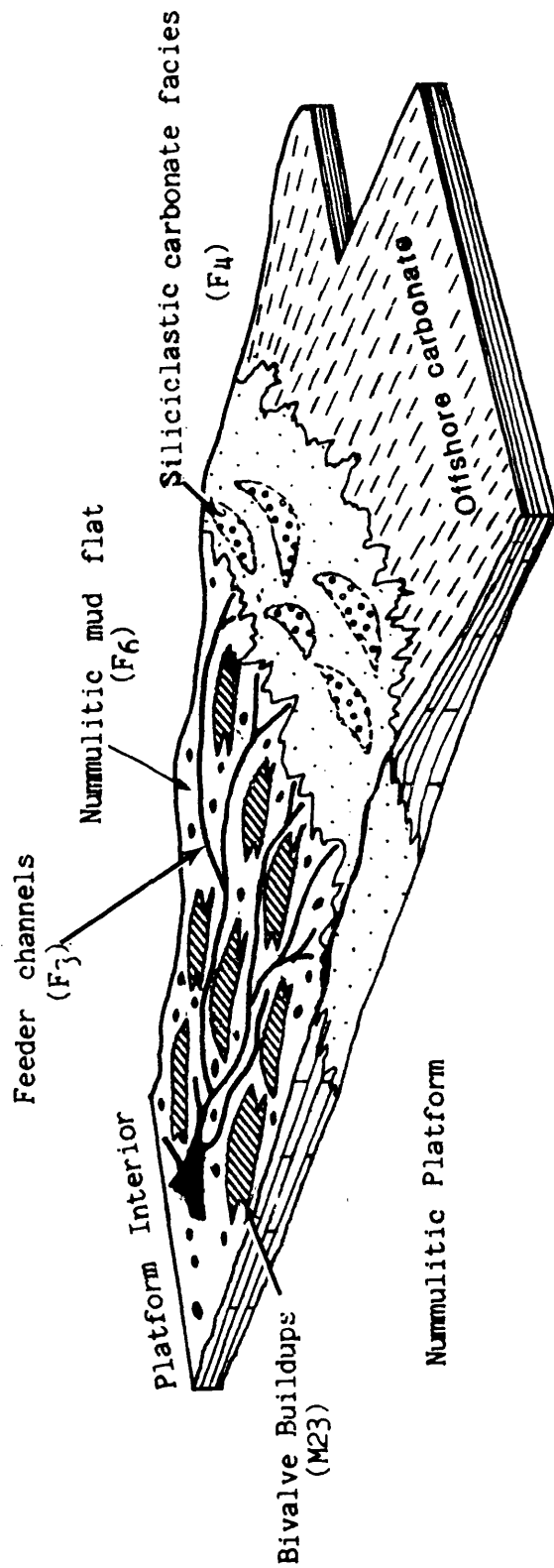


Fig. (6-12): Inferred idealized diagram illustrating the bivalve build up facies on a nummulitic carbonate platform, crossed by feeder channels. Note relationship between the bivalval facies and the other facies.

seaward as synsedimentary boulders. Renewal of the tectonic pulses was responsible for the upwards reappearance of this microfacies. The wide nature of the platform and the abundant occurrence of the bivalve fauna has contributed to the accumulation of wide patchy bivalve packstone build-ups (M23F5). These build-ups contain infauna bivalves and reflect intermittently to slightly agitated water energy. The molluscan framework of these buildups sometimes contain bryozoans which encouraged trapping of nummulites and other gastropod shells (M24F5), (Fig. 6-11). In section 16, a lithoclast and bivalve rubble wackestone (M25F5) which accumulated at the base of the build-up has acted as an initial thicket for the growth of the build-up. A similar accumulation of molluscan build-ups was recorded by Sander, 1936; Schwarzacher, 1948; Banerjee, 1959; Illing *et al*, 1965; Wilson, 1975 and Scholle *et al*, 1983.

In the East Helwan area, the build-ups are topped (Fig. 6-11) by the bivalve lithoclast wackestone rubble which could represent the subaerial exposure of these particular areas. However, the unfossiliferous marl in the Beni Suef area which occurs above the bivalve build-up might reflect the progradation of the shore sediments.

6.6 Nummulitic Facies (F6)

6.6.1 Description

This facies (Fig. 6-13) is yellowish to white on fresh surfaces (Plate 6-8,A) and has a pale greyish green or brownish colour on weathered surfaces (Plate 6-8,B). The thickness ranges from 1.7 to 7 meters and can be repeated in different horizons within a vertical succession. The facies is represented by dense beds of nummulites with a detrital quartz content. The southern sections of the studied basin show an upward increase in grain size, while the northern sequences are normally graded (Plate 6-8,C). The facies is sometimes overlain by the bivalve lithoclastic wackestone microfacies which also contains some bioclastic sandy pockets. The biotic content includes operculines (large foraminifera), bryozoa, echinoderms, serpulid worms, occasional molluscs, and microforaminifera. Pellets commonly occur in this facies. The depositional texture for this facies ranges from wackestone to packstone. This texture may reflect deposition in intermittently to slightly agitated water conditions. This facies is represented by massive and large wedged beds which have a sharp contact with the underlying Bivalve Facies (F5) and the overlying Facies.

6.6.2 Distribution

The facies is encountered in section 61, 60, 51 and 10, within the upper part of the Tarbul Member in Beni Suef

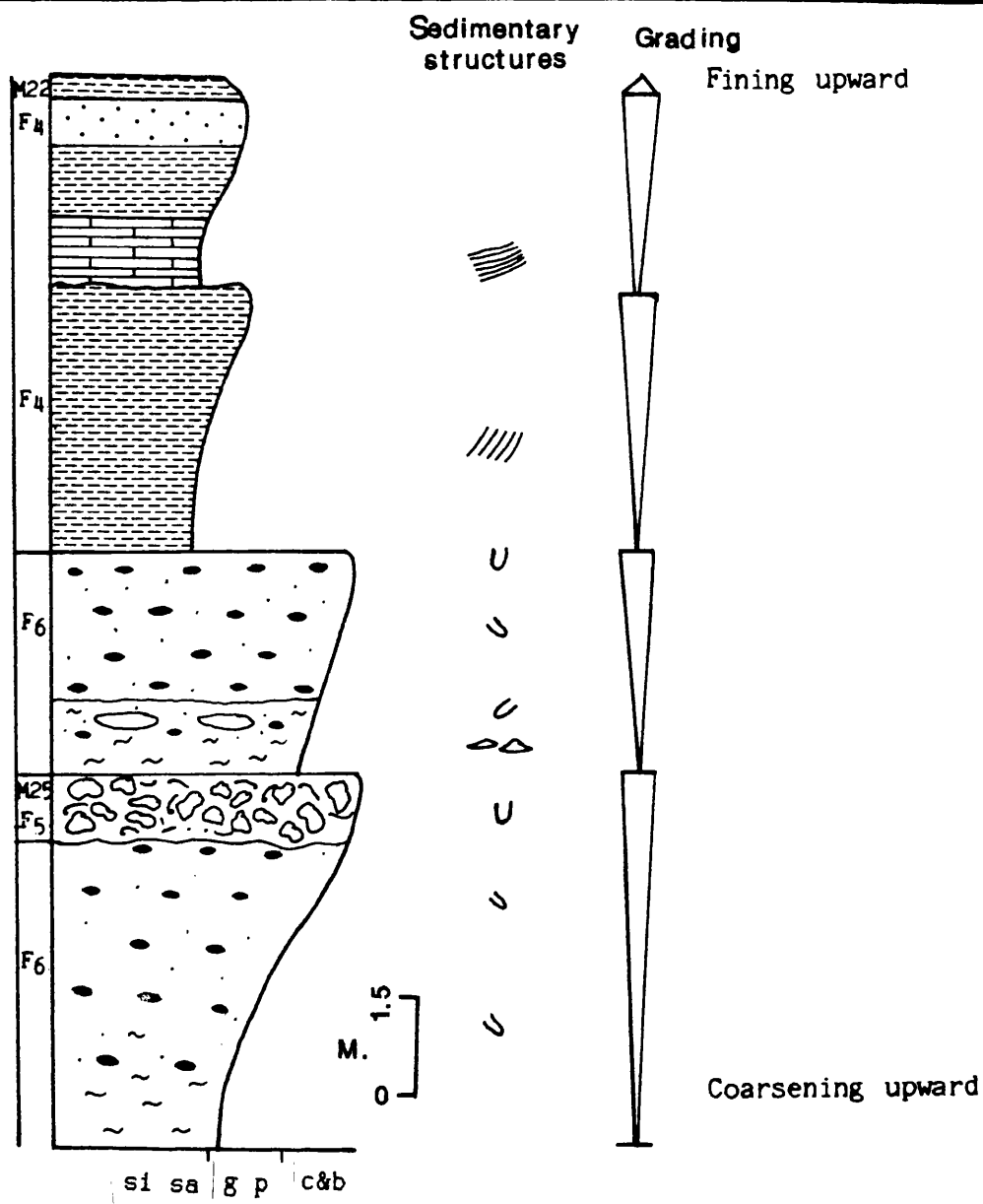


Fig. (6-13): Graphic log of the sequence of nummulitic facies (F6) and facies associations in section 61.

Plate (6-8) : (Nummulite facies "F6")

- A - Nummulite facies (F6) in fresh surface with dense shells of nummulites and few bivalves.
- B - Nummulite facies (F6) with pale-grayish green to brownish colour on weathered surface .
- C - Normally graded nummulitic sequences at east of El-Tebbin area , (northern part of the studied basin) .



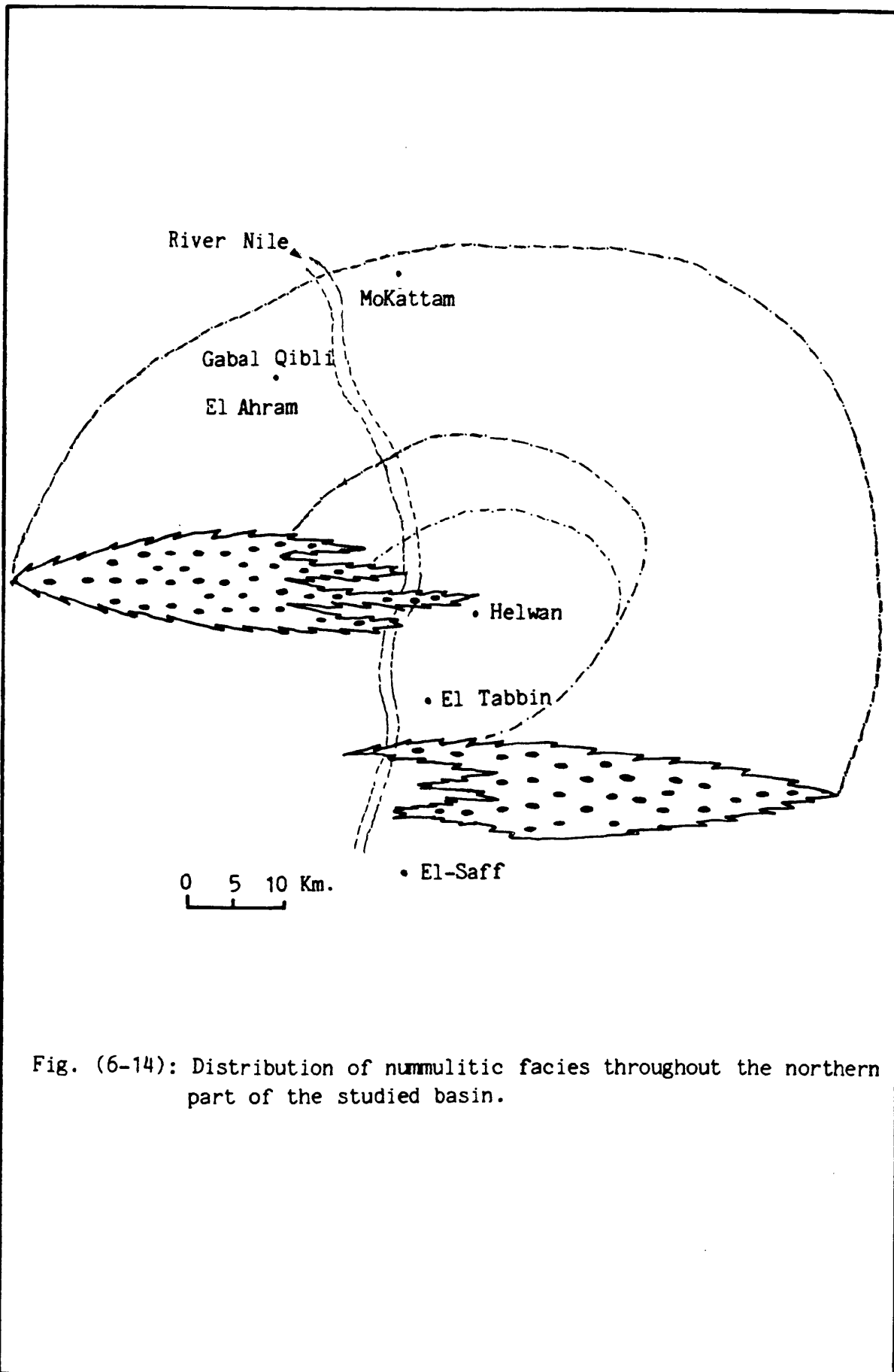


Fig. (6-14): Distribution of nummulitic facies throughout the northern part of the studied basin.

to the El Saff area. It also extends westward in section 82 of Birket Qarun and Gar Gehannam sections. The maximum recorded thickness of that facies is at Gabal Hamret Shibun (Section 61). This thickness decreases away towards the south; east; and the north-western directions. In the northern parts of the studied basin, the facies is concentrated towards the periphery of the basin in thick wedges which thin towards the inner parts of the studied basin, where it is repeated in different beds. The facies occurs in sections 44, 56, 48, 4, 49, 16, 17, 18, 64 and 40. Thus this forms an almost arch-shaped body (from south Mokattam through Gabal Giushi, south east Helman and the El Saff areas) which spills out in different tongues towards the basin centre (Fig.6-14). The microfacies is represented also in the central part of the basin by a very thick sequence. This is characterized by deformational slump structures which are noticed in very wide areas.

6.6.3 Microfacies associations

The following microfacies (Plate 6-9) have been recorded which are associated with the nummulitic facies (F6):-

1. Nummulitic arenaceous lime-wackestone to packstone microfacies (M27F6)
2. Nummulitic echinodermal bryozoan lime-packstone microfacies (M28F6)

6.6.3.1 Nummulitic arenaceous lime-wackestone-to-packstone
microfacies (M27F6)

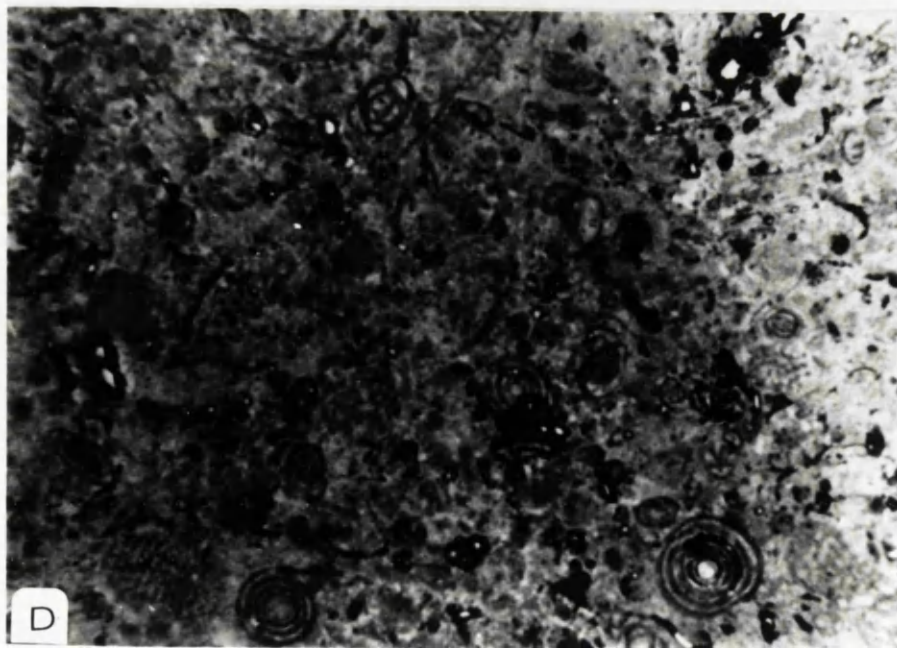
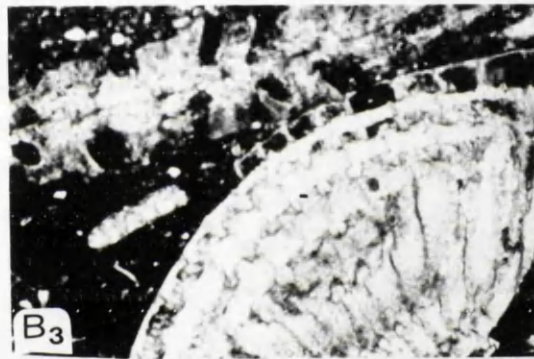
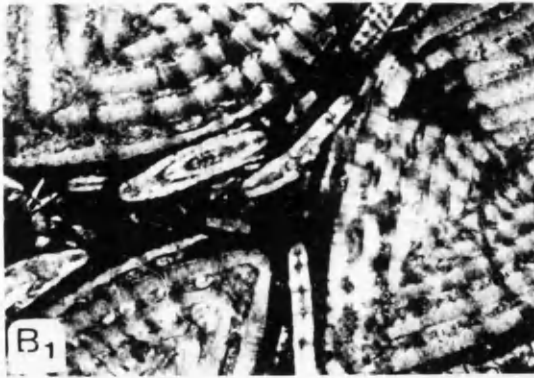
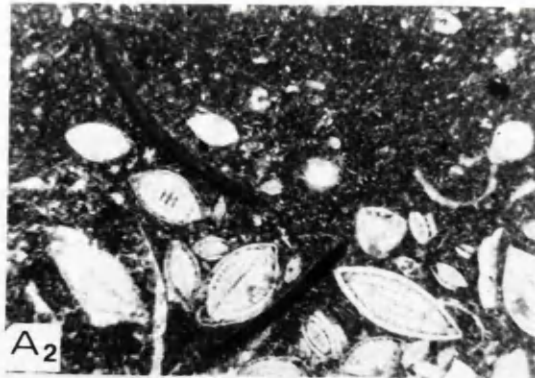
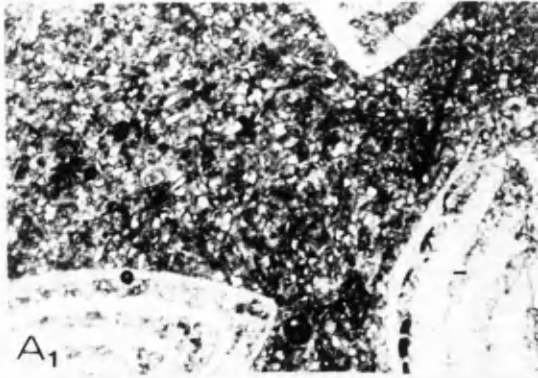
The microfacies (Plate 6-9,A) is represented by massive lenses and tongues in section 61, 60, 10 and 82. It reaches about 6.2 meters thick and its thickness decreases upwards. The main constituents are *Nummulites striatus* (4-20%), operculines (1-4%), gastropods (up to 15%), pelecypods (2-4%), bioclastic debris (20-25%) and detrital quartz (7-25%). These components are embedded in a lime mud matrix (about 19-57%). The shell fragments are replaced by sparry calcite. The detrital quartz grains are angular to subangular, of medium to fine sand sizes. The Nummulites and quartz detritus increase upwards in grain size. Miliolid rich nummulitic submicrofacies is also recorded in places (Plate 6-9,D). The microfacies is highly bioturbated with inclined burrowing. It reflects probably deposition in slightly agitated water with an energy index of (EI)=3.

6.6.3.2 Nummulitic echinodermal bryozoan lime-wackestone-
packstone microfacies (M28F6)

This microfacies (Plate 6-9,B) is well represented in the northern part of the studied basin. It forms hard massive lenses or sheets (1-5 meters thick) at Gabal Giushi, section 56, 48, 4, 49, 51, 16, 17, 18, 51 and 40. In the east Helwan area, it forms a very thick repeated succession with slump structures. The main constituents

Plate (6-9) ; (Nummulitic microfacies association "F6")

- A1 - N.arenaceous lime-wackestone packstone microfacies (M27). the matrix around the nummulite shells is made of quartz sandy detritals . X20 .
- A2 - Normal grading in thin section of nummulitic facies composed of nummulite and bioclasts (echinoderms spines and molluscs) . X12 .
- B - N.echinodermal bryozoan lime wackestone-packstone microfacies (M28), X20. B1,with nummulite (larger) and oprculina (smaller).. shells . B2, with echinodermes spine. B3, with bryozoa and bryozoan coated nummulites.
- C - Algal pigments within the nummulitic shell chambers appear as dark rounded spots. X80.
- D - Miliolid rich subnummulitic microfacies occurs towards the shallow parts of the nummulitic shelf . X30 .



are nummulites (9-50%), detrital quartz (5-7%), echinoderms (3-12%), Bryozoa (5-10%), shell fragments (3-8%), benthonic foraminifera (up to 2%), and rare miliolids. The components are embedded in a lime-mud matrix (up to 60%). The nummulite shells are always represented by small sized (0.2-0.4 cm) shells. The nummulites recorded in the Wadi Hof area are found to have micro algal pigments (Plate 6-9,C) within their shell chambers. This pigment allows use of the more penetrating light rays. As photosynthetic organisms are susceptible to destruction by intense light, this could reflect a deeper depositional environment for this particular locality (Tappan and Loeblich, 1971). In the same area, the percentage of nummulite shells is noticed to increase upward in a vertical section which may reflect upward coarsening of the sediment. The microfacies is generally bioturbated and has more gravel size, terrigenous material near the top. The microfacies indicates deposition in a slightly agitated water with an energy index (EI) of 3.

6.6.4 Depositional environment of the Nummulitic facies

(F6)

The occurrence of small shell nummulites with bryozoa molluscan shells, and some benthonic foraminifera within the deposits of this facies as well as the above mentioned characters for the microfacies association, may represent a shelf or upper platform for this facies. Pokorny, 1963,

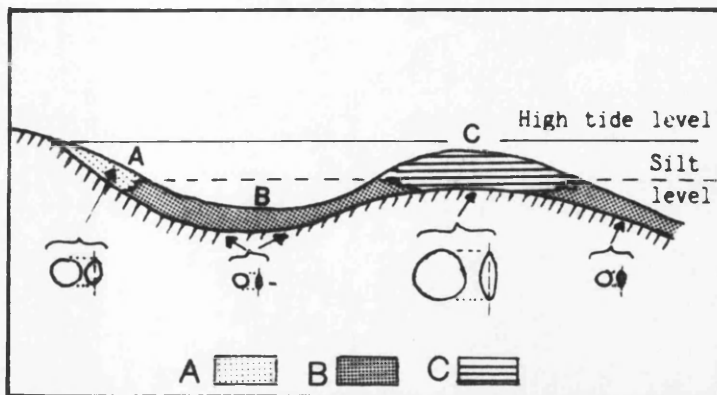


Fig. (6-15): Distribution of nummulites according to their size variation in the neritic zone.

- A - Middle size N. facies.
- B - Small size N. facies.
- C - Larger (or bigger) N. facies
(after Nemkov, 1962).

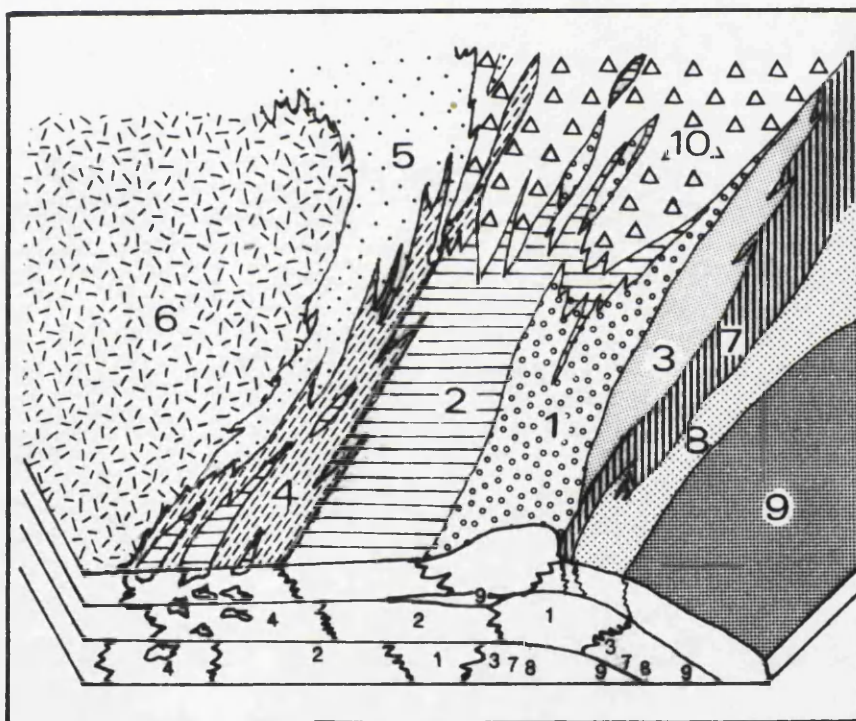


Fig. (6-16): Distribution of small nummulites around nummulitic banks.

- 1. Large shells of N. bank facies
- 2. Facies of small nummulites
- 3. Facies of thin-shells of nummulites
- 4. Lagoonal facies with Orbitolites and Alviolines
- 5. Miliolid facies
- 6. Evaporite and Dolomites
- 7. Facies with Operculina (after Arni, 1965)
- 8. Micro-benthonic foraminifera facies
- 9. Pelagic Globigerines facies
- 10. Peneroplidae facies

stated that the family Nummulitidae is limited to shallower parts of the neritic zone and to the bathyal facies. Houbolt, 1957, and Tlell, 1972, reported nummulites rich limestone in water depths ranging from 14 to 20 meters. Arni, 1965, recorded (Fig. 6-16) the small thin nummulites behind the bank's edge, and if mixed with *operculina*, to occur in the offbank facies. The same phenomenon was recorded by Nemkov, 1962; Bignot, 1972 and Decrouez and Lanterno, 1979 (Fig. 6-15). The facies characters of the Nile Valley Egypt strongly support the distribution concept of this facies from the inner shelf, with the nummulitic arenaceous wackestone (M27F6) microfacies, through the outer shelf, with the nummulitic echinodermal bryozoan wackestone-packstone (M28F6) microfacies (Fig. 6-17).

The shallow part of the shelf is characterized by the miliolid rich submicrofacies (Plate 6-9,D). In the Atlantic and Pacific borders of North America, it is found that miliolid forams occur in shallow water zones (0-5 meters) with a temperature ranging from 0°C to 27°C (Moore et al, 1952 and Moore, 1964). Miliolid facies, also, occurs in the landward areas of the shallower parts of the shelf, when they associate nummulitic banks (Arni, 1963; Fig. 6-16) and represents the restricted platform environment (Flügel, 1982).

In the studied area, a warm restricted shallow shelf subenvironment is therefore assumed to form a nummulitic miliolid sub-microfacies. This offshore subenvironment

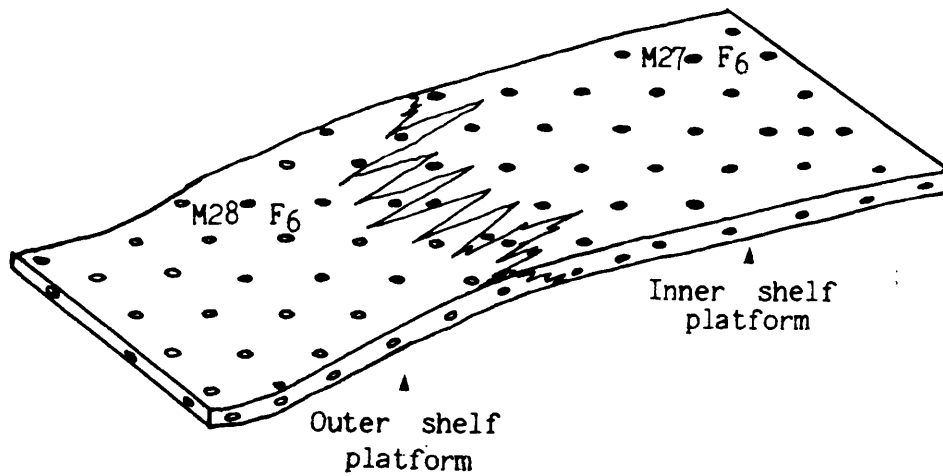


Fig. (6-17): Inferred diagrammatic representation of the nummulitic microfacies through the shelf.

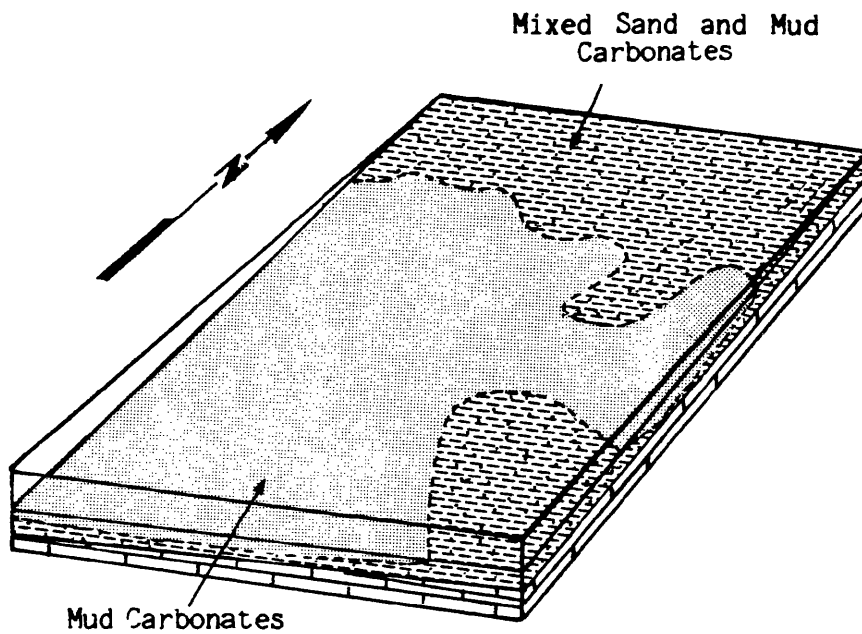


Fig. (6-18): Schematic representation of Carbonate matrix distribution in contemporaneous to the nummulitic shelf facies deposition.

occurs in patchy areas outflanking the Middle Mokattam basin. The abundant occurrence of that recorded submicrofacies offered a very distinctive field phenomenon which is used to detect the landward shore.

The occurrence of siliciclastic detritus with these nummulitic facies may reflect storm wave sedimentation which affected these facies. This can be demonstrated by the mass accumulation of the foraminifera (reported in Giushi by Abdel-Kireem, 1985) bryozoans, molluscs, echinoderms, and mud pebbles. The beds of this facies exhibit sharp or erosional boundaries. The sediment, also, contains bioclasts which may be derived from various ecological environments. Sometimes these shells occur as lag deposits.

The shelf nummulitic facies seems to have two types of matrix, both storm derived: the mixed sand and mud, and the mud, carbonate matrix (Fig. 6-18). The distribution of these types of matrix, as reported by Kulm *et al*, 1975, is mainly controlled by sediment supply and physical and organic reworking. Mud carbonate is found to occur on the middle and outer shelf (Fig. 6-18) and the mixed sand and mud carbonate, are located on the inner and outer shelf. The distribution of the recorded microfacies was found closely related to the shelf floor ground matrix. The first microfacies (M27F6) is formed on the mixed sand and mud, carbonate shelf while the other (M28F6) microfacies characterized a mud carbonate flat subenvironment. The Westphalia limestone (Pennsylvanian) of Kansas was

formed in the same way (Ball, 1971), and also the Oregon-Washington shelf (Kulm et al, 1975). Similar interpretations are also mentioned by Wilson, 1975; Johnson, 1978; Sprecht and Brenner, 1979 and Flugel, 1982.

In a palaeoecological assessment, Liebau 1980, recognized that water agitation can produce storm wave base at depths ranging from 40 to 80 and up to 200 meters in marine platform slopes.

The studied nummulitic shelf was probably sometimes affected by syndepositional tectonics which might have increased the shelf gradient. This could be demonstrated from the occurrence of slumped nummulitic facies, debris flow deposits and growth faults, associated with the deeper nummulitic facies in the deeper areas of the studied shelf.

6.7 Pelletal Facies (F7)

6.7.1 Description

The pelletal facies has a yellowish grey colour and is represented as a bedded succession of hard (30-50cm thick) and medium hardness (20-30cm) beds. The average thickness of this facies is about 20-25 meters, repeated several times in the same locality. Cross lamination and burrowing (inclined types) increase upwards. Both normal and reverse grading are recorded. The main components of this facies are the pellets mixed with some fine nummulite shells and microforaminifera, sometimes molluscs, reworked miliolids and shell fragments. The depositional texture which

characterizes this facies is mainly packstone. The facies has sharp contacts with other facies and occurs as thick lobes or sheets.

6.7.2 Distribution

The occurrence of the pelletal facies, in the studied area, is found restricted to the main central part of the studied basin. It extends from east of the El Tebbin area throughout the Wadi Hof area and northwards to Kattamia Road (sections 2, 4, 5, 16, 17, 18, 48, 49, 59, 62 and 63). In these areas the pelletal facies form the majority of the Giushi Formation of the Lower Mokattam and the Qurn Formation of the Middle Mokattam Units. The facies sediments are also represented in some tongues, in sections 51, 60 and 40, radiating towards the outside areas of the studied basin.

6.7.3 The Microfacies Association

This facies is represented by one microfacies only:-

1. Pelletal nummulitic lime-packstone microfacies (M29F7)

6.7.3.1 The pelletal nummulitic packstone microfacies

(M29F7)

This microfacies (Plate 6-10) occurs in abundance from the area between the Wadi Hof and Gabal El Maskara. This pelletal bearing facies belongs to the Qurn Formation. The microfacies also occurs with the Giushi nummulitic facies.

Plate (6-10) : (Pelletal microfacies associations "F7")

- A-- Pelletal nummulitic lime packstone microfacies (M29). Note internal structure of the original grains (mostly micro-forams) within the micritic outlines of the pellets themselves. X20 .
- B - Pelletal microfacies, at Wadi Hof area, highly densed packstone. X40 .
- C - Pelletal nummulitic packstone with bryozoa. Gabal El-Maskara, east of the El-Tebbin area. X40 .
- D - Pelletal nummulitic packstone (M29). Note recrystallization of the original micritic matrix. X40.
- E - Organized turbidite submicrofacies show some degree of stratification . The disturbed beds have residedmented intraclastic carbonates. These could be originated from long distance transport process (Stow,1986, Mutti & Normark,1987). It intercalate the pelletal microfacies at east El-Tebbin area.
- F - Dish structure associated with the turbidite sediments. The lower part shows residedmented clastic carbonate and disturbed slumps . The upper part of the photo indicates faint dish structures . These structures are believed to be formed as a result of liquefied flow mechanism (Stow,1986). Wadi Hof area.

PLATE 6-10

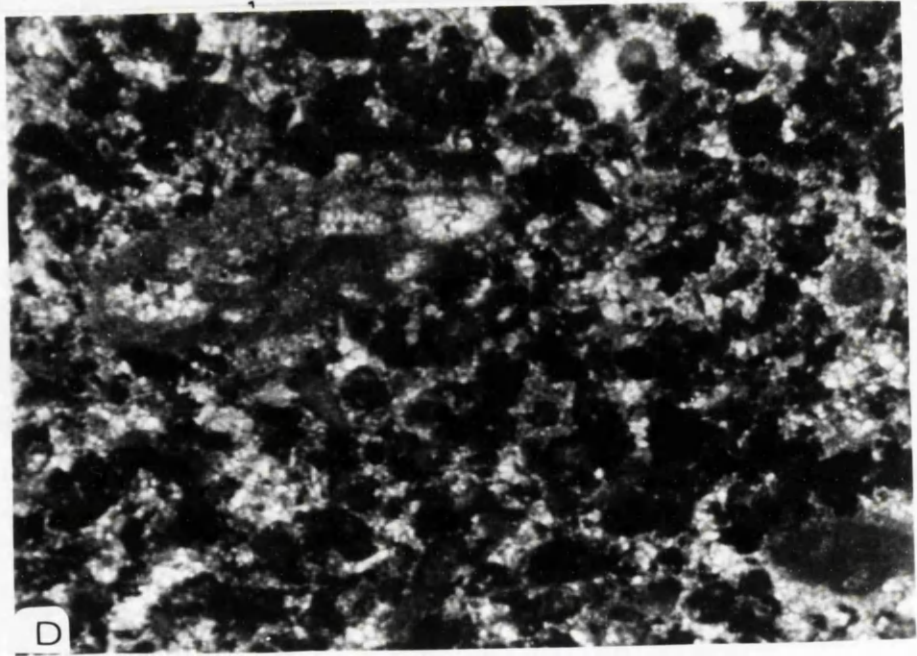
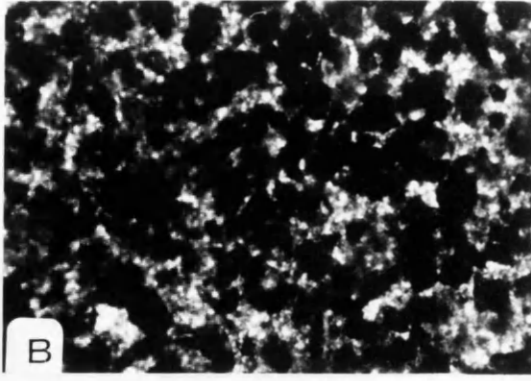
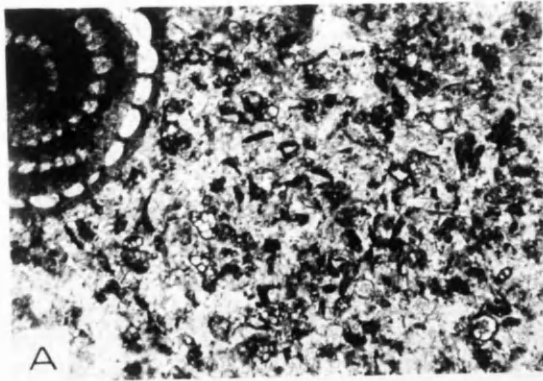
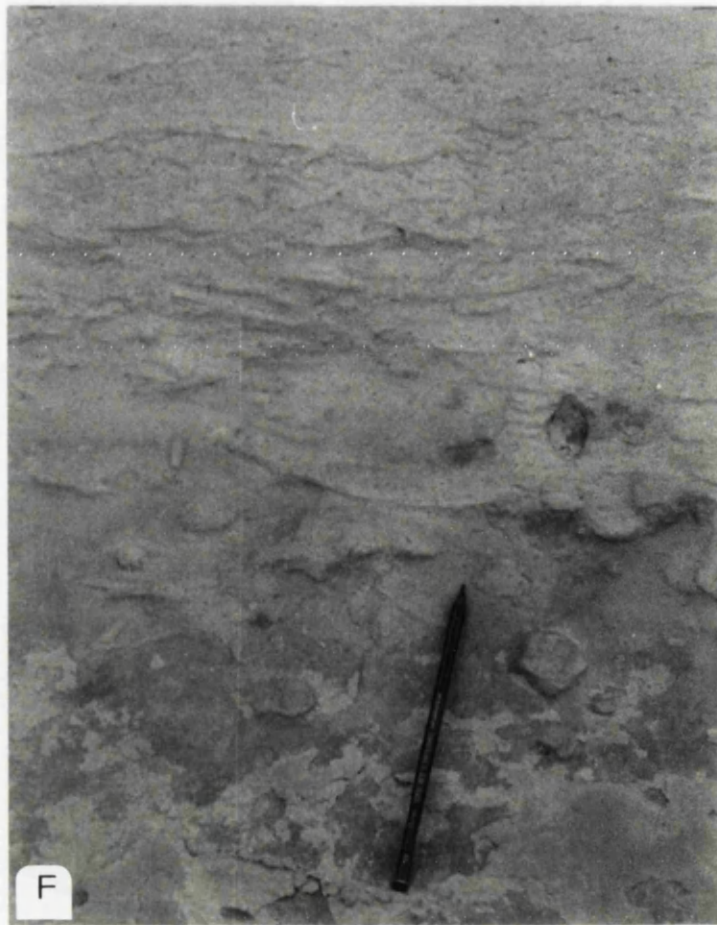
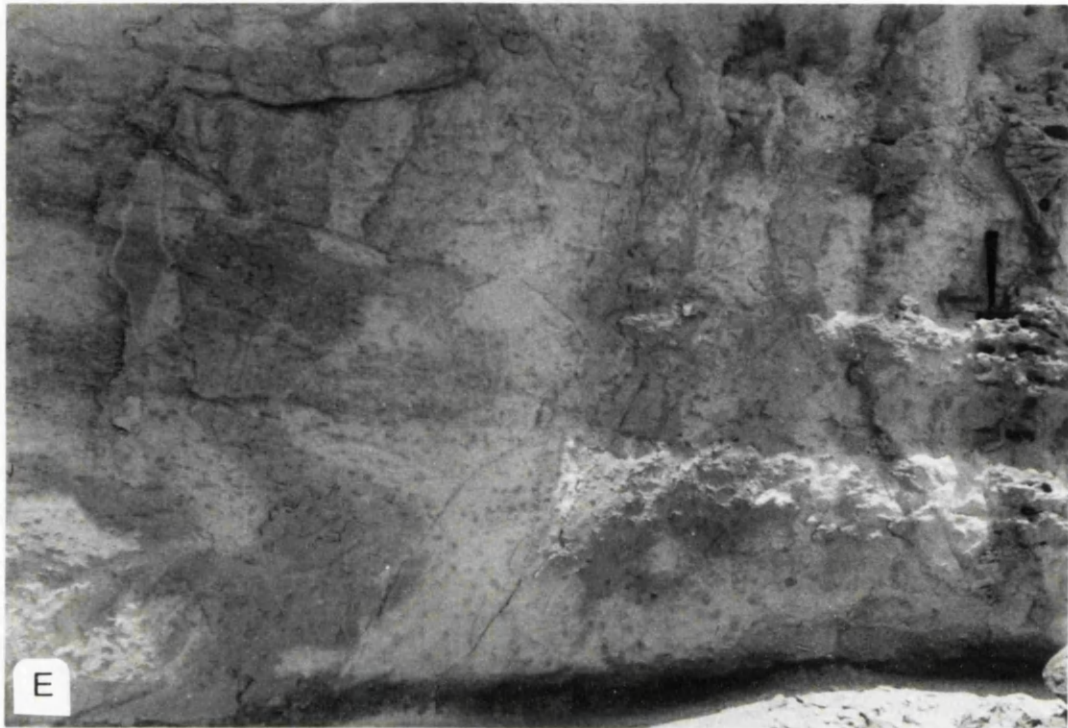


PLATE 6-10 (Continue)



It is represented by a well bedded coarsening-up carbonate sequence of thick and medium beds (25 meters thick) where the appearance of the nummulites increases towards the top of strata. This succession is followed by another fining up sequence of strata (20 meters thick) of hard (up to 70cm thick) and softer beds (up to 25cm thick). The microfacies reappears in different levels in 2 cycles when overlain by the fine bioclastic intraclastic turbidite sub-microfacies (Plate 6-10, E & F).

The main constituents of this microfacies are nummulites (1-8%), microforaminifera (3-15%), molluscan (3-10%), rare bryozoa (up to 5%), ostracods (1-3%), pellets (25-40%), and very fine shell debris (20-50%). The microfacies, also, contains lithoclasts and reworked miliolids. These grains are embedded in a micrite matrix.

The nummulite chambers contain green algae. The size of all grain components associated with this facies, is relatively smaller than the the size of the same grain types described with any other facies, in different localities. In the area of study, it was noticed, sometimes, that the internal structure of the original grains can be seen within the micrite outlines of the pellets themselves. That could lead us to believe that these pellets might have formed as a result of a primary stage of micritization of other particles or grains such as bioclastic grains, microforaminifera, and silty intraclasts. A similar conclusion was reached for

carbonates of different ages from different localities by Taylor and Illing 1969; Bathurst, 1971; and Blatt *et al*, 1972. Meanwhile, most of the recorded pellets are structureless, which could be produced as faecal materials (Leighton and Pendexter, 1962).

The grain components reflect deposition in water with energies ranging between slightly agitated and strongly agitated with an energy index (EI) of 3-5.

6.7.4 Depositional Environment of the Pelletal Facies

The microfacies association of this facies was probably deposited within a restricted shallow platform facies on a low energy nummulitic shelf (Fig. 6-19). Recent analogies are recorded from the Bahamas (Stockman *et al*, 1967; Shinn *et al*, 1969; and Ginsburg and Hardie, 1975) and the Persian gulf (Purser, 1973). Purdy, 1963 (a and b), records pelletal mud facies with the shelf lagoonal mud belt of the Bahama Bank. These pellets, in the modern shelf and lagoon carbonate, are thought to be formed under approximate limits of, near-surface, temperature from 30 C to 40 C, and salinity of 25 to 35‰ (Lees, 1975).

The restricted platform of the Giushi Formation, pelletal facies probably formed landwards of the shelf platform (Fig. 6-19) which lay to the north and east directions of the basin of deposition and was composed of miliolid and bioclastic, highly porous deposits. Sometimes, this pelletal facies is found to be mixed with the

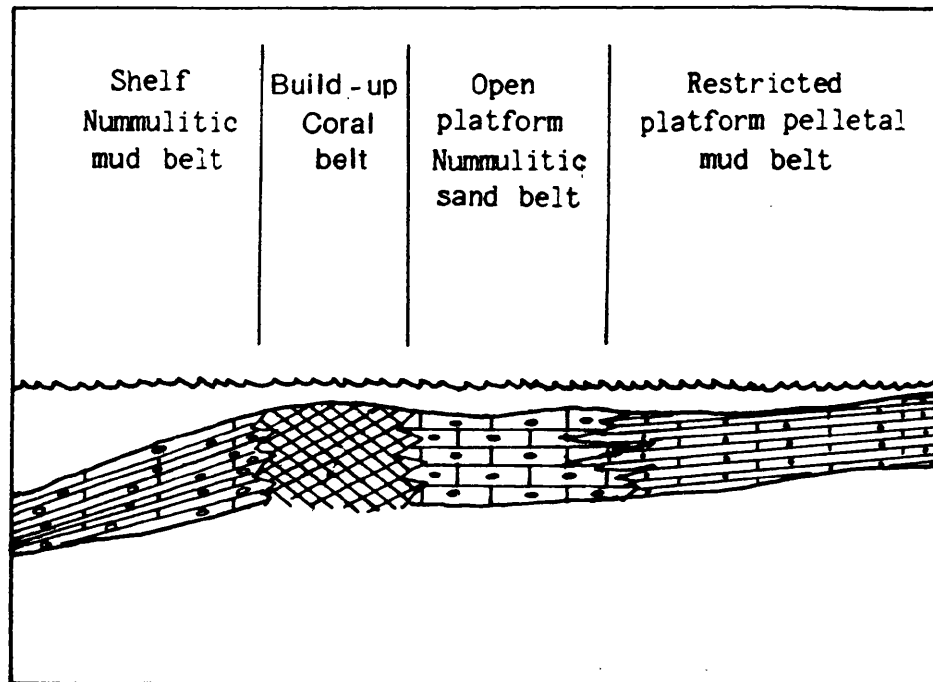


Fig. (6-19): Depositional model and distribution of the pelletal, nummulitic and coral facies along the late Eocene carbonate shelf of the Giushi formation, Nile Valley, Egypt.

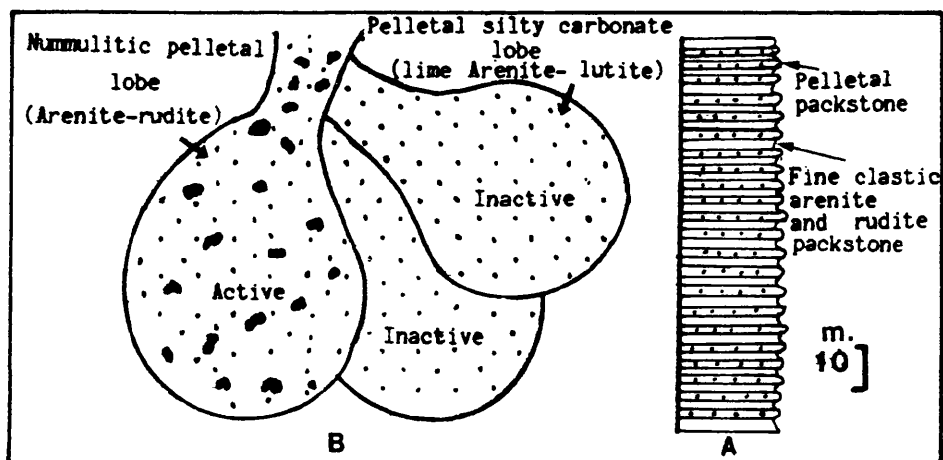


Fig. (6-20): Model of growth (A) and lateral avulsion (B) of the pelletal fan lobes, and sequence characteristic of inactive pelletal lobe of deep water plain facies.

nummulitic, open platform facies. This could be interpreted as the product of storm washover which introduced sheets of these sediments into the open sandy nummulitic platform. Such storm pelloidal deposits were described by Ball, 1967 in Florida and the Bahamas.

The concept of the restricted platform deposition of the pelletal facies, appeals in its overall treatment of the sedimentation processes of the Giushi pelletal facies in the Mokattam area, but fails to explain the occurrence of thick beds or succession of pelletal materials, having been transported primarily in suspension, in the Wadi Hof area. These thick deposits are believed to be formed in a deeper environment for some reason. Of these, the pelletal beds, in some places, intercalate with pelagic facies, slumped nummulitic, and spiculitic calcisiltite facies, which are all of deep deposition. The common occurrence of intraclasts and absence of extraclasts within that microfacies, could suggest deep water with no or only sluggish bottom currents (Wilson, 1969, 1975). The association of the pseudoplankton serpiolid may also indicate deeper water (Gall, 1983). Moreover, this could be supported from the preservation of some algal pigments of deeper water within the associated nummulitic shells (Tappan & Loeblich, 1971). Furthermore, this pelletal facies merges with turbidite deposits which reflect deeper environment (Plate 6-10, E & F).

The above mentioned facts with the facies characters,

suggest that the pelletal facies, in that particular area, must have been deposited in a deeper basin. However, the occurrence of intraclasts and reworked miliolid shells, with this pelletal facies, retains their shallower identity. That might lead to the belief that these pellets were derived from upslope shelves which flanked the deeper areas. This is clearly supported from analogous facies described by Bishop (1968) and Wilson (1975).

The intercalation of pelletal facies and both slumped and pelagic facies, may reflect accumulation during phases of tectonic activity. These phases might have disturbed the upper pelletal platform and increased the shelf gradient causing the suspended pelletal sediment spill over into the basin. That, presumably, could mean a fine reflux coming through deep fans (Fig. 6-20,B) at that time, to form this type of pelletal facies.

Isolated recorded sequences as inactive quiet lobes (Fig. 6-20 B) of completely pelletal facies and fine silty carbonate might represent a more distal phase of deep water plain deposits. A further possibility is a lateral shift in the locus of the fan sediments, leaving these thick. These inactive lobes could be demonstrated from the occurrence of finer-grained and poorly sorted pelletal deposits adjacent to more coarse pelletal ones. The finer lobes are interpreted as quite isolated suspended load deposition. However, active deposition shows more coarse material contribution due to connecting with the supplying fan

source (Rupke, 1978). These alternations of active and inactive deep fan lobes might be the result of the same tectonic activity (Moore *et al*, 1974).

6.8 The Conglomerate Debris Facies (F8)

6.8.1 Description (Fig. 6-21, Plate 6-11)

This is composed of limestone debris of thickness of up to 3-4 meters. The debris consists of subrounded to rounded clasts and the size of each clast ranges from 7 to 30cm in diameter. The debris consists of nummulitic or bioclastic limestones. The matrix contains abundant nummulite, bryzoan, echinoderms and with some molluscs. The facies is highly bioturbated with inclined burrows and cross lamination. The facies has a wedge shaped geometry. The maximum thickness is recorded in the north western sections, and decreased in a south and south easterly direction. The size and angularity of the debris decreases in a southeast direction.

6.8.2 Distribution

This facies is very distinctive in the area studied especially in the central part of the basin, Wadi Hof to south El-Tebbin area. It also occurs in sections 48, 4, 59, 5, 18, 17 and 49. The facies is up to 4.5 meters thick at section 48 and is approximately 3.5 meters in section 49. The facies extends also farther south, but decreases in thickness and grain size, towards the El-Saff to Beni-Suef areas.

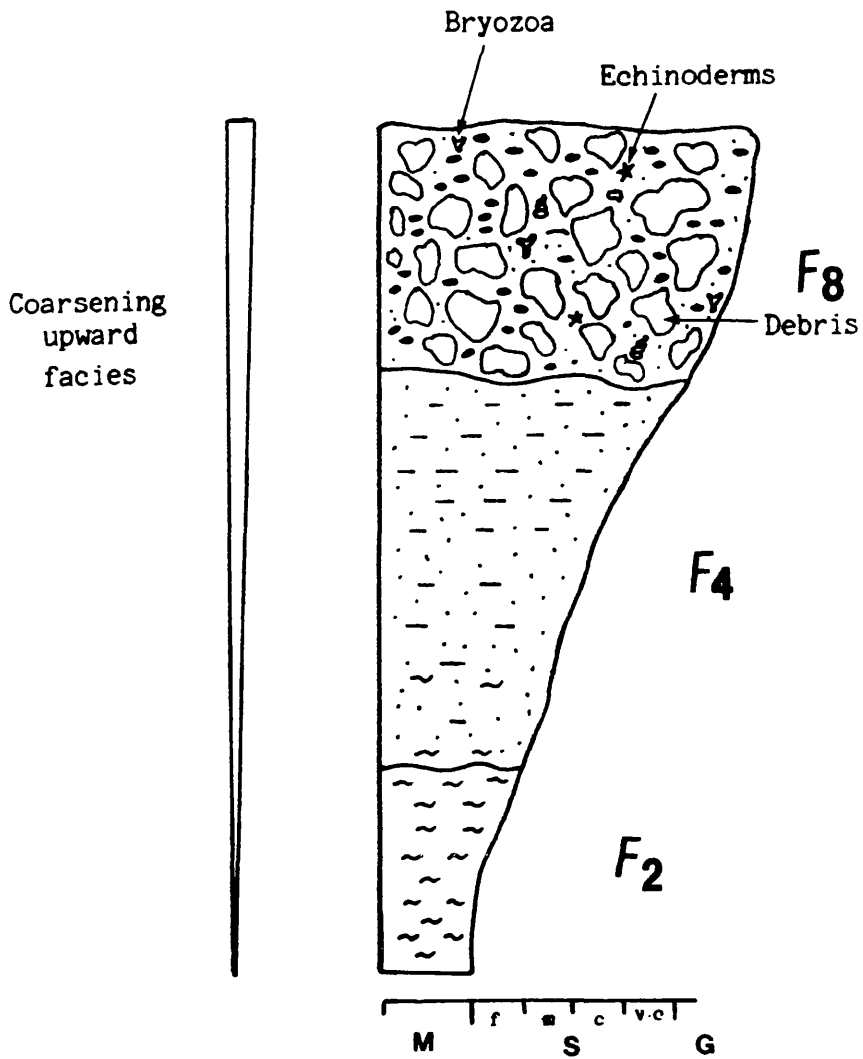


Fig. (6-21): Upward coarsening sequences of facies F₂, F₄ and F₈ in East Helwan area (section 49).

6.8.3 Microfacies association

The facies is represented by only one subfacies.

6.8.3.1 The conglomerate nummulitic lime-packstone microfacies (M30F8)

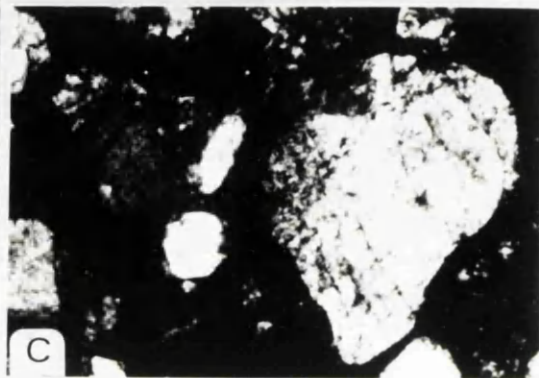
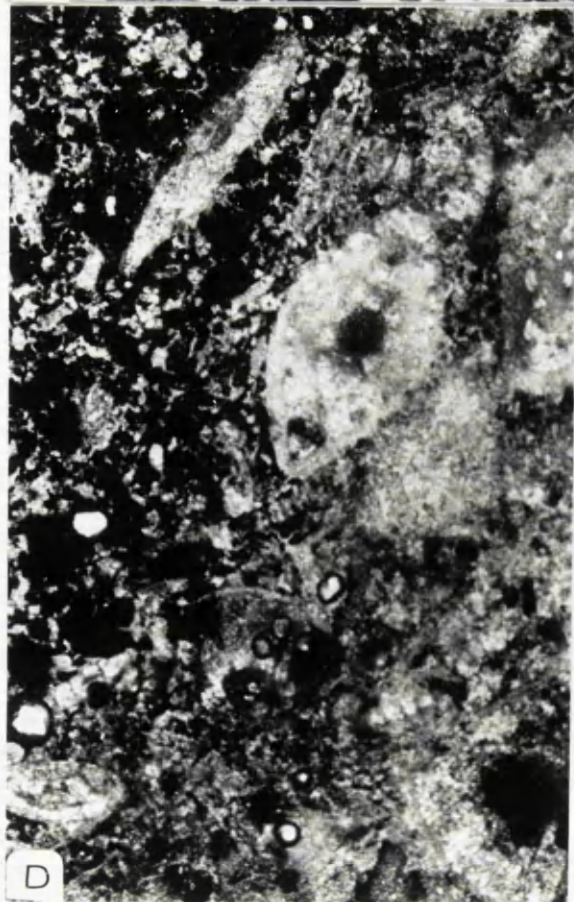
This microfacies (Plate 6-11) is well recorded, as mentioned, in the Helwan area. It can be described as a matrix supported facies, where all the debris is embedded in a matrix of nummulites (up to 50%), operculines (up to 3%), shell fragments (up to 10%), microforaminifera (up to 2%), bivalves (1%), gastropods (2%), echinoderms (up to 1%), bryozoa (1%), silty materials (4%), embedded in micrite matrix (up to 26%). The grains of the matrix have a well packed fabric with grain sizes ranging from very coarse sand to fine gravel. That fabric texture changes to wackestone in a south-east direction.

The debris themselves, contain pellets (up to 5%), operculines (up to 10%), microforaminifera (20%), bivalves (up to 5%), gastropods (up to 2%), ostracods (up to 2%), bioclasts (up to 15%), marly matrix (6%), and sparitic cement (up to 20%). Some debris has well washed grains. These grains are of coarse silty to fine sandy size with a grainstone texture.

The angularity and coarsening of debris increase in north west direction, which could suggest a north west source for all these facies. The biotic content of the debris could prove that all are derived from a unit not

Plate (6-11) : (Conglomerate facies "F8")

- A - Field photograph for the conglomerate nummulitic packstone microfacies (M30). Note the coarsing-up sequences of this microfacies. Section "48" Wadi Hof area.
- B - Close-up field photograph for the conglomerate facies at Beni Suef area. Debris are more rounded and smaller in size than in the previous (A photo) locality . Matrix is supporting the facies debris.
- C - Thin section for the nummulitic conglomerate packstone microfacies. Note occurrence of intraclasts and rare nummulites. X20 .
- D - Acetate peel, for the nummulitic conglomerate microfacies (M30) with nummulites, bryozoa, and shell fragments. X40 .



older than the Giushi Formation. The microfacies seems to be monomictic in places, but a close microscopic analysis, reveals a variety of clasts. Thus the clasts are polymictic but may have still been derived from several beds of one formation.

The facies reflects (Fig. 6-21) a general upward coarsening sequence. It overlies (Fig. 6-22,A) a slumped nummulitic and pelletal facies in the northern sections (5, 48 and 59), and marly clay with mixed sandy clastic facies, in section (49). It also underlies another coarsening up nummulitic facies (in section 49) and non-graded nummulites with slump scars in section 5 (Fig. 6-22,B). The facies also, merges with turbidite deposits in the deeper plains.

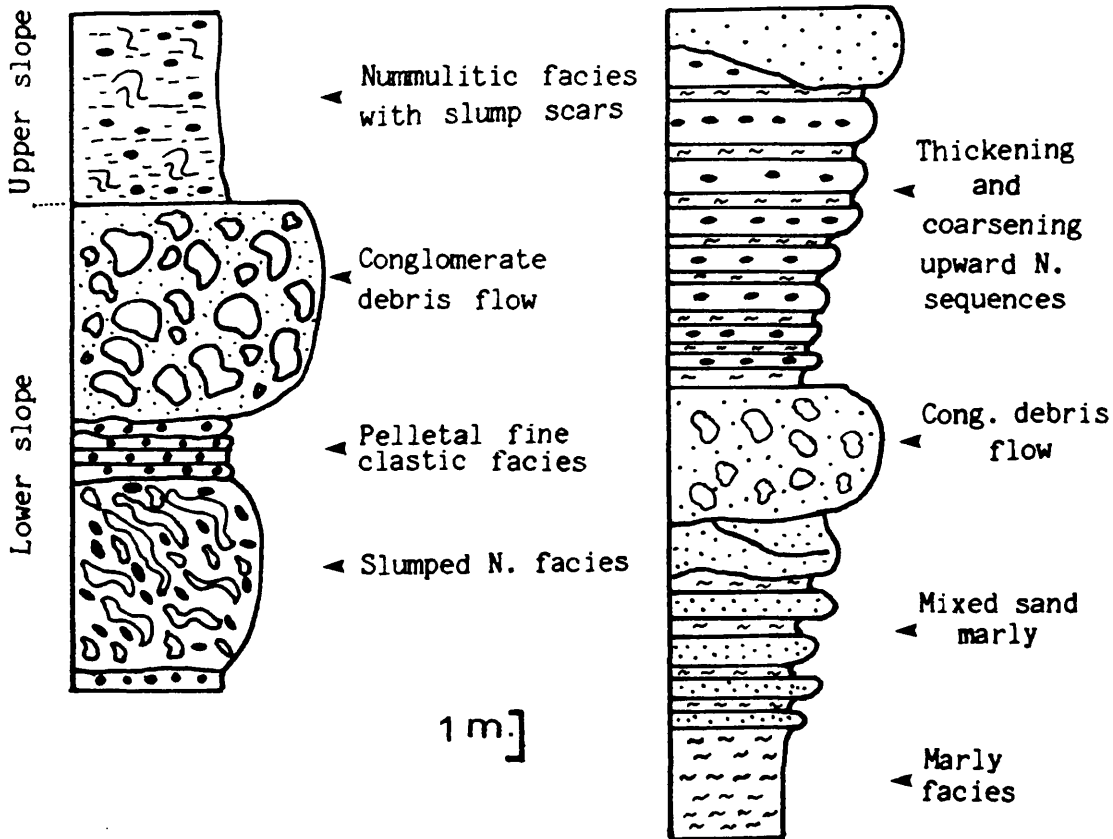
The components of this facies reflect deposition in water with energy ranging between moderately to strongly agitated and with an energy index (EI) of deposition from 4 to 5.

6.8.4 Depositional Environment of the Debris Facies (F8)

The facies characters (Fig. 6-22) and associations of the conglomerate debris facies, may represent lower (S.E.) to upper slope deposits, towards the north-west direction (Fig. 6-22,A). The lower slope sequence starts with the slumped nummulites facies and is followed by pelletal fine clastic facies, and the conglomerate debris. This debris is formed as debris flow deposits where clasts are supported by matrix. The debris is formed on the slope

Slope deposits sequences

Middle fan channel fill sequences



(A , Section 5)

(B , section 49)

Fig. (6-22): Sequences characteristic and inferred depositional environments of the debris facies. Horizontal distance between A and B is up to 20 kilometres.

which seems to be tectonically affected. The muddy nummulitic matrix helped to reduce the shear stress between the debris and grains. The slumped and debris flow facies probably formed in response to subsidence in the northern part of the studied area. The fact that there is no evidence of the Giushi Formation at the Giza pyramids supports the slumping and mass flow completely towards the southeast direction (deeper parts) on a steeper slope. The result is the formation of the thicker deposits in the new formed basin which accumulated rapidly from all the sediment brought in from all the surrounding shelves or slopes. These debris flows are capable of travelling over nearly flat slopes as low as 0.1° degree for a distance of several hundred kilometers (Embley, 1976 & Stow, 1986). Similar submarine debris flow deposits are known from the Mesozoic and Tertiary flysch in the Apennines (Italy) or from the Paleozoic of Morocco (Padgett *et al*, 1977). Dott, 1963, Elter and Trevisan, 1973 and Middleton and Hampton, 1976, all reviewed these kind of gravity flow deposits.

The occurrence of slump-scarred nummulitic facies overlying the debris flow deposits, indicates an upper slope facies.

Towards section (49), up to 20 kilometers southeast, the conglomerate debris intercalate with middle fan deposits (Fig. 6-21,B).

6.9 The Corraline Facies (F9)

6.9.1 Description

The corraline facies (Plate 6-12) is represented by a 1.5 meters thick bed of hard limestone with an abundance of corals tubes (up to 60%). These corraline colonies have a dendroid form and grow vertically. They are represented by the branched colonial type. The corallium is composed of nearly cylindrical corallites which branch irregularly in a tree-like manner. Other encrusting bryozoa, nummulites and bioclastics are represented. This facies may occur in lense or wedge shape units. The characteristic depositional texture is a boundstone. The lower surface of the facies is bored which suggests that the coral of the facies colonised a hard substrate. The facies represents deposition in moderately agitated water with an energy index (EI) of 4.

The facies overlies a siliclastic carbonate facies (F3) and underlies the nummulitic clastic facies (F6). It has sharp contact with both.

6.9.2 Distribution

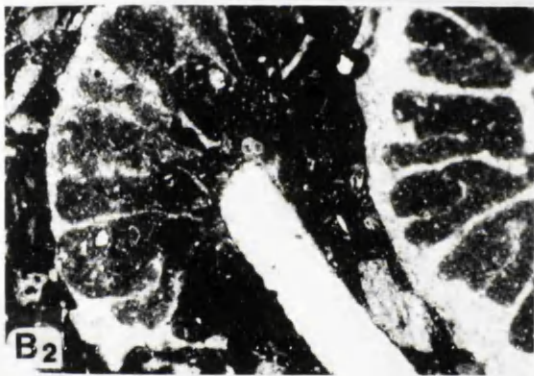
The facies is well represented in section 56 where it extends throughout the Kattamia Road, east of Maadi. The coral unit disappears towards the south and north, but extends along strike in an east-west direction. The western limits of the facies are not known. However, it extends eastwards to the vicinity of Gabal Ataqa.

Plate (6-12): (Coral facies associations "F9")

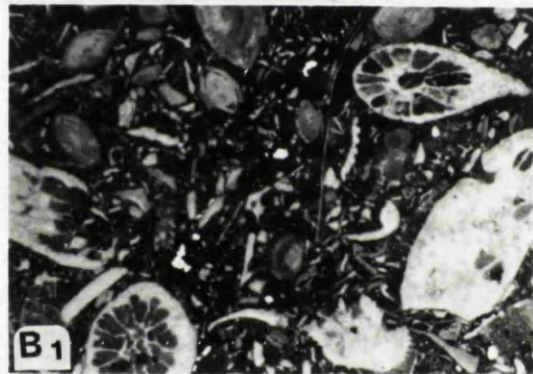
- A - An outcrop photograph of the coralline nummulitic facies (F9) composed of a branching colonized corals buildup in the Cairo Kattamia road .
- B - Acetate peel photomicrograph of coralline nummulitic boundstone to bafflestone microfacies (M31). Nummulite, bryozoa, microforaminifera, and shell debris are found to form most of the matrix components. B1 is X15, General view ; B2 is X20 ,Close up .
- C - Hand specimen from the same previous (A) coral bed indicates coral branches incrustated by bryozoan growth .
- D - Close-up microphotograph indicates that the rock is a bafflestone where baffles occur between intergrown branches of the corals. X20.



A



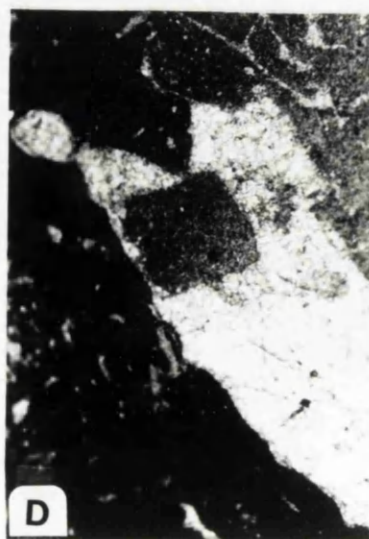
B₂



B₁



C



D

6.9.3 Microfacies association

The coral facies is represented by only one subfacies (Plate 6-12).

6.9.3.1 Corraline nummulitic lime-boundstone to bafflestone microfacies (M31F9)

This microfacies (Plate 6-12, A & B), is characterised by a white grey coloured limestone bed. It contains beside branching corals, nummulites (up to 15%), bryozoa (3-7%), microforaminifera 5%, bioclasts 16-30%, serpiolid worms (up to 3.5%) embedded in a micrite matrix. Some pellets are also associated but have a low abundance. Bryozoa are of the encrusting type (Plate 6-12, C). This facies is highly bioturbated and coral baffles are recorded (Plate 6-12, D). This microfacies of coral occurs in the upper part of the Lower Mokattam Unit (Giushi Formation). Generally the coral microfacies is believed to represent an elongate build up which started to form along the siliciclastic carbonate margin (Fig. 6-23). The microfacies has sharp contacts with the underlying and overlying facies.

The delicate, branching growth form of the studied corals indicates low wave energy and high sedimentation (James, 1983). It is believed that slightly agitated water was responsible for the deposition of this microfacies with an energy index (EI) of 3.

6.9.4 Depositional Environment of the Coral Facies

The northern platform edge of the Upper Eocene carbonate of the Nile Valley contains a coral facies which is interpreted as a build-up. Two possibilities for this facies are believed. First hypothesis is that the formation of such build-ups in the studied area occurs in four stages (Fig. 6-23). The first stage is the unaffected platform, primary stage, with a gentle slope. The nummulitic and mixed sandy facies are abundant. The second stage is indicated by the occurrence of slump structures. This stage commenced with the uplift of the upper shelf and consequently increased the shelf gradient. As a result of uplift and tilting, the shelf sediments started to move and slump basinward. In the third stage, some of the slumped sediments accumulate on the shelf edge forming an elongate submarine ridge normal to the direction of slumping. These ridges might have had a south-west north-east orientation. In the last stage, coral and encrusting organisms started to grow on the newly formed submarine ridge or bank.

The second hypothesis is that these corals flourished over a submarine paleohigh. This palaeo-ridge could be tectonically controlled. So syndepositional tectonic movement had caused that part of the shelf to be uplifted, then inhabited by corals. Confirmation of either of both hypotheses needs geophysical data which is not available.

The absence of cross-bedding and the occurrence of

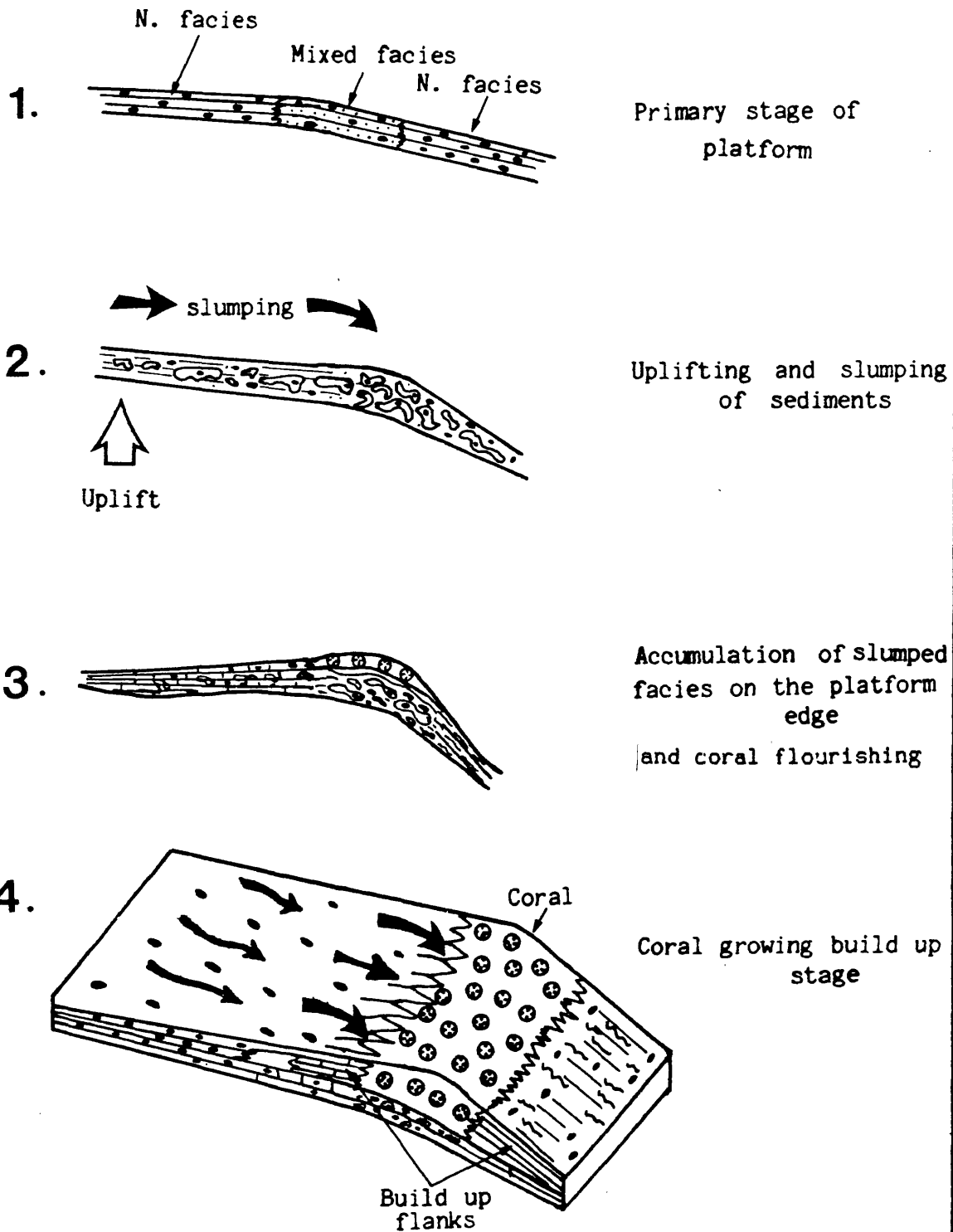


Fig. (6-23): Inferred stages of coral build-up formation on the carbonate platform edge of the Eocene Nile Valley, Egypt.

lime mud with the facies matrix might indicate that these coral build-ups are formed in relatively deep water conditions. These are also demonstrated from the recorded bafflestone textures which originate in local quiet water environments (Flügel, 1982, p.373). Generally recent branched deeper-water corals form 1m high, living colonies, in depths of 200-400m, as in Rockall Bank, Northeast Atlantic (Scoffin et al, 1980). These corals form an annular zone around the bank margin (Teichert, 1958). There is no evidence for flourishing coral build-up anywhere else in the studied area, and it is possible that they were restricted in their distribution.

6.10 The Serpulid Facies (F10)

6.10.1 Description

The serpulid worm facies (Plate 6.13) is represented at Gabal Giushi in a very hard basal bed of about 160cm. It is repeated vertically by three beds but of less widespread occurrence. The lower surface of the facies is undulating and the serpulid tubes form a very dense net. The serpulid facies bed has some infauna of bivalval shells. The shells seem to have encrusted to the bed surface with serpulids and bryozoa. The original facies which was inhabited by serpulid, contains small nummulites and microforaminifera. Most of the biotic content is of the endobiotic mode of life. The facies is also characterized by wedges which thin towards the south.

6.10.2 Distribution

The serpulid facies is best represented in the Gabal El-Giushi (section 44) with a maximum vertical thickness of 5.6 meters. It extends southward in the studied basin until it nearly disappears at south El Maadi. Owing to lack of exposure it was not possible to follow this facies eastwards.

6.10.3 Microfacies association

The following microfacies is represented:-

1. Serpulid foraminiferal lime-packstone microfacies (M32F10)

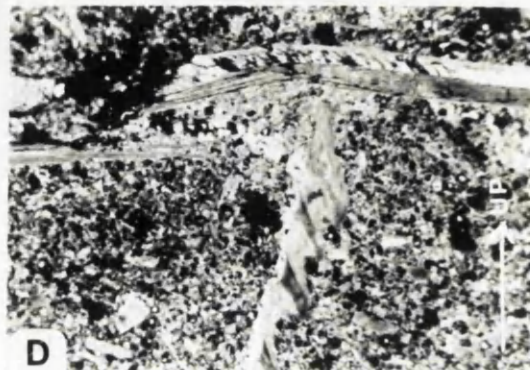
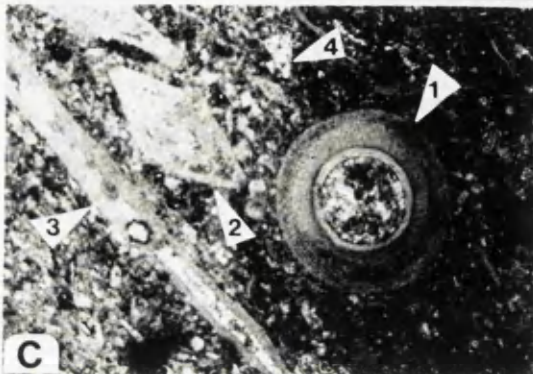
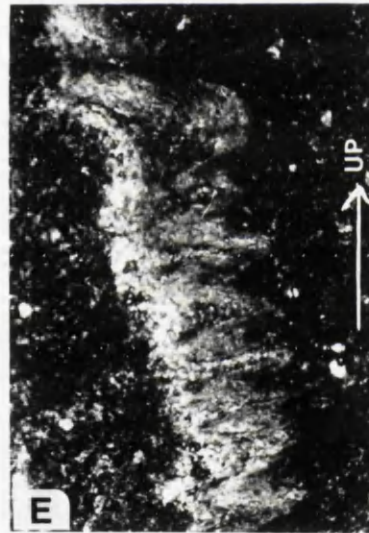
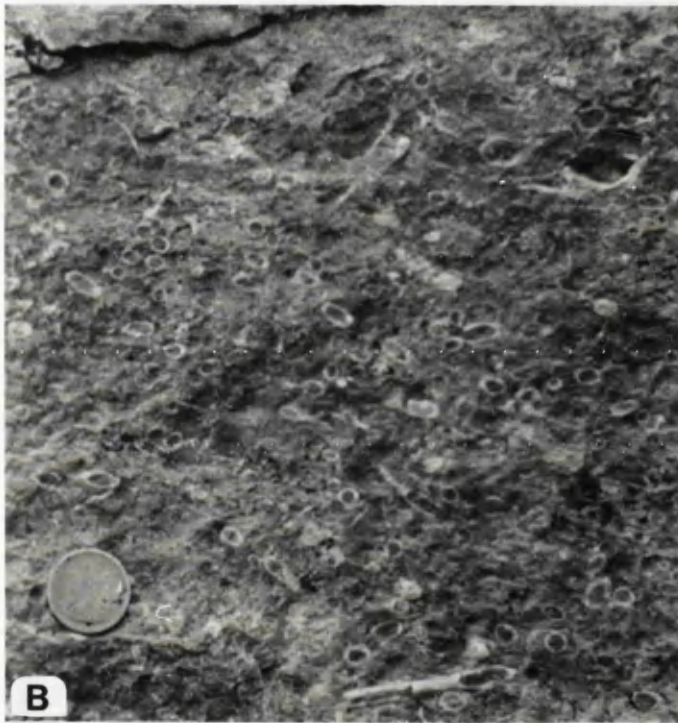
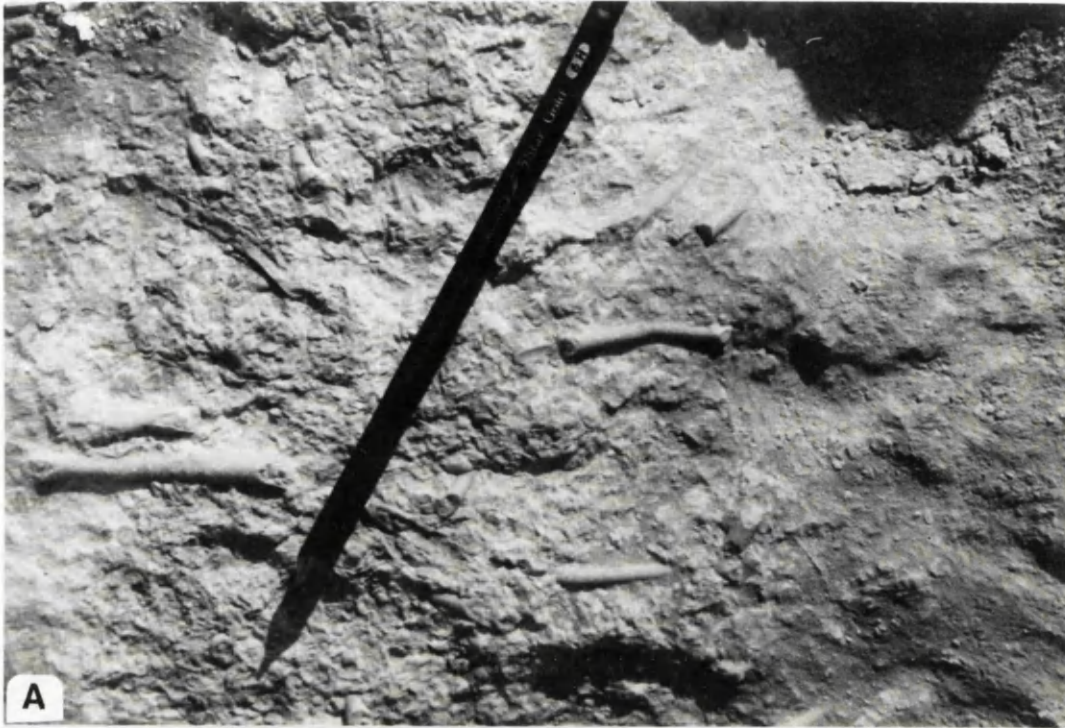
The microfacies (Plate 6-13) is represented by hard bored limestone beds. The boring is very concentrated in the lower bed (base of Giushi Formation) then began to decrease upwards in another two horizons each of nearly 1.6-2.50 meters thick. The microfacies contains (Plate 6-13, C & D), Nummulites (up to 10%), operculines (8%), microforaminifera (up to 10%), milliolid (3%), bivalve (up to 5%), gastropods (2%), bryozoa (up to 2%), echinoderms (3%), serpulid worm (5-50%), quartz detrital grains (up to 10%), bioclastic debris (up to 23%), micrite matrix (30%).

Within the lower horizon the serpulid worms become more dense upward with a reduction in the bivalve shell sizes.

In the studied area although these serpulid facies have a very limited distribution, they were found to be

Plate (6-13) : (Serpulid facies associations "F10")

- A - Highly bored limestone outcrop with dense serpulid worms of straight to slightly curved tubes. Gabal El-Giushi, east of Cairo.
- B - Fresh outcrop surface indicate the dense serpulid tubes of both longitudinal and transverse sections. Same locality as above (Coin is 2 cm. diameter) .
- C - Photomicrograph for the serpulid foraminiferal lime packstone microfacies (M32). Transverse section of serpulid worm-1; nummulites -2; operculina-3; and shell fragments-4; are shown X20.
- D - Photomicrograph of serpulid shell with spirally coiled or screw like shape . Note the way of living sheltered under bivalve shell . X30 .
- E - Photomicrograph of a screw like serpulid lives infaunally in a separate tube . X20.



very important for stratigraphic correlation. They indicate the base of the Giushi formation in Gabal El-Giushi and the Wadi Hof areas.

The serpulids recorded in section 48 are of the sessile type while the ones in section 48 are of the pseudoplanktonic type. This is believed to be a very important criterion for documenting the sea bed topography of the studied basin (see next chapter).

6.10.4 Deposition Environment of Serpulid Facies

The nature and mode of occurrence of the serpulid microfacies in section (44) suggests a hard bottom depositional subenvironment. This is probably formed on shelves with coarse surface layer. It is found that serpulid lived either as fixed epibiontic or endobiontic forams. This hardground bottom which seems to affect the Giushi limestones formed during the deposition of the nummulitic facies. It formed during a long period of interruption of sedimentation. This results in the cementation of the sediment. The bottom surface was encrusted by colonial organisms such as bryozoa, bivalves and serpulids and bored into by lithophagous animals. Two types of calcareous worm shells are recorded. The first type of shell is typically straight to slightly curved tubes. These worm shells were about 8 cm long and 0.4 cm in diameter. This type of worm preferred a colonial mode of existence (Plate 6-13, A) in turbulent waters. The basal bed of this facies at the

Giushi area of the Gabal Mokattam is inhabited by this type of serpulid worm. The second type of worm shell appears in the higher levels of the facies. This type is relatively small of up to 2cm long and 0.1cm diameter. The shell shape is spirally coiled or screw like (Plate 6-13, D & E). That type of delicate serpulid worm lives infaunally in separate sheltered tubes (Plate 6-13, D & E) and also in calm water (Cheetham, 1971).

A similar conclusion for the ecology of serpulid worms was drawn by Gall, 1983. Heckel, 1972, also mentioned that serpulid worms preferred depths ranging from neritic (20 meters) to continental slope (up to 2,000 meters) depth.

The main importance of this facies is the reflection of a long period of non or poor sedimentation when this shallow shelf was uplifted to very shallow depths and bored. In the meantime, to the south (20-25 kilometers) thick accumulations of sediment filled another subsiding basin.

6.11 Planktonic foraminiferal Facies (F11)

6.11.1 Description

The planktonic facies is composed of pale greyish green calcareous marls, to greyish white limestone. The bedded successions are formed of hard to medium beds with thickness ranges of 20 to 80cm. The strata become whiter towards the north and north west. The bedded strata are very fine cross laminated and bioturbated. Burrowing is

represented by inclined or vertical fine tubes. This planktonic foraminiferal facies contains an abundance of planktonic foraminifera and microbenthonic foraminifera. Bivalves are also recorded in different localities. Tongues of small nummulitic facies intercalate with the planktonic facies near its top. Some sponge spicules are also recorded. The facies is normally graded with an increase in the calcareous matrix towards the northwest. In the southern sections of the studied basin, the facies becomes more marly in nature. The facies yields a rich coccolith flora. It underlies the marly facies (F1) and represents the older formed facies in most of the southern part of the studied basin.

6.11.2 Distribution

The facies occurs at the base of section 60, 61, in the Beni Suef-El Wasta area. It is believed that the facies extends northward to the El-Saff area. In the west, the facies extends beneath the middle Mokattam facies. It forms the top facies of the Lower Mokattam Unit. The planktonic foraminiferal facies extends southwards to section 81.

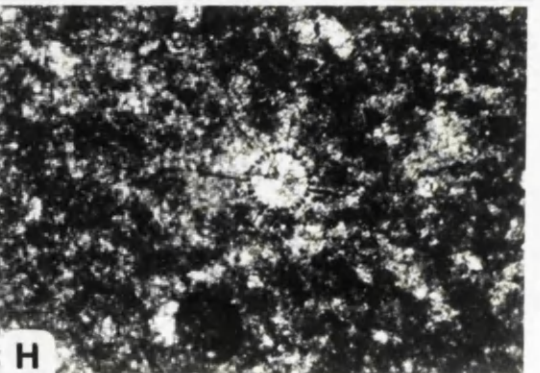
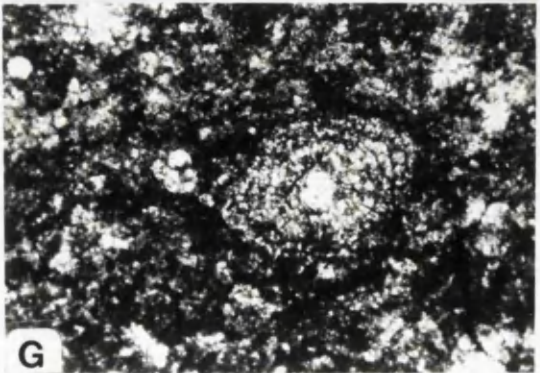
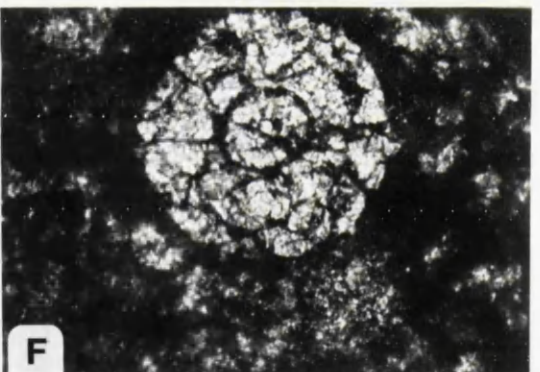
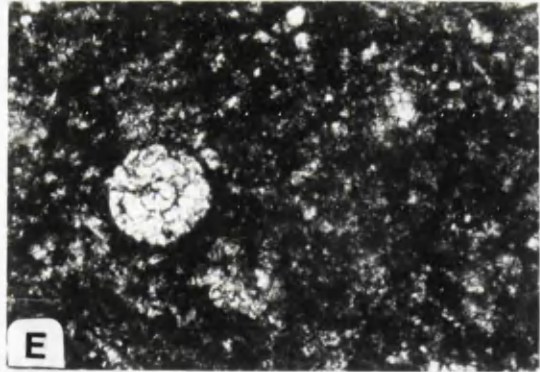
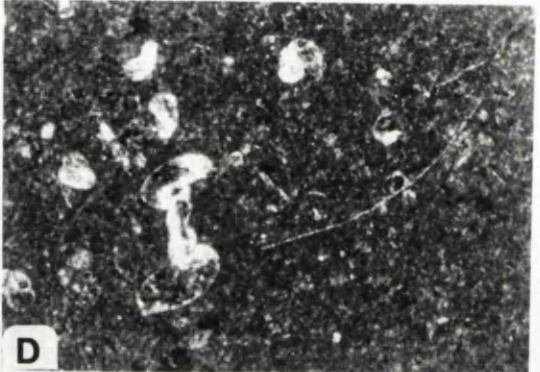
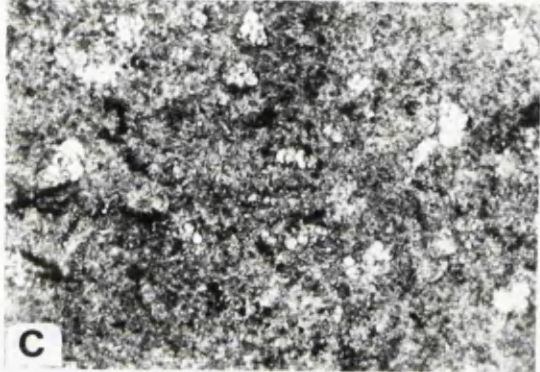
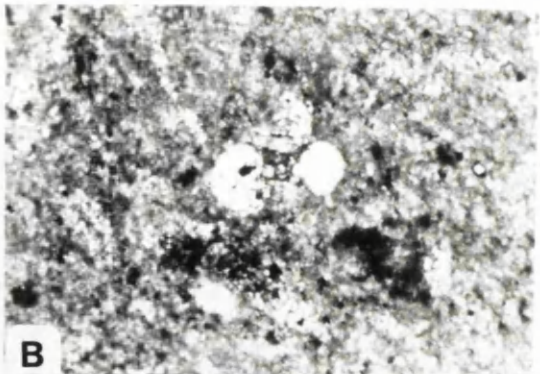
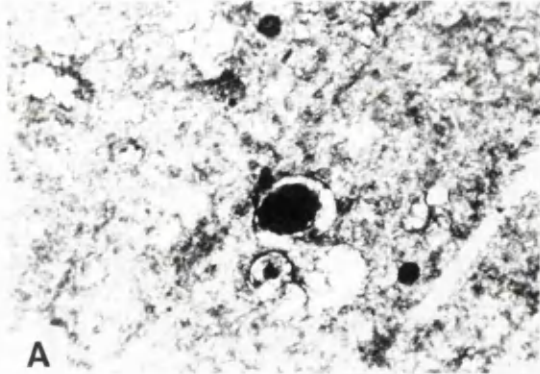
6.11.3 Microfacies Association

The planktonic foraminifera are represented by the following microfacies (Plate 6-14):-

1. Foraminiferal lime-mudstone-wackestone microfacies (M33F11)

Plate (6-14): (Foraminiferal microfacies associations "F11")

- A,B&C - Foraminiferal lime mudstone-wackestone microfacies(M33) with planktonic and few micro-benthonic shells. The middle part of the open shelf. All figures are X80 . East of Biba to El-Wasta areas .
- D - Foraminiferal lime mudstone-wackestone microfacies(M33), with inflated micro-benthonic shells, from the upper part of the open shelf facies. El-Alalma section(61), east of Beni-Suef area . X20 .
- E&F - Photomicrograph of the pelagic wackestone microfacies (M34) with calcispheres. These spheres, probably derived from planktonic algae, are distinctly larger than coccoliths. E, is X200 and f is X500 .
- G - Pelagic lime wackestone microfacies (M24) with very fine planktonic foraminifera and pelagic shells. X80 .
- H - Radiolarian , pelagic lime wackestone(M24). Radiolaria appears at the photo-center with some pelagic foraminifera. X80 .
- (Figs . E-H represent the lower part of the open shelf).



2. Pelagic lime-wackestone microfacies (M34F11)

6.11.3.1 Foraminiferal lime-mudstone-wackestone
microfacies (M33F11)

The microfacies is represented by hard, greyish white, to greenish yellow, bioturbated fine grained limestone. This limestone is exposed in Wadi Lishyab and Wadi Mâtin and extends towards the northwest. At the periphery of the basin, this microfacies is intermixed with the nummulitic facies. The thickness of each bed of these facies ranges from 30 to 60cm and even 80cm thick. The total thickness of the whole facies reaches up to 32 meters.

The main constituents (Plate 6-14, A to D) are planktonic foraminifera (2-10%), benthonic foraminifera (1-8%), shell bioclastics (from 2-3%), echinoderms (up to 4%), bivalves (2-3%) and gastropods (up to 5%), all embedded in a micritic matrix (40-90%). The matrix is disturbed by gypsum or silica veinlets. The microfacies reflects a gently agitated to intermittently agitated depositional environment with an energy index (EI) ranging from 1 to 2.

The microfacies includes well preserved species of *Globigerina*, *Globorotalia* and *Truncorotaloides*.

6.11.3.2 Pelagic lime-wackestone microfacies (M34F11)

The pelagic wackestone microfacies (Plate 6-14, E-H) is represented by marly to micritic limestone grey to greyish green in colour. These limestones occur in a rhythmically bedded 5 to 10cm thick beds. The thickness of

the whole facies reaches up to 6 meters. The pelagic facies is represented in the east El-Saff area and extends northerly to the East Helwan area. In the El-Saff area, the pelagic facies intercalate some pelletal facies with very fine bioclastic. In the east Helwan area, the pelagic facies is found to intercalate with pelletal facies and slumped nummulitic facies. The main components of this facies are mainly pelagic organisms (up to 15%), radiolaria 2%, calcispheres (up to 2%), and fine silty bioclastic (up to 7%). These components are embedded in a micrite matrix.

The pelagic facies reflects deposition in quiet or gently agitated water with an energy index (EI) of 1.

6.11.4 Depositional Environments of the Planktonic

Foraminifera

The two microfacies associations recorded here are found to be related for specific regions from the studied basin. The foraminiferal mudstone-wackestone microfacies is recorded to include the southern areas from south El-Saff to the Gabal El-Abyad section. The pelagic facies, on the other hand is represented in east El-Saff to east of the Helwan area.

The foraminiferal microfacies is believed to have been deposited on an open marine shelf on the basis of their characters. This subenvironment is equivalent to belt 2 of Wilson, 1975. Such shelves are generally wide and sedimentation is quite uniform. The water depth of these

shelves ranges from ten meters to a hundred meters deep (Wilson, 1975). The facies on that shelf is of open circulation (Flügel, 1972). That wide open marine shelf is the basal unit on which most of the southern, formed facies accumulated. The carbonate characters with the shelf facies indicate that the basin was situated towards the northwest.

The occurrence of the pelagic microfacies intercalated with the turbidite facies, slumped fine nummulitic sediments, deep pelletal facies and occurrence of lime mud all suggest deep lower basinal deposits. These pelagic deposits were diluted by the clastic reflux or input to the basin. Similar planktonic open shelf facies is described by Lowman, 1949, Pokorny, 1963, Blondeau, 1972 and Milliman, 1974.

6.12 Calcareous evaporitic shale facies (F12)

6.12.1 Description

The calcareous evaporitic shale facies (F12) represents the top capping deposits of the whole Middle Mokattam facies, in the studied basin of the Nile Valley, Egypt. It includes greenish to variegated colour shale, grey to yellowish calcareous mudstone and sandstone, and interbedded with gypsum and salty deposits. The thickness of this facies varies from 1-6 meters. The maximum thickness is recorded towards the centre of the basin. Dense bioturbation is observed in places. Turritelloid

gastropods of reduced size and operculina foraminifera are also concentrated in the central patches. Milliolid and arenaceous foraminifera are hardly recorded. The fauna as a whole are of very low diversity. Plant remains are also recorded. However, most of the outside zone of this facies are unfossiliferous. The facies is generally friable, highly weathered and very difficult to distinguish any bedding. It extends as tabular bed, on the central part, thins rapidly towards the outside zone. The facies overlies the siliciclastic and mixed sandy barrier complexes (F4). At the same time the facies underlies the Upper Mokattam facies with a sharp contact.

6.12.2 Distribution

This facies occurs at sections 39, 40, 45, 48, 56, 60, 61, 77 and 82. All of these localities represent the top facies of the studied basin. However, there was no record to this facies in the outer-frames of the basin.

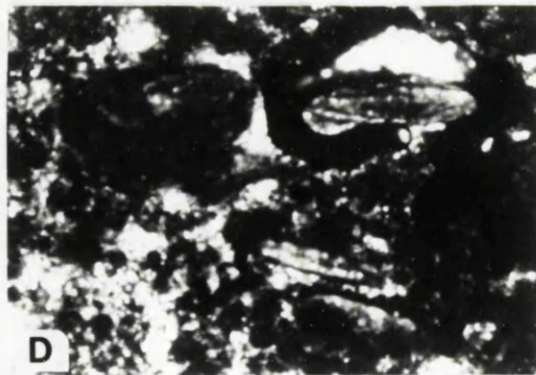
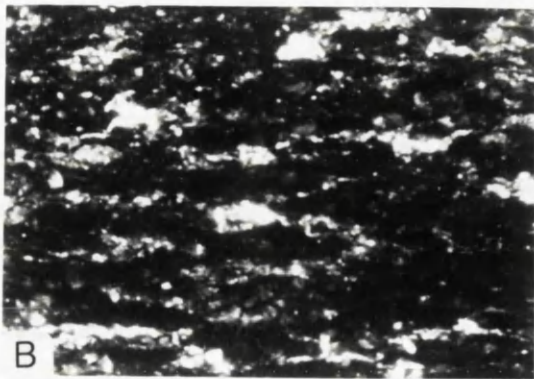
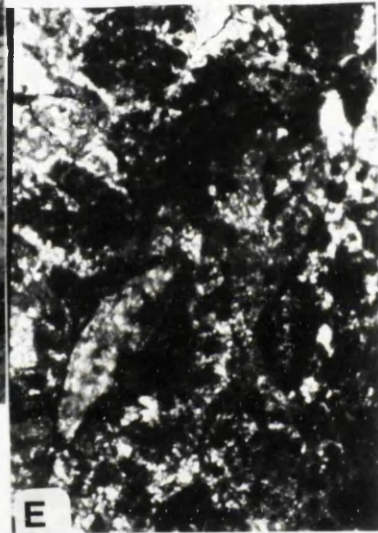
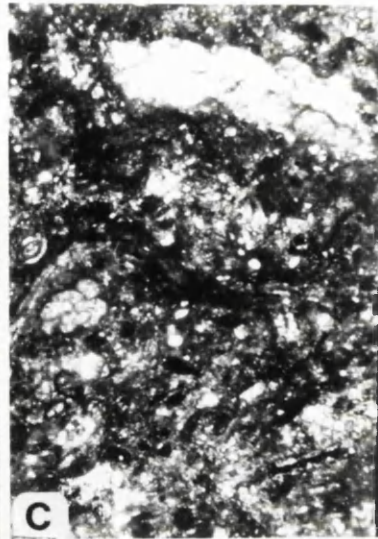
6.12.3 Microfacies Associations

Two microfacies (Plate 6-15) are recorded with this facies. Both of these microfacies are very hard to distinguish from each other in the field:

1. Unfossiliferous shale lime-mudstone wackestone microfacies (M35F12)
2. operculina shale lime-wackestone microfacies (M36F12)

Plate (6-15) : (Lagoonal microfacies associations 'F12')

- A- Outcrop photograph for the highly gypsiferous yellow shale , microfacies (M35), top of the Gabal Kattamia , East Maadi, Cairo .
- B- Photomicrograph of the unfossiliferous shale mudstone - wackestone microfacies (M35), Note occurrence of laminar fenestral fabric normal to bedding and with low detritals . X20. Gabal Shaiboun, east of Beni Suef area.
- C- The operculina shale lime - wackestone microfacies (M36) contains a mixed components of miliolids , plant remains, some microforaminiferas and bioclasts debris . X30 . Gabal Tarbūh, east of El-Wasta area .
- D- Photomicrograph of the operculina shale lime-wackestone microfacies (M36) at El-Saff area. The thin reworked operculines foraminifera are abundant as the main grains within the debris matrix . X20.
- E- Close-up photomicrograph for the previous (D) sample to show the dark micritic film around the operculina shell due to reworking processes. X25 .



6.12.3.1 The unfossiliferous shale lime-mudstone

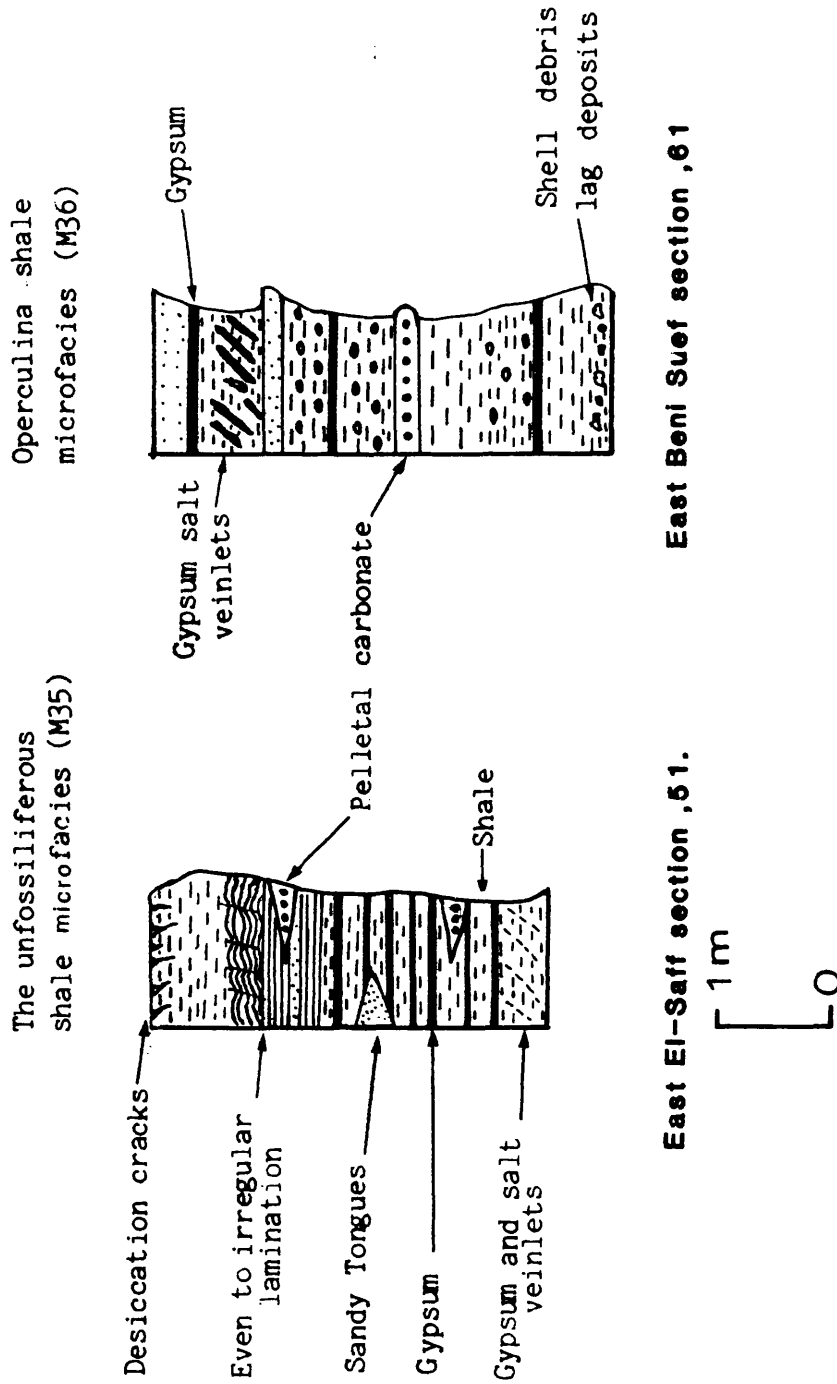
microfacies (M35F12)

The microfacies occurs in a semi-circular nature towards the outside frames of the major facies (Fig. 6-22). The microfacies is green to variegated colour or yellow unfossiliferous shale. It is interbedded with laminae and thin beds of gypsum. This gypsum and also halite cross hatch the original beds as veinlets. Even irregular laminations are hardly recorded. Fenestral fabric seems to be the main characteristic features for this microfacies. Desiccation mud polygons are sometimes preserved. Tongues of pelletal friable carbonate intercalate these deposits towards the basin centre. Calcareous sands occur and increase towards the outer periphery of the basin. On top of section 56 (Gabal Kattamia) (Plate 6-15,A), the microfacies changes completely to high gypsiferous yellow shale. The microfacies is believed to be deposited in a gently agitated water.

6.12.3.2 The operculina shale lime-wackestone microfacies

(M36F12)

This microfacies (Fig. 6-24) is concentrated towards the middle part of the basin and diminishes westwards cutting the western limit of the basin (Fig. 6-25). In this latter locality, the microfacies is fossiliferous and contains miliolids, plant remains and shell debris (Plate 6-15,C). Thin operculines increase in the central parts of



East El-Saff section, 51. East Beni Suef section, 61

Fig. (6-24): General characters of both the unfossiliferous shale microfacies (M35) and the operculina shale microfacies (36).

the basin in a completely friable shale wackestone matrix (Plate 6-15, D & E). This operculina shell has reworking features. Turretiloid gastropods, of relatively small size, are rarely found in the eastern parts of this microfacies. The microfacies is highly bioturbated. Some friable beds of pelletal deposits are intercalated with this microfacies. Gypsum laminae are sometimes interbedded with the microfacies and the whole sequence crossed by gypsum and halite veinlets. Some gypsum crystals are also embedded with facies fabric in the upper part of the microfacies. The energy index of this microfacies reflects intermittently agitated depositional water. Primary structures were very difficult to be distinguished.

6.12.4 Depositional interpretation of the calcareous evaporitic shale facies (F12)

The absence of this facies from the outer frames of the studied area, could reflect retreat in the depositional environment towards basin centre. The difficulty in facies differentiation suggest widely distributed very shallow restricted environment. The depleted nature of the biotic content could reflect the restriction of the host environment. The few number of biota recorded (with reduced sizes) were adapted to life in a hostile environment. The high content of evaporites and the facies characters all suggest a restricted lagoonal environment (Fig. 6-25).

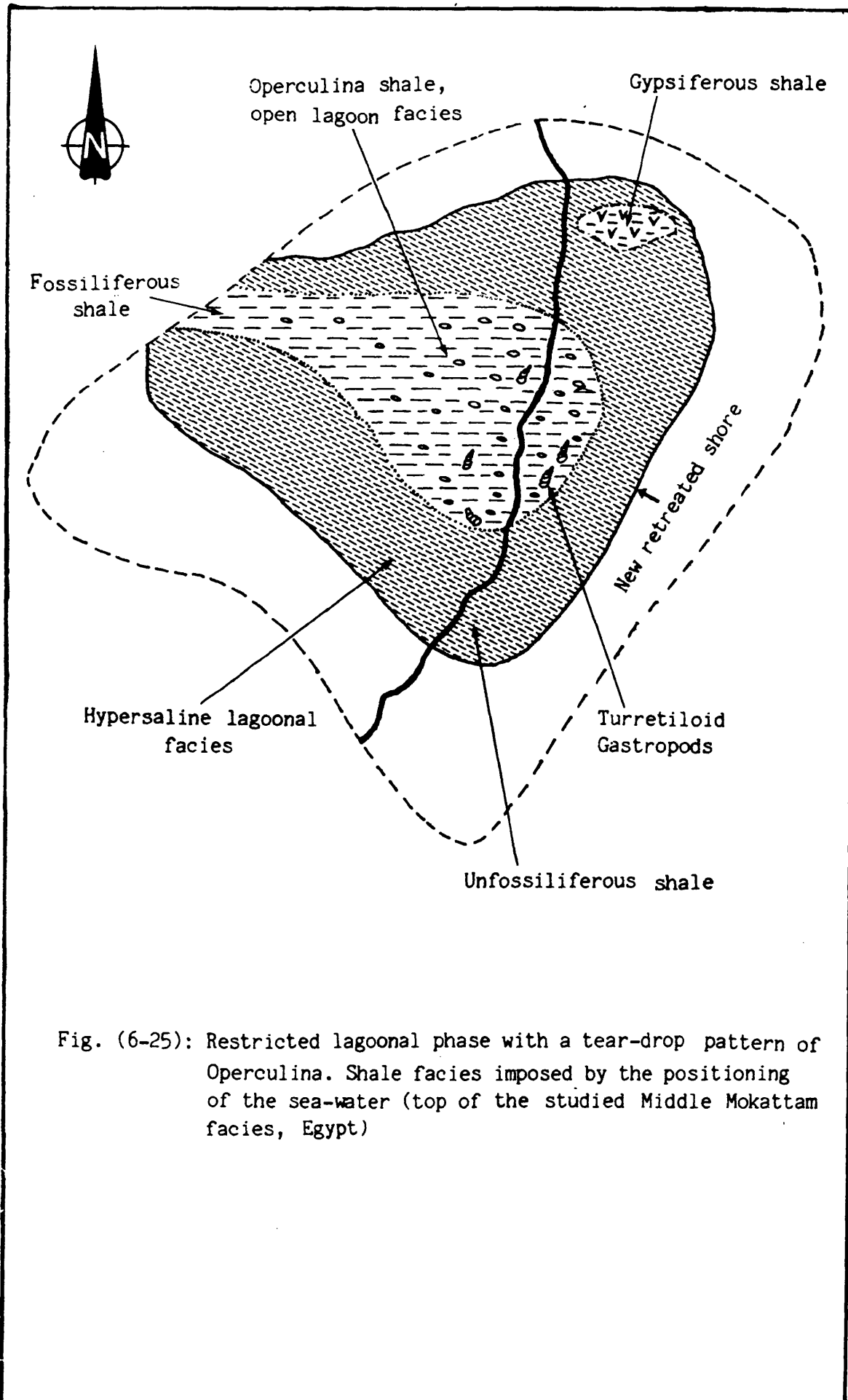


Fig. (6-25): Restricted lagoonal phase with a tear-drop pattern of Operculina. Shale facies imposed by the positioning of the sea-water (top of the studied Middle Mokattam facies, Egypt)

The unfossiliferous microfacies (M35) is believed to be deposited in a hypersaline lagoonal facies. Salinity in this part of the environment might be responsible for their biotic destitu. Restriction of shelf water with slow water circulation are believed to cause abnormal salinity and temperature extremes. Deposition of evaporites were a direct product in that case. Mud cracks suggest a subaerial drying event. The occurrence of patchy gypsiferous shale in the northern part of this microfacies could be interpreted as marsh deposits, probably developed on a palaeo high.

The fossiliferous microfacies (M36) is believed to reflect the open part of the lagoon. Most of the operculina shells could be washed in to accumulate in patchy localities. The occurrence of the survived turretiloid gastropods at the far (east) end of this facies could suggest algae-eating feeders at the back of the lagoon (Schreiber, 1986). Meanwhile the fossiliferous, western, neck of this microfacies could reflect the tidal part, connected with the shelf water. The soft pelletal mud could be formed on the high restricted areas, while the basal shelly lag could be formed in the basins and periodic storm waves. The broad expanses of this part of the lagoon was believed to damp out tidal and wave energy and consequently poor primary structures. This case looks like the facies of the epeiric seas (Enos, 1983).

Generally that lagoonal phase was believed to

represent deposition in the last stages of the basin throughout the studied area (Fig.6-25). The central part of the lagoon might be open for the biota to accumulate (Top section 51).

Attaching of that type of teara-drop pattern to the sea was towards the west. Restriction of the lagoon might be caused by physical barriers complex (F4). Increasing of these barriers around the lagoon mouth is believed to be the reason for the complete restriction which happened at the top of the facies producing mud cracks and erosional surface top of the studied facies.

BASIN ANALYSIS

CHAPTER SEVEN

7 -

BASIN ANALYSIS

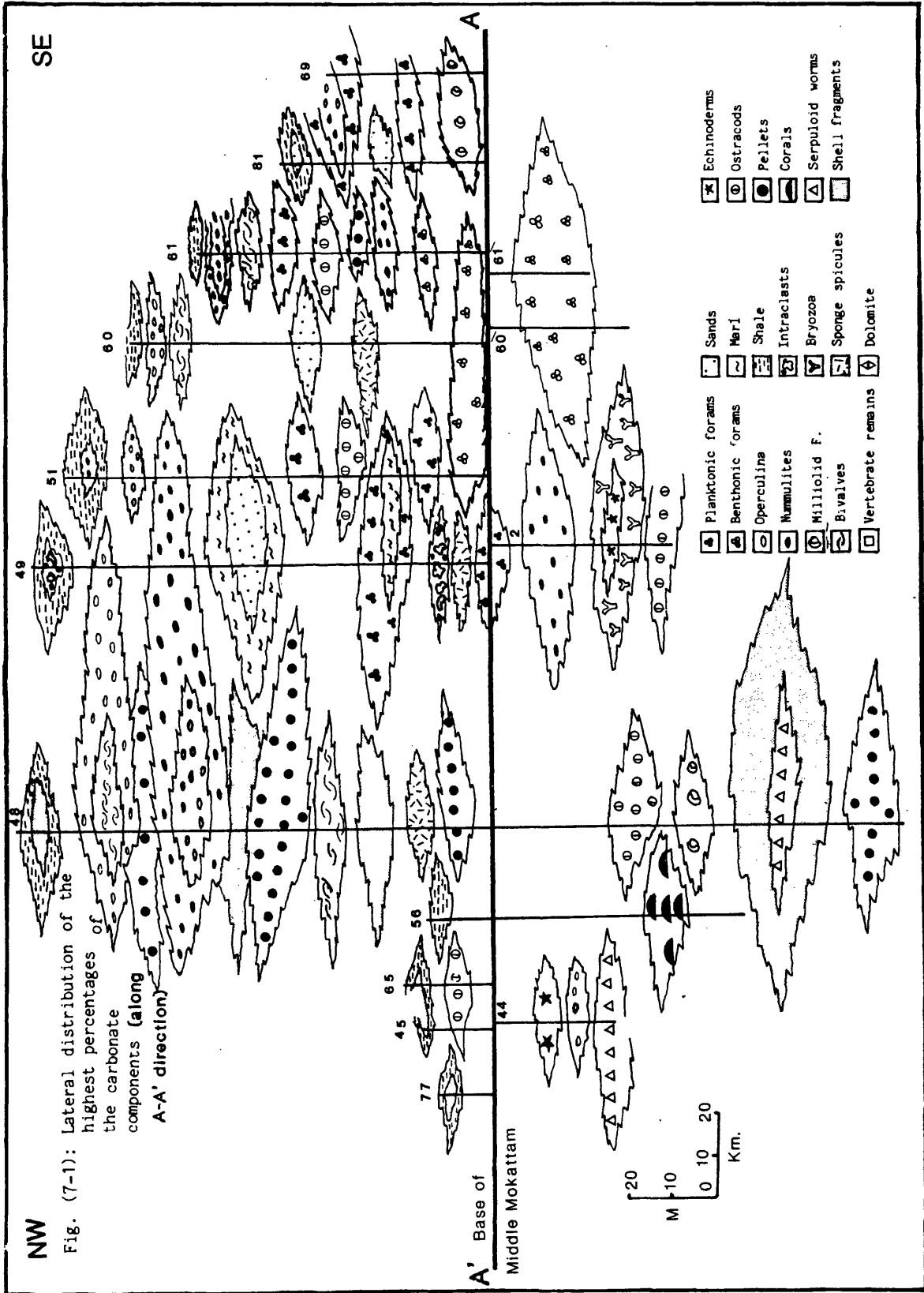
In the first part of this chapter we will discuss basin configurations. The approach used here depends upon analysis for the carbonate grains, microfacies, and the stratigraphic thickness. The second part of the chapter contains analysis of the syn-depositional deformations recorded with the Middle Mokattam facies. In the last part, the tectonism which affected the basin as well as the source of sediments which filled it are discussed.

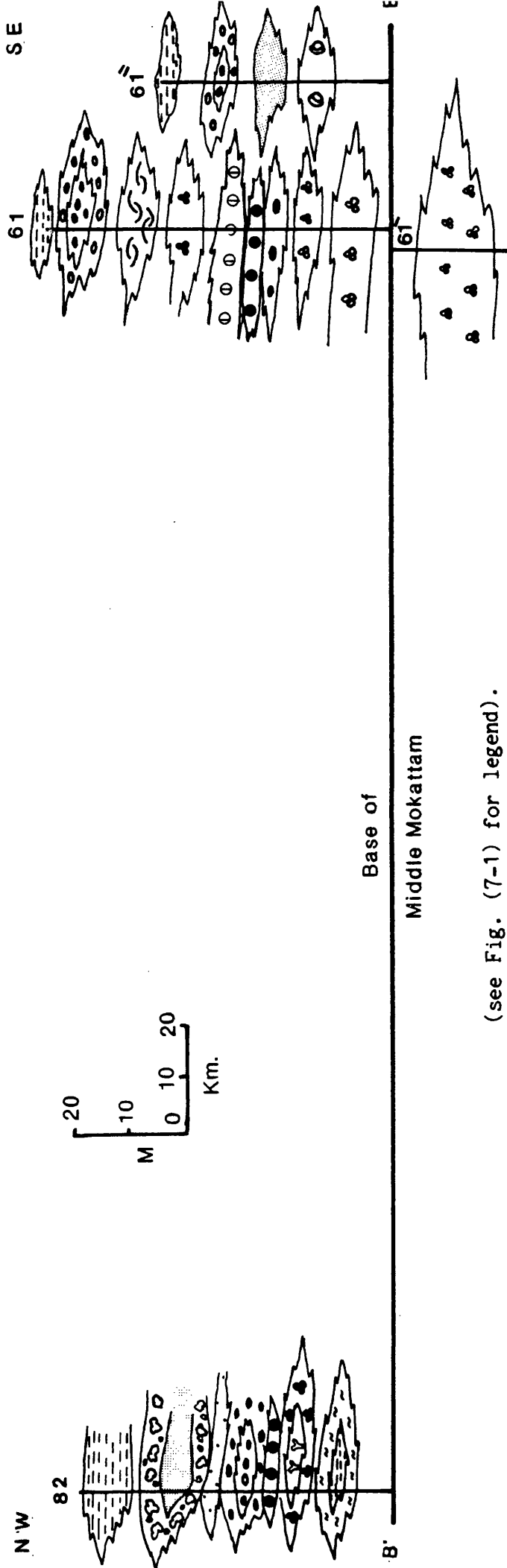
7A BASIN CONFIGURATION OF THE MIDDLE MOKATTAM FACIES

The ultimate objective of this section is to depict the solid geometry and framework control of the sedimentary basin under consideration. Therefore, we will rely on analysing the available geological informations reflected from the carbonate grains, stratigraphy and facies studies. The data will be investigated in four different orientations; and one axial and three across directions (see Figs. 2-1 and 5-3 for locations).

7A-1 ANALYSIS OF CARBONATE GRAINS AND COMMUNITIES

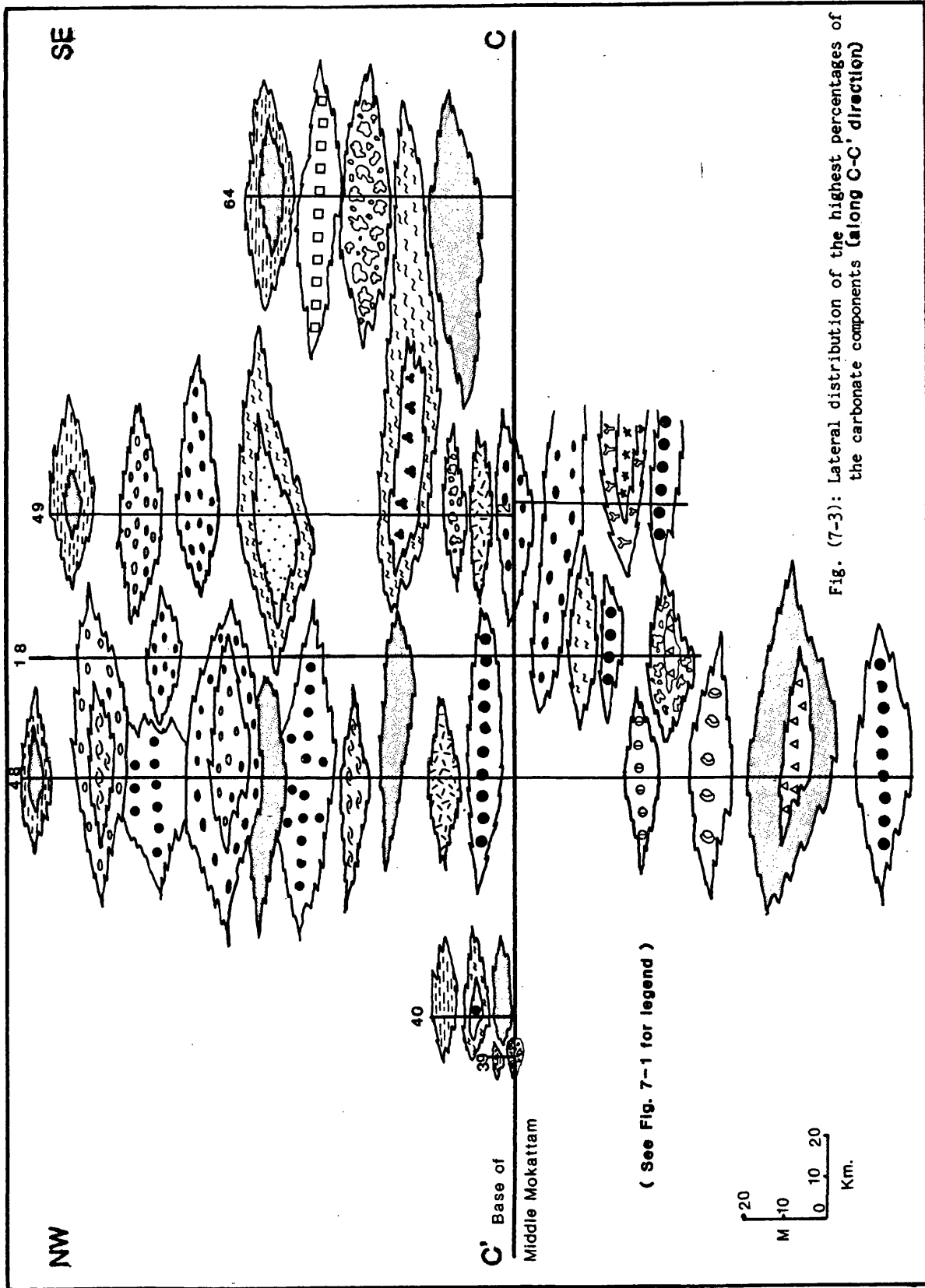
The highest percentages of the counted carbonate grains throughout the studied basin are analysed (Figs 7-1 to 7-4) to examine their lateral variations along the four different directions. The carbonate grain types in general include the skeletal carbonate grains, the non-skeletal carbonate grains and the terrigenous content.





(see Fig. (7-1) for legend).

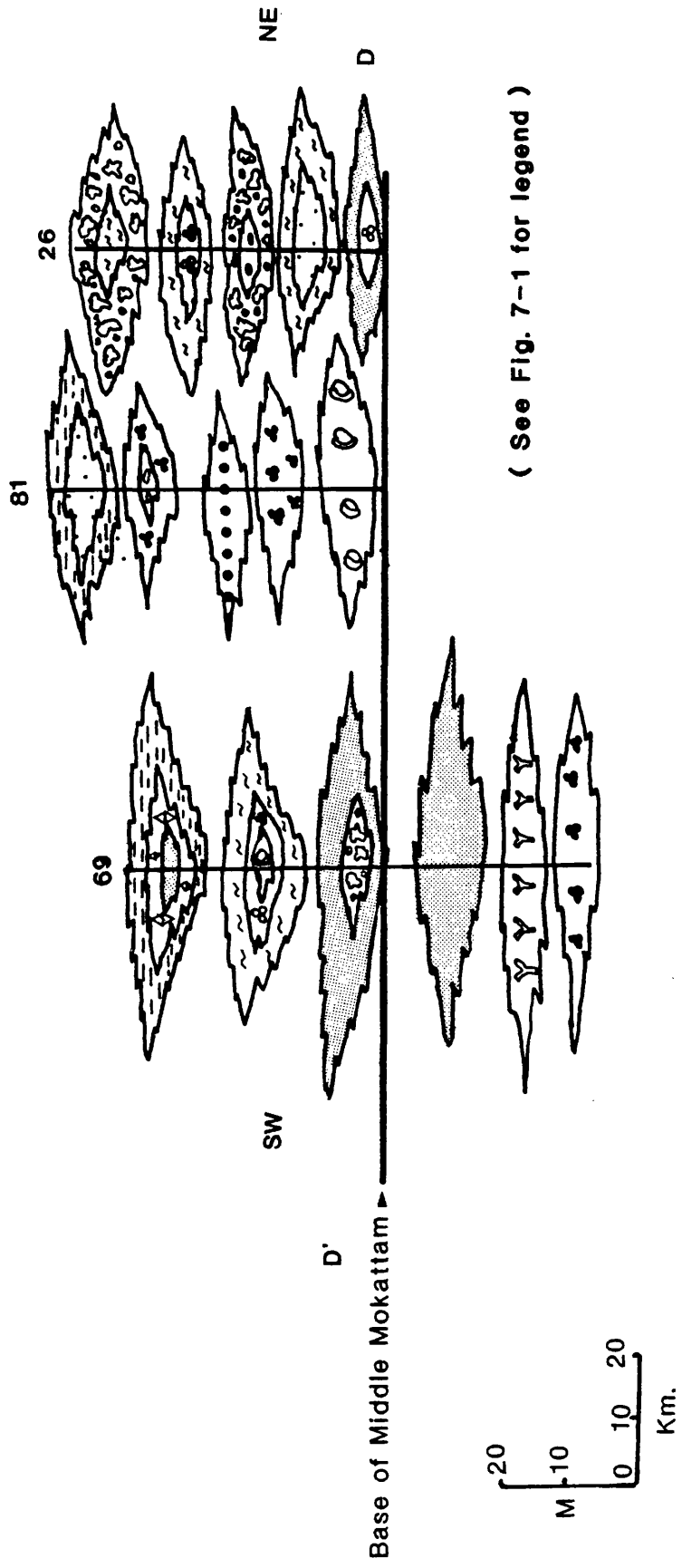
Fig. (7-2): Lateral distribution of the highest percentages of the carbonate components (along B-B' direction).



(See Fig. 7-1 for legend)

Fig. (7-3): Lateral distribution of the highest percentages of the carbonate components (along C-C' direction)

Fig. (7-4): Lateral distribution of the highest percentages of the carbonate components (along D-D' direction).



The skeletal carbonate grains of the facies filled the basin, are represented mainly by bioclasts (shell debris), large benthonic forams (nummulites, operculines and gypsinids), micro-benthonic forams, planktonic foraminifers, ostracods, bivalves, gastropods, bryozoans, echinoderms, corals, sponge spicules, calcareous green and red algae, vertebrate remains and serpulid worms. Bioclasts or shell debris which are derived from the fragmentation of many varieties of fossils form the bulk of the recognised skeletal grains. The highest percentages of the bioclastic debris (60-80%) are concentrated in sections 17, 48, 49 and 51. The occurrence of these fragmented shell skeletal is believed to be brought into the basin by channel wash. Nummulites are the second highest components (up to 40-50%) of the counted carbonate grains in the basin sediment. These flourished on the outside shelf and were carried in sediment tongues to the inner basin. Corals, also, are represented by 30-50% of the carbonate grains and are concentrated in one locality (section 56) as coral build-ups (see also section 6-9 of chapter 6). Bivalves, microforaminifers and operculines are represented by 10-20% of the sediment carbonate grains (as higher counted percentages) and distributed in variable areas all over the studied basin. Bryozoa and echinoderms occur, as high counted percentage of 6-12%, with the shelf sediments of the studied basin. However the highest percentage of the remainder skeletal grains are represented by less than 5% of the counted carbonate constituents and documented in patchy areas throughout the basin.

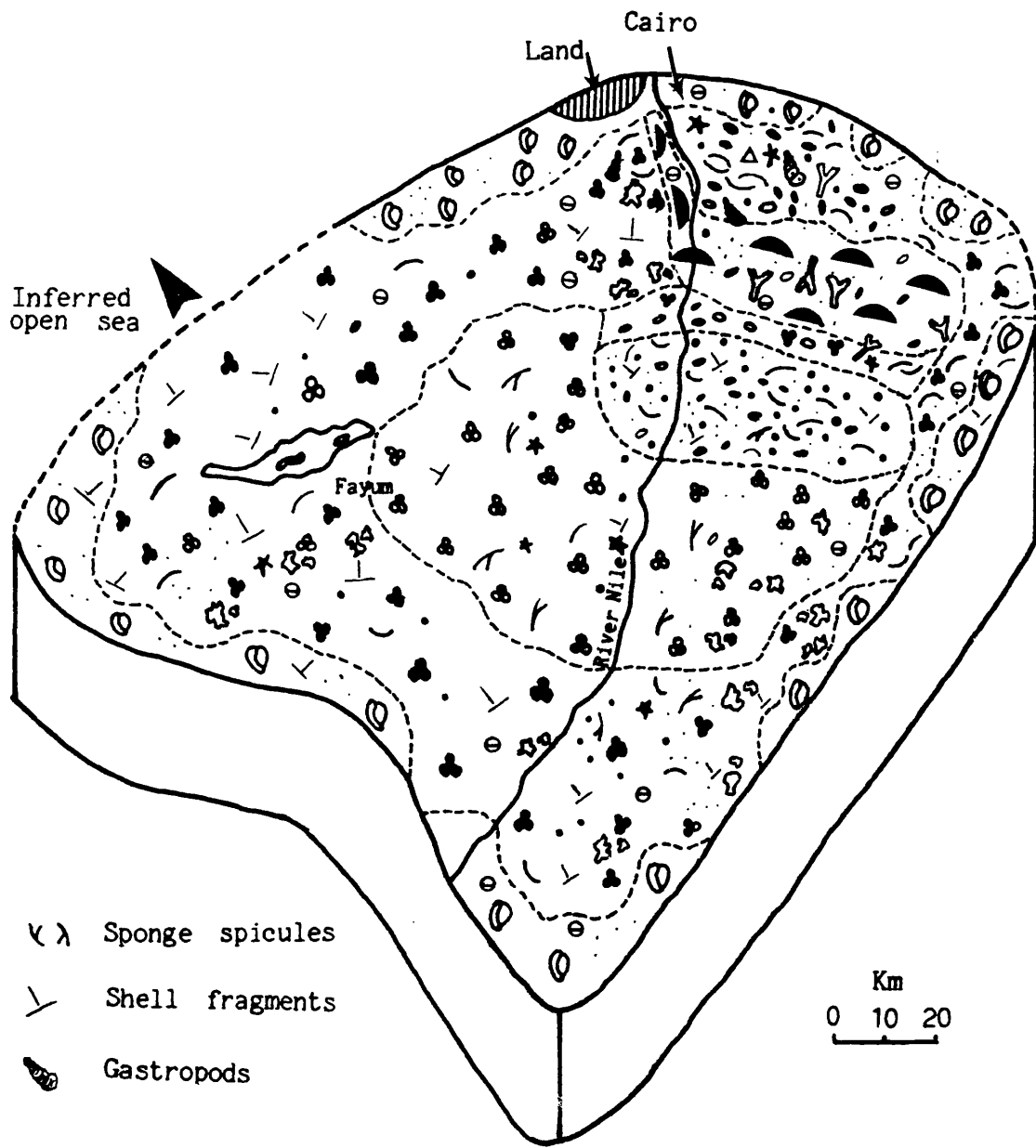
The non-skeletal carbonate grains, recorded in the facies of the studied basin of the Northern Nile Valley and the Fayum areas, are represented by pellets, lithoclasts and terrigenous contents. The highest percentage of pellets reaches up to 40% and is found to be restricted to the main central part of the studied basin. The lithoclasts (Folk, 1962), which include both intraclasts and extraclasts, are represented by a high percentages value of 10-60%. Intraclasts are found in section 49 and increase eastwards towards section 50. Extraclasts are recorded in sections 49, 48, 16, 17, 18 and as small lenses in the Beni suef and Pyramids areas. Generally, the size and angularity of the particles decrease towards the basin centre. Terrigenous content in the study area consists mainly of quartz. The highest percentages reach about 25-30% in the southern parts of the studied area (Fig. 7.1). It is also noticed that the terrigenous content increased upwards in section 61 and 49. The size and roundness of the detrital grains decrease towards the centre of the studied basin from rounded larger quartz grains (of reworked beach sand) to silty-size angular quartz grains (represent a windblown dust from storms). This latter suggestion is also supported by other workers like Porter and Fuller, 1959; Krumbein and Sloss, 1963; Shinn, 1973; Kukal and Saadallah, 1973 and Wilson, 1975.

Generally, very little can be gained from the lateral and vertical distribution of the high percentages of the carbonate grains in the studied area. However, correlation is made using similarities in certain zones. These correlations are shown in Figs. 7.1-7.4. Therefore, it is noticed that the matching of the

upper zone in almost all correlated directions (Figs 7-1 to 7.4) reflects a very closely similar depositional conditions.

In the meantime, by studying the distribution of the different carbonate grains throughout the datum plane will lead to detect or trace the regional topography of the basin floor at its time of deposition. This is achieved by dealing with these carbonate grains as communities. The term community is used here for a group of organisms living together, and linked by their effect on one another and response to the environment they share (Whittaker, 1970 and McKerrow, 1978). No previous attempts have been made to reconstruct the Middle Mokattan basin floor of the northern Nile Valley and the Fayum areas from the carbonate grain communities. The purpose of this section is to present data on both the presence and relative frequencies of the carbonate grains, on that particular plane, at the base of the Middle Mokattam basin and to derive autecological and synecological information from these data. The abundance of the different carbonate grains throughout the datum plane of the studied basin permits a reasonable construction for the bottom communities.

The data show a serial change in the abundance of the carbonate grains that reflects different sea floor conditions during the life of the datum plane. The resulting carbonate grains from different localities throughout the studied datum will then be treated as a single assemblage as though it reflects different communities, and a set of environmental factors that existed simultaneously. On the basis of the previous consideration, the studied carbonate grains assemblage, throughout the studied datum of the basin, are found to be



(For symbols, see Fig. (7-1), except if stated here).

Fig. (7-5): Areal distribution of the carbonate grains on the studied datum of Northern Nile Valley and the Fayum Basin.

Ginsburg & Schroeder, 1973; Ziegler, et.al., 1973 and McKerrow, 1978).

b) The Coral Community (Fig.7-6.2)

The coral community is unknown outside of elongated sector of the Kattamia road through Wadi Digla (east of the Maadi area) spreading eastwards. It is presumably grade laterally into shallow platform (northwards) and microbenthonic communities (southwards). The principal and characteristic elements of the community are: *Hornera* (Bryozoa, erect colony); *Smittina* (Bryozoa, encrusting colony); and dendroid and phaceloid corals, as a main component. This community seems to prefer to flourish on a carbonate build-up relief. The size and distribution of that coral community suggest that their formation was favoured by slightly deep water, away from sea level. Similar examples for coral communities were described by Valentine, 1973; Frost, 1977 and McKerrow, 1978.

c) Bioclastic-Mud Community

The bioclastic mud community (Fig. 7-6.3) is restricted to the area laying between the Wadi Hof and El-Tebbin, east of Helwan. It is composed of silty-size types of fossil skeletons and shell debris. Very fine nummulites and operculines are quite common but are always of small sizes. Serpulids functioned as pseudoplankton annelids, which were probably attached to weed or to floating objects during life are also present suggesting that they sank to the deeper substrate where they rested undisturbed. The bottom was formed of carbonate mud. The occurrence of slumped muds, limy sediments and conglomerate suggest that the topography of the submarine surrounding slopes favoured

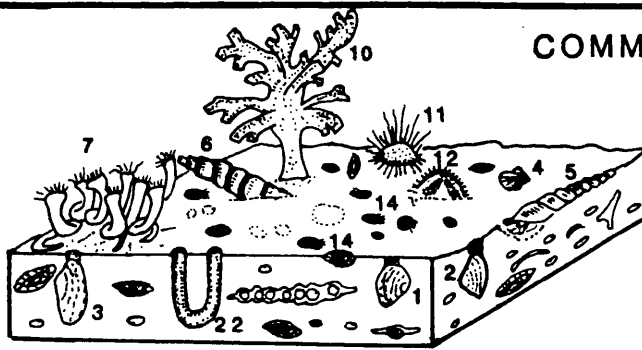
Fig.(7-6): Communities of the important carbonate skeletal on the studied datum plane .

- 1- Lucina cf. gurnaensis (Bivalves) .
- 2- Arcopagia grandis (Bivalves) .
- 3- Macrosolen uniradiatus (Bivalves) .
- 4- Mimachlamys solarium (Bivalves) .
- 5- Turritella desrtica (Gastropoda) .
- 6- Turritella imbricata (Gastropoda) .
- 7- Serpulids (Sessile Annelids) .
- 8- Hornera (Bryozoa , erect colony) .
- 9- Smittina (Bryozoa , encrusting colony) .
- 10- Flustra (Bryozoa) .
- 11- Echinolampas ovalis (Echinodermata) .
- 12- Anisaster gibberulus (Echinodermata) .
- 13- Serpulids (Pseudoplankton Annelids) .
- 14- Nummulites striatus (Foraminifera) .
- 15- Bulimina , Bolivina , Uvigerina , Robulus (Micro-benthonic Foraminifera) .
- 16- Rassilina (Milliolid Foraminifera) .
- 17- Hantkenina (Planktonic Foraminifera) .
- 18- Globigerinatheka seminvoluta (Planktonic Foraminifera) .
- 19- Endobiotic Worms (Annelids) .
- 20- Pelletal bioclastic debris .
- 21- Corals (Dendroid and phaceloid corals) .
- 22- Boring Worm U-shape tralles .

COMMUNITY NUMBERS

COMMUNITY TYPES

1 →



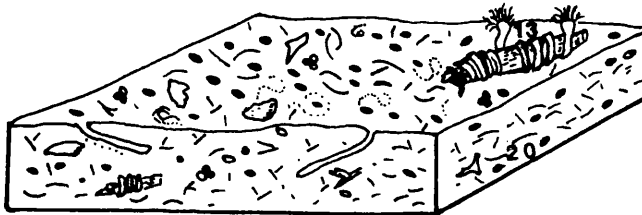
PLATFORM
COMMUNITY

2 →



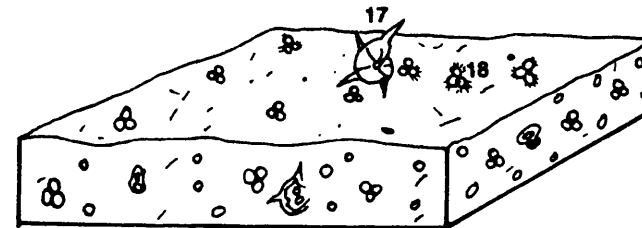
CORAL
COMMUNITY

3 →



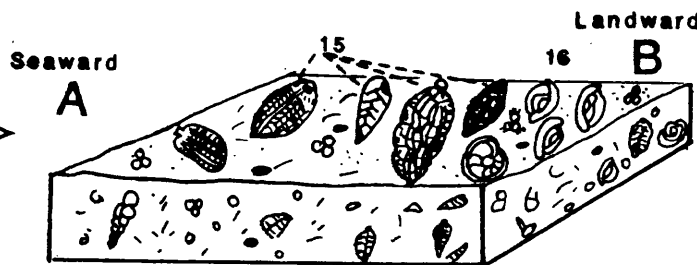
BIOCLASTIC-MUD
COMMUNITY

4 →



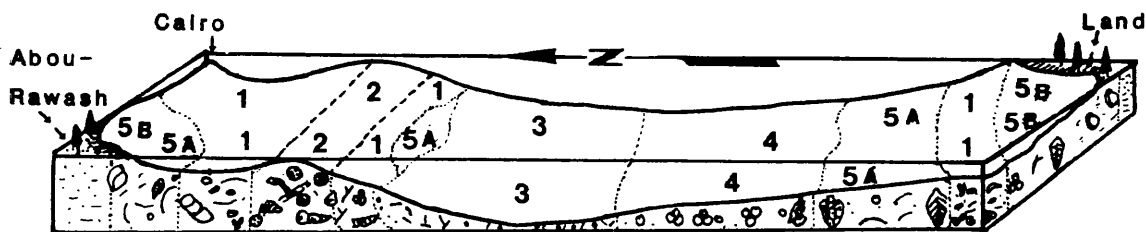
PLANKTONIC
FORAM
COMMUNITY

5 →



MICRO
BENTHONIC
COMMUNITY

Fig. (7-6)



(NOT TO SCALE)

Fig.(7-7): Reconstruction of the Middle Mokattam facies bottom , in terms of skeletal grain Communities . The numbers on this Fig. refer to community numbers of Fig.7-6 .

gravitational slumping. All of the above characters suggest a basinal environment for that community. Nowhere else in the studied basin is the bioclastic-mud community recorded. A basinal environment for such a community was also suggested by McKerrow, 1978 from the Late Devonian deposits of Saltern Cove in South Devon and supported by the work of Gray et.al., 1981.

d) Planktonic Foraminifera Community

The planktonic foraminifera community is concentrated in the Beni-Suef to El-Saff area. It is the lateral continuation of the bioclastic-mud community (Fig. 7. 6-4). The community consists of *Hantkenina* sp. and other forms of planktonic foraminifera shells. The substratum formed of carbonate mud. Some sponge-spicules are present with the skeletons of that community. It is believed from the above characters that the planktonic population generally predominant in the outer shelf subenvironment. This interpretation for planktonic foraminifera community is also suggested by Pokorny, 1963, Milliman, 1974 and Gall, 1983.

e) Micro-Benthonic Foraminifera Community (Fig. 7. 6-5)

This community occurs in the southern parts of the studied area and the eastern parts of the pyramids plateau. The community is distinguished into two populations, the mid and the shallow shelf subcommunities. The mid shelf subcommunity (Fig. 7. 6-5A) contains *Bulimina*, *Bolivina*, *Uvigerina*, *Robulus*, *Lenticulina* and *Dentalina* species. All living benthos occur in shallow waters with maximum depths of 35M. except species of *Bolivina* which are related to shelf zones with depths ranging from zero to 200M.

(Murray, 1973). *Nodosaria* characterizes the inner shelf and is replaced by upper continental slope assemblage of buliminids (Lowman, 1949 and Pokorny, 1963).

The shallow shelf subcommunity (Fig. 7. 6-5B) occurs towards the outside periphery of the basin. It is composed of *Rassilina* and other miliolid benthonic foraminifera. The miliolid subcommunity are common in the restricted shallow shelf environment (Coogan, 1972; Milliman 1974 and Wilson, 1975). The pyramids area, eastern, and south-eastern corners of the studied area were occupied by this miliolid population.

The micro-benthonic foraminifera community, in general, is most productive in near shore and in mid-shelf areas (Milliman, 1974).

As most of the marine biologists have long recognized a high degree of association occurs between the distribution of species and the substrate (e.g. see Jones, 1952; Pratt, 1953; Southward, 1957; Stickney and Stringer, 1957; Sanders, 1958 and Gray et. al., 1981). Therefore, the above mentioned communities were used to construct the datum plane, sea bottom, topography (Fig. 7.7). The inferred basin floor relief, as based on the distribution of assemblage communities, will be compared with the results of the sections discussed below.

7A-2 Basin Detection From Microfacies

In this section, we will base our models on the facies association revealed on the datum plane. Consequently, these models will emphasize their environments. The visual models of environments will help us to determine their relationships of environments with each other and to picture the idealized nature of the basin floor (datum plane).

The establishment of simplified models has contributed greatly to the sedimentology of the studied basin of the northern Nile Valley and the Fayum areas. On the investigated plane, a limited number of facies models has been developed; each represents a particular environment. Five facies and microfacies are recorded (Fig. 7.8A). These are: the nummulitic arenaceous wackestone microfacies (M27 F6); the nummulitic echinodermal bryozoan microfacies (M28 F6); the coralline facies (F9); the planktonic foraminiferal mud-wackestone microfacies (M33 F11) and the pelagic foraminiferal wackestone microfacies (M34 F11). These facies and microfacies were presumably associated at the time of deposition of the datum plane.

As has been argued in the previous chapters (ch.6), the above mentioned facies and microfacies are found to represent six environments and sub-environments (Fig.7.8,B). The relationship between these environments reflect a reasonable understanding of the complex nature of the studied datum. Fig. 7-9 summarizes the inferred depositional model of the basin bottom topography at the time of deposition of the datum plane. The southern part of the basin can be described as a ramp which dipped gently towards the basin. It is a wide floor (up to 12Km. long) with very gradual,

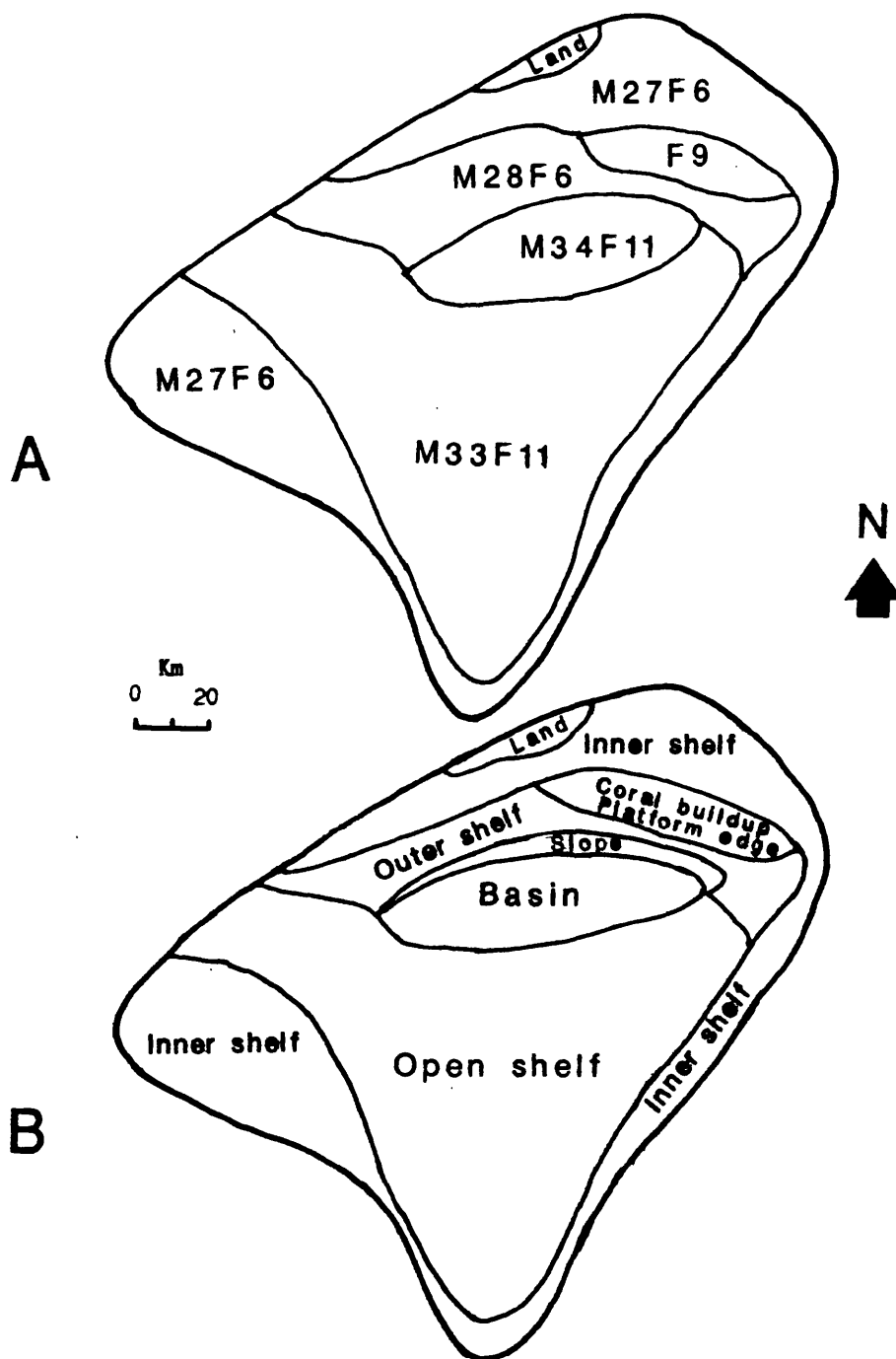


Fig. (7-8): Areal distribution of the studied facies and microfacies (A); and their depositional environments (B) throughout the datum plane of the basin.

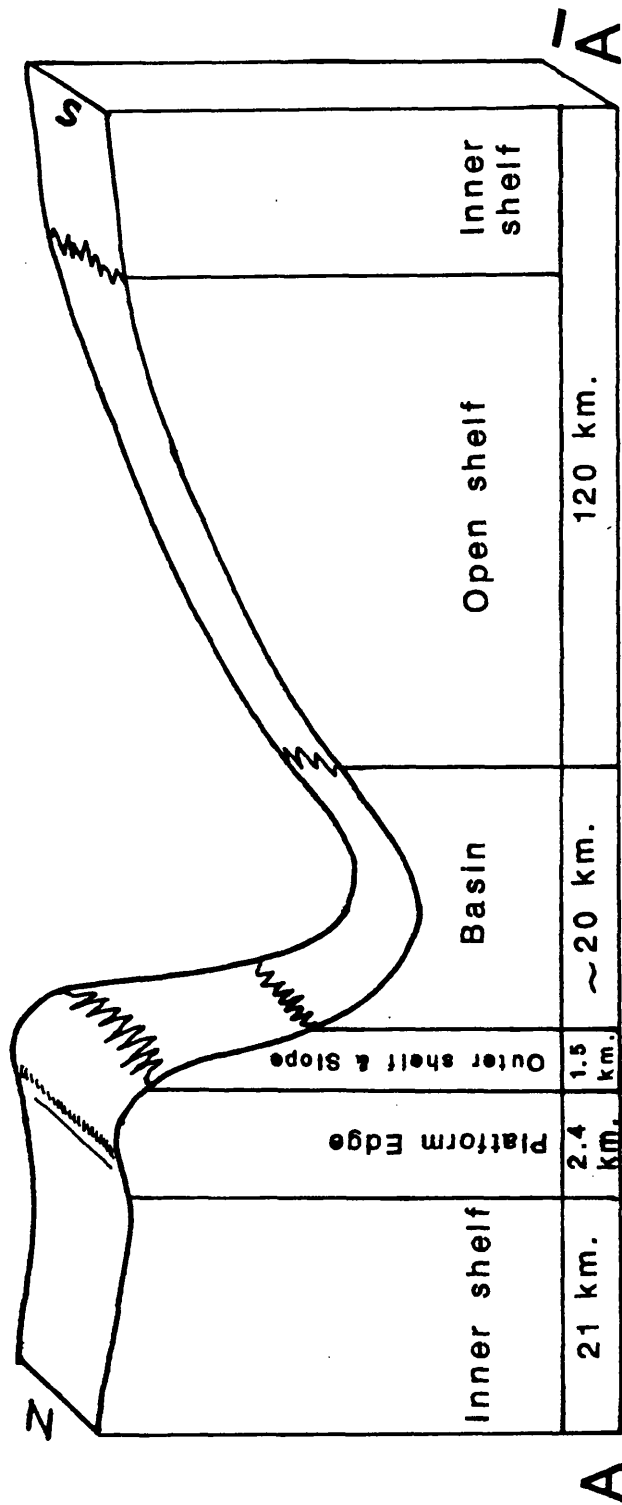


Fig. 7-9): Diagrammatic representation for the depositional environments responsible for the formation of the datum plane along nearly S-N direction (A-A').

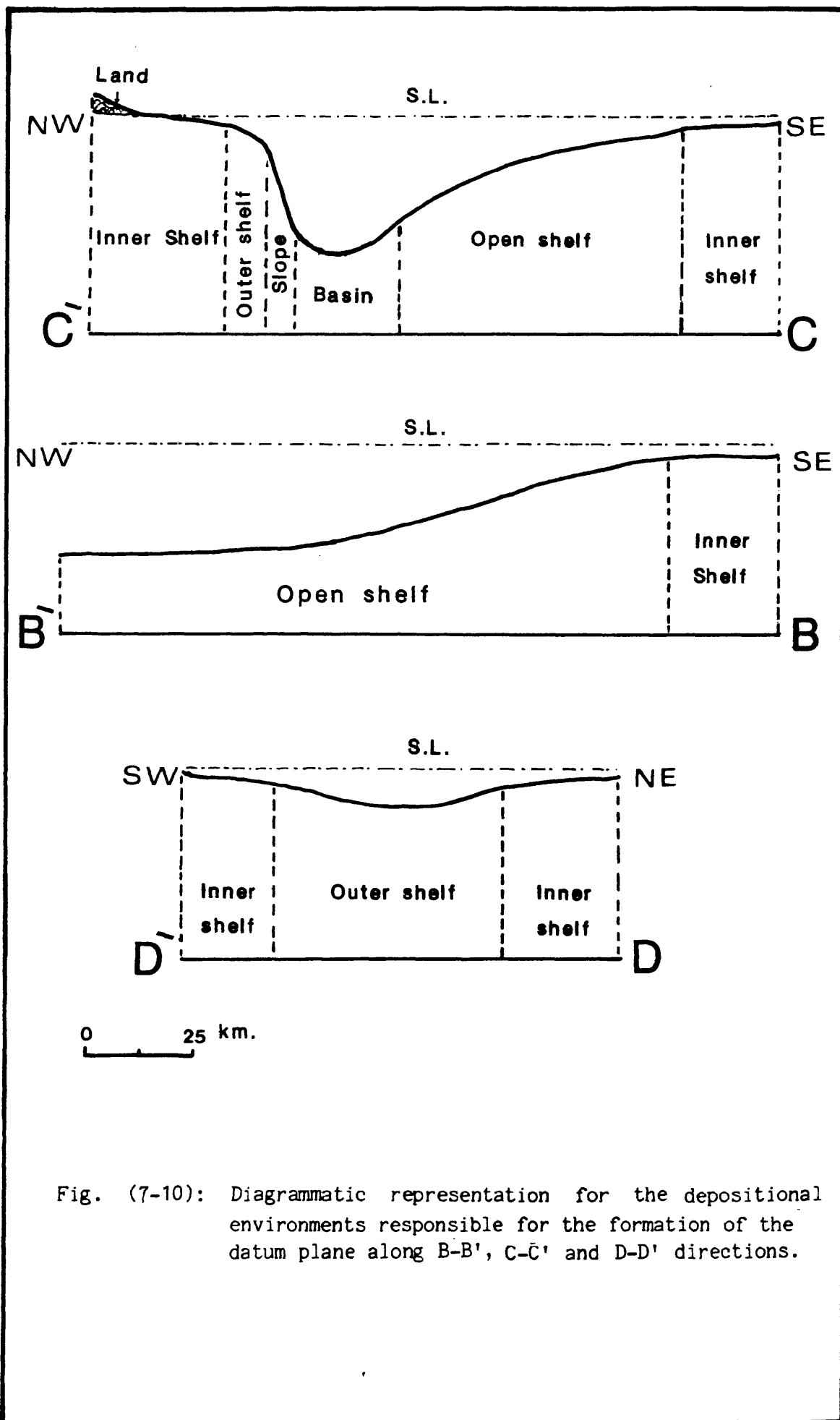


Fig. (7-10): Diagrammatic representation for the depositional environments responsible for the formation of the datum plane along B-B', C-C' and D-D' directions.

hardly recognized, facies changes probably due to its regular gentle slope. The northern part of the basin, as reflected from Fig. 7.9 along the main axial direction (A-A), represents a platform with a distinctive platform edge (coral build-up) and a moderately steep slope. Facies changes occur sharply within relatively narrow zones. Along the C-C direction (Fig.7.10) the basin slope is very steep and no build-ups exist. Meanwhile, farther to the northwest direction the inner shelf grades to a land area (Abou-Rawash). It seems obvious that the studied basin was opening to the sea in approximately western to north-western direction (Fig.7.8) along the B-B trend (Fig.7-10).

7A-3 Stratigraphic Thickness and Basin Configuration

In this section, basin configuration and the attitude of the datum plane will be discussed, with reference to stratigraphy. In this respect we will try to use a higher marker as a new datum. This higher marker is assumed to be approximately horizontal so that the underlying main datum and the associated beds become warped (Conybeare, 1979,p.162). The new datum is selected as a chronostratigraphic marker which tops the Middle Mokattam Unit facies.

The results obtained are abridged in figures 7-11,a,b,c and d. These figures reflect the basse topography of both the Ginshi and the Middle Mokattam basin. This is carried out using a carefully pre-chosen stratigraphic logs. The data were plotted to the new datum marker and correlation figures were constructed (Fig. 7-11). Using these figures it is found that the stratigraphic thickness of the Middle Mokattam Unit increase in deeper sections than shallow. This fact is used to calculate the

A

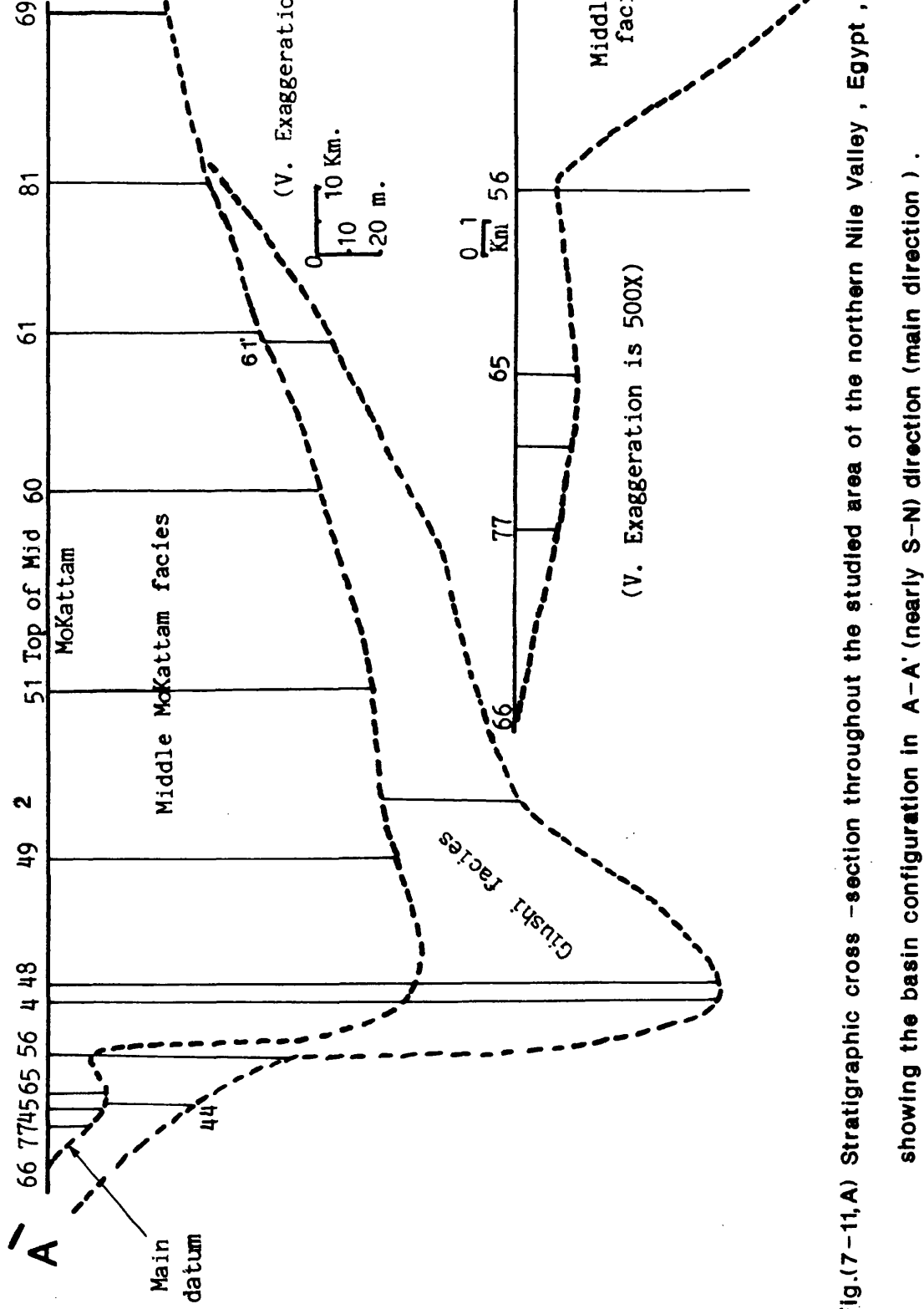


Fig.(7-11,A) Stratigraphic cross-section throughout the studied area of the northern Nile Valley, Egypt, showing the basin configuration in A-A' (nearly S-N) direction (main direction).

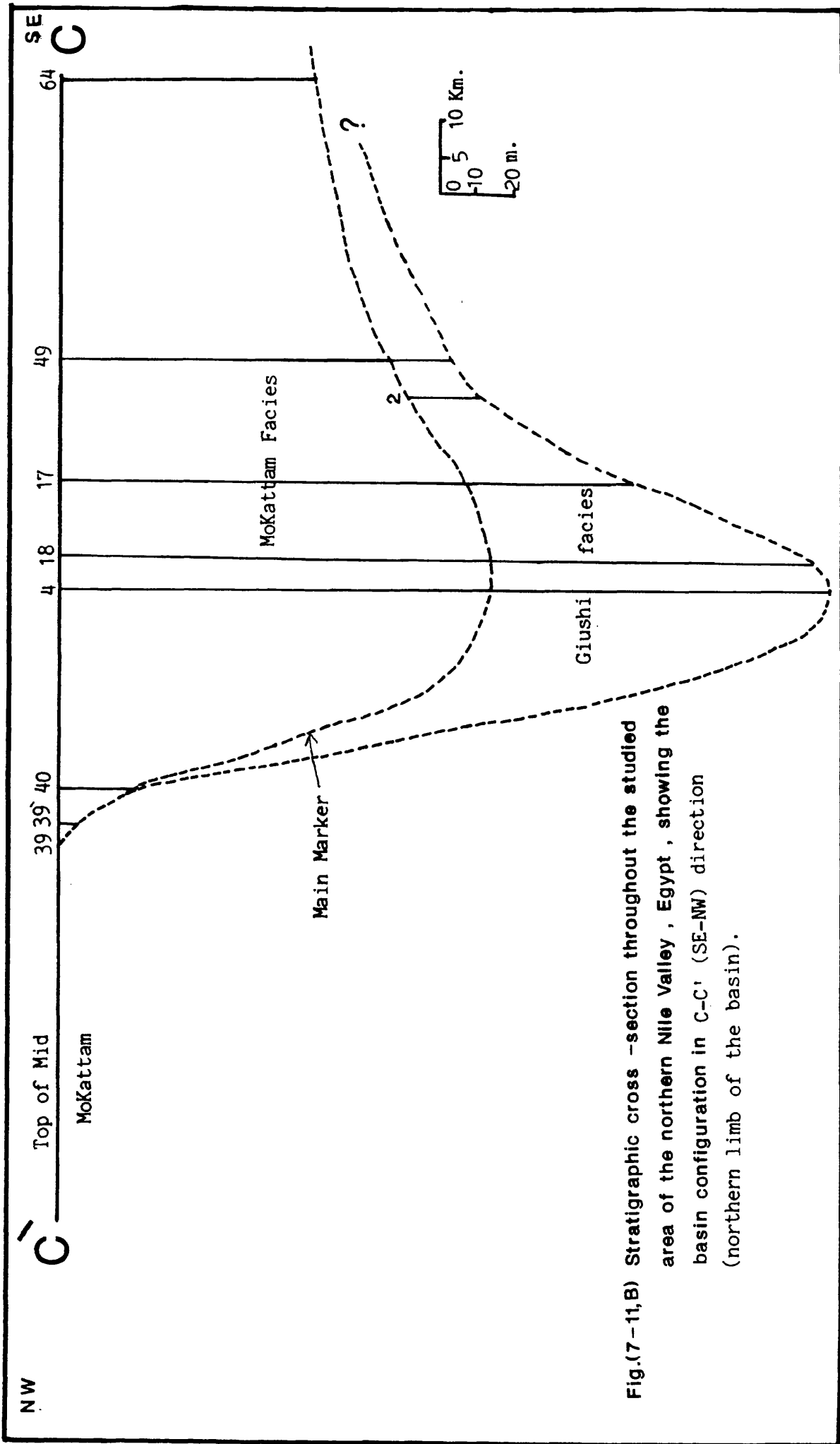


Fig.(7-11,B) Stratigraphic cross -section throughout the studied area of the northern Nile Valley , Egypt , showing the basin configuration in C-C' (SE-NW) direction (northern limb of the basin).

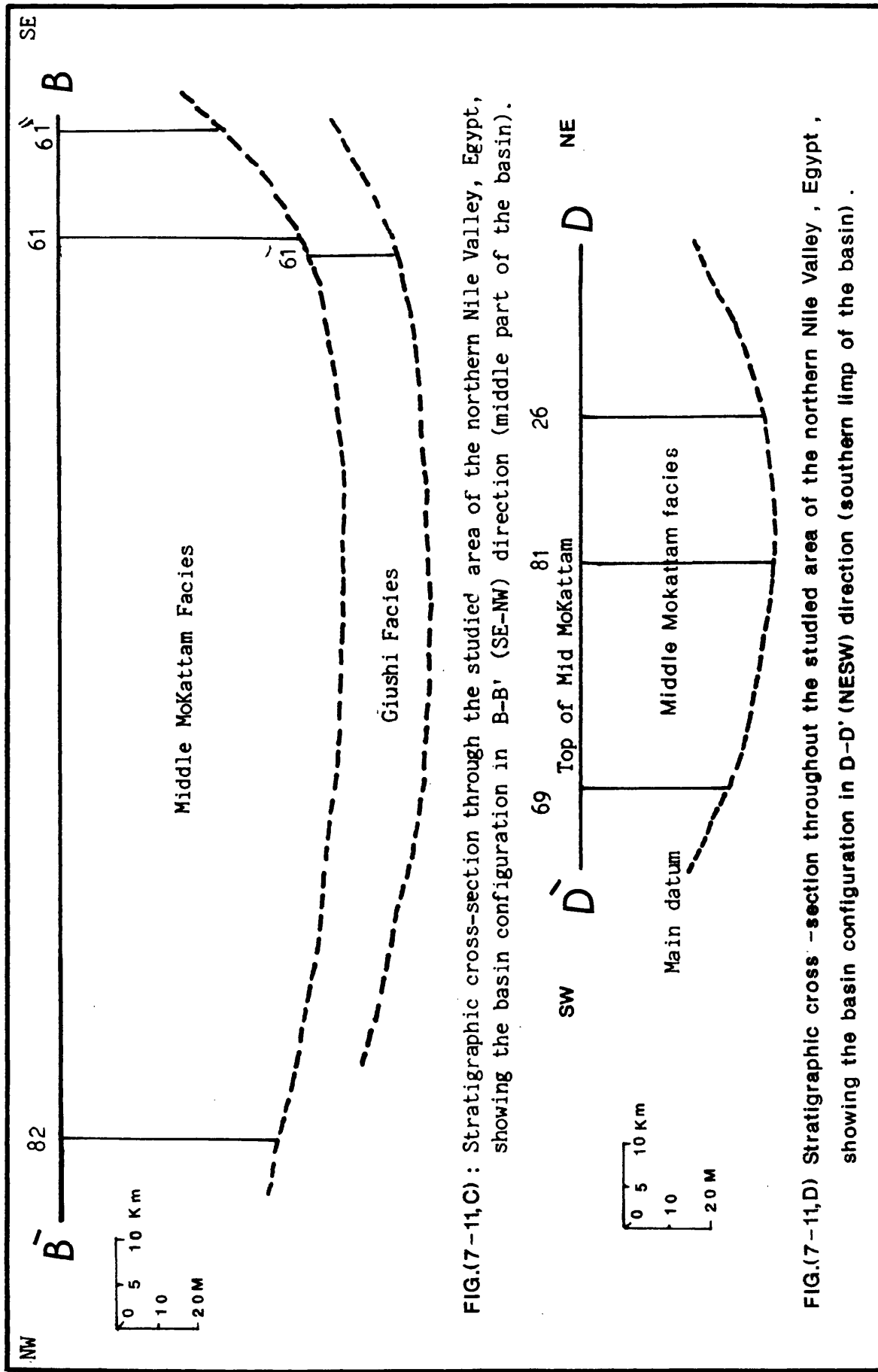


FIG.(7-11,C) : Stratigraphic cross-section through the studied area of the northern Nile Valley, Egypt, showing the basin configuration in B-B' (SE-NW) direction (middle part of the basin).

FIG.(7-11,D) Stratigraphic cross-section throughout the studied area of the northern Nile Valley, Egypt, showing the basin configuration in D-D' (NESW) direction (southern limb of the basin).

dip angles of the basin floor in different localities. As the Middle Mokattam sediments cross from section 61 to section 60, the facies thicken from an average of about 62 to nearly 81 metres; in one transection over a distance of 23.5Km. Accordingly, the southern part of the studied basin was believed to be nearly wide regular shelf (Fig. 7-11,A) dipping northwards (basinward). This dip could be of a very gentle (about 0.04°) gradient for a distance of about 100Km. long, as reflected from the axial section Fig. 7-11,A. The nature of this southern shelf indicated that it may have been formed as a small gulf or inlet farther south (Fig.7-11,D) and subsequently widened, in shape, northwards to reach a maximum of about 132 Km. (section B-B, Fig. 7-11,B).

The eastern and western peripheries of the shelf may have had an original dip of 0.02° which increased in the eastern side to 0.8° . This broad and gentle nature of this part of the studied basin has led us to believe in a ramp form for that southern shelf. This view is supported by the gradual changes in facies and the difficulty in developing a pronounced contrast between shelf facies at base of the studied facies. For this nature of the southern seaward sloping surface, it is believed that there was no sharp shelf edge. Instead there may have been a gradual and probably regular increase in the water depth.

The topography of the previous shelf breaks northwards, at lower latitudes, with a relative increase in dip (0.12°) forming a basin leading slope (Fig. 7-11,2). The eastern slope of the basin was dipping (about 0.2°) seaward (Fig.7-11,C). The ancient rimmed western and northern margins were probably more relatively

steeper (0.68 to 0.7 basinward dip).

A sub-sea paleotopographic high is recognized from the inferred base-line of the studied basin forming the northern margin. That margin leads to platform extending landwards to cover the far ends of the western, northern and eastern parts of the studied area (Figs.7-11, a and c). The north-western basin slope seemed to have had a more or less regular gradient up till it met with the ground surface at section 39 (Fig. 7-11,C). This could suggest a paleo-high and land area in that direction during the deposition of the studied Middle Mokattam facies.

7.A-4 Evaluation of the Used Methods in Estimating Basin

Configuration

One of the objectives of this chapter is to provide an accurate construction for the depositional basin paleo-slope of the studied Middle Mokattam facies in northern Nile Valley, Egypt. This has been argued in the previous sections (7.1-7.3) using three representative methods or models concluded in figures 7.5, 7.7, 7.9, 7.10 and 7.11. Here we can discuss these results to evaluate their use and to look for the right approach to understand the basin configuration.

The shallow restricted parts of the platform were ideally reflected in the grain-community scheme (as miliolid sub-community) whereas both the facies and thickness models were less accurate or nearly failed.

All of the used methods were able to depict both the sub^earial and submarine paleo-highs; in Abou-Rawash and the coral buildup base, respectively.

Both of the facies and thickness models had the platform slope (Figs. 7.9, 7.10 and 7.11) identify represented where this slope was only inferred from the data proceeding from the grain-community model.

The deeper trough part of the studied basin was confirmed and detected from all of the used, three, methods. The general nature of the shelf as a regular ramp had been figured out from either the facies or the stratigraphic studies. Meanwhile, a gentle change in the sea bottom topography level (or base levels) of shelf plates throughout the same ramp can be noticed from the grain-community model (Figs. 7.5 and 7.7). This is expressed in the existence of two different communities in a presumably regular shelf; the microbenthonic and the planktonic foraminiferal communities (Fig. 7.5).

The connection between the inferred shoreline trend with the open ocean is well evidenced, using both the grain, to be approximately towards the west direction community (Fig. 7.5) and the facies (Figs. 7.10, B-B) models.

However, this opening, at the same trend (7.10, B-B), had been obscured throughout the model of stratigraphic thickness (Fig. 7.11, C). Thus the apparent occurrence of a down curved basin floor (which dips towards the S.E. in its northwestern part and towards N.W. in the southeastern parts) is taken as an evidence of the existence of an outerbasinal discrete high. The highs, therefore, appear to have been unstable during the time interval covered by the Middle Mokattam facies. This relationship provides evidence of syn-sedimentary uplifting which cause upwarping of the basin floor (Fig. 11-3). The angles of

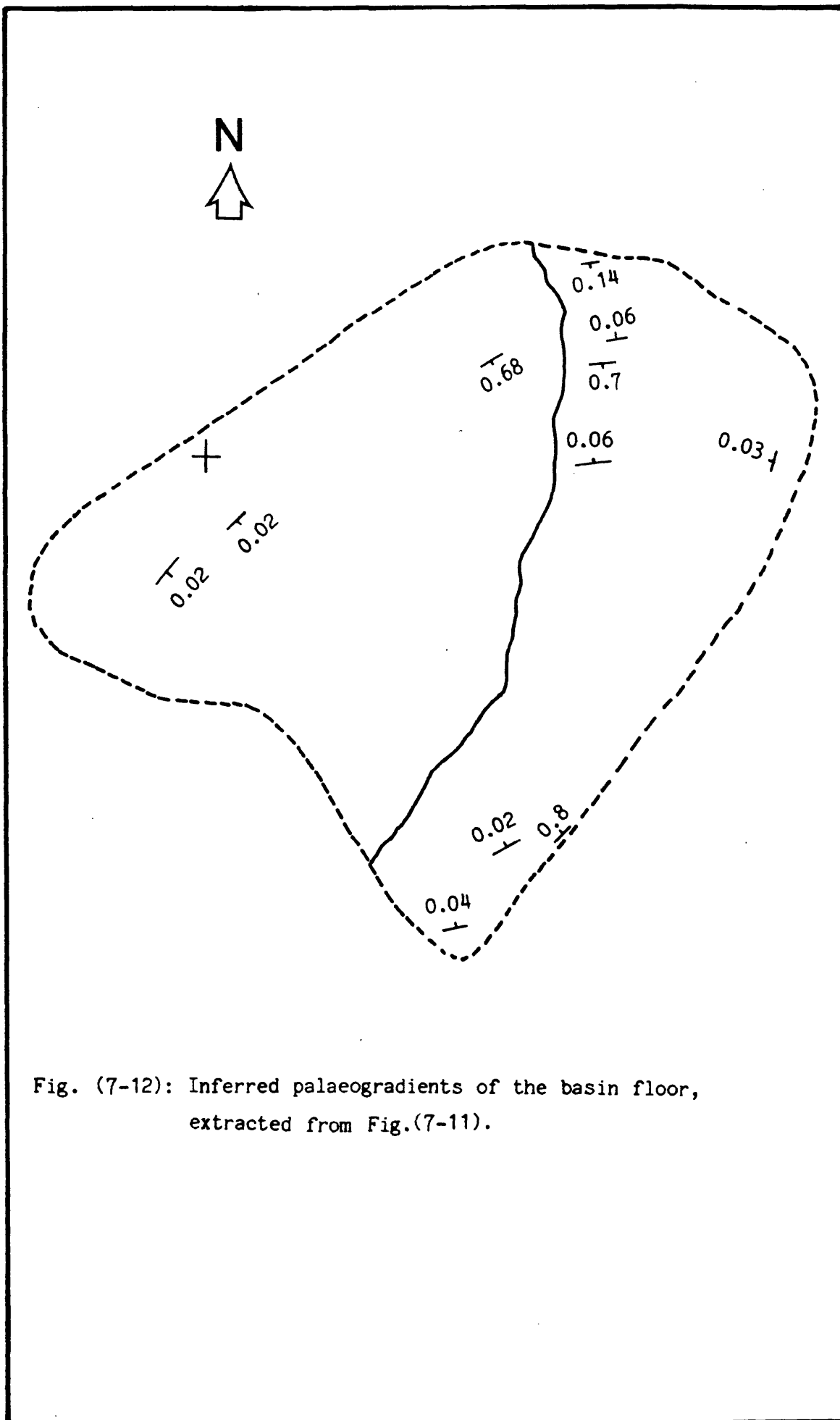


Fig. (7-12): Inferred palaeogradients of the basin floor, extracted from Fig.(7-11).

the basin floor gradient (Fig.7-12) can be realistically estimated from the stratigraphic representation of the basin floor shape (Fig.7.11).

A significant problem arises from the stratigraphic model interpretation of basin shape (Fig.7.11). This problem originates from the gaps of the unsampled areas between logs. This could mean any positive or negative topographic events, which could have occurred between these sections throughout the studied area. However, this could be answered from the lateral extension and variation of both grains and facies on either the grain-community or the facies models (Figs. 7.7 and 7.9).

From the above arguments, it seems obvious that each of the proposed methods of basin configuration depends completely on the other two models and could be vital and supportive to each other. This is unlike what most basin analysts are accustomed to, i.e. using only one method to shape any basin for exploration (see Conybeare, 1978 and Miall, 1984). Therefore, the author would like to commend the use of all of the three mentioned models (in 7-1, 7-2 and 7-3), to minimize any obscured events during restoring the basin shape. The objective of using the three models is to detect and construct the paleo-shape and nature of the basin of deposition. Consequently, a better understanding to the basin framework will be achieved. This could be a useful approach to give a realistic preliminary prediction for exploration and reservoir assessments especially before drilling commitments.

7B SYN-DEPOSITIONAL DEFORMATION STRUCTURES FROM THE MIDDLE

MOKATTAM OF EGYPT

Various types of syn-depositional-deformation structures have been observed within the sedimentary sequences described from the northern Nile Valley and the Fayum Basin of Egypt (for the first time in this work). These deformation structures include various types of slumps, gravity block sliding, gravity grain and debris flow, syn-depositional unconformity, growth faults and fluidized flow-escape pipes. They vary considerably in scale and their significance in affecting the depositional characteristics of the basin vary from being localized to regional in extent.

7B-1 Slump Structures

Slumping is the movement of semi-consolidated deposits, as sedimentary mass, by gravity. This movement occurred along a basal shear surface while retaining some internal structures, i.e. bedding (Flügel, 1982). It emphasizes the internal disturbance and folded shear planes (Stow, 1986).

The slumped beds occur in the northern part of the study basin at the east Helwan area. There are three main slump sequences which are traceable for a number of kilometers. They consist of fine bioclastic carbonate mud and small size nummulitic facies. Slumping in these horizons has disaggregated and partially homogenized the sediments. Each slumped horizon occurs as a deformed zone between undisturbed beds (Plate 7-1). These are varied and include pelagic facies, fine grained turbidites, and pelletal lobes. A glide plane, which may correspond with a bedding plane for much of its length, separates

Plate (7-1): Slumped beds occur as deformed horizons between undisturbed beds , east of the Wadi Hof area (looking towards the south direction) .

PLATE (7-1)



m. 4
2
0

Plate (7-2): Slump deformation styles inside one meter thick bed , with vertical dislocated and convoluted beds (right side of the hammer) . Folded and distorted structures are also shown in the left side of the photo . Flow direction was towards the right side of photo .

PLATE (7-2)



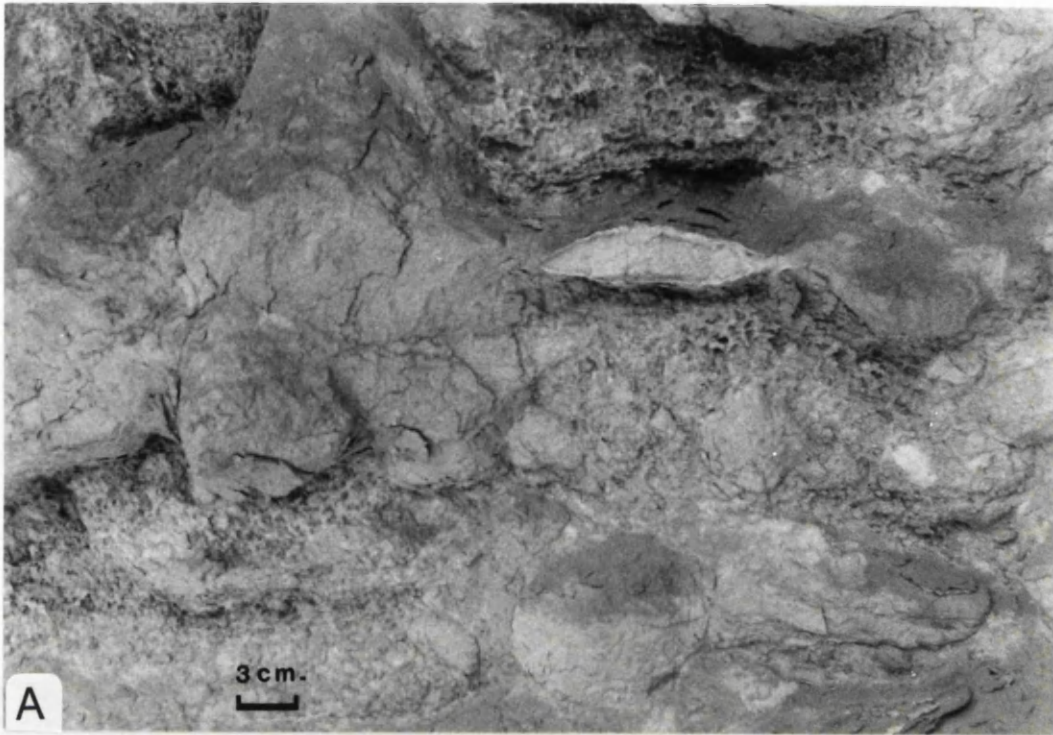
slumping beds from underlying stable deposits. The upper surface of the slumped zone displays irregular topography. This overlain by planar erosion surface. The deformational style within each single slump varies from simple sliding of intact sets of layers, to intensive slumped folds; dislocated beds; convoluted, distorted beds (plate 7-2); slumped balls (plate 7-3); boudinage and rolled up structures (Fig.7-13). Individual slumps vary in thickness from less than 10cm to many meters. The slumped horizons described above comprise about 50% of the Qurn formation deposits (in the deeper parts of the basin). Meanwhile, slumps occur in centimetric scale to a few metres on the southern and eastern shelves.

Downslope slumping of sediment is now well documented from recent sequences (e.g. Saxov and Nieuwenhuis, 1982) and occurrences in ancient sequences have been reviewed by Allen (1982). These syn-sedimentary disturbances of sediment are relatively common in the stratigraphic record and occur in all depositional environments (Farrell, 1984). However, slumps and disturbed zones are often described from ancient deep-water deposits (Woodcock, 1976; Pickering, 1982; Macdonald & Tanner, 1983). The alternation of slumped and undisturbed zones implies intermittent instability of the sediment pile in an area of turbidite and pelagic sedimentation. Slumping may have been initiated by earthquake activity that accompanied movement on the basin-bounding faults and the propagation of extensional planes to the northwest of the basin.

Plate (7-3): A- Slump balls and distorted styles in muddy matrix rich in small (2-3 mm.) nummulites . Base of the Qurn Formation , east of the Helwan area .

B- Soft sediment deformations have been initiated on a basal palaeoslope dipping basinwards (where man stands). Field photograph at the basin plane in Wadi Hof area .

PLATE (7-3)



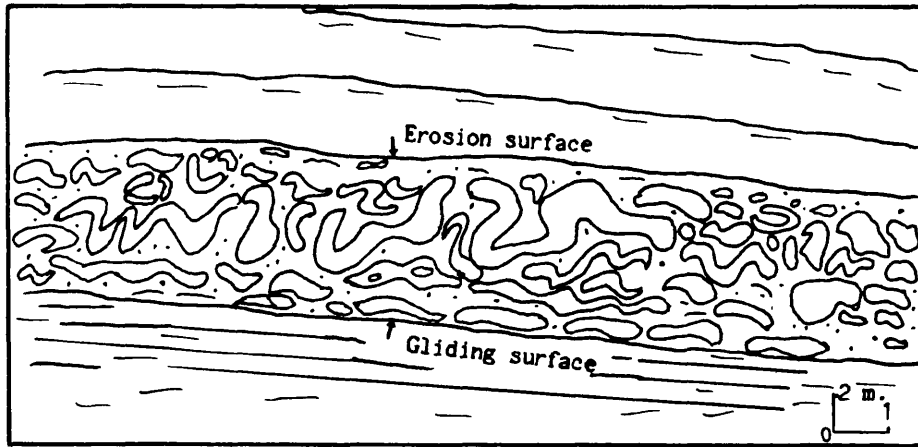


Fig. (7-13): Slumped horizon in a nummulitic facies. These structures show signs of disaggregation. Slumped folds, distorted, and rolled-up deformation occur. Beneath the slump is a basal gliding surface and above it a planar erosion surface upon which sediment was deposited.

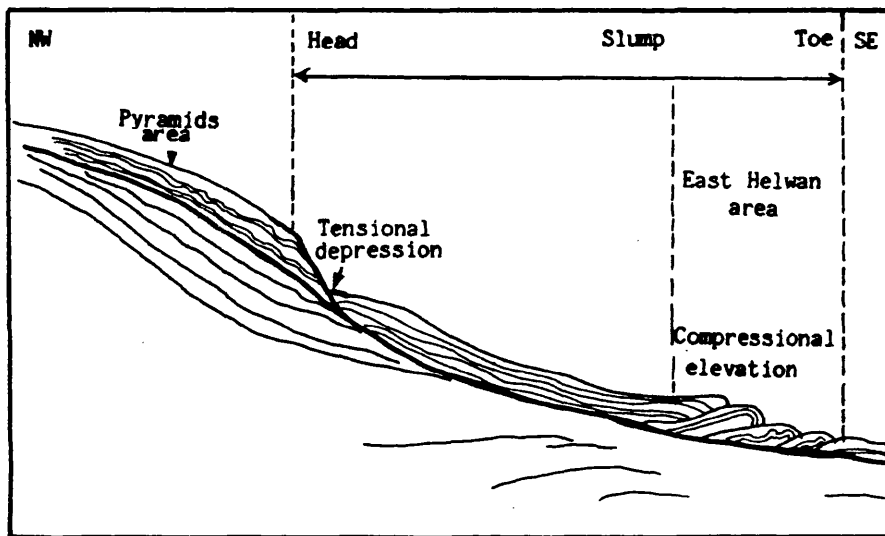


Fig. (7-14): Idealised cross-section of the submarine failure in the Middle MoKattam basin, Egypt (simplified after Lewis, 1971).

Evidence from ancient rocks, that slumping of soft sediments occurs on gentle slopes is supported by continuous seismic profiles from the gently dipping upper continental slope east of North Island, New Zealand (Lewis, 1971). Since slumping increases the thickness of the soft sediments basinwards (Lewis, 1971), that could demonstrate the recorded thickening of the Qurn formation in the deeper areas of the basin, at the toe of the slump. Meanwhile, thinning and partly missing of the Giushi facies around the Giza pyramids area may point towards the head of the slump (Fig.7-14) at this area. The movement direction of the slump sheets is assumed to have been perpendicular to the mean axis of slump folds (Jones, 1940; Woodcock, 1979). The mean direction of the palaeoslope strike around the deeper area of the studied basin is estimated (Fig.7-15) using the movement direction of slumps. This result is supported by the palaeo-reconstruction of the basin configuration (Section 7,A).

7B-2 Gravity Block Sliding

Sliding means the downslope displacement of a semi-consolidated sediment mass along a basal shear plane while retaining some internal (bedding) coherence. It emphasizes the lateral displacement along simple or slightly rotational shear planes with little internal disturbance (Saxov and Nieuwenhuis, 1982; Stow, 1986).

Gravity block sliding occurs twice in the vertical sequences of the studied basin. The lower sliding zone associated the basal beds of the Wadi Hof section. It is represented by very large slided blocks, some of which (Plate 7-4) reach up to one kilometre wide, 40 metres thick and extends to about 5 kilometres

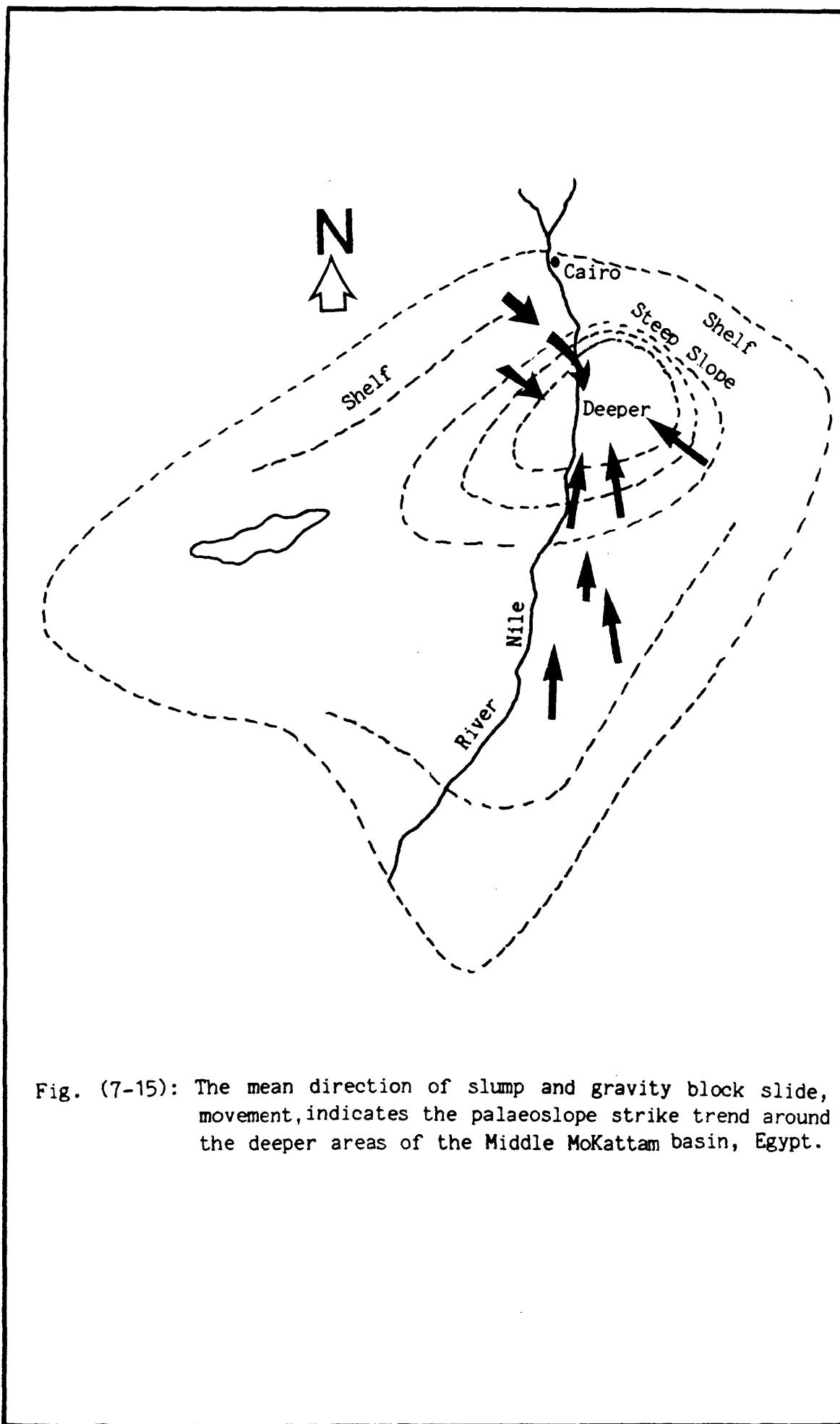
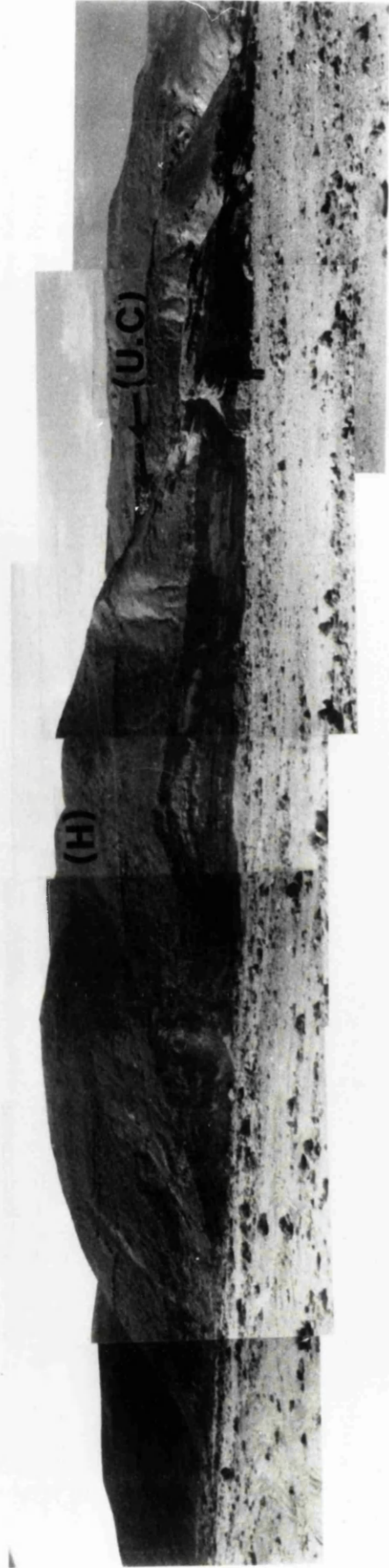


Fig. (7-15): The mean direction of slump and gravity block slide, movement, indicates the palaeoslope strike trend around the deeper areas of the Middle MoKattam basin, Egypt.

**Plate (7-4): Gravity block slide characterized by lower steep , mega
slide , carbonate mass (S) overlaid by horizontal sequence
(H) . Both are separated by syndepositional unconformity
(U.C) .**

PLATE (7-4)



long in a N.W. direction. The basal sliding rotational plane is dipping 20 degree basinward (at the basin plane, plate 7-3). The rocks of this sliding block reflects a nummulitic facies components. The internal beds are characterized by some deformations such as thrust faults, overfolding, slumping and over-riding of beds. These could be formed as compressional structures which normally associate the toe area (Fig.7-14) in a basinward direction (Lewis, 1971). The produced compressional elevation (Fig.7-14) might represent an active factor which demonstrates for thickening of basinal deposits recorded.

The upper gravity sliding zone occurs as horizons of blocks or elongate boulders of dolomite bivalval facies. These slided blocks are relatively smaller (nearly up to 4 metres long; 3 metres wide and 1 metre thick) compared with the lower sliding zone. The best example of this zone is the middle part of the Wadi Garawi facies in the deeper, basinal areas.

These gravity block sliding and slumping processes are found to be occurred on the basin slope of low gradient. This gradient of the slope some time before the flow was up to 6 vertical to 500 horizontal, i.e. an angle of about 0.68 degree (as estimated in the previous part of this chapter or by restoring the slumped sequence). However, these processes were described as very widespread on slopes of all gradients starting from 0.0022 (recorded by Komar, 1972) to greater than 0.5 (Stow, 1986).

7B-3 Gravity Grain and Debris Flow

Those terms mean the gravity or mass flows of mixtures of sediment and fluid in which bedding coherence is destroyed and the individual grains move in a fluid medium (Dott, 1963;

Plate (7-5): Grain flow deposits moving down submarine slope . Basal rotational shear indicates flow direction towards the right side of plate . (Deposits are up to 20m. thick) .

PLATE (7-5)

Flow direction



Middleton and Hampton, 1976). Grain flow caused by grain to grain interactions, while debris flow is characterized by matrix supports of the clasts (Crevello & Schlager, 1980; Naylor, 1981; Flugel, 1982; Stow, 1986 and Cas & Landis, 1987).

Grain flow deposits, in the study area, are represented by (up to 20M) thick massive beds outcrop at Wadi Hof area (plate 7-5). They are composed of a complete clasts supported mass of nummulitic and pelletal facies. Grains are poorly sorted (few millimetres up to 50cm. diameter). Orientation of grains are parallel to flow direction. That flow was towards the basin centre as indicated from the basal rotational shear and slump directions (plate 7-5). The base of the grain flow deposits is generally flat with scours and injection structures. Reverse grading also occurs near the base. Fluidization escape-cavities and faint dish-shaped laminae occur on the top half of the flow deposit. These could indicate that the excess pore pressure is dissipated and the flow came to sudden halt or freezed (Stow, 1986). Debris flow deposits are represented by highly concentrated thick deposits (up to 50 metres) of matrix supported clasts (plate 7-6). These clasts are varied in size (few centimetres up to 0.7 metres) and are of nummulitic facies origin. Beds are generally massive and vertically characterized to 3 horizons which reflect successive flow planes. Slump deposits are usually associated with these sediments. Flow direction is believed to be towards deeper localities. These debris flow deposits are well exposed in the studied basin at Wadi Hof east of the Helwan area and in north east of the Beni-Suef.

**Plate (7-6): A- Debris flow deposits with matrix supported clasts . Gabal
Tarbul northeast of the Beni-Suef area .**

**B- Debris flow sequences in deeper Wadi Hof area east of
Helwan , Cairo . Note the formation of highly concentrated
thick deposits with matrix supported debris .**



The thick recorded gravity grain and debris flow deposits indicate that the flows were formed on more gentle slopes (Watkins and Kraft, 1978). These gravity flows were capable of travelling for long distances over those very low angles basin slopes of 0.5 to 2 degrees (Flugel, 1982). They might probably initiated by seismic shock, slumping and as a result of rapid sedimentation (Stow, 1986).

7B-4 Syndepositional Unconformities

This type of deformation was formed during the deposition of the Middle Mokattam facies in the studied area. It occurs within the sequence of the basinal as well as the shelf deposits. Both the angular unconformity and disconformity are represented.

Angular unconformity is represented by a surface of syndepositional erosion of soft sediment deformation. The underlying beds of the unconformity surface had been tilted or folded due to soft deformations. Examples of that type of syndepositional unconformity are found in the basinal facies at Wadi Hof and east of El-Tebbin areas. In these localities, the lower beds were tilted and folded due to gravity block slide thin overlaid by another horizontal strata (see plate 7-4). Such that unconformity occurred when the shelf floor, soft beds, had slid due to gravity towards the basin. Contemporaneously, an upper horizontal beds were deposited. In East of the Beni Suef area at the basal beds of Gabal Tarbul Abou-Khashirat, another example of the angular unconformity is recorded.

The disconformity type is represented in the deeper facies of the studied basin, east of the Helwan area, in different levels. In this example, the shelf sediments were brought in to

intercalate horizontally the basinal facies either by slumping or by flow as debrite and grain flow facies. Age mixing is usually recorded with these levels of syndepositional unconformity.

Generally both of the unconformity types change to each other throughout the basin.

7.B-5 Growth Faults

Growth faults are important syn-sedimentary faults which have been widely recognised in the studied area (plate 7-7). They are listric normal faults which were active sometimes during sediment deposition.

The faults occur in the basal facies of the Middle Mokattam Unit of the Nile Valley of Egypt. They are exposed at Wadi Hof and Wadi Abu Selley areas of the east of Helwan. This succession comprises of up to 204m of carbonates. Growth faults have been detected at the lower part of this succession between El-Maadi Kattammia Road and east El-Tebbin area. The majority of these examples have a general northwest - southeast direction. Some few examples were directed nearly east west. These faults affect an 50-80m interval, and the overlying strata can be seen unaffected by the faulting (plate 7-7). They are considered as listric faults. These listric faults (plate 7-10) flatten from about 60 into bedding plane faults. These faults were interpreted as gravity slide growth faults. Greater thickness of carbonates occurs on the downthrown side basinward of the synthetic faults (plate 7-7). At the top of the faulted interval the dipping faulted beds are truncated in the distal parts of each fault block and some of the material eroded from these sites appears to have been redeposited in depressions immediately adjacent to the fault on the downthrown side. The localized carbonate dominated facies on the downthrown side of each fault, suggests that movements along the fault created a localized depression in the depositional slope which became a prime site for the accumulation of clastic carbonate sediment. Differential sedimentation of this

Plate (7-7): Syndepositional growth faults with the basinal carbonate deposits at Wadi Hof area . Faults are of the listric type . The upper horizontal bed indicate end of the growth deformation event .

PLATE (7-7)



nature may have perpetuated the fault movements for sometime causing the fault to grow until the locus of sedimentation shifted away from this area. Repetition of these growth faults downslope create deepening in the trough area of the basin. Evidence for the sedimentation during faulting is clear for the larger scale faults.

It is believed that these growth faults were formed due to rejuvenation of the deep seated faults during deposition of the Middle Mokattam facies. The recognition of growth faults in the northern Nile Valley basin has considerable potential significance for the lateral extent and thickness of the carbonate sediment. Although the recorded faults are limited to the central area, they clearly influenced sedimentation and the resultant facies patterns.

7,B-6 Fluidized Flow/Escape Features

These types of structures are represented, within the basin sediments, in form of flow escape pipes, liquified scape cavities (plates 7-8 & 9) and dish structures (plate 6-10,F). These are associated with both Giush and the Middle Mokattam facies. Dish structure occurs at Wadi Abou Serria-Suez road (section 49) and described previously in chapter 6 (article 6-7) associated with the pelletal facies (F7).

Plate (7-8): Fluidized escape pipes associated with the grain flow deposits formed at the deeper edge of a gravity block slide . These soft sediment deformations were formed at the sediment water interface in Wadi Hof basinal carbonates .

PLATE (7-8)



**Plate (7 - 9) : Close up of the fluid escape pipes at the same locality
of the previous plate (7 - 8) . Escape cavities are also
shown on the upper left of photograph .**

PLATE (7-9)



Flowescape pipes and liquifiedescape cavities are abundantly formed in medium to very coarse debris and grain flow deposits. Examples of these structures are recorded at Wadi Hof and east of Helwan areas (plate 6-9). Fluidized escape flow structures are post-depositional structures which formed in unconsolidated sediments as a result of pore-waterescape. (Reineck & Singh, 1980, P.92). This occurred when the fluid of the loosely packed framework of the flow grain and debris deposits is displaced upward with more tightly packed grains and intruded as pipes into the adjacent soft debris. Liquifiedescape cavities are usually recorded near the top of the grain flow deposits (plate 7-5) and associated with the flow pipes (plate 7-8 & 9).

These types of fluidizedescapes features are believed to be formed due to highest discharge rates at the water sediment contact (Lowe, 1975 & 1978; an Reineck & Singh, 1980, P.94). Also, recording of these structures in the Middle Mokattam deposits demonstrate for a quick rate of deposition.

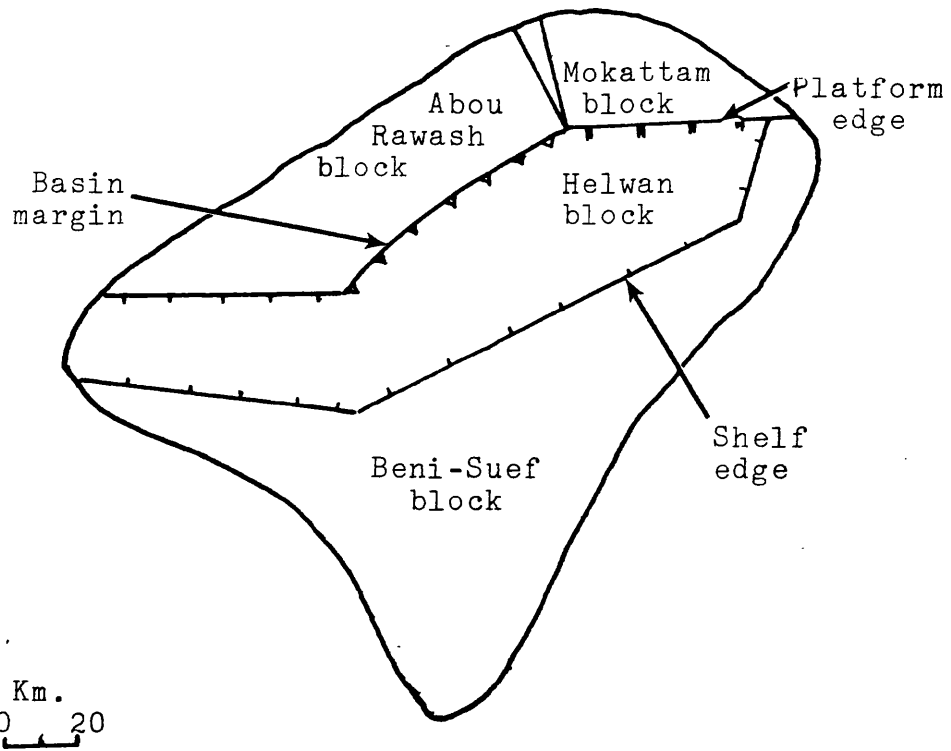
7-C TECTONIC INFLUENCE AND BASIN SEDIMENTATION

As reported in all literatures on the structural framework of Egypt, the area of study is included within the Eocene structural stage of Sigaev (1959). It is also located entirely in stable shelf zone of Egypt (Henson, 1951; Said, 1961 and 1962) while the northwestern borders of the area occur along the stable-unstable shelf contact of Said (1961 and 1962). The stable shelf

sediments are believed to be deposited on a peneplaned basement complex (Shukri and Said, 1944). The (stable - unstable) shelf was covered by northwestern shallow sea spreading out from elements of the paleo-Tethyan geosynclinal system. The general dip of the depositional shelf was believed to be towards the northwest direction (Said, 1962, and El-Shazly, 1977).

The detailed investigations carried out in this study indicate synchronous events of uplift and subsidence during the deposition of the Middle Mokattam facies. The basin exhibits abundant evidence of synchronous tectonic uplift and sedimentation. Features such as: growth faults, syn-tectonic unconformities, debris and mass gravity flow deposits, testify to a direct link between sedimentation and tectonism. This is also demonstrated (chapter 6) from: (1) the nature of the tectonically controlled marginal marl (F1) and channel fan (F3) facies: (2) The occurrence of submerged paleohigh underneath the coral buildup facies; the slumping and disappearance of the Giushi facies from ^{the} /uplifted (pyramids; N.W.) area towards the deeper subsided (Helwan; S.E.) locality and (3) the accumulation of a huge thickness of sediments in the subsided basin while thinned or disappeared towards the uplifted blocks. Repetition of soft sediment deformations at different levels highlights the episodic nature of uplift in the external parts of the basin.

A



B

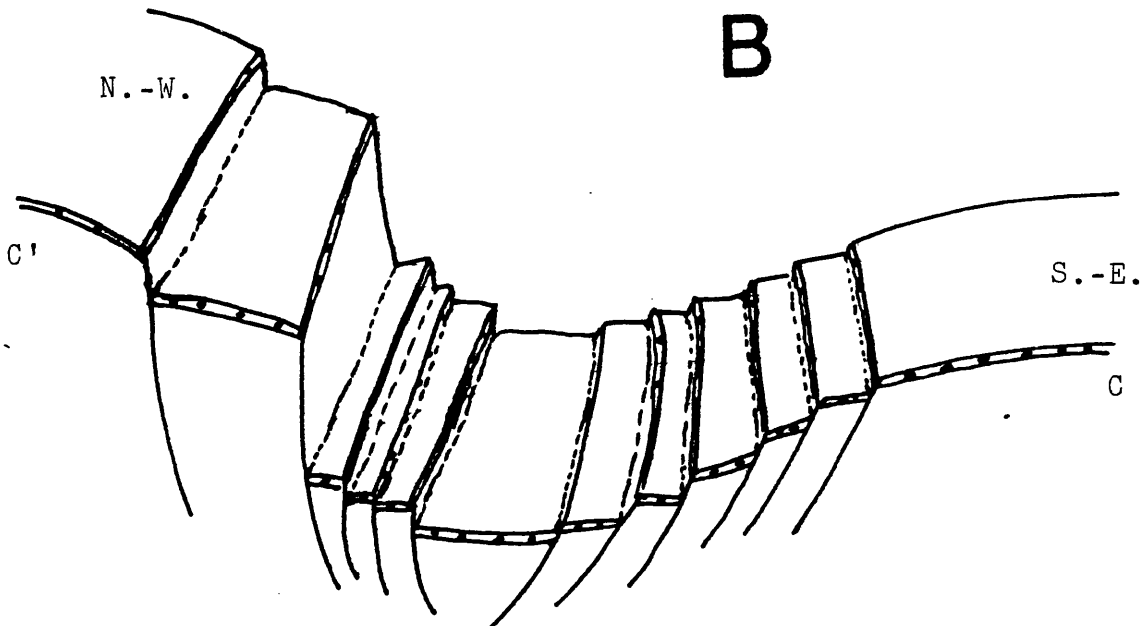


Fig.(7-16): Inferred major block faulted units "A" and framework of the deep seated subblocks "B" ,which constructed the Middle Mokattam basin in the Northern Nile Valley Egypt .

The uplift and subsidence were behind the unstable conditions which articulated the basin shelf into four principal faulted blocks (Fig 7-16,A). The northern block (Mokattam) was submergently uplifted and detached as isolated platform. The second block was the northwestern part (Abou Rawash complex) which succeeds older deposits with compressive northwestern folds. These folds are known as the Syrian arc system (Shukri, 1954) and have a steeper dip in the southern flanks (Said, 1962), which form the northwestern slope margin of the Middle Mokattam basin. This slope margin accelerated the slumping and block sliding processes of the predeposited soft sediments of the Giushi facies in that area to either redeposited slope facies or glided deeply basinward. This block is believed to be plunged southwesterly where a clastic channels established. The most uplifted northwestern corner of the Abou Rawash remained eroded land.

The southern block (Beni Suef - El Saf) was a wide shelf gently dipping northwards. This was affected by seismically triggered pulses due to the uplift and subsidence in the adjacent blocks.

The central block subsided and deepened as trough then received rapid resedimentation of gravity flow deposits and fan lobes.

Plate (7-10): Listric fault (A- Close view & B- General appearance) which occurs during the deposition of the Middle Mokattam (light) facies along the basin floor of the Lower Mokattam (dark) facies . Wadi Abou Serriaa - Suez Road , east of the Helwan area .

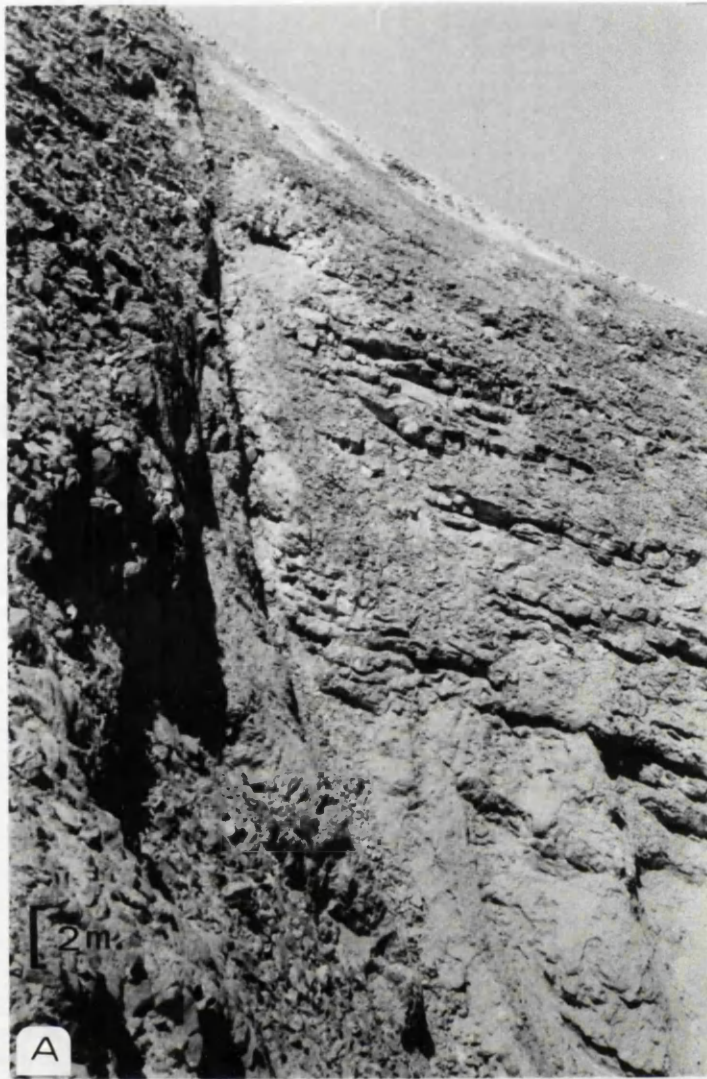


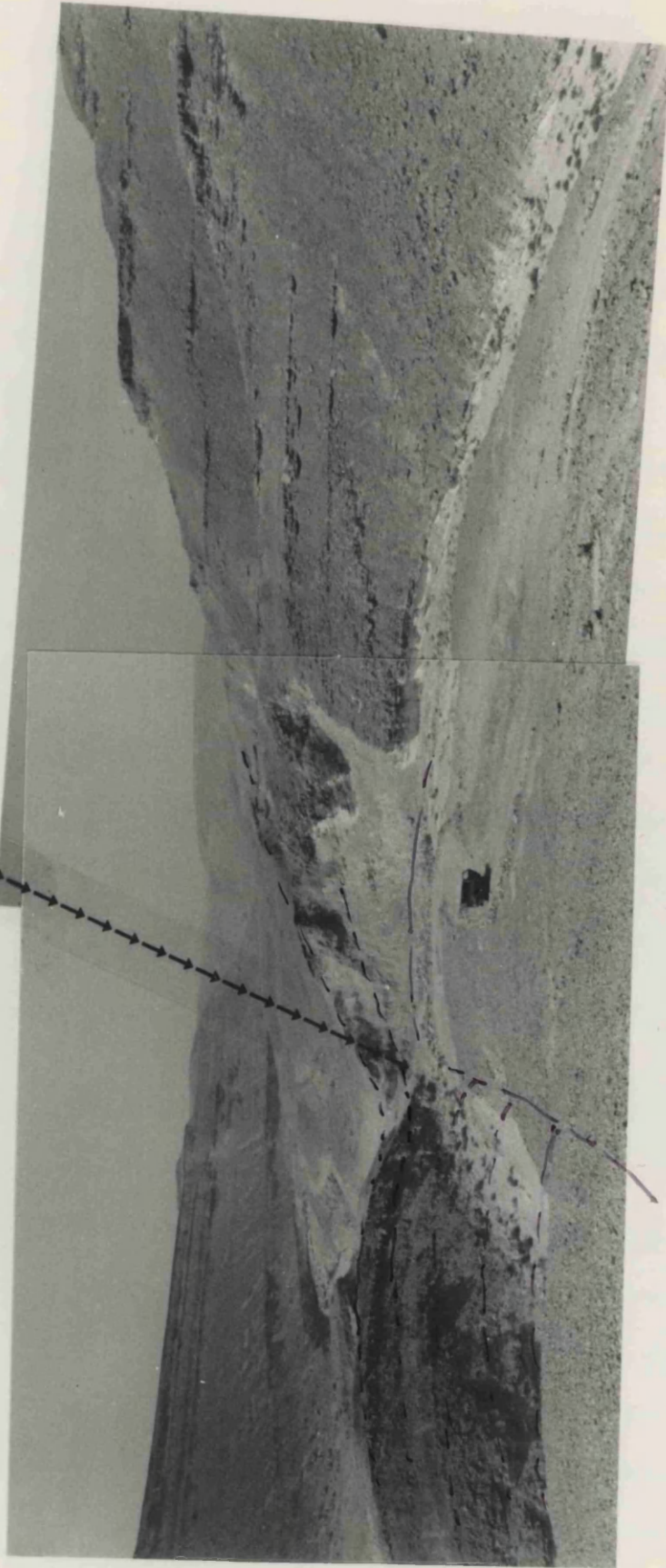
Plate (7-11): Rotational fault in the deeper Wadi Hof Area . The fault plane has a NW-SE direction and its down throw of about 8 meters towards the NE direction . (A- General view & B- Close view to show the soft sediment deformations in the down throw side) .



**Plate (7-12): Panoramic view to show deep seated "Blind structures",
Wadi Hof area .**

PLATE (7-12)

Blind structures



These subsidences and uplifts are believed to be controlled by the rejuvenation of deep-seated faults (Said, 1962 and Salem, 1976) during the deposition of the Middle Mokattam unit. Such rejuvenation of old structural elements has culminated in the subsiding depositional area. Evidence of this syndepositional faults are recorded in the basinal area of east Helwan and Wadi Hof (plates 7-10 to 7-12). Two types of structures are recognised ; visible and blind structures. The visible deep structures are those reflected on the facies surface either as listric (plate 7-10) or rotational (pl.7-11) faults. The blind structures (plate 7-12) are produced above deep seated structures and are predicted by sinking of the overlying facies. The major trends of these types of structures are NW-SE and SW-NE directions. Mechanism of such structures is explained by Gibbs (1984) and is believed to be formed due to the extensional tectonism. Migration of these faults towards the deeper areas increased the depostional axis in the trough area of the basin. Therefore the basin is fragmented into large numbers of smaller tilted blocks. The relative displacement of the deep seated blocks (Fig 7-16, B) was responsible for creating the basin slope. Consequently the dip of the northern and northwestern parts of the basin have changed towards the south and southwestern directions. Recurring uplift of the northwestern (Abou Rawash) block has steepened the adjacent marginal slope basinwards and readjusted the bottom subblocks which in turn constructed the basin framework. This is supported from the following selected subsurface and geophysical data (Fig 7-17): (1) Salem (1976) around the Fayum area, southwest part of the basin; (2) Awad

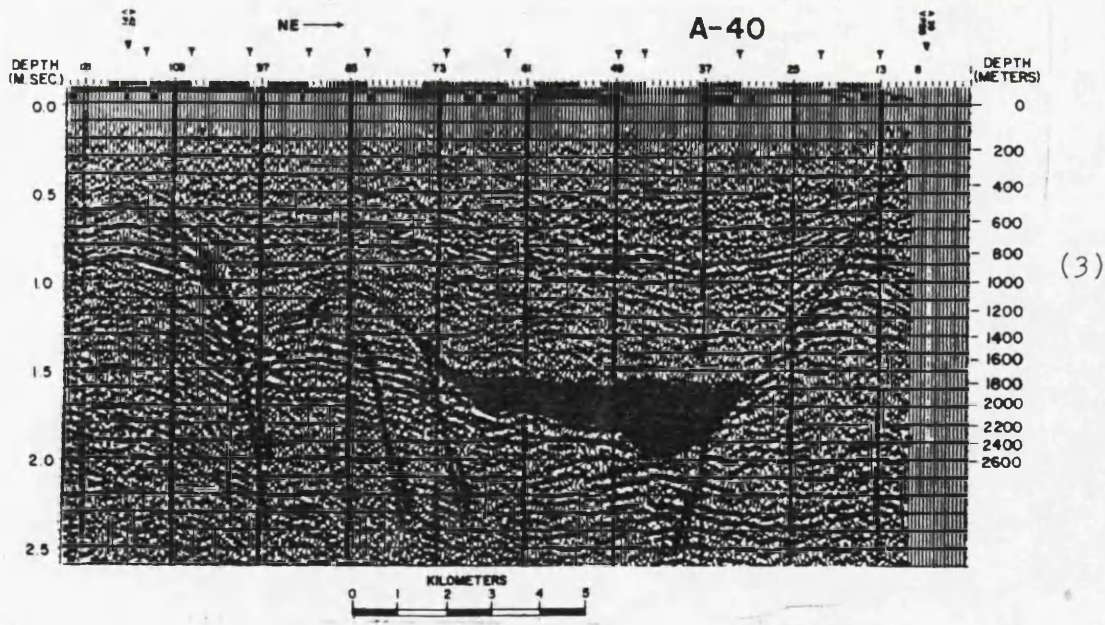
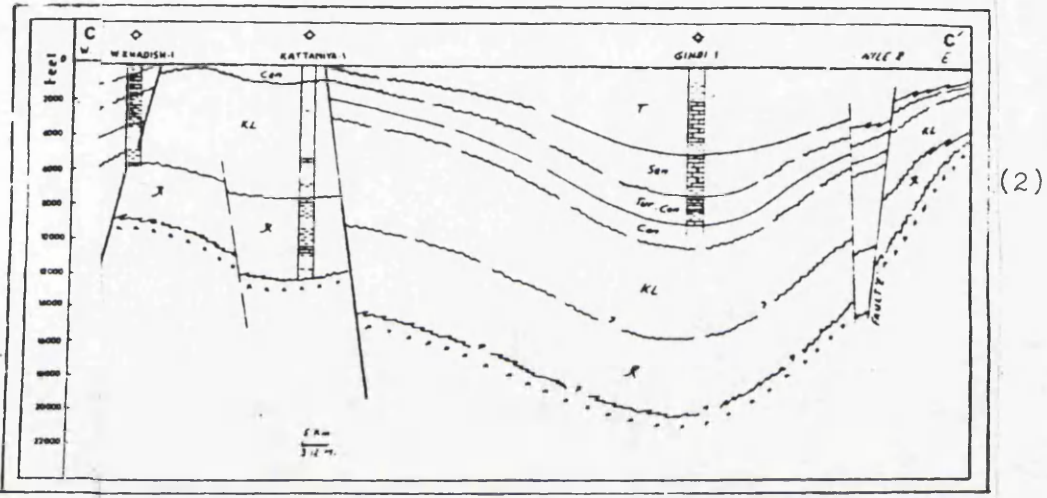
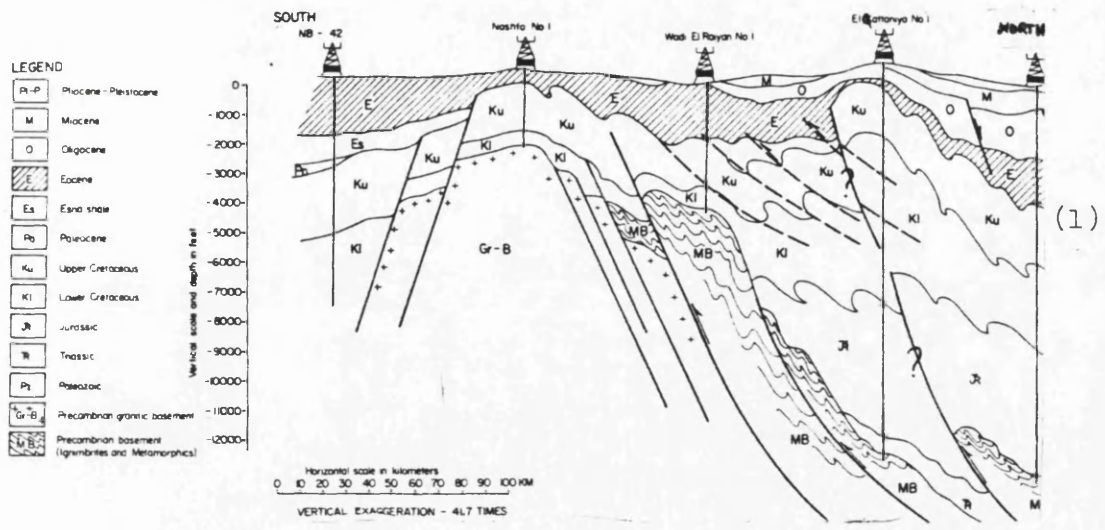


Fig (7-17): Subsurface and geophysical evidence for the deep seated faulted subblocks and the basin framework ; data compiled from defferent sources :

- 1) Cross section from Wadi El Rayan (S.)to Ghard El Qattaniya (N.) ,S-W part of the basin (Salem,1976)
- 2) NW-SE section across X'-X (in fig. 2-1) parallel to the basin centre (Awad , 1984)
- 3) Seismic section on E-W direction north of Cairo (Bentz & Hughes , 1981)

(1984) across the central part of the basin, section X-X' which can be followed in Fig 2-1; and from (3) Bentz & Gutman (1977) and Bentz & Hughes (1981), around the northern limb of the basin north of Cairo.

It is suggested that the gradual uplift of the Adou Rawash and the northern blocks was responsible for the depositional depocentre migration towards the south and south-west and swung the shore line to west of the Fayum area.

Finally the studied extensional basin is no longer considered a stable shelf as thought (Henson, 1951, Said, 1962); however the above syn-tectonic evidence could demonstrate for unstable episodes.

7-D THE MIDDLE MOKATTAM BASIN AND SOURCE OF SEDIMENTS

The broad geographical framework of sediment supply and environment is dependent on tectonics. The movement that affected Africa were epeirogenic, giving a structural pattern of broad basins separated by irregular swells. The plateaus and swells were intermittently uplifted denuded, with the result that they now consist largely of old rocks which were formerly deep seated. The basins were the receptacles of thick continental deposits representing the material eroded from the uplifted swells (Said, 1981, P.526).

The Middle Mokattam basin supply of sediments is completely depended on the affected tectonism. As it was argued (7-C) that the basin was formed as a result of synchronous subsidence and uplift tectonism. By analysing the basin production of facies, it is found that the sediment is supplied, to the Middle Mokattam basin, from two sources: (i) Intrabasinal, and (ii) Extra basinal sources.

(i) Intrabasinal Source of Sediment:

This intrabasinal source in the Middle Mokattam basin is mainly formed by erosion of materials previously deposited within the basin. Most of these materials were of the gravity - displaced type. This was tectonically controlled as demonstrated before. The basin received a huge amount of the gravity displaced sediments from the surrounding shelves. The main source of these sediments was from the northwestern block which was mostly tectonically tilted basinward. Therefore the soft sediments of the Giushi facies south and southwest of the Giza pyramids were completely displaced under gravity towards the subsided basin. Subaqueous slumping, grain and debris flow, and gravity block sliding, are a strong evidence for this gravity displaced sediments. Moreover that, the drastic movement which caused the uplifting and subsidence along rejuvenated deep-seated faults, has contributed, as a generous source for deformed materials, by debris and broken blocks from the inner shelf break.

Resedimentation of these deposits in the basinal area produced the Qurn facies in the Helwan-Wadi Hof area.

Additional deposits formed also from intrabasinal source, are demonstrated in chapter 6. The pelletal facies (F7) which washed from the upslope shelves and flanked to the deeper areas, was a remarkable of basin redeposits. Also the upper shelf deposits, F3 M11 and F3 M15, which reworked and washed down slope as slope wash lobes in the outer shelf deposits, were another source for the basin fill sediments.

(ii) Extrabasinal Source of Sediment

The contemporaneous uplifting tectonism which associated the Mokattam facies has much influence on the sediment supply to the basin. The basin study highlighted the presence of four distinctive paleohighs in the external parts of the basin (Fig 7-18). These are: (1) The Wadi Araba in the southeast borders; (2) The Gabal Ataqa and northern Galala plateau in the NE corner of the basin; (3) The Abou Rawash paleohigh in the northwestern part of the basin; and (4) The Wadi El Rayan paleohigh in the southwestern part of the basin. Some of these blocks are of sizeable dimensions and have been active for long time. The blocks were especially active during Late Eocene (Said, 1962, P.185). The geological sequences of all these paleohighs indicate that they were submerged until the end of Middle Eocene, then uplifted before the deposition of the Middle

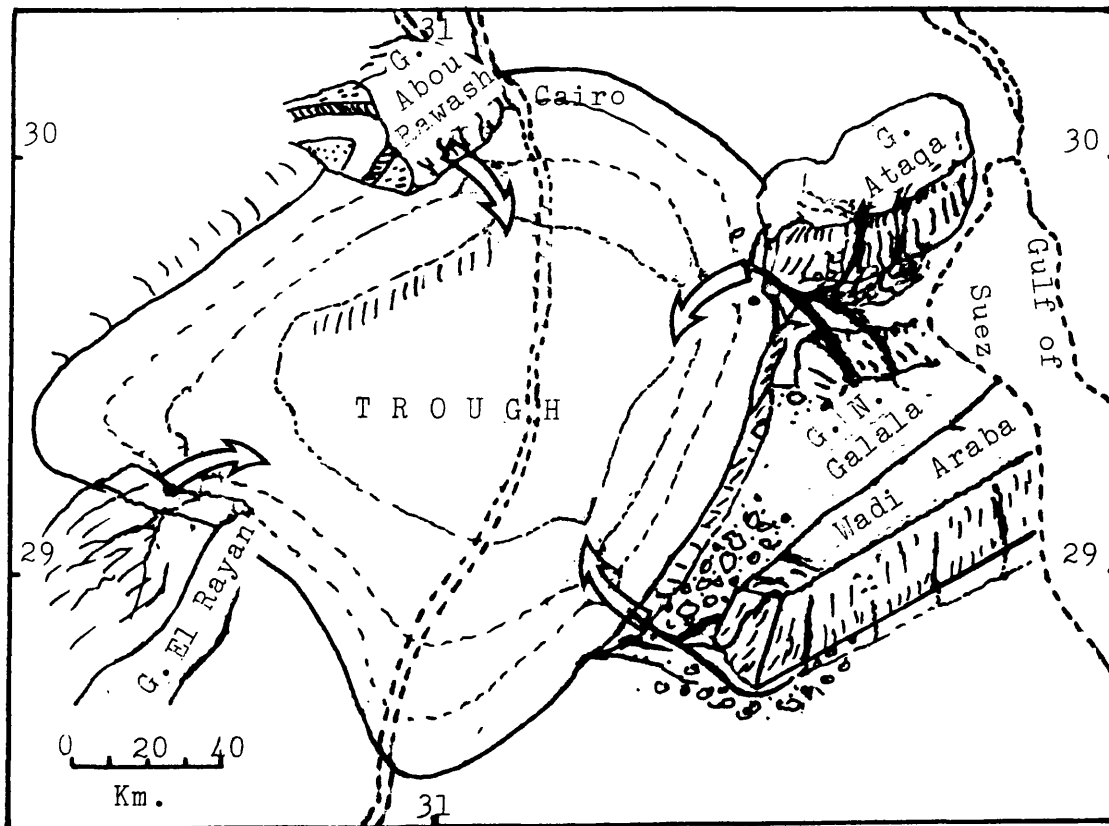


Fig.(7-18): Reconstruction of the paleo-provenance and source areas for the Middle Mokattam basin, sediments. Note the occurrence of deep channel system as the main sediment input (arrows) to the basin.

Mokattam facies and continued to rise synchronously with it. Erosion of these uplifted blocks caused the development of the siliciclastic-carbonate of the studied basin. Some of the paleohighs were block faulted and suffered an epeirogenic upheaval. Severe erosion has left these blocks with older sediments on the ground surface; Upper Cretaceous in Abou Rawash and even Carboniferous in Wadi Araba (Fig 1-4). Huge amounts of this eroded sediments were delivered to the Middle Mokattam basin.

Wadi Araba paleohigh was one of the most important sources for the basin deposits. This paleohigh covers an area of 2950 square kilometre, and uplifted by early Late Eocene block faulting tectonism (Said, 1962). The eroded Eocene to Cretaceous sediments was about 1060 metres thick (upto 600m. thick of middle-lower Eocene and 460 of Paleocene and Cretaceous deposits). That is excluding an unaccounted Jurassic and Triassic sequence of upto 653m. thick (only recorded in Gabal Ataq, Said, 1963, P.185) due to unavailability of local subsurface data. Therefore, the sediment contribution from the erosion of Middle Eocene to Cretaceous cover rocks of the Wadi Araba paleohigh is given as 3127 cubic kilometre. This calculation suggests that sediment supply to the Middle Mokattam basin may have been derived from the erosion of Cretaceous - Middle Eocene cover rocks or older.

The possible sediment supply pathways to the shelf and trough environments were a deep channel system summarised in fig. 7-18. The preservation of the Middle Mokattam upper channel sediments on the south-east margin of the studied basin (plate 6-4) suggest that channel systems existed at least during the earlier late stages of basin fill. Detailed discussion about the nature of these channels was given in chapter 6 (article 6-3-4). It is believed that transportation of the eroded materials from the four different paleohighs through the deep channel systems and redeposition in the basin, was responsible for creating different synchronous rock formations (Beni Suef, Birket Qarun, Saqqara, and Wadi Garawi formations). As suggested in chapter 6 it is believed that siliciclastic detritals were deposited into the nummulitic shelf by means of storm wave sedimentation (article 6-6-4). Also, emergent barrier islands or linear barrier complex with offshore, swash bars, and beach fore shore deposits were acting to supply basin sediments during the late stages of filling the Middle Mokattam basin in the northern Nile Valley, Egypt.

**DEPOSITIONAL EVOLUTION
OF
THE MIDDLE MOKATTAM
BASIN**

CHAPTER EIGHT

8 - DEPOSITIONAL EVOLUTION OF THE MIDDLE MOKATTAM BASIN

The aim of this chapter is to conclude the development history of the Middle Mokattam Basin from the time of its origin to the present.

The analysis of the marine carbonate sequence of the Middle-Late Eocene boundary and early Late Eocene rocks in the northern Nile Valley Basin, lead to the identification of 12 major facies (Figs. 8-1, A, B, C, and D). These are:

1. The Marly Basin margin facies (F1).
2. The Upper platform Marly clay facies (F2).
3. The Wavy modular carbonate fan facies (F3).
4. The mixed siliciclastic carbonate of the Barrier complex facies (F4).
5. The Bivalval Build-up carbonate facies (F5).
6. The Inner and Outer shelf- Nummulitic facies (F6).
7. The fan lobes pelletal facies (F7).
8. The conglomerate debris of slope flow facies (F8).
9. The Coral build-up facies (F9).
10. The serpulid rich hard-ground bottom facies (F10).
11. The open shelf planktonic, and basinal pelagic, foraminiferal facies (F11).
12. The lagoonal shale facies (F12).

By the end of the Middle Eocene and beginning of Late Eocene times, a shelf carbonate basin prevailed to produce the basal part of the Giushi Formation. This shelf was distinguished by a

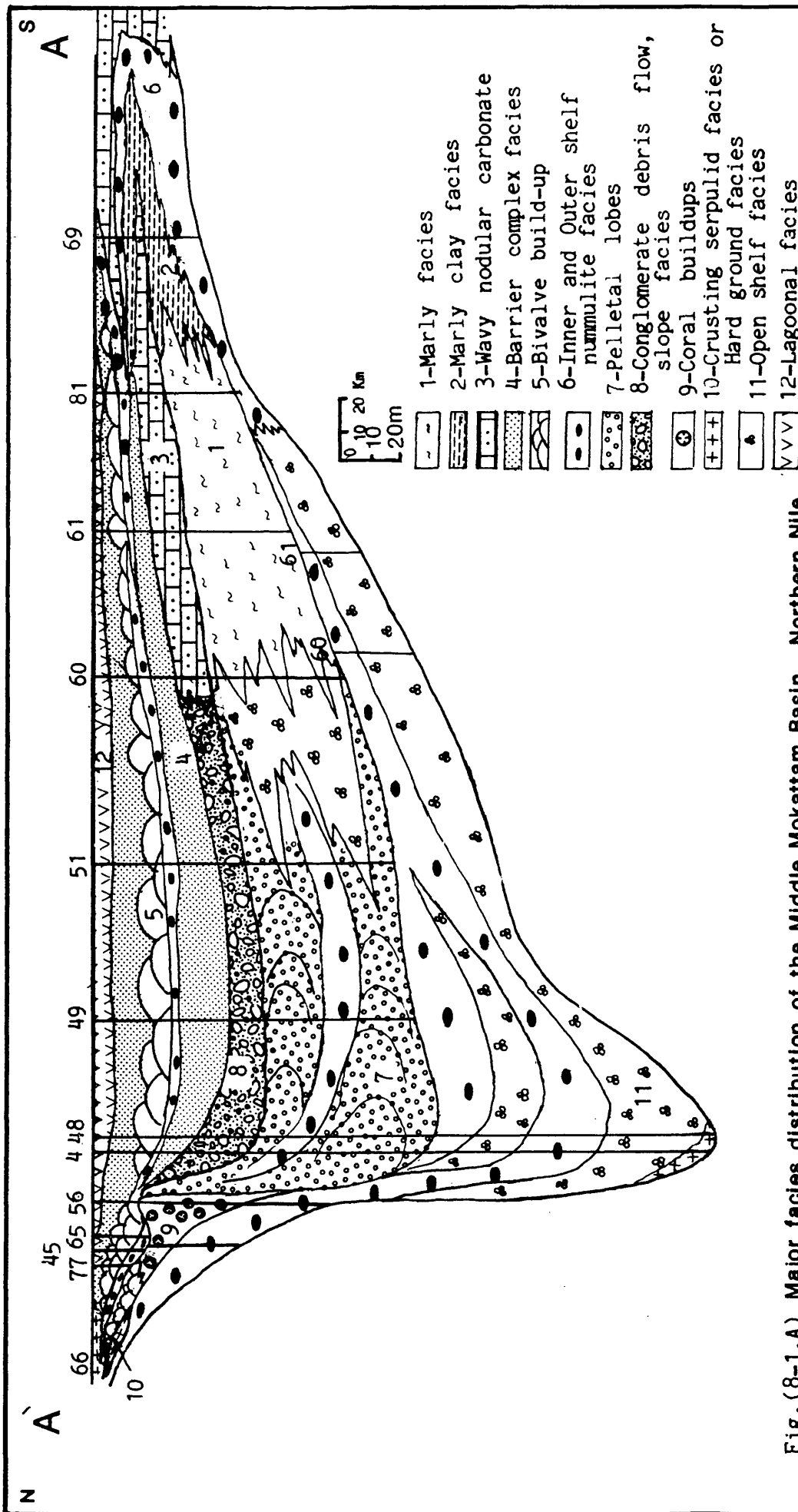


Fig. (8-1,A) Major facies distribution of the Middle Mokattam Basin , Northern Nile Valley and the Fayum, Egypt. Facies correlations along A-À nearly S-N, direction (main direction) .

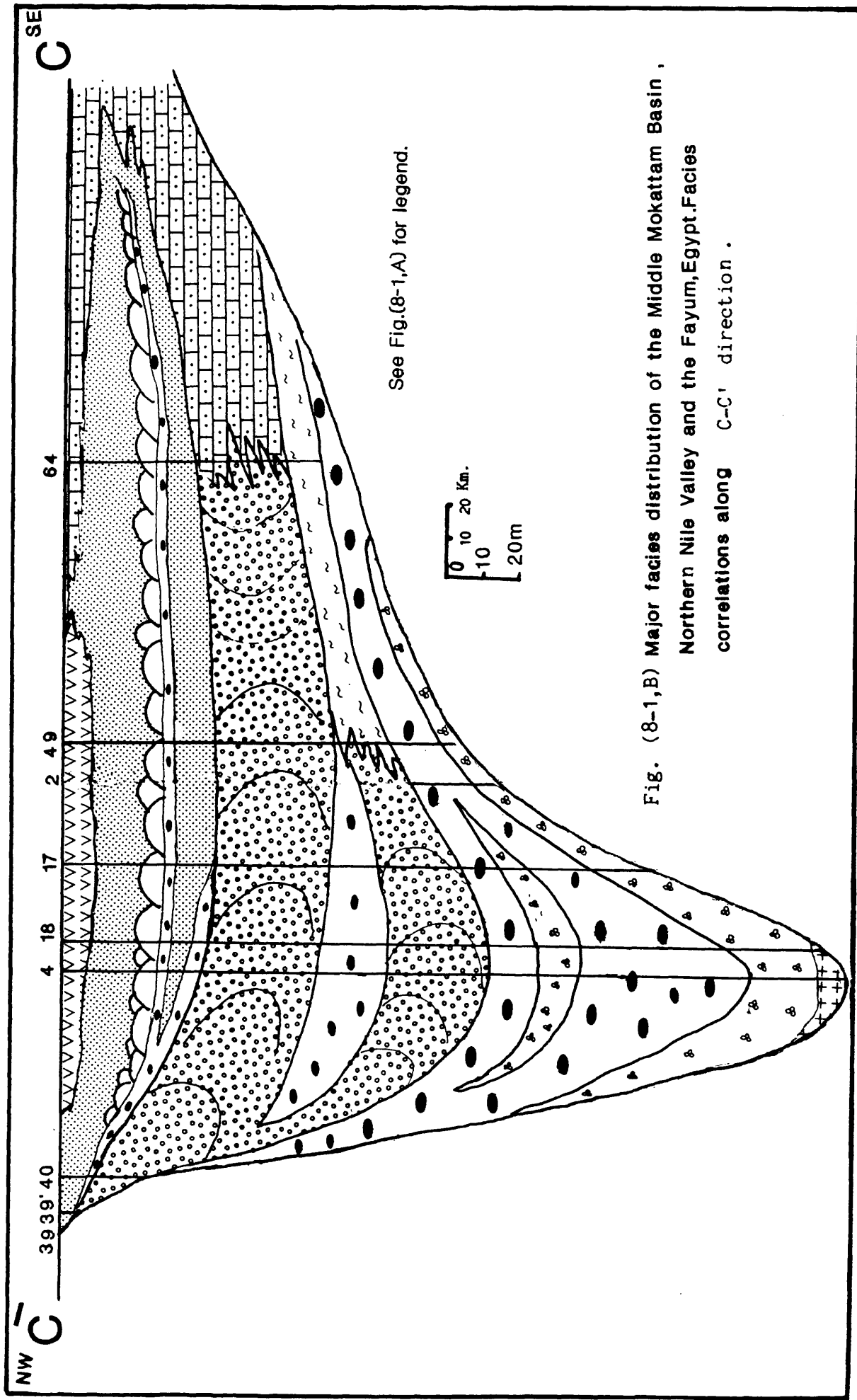
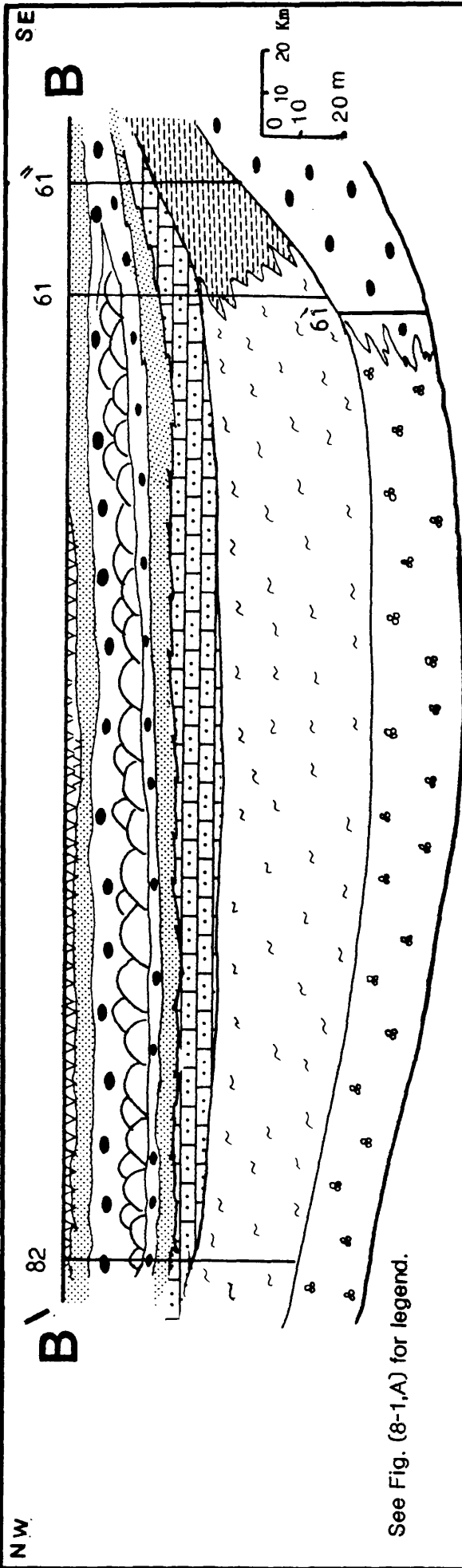
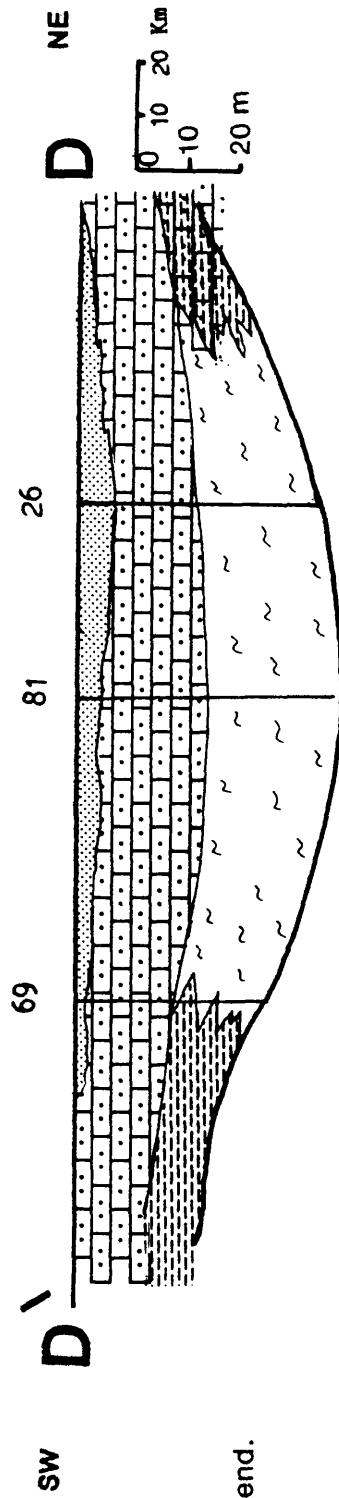


Fig. (8-1,B) Major facies distribution of the Middle Mokattam Basin ,
 Northern Nile Valley and the Fayum, Egypt. Facies
 correlations along C-C' direction .



See Fig. (8-1,A) for legend.

Fig. (8-1,C) Major facies distribution of the Middle Mokattam Basin , Northern Nile Valley and the Fayum, Egypt. Facies correlations along B-B' (NWSE) direction (middle part of the basin)

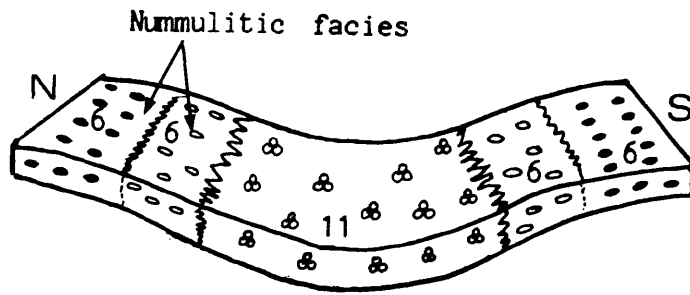


See Fig.(8-1,A) for legend.

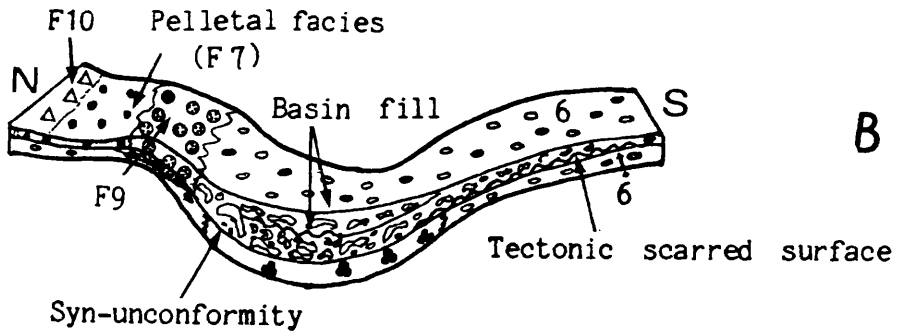
Fig. (8-1,D) Major facies distribution of the Middle Mokattam Basin, Northern Nile Valley and Fayum, Egypt. Facies correlations along D-D' (NE-SW) direction (southern limb of the basin) .

central depression surrounded by a semi-enclosed shallow platform. On the shallow platform a Nummulitic facies (F6) accumulated in both its inner and outer shelf microfacies (Fig. 8.2A) producing most of the external limbs of the Giushi facies. The deeper parts was characterized by the deposition of planktonic and pelagic facies (F11) towards the central part of the studied basin. These facies reflect quite undisturbed depositional conditions at the early stages of the Giushi formation.

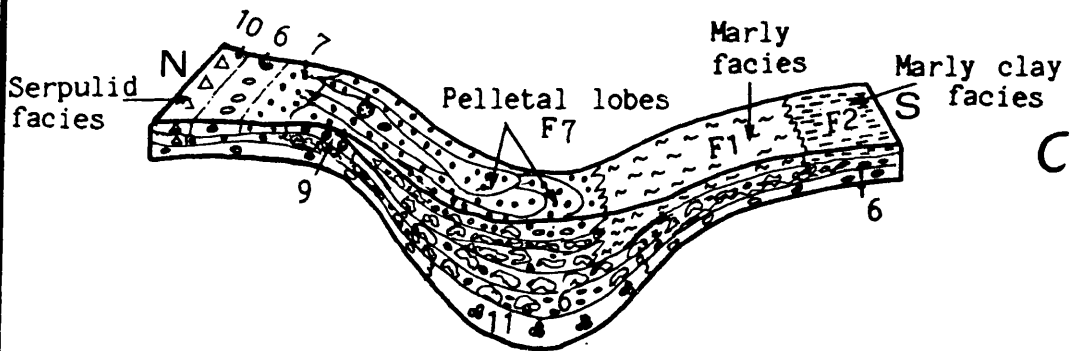
During the early Late Eocene (Fig.8.2B), the studied basin was affected by syn-tectonic movements. These movements resulted in uplifting the north-western parts of the area of study and deepening the basinal parts (probably by rejuvenating older structures). This deepening, in the central part of the study areas, was caused by a series of syn-depositional listric and antithetic faults followed by a drastic disturbance to the shelf nummulitic facies. This disturbance was reflected in a huge sliding and slumping or even flow of the unconsolidated sediments to fill the new formed basin. That gave rise to the thick Giushi facies accumulation, now observed in Wadi Hof area. The uplifted northern and north-western parts overruled the deposition of nummulitic facies on the northern platform. The main effect was a complete shallowing in the inner shelf area (top of the upper platform) with increasing the mud feeding populations producing an intensive amounts of pelletal deposits (F7) which mixed with nummulitic facies in Gabal El-Giushi. The more shallower parts were also inhabited by miliolid forams and encrusting organisms as a hard substrata. This new formed



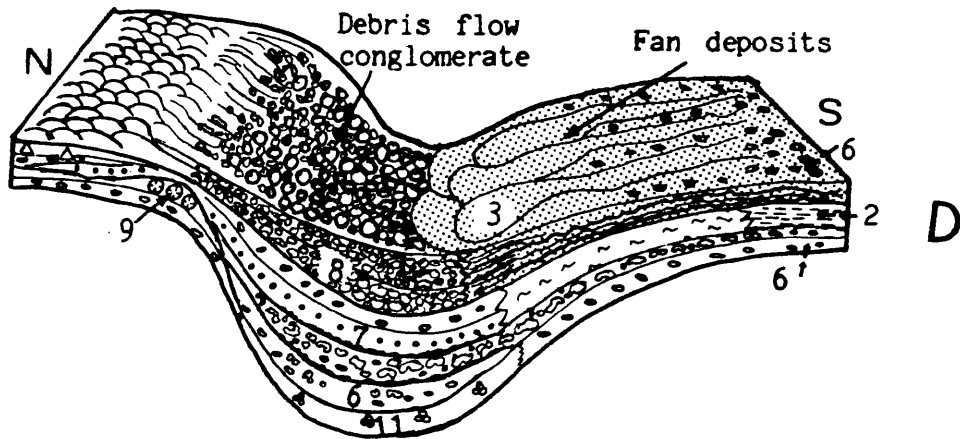
A



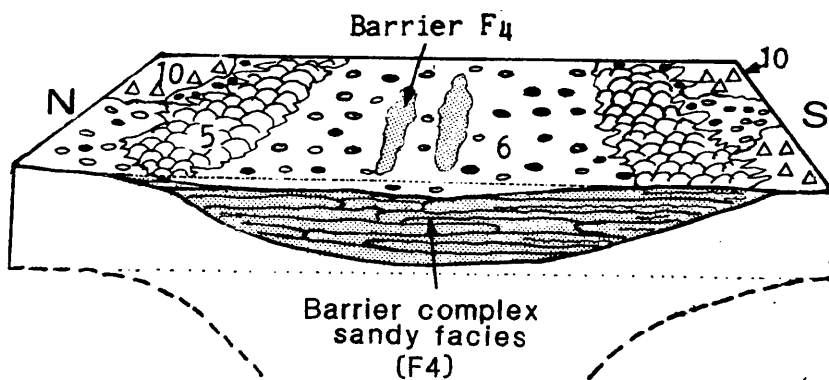
B



C



D



E

Fig (8-2) contd.

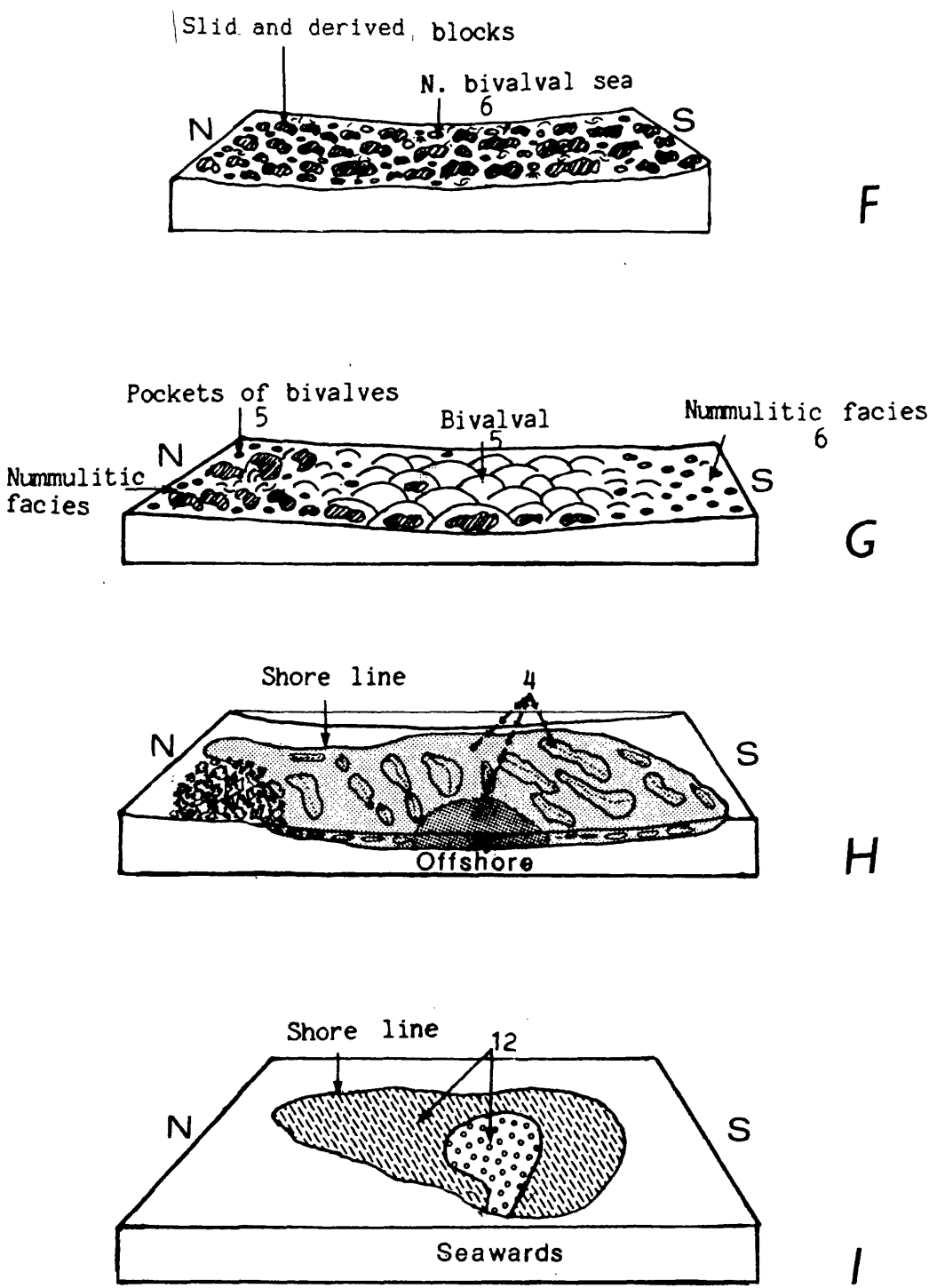


Fig. (8-2): Depositional model indicating the depositional history and developing of the Middle MoKattam Unit A and B, top of Giushi Formation, C, lower members of Middle MoKattam phase, D-I, the upper members of the Middle MiKattam.

environment was ideal for serpulid colonies (Facies 10) to grow as fixed to the hard substrata while the endobiontic serpulid forms bored into it. The north-western part of the area of study (Abou-Rawash - Giza Pyramids area) were uplifted as a land area. Moreover, a reflux of storm deposits interrupted the deposition of the shelf nummulitic facies and mixed with it. Finally the deposition ended with accumulation of sandy nummulitic deposits on the intra shelf break of slope to form a topographically elevated submarine sheets. These sheets acted as a basal substrata on which coral facies (F9) developed on near the end of that stage. However, the southern part of the basin (From El-Saff to south of the Beni Suef areas) was still covered by the open shelf sea developing an excess of the nummulitic and planktonic facies, with a remarkable tectonically scarred base. That phase of deposition marked the end of the Giushi facies development in most of the studied basin while deposition of this unit was still (taking place) building up in the northern parts (from Maadi to Gabal Mokattam area) of the upper platform.

In the Priabonian times, a more extensive tectonic phase was possibly renewed marking the beginning of the Middle Mokattam facies. This movement is recorded by some depositional events within the consequent facies of the northern Nile Valley basin (Fig. 8-2C). Uplifting of the northern parts continued and new subsidgence for the central basinal axis caused the sea water to flood over producing local transgression in many parts of the southern, south-eastern, south-western and western limbs of the Middle Mokattam basin. Sediments on the southern part of the ramp shelf were only stirred on and redeposited producing a

basinal marginal marl facies (F1). The upper parts of shelf were occupied by an upper platform on which the marly-clayfacies (F2) was developed. The new basinal area was covered by a pelagic facies (F11). In these mentioned areas, the Qurn Member of the Beni Suef-Formation and the Birket Qàrun Formation were developed.

The northern parts of the platform in the Mokattam (Giusi) area were uplifted and slightly tilted (towards the south) basinwards. This syn-depositional disturbance caused the shelf unconsolidated sediment to wash over towards the new deeper basin. Most of the pelletal sediments and suspended shelf materials were also swept from the inner shelf pouring into a shelf slope fans to fill in the deeper basin. Deposition of the shelf pelletal reflux as sheets over the platform-edge caused abandonment of the coral facies. The inner shelf nummulitic facies was left inhabited by serpulid and boring organisms.

The subsiding, deeper areas were filled by intercalated cycles of reworked pelletal lobes together with outer shelf nummulitic facies which slumped southwards. Different syn-depositional tectonic pulses were believed to account for the repeated cycles of these pelletal fan lobes and slumped stages. The supplying of basinal-fill sediments from the surrounding uplifted areas gave rise to a rapid accumulation of the Qurn Formation facies in the Helwan-Wadi Hof area.

A third syn-depositional tectonic phase resulted in syn-depositional tilting of the depositional surface, and development of localised syn-tectonic unconformities at the inner basin margin, observed at the eastern side of Gabal Hof.

Deepening of the basinal area results in infill of the marine basin. This infilling phase resulted from the supply of submarine coarse rock fragments as syn-conglomeratic debris flows (F8) to the deeper basin, and the progradation of the shore-line facies as siliciclastic fans (F3) produced from the uplifted surroundings of the basin (Fig. 8-2,D).

Intensive regression of the shore line produced barrier complex sandy facies (F4) which migrated to fill and flatten most of the depositional basin (Fig. 8-2,E). Since global sea-level is interpreted to be rising through the Priabonian (Vail and Hardenbol, 1979), these progradational sedimentary systems suggests that sediment supply rates, by that time, exceeded the subsidence rate.

Flourishing of the nummulitic facies (F6) to survive upon the new formed shallow, nearly flat, shelf depositional surface reflects that the basinal depths apparently remained relatively constant for a short time. This implies an overall balance between sedimentation and subsidence rates. That environmental conditions seemed to be appetizing for bivalval facies (F5) to accumulate on the flat inner margins (Fig. 8-2,E), as observed in both Gabal Shaibun of the Beni Suef and Gabal Giushi of the Mokattam areas. The introduction of both locally-derived and exotic large dolomite boulders and clasts as block sliding (Fig. 8-2,F), signals renewed uplifting and reworked deformation pulses. These seismic shocks resulted in a submarine brecciation terminating the Giushi facies in both Gabal Giushi and Kattamia. This deformation episode which was of short duration was followed by a tectonically quiescent interval. Deposition during this

interval took place on an outer-flat surface, rich with large dolomitic boulders as cores or nuclei on which bivalval buildups accumulated (F5), in a shoaling-up basin (Fig. 8-2,G). On the northern inner parts (Mokattam and Kattamia areas) bivalves only accumulated as pockets between the brecciated surface for being relatively shallower than the basin central parts.

The last stage of deposition of the Middle Mokattam basin was caused by an increase of the rate of sediments supply which exceeded the rate of subsidence and resulted in the infill of the marine basin. This infilling phase ultimately results in completing of the progradation of the shoreline barrier sandy complex facies (F4) (Fig. 8-2,H). This progradation might also be related to renewed uplifting episodes, generating extensive coarse clastic reflux. The uplifting, that time, generated from the north-western corner (Abou-Rawash Massive). This uplifting resulted in syn-sedimentary shifting of the axial-depositional centre southwards to El-Saff-El-Kurrimat areas. Barrier complexes prograded around the basin mouth area in the Fayum area, caused partial closing to basin of deposition from the open sea. This final closing of the sea water on the last time of the Mokattam facies deposition developed a restricted lake producing lagoonal facies (F12), (Fig. 8-2,I).

Increase of uplifting rate caused the subaerial erosion of the north-western part and regression of the sea from South Pyramids area producing sheets of conglomerate channels towards the uplifting centre. This followed by more advancing of the shore barriers probably due to farther uplifting and temporary retreat of the sea shore, causing restricting of the late basin lake and

developed of restricted lagoonal facies (F12), (Fig. 8-2,1). By that stage the last sediments of the Middle Mokattam Unit have been deposited. Then the filling-up history and depositional story of the Egyptian Middle Mokattam basin, in the northern Nile Valley and the Fayum province, were ended and completed.

* * * *

**GENERAL SUMMARY
AND
RECOMENDATIONS**

CHAPTER NINE**9. GENERAL SUMMARY & Recommendations****9.1. GENERAL SUMMARY & CONCLUSIONS**

In order to study in detail the Middle - Late Eocene carbonates of the Nile Valley in northern Egypt, an area of about 15,375 square kilometers, lying north of Maghagha (between longitudes $30^{\circ} 30'$ and $32^{\circ} 00'$ East and latitudes $28^{\circ} 40'$ and $30^{\circ} 10'$ North) has been chosen. The area was subjected to basinal analysis including its stratigraphy and sedimentology. lithostratigraphically, the Middle - Late Eocene succession was subdivided from base to top into the Lower Mokattam Unit, the Middle Mokattam Unit, and the Upper Mokattam Unit, the Middle Mokattam Unit only was studied in detail, and was further subdivided into five rock formations, namely; the Beni-Suef Formation, the Qurn Formation, the Wadi Garawi Formation, Birket Qarun Formation and Saqqara Formation. The Beni-Suef Formation (includes the Qurn Member at base and the Tarbul Member at top) was found to cover the southern parts of the studied area. The Birket Qarun Formation covers the western parts while Saqqara Formation extends throughout the north-western and northern parts of the studied area. Both the Qurn and the Wadi Garawi Formations were found to cover the central and north-eastern parts. These rock units were correlated throughout the studied area. The biostratigraphy is based on the calcareous nannoplanktons and both micro and larger Foraminifera. Range distributions for species of these groups were investigated. The faunal contents of the northern Nile Valley

and the Fayum areas, were assigned to biozones and correlated with the standard known biozones. Five nannoplankton zones were recognised. These are the *Discoaster tani nodifer* Zone (Middle Eocene), *Discoaster saipanensis* Zone (Middle - Eocene), *Chaismolithus oamaruensis* Zone (Middle - Late Eocene), *Isthmolithus recurvus* Zone (Late Eocene), and *Sphenolithus pseudoradins* Zone (Late Eocene). Five biozones based on planktonic foraminifera were recognised; *Morozovella lehneri* Zone (Middle Eocene), *Orbulinoides beckmanni* Zone (Middle Eocene), *Truncorotaloides rohri* Zone (Middle Eocene), *Globigerinatahka semiinvoluta* Zone (Late Eocene) and *Turborotalia cerrozulensis* Zone (Late Eocene). Four Nummulitic Zonations were also established. These are :- *Nummulites gizehensis* Zone (Middle Eocene), *Nummulites beaumonti* Zone (Middle Eocene), *Nummulites striatus* Zone (Middle - Late Eocene) and *Nummulites fabianii* Zone (Late Eocene). Accordingly the age of the Lower Mokattam Unit in the studied area is considered to range from Middle to early Late Eocene. The whole succession identified in this thesis as the Middle Mokattam Unit is considered to be of Late Eocene (Priabonian) age. The Upper Mokattam Unit is also believed to be of Late Eocene age. The Bartonian, of Egypt, is also re-evaluated and reduced in rank to constitute a later stage of the Middle Eocene. Onlap - offlap relationships are recorded also from the outer margins of the studied basin and discussed for the extensive south-eastern and north-western areas of the basin. The different rock Formations of the Middle Mokattam Unit were correlated, using the unit lower boundary as a datum,

throughout the studied area of the northern Nile Valley, Egypt. An isopach map for the Middle Mokattam Unit facies is constructed and the outline shape of the basin of deposition is also detected. For the detailed sedimentological study, 82 columnar sections covering the different rock units were measured, 24 of these were sampled and studied. Careful counting of all the carbonate components was carried out and the different percentages of the different carbonate grains were calculated. The vertical variations, in percentages of the different components, were traced for each collected section (Appendix E). The carbonate analysis revealed the occurrence of 12 major carbonates facies. These are marl (F1), marly clay (F2), the wavy bedded carbonate (F3), mixed sandy clay (F4), the bivalve carbonate (F5), the nummulitic carbonate (F6), the pelletal carbonate (F7), the conglomerate debris (F8), the coralline carbonate (F9), the serpulid (F10), the planktonic foraminiferal carbonate (F11) and the calcareous evaporitic shale (F12), facies. In addition to these, 36 microfacies associations were identified and used to interpret the depositional environments and construct models for the deposition of the Middle Mokattam facies.

New approach for the interpretation of the basin configuration is proposed based on carbonate grain communities, facies and microfacies, and the stratigraphical thickness of rock units.

Syn depositional soft sediment deformation features are recorded and described from the studied basin. These include :- gravity block slides, slumps, debris and grain flows, fluid - escape structures, syn-depositional unconformities, and growth fault structures. These features have been used to interpret the

pattern of syndepositional subsidences in the deeper zones of the basinal area. This if is suggested was controlled by the rejuvenation of deep-seated faults during the deposition of the Middle Mokattam Unit, due to extensional tectonics. Recurring uplift of north-western, Abou-Rawash, block had steepened the adjacent marginal slope basinwards and readjusted the bottom sub-blocks which in turn constructed the basin framework and hence controlled the depositional processes.

The sedimentological history of the carbonate succession in the studied area has been discussed briefly (Fig. 8-2). It is believed that by the end of the Middle Eocene and the starting of early Late Eocene a wide and relatively quiet shelf environment in nummulitic sea prevailed. The central parts of that shelf were gently concave and were receiving pelagic facies deposition. Under these conditions a part of the Giushi Formation was deposited.

Later, the area of study was subjected to unstable conditions which particulated the basin into four distinctive blocks. The northern block was uplifted and detached as isolated platform with nummulitic shelf on top and coral buildup on the platform edge. Later, also on the shallow parts of the platform shelf serpiolid worms and bivalves flourished. Under these conditions the northern parts of the Giushi Formation was completed. The second block was the north-western part which steeply inclined south-easterly forming slope margin and drifting most of its predeposited soft sediments of the Giushi Formation which either redeposited as slope facies or glided deeply basinward. Plunging of that block south-westerly was suitable for deep clastic

channel fan deposition of Saqqara Formation, while the most uplifted north-western corner (Abou Rawash) remained eroded land.

The central block subsided and deepened as trough, then received rapid resedimentation of soft sediments, drifted and glided from the upper margins. Debris and grain flow also accumulated. Shelf wash lobes and land-derived, clastic, pro-graded fans and barrier complex. This subenvironment produced the Qurn Formation. The nummulitic sea has also pro-graded and followed by another tectonic instability which was responsible for gravity sliding phase to cover most of the basin areas. This was followed by bivalval buildup, channel fans, barrier complex and lagoonal facies. This condition leads to the deposition of the Wadi Garawi Formation.

The southern block was a wide shelf gently dipping northwards. The surrounding inner part of the shelf was still nummulitic sea with bivalves which produced the Giushi Formation in this area. Divergent of a deep shelf margin marls landward has occurred due to basin instability and uplifting of the northern and north-western blocks. This produced marls and marly clay facies of the Qurn Member of the Beni-Suef Formation. Deep clastic channel fans from the (Wadi El-Rayan and Wadi-Araba) paleohighs, followed by convergent shore line and barrier complex pro-graded from the paleohighs. Then shelf, conditions with nummulite and bivalve buildups, environment prevailed. These shallowing sea environments invaded by another barrier progradation phase ended with restricted lagoonal environment and the upper member of the Beni-Suef Formation was developed. This

later condition marked the end of the Middle Mokattam facies throughout the studied area.

9.2. Recommendations for Further Research

- (i) Geophysical investigations are needed to confirm the basin configuration described and also to detect the position of postulated deep seated faults. Therefore a detailed study for the geometries of these faults may lead to identify the actual affected tectonism during deposition.
- (ii) Also a detailed analysis of the Lower and Upper Mokattam basins is also necessary.
- (iii) The requisition of subsurface borehole data would also provide invaluable information concerning the history of basin development in northern Egypt. A more vigorous analysis of the subsidence history of Tertiary basins in Egypt is required to test some of the hypotheses resulting from this study.
- (iv) Regional Hydro-dynamic studies and vector analysis may lead to a full understanding to the paleo Eocene sea, and will help to construct paleogeographic maps. The channel systems which were involved in filling the Eocene basins in Northern Egypt, also need more detailed studies.

(v) Diagenetic study for the northern Nile Valley basin may provide information of the effects on diagenesis of burial history for the basin components. This may clarify the different diagenetic stages which deposits have passed through on their journey from land to basin.

It will also provide invaluable senses to understand the uplifting episodes and confirm basin evolution. The field sampling program would be required, although the database would be augmented by existing sample collections at the University of Minia in Egypt.

(vi) The application of magnetostratigraphical dating techniques may allow more accurate resolution of intervals of tectonic activity and inactivity. These methods would be more refined than the biostratigraphical dating techniques used herein, and may reveal gaps in the sedimentary records that have been overlooked in this study.

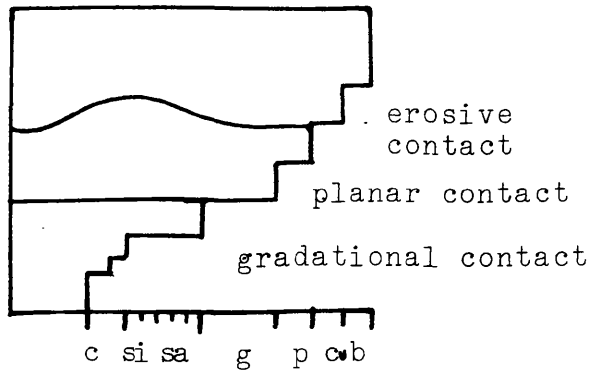
APPENDICES

Appendix (A-1): Approximate Geographic Co-ordinates for
the most important location names in the
study area, cited in this thesis .

Location	Latitude (N)		Longitude (E)	
Abou Rawash	30	02	31	06
Abou Salleh	29	11	31	12
Abou Serriaa	29	45	31	39
Beni Mazar	28	30	30	50
Beni Suef	29	05	31	06
Biba	28	56	30	59
Birket Qarun	29	27	30	40
El Alalma	29	07	31	10
El Fashn	28	52	30	56
El Gabal Ahmar	28	18	31	09
El Kurrimat	29	17	31	20
El Medawara	29	10	30	22
El Mishigeiga	29	08	30	29
El Saff	29	37	31	19
El Tebbin	29	41	31	20
El Wasta	29	20	31	12
Fayum	29	20	30	45
Gabal khashirat	29	12	31	22
Gabal Abyad	28	45	31	02
Gabal Ataga	29	59	32	18
Gabal Diya	28	38	30	58
Gabal El Maskara	29	44	31	34
Gabal El Merair	28	32	31	03
Gabal Gar Gehannam	29	18	30	07
Gabal Gibbo	29	51	31	33
*Gabal Hamrai	29	26	31	23
Gabal Hof	29	54	31	20
Gabal Kattamia	29	58	31	24
Gabal Qibli El- Ahram	29	58	30	08
Gabal Shaibun	29	05	31	15
Gabal Tarbul	29	18	31	19
*Gabal Hadid	28	46	31	04

Appendix (A-2): Approximate Geographic Co-ordinates (Cont.)

Location	Latitude (N)		Longitude (E)	
	•	\	•	\
Gabal Um Rakaba	28	58	31	09
Giushi (Gabal)	30	01	31	17
Giza Pyramids	29	58	31	06
Helwan	29	51	31	20
Kalamcha	29	10	30	50
Maadi	29	57	31	17
Maghagha	28	39	30	47
Mokattam	30	02	31	17
Northern Galala	29	16	32	00
Qasr El Sagha	29	36	30	50
Saggara	29	51	31	12
Southern Galala	28	45	32	20
The Citadil	30	02	31	16
Wadi Abou Moliyssatt	29	48	31	19
Wadi Abou Kashirat	29	10	31	22
Wadi Abou Treifi	29	02	31	14
Wadi Araba	29	08	32	32
Wadi Bayad	29	03	31	15
Wadi Digla	29	58	31	28
Wadi El Aghbig	29	13	31	25
Wadi El Arhab	28	52	31	20
Wadi El Rayan	29	09	30	22
Wadi Garawi	29	47	31	22
Wadi Hof	29	53	31	20
Wadi Lishyab	29	10	31	15
Wadi Matin	29	12	31	16
Wadi Mowillah	28	55	30	30
Wadi Sannure	28	48	31	25
Wadi Sisaba	29	47	31	34
Zaafarana	29	06	32	38

lithological key

Wentworth Scale

	Mudstone
	Shale
	Marl
	Limestone
	Dolomite
	Pebble-supported Conglomerate
	Matrix-supported Conglomerate
	Sandstone
	Intraclasts
	Pellets
	Evaporites

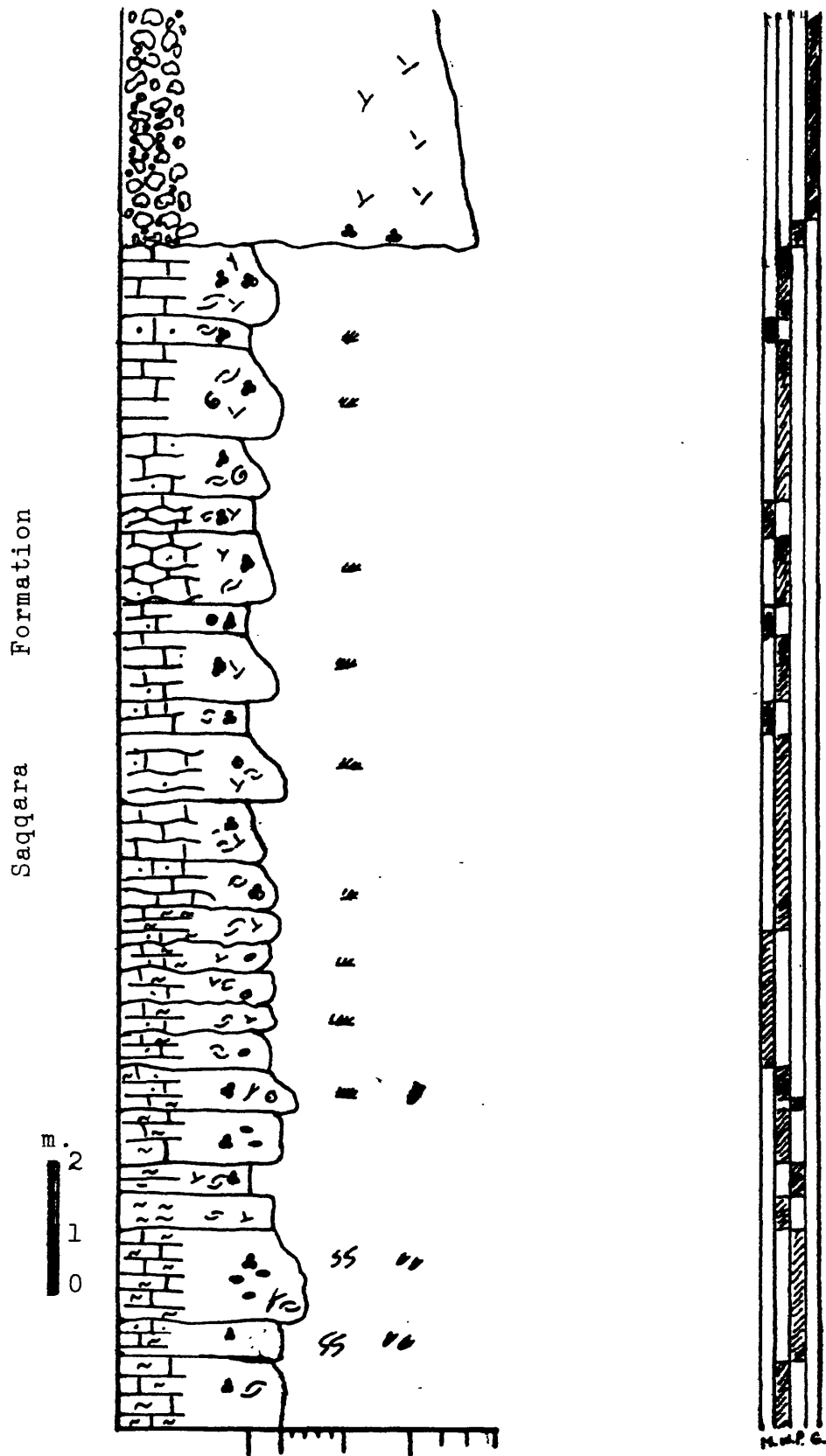
Sedimentary structures & key

	desiccation cracks
	slight bioturbation
	intense bioturbation
	burrows (vertical, inclined and horizontal)
	palaeocurrents
	slump structures
	graphity block slide
	grain & debris flow
	ripples
	cross lamination
	lenticular bedding
	wavy bedding
	cross bedding
	M. Mudstone
	W. Wackestone
	P. Packstone
	G. Grainstone
	B. Boundstone
	Dish Structures

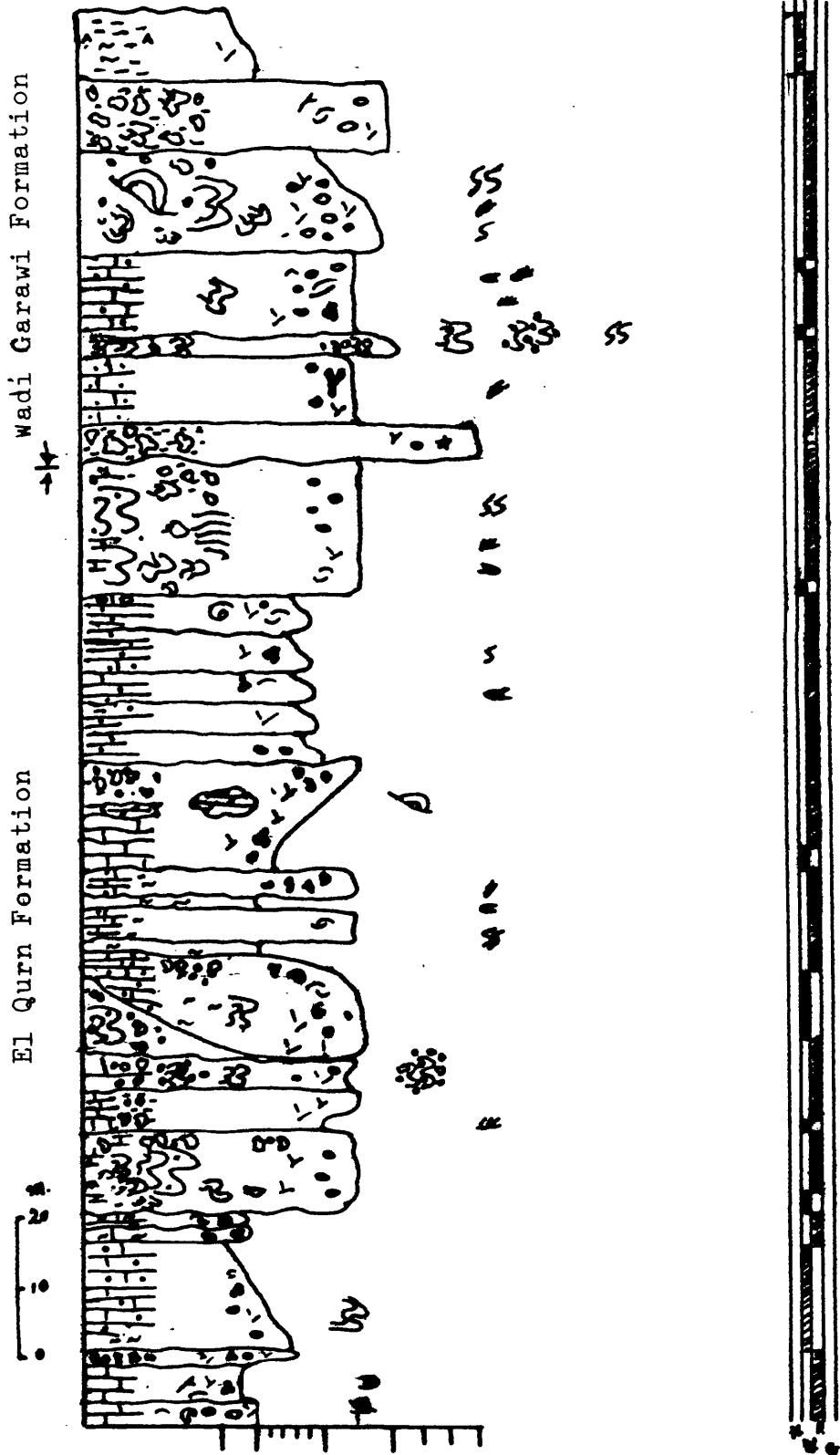
Palaentological key

	planktonic foraminifera
	micro-benthonic foram.
	milioides
	nummulites
	operculina
	bivalves
	gastropodes
	bryozoa
	echinoderms
	corals
	ostracods
	sponge spicules
	bioclasts
	vertebrate remains
	serpiolid worms

Appendix (B-2) : Log section NO ."40"at Gabal Gibli El-Ahram ; South Giza Pyramids (P) .

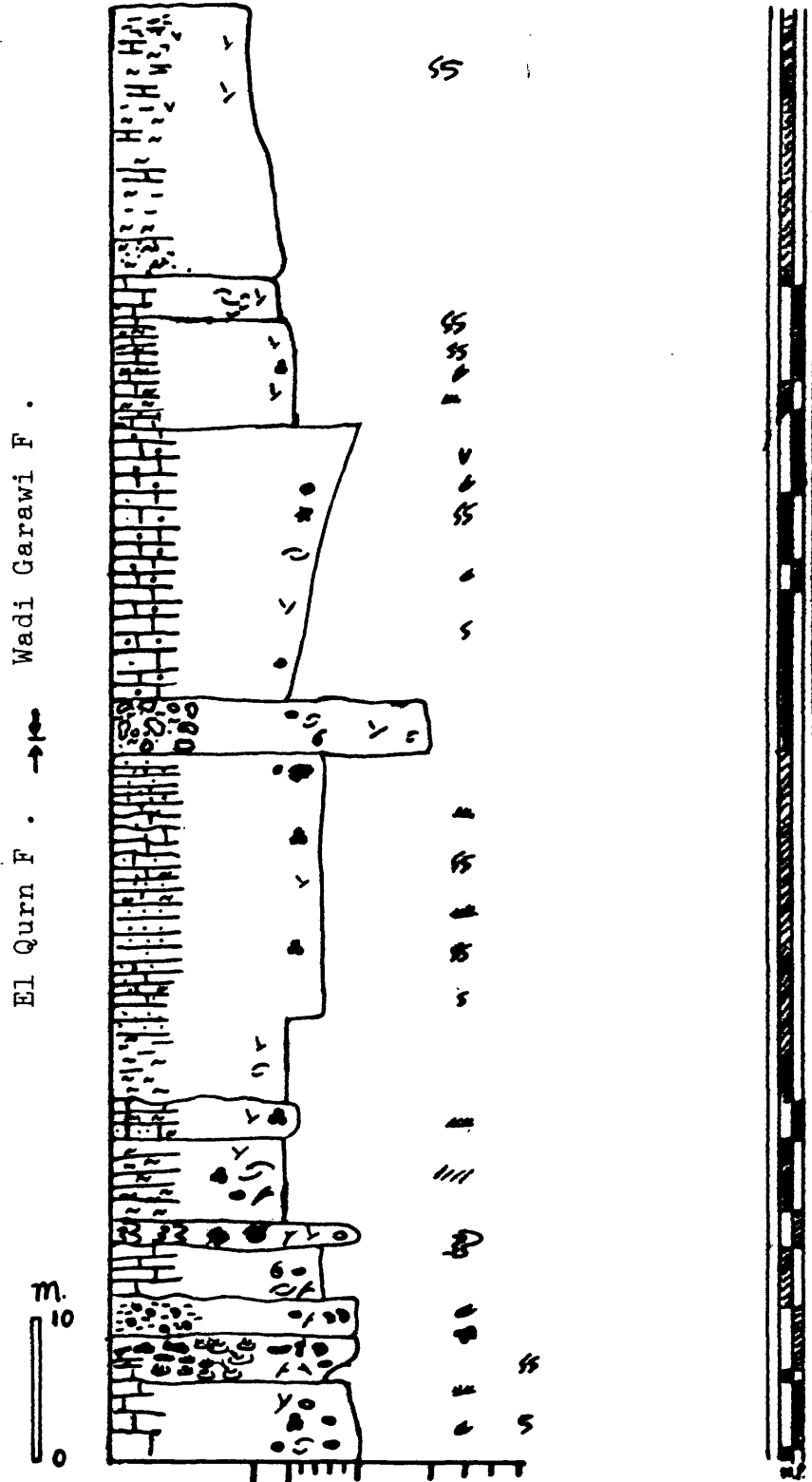


Appendix (B-3) : Log section No ."48" at Wadi Hof (WF).



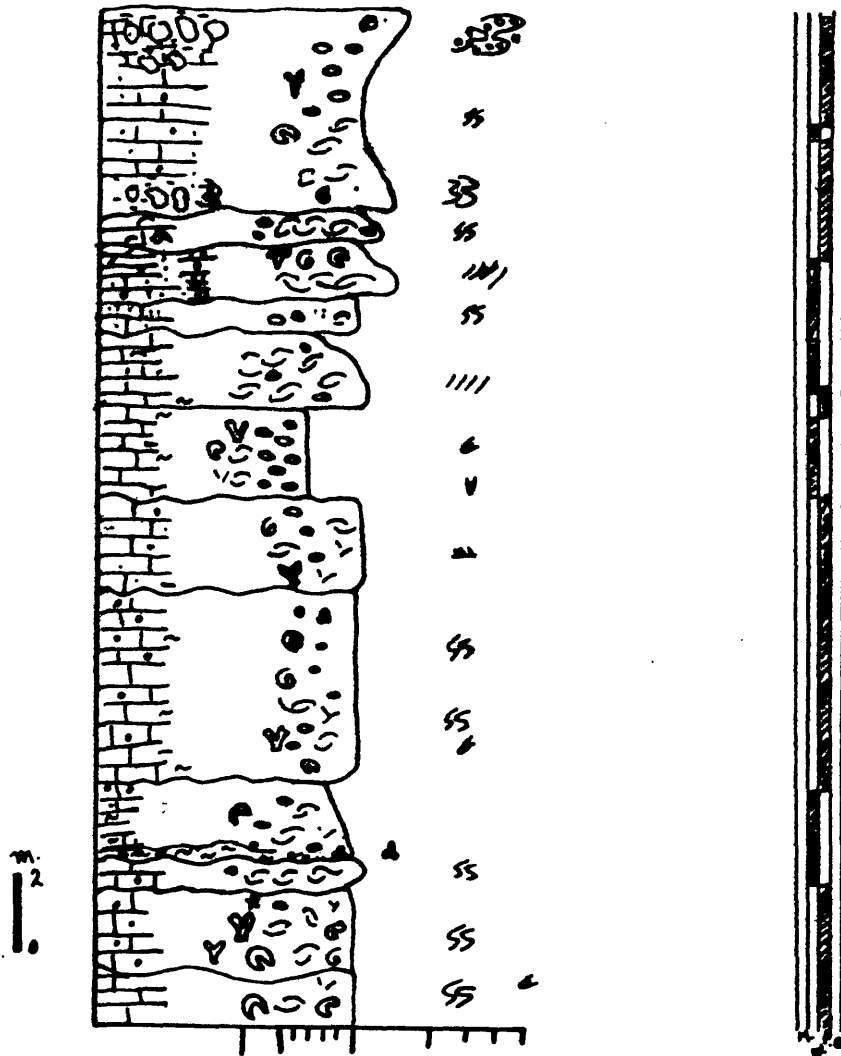
Appendix (B-4) : Log section NO."49" at Gabal El

Maskara , East of Helwan(H) .



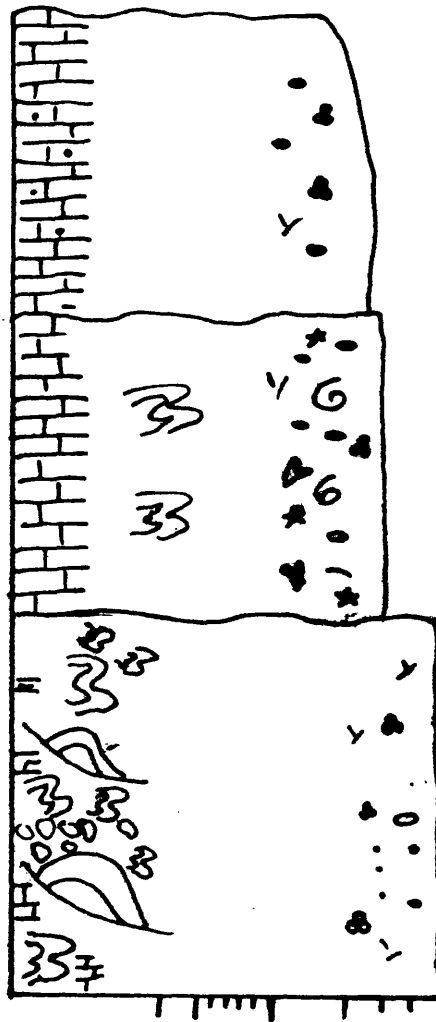
Appendix (B-5) ; Log Section No . "44" at Gabal El
 Giushi , in Mokattam area, east
 of Cairo (MG) .

Giushi Formation



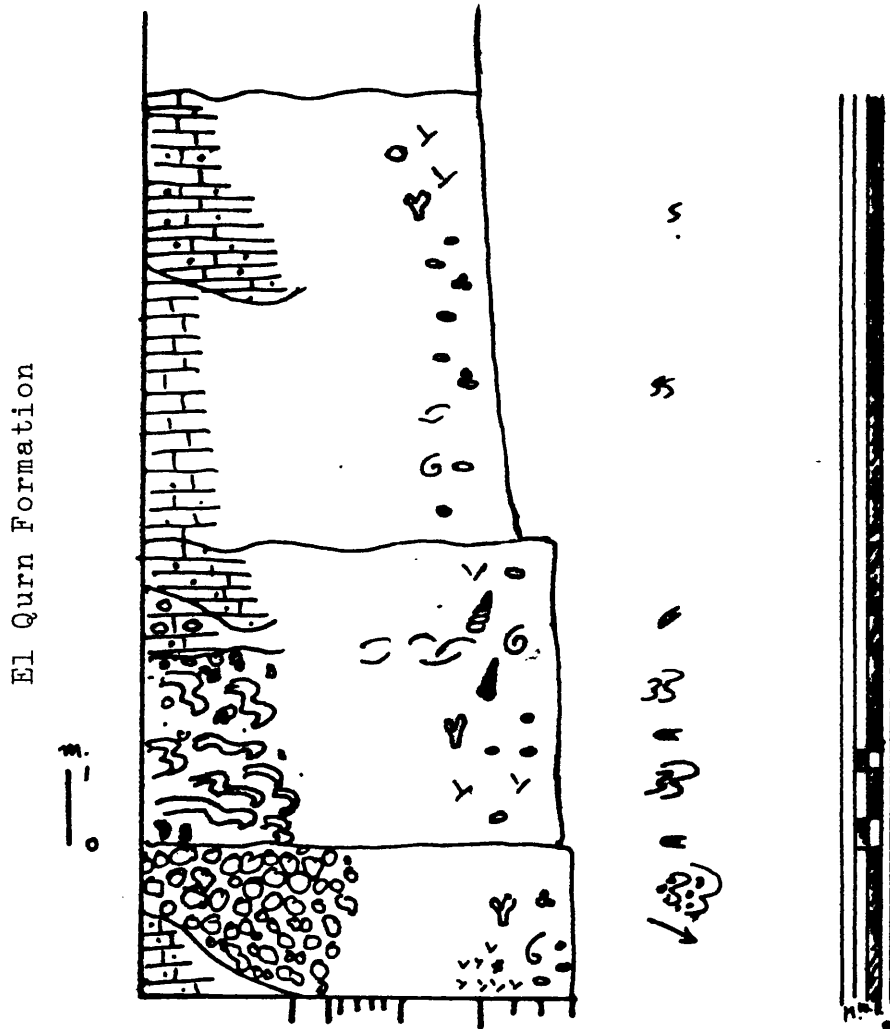
Appendix (B-6) : Log Section No. "2" at Abou Seria
Road , East El Tebbin .

Giushi Formation



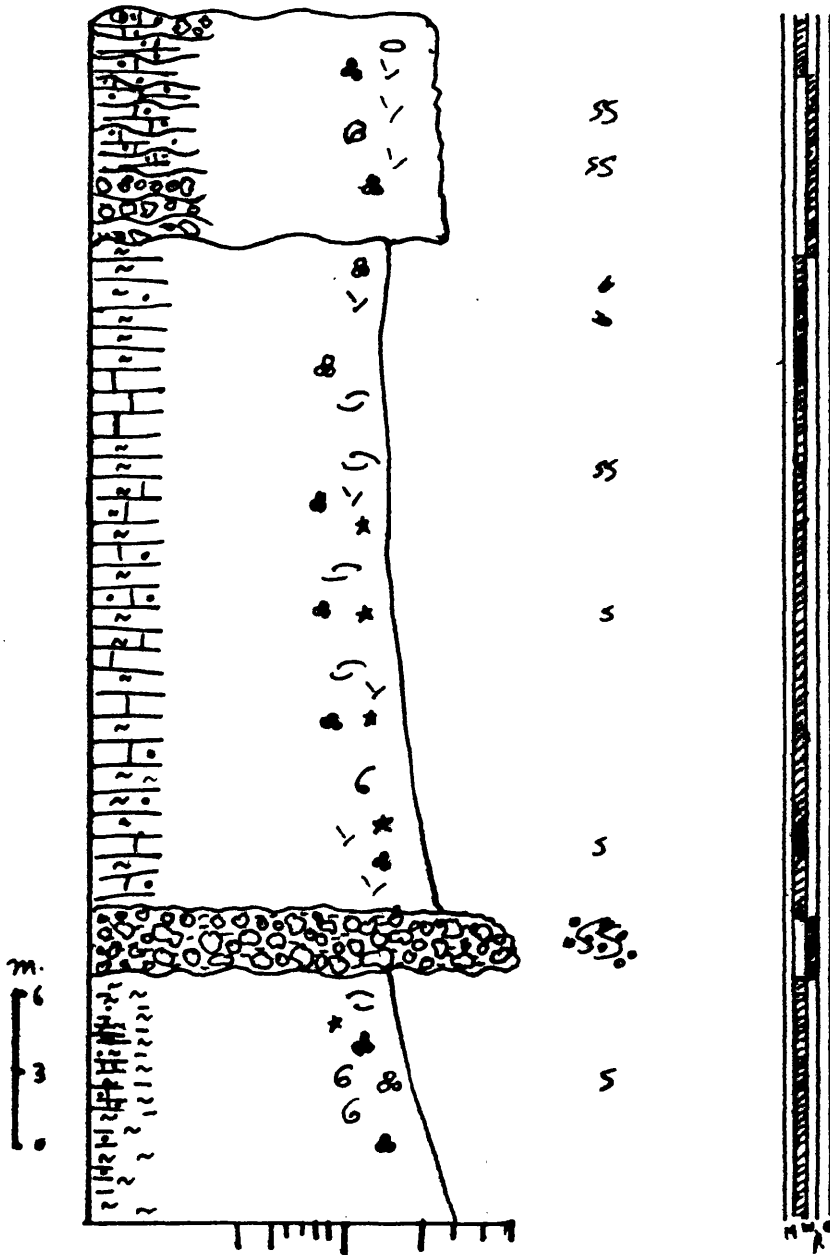
SS
↑
SS

Appendix (B-8) : Log section No."5" at Tabit Wadi
Hof , N . E . of Helwan .



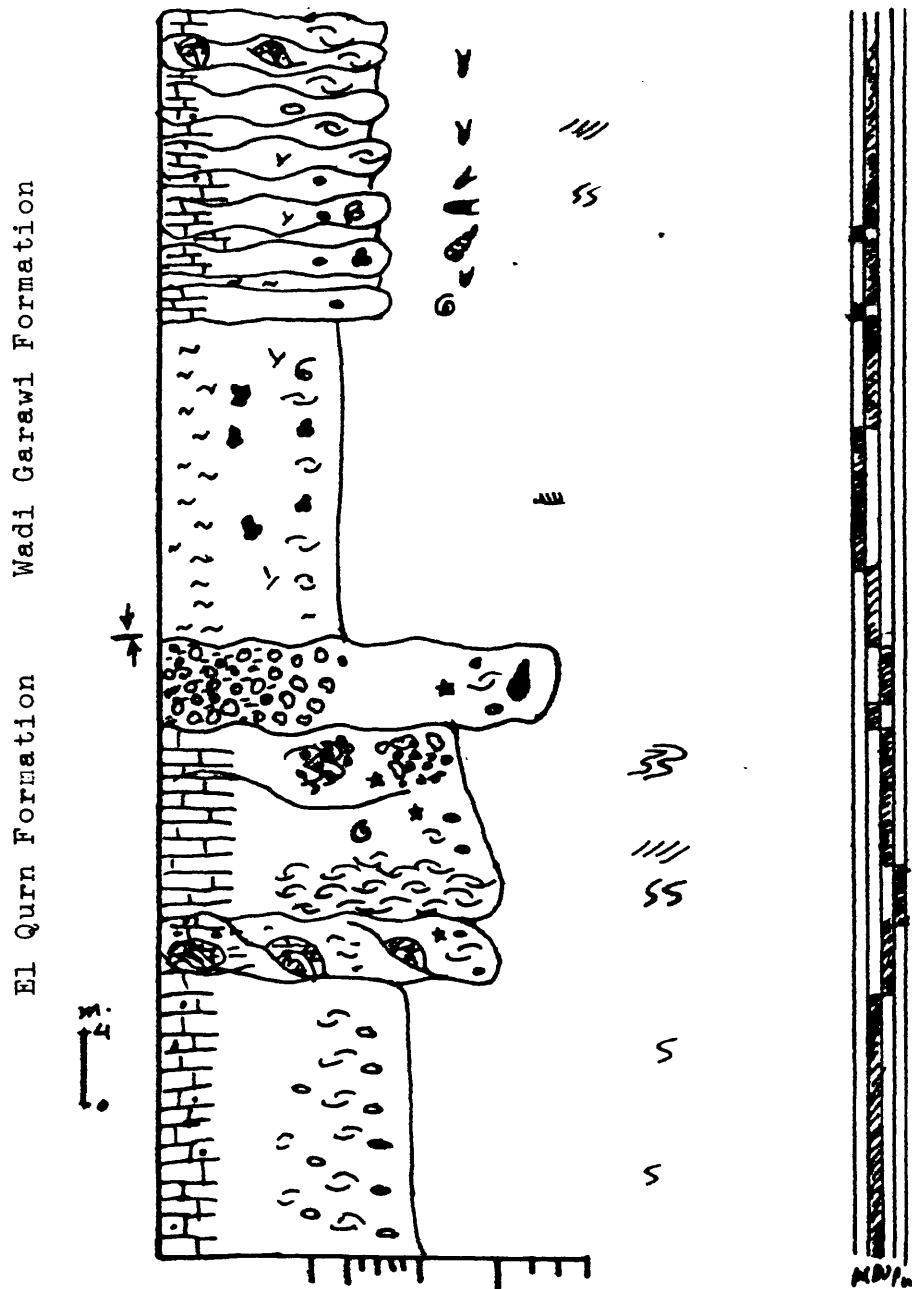
Appendix (B-9) : Log Section No. "10" at Wadi El
Aghbage , east of Beni Suef .

Middle Mokattam Unit



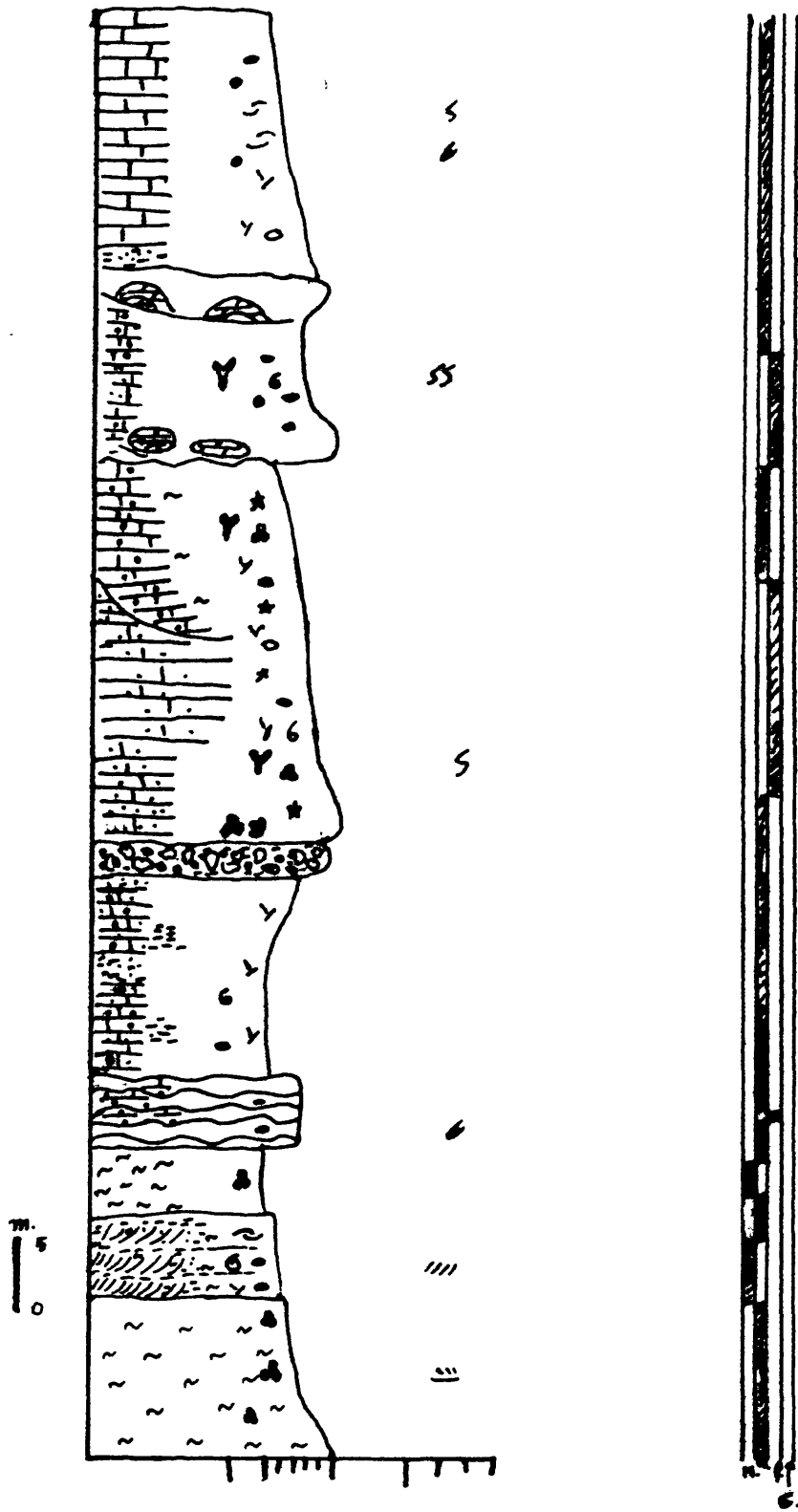
Appendix (B-10) : Log graph for Section "16" at

Gabal Gibo, E.Helwan .



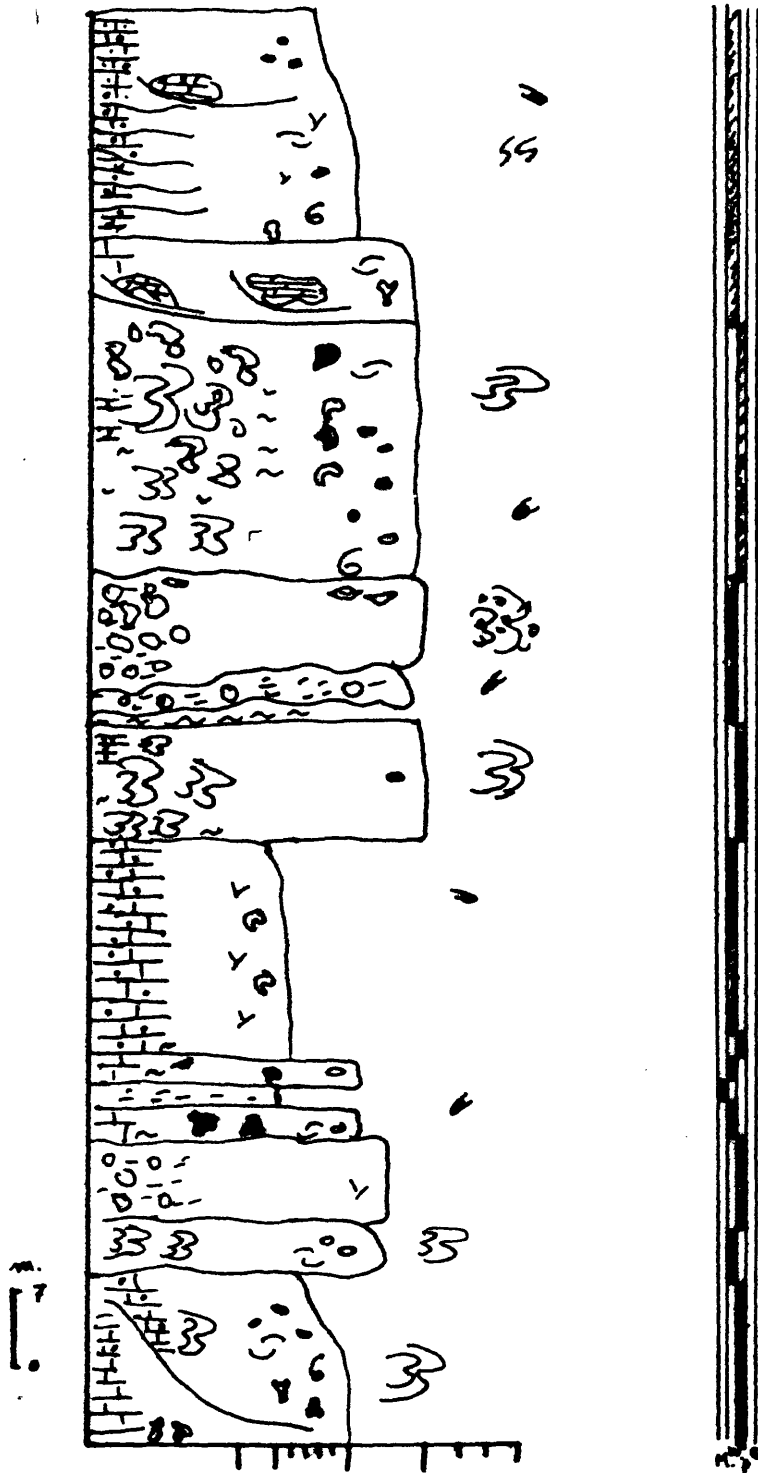
Appendix (B-11) : Log Section No "17" at deeper Wadi
Hof , east of Helwan .

El Qurn Formation

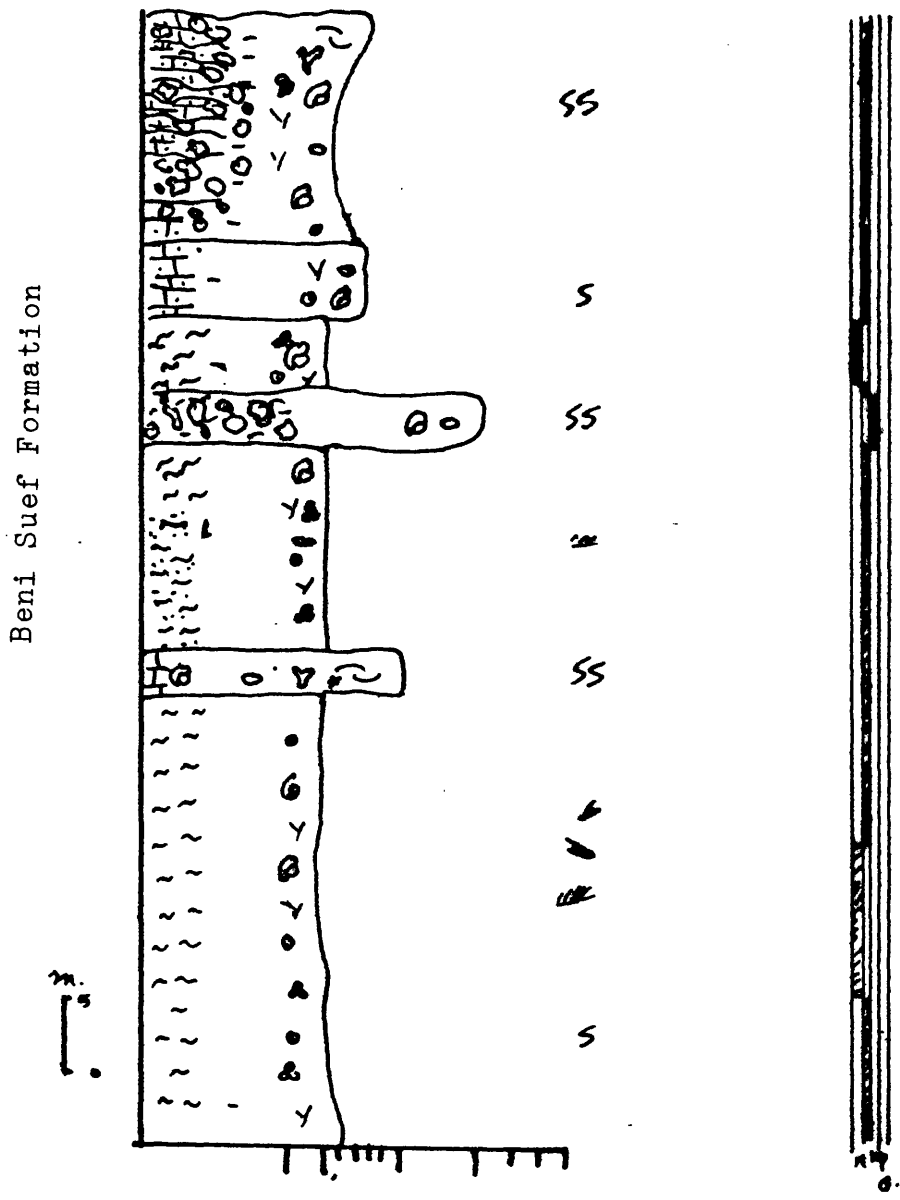


Appendix (B-12) : Log Section No. "18" N.E of
the Helwan area .

El Qurn Formation



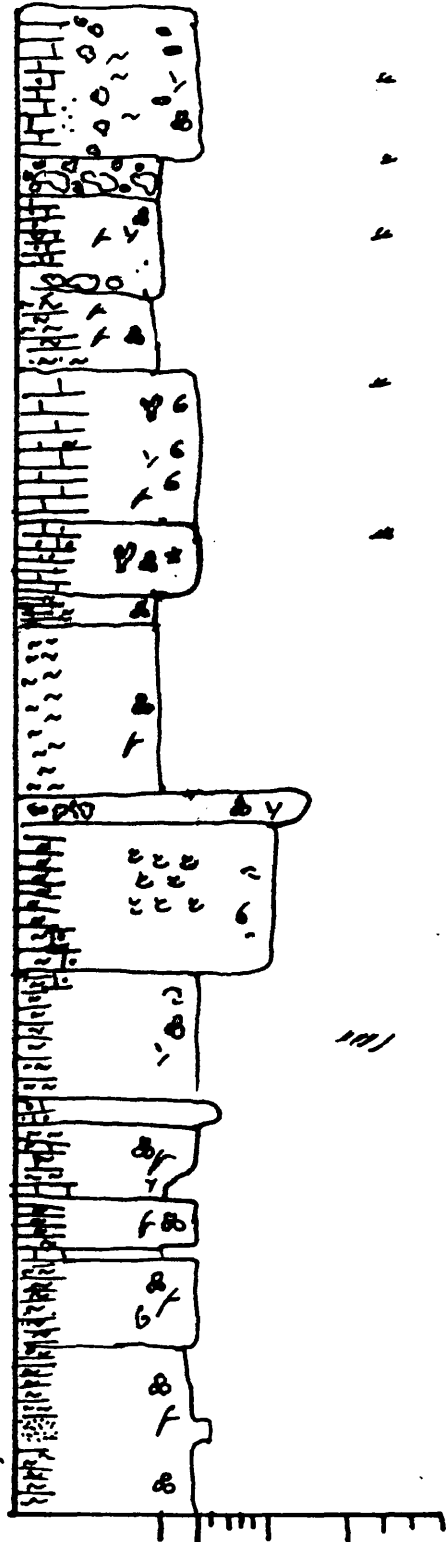
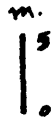
Appendix (B-13) : Log Section No"26" at Wadi El
Arhab , S.E of Beni Suef .



Appendix (B-15) : Log Section No. "15" at east

El Saff area .

Beni Suef Formation

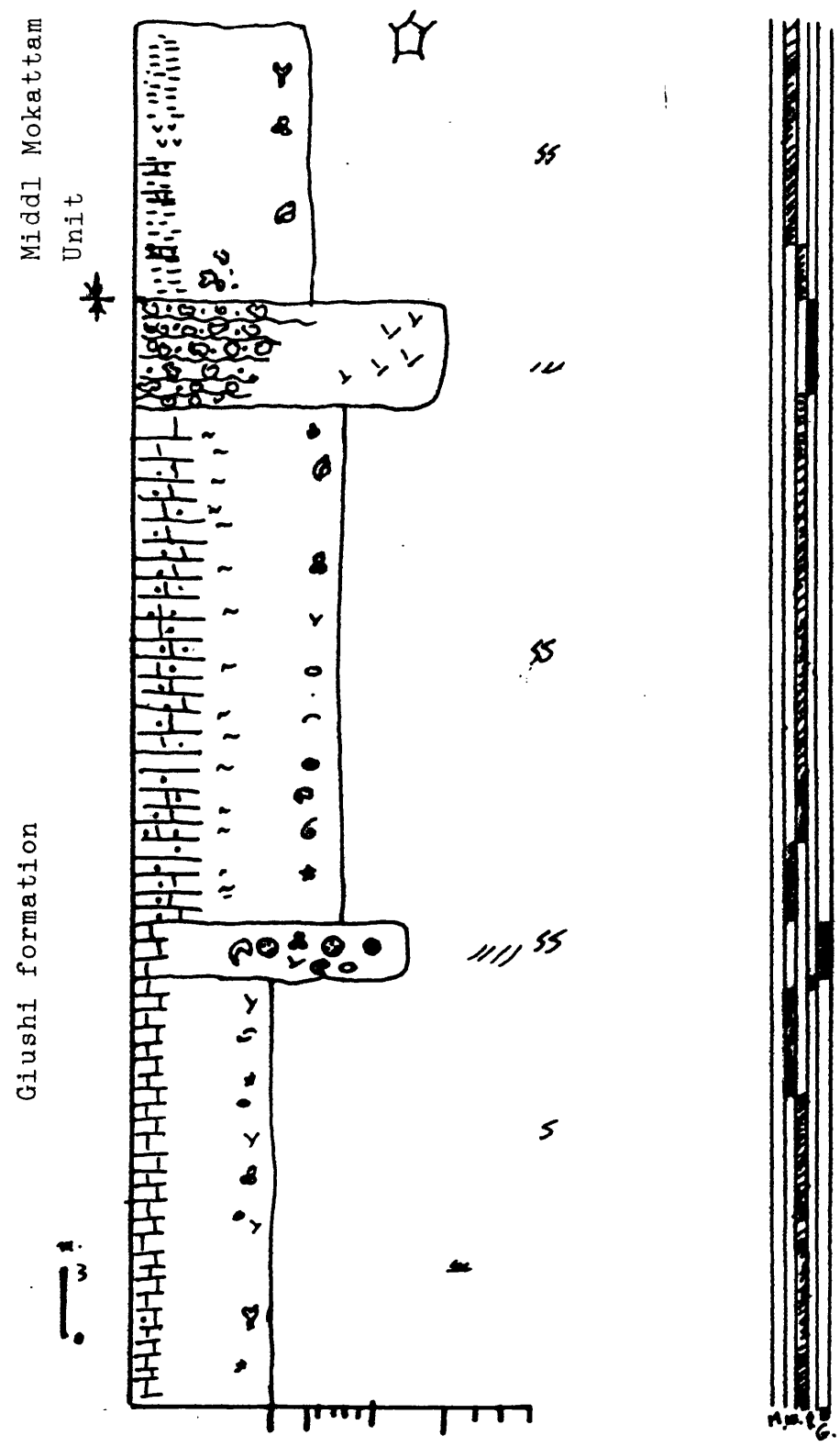


101



M.P.G.

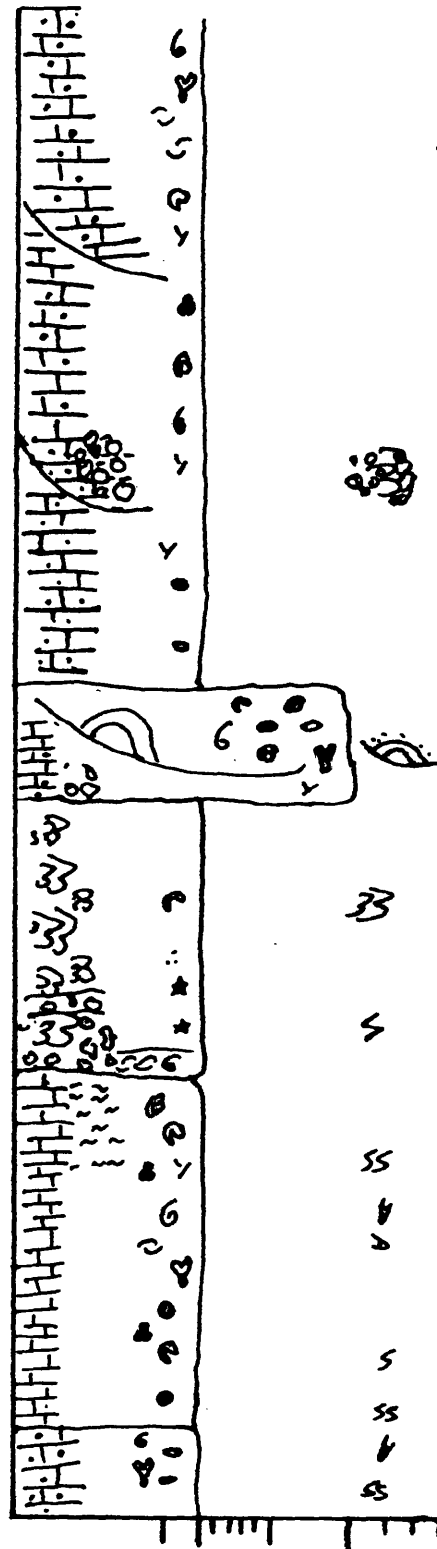
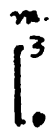
Appendix (B-16) : Log Section No "56" at Kattamia Road .



Appendix (B-17) : Log Section No "59" at east of Wadi

Hof area .

El Qurn Formation



SS
↓
↓



SS

S

SS

↓
↓

S

SS

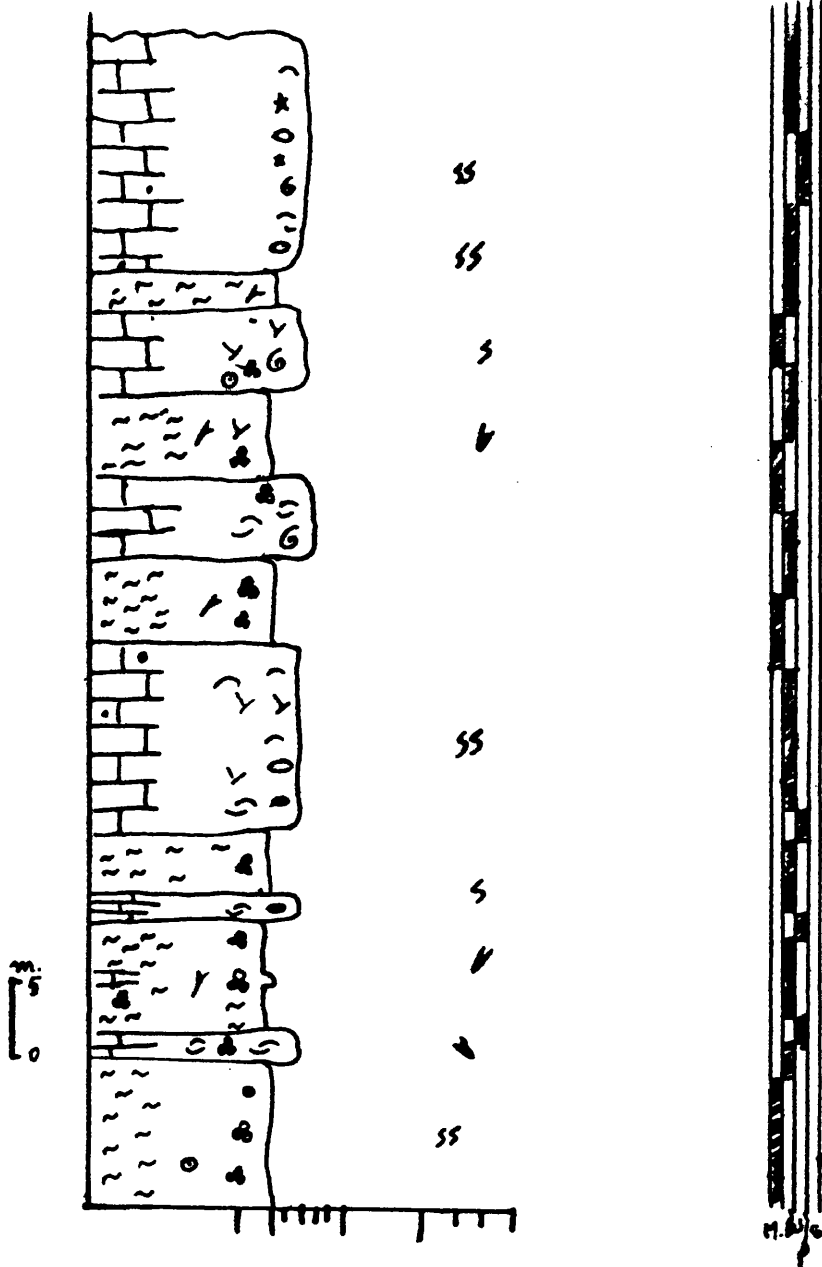
↓
↓

SS



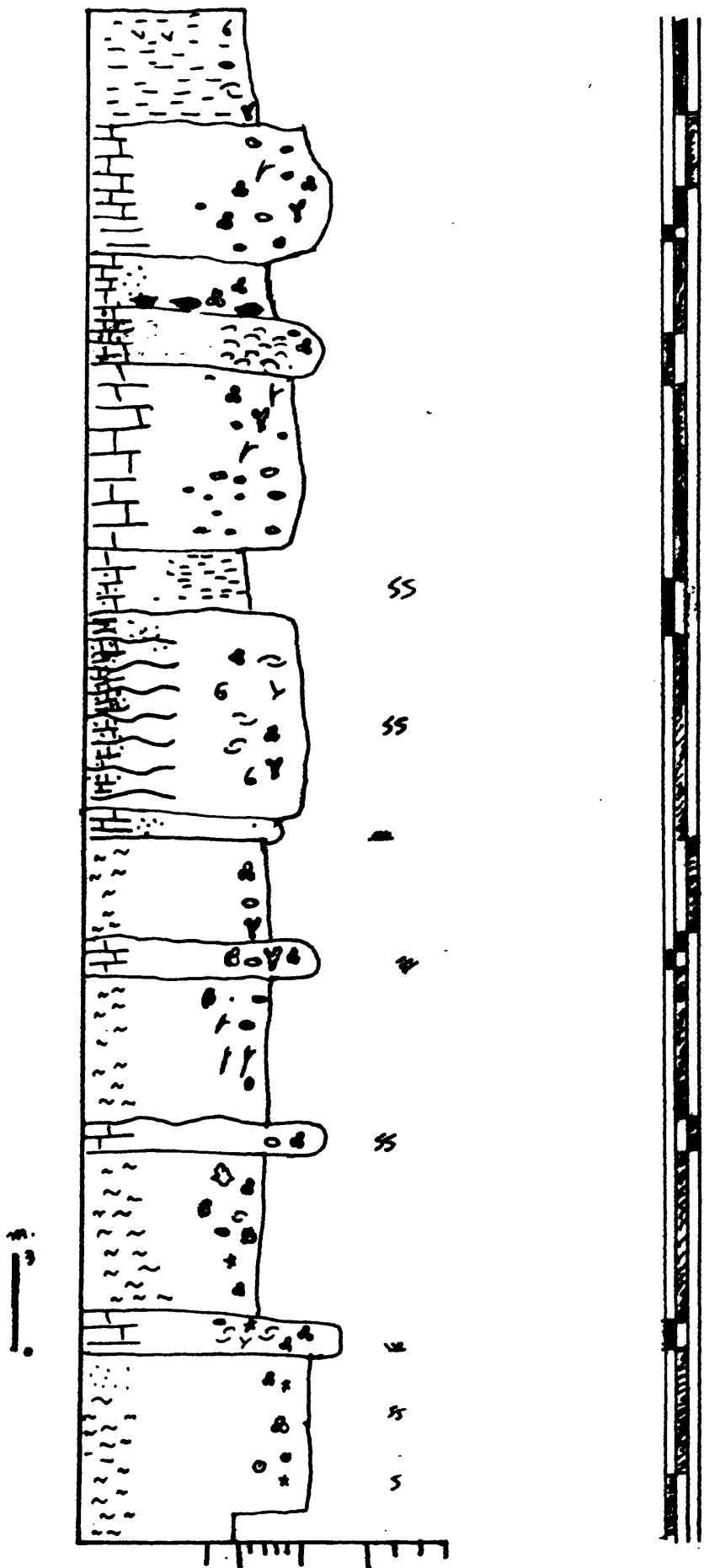
Appendix (B-18) : Log Section No"60" at Gabal Tarbul
 east El Wasta (T .) .

Beni Suef Formation



Appendix (B-19) : Log Section "61" at Gabal Shaibun (SH).

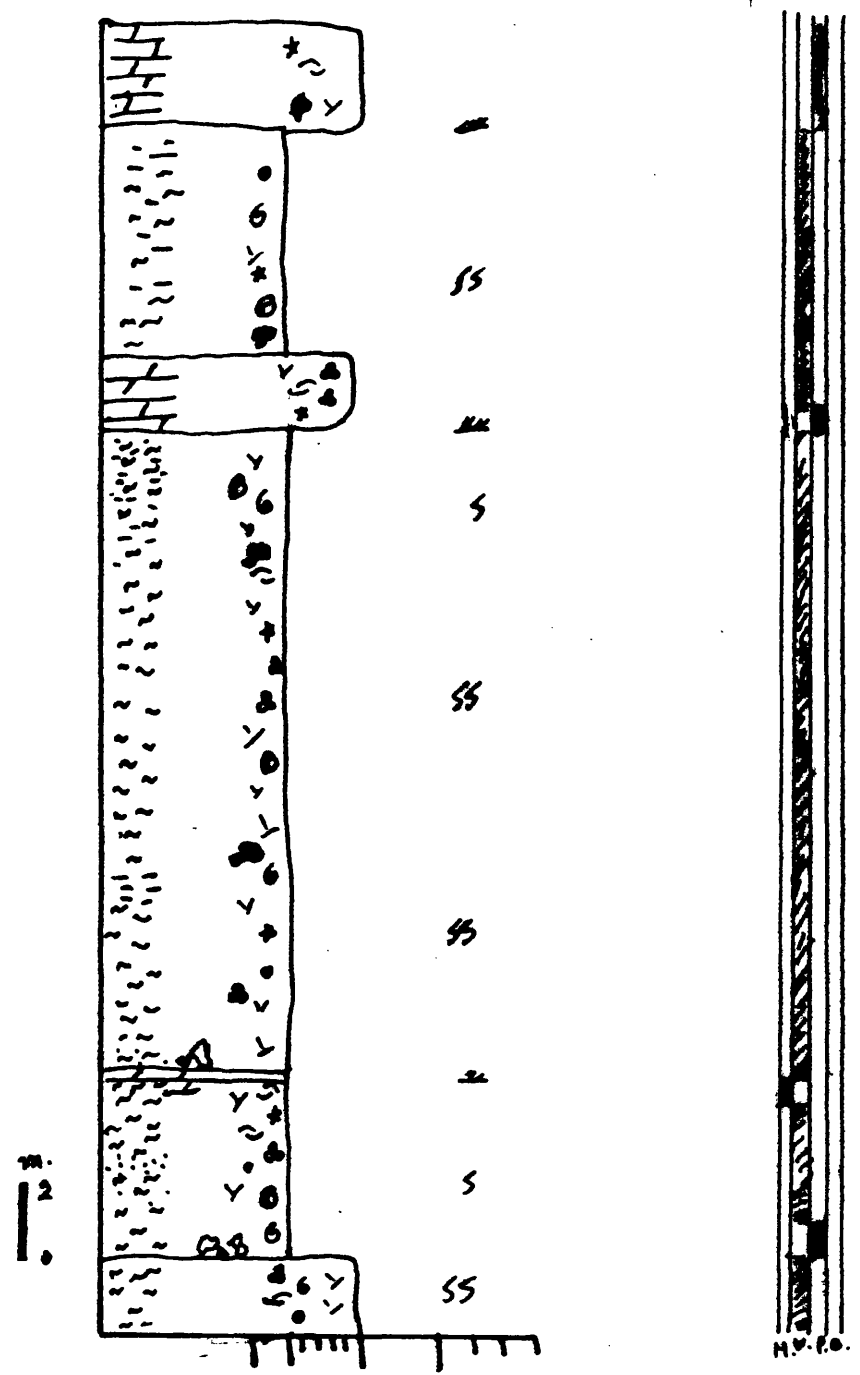
Beni Suef Formation



Appendix (B-20) : Log Section No. "69" at Gabal

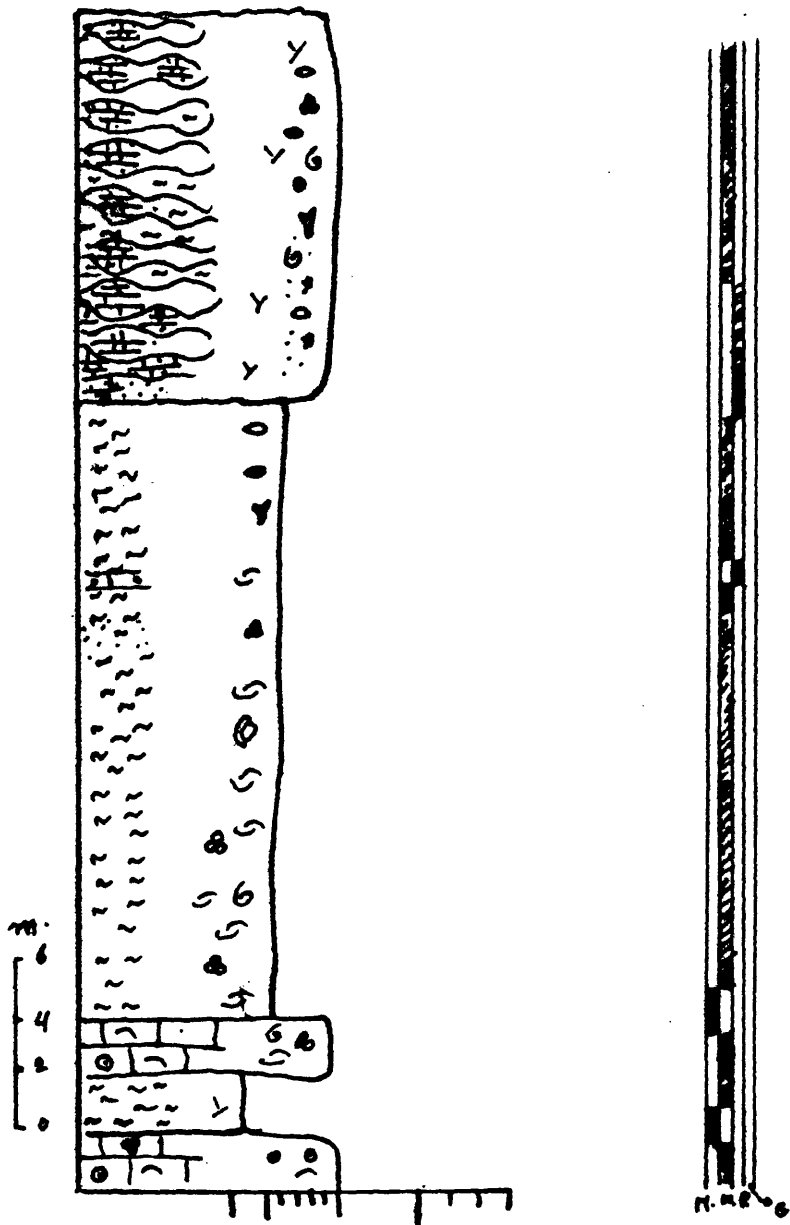
Abyad and Wadi Ridan entrance.

Middle Mokottam Unit



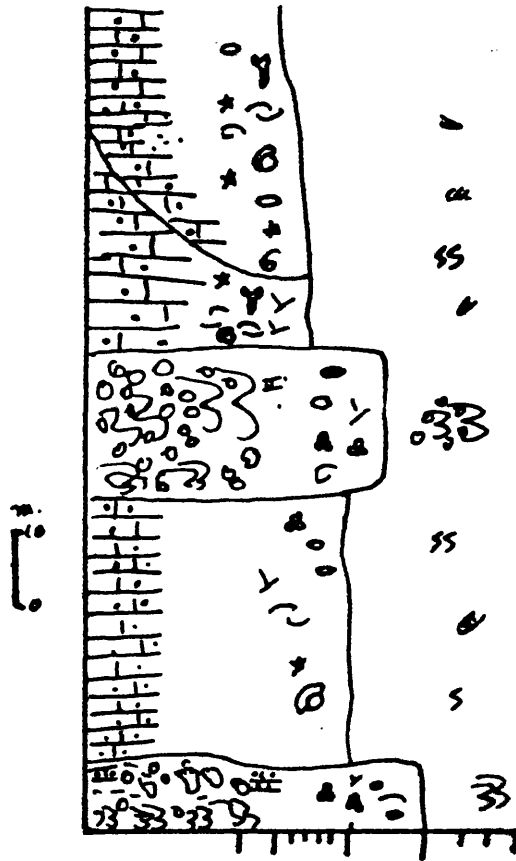
Appendix (B-21) ; Log Section No. "81" ,
Gabal El Mashash, east of
Beni Suef (MSH.) .

Beni Suef Formation



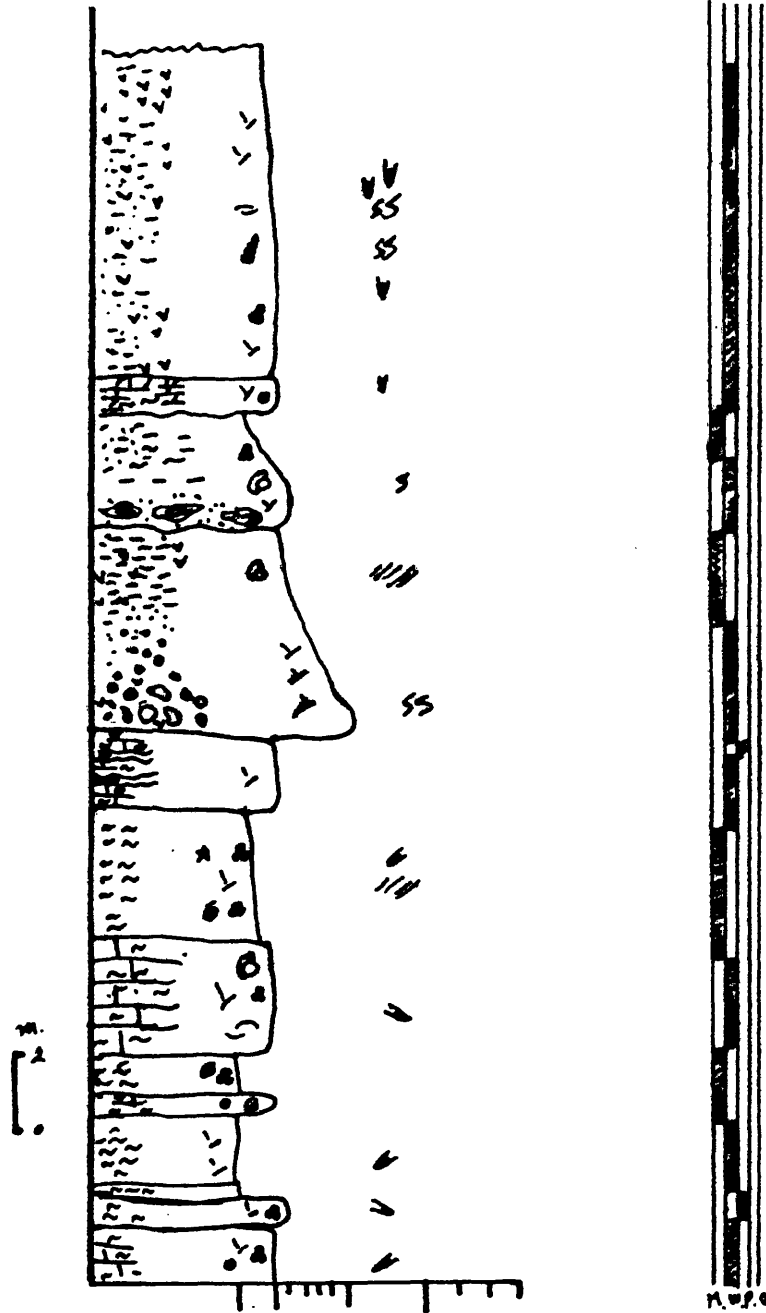
Appendix (B-24) : Log section No. "79" El Maskara Scarpe ,E. of El Tebbin .

El Qurn Formation



Appendix (B-25) : Log Section No."45" at El Mokattam
Hotel , Gabal Mokattam .

Middle Mokattam Unit



APPENDIX (C-4): POINT COUNTING DATA OF SECTION "50" CALCULATED TO A CUMULATIVE PERCENTAGE

X	Y ₁	Y ₂	Y ₃	Y ₅	Y ₆	Y ₇	Y ₈	Y ₉	Y ₁₀	Y ₁₁	Y ₁₄	Y ₁₇	Y ₁₈	Y ₂₀	Y ₂₂	Y ₂₄	Y ₂₆
35	0.0	0.0	8.0	8.0	18.0	20.0	20.0	20.0	20.0	20.0	20.0	40.0	80.0	80.0	80.0	80.0	100.0
36	0.0	0.0	8.0	8.0	18.0	20.0	20.0	20.0	20.0	20.0	20.0	40.0	80.0	80.0	80.0	80.0	100.0
6	0.0	13.0	23.0	23.0	33.0	38.0	42.0	42.0	42.0	42.0	42.0	42.0	72.0	72.0	72.0	72.0	100.0
9	1.0	15.0	21.0	34.0	34.0	34.0	42.0	42.0	43.0	43.0	46.0	46.0	66.0	66.0	66.0	66.0	100.0
11	0.0	14.0	20.0	34.0	34.0	34.0	42.0	42.0	43.0	43.0	46.0	46.0	66.0	66.0	66.0	66.0	100.0
12	0.0	13.0	19.0	34.0	34.0	35.0	42.0	42.0	43.0	43.0	46.0	46.0	66.0	66.0	66.0	66.0	100.0
15	4.0	6.0	21.0	25.0	40.0	40.0	43.0	43.0	43.0	43.0	45.0	45.0	75.0	75.0	75.0	75.0	100.0
22	4.0	3.0	8.0	8.0	12.0	12.0	12.0	12.0	12.0	12.0	12.0	12.0	12.0	72.0	72.0	72.0	100.0
24	4.0	0.0	0.0	0.0	10.0	10.0	10.0	10.0	10.0	10.0	10.0	10.0	50.0	50.0	50.0	50.0	100.0
29	4.0	0.0	0.0	0.0	3.0	3.0	3.0	3.0	3.0	3.0	3.0	3.0	80.0	80.0	80.0	80.0	100.0
31	9.0	0.0	0.0	6.0	20.0	30.0	30.0	30.0	30.0	30.0	30.0	50.0	80.0	80.0	80.0	80.0	100.0
36	1.0	0.0	4.0	4.0	45.0	45.0	47.0	47.0	47.0	47.0	47.0	72.0	92.0	92.0	92.0	92.0	100.0
39	1.0	2.0	12.0	12.0	15.0	15.0	15.0	15.0	15.0	15.0	15.0	15.0	85.0	85.0	85.0	85.0	100.0
79	9.0	0.0	0.0	10.0	18.0	24.0	25.0	25.0	25.0	25.0	28.0	50.0	85.0	100.0	100.0	100.0	100.0
41	6.0	0.0	0.0	8.0	14.0	18.0	18.0	18.0	18.0	18.0	18.0	58.0	78.0	78.0	78.0	78.0	100.0
48	6.0	4.0	12.0	12.0	19.0	22.0	25.0	25.0	25.0	27.0	29.0	29.0	89.0	89.0	100.0	100.0	100.0
55	6.0	20.0	20.0	20.0	30.0	33.0	33.0	40.0	40.0	40.0	40.0	40.0	80.0	90.0	100.0	100.0	100.0
57	2.0	0.0	0.0	50.0	50.0	50.0	53.0	53.0	53.0	53.0	53.0	78.0	88.0	88.0	88.0	100.0	100.0
59	2.0	8.0	23.0	26.0	32.0	35.0	39.0	39.0	39.0	39.0	39.0	39.0	69.0	69.0	69.0	100.0	100.0
59	8.0	0.0	45.0	45.0	53.0	58.0	63.0	63.0	63.0	63.0	64.0	70.0	80.0	80.0	80.0	80.0	100.0
66	8.0	3.0	28.0	32.0	52.0	57.0	59.0	59.0	59.0	59.0	59.0	59.0	84.0	84.0	84.0	84.0	100.0
68	8.0	0.0	10.0	10.0	18.0	20.0	29.0	29.0	29.0	29.0	29.0	29.0	75.0	75.0	75.0	75.0	100.0
73	8.0	0.0	20.0	20.0	24.0	34.0	34.0	34.0	34.0	34.0	34.0	34.0	74.0	74.0	74.0	74.0	100.0
74	4.0	0.0	5.0	5.0	10.0	10.0	10.0	10.0	10.0	10.0	10.0	10.0	70.0	70.0	70.0	70.0	100.0
79	4.0	7.0	15.0	18.0	25.0	25.0	27.0	27.0	27.0	27.0	27.0	27.0	67.0	67.0	67.0	67.0	100.0
81	2.0	0.0	4.0	4.0	11.0	15.0	15.0	15.0	15.0	15.0	15.0	15.0	75.0	75.0	75.0	75.0	100.0
82	2.0	0.0	4.0	12.0	22.0	25.0	27.0	27.0	27.0	27.0	30.0	30.0	70.0	70.0	70.0	70.0	100.0
84	2.0	8.0	10.0	10.0	10.0	17.0	17.0	17.0	17.0	17.0	17.0	17.0	90.0	90.0	100.0	100.0	100.0
88	2.0	3.0	10.0	16.0	21.0	23.0	27.0	27.0	27.0	27.0	29.0	29.0	89.0	89.0	89.0	89.0	100.0
91	2.0	8.0	23.0	33.0	43.0	43.0	50.0	50.0	50.0	50.0	50.0	50.0	70.0	70.0	70.0	70.0	100.0
94	2.0	28.0	28.0	33.0	43.0	43.0	47.0	47.0	47.0	47.0	47.0	47.0	67.0	67.0	67.0	67.0	100.0
97	2.0	0.0	6.0	6.0	21.0	21.0	21.0	21.0	21.0	21.0	21.0	21.0	67.0	67.0	67.0	67.0	100.0
100	2.0	10.0	15.0	23.0	28.0	28.0	30.0	30.0	30.0	30.0	30.0	30.0	70.0	70.0	70.0	70.0	100.0
101	0.0	16.0	20.0	26.0	28.0	28.0	31.0	36.0	36.0	36.0	36.0	36.0	66.0	66.0	66.0	66.0	100.0
101	5.0	16.0	20.0	26.0	26.0	28.0	31.0	36.0	36.0	36.0	36.0	36.0	66.0	66.0	66.0	66.0	100.0

////

APPENDIX (C-6): POINT COUNTING DATA OF SECTION "2" CALCULATED TO A CUMULATIVE PERCENTAGE.

X	Y ₁	Y ₃	Y ₆	Y ₉	Y ₁₇	Y ₁₈	Y ₂₂	Y ₂₆
0	0.0	25.0	35.7	35.0	35.0	60.0	60.0	100.0
	3.4	25.0	35.0	35.0	60.0	60.0	60.0	100.0
	10.8	10.0	45.0	47.0	59.0	63.0	63.0	100.0
	16.8	10.0	27.0	27.0	30.0	33.0	53.0	100.0
	23.3	11.0	18.5	18.5	40.5	43.0	43.0	100.0
	25.8	11.0	18.5	18.5	40.5	43.0	43.0	100.0

APPENDIX (C-7): POINT COUNTING DATA OF SECTION "4" CALCULATED TO A CUMULATIVE PERCENTAGE

X	Y1	Y2	Y3	Y4	Y6	Y7	Y8	Y9	Y11	Y15	Y16	Y17	Y18	Y19	Y20	Y22	Y24	Y26
5	2.0	2.0	2.0	12.0	15.0	14.5	21.5	22.5	23.5	23.5	24.0	60.0	63.0	63.0	63.0	63.0	100.0	100.0
15	2.0	2.0	2.0	12.0	15.0	14.5	21.0	22.5	23.5	23.5	24.0	60.0	63.0	63.0	63.0	63.0	100.0	100.0
50	1.0	1.0	1.0	3.0	3.0	3.0	4.0	5.0	5.0	5.0	5.0	45.0	51.0	51.0	51.0	51.0	51.0	100.0
70	0.0	0.0	0.0	0.0	0.0	0.0	0.5	0.5	1.0	1.0	1.0	30.0	51.0	51.0	60.0	60.0	100.0	100.0
95	1.5	1.5	4.5	5.5	5.5	5.5	5.5	6.0	6.5	6.5	6.5	30.5	46.5	46.5	46.5	46.5	100.0	100.0
110	4.0	6.0	11.0	11.5	12.5	12.5	13.5	16.5	16.5	20.5	20.5	56.5	62.5	65.5	69.5	89.5	100.0	100.0
153	0.0	0.0	10.0	10.0	11.0	12.0	12.5	12.5	13.5	13.5	13.5	53.5	59.5	60.5	60.5	62.5	100.0	100.0
160	0.0	0.0	10.0	10.0	11.0	12.0	12.5	12.5	13.5	13.5	13.5	53.5	59.5	60.5	60.5	62.5	100.0	100.0

8
////

APPENDIX (C-10): POINT COUNTING DATA OF SECTION "16" CALCULATED TO A CUMULATIVE PERCENTAGE.

X	Y ₁	Y ₂	Y ₃	Y ₄	Y ₆	Y ₇	Y ₉	Y ₁₃	Y ₁₄	Y ₁₇	Y ₁₈	Y ₂₀	Y ₂₂	Y ₂₄	Y ₂₅	Y ₂₆
0.0	16.0	19.0	22.0	23.0	23.0	23.0	25.0	26.0	26.0	26.0	76.0	75.0	76.0	100.0	100.0	100.0
6.0	16.0	19.0	22.0	23.0	23.0	23.0	25.0	26.0	26.0	26.0	76.0	76.0	76.0	100.0	100.0	100.0
16.0	10.0	10.0	10.0	10.0	10.0	10.0	10.0	10.0	10.0	10.0	10.0	30.0	100.0	100.0	100.0	100.0
26.0	0.0	0.0	12.0	12.0	42.0	45.0	45.0	45.0	45.0	45.0	60.0	60.0	80.0	80.0	80.0	100.0
29.0	0.0	0.0	0.0	0.0	0.0	0.0	0.0	0.0	0.0	0.0	22.0	30.0	40.0	40.0	100.0	100.0
34.0	2.0	2.0	27.0	27.0	29.0	30.0	32.0	32.0	34.0	44.0	52.0	52.0	82.0	82.0	82.0	100.0
44.0	0.0	0.0	10.0	10.0	10.0	14.0	16.0	16.0	18.0	48.0	60.0	60.0	75.0	75.0	75.0	100.0
59.0	2.0	2.0	7.0	9.0	17.0	34.0	35.0	35.0	37.0	47.0	54.0	55.0	60.0	68.0	68.0	100.0
64.0	2.0	2.0	7.0	9.0	17.0	34.0	35.0	35.0	37.0	47.0	54.0	55.0	60.0	68.0	68.0	100.0

APPENDIX (G-II): POINT COUNTING DATA OF SECTION "17" CALCULATED TO A CUMULATIVE PERCENTAGE

X	Y1	Y2	Y3	Y4	Y6	Y7	Y8	Y9	Y17	Y18	Y19	Y20	Y21	Y22	Y25	Y26
16	0.0	0.0	15.0	15.0	35.0	37.0	37.0	37.0	50.0	60.0	60.0	60.0	60.0	72.0	72.0	100.0
5.0	0.0	0.0	15.0	15.0	35.0	37.0	37.0	37.0	50.0	60.0	60.0	60.0	60.0	72.0	72.0	100.0
10.0	0.0	1.0	5.0	5.0	11.0	14.0	14.0	14.0	25.0	43.0	43.0	53.0	53.0	53.0	100.0	100.0
15.0	0.0	0.0	6.0	8.0	8.0	8.0	11.0	12.0	27.0	42.0	42.0	50.0	50.0	72.0	72.0	100.0
44.0	3.0	3.0	11.0	13.0	26.0	36.0	36.0	38.0	68.0	78.0	83.0	83.0	83.0	100.0	100.0	100.0
49.0	2.0	2.0	9.0	12.0	17.0	20.0	24.0	27.0	42.0	58.0	58.0	65.0	65.0	75.0	75.0	100.0
54.0	10.0	12.0	12.0	12.0	15.0	16.0	18.0	18.0	18.0	39.0	39.0	56.0	56.0	100.0	100.0	100.0
59.0	6.0	7.0	7.0	7.0	7.0	7.0	8.0	10.0	14.0	31.0	31.0	59.0	63.0	100.0	100.0	100.0
66.0	0.0	0.0	6.0	7.0	7.0	7.0	7.0	7.0	23.0	45.0	45.0	51.0	58.0	70.0	70.0	100.0
69.0	0.0	0.0	4.0	5.0	7.0	16.0	16.0	17.0	34.0	47.0	47.0	56.0	61.0	75.0	75.0	100.0
72.0	2.0	4.0	9.0	11.0	19.0	21.0	22.0	23.0	32.0	44.0	44.0	50.0	60.0	72.0	72.0	100.0
74.0	0.0	0.0	8.0	14.0	14.0	14.0	16.0	16.0	16.0	44.0	44.0	64.0	64.0	82.0	82.0	100.0
79.0	11.0	11.0	11.0	11.0	11.0	11.0	11.0	11.0	17.0	54.0	54.0	80.0	80.0	100.0	100.0	100.0
89.0	0.0	0.0	0.0	0.0	0.0	0.0	0.0	0.0	2.0	16.0	16.0	32.0	47.0	100.0	100.0	100.0
96.0	3.0	3.0	3.0	3.0	3.0	3.0	3.0	3.0	3.0	13.0	13.0	20.0	20.0	100.0	100.0	100.0
98.0	3.0	3.0	3.0	3.0	3.0	3.0	3.0	3.0	3.0	13.0	13.0	20.0	20.0	100.0	100.0	100.0

APPENDIX (C-12): POINT COUNTING DATA OF SECTION "18" CALCULATED TO A CUMULATIVE PERCENTAGE

X	Y1	Y3	Y4	Y6	Y7	Y8	Y9	Y14	Y16	Y17	Y18	Y19	Y20	Y22	Y24	Y25	Y26
24	0	0	32	35	37	37	39	39	39	59	59	61	61	61	72	78	100
0	0	32	35	35	37	37	39	39	39	59	59	61	61	61	72	78	100
4	0	2	2	2	2	2	2	2	2	57	69	69	69	79	79	79	100
6	0	1	2	2	2	2	2	2	2	37	44	44	44	59	59	80	100
9	0	12	12	26	32	32	32	32	32	32	40	40	50	50	50	100	100
10	0	6	9	9	11	11	11	11	11	15	19	19	36	72	72	100	100
14	0	4	6	7	7	25	25	25	25	28	28	28	28	51	51	51	100
15	0	6	9	9	9	11	11	11	11	15	19	19	35	59	59	59	100
18	0	12	12	26	32	32	32	32	32	32	40	40	50	50	50	100	100
21	0	6	9	9	11	11	11	11	11	15	19	19	35	59	59	59	100
25	0	14	16	16	16	19	19	19	19	26	26	34	48	68	68	68	100
29	0	30	37	37	45	47	47	47	50	50	62	62	62	69	69	69	100
40	0	14	14	14	14	14	14	14	14	14	21	21	43	70	70	70	100
46	0	39	47	48	48	49	49	49	53	53	55	55	55	77	77	77	100
47	0	9	10	10	10	10	10	10	10	10	22	22	22	40	40	40	100
50	0	2	2	15	27	27	30	30	30	41	51	51	51	77	77	77	100
51	0	11	13	28	29	29	29	29	29	29	36	36	61	82	82	82	100
57	0	47	17	17	17	19	20	22	24	32	37	37	42	52	70	70	100
58	0	7	7	11	11	11	11	11	11	16	16	16	33	53	53	53	100
64	0	6	7	7	7	9	13	13	13	18	31	31	58	85	85	85	100
71	0	12	16	19	21	22	22	24	27	40	54	54	71	83	83	83	100
86	0	8	11	14	18	20	21	22	23	31	48	48	52	70	70	70	100
108	0	9	12	15	17	16	13	18	24	31	43	43	63	73	73	73	100
126	0	9	12	15	17	16	13	18	24	31	43	43	63	73	73	73	100
129	0	9	12	15	17	16	13	18	24	31	43	43	63	73	73	73	100

APPENDIX (C-14) : POINT COUNTING DATA OF SECTION "36" CALCULATED TO A CUMULATIVE PERCENTAGE

X	Y1	Y2	Y3	Y4	Y6	Y7	Y8	Y9	Y11	Y18	Y20	Y21	Y22	Y24	Y26
0.0	3.0	5.0	10.0	12.0	14.0	17.0	19.0	20.0	22.0	39.0	45.0	52.0	66.0	91.0	100.0
3.0	3.0	5.0	10.0	12.0	14.0	17.0	19.0	20.0	22.0	39.0	45.0	52.0	66.0	91.0	100.0
8.0	6.0	8.0	8.0	9.0	11.0	14.0	16.0	19.0	20.0	31.0	39.0	44.0	61.0	91.0	100.0
13.0	7.0	8.0	8.0	8.0	9.0	9.0	11.0	13.0	17.0	31.0	48.0	56.0	79.0	100.0	100.0
16.0	7.0	8.0	8.0	8.0	9.0	9.0	11.0	13.0	17.0	31.0	48.0	56.0	79.0	100.0	100.0

APPENDIX (C-16): POINT COUNTING DATA OF SECTION "56" CALCULATED TO A CUMULATIVE PERCENTAGE

X	Y1	Y2	Y3	Y4	Y6	Y7	Y8	Y9	Y10	Y14	Y16	Y17	Y18	Y20	Y22	Y24	Y26
8	2.0	3.0	3.0	3.0	3.0	3.0	4.0	5.0	5.0	5.0	5.0	18.0	32.0	38.0	78.0	78.0	100.0
10.0	2.0	3.0	3.0	3.0	3.0	3.0	4.0	5.0	5.0	5.0	5.0	18.0	32.0	38.0	78.0	78.0	100.0
20.0	3.0	5.0	6.0	7.0	9.0	10.0	13.0	14.0	14.0	14.0	16.0	26.0	38.0	46.0	66.0	66.0	100.0
21.0	4.0	4.0	10.0	12.0	14.0	15.0	17.0	19.0	19.0	20.0	20.0	37.0	53.0	64.0	80.0	80.0	100.0
31.0	3.0	4.0	7.0	8.0	10.0	11.0	14.0	15.0	15.0	17.0	17.0	38.0	48.0	69.0	74.0	84.0	100.0
33.0	2.0	2.0	10.0	14.0	15.0	15.0	16.0	17.0	53.0	54.0	54.0	57.0	75.0	75.0	100.0	100.0	100.0
51.0	4.0	4.0	6.0	7.0	9.0	10.0	11.0	13.0	13.0	15.0	18.0	29.0	36.0	45.0	65.0	75.0	100.0
61.0	4.0	4.0	6.0	7.0	9.0	10.0	11.0	13.0	13.0	15.0	18.0	29.0	36.0	45.0	65.0	75.0	100.0

////

APPENDIX (C-17): POINT COUNTING DATA OF SECTION "59" CALCULATED TO A CUMULATIVE PERCENTAGE

X	Y1	Y2	Y3	Y4	Y6	Y7	Y8	Y9	Y10	Y14	Y15	Y16	Y17	Y18	Y20	Y22	Y25	Y26
7	1.0	3.0	5.0	15.0	18.0	20.0	23.0	27.0	27.0	27.0	27.0	27.0	30.0	46.0	67.0	87.0	87.0	100.0
	1.0	3.0	5.0	15.0	18.0	20.0	23.0	27.0	27.0	27.0	27.0	27.0	30.0	46.0	67.0	87.0	87.0	100.0
	2.0	4.0	20.0	24.0	28.0	31.0	33.0	33.0	33.0	33.0	33.0	35.0	42.0	70.0	76.0	85.0	85.0	100.0
	0.0	0.0	10.0	13.0	13.0	13.0	13.0	13.0	13.0	13.0	13.0	13.0	13.0	20.0	20.0	20.0	100.0	100.0
	7.0	8.0	38.0	39.0	41.0	45.0	46.0	49.0	50.0	52.0	53.0	54.0	76.0	81.0	83.0	83.0	83.0	100.0
	0.0	0.0	27.0	34.0	34.0	34.0	35.0	37.0	37.0	39.0	39.0	39.0	39.0	79.0	79.0	79.0	79.0	100.0
	0.0	0.0	27.0	34.0	34.0	34.0	35.0	37.0	37.0	39.0	39.0	39.0	39.0	79.0	79.0	79.0	79.0	100.0

////

APPENDIX (C24D): POINT COUNTING DATA OF SECTION "79" CALCULATED
TO A CUMULATIVE PERCENTAGE "

X	Y ₁	Y ₂	Y ₃	Y ₄	Y ₆	Y ₇	Y ₈	Y ₉	Y ₁₇	Y ₁₈	Y ₂₀	Y ₂₁	Y ₂₂	Y ₂₆
0.0	2.0	3.0	22.0	29.0	35.0	36.0	40.0	42.0	60.0	70.0	70.0	70.0	76.0	100.0
3.0	2.0	3.0	22.0	29.0	35.0	36.0	40.0	42.0	60.0	70.0	70.0	70.0	76.0	100.0
9.0	4.0	4.0	19.0	27.0	51.0	33.0	30.0	39.0	57.0	72.0	75.0	78.0	91.0	100.0
54.0	18.0	21.0	21.0	21.0	26.0	28.0	28.0	28.0	28.0	41.0	52.0	52.0	100.0	100.0
69.0	6.0	7.0	16.0	27.0	26.0	30.0	32.0	34.0	42.0	52.0	52.0	52.0	59.0	100.0
99.0	17.0	22.0	22.0	22.0	28.0	31.0	31.0	31.0	31.0	49.0	58.0	58.0	100.0	100.0
105.0	4.0	4.0	10.0	14.0	17.0	19.0	21.0	23.0	40.0	54.0	58.0	60.0	73.0	100.0
107.0	4.0	4.0	10.0	14.0	17.0	19.0	21.0	23.0	40.0	54.0	58.0	60.0	73.0	100.0

8

Appendix (D-I): Computer program used for graphic analysis of
the different carbonate components from the
point counting .

```

PROGRAM FATHY
  DIMENSION X(50),Y1(50),Y2(50),Y3(50),Y4(50)
*,Y5(50),Y6(50),Y7(50),Y8(50),Y9(50),Y10(50)
*,Y11(50),Y12(50),Y13(50),Y14(50),Y15(50),Y16(50)
*,Y17(50),Y18(50),Y19(50),Y20(50),Y21(50),Y22(50)
*,Y23(50),Y24(50),Y25(50),Y26(50),Y27(50)
  CALL PAGE(50,0,29,0)
  CALL PICSIZ(25,0,5,0)
  CALL CVTYPE(3)
  CALL SCALES(0,0,10,0,1,0,0,10,0,1)
  CALL AXES('SAMPLE LOCATION',15,'PERCENTAGE',17)
  CALL YAXIS(0,0,10,0,10,0,'PERCENTAGE',10)
  READ(5,*)N
  READ(5,*)(X(I),Y1(I),Y2(I),Y3(I),Y4(I),Y5(I),
*,Y6(I),Y7(I),Y8(I),Y9(I),Y10(I),Y11(I),
*,Y12(I),Y13(I),Y14(I),Y15(I),Y16(I),Y17(I),
*,Y18(I),Y19(I),Y20(I),Y21(I),Y22(I),Y23(I),
*,Y24(I),Y25(I),Y26(I),
*,Y27(I),I=1,N)
  CALL BRKN CV(X,Y1,N,6)
  CALL BRKN CV(X,Y2,N,4)
  CALL BRKN CV(X,Y3,N,2)
  CALL BRKN CV(X,Y4,N,1)
  CALL BRKN CV(X,Y5,N,-1)
  CALL BRKN CV(X,Y6,N,5)
  CALL BRKN CV(X,Y7,N,-1)
  CALL BRKN CV(X,Y8,N,3)
  CALL BRKN CV(X,Y9,N,-2)
  CALL BRKN CV(X,Y10,N,-6)
  CALL BRKN CV(X,Y11,N,-3)
  CALL BRKN CV(X,Y12,N,6)
  CALL BRKN CV(X,Y13,N,4)
  CALL BRKN CV(X,Y14,N,2)
  CALL BRKN CV(X,Y15,N,1)
  CALL BRKN CV(X,Y16,N,-1)
  CALL BRKN CV(X,Y17,N,5)
  CALL BRKN CV(X,Y18,N,-1)
  CALL BRKN CV(X,Y19,N,3)
  CALL BRKN CV(X,Y20,N,-2)
  CALL BRKN CV(X,Y21,N,-0)
  CALL BRKN CV(X, Y22,N,-3)
  CALL BRKN CV(X,Y23,N,6)
  CALL BRKN CV(X,Y24,N,4)
  CALL BRKN CV(X,Y25,N,2)
  CALL BRKN CV(X,Y26,N,1)
  CALL DRAW CV(X,Y27,N,0)
  CALL SET KY('L','W',55,3)
  CALL BLNK KY
  CALL LINE KY(6,'Y1 ',3)
  CALL BLNK KY
  CALL LINE KY(4,'Y2 ',3)
  CALL BLNK KY
  CALL LINE KY(2,'Y3 ',3)
  CALL BLNK KY
  CALL LINE KY( 1,'Y4 ',3)
  CALL BLNK KY
  CALL LINE KY(-1,'Y5 ',3)
  CALL BLNK KY
  CALL LINE KY( 5,'Y6 ',3)
  CALL BLNK KY

```

.... (Continued)

(D-1 Continue)

```
CALL LINE KY(-1,'Y7',3)
CALL BLNK KY
CALL LINE KY(3,'Y8',3)
CALL BLNK KY
CALL LINE KY(-2,'Y9',3)
CALL BLNK KY
CALL LINE KY(-6,'Y10',3)
CALL BLNK KY
CALL LINE KY(-3,'Y11',3)
CALL BLNK KY
CALL LINE KY(6,'Y12',3)
CALL BLNK KY
CALL LINE KY(4,'Y13',3)
CALL BLNK KY
CALL LINE KY(2,'Y14',3)
CALL BLNK KY
CALL LINE KY(1,'Y15',3)
CALL BLNK KY
CALL LINE KY(-1,'Y16',3)
CALL BLNK KY
CALL LINE KY(5,'Y17',3)
CALL BLNK KY
CALL LINE KY(-1,'Y18',3)
CALL BLNK KY
CALL LINE KY(3,'Y19',3)
CALL BLNK KY
CALL LINE KY(-2,'Y20',3)
CALL BLNK KY
CALL LINE KY(-6,'Y21',3)
CALL BLNK KY
CALL LINE KY(-3,'Y22',3)
CALL BLNK KY
CALL LINE KY(6,'Y23',3)
CALL BLNK KY
CALL LINE KY(4,'Y24',3)
CALL BLNK KY
CALL LINE KY(2,'Y25',3)
CALL BLNK KY
CALL LINE KY(1,'Y26',3)
CALL BLNK KY
CALL LINE KY(0,'Y27',3)
CALL BLNK KY
CALL ENDPLT
STOP
END
```



```

PROGRAM FATHYKY
DIMENSION X(50),Y1(50),Y2(50),Y3(50),Y4(50)
*,Y5(50),Y6(50),Y7(50),Y8(50),Y9(50),Y10(50)
*,Y11(50),Y12(50),Y13(50),Y14(50),Y15(50),Y16(50)
*,Y17(50),Y18(50),Y19(50),Y20(50),Y21(50),Y22(50)
*,Y23(50),Y24(50),Y25(50),Y26(50),Y27(50),Y28(50)
CALL PAGE(50,0,29,0)
CALL PICSIZ(15,0,5,0)
CALL CVTYPE(3)
CALL SCALES(0,0,20,0,1,0,0,10,0,1)
CALL AXES('SAMPLE LOCATION',10,'PERCENTAGE',10)
READ(5,*)N
READ(5,*)(X(I),Y1(I),Y2(I),Y3(I),Y4(I),Y5(I),
*,Y6(I),Y7(I),Y8(I),Y9(I),Y10(I),Y11(I),
*,Y12(I),Y13(I),Y14(I),Y15(I),Y16(I),Y17(I),
*,Y18(I),Y19(I),Y20(I),Y21(I),Y22(I),Y23(I),
*,Y24(I),Y25(I),Y26(I),
*,Y27(I),I=1,N)
CALL BRKN CV(X,Y1,N,6)
CALL BRKN CV(X,Y2,N,4)
CALL BRKN CV(X,Y3,N,2)
CALL BRKN CV(X,Y4,N,1)
CALL BRKN CV(X,Y5,N,-1)
CALL BRKN CV(X,Y6,N,5)
CALL BRKN CV(X,Y7,N,-1)
CALL BRKN CV(X,Y8,N,3)
CALL BRKN CV(X,Y9,N,-2)
CALL BRKN CV(X,Y10,N,-6)
CALL BRKN CV(X,Y11,N,-3)
CALL BRKN CV(X,Y12,N,6)
CALL BRKN CV(X,Y13,N,4)
CALL BRKN CV(X,Y14,N,2)
CALL BRKN CV(X,Y15,N,1)
CALL BRKN CV(X,Y16,N,-1)
CALL BRKN CV(X,Y17,N,5)
CALL BRKN CV(X,Y18,N,-1)
CALL BRKN CV(X,Y19,N,3)
CALL BRKN CV(X,Y20,N,-2)
CALL BRKN CV(X,Y21,N,-6)
CALL BRKN CV(X,Y22,N,-3)
CALL BRKN CV(X,Y23,N,6)
CALL BRKN CV(X,Y24,N,4)
CALL BRKN CV(X,Y25,N,2)
CALL BRKN CV(X,Y26,N,1)
CALL BRKN CV(X,Y27,N,6)
CALL SET KY('L', 'W', 55, 20)
CALL BLNK KY
CALL LINE KY(6, 'MICRO-FORAMS', ',20)
CALL BLNK KY
CALL LINE KY(4, 'MILLIOLIDS', ',20)
CALL BLNK KY
CALL LINE KY(2, 'NUMMULITES', ',20)
CALL BLNK KY
CALL LINE KY(, 'OPERCULINA', ',20)
CALL BLNK KY
CALL LINE KY(-1, 'LEBENTHONIC FORAMS', ',20)
CALL BLNK KY
CALL LINE KY( 5, 'BIVALVES', ',20)
CALL BLNK KY
CALL LINE KY(-1, 'GASTROPODES', ',20)
CALL BLNK KY

```

... (Continued)

(D-2 Continue)

CALL LINE KY(3, 'BRYOZOA ' ,20)
 CALL BLNK KY
 CALL LINE KY(-2, 'ECHINODERMS ' ,20)
 CALL BLNK KY
 CALL LINE KY(-6, 'CORALS ' ,20)
 CALL BLNK KY
 CALL LINE KY(-3, 'OSTRACODS ' ,20)
 CALL BLNK KY
 CALL LINE KY(6, 'SPONGE SPICULES ' ,20)
 CALL BLNK KY
 CALL LINE KY(4, 'CORALLINE ALGAE ' ,20)
 CALL BLNK KY
 CALL LINE KY(2, 'GREEN ALGAE ' ,20)
 CALL BLNK KY
 CALL LINE KY(1, 'ALGAL COATED GRAINS ' ,20)
 CALL BLNK KY
 CALL LINE KY(-1, 'SERPIOLID WORMS ' ,20)
 CALL BLNK KY
 CALL LINE KY(5, 'PELLETS ' ,20)
 CALL BLNK KY
 CALL LINE KY(-1, 'BIOCLASTIS ' ,20)
 CALL BLNK KY
 CALL LINE KY(3, 'MICRITE ENVELOPES ' ,20)
 CALL BLNK KY
 CALL LINE KY(-2, 'INTRACLAST ' ,20)
 CALL BLNK KY
 CALL LINE KY(-6, 'QUARTZ DETRITALS ' ,20)
 CALL BLNK KY
 CALL LINE KY(-3, 'MUD/SILTY MATRIX ' ,20)
 CALL BLNK KY
 CALL LINE KY(6, 'SPARITE ' ,20)
 CALL BLNK KY
 CALL LINE KY(4, 'MICROSPARITE ' ,20)
 CALL BLNK KY
 CALL LINE KY(2, 'DOLOMITE ' ,20)
 CALL BLNK KY
 CALL LINE KY(1, 'MICRITE ' ,20)
 CALL BLNK KY
 CALL LINE KY(6, 'VERTEBRATE REMAINS ' ,20)
 CALL BLNK KY
 CALL ENDPLT
 STOP
 END

Appendix (D.3): Computer program (1).

```

PROGRAM FATHY1
  DIMENSION X(50),Y1(50),Y2(50),Y3(50),Y4(50)
  *,Y5(50),Y6(50),Y7(50),Y8(50),Y9(50),Y10(50)
  *,Y11(50),Y12(50),Y13(50),Y14(50),Y15(50),Y16(50)
  *,Y17(50),Y18(50),Y19(50),Y20(50),Y21(50),Y22(50)
  *,Y23(50),Y24(50),Y25(50),Y26(50),Y27(50)
  CALL PAGE (50,0,29,0)
  CALL PICSIZ(5,0,14,0)
  CALL CVTYPE(3)
  CALL SCALES(0,0,15,0,1,0,0,100,0,1)
  CALL AXES('SAMPLE LOCATION',15,'PERCENTAGE',10)
  CALL YAXIS(0,0,100,0,15,0,'PERCENTAGE',10)
  READ(5,*)N
  READ(5,*)(X(I),Y1(I),Y3(I),Y4(I),Y6(I),Y7(I),Y8(I),
  *,Y11(I),Y14(I),Y18(I),Y21(I),Y22(I),
  *,Y26(I),I=1,N)
  CALL BRKN CV(X,Y1,N,6)
  CALL BRKN CV(X,Y3,N,4)
  CALL BRKN CV(X,Y4,N,2)
  CALL BRKN CV(X,Y6,N,1)
  CALL BRKN CV(X,Y7,N,-1)
  CALL BRKN CV(X,Y8,N,5)
  CALL BRKN CV(X,Y11,N,3)
  CALL BRKN CV(X,Y14,N,-6)
  CALL BRKN CV(X,Y18,N,-3)
  CALL BRKN CV(X,Y21,N,6)
  CALL BRKN CV(X,Y22,N,4)
  CALL DRAW CV(X,Y26,N,0)
  CALL SET KY('L','W',12,3)
  CALL LINE KY(6,'Y1',3)
  CALL LINE KY(4,'Y3',3)
  CALL LINE KY(2,'Y4',3)
  CALL LINE KY(1,'Y6',3)
  CALL LINE KY(-1,'Y7',3)
  CALL LINE KY(5,'Y8',3)
  CALL LINE KY(3,'Y11',3)
  CALL LINE KY(-2,'Y14',3)
  CALL LINE KY(-6,'Y18',3)
  CALL LINE KY(-3,'Y21',3)
  CALL LINE KY(6,'Y22',3)
  CALL LINE KY(0,'Y26',3)
  CALL TITLE('B','C',
  FIG. ( ) VERTICAL VARIATION OF CARBONA
  *TE MICROFACIES OF SECTION "40",76)
  CALL ENDPLT
  STOP
  END

```

Appendix (D.4): Computer program (2).

```

PROGRAM FATHY2
DIMENSION X(50),Y1(50),Y2(50),Y3(50),Y4(50)
*,Y5(50),Y6(50),Y7(50),Y8(50),Y9(50),Y10(50)
*,Y11(50),Y12(50),Y13(50),Y14(50),Y15(50),Y16(50)
*,Y17(50),Y18(50),Y19(50),Y20(50),Y21(50),Y22(50)
*,Y23(50),Y24(50),Y25(50),Y26(50),Y27(50)
CALL PAGE (105.0,29.0)
CALL PICSIZ(99.65,25.0)
CALL CVTYPE(3)
CALL SCALES(0.0,199.3,1,0.0,100.0,1)
CALL AXES('SAMPLE LOCATION',15,'PERCENTAGE',10)
CALL YAXIS(0.0,100.0,199.3,'PERCENTAGE',10)
READ(5,*)N
READ(5,*)(X(I),Y1(I),Y3(I),Y4(I),Y6(I),Y7(I),Y8(I),
*,Y9(I),Y11(I),Y12(I),Y14(I),Y18(I),Y21(I),Y22(I),
*,Y26(I),I=1,N)
CALL BRKN CV(X,Y1,N,6)
CALL BRKN CV(X,Y3,N,4)
CALL BRKN CV(X,Y4,N,2)
CALL BRKN CV(X,Y6,N,1)
CALL BRKN CV(X,Y7,N,-1)
CALL BRKN CV(X,Y8,N,5)
CALL BRKN CV(X,Y9,N,-1)
CALL BRKN CV(X,Y11,N,3)
CALL BRKN CV(X,Y12,N,-2)
CALL BRKN CV(X,Y14,N,-6)
CALL BRKN CV(X,Y18,N,-3)
CALL BRKN CV(X,Y21,N,6)
CALL BRKN CV(X,Y22,N,4)
CALL DRAW CV(X,Y26,N,0)
CALL SET KY('L','W',14,3)
CALL LINE KY(6,'Y1 ',3)
CALL LINE KY(4,'Y3 ',3)
CALL LINE KY(2,'Y4 ',3)
CALL LINE KY( 1,'Y6 ',3)
CALL LINE KY(-1,'Y7 ',3)
CALL LINE KY( 5,'Y8 ',3)
CALL LINE KY(-1,'Y9 ',3)
CALL LINE KY( 3,'Y11 ',3)
CALL LINE KY(-2,'Y12 ',3)
CALL LINE KY(-6,'Y14 ',3)
CALL LINE KY(-3,'Y18 ',3)
CALL LINE KY(6,'Y21 ',3)
CALL LINE KY(4,'Y22 ',3)
CALL LINE KY( 0,'Y26 ',3)
CALL TITLE('B','C','
FIG. ( ) VERTICAL VARIATION OF CARBONA
*TE MICROFACIES OF SECTION "48" (76)
CALL ENDPLT
STOP
END

```

```

PROGRAM FATHY3
DIMENSION X(50),Y1(50),Y2(50),Y3(50),Y4(50)
*,Y5(50),Y6(50),Y7(50),Y8(50),Y9(50),Y10(50)
*,Y11(50),Y12(50),Y13(50),Y14(50),Y15(50),Y16(50)
*,Y17(50),Y18(50),Y19(50),Y20(50),Y21(50),Y22(50)
*,Y23(50),Y24(50),Y25(50),Y26(50),Y27(50)
CALL PAGE (50,0,29,0)
CALL PICSIZ(44,7,14,0)
CALL CVTYPE(3)
CALL SCALES(0,0,134,1,1,0,0,100,0,1)
CALL AXES('SAMPLE LOCATION',15,'PERCENTAGE',10)
CALL YAXIS(0,1,100,0,134,1,'PERCENTAGE',10)
READ(5,*)N
READ(5,*)(X(I),Y1(I),Y2(I),Y3(I),Y4(I),Y5(I),
*,Y6(I),Y7(I),Y8(I),Y9(I),Y11(I),Y12(I),Y18(I),
*,Y20(I),Y21(I),Y22(I),Y26(I)),I=1,N)
CALL BRKN CV(X,Y1,N,6)
CALL BRKN CV(X,Y2,N,4)
CALL BRKN CV(X,Y3,N,2)
CALL BRKN CV(X,Y4,N,1)
CALL BRKN CV(X,Y5,N,-1)
CALL BRKN CV(X,Y6,N,5)
CALL BRKN CV(X,Y7,N,-1)
CALL BRKN CV(X,Y8,N,3)
CALL BRKN CV(X,Y9,N,-2)
CALL BRKN CV(X,Y11,N,-6)
CALL BRKN CV(X,Y12,N,-3)
CALL BRKN CV(X,Y18,N,6)
CALL BRKN CV(X,Y20,N,4)
CALL BRKN CV(X,Y21,N,2)
CALL BRKN CV(X,Y22,N,1)
CALL DRAW CV(X,Y26,N,0)
CALL SET KY('L','W',16,3)
CALL LINE KY(6,'Y1',3)
CALL LINE KY(4,'Y2',3)
CALL LINE KY(2,'Y3',3)
CALL LINE KY(1,'Y4',3)
CALL LINE KY(-1,'Y5',3)
CALL LINE KY(5,'Y6',3)
CALL LINE KY(-1,'Y7',3)
CALL LINE KY(3,'Y8',3)
CALL LINE KY(-2,'Y9',3)
CALL LINE KY(-6,'Y11',3)
CALL LINE KY(-3,'Y12',3)
CALL LINE KY(6,'Y18',3)
CALL LINE KY(4,'Y20',3)
CALL LINE KY(2,'Y21',3)
CALL LINE KY(1,'Y22',3)
CALL LINE KY(0,'Y26',3)
CALL TITLE('B','C',
*,TE MICROFACIES OF SECTION "49",76)
CALL ENDPLT
STOP
END

```

FIG. () VERTICAL VARIATION OF CARBONA

```

PROGRAM FATHY4
DIMENSION X(5),Y1(50),Y2(50),Y3(50),Y4(50)
*,Y5(50),Y6(50),Y7(50),Y8(50),Y9(50),Y10(50)
*,Y11(50),Y12(50),Y13(50),Y14(50),Y15(50),Y16(50)
*,Y17(50),Y18(50),Y19(50),Y20(50),Y21(50),Y22(50)
*,Y23(50),Y24(50),Y25(50),Y26(50),Y27(50)
CALL PAGE (50.0,29.0)
CALL PICSIZ(33.83,14.0)
CALL CVTYPE(3)
CALL SCALES(0.0,101.5,1,0.0,100.0,1)
CALL AXES('SAMPLE LOCATION',15,'PERCENTAGE',10)
CALL YAXIS(0.0,100.0,101.5,'PERCENTAGE',10)
READ(5,*)N
READ(5,*)(X(I),Y1(I),Y2(I),Y3(I),Y5(I),Y6(I),
*,Y7(I),Y8(I),Y9(I),Y10(I),Y11(I),Y14(I),Y17(I),
*,Y18(I),Y20(I),Y22(I),Y24(I),Y26(I),I=1,N)
CALL BRKN CV(X,Y1,N,6)
CALL BRKN CV(X,Y2,N,4)
CALL BRKN CV(X,Y3,N,2)
CALL BRKN CV(X,Y5,N,1)
CALL BRKN CV(X,Y6,N,-1)
CALL BRKN CV(X,Y7,N,5)
CALL BRKN CV(X,Y8,N,-1)
CALL BRKN CV(X,Y9,N,3)
CALL BRKN CV(X,Y10,N,-2)
CALL BRKN CV(X,Y11,N,-6)
CALL BRKN CV(X,Y14,N,-3)
CALL BRKN CV(X,Y17,N,-5)
CALL BRKN CV(X,Y18,N,6)
CALL BRKN CV(X,Y20,N,4)
CALL BRKN CV(X,Y22,N,2)
CALL BRKN CV(X,Y24,N,1)
CALL DRAW CV(X,Y26,N,0)
CALL SET KY('L','W',17,3)
CALL LINE KY(6,'Y1',3)
CALL LINE KY(4,'Y2',3)
CALL LINE KY(2,'Y3',3)
CALL LINE KY(1,'Y5',3)
CALL LINE KY(-1,'Y6',3)
CALL LINE KY(5,'Y7',3)
CALL LINE KY(-1,'Y8',3)
CALL LINE KY(3,'Y9',3)
CALL LINE KY(-2,'Y10',3)
CALL LINE KY(-6,'Y11',3)
CALL LINE KY(-3,'Y14',3)
CALL LINE KY(-5,'Y17',3)
CALL LINE KY(6,'Y18',3)
CALL LINE KY(4,'Y20',3)
CALL LINE KY(2,'Y22',3)
CALL LINE KY(1,'Y24',3)
CALL LINE KY(0,'Y26',3)
CALL TITLE('B','C',
*,TE MICROFACIES OF SECTION "50",76)
CALL ENDPLT
STOP
END

```

FIG. () VERTICAL VARIATION OF CARBONA

```

PROGRAM FATHY5
DIMENSION X(50),Y1(50),Y2(50),Y3(50),Y4(50)
*,Y5(50),Y6(50),Y7(50),Y8(50),Y9(50),Y10(50)
*,Y11(50),Y12(50),Y13(50),Y14(50),Y15(50),Y16(50)
*,Y17(50),Y18(50),Y19(50),Y20(50),Y21(50),Y22(50)
*,Y23(50),Y24(50),Y25(50),Y26(50),Y27(50)
CALL PAGE (50.0,29.0)
CALL PICSIZ(10.03,14.0)
CALL CVTYPE(3)
CALL SCALES(0.0,30.1,1,0.0,100.0,1)
CALL AXES('SAMPLE LOCATION',15,'PERCENTAGE',10)
CALL YAXIS(0.0,100.0,30.1,'PERCENTAGE',10)
READ(5,*)N
READ(5,*)(X(I),Y1(I),Y2(I),Y3(I),Y4(I),Y6(I),
*,Y7(I),Y8(I),Y9(I),Y11(I),Y16(I),Y18(I),
*,Y21(I),Y22(I),Y26(I),I=1,N)
CALL BRKN CV(X,Y1,N,6)
CALL BRKN CV(X,Y2,N,4)
CALL BRKN CV(X,Y3,N,2)
CALL BRKN CV(X,Y4,N,1)
CALL BRKN CV(X,Y6,N,-1)
CALL BRKN CV(X,Y7,N,5)
CALL BRKN CV(X,Y8,N,-1)
CALL BRKN CV(X,Y9,N,3)
CALL BRKN CV(X,Y11,N,-2)
CALL BRKN CV(X,Y16,N,-6)
CALL BRKN CV(X,Y18,N,-3)
CALL BRKN CV(X,Y21,N,6)
CALL BRKN CV(X,Y22,N,4)
CALL DRAW CV(X,Y26,N,0)
CALL SET KY('L','W',14,3)
CALL LINE KY(6,'Y1',3)
CALL LINE KY(4,'Y2',3)
CALL LINE KY(2,'Y3',3)
CALL LINE KY(1,'Y4',3)
CALL LINE KY(-1,'Y6',3)
CALL LINE KY(-1,'Y7',3)
CALL LINE KY(3,'Y8',3)
CALL LINE KY(-2,'Y9',3)
CALL LINE KY(-6,'Y11',3)
CALL LINE KY(-3,'Y16',3)
CALL LINE KY(6,'Y18',3)
CALL LINE KY(4,'Y21',3)
CALL LINE KY(2,'Y22',3)
CALL LINE KY(0,'Y26',3)
CALL TITLE('B','C',)
*TE MICROFACIES OF SECTION "44",76)
CALL ENDPLT
STOP
END

```

FIG. () VERTICAL VARIATION OF CARBONA

Appendix (D.8): Computer program (6)

```

PROGRAM FATHY6
DIMENSION X(50),Y1(50),Y2(50),Y3(50),Y4(50)
*,Y5(50),Y6(50),Y7(50),Y8(50),Y9(50),Y10(50)
*,Y11(50),Y12(50),Y13(50),Y14(50),Y15(50),Y16(50)
*,Y17(50),Y18(50),Y19(50),Y20(50),Y21(50),Y22(50)
*,Y23(50),Y24(50),Y25(50),Y26(50),Y27(50)
CALL PAGE (50,0,29,0)
CALL PICSIZ(8,6,14,0)
CALL CVTYPE(3)
CALL SCALES(0,0,25,8,1,0,0,100,0,1)
CALL AXES('SAMPLE LOCATION',15,'PERCENTAGE',10)
CALL YAXIS(0,100,0,25,8,'PERCENTAGE',10)
READ(5,*)N
READ(5,*)(X(I),Y1(I),Y3(I),Y8(I),Y9(I),Y17(I),Y18(I),
*,Y22(I),Y26(I),I=1,N)
CALL BRKN CV(X,Y1,N,6)
CALL BRKN CV(X,Y3,N,4)
CALL BRKN CV(X,Y8,N,2)
CALL BRKN CV(X,Y9,N,1)
CALL BRKN CV(X,Y17,N,-1)
CALL BRKN CV(X,Y18,N,5)
CALL BRKN CV(X,Y22,N,-1)
CALL DRAW CV(X,Y26,N,0)
CALL SET KY('L','W',8,3)
CALL LINE KY(6,'Y1',3)
CALL LINE KY(4,'Y3',3)
CALL LINE KY(2,'Y8',3)
CALL LINE KY(1,'Y9',3)
CALL LINE KY(-1,'Y17',3)
CALL LINE KY(5,'Y18',3)
CALL LINE KY(-1,'Y22',3)
CALL LINE KY(0,'Y26',3)
CALL TITLE('B','C',
*,TE MICROFACIES OF SECTION " 2",76)
CALL ENDPLT
STOP
END

```

FIG. () VERTICAL VARIATION OF CARBONA


```

PROGRAM FATHY7
DIMENSION X(50),Y1(50),Y2(50),Y3(50),Y4(50)
*,Y5(50),Y6(50),Y7(50),Y8(50),Y9(50),Y10(50)
*,Y11(50),Y12(50),Y13(50),Y14(50),Y15(50),Y16(50)
*,Y17(50),Y18(50),Y19(50),Y20(50),Y21(50),Y22(50)
*,Y23(50),Y24(50),Y25(50),Y26(50),Y27(50)
CALL PAGE(60.,29.0)
CALL PICSIZ(53.33,14.0)
CALL CVTYPE(3)
CALL SCALES(0.0,160.0,1,0.0,100.0,1)
CALL AXES('SAMPLE LOCATION',15,'PERCENTAGE',10)
CALL YAXIS(0.0,100.0,160.0,'PERCENTAGE',10)
READ(5,*)N
READ(5,*)(X(I),Y1(I),Y2(I),Y3(I),Y4(I),Y6(I),
*,Y7(I),Y8(I),Y9(I),Y11(I),Y15(I),Y16(I),
*,Y17(I),Y18(I),Y19(I),Y20(I),Y22(I),Y24(I),
*,Y26(I),I=1,N)
CALL BRKN CV(X,Y1,N,6)
CALL BRKN CV(X,Y2,N,4)
CALL BRKN CV(X,Y3,N,2)
CALL BRKN CV(X,Y4,N,1)
CALL BRKN CV(X,Y6,N,-1)
CALL BRKN CV(X,Y7,N,5)
CALL BRKN CV(X,Y8,N,-1)
CALL BRKN CV(X,Y9,N,3)
CALL BRKN CV(X,Y11,N,-2)
CALL BRKN CV(X,Y15,N,-6)
CALL BRKN CV(X,Y16,N,-3)
CALL BRKN CV(X,Y16,N,6)
CALL BRKN CV(X,Y18,N,4)
CALL BRKN CV(X,Y19,N,2)
CALL BRKN CV(X,Y20,N,1)
CALL BRKN CV(X,Y22,N,-1)
CALL BRKN CV(X,Y24,N,5)
CALL DRAW CV(X,Y26,N,0)
CALL SET KY('L','W',18,3)
CALL LINE KY(6,'Y1',3)
CALL LINE KY(4,'Y2',3)
CALL LINE KY(2,'Y3',3)
CALL LINE KY(1,'Y4',3)
CALL LINE KY(-1,'Y6',3)
CALL LINE KY(5,'Y7',3)
CALL LINE KY(-1,'Y8',3)
CALL LINE KY(3,'Y9',3)
CALL LINE KY(-2,'Y11',3)
CALL LINE KY(-6,'Y15',3)
CALL LINE KY(-3,'Y16',3)
CALL LINE KY(6,'Y17',3)
CALL LINE KY(4,'Y18',3)
CALL LINE KY(2,'Y19',3)
CALL LINE KY(1,'Y20',3)
CALL LINE KY(-1,'Y22',3)
CALL LINE KY(5,'Y24',3)
CALL LINE KY(0,'Y26',3)
CALL TITLE('B','C',
          FIG.( ) VERTICAL VARIATION OF CARBONA
          *TE MICROFACIES OF SECTION " 4" (76)
CALL ENDPLT
STOP
END

```

```

PROGRAM FATHY8
DIMENSION X(50),Y1(50),Y2(50),Y3(50),Y4(50)
*,Y5(50),Y6(50),Y7(50),Y8(50),Y9(50),Y10(50)
*,Y11(50),Y12(50),Y13(50),Y14(50),Y15(50),Y16(50)
*,Y17(50),Y18(50),Y19(50),Y20(50),Y21(50),Y22(50)
*,Y23(50),Y24(50),Y25(50),Y26(50),Y27(50)
CALL PAGE (50,0,29,0)
CALL PICSIZ(4,0,14,0)
CALL CVTYPE(3)
CALL SCALES(0,0,12,0,1,0,0,100,0,1)
CALL AXES('SAMPLE LOCATION',15,'PERCENTAGE',10)
CALL YAXIS(0,0,100,0,12,0,'PERCENTAGE',10)
READ(5,*)N
READ(5,*)(X(I),Y1(I),Y3(I),Y4(I),Y6(I),Y7(I),
*,Y8(I),Y9(I),Y11(I),Y15(I),Y17(I),Y18(I),Y19(I),
*,Y20(I),Y22(I),Y24(I),I=1,N)
CALL BRKN CV(X,Y1,N,6)
CALL BRKN CV(X,Y3,N,4)
CALL BRKN CV(X,Y4,N,2)
CALL BRKN CV(X,Y6,N,1)
CALL BRKN CV(X,Y7,N,-1)
CALL BRKN CV(X,Y8,N,5)
CALL BRKN CV(X,Y9,N,-1)
CALL BRKN CV(X,Y11,N,3)
CALL BRKN CV(X,Y15,N,-2)
CALL BRKN CV(X,Y17,N,-6)
CALL BRKN CV(X,Y18,N,-3)
CALL BRKN CV(X,Y19,N,6)
CALL BRKN CV(X,Y20,N,4)
CALL BRKN CV(X,Y22,N,2)
CALL DRAW CV(X,Y24,N,0)
CALL SET KY('L','W',15,3)
CALL LINE KY(5,'Y1',3)
CALL LINE KY(4,'Y3',3)
CALL LINE KY(2,'Y4',3)
CALL LINE KY(1,'Y6',3)
CALL LINE KY(-1,'Y7',3)
CALL LINE KY(5,'Y8',3)
CALL LINE KY(-1,'Y9',3)
CALL LINE KY(3,'Y11',3)
CALL LINE KY(-2,'Y15',3)
CALL LINE KY(-6,'Y17',3)
CALL LINE KY(-3,'Y18',3)
CALL LINE KY(6,'Y19',3)
CALL LINE KY(4,'Y20',3)
CALL LINE KY(2,'Y22',3)
CALL LINE KY(0,'Y24',3)
CALL TITLE('B','C',
*TE MICROFACIES OF SECTION " 5" (76)
CALL ENDPLT
STOP
END

```

FIG. () VERTICAL VARIATION OF CARBONA

Appendix(D.11): Computer program (9)

```

PROGRAM FATHY9
DIMENSION X(50),Y1(50),Y2(50),Y3(50),Y4(50)
*,Y5(50),Y6(50),Y7(50),Y8(50),Y9(50),Y10(50)
*,Y11(50),Y12(50),Y13(50),Y14(50),Y15(50),Y16(50)
*,Y17(50),Y18(50),Y19(50),Y20(50),Y21(50),Y22(50)
*,Y23(50),Y24(50),Y25(50),Y26(50),Y27(50)
CALL PAGE (50.0,29.0)
CALL PICSIZ(16.0,14.0)
CALL CVTYPE(3)
CALL SCALES(0.0,48.0,1.0,0.0,100.0,1)
CALL AXES('SAMPLE LOCATION',15,'PERCENTAGE',10)
CALL YAXIS(0.0,100.0,48.0,'PERCENTAGE',10)
READ(5,*)N
READ(5,*)(X(I),Y1(I),Y2(I),Y3(I),Y6(I),Y7(I),Y9(I),
*,Y11(I),Y15(I),Y17(I),Y18(I),Y22(I),
*,Y24(I),I=1,N)
CALL BRKN CV(X,Y1,N,6)
CALL BRKN CV(X,Y2,N,4)
CALL BRKN CV(X,Y3,N,2)
CALL BRKN CV(X,Y6,N,1)
CALL BRKN CV(X,Y7,N,- )
CALL BRKN CV(X,Y9,N,5)
CALL BRKN CV(X,Y11,N,-1)
CALL BRKN CV(X,Y15,N,3)
CALL BRKN CV(X,Y17,N,-2)
CALL BRKN CV(X,Y18,N,-6)
CALL BRKN CV(X,Y22,N,-3)
CALL DRAW CV(X,Y24,N,0)
CALL SET KY('L','W',12,3)
CALL LINE KY(6,'Y1 ',3)
CALL LINE KY(4,'Y2 ',3)
CALL LINE KY(2,'Y3 ',3)
CALL LINE KY( 1,'Y6 ',3)
CALL LINE KY(-1,'Y7 ',3)
CALL LINE KY( 5,'Y9 ',3)
CALL LINE KY(-1,'Y11 ',3)
CALL LINE KY( 3,'Y15 ',3)
CALL LINE KY(-2,'Y17 ',3)
CALL LINE KY( -6,'Y18 ',3)
CALL LINE KY(-3,'Y22 ',3)
CALL LINE KY( 0,'Y24 ',3)
CALL TITLE('B','C',0
FIG.( ) VERTICAL VARIATION OF CARBONA
*,TE MICROFACIES OF SECTION "10" ',76)
CALL ENDPLT
STOP
END

```

Appendix (D.12) : Computer program (10)

```

PROGRAM FATHY10
DIMENSION X(50),Y1(50),Y2(50),Y3(50),Y4(50)
*,Y5(50),Y6(50),Y7(50),Y8(50),Y9(50),Y10(50)
*,Y11(50),Y12(50),Y13(50),Y14(50),Y15(50),Y16(50)
*,Y17(50),Y18(50),Y19(50),Y20(50),Y21(50),Y22(50)
*,Y23(50),Y24(50),Y25(50),Y26(50),Y27(50)
CALL PAGE (50,0,29,0)
CALL PICSIZ(21,33,14,0)
CALL CVTYPE(3)
CALL SCALES(0,0,64,0,1,0,0,100,0,1)
CALL AXES('SAMPLE LOCATION',15,'PERCENTAGE',10)
CALL YAXIS(0,0,100,0,64,0,'PERCENTAGE',10)
READ(5,*)N
READ(5,*)(X(I),Y1(I),Y2(I),Y3(I),Y4(I),Y6(I),
*,Y7(I),Y9(I),Y13(I),Y14(I),Y17(I),Y18(I),Y20(I),
*,Y22(I),Y24(I),Y25(I),Y26(I),I=1,N)
CALL BRKN CV(X,Y1,N,6)
CALL BRKN CV(X,Y2,N,4)
CALL BRKN CV(X,Y3,N,2)
CALL BRKN CV(X,Y4,N,1)
CALL BRKN CV(X,Y6,N,-1)
CALL BRKN CV(X,Y7,N,5)
CALL BRKN CV(X,Y9,N,-1)
CALL BRKN CV(X,Y13,N,3)
CALL BRKN CV(X,Y14,N,-2)
CALL BRKN CV(X,Y17,N,-6)
CALL BRKN CV(X,Y18,N,-3)
CALL BRKN CV(X,Y20,N,6)
CALL BRKN CV(X,Y22,N,4)
CALL BRKN CV(X,Y24,N,2)
CALL BRKN CV(X,Y25,N,1)
CALL DRAW CV(X,Y26,N,0)
CALL SET KY('L','W',16,3)
CALL LINE KY(6,'Y1',3)
CALL LINE KY(4,'Y2',3)
CALL LINE KY(2,'Y3',3)
CALL LINE KY(1,'Y4',3)
CALL LINE KY(-1,'Y6',3)
CALL LINE KY(5,'Y7',3)
CALL LINE KY(-1,'Y9',3)
CALL LINE KY(3,'Y13',3)
CALL LINE KY(-2,'Y14',3)
CALL LINE KY(-6,'Y17',3)
CALL LINE KY(-3,'Y18',3)
CALL LINE KY(6,'Y20',3)
CALL LINE KY(4,'Y22',3)
CALL LINE KY(2,'Y24',3)
CALL LINE KY(1,'Y25',3)
CALL LINE KY(0,'Y26',3)
CALL TITLE('B','C',)
*TE MICROFACIES OF SECTION "16" (76)
CALL ENDPLT
STOP
END

```

FIG. () VERTICAL VARIATION OF CARBONA

```

PROGRAM FATHY11
DIMENSION X(50),Y1(50),Y2(50),Y3(50),Y4(50)
*,Y5(50),Y6(50),Y7(50),Y8(50),Y9(50),Y10(50)
*,Y11(50),Y12(50),Y13(50),Y14(50),Y15(50),Y16(50)
*,Y17(50),Y18(50),Y19(50),Y20(50),Y21(50),Y22(50)
*,Y23(50),Y24(50),Y25(50),Y26(50),Y27(50)
CALL PAGE (50,0,29,0)
CALL PICSIZ(32,66,14,0)
CALL CVTYPE(3)
CALL SCALES(0,0,98,0,1,0,0,100,0,1)
CALL AXES('SAMPLE LOCATION',15,'PERCENTAGE',10)
CALL YAXIS(0,0,100,0,98,0,'PERCENTAGE',10)
READ(5,*)N
READ(5,*)(X(I),Y1(I),Y2(I),Y3(I),Y4(I),Y6(I),
*,Y7(I),Y8(I),Y9(I),Y17(I),Y18(I),Y19(I),
*,Y20(I),Y21(I),Y22(I),Y25(I),Y26(I),I=1,N)
CALL BRKN CV(X,Y1,N,6)
CALL BRKN CV(X,Y2,N,4)
CALL BRKN CV(X,Y3,N,2)
CALL BRKN CV(X,Y4,N,1)
CALL BRKN CV(X,Y6,N,-1)
CALL BRKN CV(X,Y7,N,5)
CALL BRKN CV(X,Y8,N,-1)
CALL BRKN CV(X,Y9,N,3)
CALL BRKN CV(X,Y17,N,-2)
CALL BRKN CV(X,Y18,N,-6)
CALL BRKN CV(X,Y19,N,-3)
CALL BRKN CV(X,Y20,N,6)
CALL BRKN CV(X,Y21,N,4)
CALL BRKN CV(X,Y22,N,2)
CALL BRKN CV(X,Y25,N,1)
CALL DRAW CV(X,Y26,N,0)
CALL SET KY('L','W',16,3)
CALL LINE KY(6,'Y1',3)
CALL LINE KY(4,'Y2',3)
CALL LINE KY(2,'Y3',3)
CALL LINE KY(1,'Y4',3)
CALL LINE KY(-1,'Y6',3)
CALL LINE KY(5,'Y7',3)
CALL LINE KY(-1,'Y8',3)
CALL LINE KY(3,'Y9',3)
CALL LINE KY(-2,'Y17',3)
CALL LINE KY(-6,'Y18',3)
CALL LINE KY(-3,'Y19',3)
CALL LINE KY(6,'Y20',3)
CALL LINE KY(4,'Y21',3)
CALL LINE KY(2,'Y22',3)
CALL LINE KY(1,'Y25',3)
CALL LINE KY(0,'Y26',3)
CALL TITLE('B','C',)
FIG.( ) VERTICAL VARIATION OF CARBONA
*,TE MICROFACIES OF SECTION "17",76)
CALL ENDPLT
STOP
END

```

Appendix (D.14): Computer program (12)

```

PROGRAM FATHY12
DIMENSION X(50),Y1(50),Y2(50),Y3(50),Y4(50)
*,Y5(50),Y6(50),Y7(50),Y8(50),Y9(50),Y10(50)
*,Y11(50),Y12(50),Y13(50),Y14(50),Y15(50),Y16(50)
*,Y17(50),Y18(50),Y19(50),Y20(50),Y21(50),Y22(50)
*,Y23(50),Y24(50),Y25(50),Y26(50),Y27(50)
CALL PAGE (50.0,29.0)
CALL PICSIZ(43.0,14.0)
CALL CVTYPE(3)
CALL SCALES(0.0,129.0,1.0,0.0,100.0,1)
CALL AXES('SAMPLE LOCATION',15,'PERCENTAGE',10)
CALL YAXIS(0.0,100.0,129.0,'PERCENTAGE',10)
READ(5,*)N
READ(5,*)(X(I),Y1(I),Y3(I),Y4(I),Y6(I),Y7(I),
*,Y8(I),Y9(I),Y14(I),Y16(I),Y17(I),Y18(I),
*,Y19(I),Y20(I),Y22(I),Y24(I),Y25(I),Y26(I),I=1,N)
CALL BRKN CV(X,Y1,N,6)
CALL BRKN CV(X,Y3,N,4)
CALL BRKN CV(X,Y4,N,2)
CALL BRKN CV(X,Y6,N,1)
CALL BRKN CV(X,Y7,N,-1)
CALL BRKN CV(X,Y8,N,5)
CALL BRKN CV(X,Y9,N,-1)
CALL BRKN CV(X,Y14,N,3)
CALL BRKN CV(X,Y16,N,-2)
CALL BRKN CV(X,Y17,N,-6)
CALL BRKN CV(X,Y18,N,-3)
CALL BRKN CV(X,Y19,N,6)
CALL BRKN CV(X,Y20,N,4)
CALL BRKN CV(X,Y22,N,2)
CALL BRKN CV(X,Y24,N,1)
CALL BRKN CV(X,Y25,N,-1)
CALL DRAW CV(X,Y26,N,0)
CALL SET KY('L','W',17,3)
CALL LINE KY(5,'Y1',3)
CALL LINE KY(4,'Y3',3)
CALL LINE KY(2,'Y4',3)
CALL LINE KY(-1,'Y6',3)
CALL LINE KY(-1,'Y7',3)
CALL LINE KY(5,'Y8',3)
CALL LINE KY(-1,'Y9',3)
CALL LINE KY(3,'Y14',3)
CALL LINE KY(-2,'Y16',3)
CALL LINE KY(-6,'Y17',3)
CALL LINE KY(-3,'Y18',3)
CALL LINE KY(6,'Y19',3)
CALL LINE KY(4,'Y20',3)
CALL LINE KY(2,'Y22',3)
CALL LINE KY(1,'Y24',3)
CALL LINE KY(-1,'Y25',3)
CALL LINE KY(0,'Y26',3)
CALL TITLE('B','C',
*,TE MICROFACIES OF SECTION "18" (76)
CALL ENDPLT
STOP
END

```

FIG. () VERTICAL VARIATION OF CARBONA

Appendix (D.15): Computer program (13)

```

PROGRAM FATHY13
DIMENSION X(50),Y1(50),Y2(50),Y3(50),Y4(50)
*,Y5(50),Y6(50),Y7(50),Y8(50),Y9(50),Y10(50)
*,Y11(50),Y12(50),Y13(50),Y14(50),Y15(50),Y16(50)
*,Y17(50),Y18(50),Y19(50),Y20(50),Y21(50),Y22(50)
*,Y23(50),Y24(50),Y25(50),Y26(50),Y27(50)
CALL PAGE (50,0,29,0)
CALL PICSIZ(23,66,14,0)
CALL CVTYPE(3)
CALL SCALES(0,0,71,0,1,0,0,100,0,1)
CALL AXES('SAMPLE LOCATION',15,'PERCENTAGE',10)
CALL YAXIS(0,0,100,0,71,0,'PERCENTAGE',10)
READ(5,*)N
READ(5,*)(X(I),Y1(I),Y2(I),Y3(I),Y4(I),Y6(I),
*,Y7(I),Y8(I),Y9(I),Y11(I),Y18(I),Y20(I),Y21(I),
*,Y22(I),Y24(I),Y26(I),I=1,N)
CALL BRKN CV(X,Y1,N,6)
CALL BRKN CV(X,Y2,N,4)
CALL BRKN CV(X,Y3,N,2)
CALL BRKN CV(X,Y4,N,1)
CALL BRKN CV(X,Y6,N,-1)
CALL BRKN CV(X,Y7,N,5)
CALL BRKN CV(X,Y8,N,-1)
CALL BRKN CV(X,Y9,N,3)
CALL BRKN CV(X,Y11,N,-2)
CALL BRKN CV(X,Y18,N,-6)
CALL BRKN CV(X,Y20,N,-3)
CALL BRKN CV(X,Y21,N,6)
CALL BRKN CV(X,Y22,N,4)
CALL BRKN CV(X,Y24,N,2)
CALL DRAW CV(X,Y26,N,0)

CALL SET KY('L','W',15,3)
CALL LINE KY(6,'Y1',3)
CALL LINE KY(4,'Y2',3)
CALL LINE KY(2,'Y3',3)
CALL LINE KY(1,'Y4',3)
CALL LINE KY(-1,'Y6',3)
CALL LINE KY(5,'Y7',3)
CALL LINE KY(-1,'Y8',3)
CALL LINE KY(3,'Y9',3)
CALL LINE KY(-2,'Y11',3)
CALL LINE KY(-6,'Y18',3)
CALL LINE KY(-3,'Y20',3)
CALL LINE KY(6,'Y21',3)
CALL LINE KY(4,'Y22',3)
CALL LINE KY(2,'Y24',3)
CALL LINE KY(0,'Y26',3)
CALL TITLE('B','C',
FIG.( ) VERTICAL VARIATION OF CARBONA
*TE MICROFACIES OF SECTION "26" (76)
CALL ENDPLT
STOP
END

```

```

PROGRAM FATHY14
DIMENSION X(50),Y1(50),Y2(50),Y3(50),Y4(50)
*,Y5(50),Y6(50),Y7(50),Y8(50),Y9(50),Y10(50)
*,Y11(50),Y12(50),Y13(50),Y14(50),Y15(50),Y16(50)
*,Y17(50),Y18(50),Y19(50),Y20(50),Y21(50),Y22(50)
*,Y23(50),Y24(50),Y25(50),Y26(50),Y27(50)
CALL PAGE (50,0,29,0)
CALL PICSIZ(5,33,14,0)
CALL CVTYPE(3)
CALL SCALES(0,0,16,0,1,0,0,100,0,1)
CALL AXES('SAMPLE LOCATION',15,'PERCENTAGE',10)
CALL YAXIS(0,0,100,0,16,0,'PERCENTAGE',10)
READ(5,*)N
READ(5,*)(X(I),Y1(I),Y2(I),Y3(I),Y4(I),Y6(I),
*,Y7(I),Y8(I),Y9(I),Y11(I),Y18(I),Y20(I),Y21(I),
*,Y22(I),Y24(I),Y26(I),I=1,N)
CALL BRKN CV(X,Y1,N,6)
CALL BRKN CV(X,Y2,N,4)
CALL BRKN CV(X,Y3,N,2)
CALL BRKN CV(X,Y4,N,1)
CALL BRKN CV(X,Y6,N,-1)
CALL BRKN CV(X,Y7,N,5)
CALL BRKN CV(X,Y8,N,-1)
CALL BRKN CV(X,Y9,N,3)
CALL BRKN CV(X,Y11,N,-2)
CALL BRKN CV(X,Y18,N,-6)
CALL BRKN CV(X,Y20,N,-3)
CALL BRKN CV(X,Y21,N,6)
CALL BRKN CV(X,Y22,N,4)
CALL BRKN CV(X,Y24,N,2)
CALL DRAW CV(X,Y26,N,0)
CALL SET KY('L','W',15,3)
CALL LINE KY(6,'Y1',3)
CALL LINE KY(4,'Y2',3)
CALL LINE KY(2,'Y3',3)
CALL LINE KY(1,'Y4',3)
CALL LINE KY(-1,'Y6',3)
CALL LINE KY(5,'Y7',3)
CALL LINE KY(-1,'Y8',3)
CALL LINE KY(3,'Y9',3)
CALL LINE KY(-2,'Y11',3)
CALL LINE KY(-6,'Y18',3)
CALL LINE KY(-3,'Y20',3)
CALL LINE KY(6,'Y21',3)
CALL LINE KY(4,'Y22',3)
CALL LINE KY(2,'Y24',3)
CALL LINE KY(0,'Y26',3)
CALL TITLE('B','C',
*,TE MICROFACIES OF SECTION "36",76)
FIG.( ) VERTICAL VARIATION OF CARBONA
CALL ENDPLT
STOP
END

```



```

PROGRAM FATHY15
DIMENSION X(50),Y1(50),Y2(50),Y3(50),Y4(50)
*,Y5(50),Y6(50),Y7(50),Y8(50),Y9(50),Y10(50)
*,Y11(50),Y12(50),Y13(50),Y14(50),Y15(50),Y16(50)
*,Y17(50),Y18(50),Y19(50),Y20(50),Y21(50),Y22(50)
*,Y23(50),Y24(50),Y25(50),Y26(50),Y27(50)
CALL PAGE(50,0,29,0)
CALL PICSIZ(34,46,14,0)
CALL CVTYPE(3)
CALL SCALES(0,0,103.4,1,0,0,100,0,1)
CALL AXES('SAMPLE LOCATION',15,'PERCENTAGE',10)
CALL YAXIS(0,0,100,0,103.4,'PERCENTAGE',10)
READ(5,*)N
READ(5,*)(X(I),Y1(I),Y3(I),Y4(I),
*,Y6(I),Y7(I),Y8(I),
*,Y12(I),Y17(I),
*,Y18(I),Y20(I),Y21(I),Y22(I),
*,Y25(I),Y26(I),
*,Y27(I),I=1,N)
CALL BRKN CV(X,Y1,N,6)
CALL BRKN CV(X,Y3,N,2)
CALL BRKN CV(X,Y4,N,1)
CALL BRKN CV(X,Y6,N,5)
CALL BRKN CV(X,Y7,N,-1)
CALL BRKN CV(X,Y8,N,3)
CALL BRKN CV(X,Y12,N,6)
CALL BRKN CV(X,Y17,N, )
CALL BRKN CV(X,Y18,N,-1)
CALL BRKN CV(X,Y20,N,-2)
CALL BRKN CV(X,Y21,N,-6)
CALL BRKN CV(X,Y22,N,-3)
CALL BRKN CV(X,Y25,N,2)
CALL BRKN CV(X,Y26,N, )
CALL DRAW CV(X,Y27,N,0)
CALL SET KY('L','W',15,3)
CALL LINE KY(6,'Y1',3)
CALL LINE KY(2,'Y3',3)
CALL LINE KY(1,'Y4',3)
CALL LINE KY(5,'Y6',3)
CALL LINE KY(-1,'Y7',3)
CALL LINE KY(3,'Y8',3)
CALL LINE KY(6,'Y12',3)
CALL LINE KY(5,'Y17',3)
CALL LINE KY(-1,'Y18',3)
CALL LINE KY(-2,'Y20',3)
CALL LINE KY(-6,'Y21',3)
CALL LINE KY(-3,'Y22',3)
CALL LINE KY(2,'Y25',3)
CALL LINE KY(1,'Y26',3)
CALL LINE KY(0,'Y27',3)
CALL TITLE('B','C',,
*,TE MICROFACIES OF SECTION "51",76)
CALL ENDPLT
STOP
END

```

FIG. () VERTICAL VARIATION OF CARBONA

```

PROGRAM FATHY16
DIMENSION X(50),Y1(50),Y2(50),Y3(50),Y4(50)
*,Y5(50),Y6(50),Y7(50),Y8(50),Y9(50),Y10(50)
*,Y11(50),Y12(50),Y13(50),Y14(50),Y15(50),Y16(50)
*,Y17(50),Y18(50),Y19(50),Y20(50),Y21(50),Y22(50)
*,Y23(50),Y24(50),Y25(50),Y26(50),Y27(50)
CALL PAGE (50,0,29,0)
CALL PICSIZ(20,33,14,0)
CALL CVTYPE(3)
CALL SCALES(0,0,61,0,1,0,0,100,0,1)
CALL AXES('SAMPLE LOCATION',15,'PERCENTAGE',10)
CALL YAXIS (0,0 100,0,61,0,'PERCENTAGE',10)
READ(5,*)N
READ(5,*)(X(I),Y1(I),Y2(I),Y3(I),Y4(I),Y6(I),
*,Y7(I),Y8(I),Y9(I),Y10(I),Y14(I),Y16(I),
*,Y17(I),Y18(I),Y20(I),Y22(I),Y24(I),Y26(I),I=1,N)
CALL BRKN CV(X,Y1,N,6)
CALL BRKN CV(X,Y2,N,4)
CALL BRKN CV(X,Y3,N,2)
CALL BRKN CV(X,Y4,N,1)
CALL BRKN CV(X,Y6,N,-1)
CALL BRKN CV(X,Y7,N,5)
CALL BRKN CV(X,Y8,N,-1)
CALL BRKN CV(X,Y9,N,3)
CALL BRKN CV(X,Y10,N,-2)
CALL BRKN CV(X,Y14,N,-6)
CALL BRKN CV(X,Y16,N,-3)
CALL BRKN CV(X,Y17,N,6)
CALL BRKN CV(X,Y18,N,4)
CALL BRKN CV(X,Y20,N,2)
CALL BRKN CV(X,Y22,N,1)
CALL BRKN CV(X,Y24,N,1)
CALL DRAW CV(X,Y26,N,0)
CALL SET KY('L','W',17,3)
CALL LINE KY(6,'Y1',3)
CALL LINE KY(4,'Y2',3)
CALL LINE KY(2,'Y3',3)
CALL LINE KY(1,'Y4',3)
CALL LINE KY(-1,'Y6',3)
CALL LINE KY(5,'Y7',3)
CALL LINE KY(-1,'Y8',3)
CALL LINE KY(3,'Y9',3)
CALL LINE KY(-2,'Y10',3)
CALL LINE KY(-6,'Y14',3)
CALL LINE KY(-3,'Y16',3)
CALL LINE KY(6,'Y17',3)
CALL LINE KY(4,'Y18',3)
CALL LINE KY(2,'Y20',3)
CALL LINE KY(1,'Y22',3)
CALL LINE KY(-1,'Y24',3)
CALL LINE KY(0,'Y26',3)
CALL TITLE('B','C',
*,TE MICROFACIES OF SECTION "56",76)
CALL ENDPLT

```

FIG. () VERTICAL VARIATION OF CARBONA

```

STOP
END

```

Appendix (D.19): Computer program (17)

```

PROGRAM FATHY17
DIMENSION X(50),Y1(50),Y2(50),Y3(50),Y4(50)
*,Y5(50),Y6(50),Y7(50),Y8(50),Y9(50),Y10(50)
*,Y11(50),Y12(50),Y13(50),Y14(50),Y15(50),Y16(50)
*,Y17(50),Y18(50),Y19(50),Y20(50),Y21(50),Y22(50)
*,Y23(50),Y24(50),Y25(50),Y26(50),Y27(50)
CALL PAGE(50,0,29,0)
CALL PICSIZ(20,33,14,0)
CALL CVTYPE(3)
CALL SCALES(0,0,61,0,1,0,0,100,0,1)
CALL AXES('SAMPLE LOCATION',15,'PERCENTAGE',10)
CALL YAXIS(0,0,100,0,61,0,'PERCENTAGE',10)
READ(5,*)N
READ(5,*)(X(I),Y1(I),Y2(I),Y3(I),Y4(I),Y6(I),
*,Y7(I),Y8(I),Y9(I),Y10(I),Y14(I),Y15(I),
*,Y16(I),Y17(I),Y18(I),Y20(I),Y22(I),Y25(I),
*,Y26(I),I=1,N)
CALL BRKN CV(X,Y1,N,6)
CALL BRKN CV(X,Y2,N,4)
CALL BRKN CV(X,Y3,N,2)
CALL BRKN CV(X,Y4,N,1)
CALL BRKN CV(X,Y6,N,-1)
CALL BRKN CV(X,Y7,N,5)
CALL BRKN CV(X,Y8,N,-1)
CALL BRKN CV(X,Y9,N,3)
CALL BRKN CV(X,Y10,N,-2)
CALL BRKN CV(X,Y14,N,-6)
CALL BRKN CV(X,Y15,N,-3)
CALL BRKN CV(X,Y16,N,6)
CALL BRKN CV(X,Y17,N,4)
CALL BRKN CV(X,Y18,N,2)
CALL BRKN CV(X,Y20,N,1)
CALL BRKN CV(X,Y22,N,-1)
CALL BRKN CV(X,Y25,N,5)
CALL DRAW CV(X,Y26,N,0)
CALL SET KY('L','W',18,3)
CALL LINE KY(6,'Y1',3)
CALL LINE KY(4,'Y2',3)
CALL LINE KY(2,'Y3',3)
CALL LINE KY(1,'Y4',3)
CALL LINE KY(-1,'Y6',3)
CALL LINE KY(5,'Y7',3)
CALL LINE KY(-1,'Y8',3)
CALL LINE KY(3,'Y9',3)
CALL LINE KY(-2,'Y10',3)
CALL LINE KY(-6,'Y14',3)
CALL LINE KY(-3,'Y15',3)
CALL LINE KY(6,'Y16',3)
CALL LINE KY(4,'Y17',3)
CALL LINE KY(2,'Y18',3)
CALL LINE KY(1,'Y20',3)
CALL LINE KY(-1,'Y22',3)
CALL LINE KY(5,'Y25',3)
CALL LINE KY(0,'Y26',3)
CALL TITLE('B','C',
FIG.( ) VERTICAL VARIATION OF CARBONA
*TE MICROFACIES OF SECTION "59",76)
CALL ENDPLT

```

```

STOP
END

```

Appendix (D.20): Computer program (18)

```

PROGRAM FATHY18
DIMENSION X(50),Y1(50),Y2(50),Y3(50),Y4(50)
*,Y5(50),Y6(50),Y7(50),Y8(50),Y9(50),Y10(50)
*,Y11(50),Y12(50),Y13(50),Y14(50),Y15(50),Y16(50)
*,Y17(50),Y18(50),Y19(50),Y20(50),Y21(50),Y22(50)
*,Y23(50),Y24(50),Y25(50),Y26(50),Y27(50)
CALL PAGE(50,0,29,0)
CALL PICSIZ(3),43,14,0)
CALL CVTYPE(3)
CALL SCALES(0,0,91.3,1,0,0,100,0,1)
CALL AXES('SAMPLE LOCATION',15,'PERCENTAGE',10)
CALL YAXIS(0,0,100,0,91.3,'PERCENTAGE',10)
READ(5,*)N
READ(5,*)(X(I),Y1(I),Y3(I),Y4(I),
*,Y6(I),Y7(I),Y9(I),
*,Y12(I),Y17(I),
*,Y18(I),Y20(I),Y21(I),Y22(I),
*,Y25(I),Y26(I),
*I=1,N)
CALL BRKN CV(X,Y1,N,6)
CALL BRKN CV(X,Y3,N,2)
CALL BRKN CV(X,Y4,N,1)
CALL BRKN CV(X,6,N,5)
CALL BRKN CV(X,Y7,N,-1)
CALL BRKN CV(X,Y9,N,-2)
CALL BRKN CV(X,Y12,N,6)
CALL BRKN CV(X,Y17,N,5)
CALL BRKN CV(X,Y18,N,-1)
CALL BRKN CV(X,Y20,N,-2)
CALL BRKN CV(X,Y21,N,-6)
CALL BRKN CV(X,Y22,N,-3)
CALL BRKN CV(X,Y25,N,2)
CALL DRAW CV(X,Y26,N,0)
CALL SET KY('L','W',14,3)
CALL LINE KY(6,'Y1',3)
CALL LINE KY(2,'Y3',3)
CALL LINE KY(1,'Y4',3)
CALL LINE KY(5,'Y6',3)
CALL LINE KY(-1,'Y7',3)
CALL LINE KY(-2,'Y9',3)
CALL LINE KY(6,'Y12',3)
CALL LINE KY(5,'Y17',3)
CALL LINE KY(-1,'Y18',3)
CALL LINE KY(-2,'Y20',3)
CALL LINE KY(-6,'Y21',3)
CALL LINE KY(-3,'Y22',3)
CALL LINE KY(2,'Y25',3)
CALL LINE KY(0,'Y26',3)
CALL TITLE('B','C',, FIG.( ) VERTICAL VARIATION OF CARBONA
*TE MICROFACIES OF SECTION "60",76)
CALL ENDPLT
STOP
END

```

PROGRAM FATHY19

```

DIMENSION X(50),Y1(50),Y2(50),Y3(50),Y4(50)
*,Y5(50),Y6(50),Y7(50),Y8(50),Y9(50),Y10(50)
*,Y11(50),Y12(50),Y13(50),Y14(50),Y15(50),Y16(50)
*,Y17(50),Y18(50),Y19(50),Y20(50),Y21(50),Y22(50)
*,Y23(50),Y24(50),Y25(50),Y26(50),Y27(50)
CALL PAGE(50,0,29,0)
CALL PICSIZ(26,6,14,0)
CALL CVTYPE(3)
CALL SCALES(0,0,80,0,1,0,0,100,0,1)
CALL AXES('SAMPLE LOCATION',15,'PERCENTAGE',10)
CALL YAXIS(0,0,100,0,80,0,'PERCENTAGE',10)
READ(5,*)N
READ(5,*)(X(I),Y1(I),Y2(I),Y3(I),Y4(I),
*,Y6(I),Y7(I),Y8(I),Y9(I),Y11(I),
*,Y12(I),Y17(I),
*,Y18(I),Y20(I),Y21(I),Y22(I),
*,Y24(I),Y25(I),Y26(I),
*I=1,N)
CALL BRKN CV(X,Y1,N,6)
CALL BRKN CV(X,Y2,N,4)
CALL BRKN CV(X,Y3,N,2)
CALL BRKN CV(X,Y4,N,1)
CALL BRKN CV(X,Y6,N,5)
CALL BRKN CV(X,Y7,N,-1)
CALL BRKN CV(X,Y8,N,3)
CALL BRKN CV(X,Y9,N,-2)
CALL BRKN CV(X,Y11,N,-3)
CALL BRKN CV(X,Y12,N,6)
CALL BRKN CV(X,Y17,N,5)
CALL BRKN CV(X,Y18,N,-1)
CALL BRKN CV(X,Y20,N,-2)
CALL BRKN CV(X,Y21,N,-6)
CALL BRKN CV(X,Y22,N,-3)
CALL BRKN CV(X,Y24,N,4)
CALL BRKN CV(X,Y25,N,2)
CALL DRAW CV(X,Y26,N,0)
CALL SET KY('L','W',18,3)
CALL LINE KY(6,'Y1',3)
CALL LINE KY(4,'Y2',3)
CALL LINE KY(2,'Y3',3)
CALL LINE KY(1,'Y4',3)
CALL LINE KY(5,'Y6',3)
CALL LINE KY(-1,'Y7',3)
CALL LINE KY(3,'Y8',3)
CALL LINE KY(-2,'Y9',3)
CALL LINE KY(-3,'Y11',3)
CALL LINE KY(6,'Y12',3)
CALL LINE KY(5,'Y17',3)
CALL LINE KY(-1,'Y18',3)
CALL LINE KY(-2,'Y20',3)
CALL LINE KY(-6,'Y21',3)
CALL LINE KY(-3,'Y22',3)
CALL LINE KY(4,'Y24',3)
CALL LINE KY(2,'Y25',3)
CALL LINE KY(0,'Y26',3)
CALL TITLE('B','C',
*TE MICROFACIES OF SECTION "61",76)
CALL ENDPLT
STOP
END

```

FIG. () VERTICAL VARIATION OF CARBONA

Appendix (D.22): Computer program (20)

```

PROGRAM FATHY2G
DIMENSION X(50),Y1(50),Y2(50),Y3(50),Y4(50)
*,Y5(50),Y6(50),Y7(50),Y8(50),Y9(50),Y10(50)
*,Y11(50),Y12(50),Y13(50),Y14(50),Y15(50),Y16(50)
*,Y17(50),Y18(50),Y19(50),Y20(50),Y21(50),Y22(50)
*,Y23(50),Y24(50),Y25(50),Y26(50),Y27(50)
CALL PAGE(50,0,29,0)
CALL PICSIZ(12,60,14,0)
CALL CVTYPE(3)
CALL SCALES(0,0,38,0,1,0,0,100,0,1)
CALL AXES('SAMPLE LOCATION',15,'PERCENTAGE',10)
CALL YAXIS(0,0,100,0,38,0,'PERCENTAGE',10)
READ(5,*)N
READ(5,*)(X(I),Y1(I),Y2(I),Y3(I),
*,Y6(I),Y7(I),Y9(I),Y11(I),
*,Y18(I),Y20(I),Y21(I),Y22(I),
*,Y25(I),Y26(I),
*I=1,N)
CALL BRKN CV(X,Y1,N,6)
CALL BRKN CV(X,Y2,N,4)
CALL BRKN CV(X,Y3,N,2)
CALL BRKN CV(X,Y6,N,5)
CALL BRKN CV(X,Y7,N,-1)
CALL BRKN CV(X,Y9,N,-2)
CALL BRKN CV(X,Y11,N,-3)
CALL BRKN CV(X,Y18,N,-1)
CALL BRKN CV(X,Y20,N,-2)
CALL BRKN CV(X,Y21,N,-6)
CALL BRKN CV(X,Y22,N,-3)
CALL BRKN CV(X,Y25,N,2)
CALL DRAW CV(X,Y26,N,0)
CALL SET KY('L','W',13,3)
CALL LINE KY(6,'Y1 ', )
CALL LINE KY(4,'Y2 ',3)
CALL LINE KY(2,'Y3 ',3)
CALL LINE KY( 5,'Y6 ',3)
CALL LINE KY(-1,'Y7 ',3)
CALL LINE KY(-2,'Y9 ',3)
CALL LINE KY(-3,'Y11',3)
CALL LINE KY(-1,'Y18',3)
CALL LINE KY(-2,'Y20',3)
CALL LINE KY(-6,'Y21',3)
CALL LINE KY(-3,'Y22',3)
CALL LINE KY(2,'Y25',3)
CALL LINE KY(0,'Y26',3)
CALL TITLE('B','C', )
*TE MICROFACIES OF SECTION "69",76)
CALL ENDPLT
STOP
END

```

FIG. () VERTICAL VARIATION OF CARBONA

Appendix (D.23): Computer program (21)

```

PROGRAM FATHY21
DIMENSION X(50),Y1(50),Y2(50),Y3(50),Y4(50)
*,Y5(50),Y6(50),Y7(50),Y8(50),Y9(50),Y10(50)
*,Y11(50),Y12(50),Y13(50),Y14(50),Y15(50),Y16(50)
*,Y17(50),Y18(50),Y19(50),Y20(50),Y21(50),Y22(50)
*,Y23(50),Y24(50),Y25(50),Y26(50),Y27(50)
CALL PAGE(50.0,29.0)
CALL PICSIZ(18.46,14.0)
CALL CVTYPE(3)
CALL SCALES(0.0,55.4,1.0,0.0,100.0,1)
CALL AXES('SAMPLE LOCATION',15,'PERCENTAGE',10)
CALL YAXIS(0.0,100.0,55.4,'PERCENTAGE',10)
READ(5,*)N
READ(5,*)(X(I),Y1(I),Y2(I),Y3(I),Y4(I),
*,Y6(I),Y7(I),Y8(I),Y9(I),Y11(I),
*,Y17(I),
*,Y18(I),Y20(I),Y21(I),Y22(I),
*,Y26(I),
*,I=1,N)
CALL BRKN CV(X,Y1,N,6)
CALL BRKN CV(X, Y2,N,4)
CALL BRKN CV(X,Y3,N,2)
CALL BRKN CV(X,Y4,N,1)
CALL BRKN CV(X,Y6,N,5)
CALL BRKN CV(X,Y7,N,-1)
CALL BRKN CV(X,Y8,N,3)
CALL BRKN CV(X,Y9,N,-2)
CALL BRKN CV(X,Y11,N,-3)
CALL BRKN CV(X,Y17,N,5)
CALL BRKN CV(X,Y18,N,-1)
CALL BRKN CV(X,Y20,N,-2)
CALL BRKN CV(X,Y21,N,-6)
CALL BRKN CV(X, Y22,N,-3)
CALL DRAW CV(X,Y26,N,0)
CALL SET KY('L','W',15,3)
CALL LINE KY(6,'Y1 ',3)
CALL LINE KY(4,'Y2 ',3)
CALL LINE KY(2,'Y3 ',3)
CALL LINE KY( 1,'Y4 ',3)
CALL LINE KY( 5,'Y6 ',3)
CALL LINE KY(-1,'Y7 ',3)
CALL LINE KY( 3 'Y8 ',3)
CALL LINE KY(-2,'Y9 ',3)
CALL LINE KY(-3,'Y11 ',3)
CALL LINE KY(5,'Y17 ',3)
CALL LINE KY(-1,'Y18 ',3)
CALL LINE KY(-2,'Y20 ',3)
CALL LINE KY(-6 'Y21 ',3)
CALL LINE KY(-3,'Y22 ',3)
CALL LINE KY(3,'Y26 ',3)
CALL TITLE('B','C',
FIG. ( ) VERTICAL VARIATION OF CARBONA
*TE MICROFACIES OF SECTION "81" (76)
CALL ENDPLT
STOP
END

```

```

PROGRAM FATHY22
DIMENSION X(50),Y1(50),Y2(50),Y3(50),Y4(50)
*,Y5(50),Y6(50),Y7(50),Y8(50),Y9(50),Y10(50)
*,Y11(50),Y12(50),Y13(50),Y14(50),Y15(50),Y16(50)
*,Y17(50),Y18(50),Y19(50),Y20(50),Y21(50),Y22(50)
*,Y23(50),Y24(50),Y25(50),Y26(50),Y27(50)
CALL PAGE(50,0,29,0)
CALL PICSIZ(24,0,14,0)
CALL CVTYPE(3)
CALL SCALES(0,0,57,0,1,0,0,100,0,1)
CALL AXES('SAMPLE LOCATION',15,'PERCENTAGE',10)
CALL YAXIS(0,0,100,0,57,0,'PERCENTAGE',10)
READ(5,*)N
READ(5,*)(X(I),Y1(I),Y3(I),Y4(I),
*,Y6(I),Y7(I),Y8(I),
*,Y9(I),Y11(I),Y17(I),
*,Y18(I),Y20(I),Y21(I),Y22(I),
*,Y26(I),
*I=1,N)
CALL BRKN CV(X,Y1,N,6)
CALL BRKN CV(X,Y3,N,2)
CALL BRKN CV(X,Y4,N,1)
CALL BRKN CV(X,Y6,N,5)
CALL BRKN CV(X,Y7,N,-1)
CALL BRKN CV(X,Y8,N,-2)
CALL BRKN CV(X,Y9,N,6)
CALL BRKN CV(X,Y11,N,5)
CALL BRKN CV(X,Y17,N,-4)
CALL BRKN CV(X,Y18,N,-1)
CALL BRKN CV(X,Y20,N,-2)
CALL BRKN CV(X,Y21,N,-6)
CALL BRKN CV(X,Y22,N,-3)
CALL DRAW CV(X,Y26,N,0)
CALL SET KY('L','W',14,3)
CALL LINE KY(6,'Y1',3)
CALL LINE KY(2,'Y3',3)
CALL LINE KY(1,'Y4',3)
CALL LINE KY(5,'Y6',3)
CALL LINE KY(-1,'Y7',3)
CALL LINE KY(-2,'Y8',3)
CALL LINE KY(6,'Y9',3)
CALL LINE KY(5,'Y11',3)
CALL LINE KY(-4,'Y17',3)
CALL LINE KY(-1,'Y18',3)
CALL LINE KY(-2,'Y20',3)
CALL LINE KY(-6,'Y21',3)
CALL LINE KY(-3,'Y22',3)
CALL LINE KY(0,'Y26',3)
CALL TITLE('B','C',,
*,TE MICROFACIES OF SECTION "82",76)
CALL ENDPLT
STOP
END

```

FIG. () VERTICAL VARIATION OF CARBONA

Appendix (D.25): Computer program (23)

```

PROGRAM FATHY23
DIMENSION X(50),Y1(50),Y2(50),Y3(50),Y4(50)
*,Y5(50),Y6(50),Y7(50),Y8(50),Y9(50),Y10(50)
*,Y11(50),Y12(50),Y13(50),Y14(50),Y15(50),Y16(50)
*,Y17(50),Y18(50),Y19(50),Y20(50),Y21(50),Y22(50)
*,Y23(50),Y24(50),Y25(50),Y26(50),Y27(50),Y28(50)
CALL PAGE(50,29,0)
CALL PICSIZ(23,66,14,0)
CALL CVTYPE(3)
CALL SCALES(0,0,71,0,1,0,0,100,0,1)
CALL AXES('SAMPLE LOCATION',15,'PERCENTAGE',10)
CALL YAXIS(0,0,100,0,71,0,'PERCENTAGE',10)
READ(5,*)N
READ(5,*)(X(I),Y1(I),Y2(I),Y6(I),
*,Y7(I),Y8(I),Y9(I),
*,Y11(I),Y18(I),
*,Y20(I),Y21(I),Y22(I),Y24(I),
*,Y25(I),Y26(I),
*,Y27(I),I=1,N)
CALL BRKN CV(X,Y1,N,6)
CALL BRKN CV(X,Y2,N,2)
CALL BRKN CV(X,Y6,N,1)
CALL BRKN CV(X,Y7,N,5)
CALL BRKN CV(X,Y8,N,-1)
CALL BRKN CV(X,Y9,N,3)
CALL BRKN CV(X,Y11,N,6)
CALL BRKN CV(X,Y18,N,5)
CALL BRKN CV(X,Y20,N,-1)
CALL BRKN CV(X,Y21,N,-2)
CALL BRKN CV(X,Y22,N,-6)
CALL BRKN CV(X,Y24,N,-3)
CALL BRKN CV(X,Y25,N,2)
CALL BRKN CV(X,Y26,N,1)
CALL DRAW CV(X,Y27,N,0)
CALL SET KY('L','W',15,3)
CALL LINE KY(5,'Y1',3)
CALL LINE KY(2,'Y2',3)
CALL LINE KY(1,'Y6',3)
CALL LINE KY(5,'Y7',3)
CALL LINE KY(-1,'Y8',3)
CALL LINE KY(3,'Y9',3)
CALL LINE KY(6,'Y11',3)
CALL LINE KY(5,'Y18',3)
CALL LINE KY(-1,'Y20',3)
CALL LINE KY(-2,'Y21',3)
CALL LINE KY(-6,'Y22',3)
CALL LINE KY(-3,'Y24',3)
CALL LINE KY(2,'Y25',3)
CALL LINE KY(1,'Y26',3)
CALL LINE KY(0,'Y27',3)
CALL TITLE('B','C',0)
*TE MICROFACIES OF SECTION "64" (76)
CALL ENDPLT
STOP
END






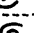



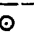
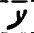


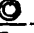
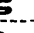

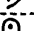
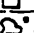
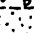
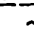



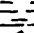



```

FIG. () VERTICAL VARIATION OF CARBONA

```

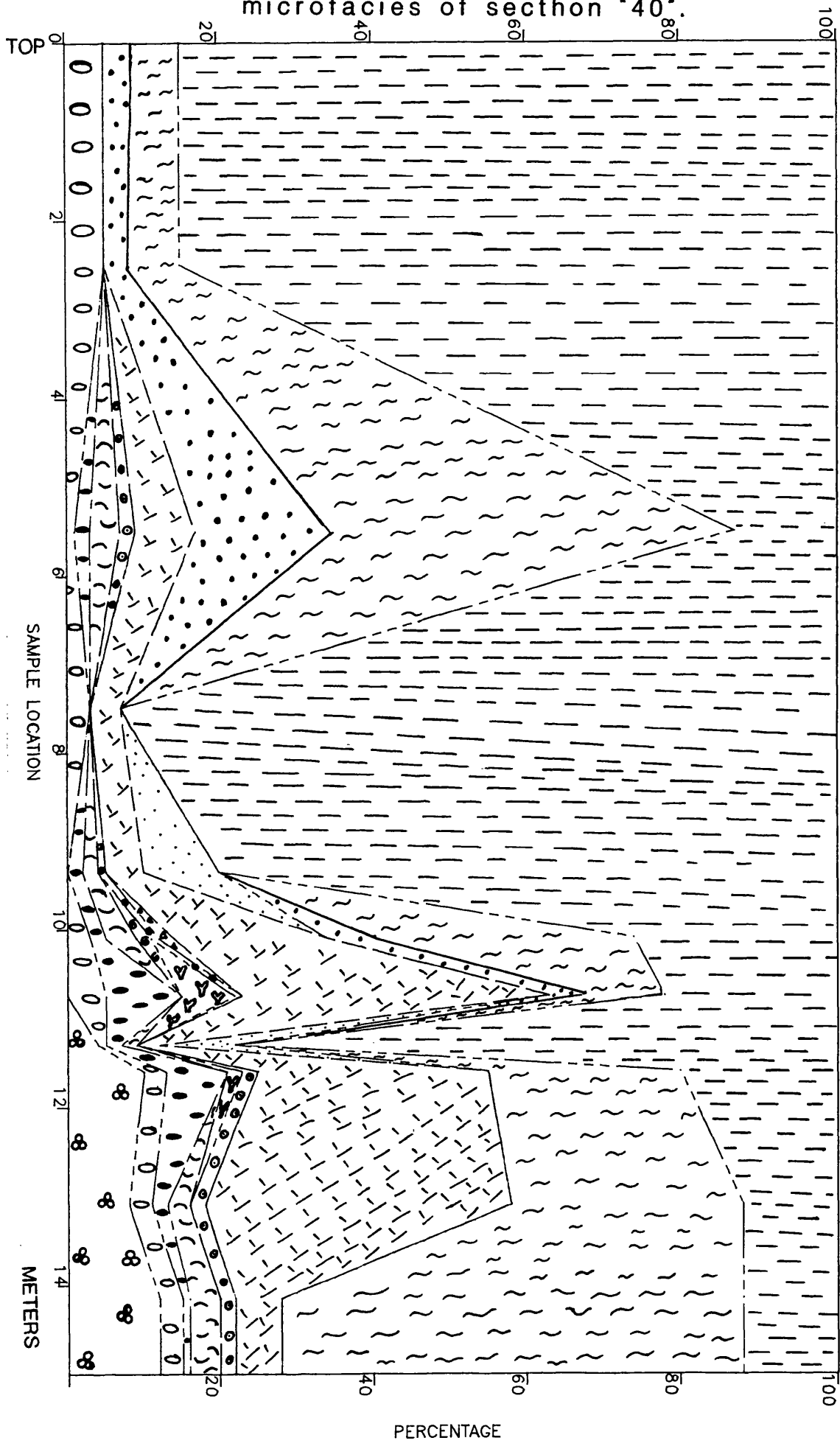
PROGRAM FATHY24
DIMENSION X(50),Y1(50),Y2(50),Y3(50),Y4(50)
*,Y5(50),Y6(50),Y7(50),Y8(50),Y9(50),Y10(50)
*,Y11(50),Y12(50),Y13(50),Y14(50),Y15(50),Y16(50)
*,Y17(50),Y18(50),Y19(50),Y20(50),Y21(50),Y22(50)
*,Y23(50),Y24(50),Y25(50),Y26(50),Y27(50)
CALL PAGE(50,0,29,0)
CALL PICSIZ(35,6,14,0)
CALL CVTYPE(3)
CALL SCALES(0,0,107,0,1,0,0,100,0,1)
CALL AXES('SAMPLE LOCATION',15,'PERCENTAGE',10)
CALL YAXIS(0,0,100,0,107,0,'PERCENTAGE',10)
READ(5,*)N
READ(5,*)(X(I),Y1(I),Y2(I),Y3(I),
*,Y4(I),Y6(I),Y7(I),
*,Y8(I),Y9(I),
*,Y17(I),Y18(I),Y20(I),Y21(I),
*,Y22(I),Y26(I),
*I=1,N)
CALL BRKN CV(X,Y1,N,6)
CALL BRKN CV(X,Y2,N,2)
CALL BRKN CV(X,Y3,N,1)
CALL BRKN CV(X,Y4,N,5)
CALL BRKN CV(X,Y6,N,-1)
CALL BRKN CV(X,Y7,N,3)
CALL BRKN CV(X,Y8,N,6)
CALL BRKN CV(X,Y9,N,5)
CALL BRKN CV(X,Y17,N,-1)
CALL BRKN CV(X,Y18,N,-2)
CALL BRKN CV(X,Y20,N,-6)
CALL BRKN CV(X,Y21,N,-3)
CALL BRKN CV(X,Y22,N,2)
CALL DRAW CV(X,Y26,N,0)
CALL SET KY('L','W',14,3)
CALL LINE KY(6,'Y1',3)
CALL LINE KY(2,'Y2',3)
CALL LINE KY(1,'Y3',3)
CALL LINE KY(5,'Y4',3)
CALL LINE KY(-1,'Y6',3)
CALL LINE KY(3,'Y7',3)
CALL LINE KY(6,'Y8',3)
CALL LINE KY(5,'Y9',3)
CALL LINE KY(-1,'Y17',3)
CALL LINE KY(-2,'Y18',3)
CALL LINE KY(-6,'Y20',3)
CALL LINE KY(-3,'Y21',3)
CALL LINE KY(2,'Y22',3)
CALL LINE KY(0,'Y26',3)
CALL TITLE('B','C',
          FIG.( ) VERTICAL VARIATION OF CARBONA
*,TE MICROFACIES OF SECTION "79",76)
CALL ENDPLT
STOP
END

```

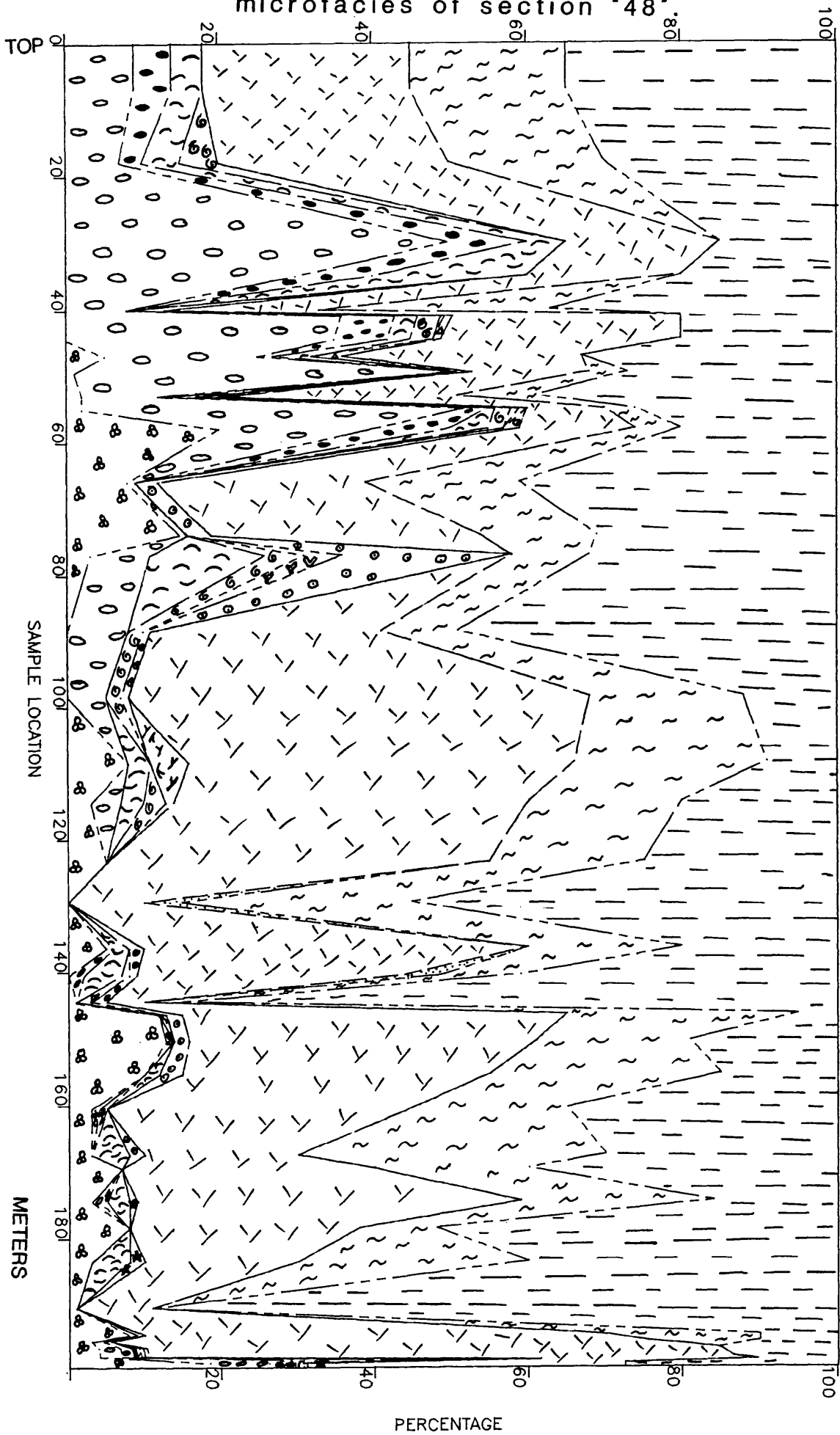
Y1		MICRO-FORAMS.
Y2		MILLIOLIDES
Y3		NUMMULITES
Y4		OPERCULINA
Y5		L.BENTHONIC FORAMS.
Y6		BIVALVES
Y7		GASTROPODES
Y8		BRYOZOA
Y9		ECHINODERMS
Y10		CORALS
Y11		OSTRACODS
Y12		SPONGE SPICULES
Y13		CORALLINE ALGAE
Y14		GREEN ALGAE
Y15		ALGAL COATED GRAINS
Y16		SERPIOLID WORMS
Y17		PELLETS
Y18		BIOCLASTIS
Y19		MICRITE ENVELOPES
Y20		INTRACLAST
Y21		QUARTZ DETRITALS
Y22		MARLEY/SILTY MATRIX
Y23		SPARITE
Y24		MICROSPARITE
Y25		DOLOMITE
Y26		MICRITE
Y27		VERTEBRATE REMAINS

Appendix (E.1): Key used in the previous point counted data , computer programs and the following vertical variation diagrams of the differnt carbonate components (Appendixes C ,D &E).

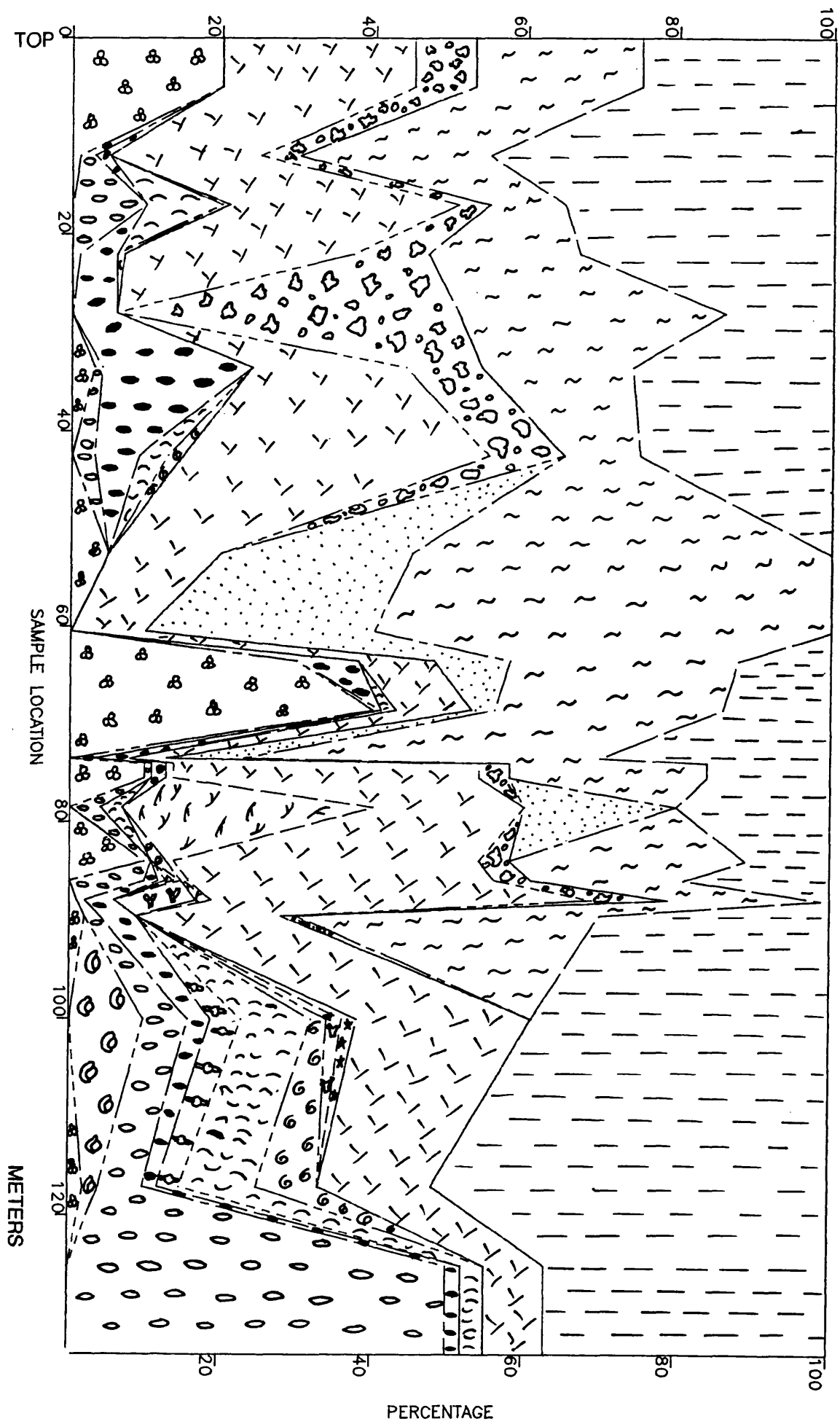
Appendix (E2): Vertical variation of the carbonate microfacies of section '40'. 411



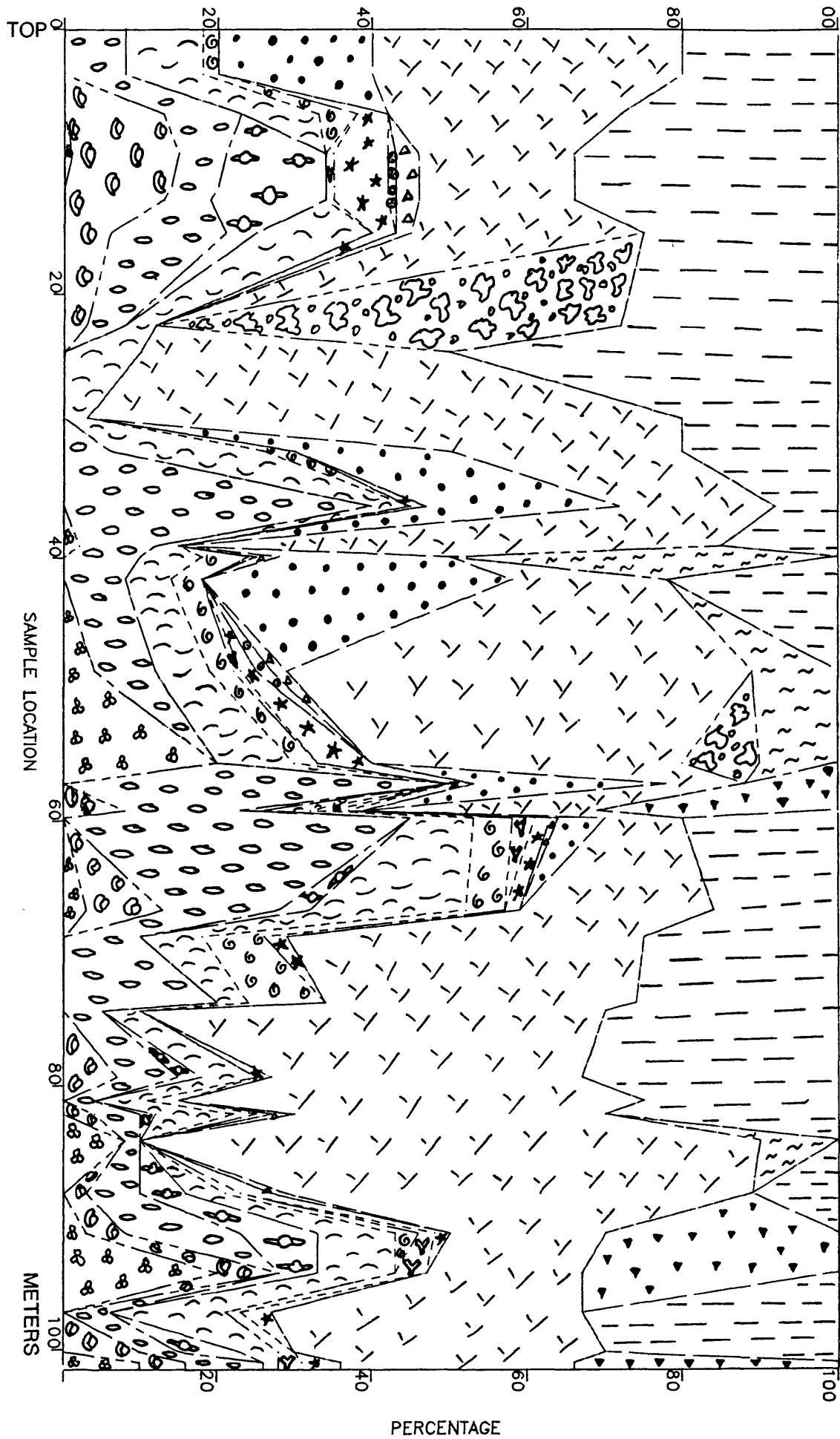
Appendix (E3): vertical variation of the carbonate microfacies of section '48'



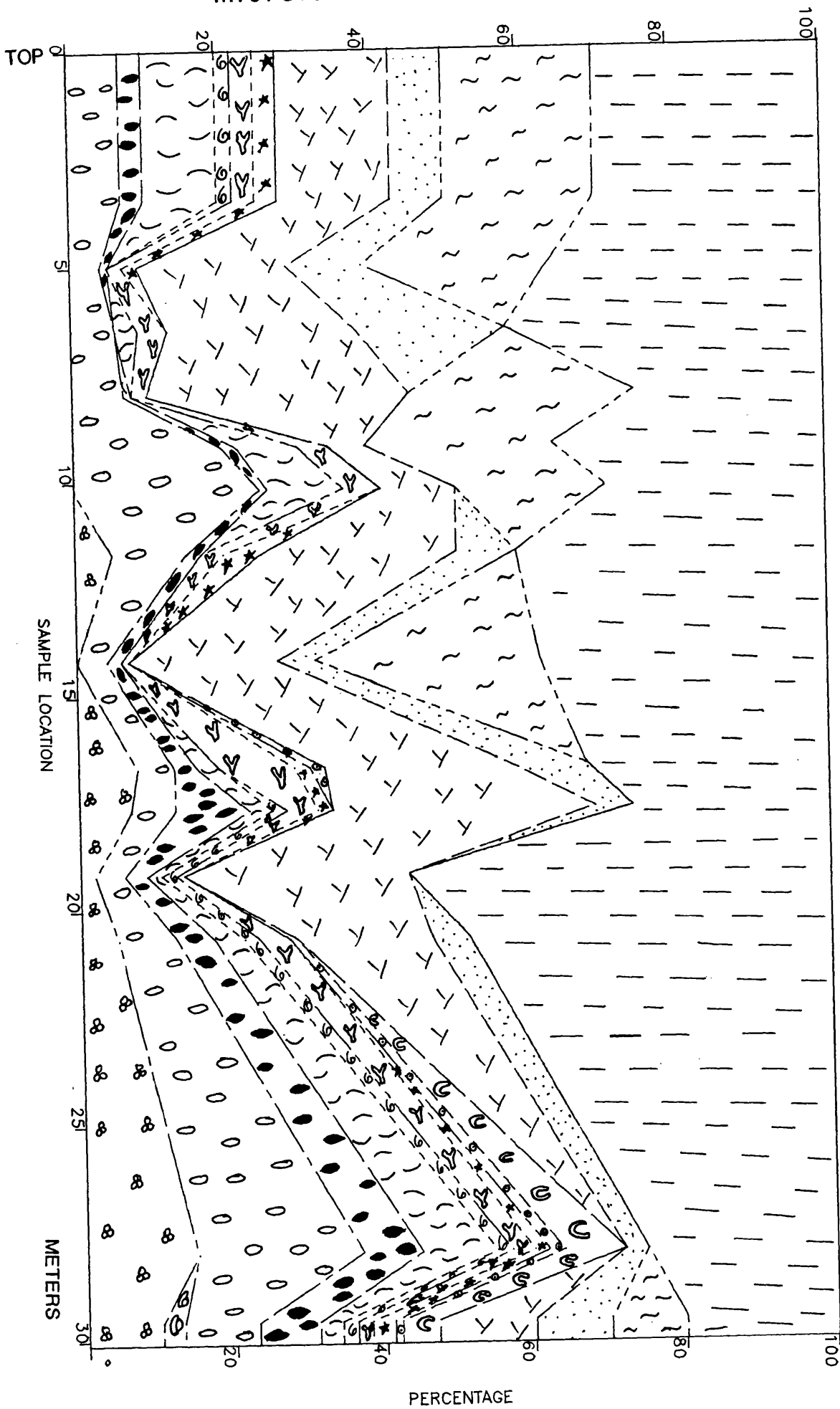
Appendix (E.4): Vertical variation of the carbonate microfacies of section '49'.



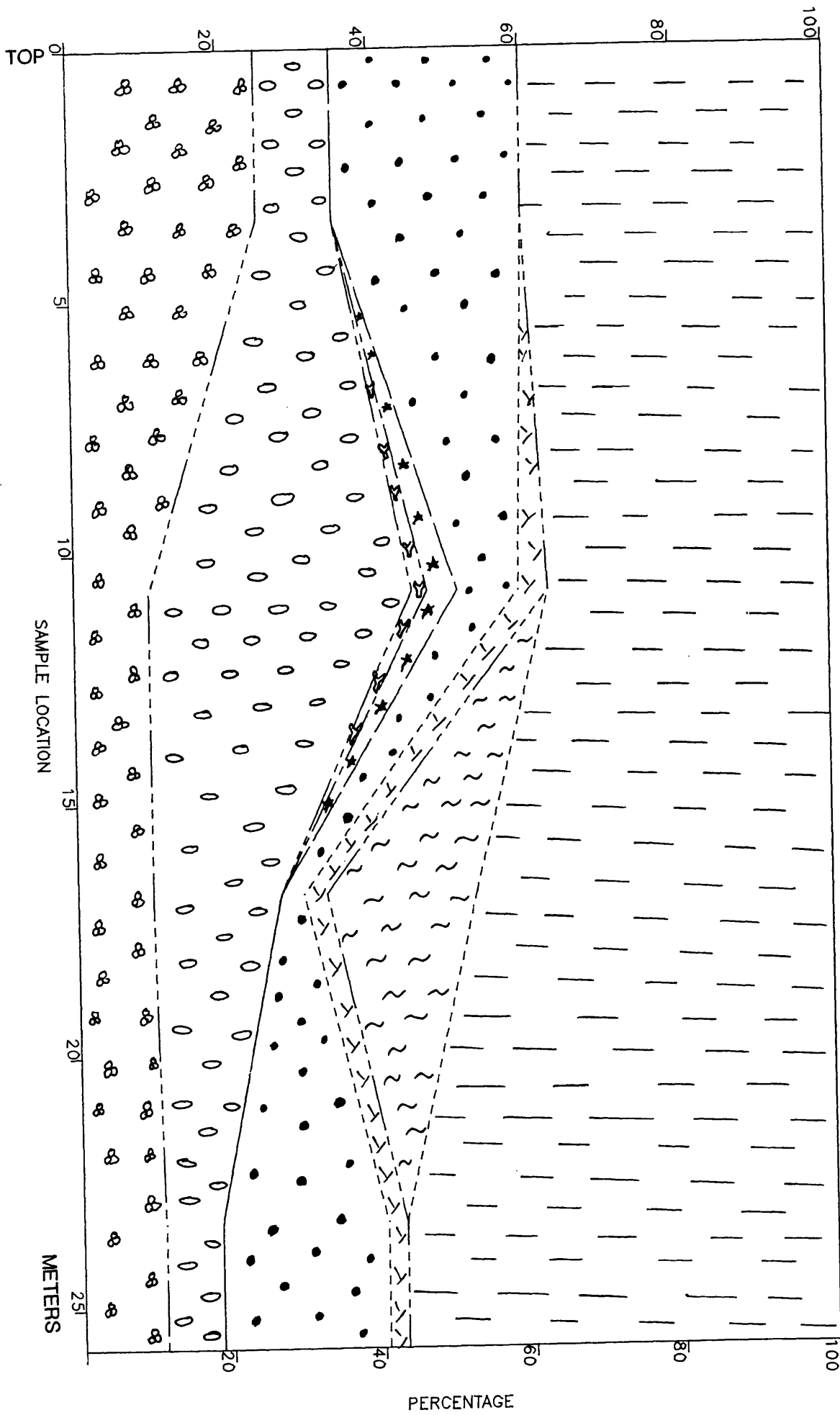
Appendix (E.5): Vertical variation of the carbonte microfacies of section '50'.



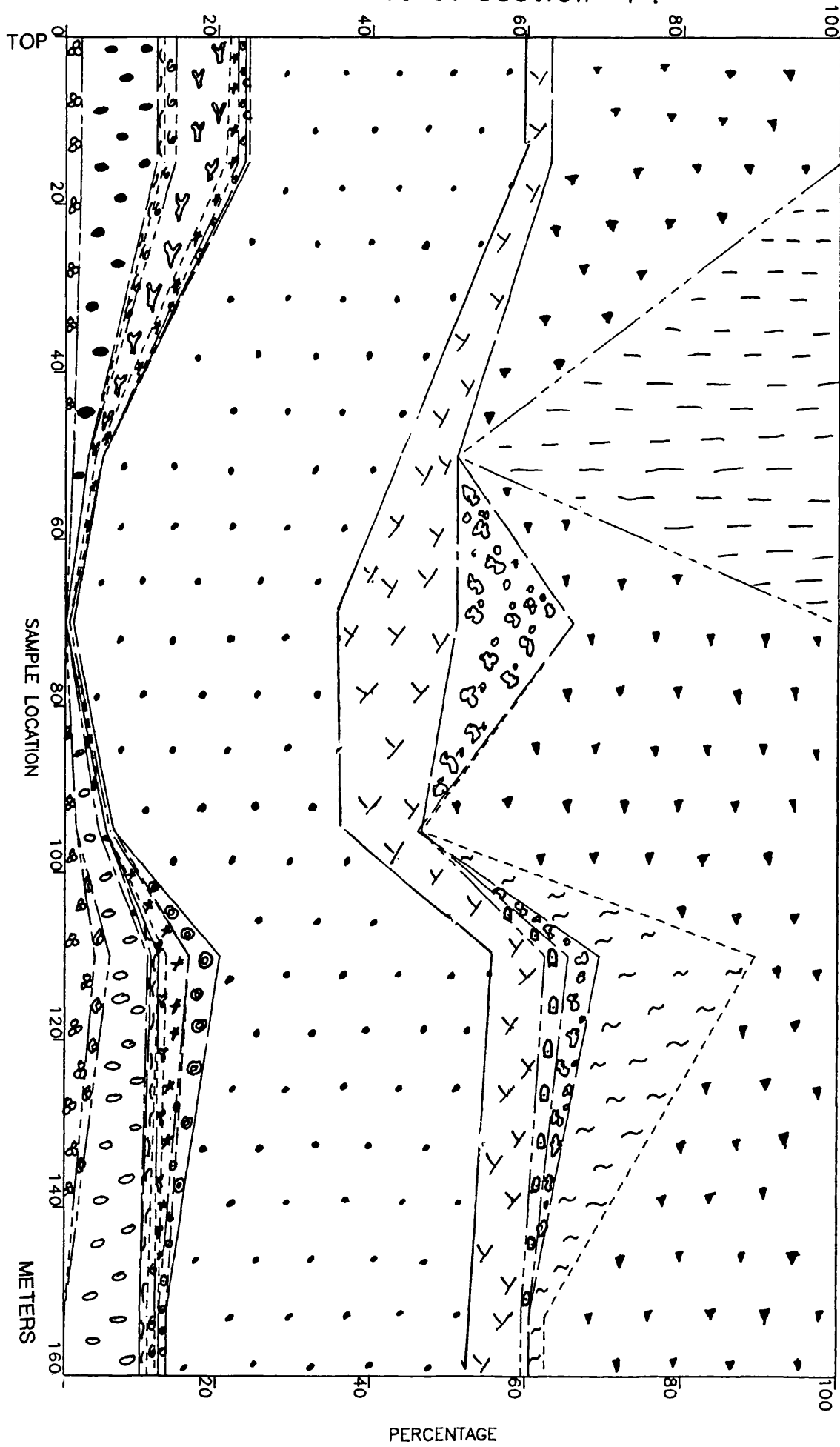
Appendix (E.6): Vertical variation of the carbonate microfacies of section '44'.



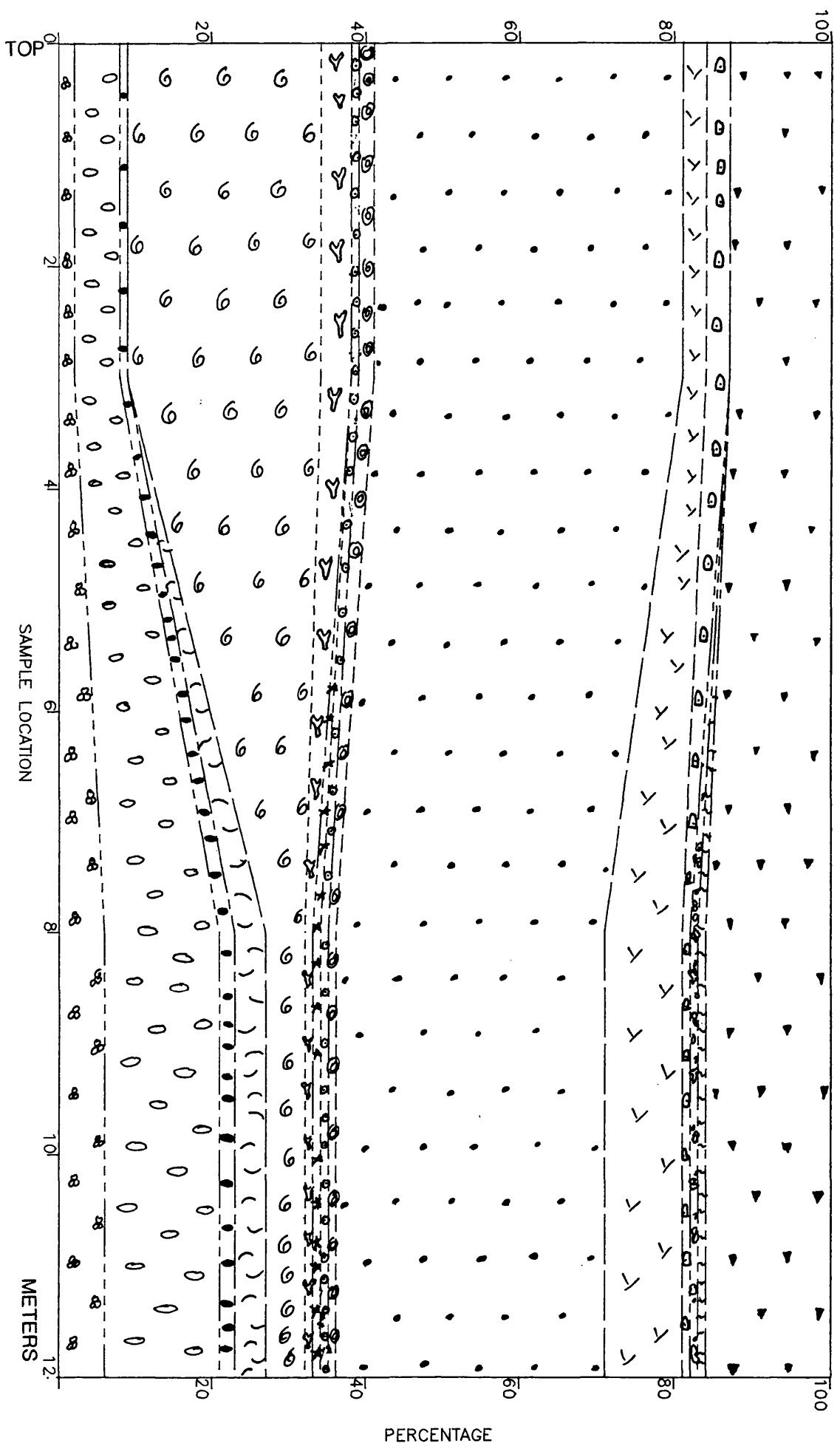
Appendix (E7): Vertical variation of the carbonate microfacies of section '2'.



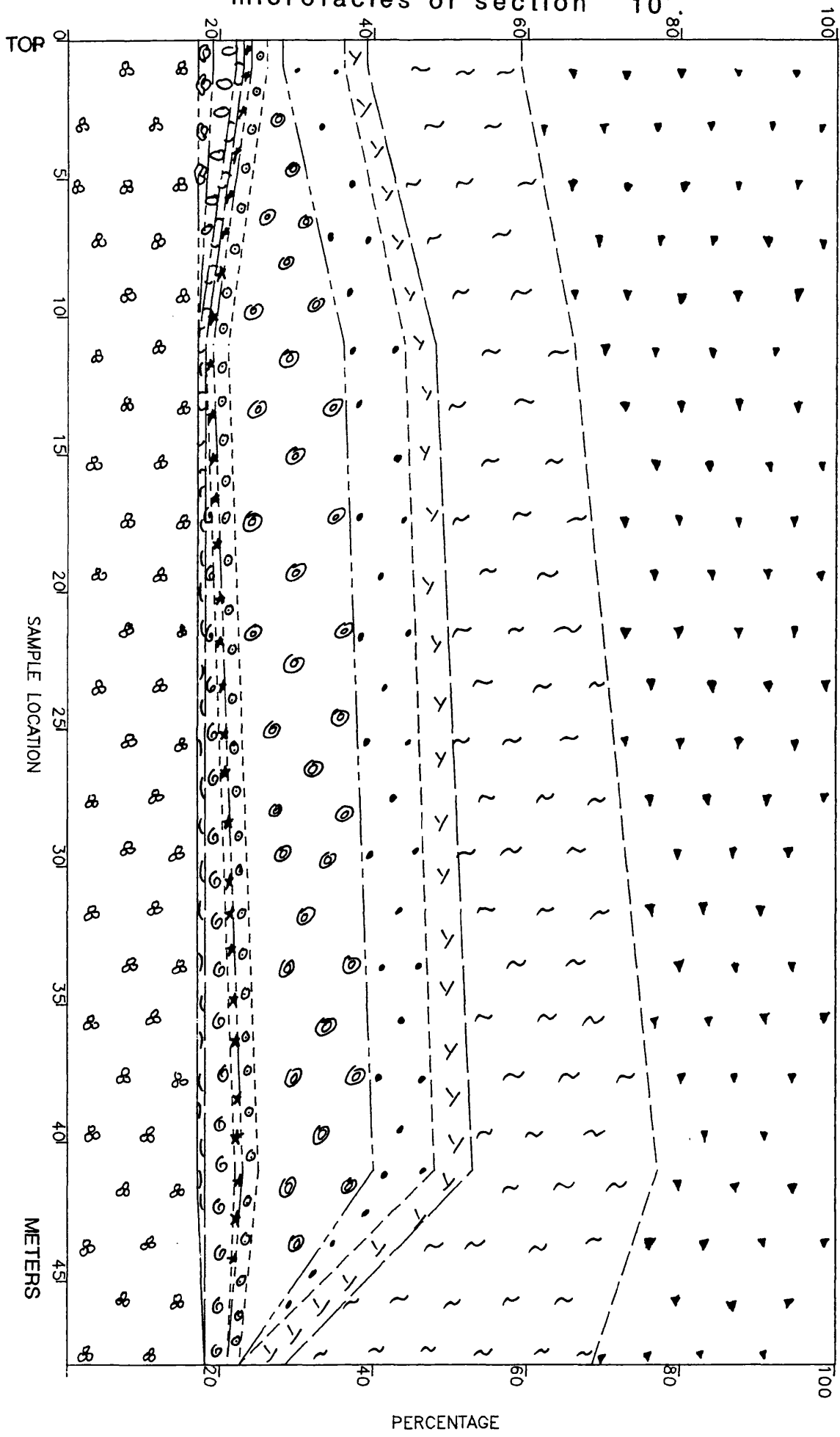
Appendix (E8): Vertical variation of the carbonate microfacies of section '4'.



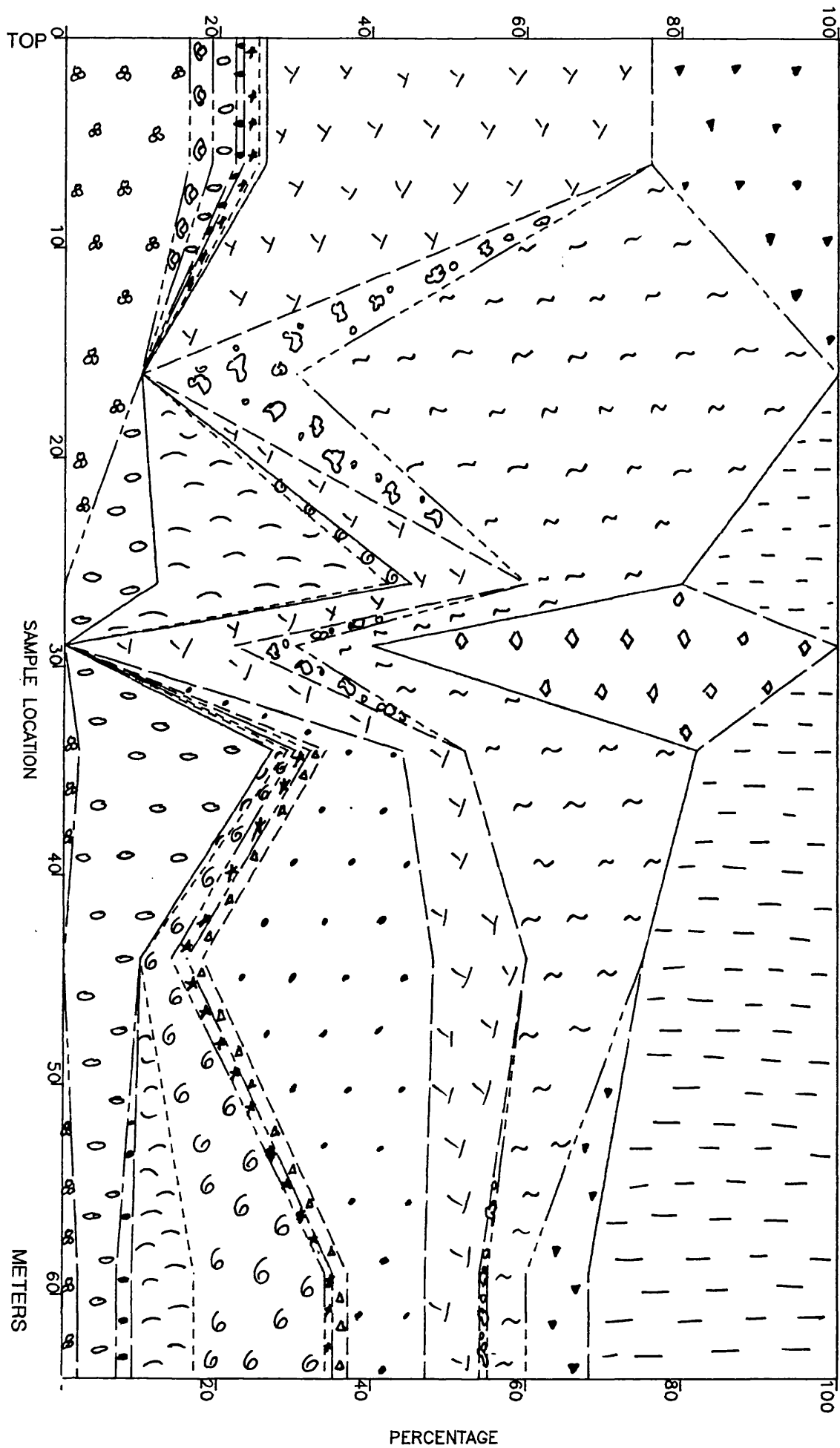
Appendix (E.9): Vertical variation of the carbonate microfacies of section '5'.



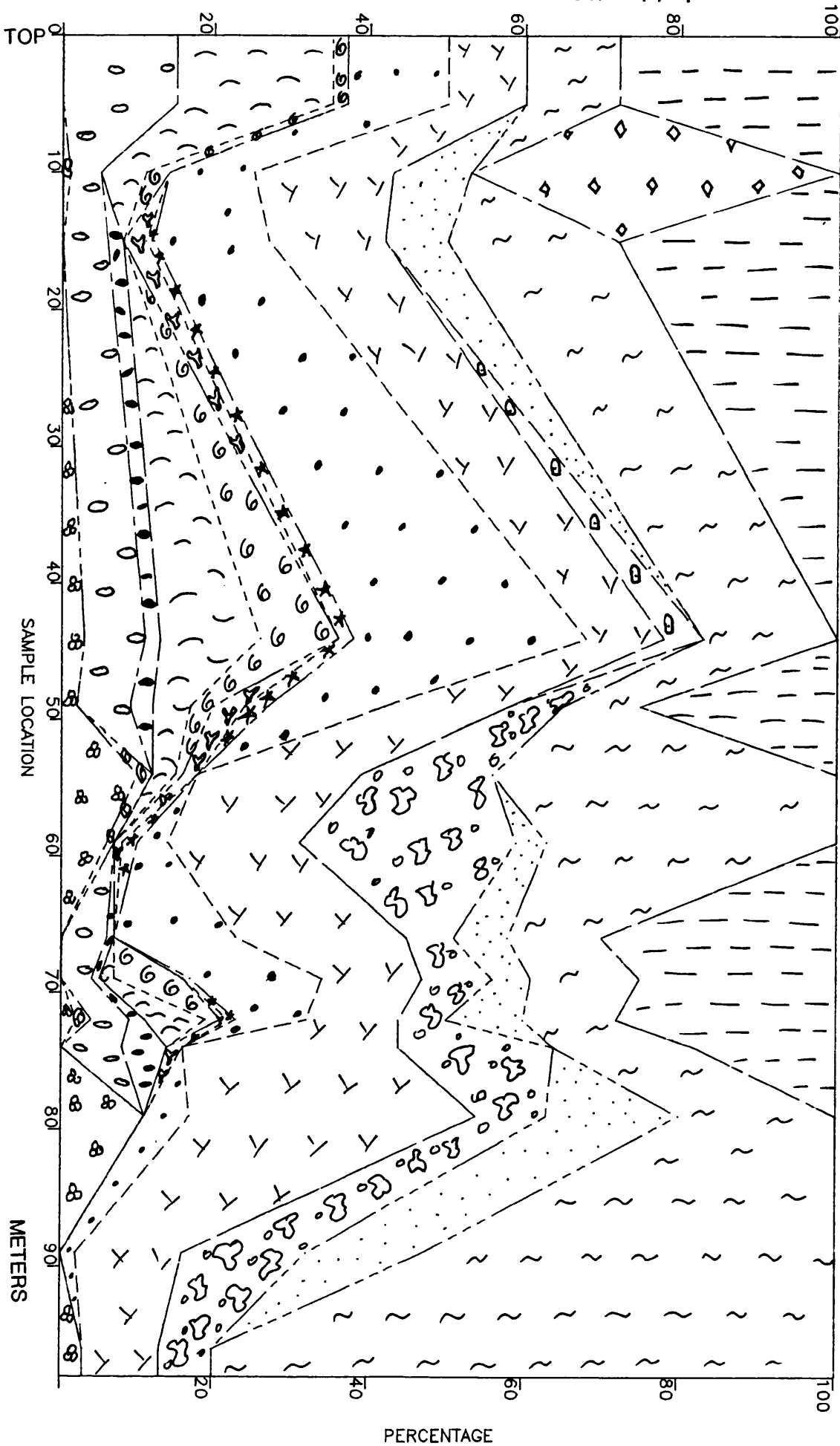
Appendix E.10: A vertical variation of the carbonate microfacies of section "10"



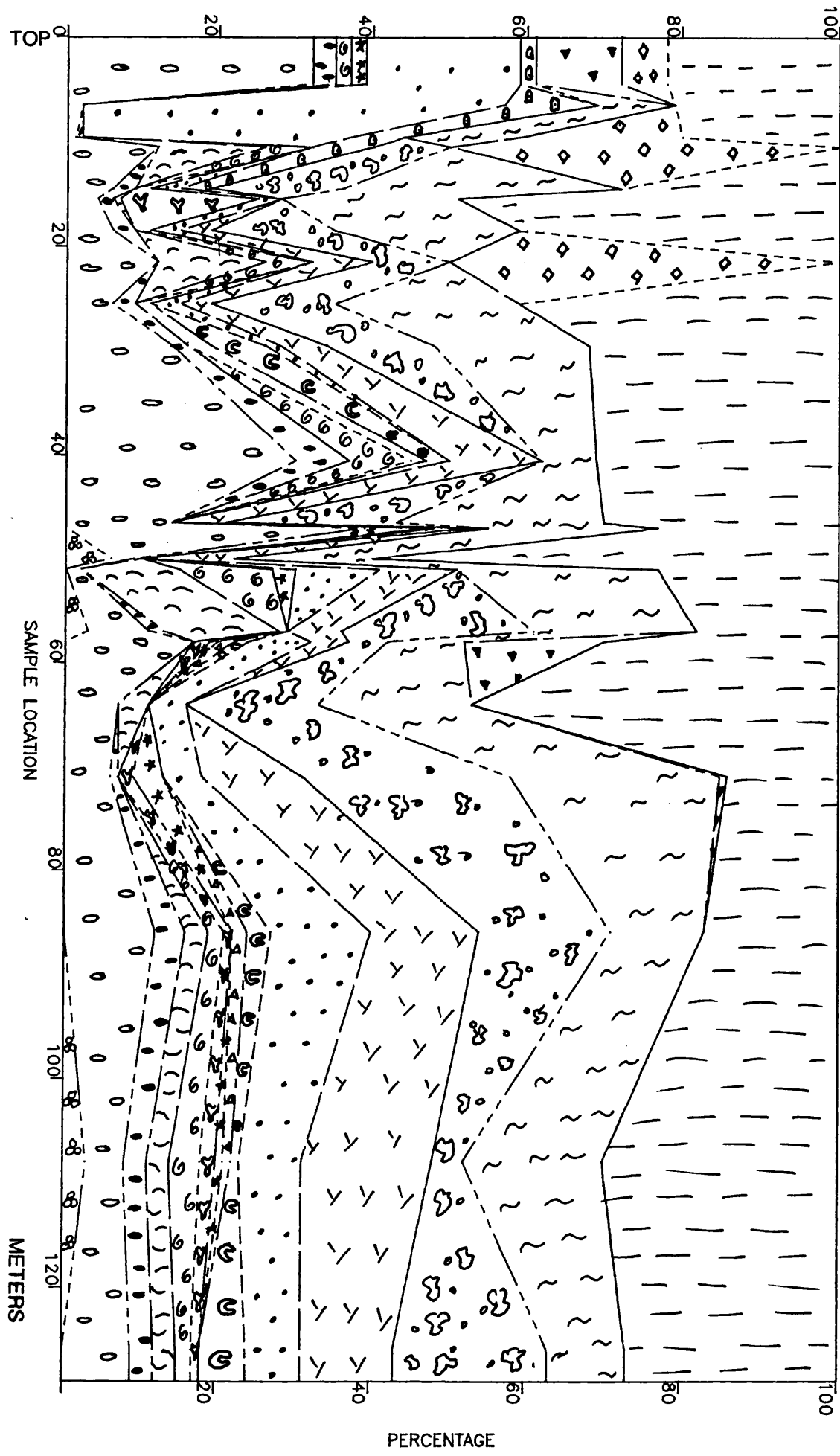
Appendix E.10: vertical variation of the carbonate microfacies of section '16'.



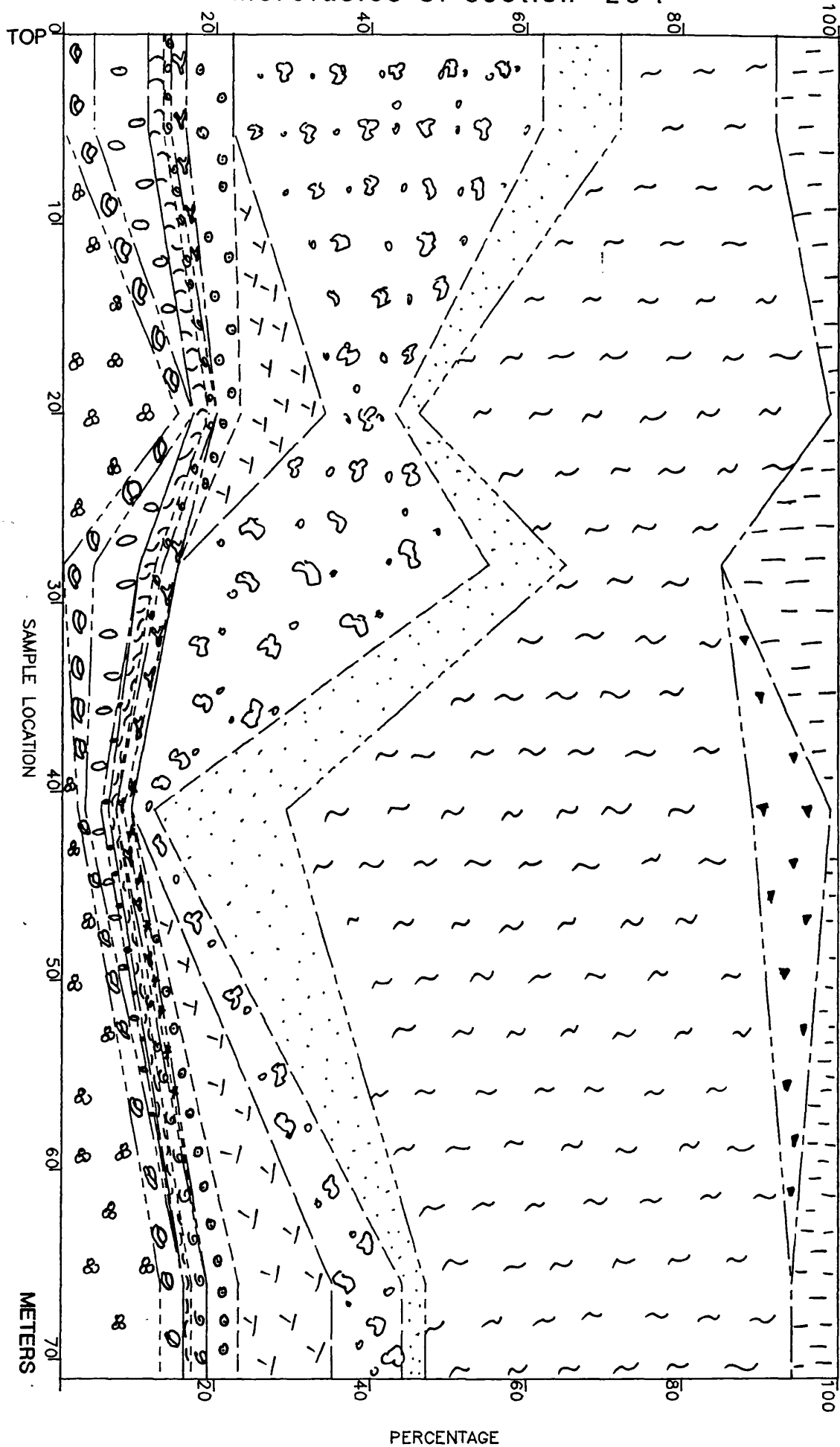
Appendix E12: Vertical variation of the carbonate microfacies of section '17'.



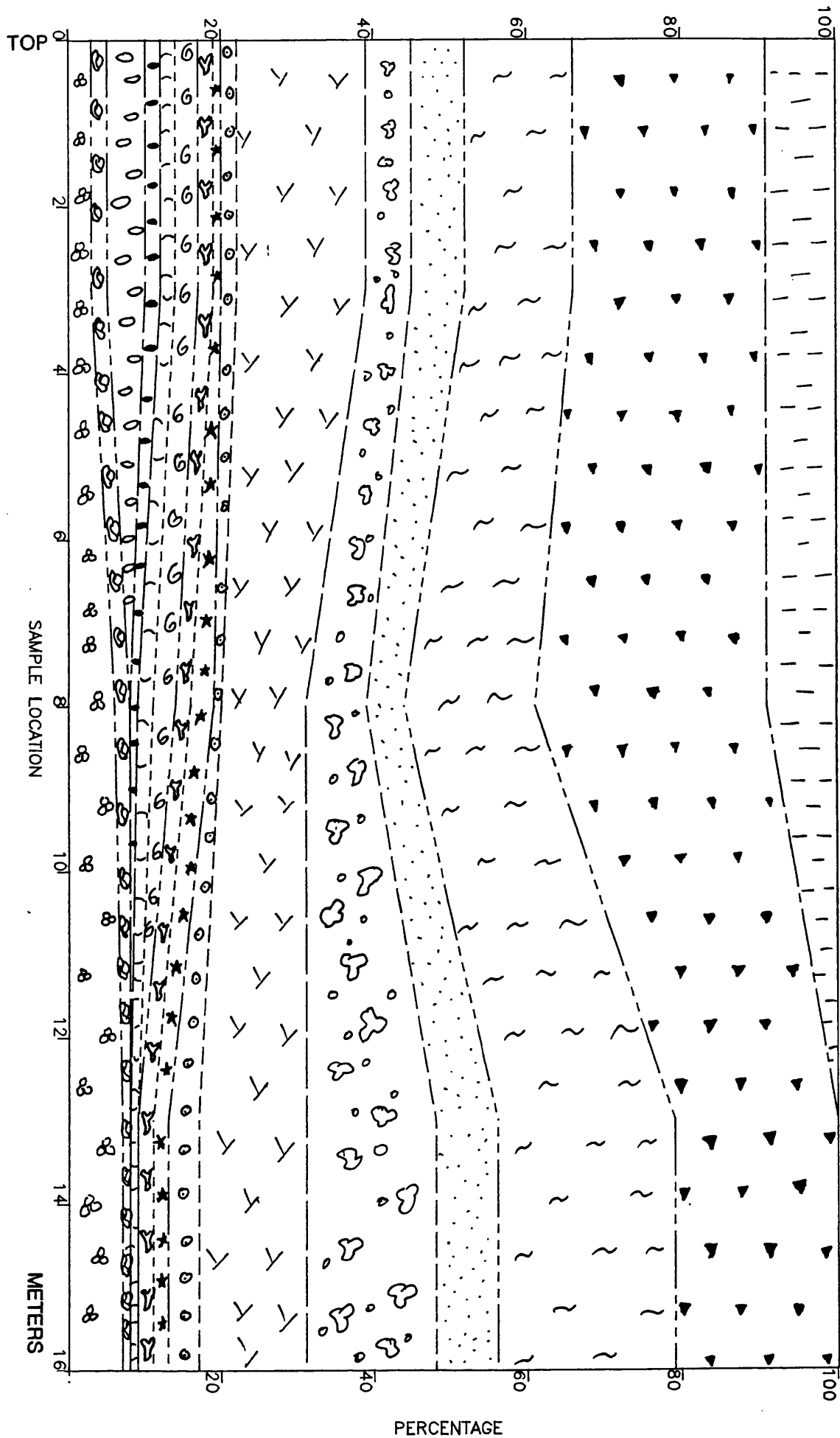
Appendix (E13): Vertical variation of the carbonate microfacies of section '18'. 422



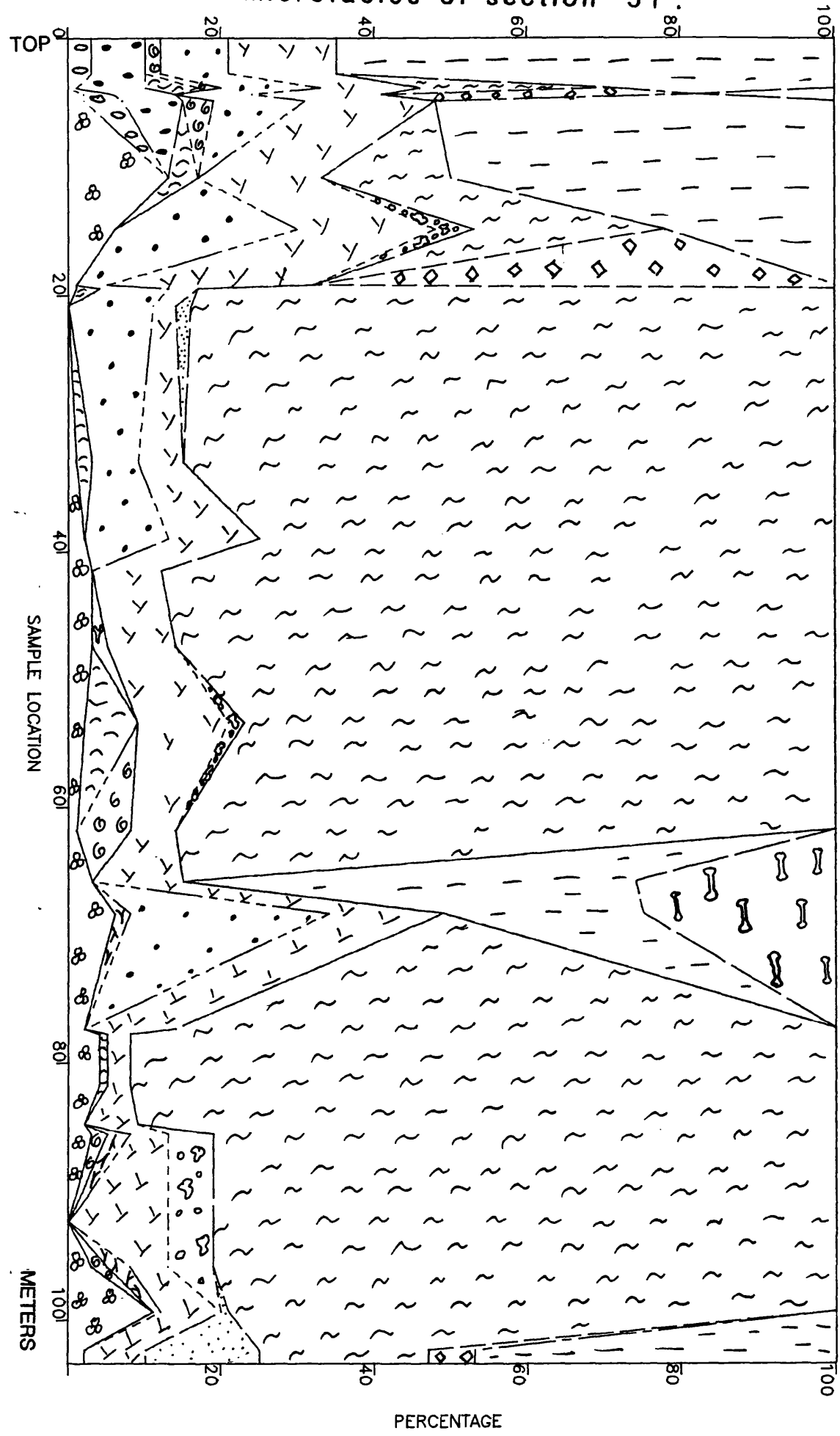
Appendix E14: Vertical variation of the carbonate microfacies of section '26'.



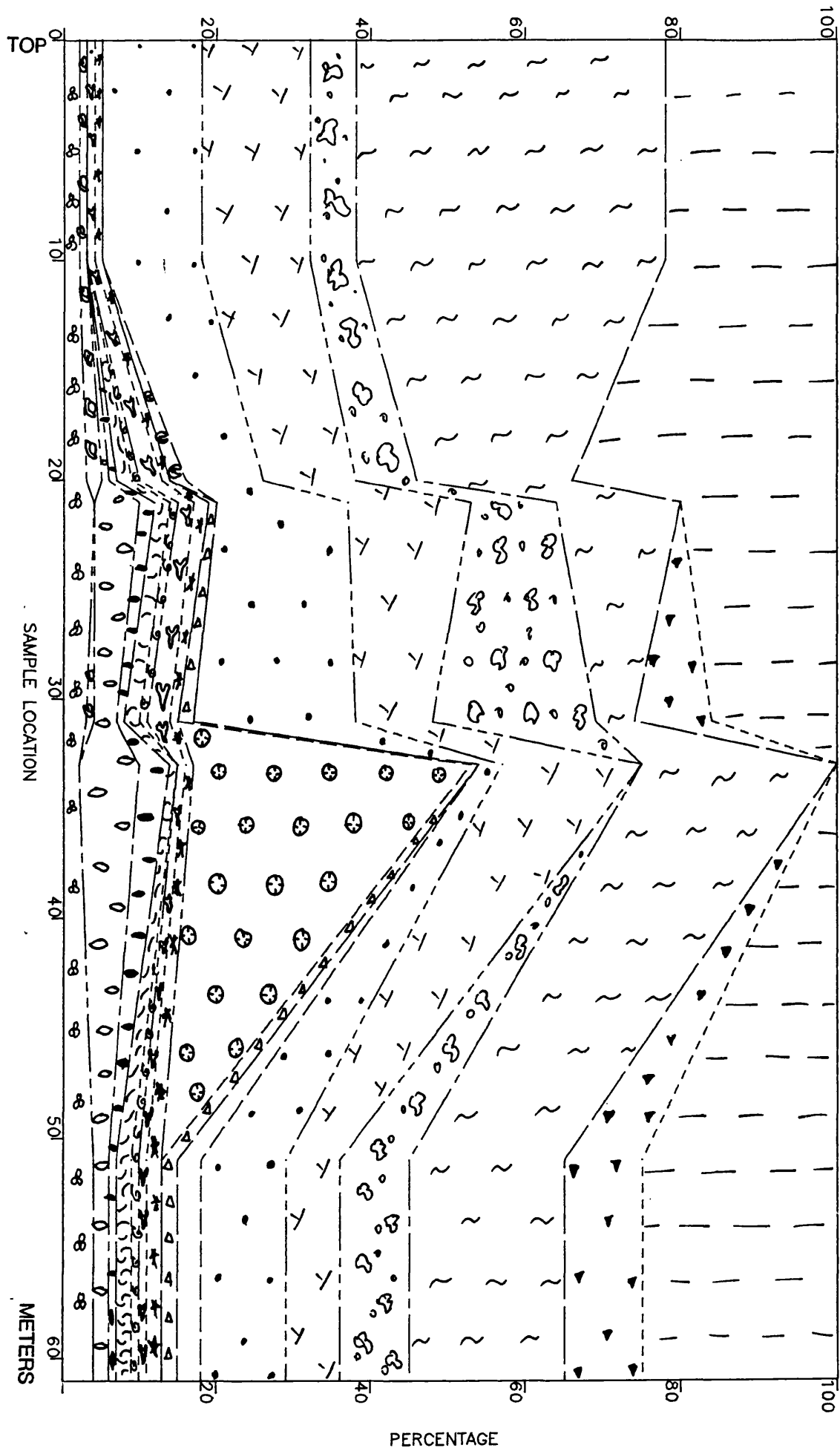
Appendix E15: Vertical variation of the carbonate microfacies of section '36'.



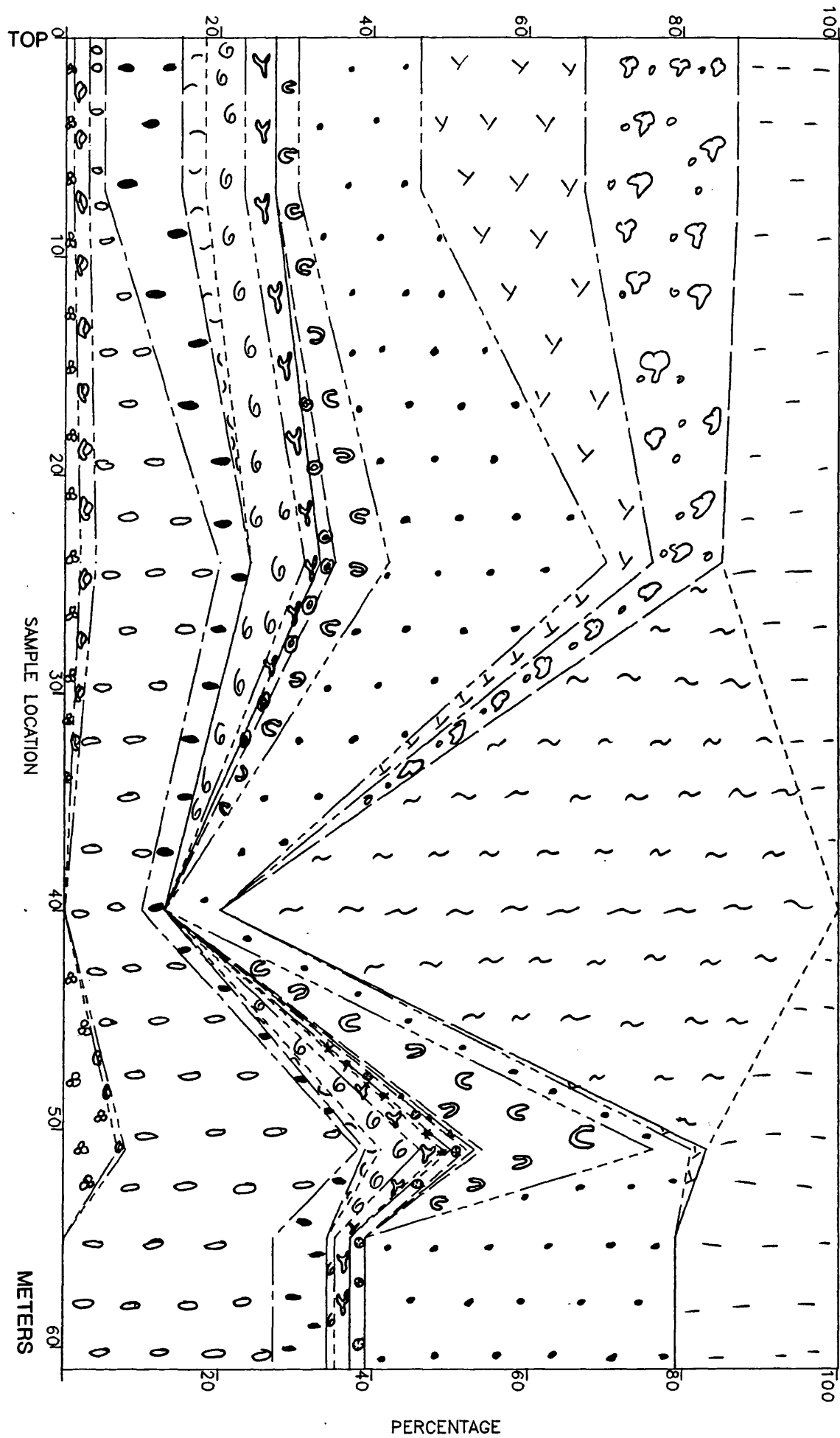
Appendix (E16): Vertical variation of the carbonate microfacies of section '51'.



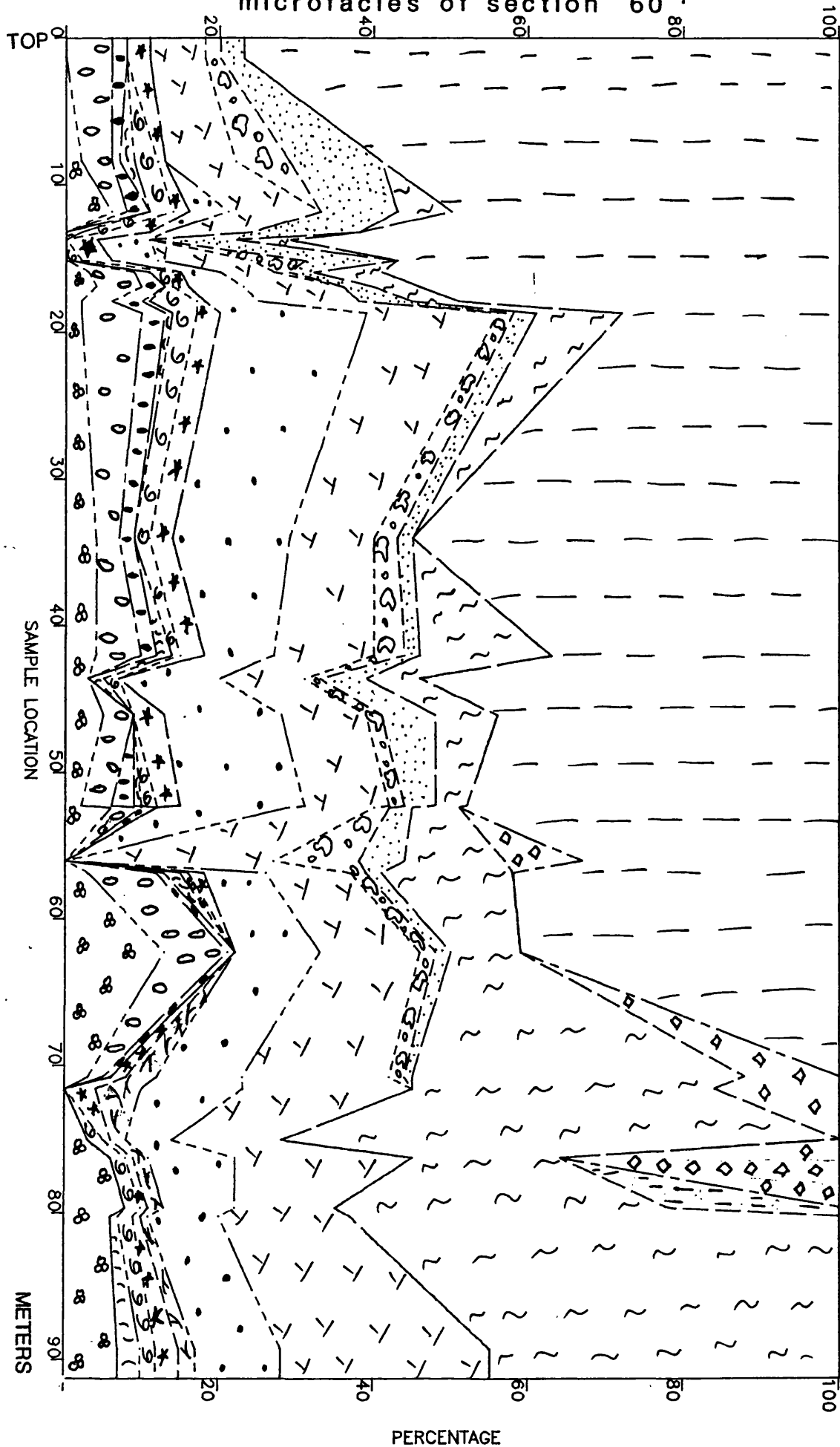
Appendix E10: Vertical variation of the carbonate microfacies of section '56'.



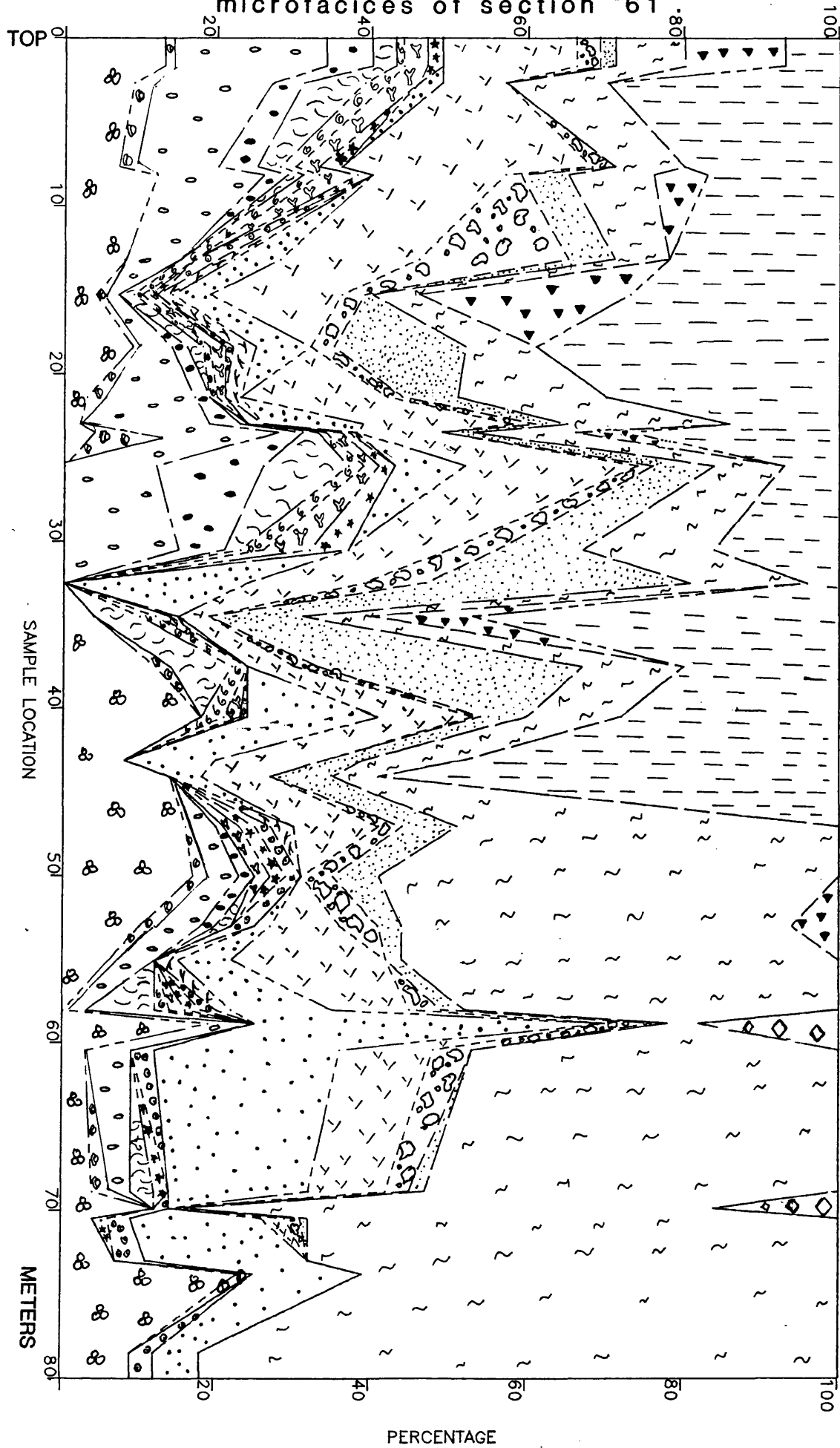
Appendix E18: Vertical variation of the carbonate microfacies of section '59'.



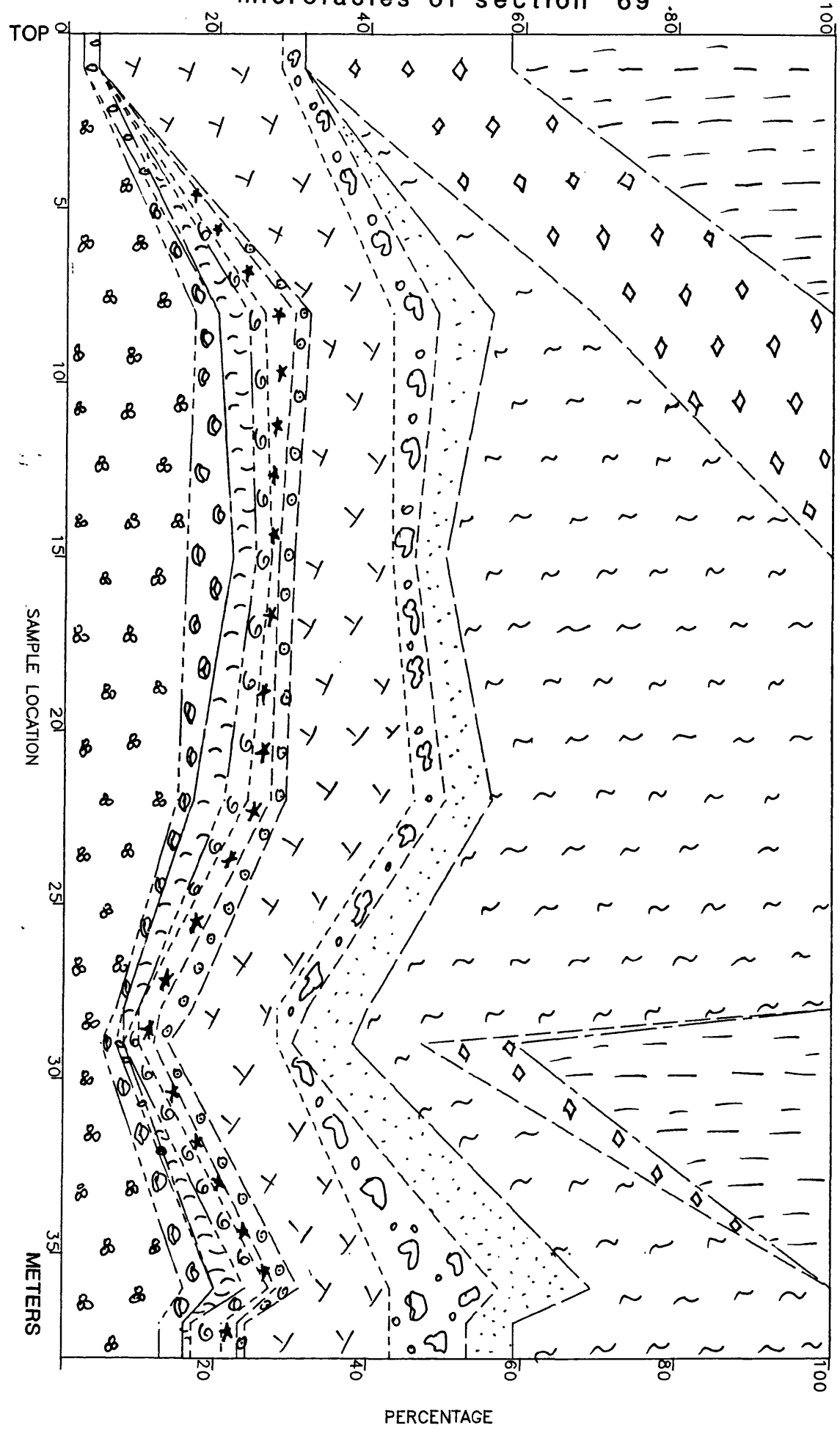
Appendix (519): vertical variation of the carbonate microfacies of section '60'.



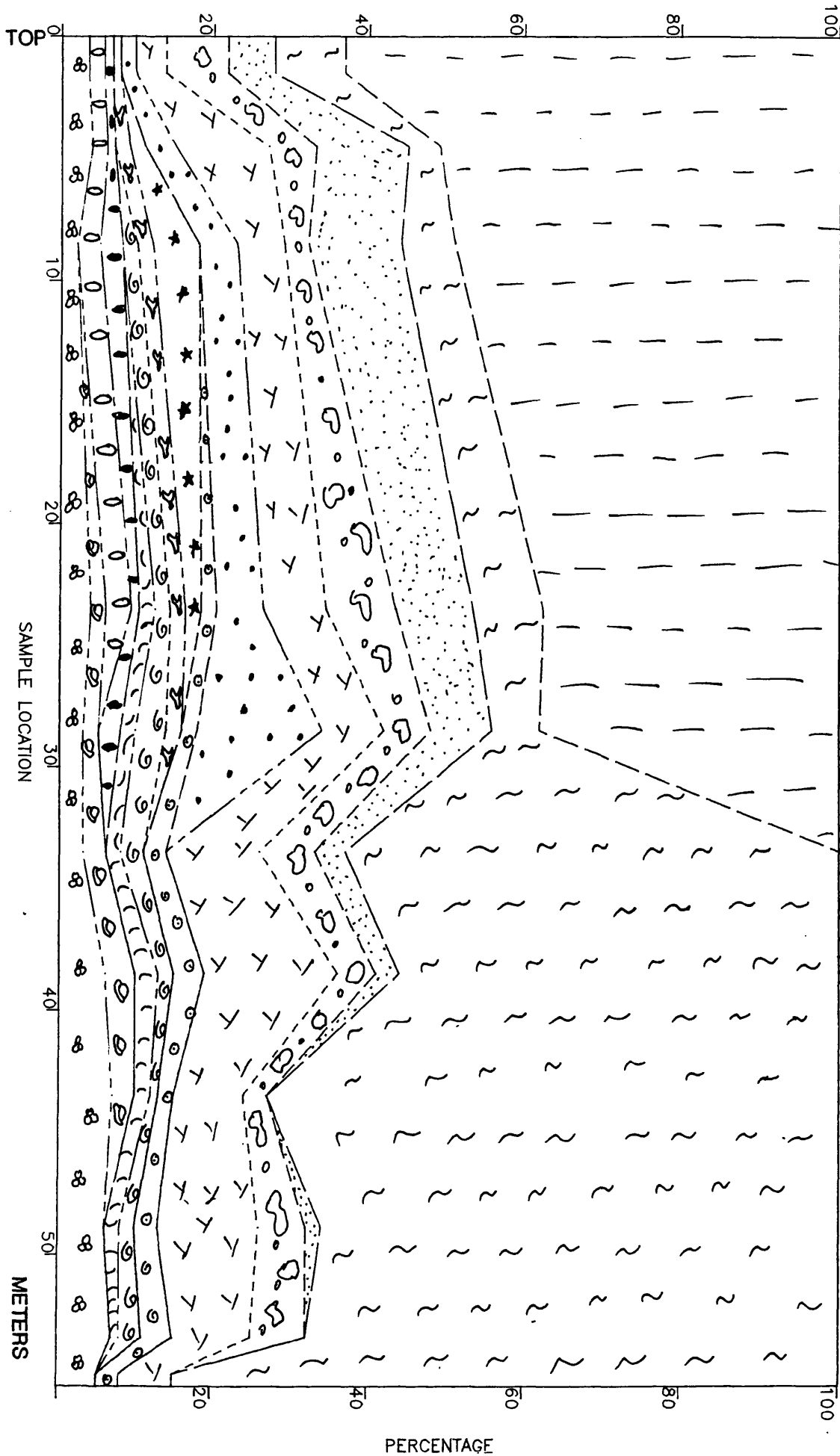
Appendix E20: Vertical variation of the carbonate microfacies of section '61'



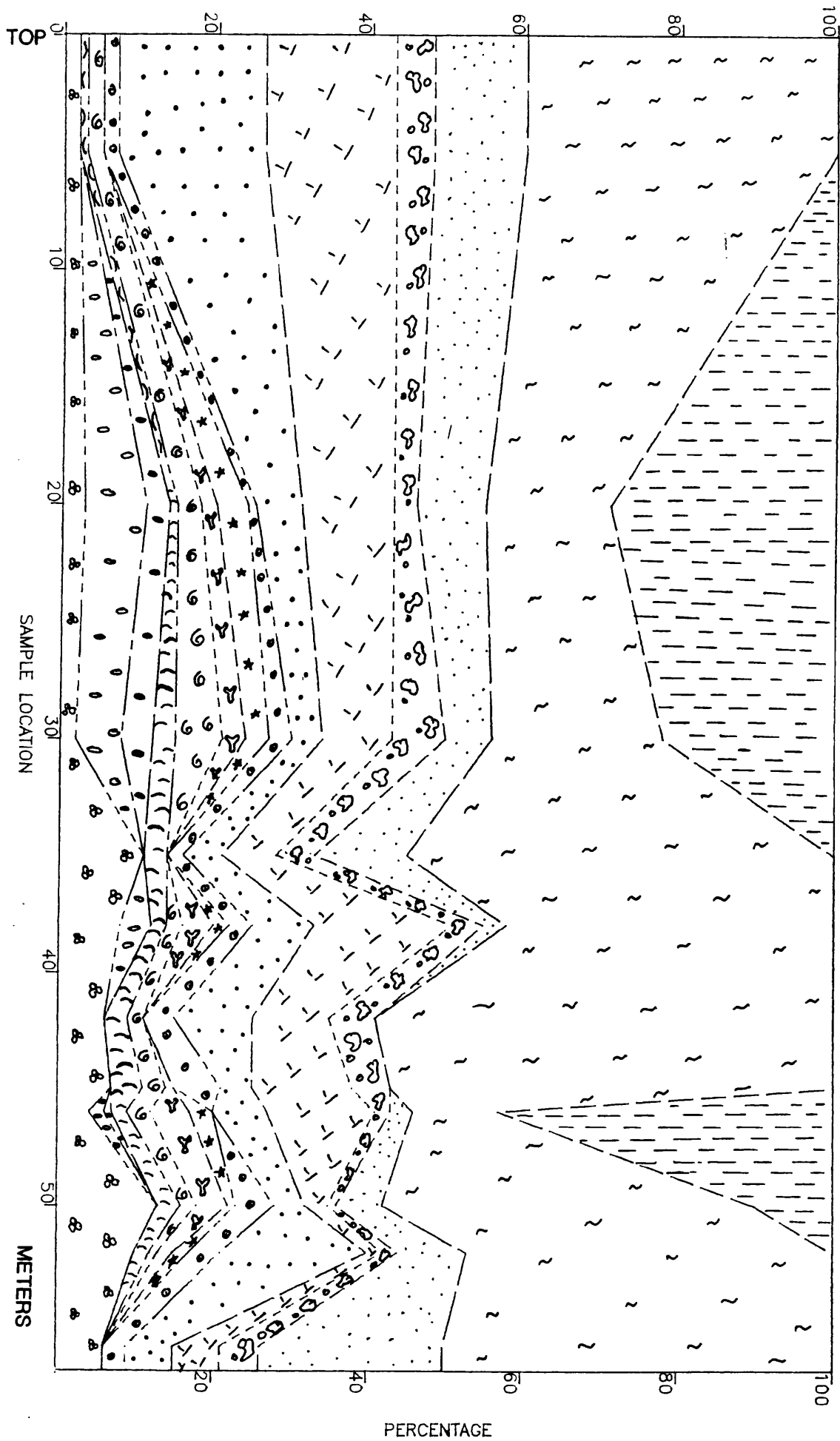
Appendix E.21: Vertical variation of the carbonate microfacies of section '69'



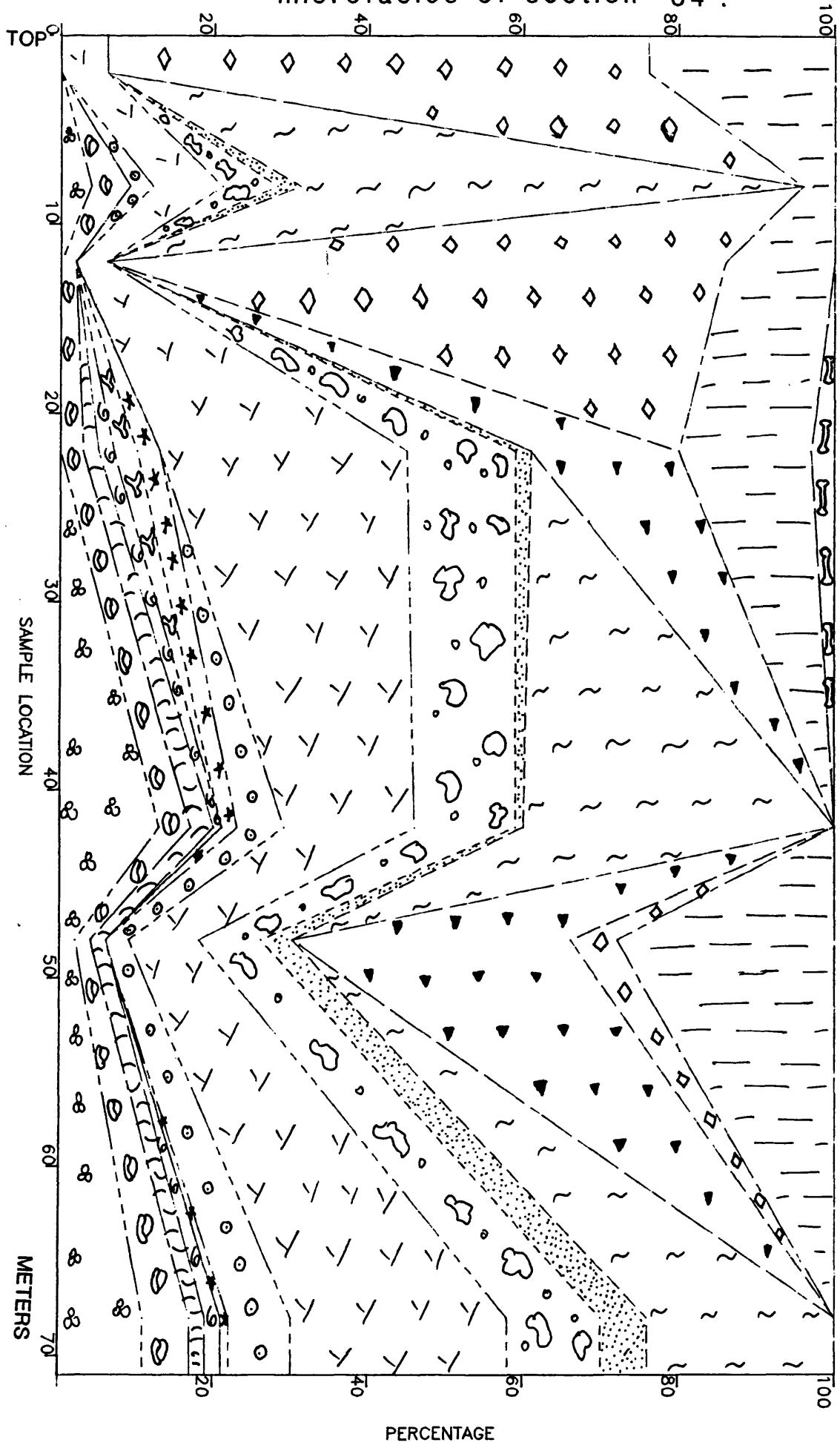
Appendix E.22: Vertical variation of the carbonate microfacies of section '81'.



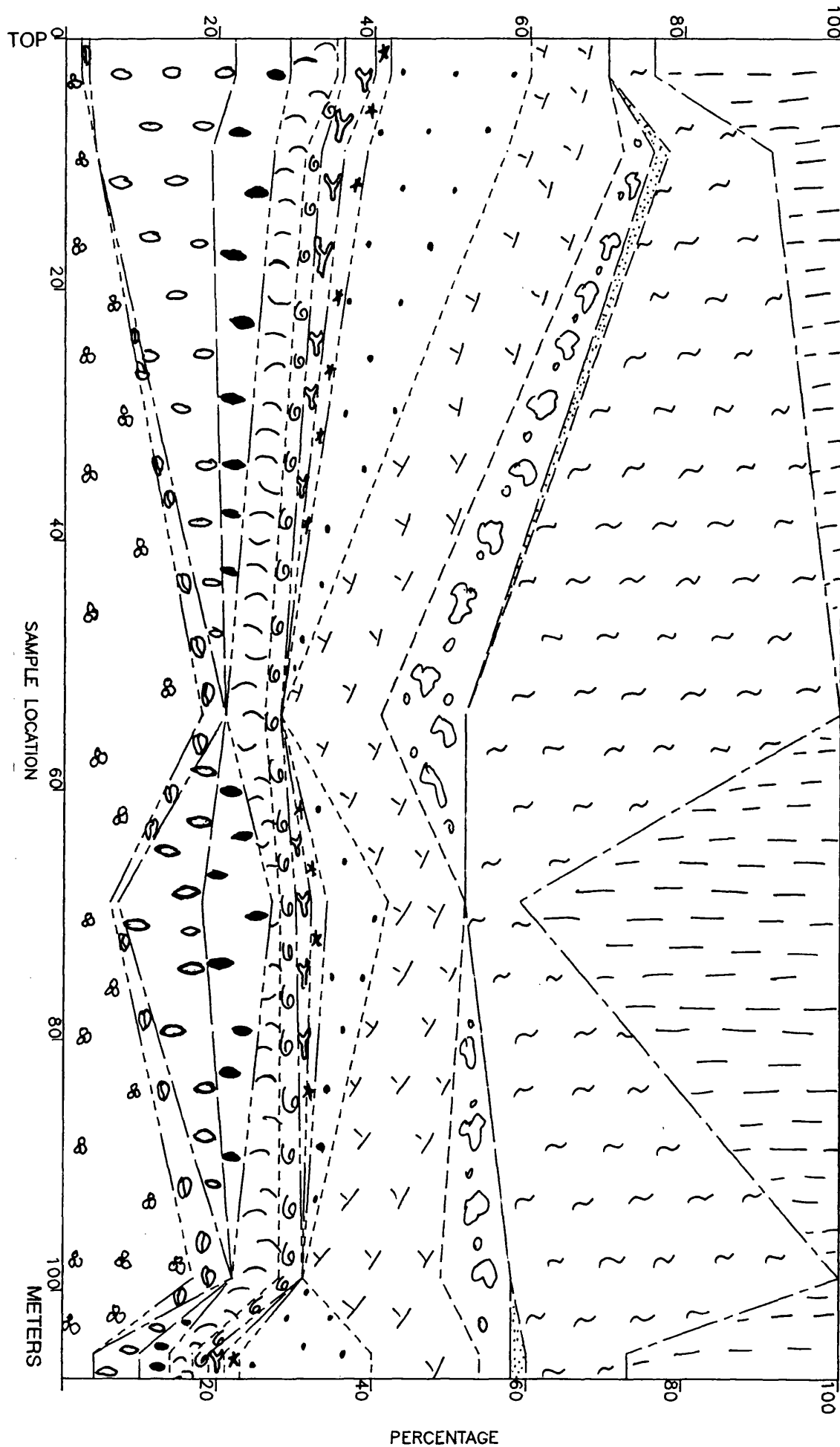
Appendix E23: Vertical variation of the carbonate microfacies of section '82'.



Appendix (E2): Vertical variation of the carbonate microfacies of section '64'.



Appendix E25: Vertical variation of the carbonate microfacies of section '79'.



REFERENCES

REFERENCES

- Abbate, E., Bortolotti, V. & Passerini, P. (1970):
Olistostromes and Olistoliths. *Sedim. Geol.*, 4,
P.521-557.
- Abdel-Kireem (1985):
Planktonic Foraminifera of Mokattam Formation (Eocene) of
Gabal Mokattam, Cairo, Egypt.
Rev. Micropaléont., Vol. 28, No 2, P77-96
- Abdou, H.F. and Abdel-Kireem, M.R. (1972):
Planktonic foraminiferal zonation of the Middle and Upper
Eocene rocks of Fayum Province, Egypt. *Proc. Vth African
Micropal. Coll. Addis Ababa*, P.15-46.
- Abdou-Soliman, F.H. (1980):
Geological studies on the area Northeast of Beni Suef,
M.Sc. Geol. Dept., Assiut Univ., Egypt.
- Aigner, T. (1982):
Event-stratification in Nummulite accumulations and in
shell beds from the Eocene of Egypt. In G. Einsele and
A. Seilacher (Eds.). *Cyclic and Event stratification*,
248-262. Springer-Verlag.
- Aigner, T.A. (1983):
Facies and origin of nummulitic buildups: an example from
the Giza Pyramids Plateau (Middle Eocene, Egypt).
N.Jb.Geol. Paläont. Abh., 166,3, P.347-368.
- Aigner, T.A. (1984):
Biofabrics as dynamic indicators in Nummulite accumulations
J. Sed. Pet., V.55, No.1, P.131-134.
- Allen, J.R.L. (1982):
Sedimentary structures. their character and physical basis.
Vol.2. Elsevier, Amsterdam.
- Anadon, P.; Cabrera, L.; Guimera, J., and Santanach, P. (1985):
Paleogene strike-slip deformation and sedimentation along
the southeastern margin of the EBRO Basin. In: Biddle,
K.T. & Christie-Blick, N. (eds): *Strike-Slip deformation,
Basin formation and sedimentation. S.E.P.M. special publ.*
No. 37, P.303-318.
- Anderson, E.J. (1973):
Community Patterns. In A.M. Ziegler, et. al (Eds.), 1973:
*Principles of benthic community analysis. Univ. of Miami,
short course, lecture notes*, P.3.1-3.11.
- Anon.. (1981):
A list of Publications of the Geological Survey, Cairo,
Egypt. P.1-39.

- 430
- Ansary, S.E. (1955):
Report on the foraminiferal fauna from the Upper Eocene of
Egypt. Publ. Inst. Désert d' Egypte, Vol. 6, P.1-160.
- Ansary, S.E. and Ismail, M.M. (1956):
The determination of the Middle-Upper Eocene boundary in
the area east of Helwan as indicated by Foraminifera.
Bull. Inst. Desert Egypte, V.6.
- Archiac, A.D. and Haime, J. (1853):
Description des animaux fossiles du groupe nummulitique
de l'Inde. Précédé d'un résumé géologique et d'une
monographie des Nummuliten. Paris.
- Arni, P. (1965):
L'évolution des Nummulitinae en tant que facteur de
modification des dépôts Littoraux, France, Bur.Rech.
Géologie et Mineralogie Mem. Vol. 32, P.7-20.
- Aubry, M.P. (1983):
Biostratigraphie du Paléogène épicontinental de l'Europe
du Nord-Ouest. Etude fondée sur les nannofossiles
calcaires. Doc. Labor. Géologie Fac. Sciences Lyon,
89,320p.
- Awad, G.M. (1984):
Habitat of Oil in Abu Gharadig and Fayum Basins, Western
Desert, Egypt. AAPG Bulletin, V.68, No. 5, P.564-573.
- Ayan, T. (1965)
Chemical staining methods used in the identification of
carbonate minerals. Bull. Min. Res. Explor. Inst. Turkey
65, 133-147, Ankara.
- Ball, J. (1939):
Contribution to the geography of Egypt. Egypt Survey Dept.,
Cairo, 300p.
- Ball, M.M. (1967):
Carbonate sandbodies of Florida and the Bahamas. J. Sed.
Pet., 37, P.556-591.
- Ball, St. M. (1971):
The Westphalia limestone of the Northern Midcontinent: a
possible Ancient storm deposit. J. Sed. Petrol. V.41, 1,
P.217-232, Tulsa.
- Bandy, O.L. (1949):
Eocene and Oligocene foraminifera from Little Stave Creeke
County, Alabama. Bull. Am.Paleontol., 32, 1-211.
- Banerjee, A. (1959):
Petrography and facies of some Upper Visean (Mississippian)
limestones in North Wales. J. Sed. Pet., V.29, P.377-390.

- Barker, M.H.S. (1945):
The stratigraphy and structures of the Eastern Desert between latitudes of Wasta and Assiut. Unpublished A.E.O. Report.
- Barron, T. (1907):
The topography and geology of the district between Cairo and Suez. Egypt. Survey Dept., Cairo, 133pp.
- Barth, T., Correns, C.W., Eskola, P., (1939):
Die Entstehung der Gesteine: New York, Springer, 422pp.
- Bassiouni, M.A., Boukhary, M.A. and Abdelmalik, W.M. (1974):
Litho and biostratigraphy of middle and upper Eocene rocks in the Minia-Beni Suef reach of the Nile Valley, Egypt. 6th. Colloq. Afric. Micropaleont., Tunis, P.101-113.
- Bathurst, R.G.C. (1970):
Problems of lithification in carbonate rocks. Proc. Geol. Ass. 81, 3, P.429-440, Leeds.
- Bathurst, R.G.C. (1971):
Carbonate sediments and their diagenesis. Developments in Sedimentology, 12, 620pp., Elsevier, Amsterdam.,
- Beadnell, H.J.L. (1905):
The topography and geology of the Fayum province of Egypt. Egypt. Survey Dept., Cairo, 101pp.
- Beckmann, J.P., El-Heiny, I., Kerdany, M.T., Said, R and Viotti, C. (1969):
Standard planktonic zones in Egypt. Proc. 1st. Int. Conf. Planktonic Microfossiles, Geneva (1967), V.1, P.92-103.
- Bentz, F.P. & Gutman, S.J. (1977):
Landsat data contributions to hydrocarbon exploration in foreign regions. Prof. pap. U.S. geol. Surv., 1015, P.83-92.
- Bentz, F.P. & Hughes, J.B. (1981):
New Reflection Seismic Evidence of Late Miocene Nile Canyon
In: Said, R. (1981): The geological evolution of the River Nile, P.131-138. Springer-Verlag.
- Berggren, W.A. Kent, D.V. and Flynn, J.J. (1985):
Paleogene geochronology and chronostratigraphy: In: Snelling N.J. Ed., The chronology of the geological record. Geol. Soc. London. Mem. 10, P.141-198.
- Bermudez, P.J. (1961):
Contribucion al estudio de las Globigerinidea de la region Caribe-Antillana (Paleoceno-Reciente). Bol. Geologia (Venezuela), Spec. Publ. 3 (Cong. Geol. Venezolano, III, Caracas, 1960, Mem. 3), P.1119-1393.

- Bigg, P.J. (1982):
Eocene planktonic foraminifera and calcareous nannoplankton of the Paris Basin and Belgium. *Rev. Micropléont.*, 25, 2, P.69-89.
- Bignot, G. (1972):
Recherches stratigraphiques sur les calcaires du Crétacé supérieur et de l'Eocène d'Istrie et des régions voisines. Essai de révision du Liburnien. *Trav. Lab. Micropal.*, Paris, No. 2, 353pp.
- Bishay, Y. (1961):
Biostratigraphic study of the Eocene in the Eastern Desert between Samalut and Assiut by the large foraminifera. *Third Arab. Petrol. Congr.*, Alexandria, vol.2, P.13.
- Bishay, Y. (1966):
Studies on the larger foraminifera of the Eocene (The Nile Valley between Assiut and Cairo, and S.W. Sinai). Ph.D. Thesis, Alexandria University.
- Bishop, W.F. (1968):
Petrology of Upper Smackover limestone in north Haynesville field, Claiborne parish, Louisiana. *Bull. Am. Ass. Pet. Geol.*, 52, 92-128.
- Bissel, H. (1957):
Combined preferential staining and cellulose peel technique *J. Sed. Petrol.* 27, 417-420.
- Bissel, H.J. & Chilingar, G.V. (1967):
Classification of sedimentary carbonate rocks. In: Chilingar, G.V., Bissell, H.J. and Fairbridge, R.W. (eds.) *Development in Sedimentology*, 9A, Carbonate rocks. Elsevier Publ. P.87-168.
- Blanckenhorn, M. (1900):
Neues zur Geologie und Paläontologie Aegyptens. II: Das Palaeogen (Eocän und Oligocän). *Z. deut. geol. Ges.*, 52: 403-479.
- Blatt, H., Middleton, G.V. & Murray, R.C. (1972):
Origin of Sedimentary Rocks, 634pp., Prentice-Hall, New Jersey.
- Blondeau, A. (1972):
Les Nummulites, Paris Librairie, Vuibert, Boulevard Saint Germain, V.63, 254pp.
- Blour, W.H. (1979):
The Cainozoic Globigerinida. 3 vols., E.J. Brill, Leiden, 1413pp.

- Blow, W.H. and Banner, F.T. (1962):
The Mid-Tertiary (Upper Eocene to Aquitanian)
Globigerinaceae. In: F.E. Eames et. al., Fundamentals
of Mid-Tertiary Stratigraphical Correlation, P.61-151.
Cambridge Univ. Press, Cambridge.
- Blow, W.H. and Saito, T. (1968):
The morphology and taxonomy of *Globigerina mexicana*
Cushman, 1925. *Micropaleontology*, 14, 357-360.
- Bolli, H.M. (1957):
Planktonic Foraminifera from the Eocene Navet and San
Fernando formations of Trinidad, B.W.I. *Bull. U.S. nat.
Mus.*, 215, P155-172.
- Bolli, H.M. (1966):
Zonation of Cretaceous to Pliocene marine sediments based
on planktonic formimifera. *Boletino Informativo
Asociación Venezolana de Geología, Minería Y Petróleo*,
9, 3-32.
- Bolli, H.M. (1972):
The genus *Globigerinatheka* Brönnimann. *J. foramin.
Res.*, 2, 109-136.
- Bolli, H.M., Loeblich, A.R. and Tappan, H. (1957):
Planktonic foraminifera families Hantkeninidae,
Orbulinidae, Globorotaliidae and Globotruncanidae.
Bull. U.S. nat. Mus., 215, 3-50.
- Bolli, H.M. & Saunders, J.B. (1985):
Oligocene to Holocene low latitude planktic foraminifera
In: Bolli, H.M. et. al. (Ed.) *Plankton Stratigraphy*,
Cambridge Univ. Press, P.155-262.
- Bolli, H.M., Saunders, J.B. and Perch-Nielsen, K. (1985):
Plankton Stratigraphy. Cambridge Univ. Press,
1032pp. (ISBN 0-521-23576-6).
- Boukhary, M.A. (1970):
Facies paleontology and Biostratigraphy of some Mesozoic
and Tertiary rocks of the Cairo-Minia Reach of the Nile
Valley. Unpublished M.Sc. Thesis, Ain Shams Univ.
- Boukhary, M.A. (1973):
Stratigraphic and Micropaleontologic studies on some
Eocene rocks from Egypt. Ph.D. Thesis, Ain Shams
University.
- Boukhary, M. and Abdelmalik, W. (1983):
Revision of the stratigraphy of the Eocene deposits in
Egypt. *N.Jb. Geol. Paläont. Mh.*, 6, 321-337.

- 40
- Boukhary, M.; Toumarkine, M.; Khalifa, H. and Arif, M. (1982):
Etude biostratigraphique a l'aide des foraminiferes
planctoniques et des ostracodes de l'Eocene de Beni Mazar,
Vallée du Nil, Egypt. 8th colloq. Afr. Micropaléont., Paris
(1980). Cahiers de Micropaleontologie, 1, P.53-64.
- Boussac, J. (1910):
Sur la presence du Priabonien en Egypt. Bull. Soc. Geol.
Fr., Paris, (série 4), tome X, P.485-486.
- Boussac, J. (1911):
Etudes paléontologiques sur le Nummulitique alpin. - Mém.
Explic. Carte géol. dét. France, P.1-437.
- Boutte, A.L. (1969):
Callahan. Carbonate sand complex, west central Texas, in
C. Moore, (Ed.), Depositional environments and
dispositional history, Lower Cretaceous shallow shelf
carbonate sequence, west central Texas: Dallas, Tex.,
Dallas Geol. Soc., P.40-74.
- Bown, T.M. (1982):
Ichnofossils and Rhizoliths of the nearshore fluvial Jebel
Qatrani Formation (Oligocene), Fayum Province, Egypt.
Palaeogeogr., Palaeoclimat., Palaeoecol., 40, P.255-309.
- Bridge, J.S. (1985):
Perspectives, Paleochannel patterns inferred from alluvial
deposits: A critical evaluation. Jor. Sed. Pet., V.55,
no. 4, P.579-589.
- Brönnimann, P. (1952):
Globigerinoida and Globigerinathea, new genera from the
Tertiary of Trinidad, B.W.I. Contrib. Cushman Faund.
foramin. Res., 3, 25-28.
- Brönnimann, P. and Bermudez, P.J. (1953):
Truncorotaloides, a new foraminiferal genus from the Eocene
of Trinidad, B.W.I. J. Paleont., 27, 817-826.
- Bruguière, J.G. (1792):
Histoire naturelle des Vers. In: Encyclopédie méthodique -
Paris, V.1, 2, P.345-757.
- Burchette, T.P. and Britton, S.R. (1985):
Carbonate facies analysis in the exploration for
hydrocarbons: a case-study from the Cretaceous of the
Middle East. Spec. Publ. Geol. Soc. London, V.18,
P.311-399.
- Cas, R.A.F. & Landis C.A. (1987):
A debris-flow deposit with multiple plug-flow channels and
associated side accretion deposits. Sedimentology,
34, P.901-910.

- Cavelier, C. and Pomerol, C. (1986):
Stratigraphy of the Paleogene.
Bull. Soc. Géol. France, 8, No. 2, P.255-265.
- Chalilov, D.M. (1956):
O pelagecheckii Fayna foraminifer Paleogenorykh otlozhenii Azerbaidjana. (On the pelagic foraminiferal fauna of the Paleogene deposits of Azerbaidjan).
Akad, Nauk Azerb. SSR, Inst. Geol. Baku, Trudy, vd. 17.
- Chateauneuf, J.J. (1980):
Palynostratigraphie et paléoclimatologie de l'Eocene supérieur et de l'Oligocène du Bassin de Paris. Mem. B.R.G.M., Orleans, 116, 390p
- Cheetham, A.H. (1971):
Functional morphology and biofacies distribution of cheilostoms Bryozoa in the Danian Stage (Paleocene) of the Southern Scandinavia. Smithsonian Contrib. Paleobiol. 6, 1-85, Washington.
- Chilingar, G.V., Bissel, H.J., and Fairbridge, R.W. (eds) (1967):
Carbonate rocks. Dev. Sedimentology, 9A (origin, occurrence and classification). 471pp, Elsevier, Amsterdam.
- Clifton, H.E., Hunter, R.E. and Phillips, R.L. (1971):
Depositional structures and processes in the non-barred, high energy nearshore.
J. Sed. Pet., 41, P.651-670.
- Cole, W.S. (1927):
A foraminiferal fauna from the Guayabal Formation in Mexico.
Bull. Am. Paleontol., 14, P.1-46.
- Coleman, J.M. (1969):
Brahmaputra River: Channel processes and sedimentation. Sediment. Geol. 3, 129-239.
- Conybeare, C.E.B. (1979):
Lithostratigraphic analysis of sedimentary Basins. Academic Press, 555p.
- Cushman, J.A. (1927):
New and interesting foraminifera from Mexico and Texas. Contrib. Cushman Lab. foramin. Res., 3, 111-119.
- Cushman, J.A. (1928):
Additional foraminifera from the Upper Eocene of Alabama. Contrib. Cushman Lab. foramin. Res., 4, P.73-79.

- Cushman, J.A. (1940):
Foraminifera; their classification and economic use.
3rd ed., Harvard Univ. Press.
- Cushman, J.A. and Bermudez, P.J. (1937):
Further new species of foraminifera from the Eocene of
Cuba. Contrib. Cushman Lab. Foramin. Res., 13, P.1-29.
- Cushman, J.A. and Jarvis, P.W. (1929):
New foraminifera from Trinidad. Contrib. Cushman Lab.
foramin. Res., V.5, 6-17.
- Cuvillier, J. (1924):
Contribution à l'étude géologique du Mokattam.
Bull. ins. Egypte, 6, P.93-102.
- Cuvillier, J. (1930):
Révision du Nummulitique Egyptien.
Mém. ins. Egypte, 16, 371pp.
- Coogan, A.H. (1972):
Recent and ancient carbonate cyclic sequences. In: Elam,
J.C. and Chuber, S. (Eds): Cyclic sedimentation in the
Permian Basin, Midland, Texas: West Texas Geol. Society,
P.5-16.
- Cordey, W.G. (1968):
Morphology and phylogeny of *Orbulinoides beckmanni* (Saito,
1962). Palaeontology, 11, 371, 375.
- Cotter, E. (1966):
Limestone diagenesis and dolomitization in the
Mississippian carbonate banks in Montana
Jour. Sed. Petrol., V.36, P.764-774.
- Crevello, P.D. & Schlager, W. (1980):
Carbonate debris sheets and turbidites, Exuma Sound,
Bahamas.
J. Sed. Petrol., 50, 4, P.1121-1148.
- Curry, D., Adams, C.G., Boulter, M.C., Dilley, F.C., Eames, F.E.,
Funnell, B.M. and Wells, M.K. (1978):
A correlation of Tertiary rocks in the British Isles. Geol.
Soc. Lond., Special Report No. 12, 72p.
- Davies, P.J., Till, R. (1968):
Stained dry cellulose peels of ancient and recent
impregnated carbonate sediments.
J. Sed. Petrol. 38/1, 234-237.
- Decrouez, D. and Lanterno, E. (1979):
Les "bancs à Nummulites" de l'Eocène mésogéen et leurs
implications.
Arch. Sc. Genève, vol. 32, Fasc.1, P.67-94.

- Dennison, J.M. and Shea, J.H. (1966):
Reliability of visual estimates of grain abundance.
J. Sed. Petrol. 36/1, 81-89.
- Dickson, J.A.D. (1965):
A modification staining technique for carbonates in thin section.
Nature, No. 4071, 6, P.587.
- Dickson, J.A.D. (1966):
Carbonate identification and genesis as revealed by staining.
J. Sed. Petrol. 36/2, 491-505.
- Dott, R.H., Jr. (1963):
Dynamics of subaqueous gravity depositional processes.
Amer. Ass. Pet. Geol. Bull. 47, P.104-129, New York.
- Dryden, A.L. (1931):
Accuracy in percentage representation of heavy mineral frequencies.
Proc. Nat. Academy of Science, U.S., 17, 233-238.
- Dunham, R.J. (1962):
Classification of carbonate rocks according to depositional texture.
Mem. Amer. Ass. Petrol. Geol. 1, 108-121, Tulsa.
- Einsele, G. (1982):
Limestone-Marl Cycles (Periodites): Dignosis, Significance, Causes - a Review. In Einsele, G. and Seilacher, A. (Eds.)
Cyclic and Event Stratification - Springer, P.8-53.
- El-Dawoody, A. (1979):
Micro and Nannopaleontology of the Middle Eocene section in El-Fashn and Areg Oasis, Egypt 5th conference on African Geology, Cairo-Egypt, Geol. Survey of Egypt.
- EL-Khoudary, R.H. (1977):
Truncorotaloides Libyaensis, a new planktonic foraminifer from Gabal Al Akhdar (Libya).
Res. Esp. Micropaleontol., 9, 327-336.
- Ellis, B.F., Messina, A.R. (1966):
Catalogue of Index Foraminifera, V.2, Nummulites. Spec. Publ. Amer. Mus. Natural History, New York.
- Ellis, B.F., Messina, A.R., Charmatz, R. and Ronai, L.E. (1969):
Catalogue of Index smaller Foraminifera, Vols. 2,3, Spec. Publ. Amer. Mus. Natural History, New York.

- El-Naggar, Z.R. (1970):
On a proposed lithostratigraphic subdivision for the Late Cretaceous Lower Early Paleogene succession in the Nile Valley, Egypt (U.A.R.).
7th Arab. Petrol. Cong. Kuwait, 64 (B.3), 1-50.
- El Shazly, E.M. (1977):
Geology of the Egyptian region. In: Nairn, A.E.M., Stehli, F.G. & Kaner, W.H. (eds.): The ocean Basins and Margins. 4A. The Eastern Mediterranean. 379-344.
- Elter, P., Trevisan, P. (1973):
Olistostromes in the tectonic evolution of the Northern Apennines. In: Gravity and Tectonics (Ed. by K.A. de Jong and R. Scholten), P.175-188. John Wiley, New York.
- Embley, R.W. (1976):
New evidence for occurrence of debris flow deposits in the deep sea. *Geology*, 4, P.371-374.
- Embrey, A.F., Klovan, E.J. (1972):
Absolute water depths limits of late Devonian Paleocological zones.
Ged. Rdsch., 61/2. 10 figs., Stuttgart.
- Enos., P. (1977):
Tamabra Limestone of the Poza Rica Trend, Cretaceous, Mexico. In: H.E. Cook and P. Enos (Eds.): Deep water carbonate Environments, p.273-314.
Spec. Publ. Soc. econ. Paleont. Miner., 25, Tulsa.
- Enos, P. (1983):
Shelf environment. In Scholle, et. al. (Eds): Carbonate depositional Environments.
268-295. *A.A.P.G. Mem.* 33.
- Fabiani, R. (1905):
Studii geo-paleontdogichi dei Colli Berici.
Atti R. Istit. Ven. Sci., Lett. Arti 64, 1805-1825.
- Fahmy, S.E. (1975):
Contribution to Eocene stratigraphy and micropaleontology in the Nile Valley, Egypt. *Proc. 5th African Coll. Micropal.*, Addis-Ababa 1972.
Rev. Espan. Micropal., 7, 3, P.293-317.
- Farag, I.A.M. and Ismail, M.M. (1959):
Contribution to the stratigraphy of Wadi Hof area (North East of Helwan).
Bull. Fac. Sci., Cairo Univ., Vol. 34, P147-168.
- Farrell, S.G. (1984):
A dislocation model applied to slump structures, Ainsa Basin, South Central Pyrenees. *Journal of Structural Geology*, V.6, No. 6, P.727-736.

- Finlay, H.J. (1939):
New Zealand foraminifera: Key species in stratigraphy.
No. 2. Trans. Proc. R. Soc. N.Z., 69, 89-128.
- Fitzgerald, D.M. (1976):
Ebb-tidal delta of the Price Inlet, South Carolina:
geomorphology, physical processes and associated shoreline
changes. In: M.O. Hayes and T.W. Kana (Eds.), Terrigenous
clastic Depositional Environments - Some Modern Examples.
Tech. Rept., 11CRD, Coastal Res. Div., Univ. South Carolina
11.143-11.157.
- Flügel, E. (1972):
Mikroproblematika in Dünnschliffen von Trias-Kalken.
Mitt. Ges. Geol. Bergbausted. 21, 957-988, Innsbruck.
- Flügel, E. (1982):
Microfacies Analysis of limestones.
Springer-Verlag, 633P., Berlin, Heidelberg, New York.
- Folk, R.L. (1962):
Petrography and Origin of Silurian Rochester and
McKenzie Shales, Morgan County, West Virginia. J. Sed.
Petrol. 32, 3, P.539-578. Tulsa.
- Forskal, P. (1775):
Descriptiones animalium. quae in itinere orientali
osservavit Petrus Forskal. Haumiae (Copenhagen).
- Fourtau, R. (1897):
Note sur stratigraphique du Mokattam.
Bull. Soc. Géol. Fr. Paris, Ser. 3, 25, P.208-211.
(1912): Sur les divisions de L'Eocene en Egypte.
C. R. Ac. Sc. Paris, T.155, P.116.
- Fourtau, R. (1912):
Sur les divisions de L'Eocene en Egypte -
C. R. Acad. Sc. Paris, 155, P.1116-1118.
- Fourtau, R. (1916):
The divisions of the Eocene of Egypt as determined by the
succession of the Echinid Faunas.
Geol. Mag., V.3 (decade 6). No. 2, P.64-68.
- Friedman, G.M. (1959):
Identification of carbonate minerals by staining methods.
J.Sed. Petrol. 29/2, 87-97.
- Frost, S.H. (1977):
Ecologic controls of Caribbean and Mediterranean Oligocene
reef coral communities. International Coral Reef
Symposium, 3. 367-373.
- Furon, R. (1968):
Geologie de L'Afrique. Vol. 1, Payot, Paris, 374P.

- Galehouse, J.S. (1971):
Point counting in Carrer, R.E. (ed.)
Procedures in Sedimentary Petrology. Wiley-interscience
P.385-407.
- Gall, J.C. (1983):
Ancient Sedimentary Environments and the Habitats of Living
organisms. Springer-Verlag, Berlin, Heidelberg, New York
Tokyo, 219pp.
- Garrison, R.E., Fischer, A.G. (1969):
Deep water limestones and radiolarites of the Alpine
Jurassic. In: G.M. Friedman (Ed.) Depositional
Environments in Carbonate Rocks.
Soc. Econ. Paleont. Min., Spec. Publ., V.14, P.20-56.
- Gebhard, G. (1982):
Glauconitic Condensation through High-Energy Events in the
Albian Near Clars (Escragnalles, Var, SE-France). In:
Einsele, G. and Seilacher, A. (Eds.): Cyclic and Event
stratification. Springer, P.286-298.
- Ghorab, M.A. and Ismail, M.M. (1957):
A microfacies study of the Eocene and Pliocene east of
Helwan. Egypt. J. Geol., Vol. 1, No.2, P105-125.
- Gibbs, A.D. (1984):
Structural evolution of extensional basin margins. J.Geol.
Soc. Lond., Vol.141, P.609-620.
- Ginsburg, R.N. & Hardie, L.A. (1975):
Tidal and Storm deposits, northeastern Andros Island,
Bahamas. In: Tidal Deposits: A Casebook of Recent Examples
and Fossil counterparts (Ed. by R.N. Ginsburg), P.201-208,
Springer-Verlag, Berlin.
- Ginsburg, R.N. and Schroeder, J.H. (1973):
Growth and submarine fossilization of algal cup reefs,
Bermuda, Sedimentology, 20, 575-614, Amsterdam.
- Gray, J., Boucot, A.J. and Berry, W.B.N. (Eds.)(1981):
Communities of the Past. Hutchinson Ross Publ. Comp.,
Stroudsburg, Pennsylvania, 623p.
- Gregory, J.W., and Barrett, B.H. (1931):
General stratigraphy. Methuen and Co. Ltd., London,
P.194-203.
- Grinnell, R.S. Jr. (1974):
Vertical orientation of shells on some Florida oyster reefs
J. Sediment. Petrol., 44, P.116-122.

- Guembel, C.W. (1868):
 Beiträge zur Foraminiferenfauna der nordalpinen älteren Eocängbilde oder der Kressenberger Nummulitenschichten. Abhandlungen Bayerische Akademie der Wissenschaften, Math. Physik Kl., 10, 579-730.
- Haak, R. and Postuma, J.A. (1975):
 The relation between the tropical planktonic Foraminiferal zonation and the Tertiary Far East Letter classification. Geol. en Mijnbouw, V.54, 5-4, P.195-198.
- Ham, W.E. (ed.) (1962):
 Classification of carbonate rocks, a symposium. Memoir 1, Am. Ass. Pet. Geol., 279pp.
- Hanna, S.S. (1974):
 Geological studies on the area East of Minia M.Sc. Thesis, Geol. Dept., Assiut Univ., Egypt.
- Haq, B.U. (1971):
 Paleogene calcareous nannoflora. Part IV: Paleogene nannoplankton biostratigraphy and evolutionary rates in Cenozoic calcareous nannoplankton: Stockholm Contributions in Geology, V.25, P.129-158.
- Haq, B.U. (1983):
 Jurassic to Recent nannofossil biochronology: and update. In: Haq, B.U. (ed.) Nannofossil biostratigraphy. Benchmark papers in Geology, V.78, Hutchinson Ross publ. co., Stroudsburg, Pa, P.358-378.
- Harland, W.B., Cox, A.V., Llewellyn, P.G., Pickton, C.A., Smith, A.G. and Walters, R. (1982):
 A geologic time scale. Cambridge Univ. Press.
- Hassan, M.Y., Issawi, B. and Zaghloûl, E.A. (1978):
 Geology of the area east of Beni Suef, Eastern Desert, Egypt. Ann. Geol. Surv. Egypt., Vol. 8, P.129-162.
- Hay W.W., Mohler, H.P., Roth, P.H., Schmidt, R.R. and Baudreaux, J.E. (1967):
 Calcareous nanoplankton zonation of the Cenozoic of the Gulf Coast and Caribbean-Antilleau area and transoceanic correlation. Trans. Gulf Coast Ass. geol. Soc., V.17, P.428-480.
- Hay, W.W., Mohler, H.P. and Wade, M.E. (1966):
 Calcareous nanofossils from Nal'chik (Northwest Caucasus). Eclog. geol. Helvet., vol. 59, P379-399, Basel.

- Hayes, M.O. (1976) Transitional coastal depositional environments (lecture notes) . In: Hayes, M. O. and Kana , T. W. (eds.), Terrigenous clastic depositional environments - Some Modern Examples . Tech. Rep. 11- CRD, Coastal Res. Div. , Univ. South Carolina , P. 1.32 - 1.112 .
- Heckel, P.H. (1972):
Possible inorganic origin for Stromatactis in calcilutite mounds in the Tully limestone, Devonian of New York.
J. Sed. Pet. 42/1, P.7-18, Tulsa.
- Hedberg (H.D.) (1937):
Foraminifera of the Middle Tertiary Carapita Formation of Northeastern Venezuela.
J. Paleont., 11, 8, P.661-697.
- Hedberg, H.D. (1976):
International stratigraphic guide: A guide to stratigraphic classification, terminology, and procedure. John Wiley, New York, 200p.
- Hedberg, H.D. (ed.) (1972(a)):
Introduction to an international guide to stratigraphic classification, terminology, and usage.
Lethaia, V.5, P.283-295.
- Hedberg, H.D. (ed.) (1972(b)):
Summary of an International guide to stratigraphic classification, terminology, and usage.
Lethaia, V.5, P.297-323.
- Hendrix, W.E. (1958):
Foraminiferal shell form, A Key to Sedimentary Environment.
J. of Paleont., V.32, 4, P.649-659.
- Henson, F.R.S. (1948):
New Trochamminidae and Verneuilinae from the Middle East.
Ann. and Mag. Nat., Ser. 11, V.14, P.605-630.
- Hesse, R. (1975):
Turbiditic and non-turbiditic mudstone of Cretaceous flysch sections of the East Alps and other basins. Sedimentology, 22, P.387-416.
- Holland, C.H. et al. (1978):
A guide to stratigraphical procedure.
Geol. Soc. London. Spec. Rep. No. 10.
- Hornibrook, N. de B. (1965):
Globigerina angiporoides n.sp from the Upper Eocene and Lower Oligocene of New Zealand and the status of Globigerina angipora Stache 1865.
N.Z. J. Geol. Geophys., 8, P.834-883.

- Hottinger, L. (1960):
Recherches sur les Alvéolines paléocènes et éocènes. *Meim suisses Paléont.* 75, 76. P.1-242.
- Houbolt, J.J.H.C. (1957):
Surface sediments of the Persian Gulf near the Qatar peninsula. Dissertation, Univ. Utrecht, 113pp. The Hague, Mouton and Co.
- Howard, J.D. & Reineck, H.E. (1981):
Depositional facies of high energy beach-to-offshore sequence, comparison with low energy sequence.
Bull. Am. pet. Geol., 65, P.807-830.
- Hubbard, D.K. and Barwis, J.H. (1976):
Discussion of tidal inlet sand deposits: examples from the South Carolina Coast. In M.O. Hayes and T.W. Kana (Eds.), *Terrigenous clastic Depositional Environments - Some Modern Examples*. Tech Rep. 11-CRD, Coastal Res. Div, Univ. South Carolina 11.128-11.142.
- Hubbard, D.K., Oeertel, G. and Nummedal, D. (1979):
The role of waves and tidal currents in the development of tidal-inlet sedimentary structures and sand body geometry; examples from North Carolina, South Carolina, and Georgia:
Jour. Sed. Pet., V.49, P.1073-1092.
- Hume, W.F. (1911):
The effects of secular oscillation in Egypt during the Cretaceous and Eocene periods.
Quart. J. Geol. Soc. London, 67:118-148.
- Hume, W.F. (1912):
Explanatory notes to accompany the Geological map of Egypt.
Egypt. Survey Dept., Cairo, 50pp.
- Hume, W.F. (1925):
Geology of Egypt, vol. I: The surface features of Egypt, their determining causes and relation to geological structure.
Egypt. Survey Dept., Cairo, 408pp.
- Illing, L.V., Wells, A.J. and Taylor, J.C.M. (1965):
Penecontemporary dolomite in the Persian Gulf.
Soc. Econ. Paleon. Min. Spec. Publ., Vol. 13, P.89-111.
- Imbrie, J. and Buchanan, H. (1965):
Sedimentary structures in modern carbonate sands of the Bahamas. In: G.V. Middleton (Ed.) *Primary Sedimentary Structures and their Hydrodynamics Interpretation*. P.149-172.
Spec. Publ. Soc. Ec. Pal. Min., 12, Tulsa.

- Ismail, M.M. and Abdel-Kireem, M.R. (1971):
Contribution to the stratigraphy of the Fayum Province.
Bull. Fac. Sci., Alexandria Univ., V.11, No. 2, P.57-63.
- Ismail, M.M. and Farag, I.A.M. (1957):
Contributions to the stratigraphy of the area East of
Helwan (Egypt).
Bull. Ins. Désert Egypte, Vol.7, No.1, P95-134.
- Jaanusson, V. (1972):
Constituent analysis of an Ordovician limestone from
Sweden.
Lethaia, 5, 217-237.
- James, N.P. (1983):
Reef environment. In: Scholle et. al (eds.): Carbonate
Depositional Environments.
A.A.P.G. Mem. 33, P.345-440.
- Johnson, H.D. (1978):
Shallow Siliciclastic Seas. In: Reading, H.G. (ed.).
Sedimentary environment and facies. P.207-258, Oxford,
Blackwell Scientific Publication.
- Jones, O.T. (1940):
The geology of the Colwyn Bay district: a study of
submarine slumping in the Salopian Period.
Q. Jl. Geol. Soc. London. 95, P.335-382.
- Jones, N.S. (1952):
The bottom fauna and the food of flatfish off the
Cumberland Coast
J. Animal Ecol., V. 21, P182-205.
- Kacharara, Z.D. (1980):
On the systematics of some representatives of
Nummulites Fabianii Group. Bull. of the Academy of
Sciences of the Georgian SSR (In Russian), Vol. 98, No.3,
P.733-736.
- Kapellos, C. and Schaub, H. (1975):
L'Urdien dans les Alpes, dans les Pyrénées et en Crimée.
Corrélation de zones à grands Foraminifériés et à
Nannoplancton. B.S.G.F., 7, XVII, No. 2.
- Katz, A. and Friedman, G.M. (1965):
The preparation of stained acetate peels for the study of
carbonate rocks.
J. Sed. Petrol. 35, 248-249.
- Kauffman, E.G. and Sohl, N.F. (1974):
Structure and evolution of Caribbean Cretaceous rudist
frameworks. Festschrift für Hans Kugler (Ed. by P.Jung),
P.1-80. Mus. Nat. Hist. Basel, Switzerland.

- Keijzer, F.G. (1945):
Outline of the geology of the eastern part of the province of Oriente, Cuba (E of 76° WL), with notes on the geology of other parts of the island. Geographische en Geologische Mededelingen. Publicaties uit het Geographisch en uit het Mineralogisch-Geologisch Instituut der Rijksuniversiteit te Utrecht. Physiographisch-Geologische Reeks. Ser. II, N.6, P.1-239.
- Keldani, E.H. (1939):
A bibliography of geology and related sciences concerning Egypt up to the end to 1939.
Survey and Mines Dept., Cairo, 428pp.
- Kenawy, A.J. (1978):
Nouvelles espèces de grands foraminifères provenant de la base de l'Éocène supérieur de la section Midawara, Province du Fayoum, Égypte.
Rev. de Microp., V21, No.2, P.59-67.
- Kenawy, A.I., Khalifa, H. and Mansour, H.H. (1978):
Biostratigraphic zonation of the Middle Eocene in the Nile Valley, based on larger foraminifera.
Bull. Fac. Sci., Assiut Univ.
- Komar, P.D. (1969):
The channelized flow of turbidity currents with application to Monterey deep-sea fan channel. J. geophys. Res., 74, P.4544-4558.
- Krasheninnikov, V.A. and Ponikarov, V.P. (1964):
Zonal stratigraphy of Paleogene in the Nile Valley. Geol. Surv. and Min. Res. Dept. Egypt, Paper No. 32, P.26P.
- Krumbein, W.C. and Sloss, L.L. (1963):
Stratigraphy and Sedimentation, 660pp., W.H. Freeman, San Francisco.
- Kukal, Z. and Saadallah, A. (1973):
Aeolin admixtures in the sediments of the N. Persian Gulf. In B.H. Purser (Ed.). The Persian Gulf, 115-122, Heidelberg: Springer.
- Kulm, L.D., Rousch, R.C., Harlett, J.C., Neudeck, R.H., Chambers, D.M., and Runge E.J. (1975):
Oregon continental shelf sedimentation: Interrelationships of facies distribution and sedimentary processes. J. Geol. 83, P.145-176.
- Kumar, N. and Sanders, J.E. (1974):
Inlet sequence: a vertical succession of sedimentary structures and textures created by the lateral migration of tidal inlets.
Sedimentology, 21, P. 491-532.

- Laporte, L.F. (1975):
Carbonate Tidal-flat Deposits of the Early Devonian
Manlius Formation of New York State. In: R.N. Ginsburg
(Ed.), Tidal Deposits. Springer-Verlag. Berlin,
Heidelberg, New York.
- Lees, A. (1975):
Possible influences of salinity and temperature on modern
shelf carbonate sedimentation Mar.Geol., 19, P.159-198.
- Leighton, M.W. and Pendexter, C. (1962):
Carbonate rock types. In: W.E. Ham (ed.) Classification of
Carbonate Rocks: A symposium, pp.33-61.
Mem. Am. Ass. Petrol. Geol., 1, Tulsa.
- Leopold, L.B., Wolman, M.G. (1957):
River channel patterns; braided, meandering and straight.
U.S. Geol. Surv. Profess. Papers, 282-B, P.39-85.
- Leopold, L.B., Wolman, M.G. and Miller, J.P. (1964):
Fluvial process in geomorphology, 522pp. San Fransisco,
London: Freeman.
- Lewis, K.B. (1971):
Slumping on a continental slope inclined at 1° - 4°.
Sedimentology, 16, P.97-110.
- Liebau, A. (1980):
Paläobathymetrie und Ökofaktoren: Flachmeer - Zonierungen.
Neues Jahrbuch.
Geol. Paläont. Abhandlungen, 160, P.173-216, Stuttgart.
- Little, O.H. (1936):
Recent geological work in the Fayium and adjoining portion
of the Nile Valley.
Bull. ins. Égypte, Vol.18, P201-240.
- Lowe, D.R. (1976):
Subaqueous liquefied and fluidized sediment flows and their
deposits. Sedimentology 23, 285-308.
- Lowe, D.R. (1975):
Water-escape structures in coarse-grained sediments.
Sedimentology 22 , 157- 204 .
- Lowman, S.W. (1949):
Sedimentary facies in Gulf Coast, A.A.P.G.,
Bull., V.33, P.1939-1997.
- Lucia, F.J. (1972):
Recognition of evaporite shoreline sedimentation.
Soc. Econ. Pal. Min. Sp. Pub., V.16, P.160-191.

- Macdonald, D.I.M. and Tanner, P.W.G. (1983):
Sediment dispersal patterns in part of a deformed Mesozoic back arc basin of South Georgia, South Atlantic.
J. Sedim. Petrol. 53, 83-104.
- Martini, E. (1970(a)):
Standard Palaeogene calcareous nannoplankton zonation.
Nature, 226, P.560-561.
- Martini, E. (1970(b)):
Imperiaster n.g. aus dem europäischen Unter-Eozän
(Nannoplankton, incertae sedis). Senckenbergiana Lethaea,
51, P.383-386.
- Martini, E. (1971):
Standard Tertiary and Quaternary calcareous nannoplankton zonation. In: A. Farinacci (ed.), Proceedings II Planktonic Conference. Roma, 1970, 2, P.739-785.
- McGowen, J.H. and Garner, L.E. (1970):
Physiographic features and stratification types of coarse-grained point bars: Modern and ancient examples.
Sedimentology, 14, 77-111.
- McKerrow, W.S. (1978):
The Ecology of Fossils.
Duckworth Co. Ltd., 384pp.
- Miall, A.D. (1984):
Principles of Sedimentary Basin Analysis. Springer-Verlag, 490P., New York, Berlin, Heidelberg, Tokyo.
- Middleton, G.V. (1970):
Experimental studies related to problems of flysch sedimentation. In: Lajoie, J. (ed.). Flysch sedimentology in North America.
Geol. Assoc., Can. Spec. Pap., 7, P.253-272.
- Middleton, G.V., Hampton, M.A. (1976):
Subaqueous sediment transport and deposition by sediment gravity flows. In Stanley, D.J. Swift, D.J.P. (eds.): Marine sediment Transport and Environmental Management, 197-218, New York: Wiley.
- Milliman, J.D. (1966):
Submarine lithification of deep-water Carbonate sediments.
Science, V.153, P.994.
- Milliman, J.D. (1974):
Marine Carbonates, recent sedimentary carbonates, Part 1. 375p., Springer-Verlag. Berlin-Heidelberg - New York.

- Moore, R.C. (1964):
Treatise on Invertebrate Paleontology Part C, Protista 2, Sarcodina, Vol. 1. The Geological Society of America and University of Kansas Press.
- Moore, D.G., Curray, J.R., Raitt, R.W. and Emmel, F.J. (1974):
Stratigraphic-seismic section correlations and implications to Bengal Fan history. In: Initial Reports of the Deep Sea Drilling Project, 22 (C.C. von der Borch, J.G. Sclater et. al.), P.403-412. U.S. Government Printing Office, Washington.
- Moore, R.C., Lalicker, C.G. and Fischer, A.G. (1952):
Invertebrate Fossils, McGraw-Hill Com. Inc 766P.
- Morgenstein, M. (1973):
Sedimentary diagenesis and rates of manganese accretion on the Waho Shelf, Kauai Channel, Hawaii, P.121 - 136. Interuniversity program of research on ferromanganese deposits of the ocean floor (unpublished). Seabed Assessment Program Inter. Dec. Ocean Exploration, Nat. Sci. Foundation, Washington, D.C.
- Mount, J. (1985):
Mixed siliciclastic and carbonate sediments: a proposed first-order textural and compositional classification sedimentology, 32. P. 435-442 .
- Müller, G. (1967):
Methods in sedimentary Petrology. 283pp.
Sed. Petrol, part I, by Engelhardt, W.V., Fuchtbauer, H., and Muller, G.
- Murray, J.W. (1973):
Distribution and Ecology of living benthic foraminiferids. Grane, Russak & Co., Inc., New York, 274P.
- Murray, J.W., Curry, D., Haynes, J.R. and King, C. (1981):
Palaeogene. In: Jenkins, D.G. and Murray, J.W. (eds.): Stratigraphical atlas of fossil foraminifera British Micropalaeontological Society/ Ellis Horwood Ltd. P228-267.
- Mutti, E. (1977):
Distinctive thin-bedded turbidite facies and related depositional environments in the Eocene Hecko Group (South Central Pyrenees, Spain). Sedimentology, 24, 107-132.
- Mutti, E and Normark, W.R. (1987):
Comparing examples of modern and ancient turbidite systems: problems and concepts. In: Leggett, J.K. and Zuffa, G.G. (eds.): Marine Clastic Sedimentology, concepts and case studies. Graham & Trotman Ltd., P.1-38.
- Mutti, E., Ricci and Lucchi, F.O. (1972):
Le torbiditi dell'appennino settentrionale: Introduzueone all'analisi di facies. Mem Soc. Geol. It. 11, 161-199.

- Nakkady, S.E. (1958):
Stratigraphic and Petroleum Geology of Egypt. Univ. Assiut,
Monograph Series No. 1.
- Naylor, M.A. (1981):
Debris flow (olistostromes) and slumping on a distal passive
continental margin the Palombini limestone-shale sequence of
the northern Apennines. *Sedimentology*, 28, P.837-852.
- Nelson, C.H. and Kulm, L.D. (1973):
Submarine fans and channels. In: *Turbidites and Deep Water
Sedimentation*, P.39-91. Spec. Publ. Soc. econ. Paleont.
Miner., 19, Tulsa.
- Nelson, C.H. and Nilsen, T. (1974):
Depositional trends of modern and ancient deep-sea fans.
In: Dott, R.H. and Shaver, R.H. (eds.): *Modern and Ancient
Geosynclinal sedimentation*. Spec. Publ. Soc. econ.
Paleont. Miner., 19, P.69-91.
- Nemkov, G.I. (1962):
Stratigraphie des couches liburniennes au nord - ouest de
la Yougoslavie. *Mém. B.R.G.M.*, 28, 2, P.711-717.
- Omara, S. and Kenawy, A.I. (1984):
Nummulites Rohlfi, a new nummulites species from the
Gizehensis group, in the early Late Eocene of the Nile
Valley, Egypt.
Rev. de Microp., V.27, No.1, P.54-60.
- Omara, S., Khalifa, H. and Youssef, M.M. (1978(b)):
Contribution to the geology of the area to the Southwest of
Beni Suef, Egypt.
Bull. Fac. Sci. Assiut Univ.
- Omara, S., Mansour, H., Youssef, M.M. and Khalifa, H.
(1978(a)):
Stratigraphy, Paleoenvironment and structural features of
the area East of Beni-Mazar, Upper Egypt.
Bull. Fac. Sci. Assiut Univ.
- Oppenheim, P. (1903):
Zur Kenntniss Alttertiärer faunen in Aegypten Lief1, *Palaeo.*
Stuttg. 30. Abth.III, No. 1, P.1-164.
- Padgett, G., Ehrlich, R., Moody, H. (1977):
Submarine debris flow deposits in an extensional setting.
Upper Devonian of Western Morocco.
J. Sed Pet. 47/2, P.811-818, Tulsa.
- Pettijohn, F.J. (1975):
Sedimentary Rocks. Harper and Row, New York, London,
628pp.

- Pettijohn, F.J. and Potter, P.N. (1964):
Atlas and Glossary of primary sedimentary structures.
370pp. Springer, Berlin-Göttingen, Heidelberg.
- Philobos, E.R. (1984):
Outline of the tectonically controlled Eocene carbonate siliciclastic sedimentation, Nile Valley and Eastern Desert, Egypt. 5th European regional meeting of sedimentology. (abst.) P.353.
- Pickering, K.T. (1982):
A Precambrian Upper Basin - Slope and Pro-delta in Northeast Finnmark, North Norway - a possible ancient upper continental slope.
J. Sedim. Petrol. 52, 171-186.
- Piper, D.J.W., Normark, W.R. and Stow, D.A.V. (1984):
The Laurentian Fan-Sohm Abyssal Plain. GeoMar. Letts, 3, P.141-146.
- Pokorny, V. (1963):
Principles of Zoological Micropalaentology. Pergamon Press, Oxford. London, New York, Paris. 652pp.
- Pomerol, C. (1980(a))
Aurersien. In les étages français et leurs stratotypes Mém B.R.G.M. 109, Orléans, P.227,231.
- Pomerol, C (1980(b)):
Marinésien. In Les étages français et leurs stratotypes. Mém B.R.G.M., 109, Orléans, P.232-237.
- Pomerol, C.H. and Premoli-Silva, I. (1986):
The Eocene-Oligocene transition events and boundary. In: Terminal Eocene Events. Developments in palaeontology and stratigraphy, Elsevier, Amsterdam.
- Porter, J.W. and Fuller, J.G.C.M. (1959):
Lower Paleozoic rocks of northern Williston basin and adjacent areas.
A.A.P.G. Bull., Vol. 43, P.124-189.
- Pratt, D.M. (1953):
Abundance and growth of venus mercenaria and Collocardia morrhuana in relation to the character of the bottom sediments.
J. Marine Res., V.12, P.60-74.
- Price, N.B. (1967):
Some geochemical observations on manganese-iron oxide from different depth environments.
Marine Geology, V.5, P.511-538.
- Proto Decima, F. and Bolli, H.M. (1970):
Evolution and variability of Orbulinoides beckmanni (Saito)
Eclog. geol. Helv., 63, P.883-905.

- Purdy, E.G. (1963(a)):
Recent calcium carbonate facies of the Great Bahama Bank.
I. Petrography and reaction groups.
J. Geol., 71, P.334-355.
- Purdy, E.G. (1963(b)):
Recent calcium carbonate facies of the Great Bahama Bank.
II. Sedimentary facies.
J. Geol., 71, P.472-497.
- Purser, P.H. (1973):
The Persian Gulf: Holocene Carbonate Sedimentation and Diagenesis in a shallow Epicontinental Sea, 471pp.
Springer-Verlag, Berlin.
- Ramsay, A.T.S. (1971):
The investigation of lower Tertiary sediments from the North Atlantic. In: A. Farianacci (ed.), Proceedings of the 11 Planktonic Conference, Roma, 1970., P.1039-1055.
- Read, J.F. (1974):
Carbonate bank and wave built platform sedimentation, Edel Province, Shark Bay, Western Australia, A.A.P.G., Bull. Memor., No. 22, P.1-60.
- Read, J.F. (1985):
Carbonate platform facies Models.
A.A.P.G. Bulletin, V.69, No. 1, P.1-21.
- Reading, H.G. (ed.) (1978):
Sedimentary environment and facies. 576pp., Oxford, Blackwell Scientific Publications.
- Reddering, J.S.V. (1983):
An inlet sequence produced by migration of a small microtidal inlet against longshore drift ; the Keurbooms inlet, South Africa. Sedimentology, 30, P.201-218.
- Reineck, H.E. and Singh, I.B. (1980):
Depositional Sedimentary Environments. Springer-Verlag. Second edition, 549pp.
- Riba, O. (1976):
Syntectonic unconformities of the Alto Cardener, Spanish Pyrenees: a genetic interpretation: Sedimentary Geology, V.15, P.213-233.
- Roveda, V. (1961):
Contributo allo studio di alcuni macroforaminiferi di Priabona. Riv. ital. Paleont. 67(2), P.153-224.
- Rupke, N.A. (1978):
Deep clastic seas. In: Reading, H.G. (ed.). Sedimentary Environments and facies. P.372-415, Blackwell Scientific Publications

- Said, R. (1961):
Tectonic framework of Egypt and its influence on
distribution of foraminifera.
Bull. Am. Assoc. Petrol. Geol., Vol. 45, P.198-218.
- Said, R. (1962):
The Geology of Egypt. Elsevier. Amsterdam. New York.
- Said, R. (1963):
Note on the biostratigraphy of the Middle and Upper
Eocene sections in Egypt. Revue de L'inst., Franc.
Petrol., vol. 18, P.1500-1503.
- Said, R. (1971):
Explanatory notes to accompany the geological map of
Egypt, The Geological Survey of Egypt, Paper 56, 123pp.
- Said, R. and EL-Shazly, E.M. (1957):
Review of Egyptian geology. Science Council, Cairo, 91 pp.
- Said, R. and Martin, L. (1964):
Cairo area Geology Excursion notes, In. Trip to Egypt,
Libya Petrol. Explor. Soc. P. 107-121.
- Saito, T. (1962):
Eocene planktonic foraminifera from itahajima (Hillsborough
Island). Trans. Proc. Paleontol. Soc. Japan.
news series, 45, P.209-225.
- Salem, R. (1976):
Evolution of Eocene - Miocene sedimentation patterns in
parts of Northern Egypt.
AAPG. Bull., vol. 60, No 1., p.34-64.
- Samanta, B.K. (1970):
Middle Eocene planktonic foraminifera from the Lakhpat,
Cutch, Western India. Micropal., 16, P.185-215.
- Sander, B. (1936):
Beitrage zur Kenntnis der Anlagerungsgefuge (rhythmische
Kalke und Dolomite aus der Trias).
Mineral. Petrol. Mitt. Vol.48, P.27-139.
- Sander, B. (1951):
Einführung in die Gefügekunde als Geologischer Körper,
2. Teil. Die Korngefügemerkmale. 409pp., Wien-innsbruck:
Springer.
- Sanders, H.L. (1958):
Benthic studies in Buzzards Bay, I; Animal-sediment
relationships: Limnol. and Ocean., V.3, p.245-258.
- Saxov, S. & Nieuwenhuis, J.K. (eds.) (1982):
Marine slumps and other Mass Movements. Plenum Press,
New York.

- Schaub, H. (1981):
Nummulites et Assiliones de la Tethys paléogène, Taxinomie,
Phylogénèse et biostratigraphie. Mémoires suisses de
Paléontologie, volume 104. Birhhäuser Editions, Bâle.
- Scholle, P.A., Bebout, D.G., and Moore, C.H. (1983):
Carbonate Depositional Environments.
A.A.P.G., Mem.33, Tulsa, Oklahoma, 708pp.
- Schreiber, B.C. (1986):
Arid Shorelines and Evaporites. In: Reading, H.G. (ed.):
Sedimentary environments and facies. Second Edition,
Blackwell, p. 189-228.
- Schumm, S.A. (1977):
The fluvial system, 338pp. New York: Wiley & Sons.
- Schumm, S.A. (1985):
Patterns of alluvial Rivers. Ann. Rev. Earth Planet.
Sci, 13, p.5-27.
- Schweinfurth, G. (1883): Uper die
Geologisch Schichtengliederung des Mokattam bei Cairo
Zeitschr. Deutsch-Geol. Gesellsch., Berlin, Bd. T. XXXV,
p.709-734, XV-XXII.
- Schwarzacher, W. (1948):
Sedimentpetrographische Untersuchungen Kalkalpiner
Gesteine, Hallstätter Kalke von Hallstatt und Ischl. Jb.
geol. Bundesanst. 91, J.g. 1946, 1-48, wien.
- Scoffin, T.P., Alexandersson, E.T., Bowes, G.E., Clokie, J.J.,
Farrow, G.F., & Milliman, J.D. (1980):
Recent, temperate, sub-photic carbonate sedimentation,
Rockall Bank, Northeast Atlantic.
J.sed. Pétról. 5012, 231-356. Tulsa.
- Sellwood, B.W. (1986):
Shallow-marine carbonate environments. In: Reading, H.C.
(1986): Sedimentary environments and facies. Second edition,
Blackwell.
- Sestini, G. (1984):
Tectonic and sedimentary history of the NE African margin
(Egypt-Libya). In: Dixon, J.E., and Robertson, A.H.F.
(eds.): The geological evolution of the Eastern
Mediterranean P.161-175.
- Shama, K. (1976):
Etude de la région du Fayoum (Égypte): la Formation d'EL
Midawarah-7e colloque Africain de Micropaléontologie,
Ile-Ife, Nigéria.

- Shama, K., Blondeau, A.; Le Calvez, Y., Perch-Nielsen, K., and Toumarkine, M. (1982):
Biostratigraphie de L'Eocene moyen de la formation El Midawarah, région de wadi El Rayan, Province du Fayoum, Egypte. Cahiers De Micropaleontologie, 1, part 3, p.91-104.
- Sherborn, C.D. (1910):
Bibliography of scientific and Technical literature relating to Egypt. National Printing Dept., Cairo, 155p.
- Shinn, E.A. (1969):
Submarine lithification of Holocene carbonate sediments in the Persian Gulf. Sedimentology, V.12, 109-144.
- Shinn, E.A. (1973):
Sedimentary accretion along the leeward, southeast coast of Qatar Peninsula, Persian Gulf, In B.H. Purser (Ed.). The Persian Gulf, Holocene carbonate sedimentation and diagenesis in a shallow epicontinental sea. Springer, P.199-209.
- Shinn, E.A.; Lloyd, R.M. & Ginsburg, R.N. (1969):
Anatomy of a modern carbonate tidal flat, Andros Island, Bahamas. J. Sed. Pet., 39, p.1202-1228.
- Shrock, R.P. (1948):
Sequence in layered rocks. 507pp., McGraw Hill, New York. Toronto. London.
- Shukri, N.M. (1954):
Remarks on the Geological structure of Egypt. Bull. Soc. Géogr. Egypte, V.27, P.65-82.
- Shukri, N.M., and Said, R. (1944):
Contribution to the Geology of the Nubian Sandstone, Part I: Field observations and mechanical analysis. Bull. Fac. Sci, No.25, P.149-172.
- Sigaev, N. A. (1959):
The main tectonic features of Egypt. Geol. Surv. Egypt, Paper 39, 25pp.
- Smith, D.B. (1974):
Sediments of upper Artesia (Guadalupian) cycle-shelf deposits of northern Guadalupe Mountains, New Mexico. Am. Ass. Pet. Geol. Bull., V.58, p.1699-1730.
- Southward, E.C. (1957):
The distribution of Polychaeta in offshore deposits in the Irish sea. J. Marine Biol. Assoc. U.K., V.18, p.243-278.
- Sprecht, R.W., Brenner, R.L. (1979):
Storm-wave genesis of bioclastic carbonates in Upper Jurassic epicontinental mudstones, East-Central Wyoming. J. Sed. Petrol. V.49, 4, p.1307-1322, Tulsa.

- Stickney, A.P. and Stringer, L.D. (1957):
A study of the invertebrate bottom fauna of Greenwich Bay,
Rhode Island. Ecology, V.38, p.11-122.
- Stockman, K.W., Ginsburg, R.N. & Shinn, E.A. (1967):
The production of lime mud by algae in south Florida.
J.sed. Pet. , 37, p.633-648.
- Stow, D.A.V. (1986):
Deep Clastic Seas. In: Reading, H.G. (ed.): Sedimentary
environments and facies. Second Edition. Blackwell,
p.399-443.
- Stow, D.A.V. & Bowen, A.J. (1980):
A physical model for the transport and sorting of
fine-grained sediments by turbidity currents.
Sedimentology, 27, p.31-46.
- Strougo, A. (1977):
Le "Biarritzien" et le Priabonien en Egypte et leurs faunes
de Bivalves. Ph. D. Thesis, Univ. Paris Sud, (Orsay).
- Strougo, A. (1979):
The Middle Eocene - Upper Eocene boundary in Egypt. Ann.
Geol. Surv. Egypt, Vol.9, p.455-470.
- Strougo, A., Abul-Nasr, R.A. and Haggag, M.A.Y. (1982):
Contribution to the age of the Middle Mokattam beds of
Egypt. N.Jb. Geol. Paläont. Mh., no. 4, p. 240-243.
- Subbotina, N.N. (1953):
Fossil foraminifers of the USSR: Globigerinidae,
Hantkeninidae, and Globorotaliidae. Trudy VNIGRI, new
series, 76, 296p. (in Russian). Translated into English by
E. Lees, Fossil foraminifera of the USSR, Globigerinidae,
Hantkeninidae and Globorotaliidae. Collet's Ltd., London
and Wellingborough, 321p.
- Tadros, S.F. (1968):
Geologic, palaeontologic and economic studies on some rocks
from Mokattam area. M.Sc. Thesis, Geology Dept., Ain Shams
Univ., 224p.
- Tappan, H. & Loeblich, A.R. (1971):
Geobiologic Implications of fossil Phytoplankton Evolution
and Time-space Distribution. In R.Kasanke and A.T. Cross,
eds., Symposium on palynology of the Late Cretaceous and
early Tertiary: Geol. Soc. America, Spec. Paper, 127,
p.247-339.
- Taylor, J.C.M. & Illing, L.V. (1969):
Holocene intertidal calcium carbonate cementation, Qatar,
Persian Gulf. Sedimentology, 12, p.69-107.

- Teichert, C. (1958):
Cold and deep-water coral banks.
Bull. Amer. Ass. Petrol. Geol. 42/5, 1064-1082. Tulsa.
- Tlell, J.W. (1972):
Surface geology of Dammax dome, Eastern Province, Saudi Arabia: M.Sc. Thesis, Texas christian Univ. p.56.
- Toumarkine, M. and Bolli, H.M. (1970):
Evolution de Globorotalia cerroazulensis (Cole) ans L'Eocène moyen et supérieur de possagno (Italie). Rev. Micropaleontol., 13, p. 131-145.
- Toumarkine, M. & Luterbacher, H. (1985):
Paleocene and Eocene planktonic Foraminifera. In Boli, H, et. al. (Ed.); Plankton stratigraphy. Cambridge University Press, p.87-154.
- Tucker, M. E. (1982):
The field discription of sedimentary rocks.
Open University Press (112pp).
- Vail, P.R. and Hardenbol, J. (1979):
Sea level changes during the Tertiary: in Ocean/continent boundaries, Oceanus, Vol. 22, No.3, p. 71-79.
- Valentine, J. W. (1973):
Evolutionary Paleoeecology of the Marine biosphere.
Prentice-Hall, Inc., 511PP.
- Van Straaten, L.M.J.U. (1971):
Origin of Solnhofen Limestone. Geol Mijnbouw 50,P3-8.
- Walker, R.G. (1978):
Deep-water sandstone facies and ancient submarine fans: Models for exploration for stratigraphic traps.
Am. Ass. Pet. Geol. Bull 62, 932-966.
- Walker, R.G., Mutti, E. (1973):
Turbidite facies and facies associations. In: G.V. Middleton, AH. Bouma (eds.). Turbidites and deep sea sedimentation. Soc. Econ. Paleont. Min., Pacific Sect., Short Course, 119-157.
- Warne, J. (1962):
A quick field or laboratory staining scheme for the differentiation of the major carbonate minerals.
J. Sed. Petrol. 32/1. 29-39.
- Watkins, D.J. and Kraft, L.M. (1978):
Stability of continental shelf and slope of Louisiana and Texas: geotechnical aspects. In: Bouma, A.H., Moore, G.T. and Coleman, J.M. (eds.): Framework, Facies and Oil-Trapping Characteristics of the Upper Continental Margin. P.267-286. Stud. Geol. Am. Ass. Pet. Geol., 7, Tulsa.

- Weinzierl, L.L and Applin, E.R. (1929):
The Claiborne formation on the Coastal Domes.
J. Paleontol., 3. 384-410.
- Weller, J.M. (1960):
Stratigraphic Principles and Practice. Harper, New York,
725pp.
- Whitaker, McD.J.H. (1974):
Ancient submarine canyons and fan valleys. In: R.H.Dott
and R.H.Shaver (eds.): Modern and Ancient Geosynclinal
Sedimentation. P.106-125.
Spec. Publ. Soc. econ. Paleont, Miner, No.19.
- Whitaker, R.H. (1970):
Communities and ecosystems, MacMillan, London, 161pp.
- Wilson, J.L. (1969):
Microfacies and sedimentary structures in deeper water lime
mudstones. In: Friedman, G.M. (ed.) Depositional Environments
in Carbonate Rocks. P.4-19. Spec. Publ. Soc.
Econ. Paleont. Miner., 14, Tulsa.
- Wilson, J.L. (1975):
Carbonate facies in geologic history. 471pp, Springer-
Verlag, Berlin, Heidelberg, New York.
- Winn, R.D.Jr. and Dott, R.H.Jr. (1979):
Deep water fan-channel conglomerates of Late Cretaceous
age, Southern Chile.
Sedimentology, No. 26, P.203-228.
- Woodcock, N.H. (1976):
Structural style in slump sheets. Ludlow Series, Powys,
Wales. J.Geol. Soc. London. 132, P.399-415.
- Woodcock, N.H. (1979):
The use of slump structures as palaeoslope orientation
estimators. Sedimentology. 26. P.83-99.
- Ziegler, A.M., Walker, K.R., Anderson, E.J., Kauffman, E.G.,
and Ginsburg, R.N. (1973):
Principles of Benthic Community Analysis, University of
Miami, notes for a short course, Miami, Florida.
- Ziegler, B. (1972):
Einführung in die Paläobiologie. Teil 1. Allgemeine
Paläontologie. 245pp., Stuttgart, Schweizbart.
- Zittel, A.K. (1883):
Beiträge zur Geologie und Palaentologie der Libyschen
Wüste und der angrenzenden Gebiete van Aegypten.
Paleontographica, 30(1):1-112.

A R A B I C S U M M A R Y

من خلال مراوح القنوات الترسيبية العميقة أو نتيجة زحف رواسب الحواجز الفتاتية المعقدة .

وأوضحت الدراسة وجود ظواهر كثيرة ودلالات متعددة لتزامن حركات الرفع مع الترسيب، فقد أمكن تسجيل شواهد كثيرة لذلك منها الفوالق البانية وعدم التوافق المتزامن مع الترسيب، وأيضاً كل من رواسب سريان الحطام المتكسّر والكتل العملاقة المتحلقة (الذاحفة تحت الجازيه) وهذه أيضاً تلقى الضوء على الطبيعة المتكررة لآحداث الرفع في الكتل المحيطة بالحوض والتي أدت بالتالى إلى إنحراف وتغيير المحور الترسيبى في الحوض من الشمال الغربى الى اتجاه الجنوب والجنوب الشرقى .

بِسْمِ اللّٰهِ الرَّحْمٰنِ الرَّحِیْمِ
 "رَبُّ اَوْ ذَعْنَى اَنْ اَشْكُرْ نِعْمَتَكَ الَّتِیْ اَنْصَبْتَ عَلَیَّ وَعَلَى وَا لِدَىَّ وَاَنْ اَعْمَلَ صَالِحًا تَرْضَاهُ
 وَاَدْخِلْنِیْ فِیْ عِبَادِكَ الصّٰلِحِیْنَ"

صدق الله العظيم

"تحليل حوض ودراسات طباقية وترسيبيه لصخور الأيوسين
 الجيرية في شمال وادي النيل بمصر"

(ملخص)

خضعت رواسب الكربونات (الصخور الجيرية) في شمال وادي النيل لدراسات
 إستراتيجية وترسيبيه قادت إلى أبحاث تحليلية حوضيه متكامله .
 وقد اشتملت الدراسات الاستراتيجية على عمل مضاهاة طباقية للمكونات الصخرية
 المثلثة (مكون بنى سويف، مكون قارون، مكون سفارة، مكون القرن، ومكون وادي
 حوف) وأقترح ضمهم تحت وحدة صخرية جامعته وهي وحدة المقطم المتوسط .

كما كشفت دراسة الكائنات الدقيقة والمشقيات الجيرية (الميكروسكوبية
 والكبيره) لتأريخ الطبقات، عن اشتقاق نطاقات حيوية تطبيقية أفادت في
 إجراء مضاهاة إستراتيجية زمنيه للوحدات الصخرية المختلفه المشمله
 في منطقة البحث، وقد تمكن الباحث أيضا من تسجيل ومناقشه ظواهر التراكب
 السحني التقدمي والتقهقري والامتداحل .

ولقد أبرزت الدراسات الاستراتيجية واستكشاف حوض ترسيبي كبير أمكن تحديده
 أبظاده ورسم شكله الخارجى حيث ضم هذه الرواسب المدروسة وسى حوض المقطم
 المتوسط، وتبلغ مساحته ١٥٣٧٥ كيلومتر مربع . وقد توصل الباحث إلى تحديد العمر
 الذى تكون فيه هذا الحوض منذ حوالى ٤٠ مليون سنة تقريبا .

وقد أدت الدراسات الترسيبيه والتحليل الكيفيه المفضله للنسب المختلفه لحبيبات
 المكونات الكربونية إلى تمييز وفرواقية ١٢ - سحنه ترسيبيه كبرى، أمكن تصنيفهم إلى ٣٦ تحت
 سحنه مترافقه، وهذه بدورها أدت إلى كشف النقاب عن البيئات الترسيبيه البحريه
 المختلفه والتي ترسبت فيها رواسب الحوض وأمتلئ بها .

وقد أدت التحاليل الأستراتيجية والترسيبيه الدقيقه وأيضا بإستعمار البيئات
 القديمه التى عاشت فيها الجماعات المختلفه من الكائنات البانيه لصخور هذه
 الكربونات، إلى الكشف عن شكل قاع الحوض الكامل وقت وبعد الترسيب
 وتمكن الباحث من رسم أشكاله تركيبيه لهذا الحوض في إتجاهات مختلفه وقد تم
 أيضا تسجيل ظواهر عديده للتشوهات الترسيبيه اللينه والتي أدت إلى كشف
 وتفسير حركات الهبوط التركيبى المصاحب للترسيب والتي تكونت نتيجة لتجدد مستمر في
 حركة الفوالق العميقه، وقد كشف البحث عن أنه بتكرار الرفع المستمر للكسبه الشماليه
 الغربيه (أبورواش الحاليه) والمجاوره للحوض - أدت إلى تشكيل وتشبيهد الهيكل التركيبى
 للحوض الترسيبى . هذه الصليات هى المسئله عن إعادة ترسيب فيض هائل من الفتاتيات
 المنقلبه سوا من الرفوف البحريه القريبه والمحيطه للحوض أو من المرتفعات اليابسه المجاوره